Studies and reports in hydrology 40

Guidebook to studies of land subsidence due to ground-water withdrawal

Prepared for the International Hydrological Programme, Working Group 8.4

Joseph F. Poland, Chairman and Editor

Unesco

Guidebook to studies of land subsidence due to ground-water withdrawal

Prepared for the International Hydrological Programme, Working Group 8.4

Joseph F. Poland, Chairman and Editor

The designations employed and the presentation of the material in this publication do not imply the expression of any opinion whatsoever on the part of the publishers concerning the legal status of any country or territory, or of its authorities, or concerning the frontiers of any country or territory

Published in 1984 by the United Nations
Educational, Scientific and Cultural Organization
7, place de Fontenoy, 75700 Paris
Printed under the direction of
the American Geophysical Union, by
Book Crafters, Chelsea, Michigan
ISBN 92-3-102213-X

© Unesco 1984

Printed in the United States of America

Preface

Although the total amount of water on earth is generally assumed to have remained virtually constant, the rapid growth of population, together with the extension of irrigated agriculture and industrial development, are stressing the quantity and quality aspects of the natural system. Because of the increasing problems, man has begun to realize that he can no longer follow a "use and discard philosophy--either with water resources or any other natural resource. As a result, the need for a consistent policy of rational management of water resources has become evident.

Rational water management, however, should be founded upon a thorough understanding of water availability and movement. Thus, as a contribution to the solution of the world's water problems, Unesco, in 1965, began the first world-wide programme of studies of the hydrological cycle--the International Hydrological Decade (IHD). The research programme was complemented by a major effort in the field of hydrological education and training. The activities undertaken during the Decade proved to be of great interest and value to Member States. By the end of that period, a majority of Unesco's Member States had formed IHD National Committees to carry out relevant national activities and to participate in regional and international co-operation within the IHD programme. The knowledge of the world's water resources had substantially improved. Hydrology became widely recognized as an independent professional option and facilities for the training of hydrologists had been developed.

Conscious of the need to expand upon the efforts initiated during the International Hydrological Decade and, following the recommendations of Member States, Unesco, in 1975, launched a new long-term intergovernmental programme, the International Hydrological Programme (IHP), to follow the Decade.

Although the IHP is basically a scientific and educational programme, Unesco has been aware from the beginning of a need to direct its activities toward the practical solutions of the world's very real water resources problems. Accordingly, and in line with the recommendations of the 1977 United Nations Water Conference, the objectives of the International Hydrological Programme have been gradually expanded in order to cover not only hydrological processes considered in interrelationship with the environment and human activities, but also the scientific aspects of multi-purpose utilization and conservation of water resources to meet the needs of economic and social development. Thus, while maintaining IHP's scientific concept, the objectives have shifted perceptibly towards a multidisciplinary approach to the assessment, planning, and rational management of water resources.

As part of Unesco's contribution to the objectives of the IHP, two publication series are issued: "Studies and Reports in Hydrology" and "Technical Papers in Hydrology." In addition to these publications, and in order to expedite exchange of information in the areas in which it is most needed, works of a preliminary nature are issued in the form of Technical Documents.

The purpose of the continuing series "Studies and Reports in Hydrology" to which this volume belongs, is to present data collected and the main results of hydrological studies, as well as to provide information on hydrological research techniques. The proceedings of symposia are also sometimes included. It is hoped that these volumes will furnish material of both practical and theoretical interest to water resources scientists and also to those involved in water resources assessments and the planning for rational water resources management.

Joseph F. Poland of U.S. Geological Survey stands near bench mark S661 southwest of Mendota in the San Joaquin Valley, California. The bench mark site subsided 9m from 1925 to 1977, because of intensive withdrawal of ground water. Signs on the power pole indicate the respective positions of the land surface in 1925, 1955, and 1977.

Contents

Preface iii

Part I Manual. The occurrence, measurement, mechanics, prediction, and control of subsidence 1

1 Introduction, by Working Group 8.4, International Hydrological Programme 3

1.1 Background information 3
1.2 Purpose and scope of guidebook 3
1.3 Occurrence of subsidence 4
1.4 Geological environments of occurrence 11
1.5 Problems and remedial steps 12
1.6 Acknowledgments 12
1.7 References 12

2 Field measurement of deformation, by Joseph F. Poland, Soki Yamamoto, and Working Group 17

2.1 Introduction 17
2.2 Vertical displacement 17
2.2.1 Precise leveling by spirit leveling 17
2.2.2 Other techniques for measuring land-surface displacement 20
2.2.3 Extensometer wells 20
2.2.3.1 Single and double pipe extensometers 20
2.2.3.2 Anchored-cable and pipe extensometers 22
2.2.3.3 Slip joints 28
2.2.3.4 Telescopic extensometer 28
2.2.3.5 Extensometer records 29
2.2.4 Other techniques of subsurface measurement 29
2.2.4.1 General 29
2.2-4.2 Casing-collar logging 30
2.2.4.3 Radioactive-bullet logging 31
2.3 Horizontal displacement 33
2.3.1 Land-surface displacement 33
2.3.2 Subsurface displacement 33
2.4 References 33

3 Mechanics of land subsidence due to fluid withdrawal, by Joseph F. Poland and Working Group 37

3.1 Introduction 37
3.2 Theory of aquifer-system compaction 38
3.3 Analysis of stresses causing subsidence 41
3.3.1 Types of stresses 41
3.3.2 Computation of stress change 43
3.4 Compressibility and storage characteristics 45
3.4.1 Stress-strain analysis 45
3.4.2 Soil-mechanics techniques 49
3.4.3 The compressibility environment 52
3.5 References 53

4 Laboratory tests for properties of sediments in subsiding areas, by A. I. Johnson and Working Group 55

4.1 Introduction 55
4.2 Field sampling 55
4.3 Composite logs of core holes 56
4.4 Methods of laboratory analysis 57
4.4.1 Particle-size distribution 58
4.4.2 Permeability 60
4.4.3 Unit weight 60
4.4.4 Specific gravity of solids 61
4.4.5 Porosity and void ratio 62
4.4.6 Moisture content 63
4.4.7 Atterberg limits 63
4.4.7.1 Liquid limit 64
4.4.7.2 Plastic limit 65
4.4.8 Consolidation 65
4.5 Results of laboratory analyses 67
4.5.1 Particle-size distribution 67
4.5.2 Sediment classification triangles 70
4.5.3 Statistical measures 70
4.5.4 Permeability 73
4.5.5 Specific gravity, unit weight, and porosity 74
4.5.6 Atterberg limits and indices 75
4.5.7 Consolidation 78
4.5.7.1 Estimating the compression index 78
4.5.7.2 Correlation of compression indices 82
4.5.7.3 Estimating coefficients of consolidation 82
4.5-7.4 Effect of soil classification 82
4.5.7.5 Relationship of consolidation characteristics and liquid limits 82
4.6 References 85

5 Techniques for prediction of subsidence, by Germán Figueroa Vega, Soki Yamamoto, and Working Group (Section 5.3.6 by Donald C. Helm) 89

5.1 Empirical methods 89
5.1.1 Extrapolation of data by naked eye 89
5.1.2 Application of some suitable curve: Nonlinear extrapolation 89
5.2 Semi-theoretical approach 93
5.2.1 Wadachi's (1939) model 93
5.2.2 Ratio of subsidence volume to liquid withdrawal 94
5.2.3 Ratio of subsidence to head decline 96
5.2.4 Clay content-subsidence relation 100
5.3 Theoretical approach 100
5.3.1 General remarks 100
5.3.2 Compressibility relationships and total potential subsidence 101
5.3.3 Differential equations of ground-water flow in an aquifer-aquitard system 102
5.3.4 Uncoupling the system and solving a simpler problem 103
5.3.5 Simplified subsidence modeling 105
5.3.6 Other types of subsidence models 106
5.3.6.1 Depth-porosity model 107
5.3.6.2 Aquitard-drainage model 110
5.3.6.3 Influence of material within the unpumped overburden 112
5.4 References 114

6 Economic and social impacts and legal considerations, by Joseph F. Poland, Laura Carbognin, Soki Yamamoto, and Working Group 119

6.1 General comments 119
6.2 Italy 119

6 Economic and social impacts and legal considerations, by Joseph F. Poland, Laura Carbognin, and Soki Yamamoto--Continued

6.3 Japan 120
6.3.1 Socioeconomic impacts 120
6.3.2 Ground-water law in Japan 121
6.4 United States 122
6.4.1 Economic and social impacts 122
6.4.1.1 Houston-Galveston area, Texas 122
6.4-1.2 San Joaquin and Santa Clara Valleys, California 123
6.4.2 Legal developments in California and Texas 123
6.5 References 125

7 Review of methods to control or arrest subsidence, by Joseph F. Poland and Working Group 127

7.1 Summary of available methods 127
7.1.1 General statement 127
7.1.2 Reduction of pumping draft 127
7.1.3 Artificial recharge of aquifers from the land surface 127
7.1.4 Repressuring of aquifers through wells 128
7.2 Review of methods used 128
7.2.1 Summary statement 128
7.2.2 Shanghai, China 129
7.2.3 Venice, Italy 129
7.2.4 Japan 129
7.2.5 United States 130
7.3 References 130

Part II Case histories of land subsidence due to ground-water withdrawal

8 Types of land subsidence, by Alice S. Allen 133

8.1 Introduction 133
8.2 The role of subsurface solution in subsidence 133
8.2.1 Salt 133
8.2.2 Gypsum 134
8.2.3 Carbonate rocks 135
8.3 The role of subsurface mechanical erosion in subsidence 135
8.4 Lateral flow as a subsidence mechanism 137
8.5 Compaction as a cause of subsidence 137
8.5.1 Loading 137
8.5.2 Drainage 138
8.5.3 Vibration 138
8.5.4 Extraction of pore fluids 138
8.5.5 Hydrocompaction 138
8.6 Tectonic subsidence 139
8.6.1 Discussion 139
8.7 References 139

9 Case histories 143

9.1 Latrobe Valley, Victoria, Australia, by C.S. Gloe 145
9.2 Shanghai, China, by S. Luxiang and B. Manfang 155
9.3 Venice, Italy, by L. Carbognin, et al. 161
9.4 Tokyo, Japan, compiled by S. Yamamoto 175
9.5 Osaka, Japan, compiled by S. Yamamoto 185

9 Case histories--Continued

9.6 Nobi Plain, Japan, compiled by S. Yamamoto 195
9.7 Niigata, Japan, compiled by S. Yamamoto 205
9.8 Mexico, D.F., Mexico, by G. E. Figueroa Vega 217
9.9 Wairakei, New Zealand, by P. F. Bixley 233
9.10 Bangkok, Thailand, compiled by S. Yamamoto 241
9.11 Alabama, U.S.A., by J. G. Newton 245
9.12 Houston-Glaveston Region, Texas, U.S.A., by R. K. Gabrysch 253
9.13 San Joaquin Valley, California, U.S.A., by J. F. Poland and B. E. Lofgren 263
9.14 Santa Clara Valley, California, U.S.A., by J. F. Poland 279
9.15 Ravenna, Italy, by L. Carbognin, et al. 291

Appendixes
A. Instrument capabilities for measuring land-surface displacement A-1
B. Capabilities of existing subsidence monitoring instruments B-1
C. List of symbols used in text, part I C-1
D. Glossary D-1
E. Metric conversion table E-1

Part I
Manual.
The occurrence, measurement, mechanics, prediction, and control of subsidence

I Introduction, by Working Group 8.4, International Hydrological Programme

1.1 BACKGROUND INFORMATION

The increasing exploitation of ground water, especially in basins filled with unconsolidated alluvial, lacustrine, or shallow marine deposits, has as one of its consequences the sinking or settlement of the land surface--land subsidence (see Glossary, Appendix D).

The occurrence of major land subsidence due to the withdrawal of ground water is relatively common in highly developed areas. Case studies on land subsidence and on remedial measures taken will be useful for developing areas facing similar problems in the future.

The problems of land subsidence were included in the programme of the International Hydrological Decade. During the Decade the major action with respect to land subsidence was the organization of the International Symposium on Land Subsidence held in Tokyo in 1969. The subject has also been retained under the framework of the International Hydrological Programme and included in the work plan for the first phase of the Programme (1975-1980) as IHP subproject 8.4.

In April 1975, the Intergovernmental Council for the International Hydrological Programme, at its first session in Paris, established a Working Group for coordination of IHP subproject 8.4, "Investigation on land subsidence due to ground-water exploitation." The Working Group members are listed below. In addition, A. I. Johnson, Vice President of the International Association of Hydrological Sciences, was the designated liaison from that international organization.

UNESCO Working Group on Land Subsidence

Due to Ground-Water Withdrawal

Mr. Joseph F. Poland, Chairman
U.S. Geological Survey
Rm. W-2528, Federal Building
2800 Cottage Way
Sacramento, California 95825

Mr. Germán Figueroa Vega
Comisión de Aguas de Valle de México
Balderas No. 55-20. Piso.
México 1, D.F.

Ms. Laura Carbognin
National Research Council
1364 San Polo
Venice, Italy 30125

Mr. Ivan Johnson
Representative of IAHS
Woodward-Clyde Consultants
2909 West 7th Avenue
Denver, Colorado,80204

Mr. Soki Yamamoto
Rissho University
4-2-16 Osaki, Shingawa-ku
Tokyo 141, Japan

1.2 PURPOSE AND SCOPE OF GUIDEBOOK

The group was asked to prepare a guidebook on subsidence due to ground-water withdrawal, paying particular attention to measures to control and arrest subsidence, the use of artificial recharge, and the repressuring of aquifers. The goal was to produce a guidebook that will serve as a guide to engineers, geologists, and hydrologists faced with the problem of land subsidence, particularly in developing countries. They may be asked to answer the questions of whether land subsidence is occurring, if so, where and at what rate, the cause or causes, and what can be done to stop it or at least slow it down. The guidebook should be of assistance in planning and undertaking the field studies.

The first session of the Working Group was held in December 1976 in connection with the Second IAHS-UNESCO International Symposium on Land Subsidence in Anaheim, California. At that meeting the group drafted the general outline of the guidebook and decided on the distribution of work.

The guidebook is organized in two parts. Part I is a manual of seven chapters on the occurrence, measurement, mechanics, prediction, and control of land subsidence due to groundwater withdrawal. It has been prepared as a joint effort of the Working Group members.

Part II is a series of invited case histories of land subsidence due to ground-water withdrawal, prepared by individual authors. The first chapter in Part II (Chapter 8) is a brief discussion of other types of land subsidence written by Ms. Alice Allen. Subsidence may occur from many other causes than withdrawal of ground water. Some occurrences are due to natural causes and some are the work of man. Anyone investigating subsidence due to ground-water withdrawal should have at least an elementary knowledge of other types of subsidence and the geologic environments in which they are likely to occur. Although the present discussion by Ms. Allen is brief, it contains 62 references, which should prove very helpful to the reader who wishes to learn more about any particular subsidence process.

The second chapter in Part II (Chapter 9) consists of 15 case histories of subsidence due to ground-water withdrawal, prepared by individual authors. These case histories cover a wide range of conditions and magnitudes of subsidence. Of the occurrences described, 12 are areas of ground-water withdrawal for use and 3 represent conditions where ground water is withdrawn as a step in obtaining a resource. These are Latrobe Valley, Australia (withdrawal to permit mining brown coal), Niigata, Japan (withdrawal to obtain natural gas), and Wairakei, New Zealand (withdrawal of hot water for geothermal power).

1.3 OCCURRENCE OF SUBSIDENCE

The chief source of information on areas of land subsidence due to ground-water withdrawal is the Questionnaire on Land-Subsidence Occurrence, Research, and Remedial Work that was distributed worldwide in 1975-78 by A. I. Johnson, then President of the International Commission of Subsurface Water of IAHS. The results of this survey are being compiled for publication by UNESCO and IAHS. Other sources of data are (1) the 15 case histories in Part II of this casebook, (2) the Proceedings of the lst International Symposium on Land Subsidence held in Tokyo, Japan, in September 1969, and (3) the Proceedings of the 2nd International Symposium on Land Subsidence held in Anaheim, California, in December 1976.

Table 1.1, based on the information listed above, summarizes information on 42 subsidence areas worldwide, of which 18 are in the United States and 10 are in Japan (Figure 1-1). Actually, Japan has the largest number of subsiding areas of any country. According to Yamamoto (1977, p. 9 and Figure 2), the number of subsiding areas in Japan has reached 40 and is still increasing. Most of the subsidence is due to ground-water withdrawal from thickly populated topographically low areas bordering the ocean. Only the 10 chief subsidence areas in Japan due to ground-water withdrawal are reported in Table 1.1 and shown in Figure 1.1. All of these border the ocean.

In terms of vertical magnitude, the subsiding areas listed in Table 1.1 range from reported minor casing protrusion in Bangkok, Thailand, and 0.15 m of subsidence in Venice, Italy, to 15 m in the Cheshire district of Great Britain where rock salt has been mined by solution since Roman times. As a result of man-induced sinkhole development in carbonate terrane in Alabama, we even have a reported maximum of 37 m. The areal extent of subsidence, worldwide, ranges from 10 km^2 in the San Jacinto Valley to 13,500 km^2 in the San Joaquin Valley, both in California (USA).

Figure 1.2 shows the geographic location of the 17 areas in the United States (exclusive of the Alabama sinkhole area) on a map of conterminous United States. Subsidence of the land surface in the 17 areas ranges from 0.3 m at Savannah, Georgia to 9 m. on the west side of the San Joaquin Valley (Los Banos-Kettleman City area) in California (Figure 1.3). Subsidence exceeding 1 metre occurs in four States: Texas, Arizona, Nevada, and California. The areal extent ranges from 10 km^2 in San Jacinto Valley, California, to 13,500 km^2 in the San Joaquin Valley. California is the State ranking number one for the dubious honor of having the largest area of subsidence --about 16,000 km^2. Close behind is Texas with 12,000 km^2; and Arizona is third with 2,700 km^2.

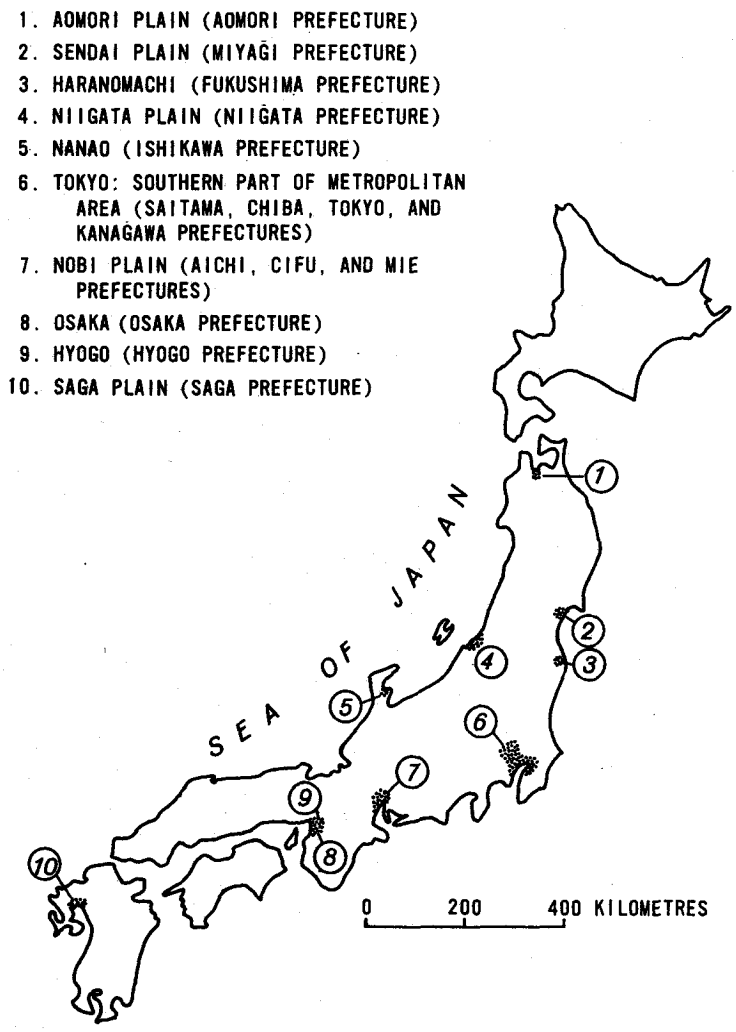

Figure 1.1 Chief subsidence areas in Japan.

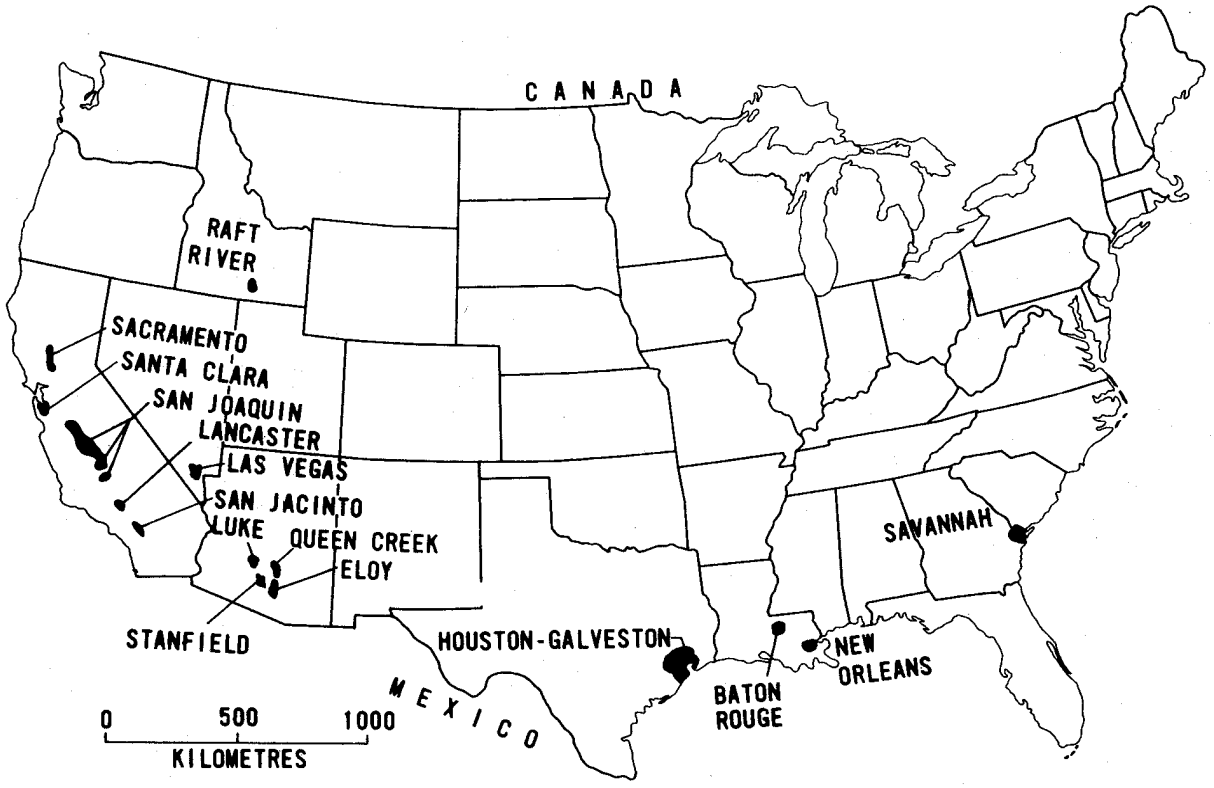

Figure 1.2 Areas of land subsidence from ground-water withdrawal, USA.

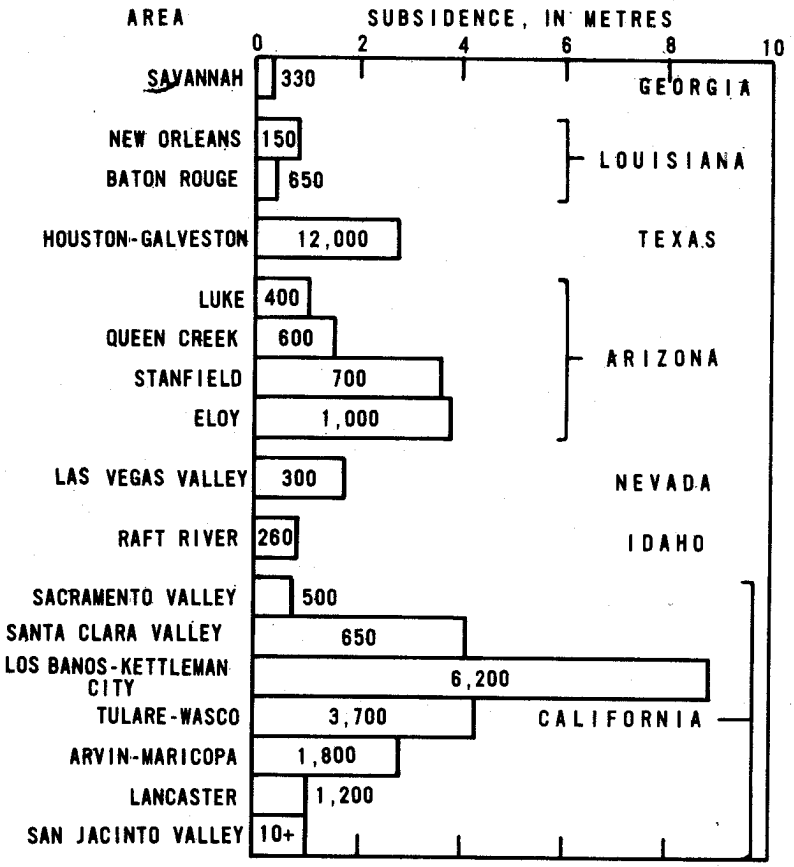

Figure 1.3 Magnitude of land subsidence from ground-water withdrawal, USA (number in column represents area in square kilometres).

Table 1.1. Areas of land subsidence due to ground-water withdrawal

Location	Depositional environment and age	Depth range of compacting beds (m)	Maximum subsidence (m)	Area of subsidence (km^2)	Time of principal occurrence	Remedial or protective measures taken	Principal reference(s)
Australia:							
Latrobe Valley.	Lacustrine and fluviatile; early Tertiary.	10-300	1.6 (1977)	100 (>0.2 m)	1961-78	Reduction in artesian ground-water pressures, necessary for mining coal. Restrictions placed on building in critical area.	Gloe (1977); Gloe, Guidebook, Ch. 9.1.
China:							
Shanghai.	Alternating fresh-water and marine; Quaternary.	3-300	2.63 (1965)	121	1921-65	Restricted use of ground water; artificial recharge by injection of treated river water into wells; adjustment of pumping pattern.	Shanghai Hydrogeological Team (1973); Luxiang and Manfang, Guidebook, Ch. 9.2.
Taipei Basin.	do.	10-240	1.9 (1974)	235	1955-74	In 1968, legal action taken to limit ground-water pumpage.	Hwang and Wu (1969); Wu (1977).
Great Britain:							
London.	London Clay of Eocene age overlying chalk aquifer of Cretaceous age.	50-100	0.35 (1976)	450	1865-1932	None.	Longfield (1932); Wilson and Grace (1942); Water Resources Board (1972).
Cheshire district.	Sandstone, marl, and rock salt; Triassic.	100-300	15 (1977)	1,500	1533-1977	Reduced pumping of brine; installed flexible foundations; regraded railways roads, canals.	Howell and Jenkins (1977); Collins (1971).
Hungary:							
Debrecen.	Fluviatile; Quaternary.	50-250	0.42 (1975)	390	1920-75	None.	Orlóczi (1969); Miskolczi (1967); Szekely (1975).
Visonta.	Fluviatile and swampy; late Cenozoic.	20-100	0.5 (1975)	40	1961-75	None.	Kesserü (1970); Kesserü (1972).
Italy:							
Po Delta.	Alluvial, lagoonal, and shallow marine; Quaternary.	100-600	3.2	2,600	1951-66	Pumping of gas-bearing water stopped by legal action.	Schrefler, Lewis, and Norris (1977); Zambon (1967); Caputo, et al (1970).
Ravenna.	Alluvial, lacustrine, and shallow marine; Neozoic.	80-500	1.20 (1977)	about 600	1955-77	None (project plans underway).	Bertoni, et al (1973); Carbognin, et al (1978); Guidebook, Ch. 9.15.
Venezia.	Alluvial, lacustrine, and shallow marine; Neozoic.	70-350	0.15 (1976)	about 400	1952-70	A 70-percent shutdown of active artesian wells including some principal ones, and construction of two river-fed aqueducts supplying mainly the industrial zone.	Gambolati and Freeze (1973); Gambolati, et al (1974); Carbognin, et al (1977) (reprinted in Guidebook as Ch. 9.3).
Japan:							
Aomori.	Alluvial and lacustrine; late Cenozoic.	0-600	0.45 (1977)	65	1958-78	Reduced withdrawal of ground water by regulation	Aomori Pref. (1974).
Sendai.	Alluvial and shallow marine; late Cenozoic.	0-300	0.57 (1977)	90	1966-78	As above and introducing water from river	
Haranomachi. City.	Alluvial and shallow marine; late Cenozoic.	100-200	2	25	1965-78+	Regulation of ground water withdrawal; constructed multipurpose dams and water-supply systems	IAHS questionnaire.
Nanao.	Alluvial and shallow marine; late Cenozoic.	0-200	0.53 (1977)	80	1972-78	Reduced withdrawal of ground water by regulation	Murakami and Takahashi (1969)

Tokyo, including Chiba, Saitama, and Kanagawa Prefectures.	Alluvial and shallow marine; late Cenozoic.	0-400 and *800-2,000	4.59 (1975)	3,420	1918-78+	Built reservoirs and canals to import surface water-from R. Tone and reduce ground-water withdrawal	Miyabe (1962); Aoki and Miyabe (1969); Ishii, et al (1977); Yamamoto, Guide book, Ch. 9.4.
Niigata	Shallow marine and marine; late Cenozoic.	0-1,000	2.65 (1965)	430	1957-78+	Reduced withdrawal of gas-bearing water by regulation; since 1973, all gas water reinjected into reservoirs.	Takeuchi et al (1969); Aoki (1977); Yamamoto, Guidebook, Ch. 9.7.
Nobi (Aichi, Gifu, and Mie Prefectures.	Alluvial and lacustrine; late Cenozoic.	0-300	1.53 (1970)	1,140	1932-78+	Diverted Aichi irrigation water and constructed dam; reduced ground-water withdrawal by regulation.	Kuwahara, et al (1977); Yamamoto, Guidebook, Ch. 9.6.
Osaka.	Alluvial and lacustrine; Quaternary.	0-400	2.88 (1970)	630	1935-70	Imported surface water from R. Yodo and reduced ground-water withdrawal.	Murayama (1969); Ikebe, et al (1970); Nakamachi (1977); Editorial Comm. (1969); Yamamoto, Guidebook, Ch. 9.5.
Hyogo.	do.	0-200	2.84 (1960)	100	1932-70	do.	
Saga.	Alluvial and shallow marine; Quaternary.	0-200	1.20 (1977)	300	1957-78+	Imported surface water; dam under construction.	Kumai, et al (1969).
México:							
México city.	Alluvial, lacustrine; Quaternary and Tertiary.	0-50	9(1978)	about 225	1891-1978	Holding withdrawal constant and undertaking delivery of surface water into the valley of Mexico to diminish and eventually eliminate ground-water overdraft.	Marsal y Mazari (1959); CHCVM (1953-1970); CAVM (1975); Figueroa-Vega, Guidebook, Ch. 9.8.
New Zealand:							
Wairakei.	Volcanic flows and breccias; Pleistocene.	250-800	6-7 (1975)	30	1952-78	None.	Stilwell, Hall, and Tawhai (1975); Bixley, Guidebook, Ch. 9.9.
South Africa:							
Far West Rand.	Dolomite Series, Paleozoic, and weathered overburden.	30-200 for overburden; 30-1,200 for dolomite.	9(overburden)	?	1959-75	Artificial recharge of dolomitic compartments with ground water pumped from mines.	Bezuidenhout and Enslin (1969); Enslin, et al (1977).
Thailand:							
Bangkok.	Alluvial and shallow marine; Quaternary.	0-200	Well casing protrusion reported.	?	1978-	None.	Piancharoen (1977); Brand and Balasubramaniam (1977); Yamamoto, Guidebook, Ch. 9.10.
United States:							
Alabama:	Carbonate terrane; unconsolidated deposits on bedrock.	10-100	37(?)	4,000 man-made sink-holes, 1-1,000 m in diameter.	1900-75	Removal of surface water; bridging of railroads and highways; removal of unconsolidated deposits.	Newton (1977); Newton, Guide book, Ch. 9.11.
Arizona**:							
Luke area.	Alluvial and lacustrine; Cenozoic	50-350	1(1967)	400	1950(?)-1978	Damaged well casings repaired	Laney, Raymond, and Winikka (1978).
Queen Creek area.	do.	50-350	1.5 (1976)	600	1950(?)-1978	Constructing major aqueduct to import Colorado River water and reducing overdraft.	Winikka and Wold (1977); Schumann (1914).

Table 1.1. Areas of land subsidence due to ground-water withdrawal--Continued

Location	Depositional environment and age	Depth range of compacting beds (m)	Maximum subsidence (m)	Area of subsidence (km^2)	Time of principal occurrence	Remedial or protective measures taken	Principal reference(s)
United States--Continued:							
Arizona--Continued:							
Stanfield area.	Alluvial and lacustrine; Cenozoic.	50-350	3.6 (1977)	700	1950(?)-78	Well casings repaired.	
Eloy area.	do.	50-350	3.8 (1977)	1,000	1950(?)-78	Well casings, highway, and railroad repaired.	Schumann and Poland (1969).
California							
Sacramento Valley.	Alluvial and fluviatile; late Cenozoic.	30-300	0.7	500	1955-78+	None.	Lofgren and Ireland (1973).
Santa Clara Valley.	Alluvial and shallow marine; late Cenozoic.	50-330	4.1 (1975)	650	1918-70	Built detention dams; increased local recharge; built levees; imported water; many damaged well casings repaired or wells replaced.	Poland (1977); Poland, Guide book, Ch. 9.14.
San Joaquin Valley							
Los Banos-Kettleman City area.	Alluvial and lacustrine; late Cenozoic.	60-900	9.0 (1977)	6,200	1930-75	Built dams and canals to import surface water and reduce ground-water withdrawal. Repaired many well casings damaged by compressive stresses.	Poland, Lofgren, Ireland, and Pugh (1975); Bull (1975); Poland and Lofgren, Guide book, Ch. 9.13.
Tulare-Wasco area.	Alluvial, lacustrine, and shallow marine; late Cenozoic.	60-700	4.3 (1970)	3,680	1930-70	do.	Lofgren and Klausing (1969); Poland and others (1975).
Arvin-Maricopa area.	Alluvial and lacustrine; late Cenozoic.	60-500	2.8 (1970)	1,800	1940-70	do.	Lofgren (1975); Poland and others (1975).
Lancaster area.	Alluvial and lacustrine; late Cenozoic.	60-300	1+ (1976)	1,200	1955-78	Damaged well casings repaired.	Lewis and Miller (1968); McMillan (1973).
San Jacinto Valley.	Alluvial; late Cenozoic.	60-300	1+ (1974)	10+	1950-75+	None.	Lofgren (1976).
Georgia:							
Savannah area.	Marine; Tertiary.	50-150	0.3	330	1933-75+	None.	Davis, Counts, and Holdahl (1977).
Idaho:							
Raft River.	Alluvial; late Cenozoic.	50-300	10.8 (1975)	260	1960-75+	None.	Lofgren (1975).
Louisiana:							
Baton Rouge.	Fluviatile and shallow marine; late Cenozoic.	120-900	0.38 (1976)	650+	1935-76+	None.	Davis and Rollo (1969); Wintz, Kazmann, and Smith (1970); Smith and Kazmann (1978).
New Orleans.	Fluviatile and shallow marine; Quaternary(?).	150-260	0.8 (1975)	150	1940-75+	None.	Rollo (1966); Kazmann and Heath (1968).
Nevada:							
Las Vegas.	Alluvial; late Cenozoic.	60-300	1-1.7 (1972)	300	1935-75+	Moved well field away from fine-grained deposits; imported Colorado River water.	Malmberg (1964); Kindling (1971).
Texas:							
Houston-Galveston area.	Fluviatile and shallow marine; late Cenozoic.	60-900	2.75 (1973)	12,000 >15 cm	1943-78	Built reservoirs and importing surface water to reduce overdraft; Subsidence Control District created.	Gabrysch and Bonnet (1975); Gabrysch, Guidebook, Ch. 9.12.

*Extraction of natural gas.
**Data chiefly from questionnaires for IAHS completed by Carl Winikka, January 1978.

1.4 GEOLOGICAL ENVIRONMENTS OF OCCURRENCE

Subsidence due to ground-water withdrawal develops principally under two contrasting environments and mechanics. One environment is that of carbonate rocks overlain by unconsolidated deposits, or old sinkholes filled with unconsolidated deposits, that receive buoyant support from the ground-water body. When the water table is lowered, the buoyant support removed, and the hydraulic gradient increased, the unconsolidated material may move downward into openings in the underlying carbonate rocks, sometimes causing catastrophic collapses of the roof. In Alabama, according to J. G. Newton (1977 and Chapter 9.11), an estimated 4,000 man-induced sinkholes have formed since 1900 in contrast to less than 50 natural collapses. In the United States manmade sinkhole occurrence is common in carbonate terranes from Florida to Pennsylvania, numbering many thousands. The individual sinkhole area is small, however, the diameter usually ranging from 1 to 100 m (Stringfield and Rapp, 1977). Carbonate terrane susceptible to sinkhole formation when the water table is lowered occurs in many parts of the world. In populated areas the formation of sinkholes can produce a variety of problems related to the maintenance of manmade structures and the pollution of water supplies. Newton discusses some of these problems in Chapter 9.11. The overall subject is broad and beyond the scope of this guidebook.

The other environment and by far the most extensive occurrence is that of young unconsolidated or semiconsolidated clastic sediments of high porosity laid down in alluvial, lacustrine, or shallow marine environments. Almost all the subsiding areas included in Table 1.1 are underlain by semiconfined or confined aquifer systems containing aquifers of sand and/or gravel of high permeability and low compressibility, interbedded with clayey aquitards of low vertical permeability and high compressibility under virgin stresses. All the compacting deposits were normally loaded, or approximately so, before man applied stresses exceeding preconsolidation stress. These aquifer systems compact in response to increased effective stress caused by artesian-head decline in the coarse-grained aquifers and time-dependent pore-pressure reduction in the fine-grained compressible aquitards, causing land-surface subsidence.

Of the principal clay minerals--montmorillonite, illite, and kaolinite--montmorillonite is the most compressible. Montmorillonite is the predominant clay mineral in the compacting aquifer systems in southwestern United States--California (Meade, 1967), south-central Arizona (Poland, 1968), and Texas (Corliss and Meade, 1964)--also in Mexico City (Marsal and Mazari, 1959). Montmorillonite comprises 60 to 80 per cent of the clay-mineral assemblage in each of these areas. Illite is the chief clay mineral in the Taipei basin (Hwang and Wu, 1969), and in the Quaternary deposits in Tokyo (Tokyo Metropolitan Govt., 1969).

Another occurrence of subsidence due to ground-water withdrawal that is not represented in Table 1.1 has developed at many sites in Sweden and Norway and probably in other glaciated areas of similar geologic and hydrologic environments. According to Broms, Fredriksson, and Carlsson (1977), most of the bedrock in Sweden is crystalline rock, favorable for construction of underground structures, especially tunnels, because of high strength and because loose and weathered parts have been removed by the glaciation. After the latest glaciation, clay and silt were deposited on a thin layer of till or sand and gravel resting on the bedrock surface, especially in bedrock depressions that commonly are indicative of tectonic zones deepened by the ice. The areas covered with clay are small but the urban regions are mostly in these areas. Deep tunnels cutting through tectonic zones act as drains, lowering the pore-water pressure first in the pervious bottom layers (confined aquifers), and then gradually (over a period of years) in the overlying clay layer. Broms and others (1977) describe damages cause by this type of subsidence and steps that can be taken to mitigate or prevent the subsidence. They can be summarized as follows:

1. Before the construction of a tunnel, by avoiding areas which can be affected by subsidence;

2. During the construction, by pregrouting;

3. After the construction, by grouting, in order to reduce the leakage or by artificial infiltration of water to maintain the pore pressure in the compressible layers.

Moreover it is often possible to decrease the subsidence in soft clays by preloading. It is also possible to preload the compressible layers in advance by temporarily lowering the groundwater level by pumping from deep wells.

1.5 PROBLEMS AND REMEDIAL STEPS

Principal problems caused by the subsidences listed in Table 1.1 are (1) differential changes in elevation and gradient of stream channels, drains, and water-transport structures, (2) failure of water-well casings due to compressive stresses generated by compaction of aquifer systems, (3) tidal encroachment in lowland coastal areas, and (4) in areas of intensive subsidence, development of tensional or compressional strain in engineering structures. Additional details on problems are discussed in the case histories of Chapter 9.

Remedial or protective measures of some sort have been taken in 10 of the 15 case-history areas and 30 of the 42 areas listed in Table 1.1. The various steps that have been taken to control or ameliorate subsidence will be discussed in Chapter 7. The methods employed and the results attained should be of interest to anyone facing a subsidence problem due to water-level decline from overpumping. In Part I of this guidebook, frequent reference will be made to pertinent case histories.

1.6 ACKNOWLEDGMENTS

Beyond the joint efforts of the Working Group, several people have assisted in preparation or review of chapters. In preparation of Table 1.1, Marcelo Lippmann assisted by contacting countries in South America concerning possible subsidence. Chapter 2 reviewers included R. K. Gabrysch, R. L. Ireland, R. L. Laney, H. H. Schumann, and especially F. S. Riley, for his many helpful suggestions. Chapter 3 was reviewed in detail by D. C. Helm, who also made a major contribution to Chapter 5. He is the author of section 5.3.6, including discussion of the depth-porosity model and the aquitard-drainage model. J. A. daCosta was very helpful in editorial review of several chapters and case histories. Also, we are indebted to Mrs. Margaret Farmer for her patient and careful typing and retyping of manuscript drafts.

1.7 REFERENCES

AOKI, S. 1977. Land Subsidence in Niigata. IAHS/AISH Pub. No. 121, p. 105-112.

AOKI, S., and MIYABE, N. 1969. Studies on partial compaction of soil layer in reference to land subsidence in Tokyo. IAHS/AISH Pub. No. 89, p. 354-360.

AOMORI PREFECTURE. 1974. Report on water balance study in Aomori region. Environment and Health Dept., p. 1-111 (in Japanese).

BERTONI, W., CARBOGNIN, L., GATTO, P., and MOZZI, G. 1973. Note interpretative preliminari sulle cause della subsidenza in atto a Ravenna. C.N.R., Lab. per lo Studio della Dinamica delle Gradi Masse, Tech. Rept. 65, Venezia.

BEZUIDENHOUT, C. A., and ENSLIN, J. F. 1969. Surface subsidence and sinkholes in the dolomitic areas of the Far West Rand, Transvaal, Republic of South Africa, in Tison, L. J., ed., Land Subsidence, V. 2. IAHS/AISH Pub. No. 89, p. 482-495.

BROMS, B. B., FREDRICKSSON, ANDERS. 1977. Land subsidence in Sweden due to water-leakage into deep-lying tunnels and its effects on pile-supported structures. IAHS/AISH Pub. No. 121, p. 375-387.

BUREAU OF CONSTRUCTION, TOKYO METROPOLITAN GOVERNMENT, 1969. Land Subsidence and flood control measures in Tokyo. p. 1-40.

CARBOGNIN, L., GATTO, P., MOZZI, G., GAMBOLATI, G., and RICCARI, G. 1977. New trend in the subsidence of Venice. IAHS/AISH Pub. No. 121, p. 65-81.

CARBOGNIN, L., GATTO, P., MOZZI, G., and GAMBOLATI, G. 1978. Land subsidence of Ravenna and its similarities with the Venice case. American Soc. Civil Engineers, Proceedings of Eng. Found. Conf. on Evaluation and Prediction of Subsidence, Pensacola Beach, Florida. Jan. 1978.

COLLINS, J. F. N. 1971. Salt: A policy for the control of salt extraction in Cheshire. Chesire County Council.

COMISIÓN HIDRÓLOGICA DE LA CUENCA DEL VALLEY DE MÉXICO, SRH. 1953-70. Boletín de Mecánica de Suelos del Núm. 1-6. Mexico.

COMISIÓN DE AGUAS DEL VALLE DE MÉXICO, SRH. 1975. Boletin de Mecánica de Suelos Núm. 7, 289 pp.

CORLISS, J. B., and MEADE, R. H. 1964. Clay minerals from an area of land subsidence in the Houston-Galveston Bay area, Texas, in Geological Survey Research 1964. U.S. Geol. Survey Prof. Paper 501-C, p. C79-C81.

DAVIS, G. H., COUNTS, H. B., and HOLDAHL, S. R., 1977. Further examination of subsidence at Savannah, Georgia, 1955-1975. IAHS/AISH Pub. No. 121, p. 347-354.

DAVIS, G. H., and ROLLO, J. R., 1969. Land subsidence related to decline of artesian head at Baton Rouge, Lower Mississippi Valley, USA, in Tison, L. J., ed., Land Subsidence, V. 1. IAHS/AISH Pub. No. 88, p. 174-184.

EDITORIAL COMM. FOR TECHNICAL REPORT ON OSAKA LAND SUBSIDENCE. 1969. Report on land subsidence in Osaka, p. 1-148.

ENSLIN, J. F., KLEYWEGT, R. J., BEUKES, J. H. T., and GORDON-WELSH, J. F., 1977. Artificial recharge of dolomitic ground-water compartments in the Far West Rand gold fields of South Africa. IAHS/AISH Pub. No. 121, p. 495-506.

GABRYSCH, R. K., and BONNET, C. W. 1975. Land-surface subsidence in the Houston-Galveston region, Texas. Texas Water Development Board Report 188, 19 p.

GAMBOLATI, G., and FREEZE, R. A. 1973. Mathematical simulation of subsidence of Venice, 1, Theory. Water Resources Research, v. 9, no. 3, p. 721-733.

GAMBOLATI, G., GATTO, P., and FREEZE, R. A. 1974. Mathematical simulation of subsidence of Venice, 2, Results. Water Resources Research, v. 10, no. 3, p. 563-577.

GLOE, C. S. 1977. Land subsidence related to brown coal open cut operations, Latrobe Valley, Victoria, Australia. IAHS/AISH Pub. No. 121, p. 399-401.

HOWELL, F. T., and JENKINS, P. L. 1977. Some aspects of the subsidences in the rocksalt districts of Cheshire, England. IAHS/AISH Pub. No. 121, p. 507-520.

HWANG, JUI-MING, and WU, CHIAN-MIN. 1969. Land subsidence problems in Taipei Basin, in Tison, L. J., ed., Land Subsidence, V. 1. IAHS/AISH Pub. No. 88, p. 21-34.

IKEBE, N., WATSU, J. I., TAKENAKA, J. 1970. Quaternary geology of Osaka with special reference to land subsidence. Jour. Geosc., Osaka City Univ., 13, p. 39-98.

ISHI, M., KURAMOCHI, F., and ENDO, T. 1977. Recent tendencies of the land subsidence in Tokyo. IAHS/AISH Pub. No. 121, p. 25-34.

KAZMANN, R. G., and HEATH, M. M. 1968. Land subsidence related to ground-water offtake in the New Orleans area. Gulf Coast Assoc. Geological Societies Trans., v. xviii, p. 108-113.

KESSERÜ, ZSOLT. 1970. Felszini süllyedés vizszintsüllyesztés követ-keztében (Land subsidence due to the effect of sinking the ground-water table). Magyar Tudományos Akadémia IV; Bányavizvédelmi Konferencíaja, Budapest IV. Conference of mine-drainage networks, Hungarian Academy of Sciences, Budapest, I.a/Vol. no. 3.

KESSERÜ, ZSOLT. 1972. Forecasting potential building damages due to the effect of sinking the underground-water table. II. International Conference of mining Geodesy, Budapest, Vol. V.

KUMAI, H., SAYAMA, M., SHIBASAKI, T., and UNO, K. 1969. Ground sinking in Shiroishi Plain Saga Prefecture. IAHS/AISH Pub. No. 89, p. 645-657.

KUWAHARA, T., UESHITA, K., and IIDA, K. 1977. Analysis of land subsidence in Nobi Plain. IAHS/AISH Pub. No. 121, p. 55-64.

LANEY, R. L., RAYMOND, R. H., and WINIKKA, C. C. 1978. Maps showing water-level declines, land subsidence, and earth fissures in south-central Arizona. U.S. Geol. Survey Water-Resources Investigations Report 78-83, 2 maps.

LEWIS, R. E., and MILLER, R. E. 1968. Geologic and hydrologic maps of the southern part of Antelope Valley, California. U.S. Geol. Survey report, 13 p.

LOFGREN, B. E. 1975. Land subsidence and tectonism, Raft River Valley, Idaho. U.S. Geol. Survey open-file report 75-585, 21 p.

LOFGREN, B. E. 1976. Land subsidence and aquifer-system compaction in the San Jacinto Valley, Riverside County, California--A progress report. U.S. Geol. Survey Journal of Research, v. 4, no. 1, p. 9-18.

LOFGREN, B. E., and IRELAND, R. L. 1973. Preliminary investigation of land subsidence in the Sacramento Valley, California. U.S. Geol. Survey open-file report, 32 p.

LONGFIELD, T. E. 1932. The subsidence of London. Ordnance Survey, Prof. Papers, new ser., no. 14.

McMILLAN, J. F. 1973. Land subsidence--Antelope Valley area of Los Angeles County. Dept. of County Engineer, Survey Div., Los Angeles, Calif., 11 p.

MALMBERG, G. T. 1964. Land subsidence in Las Vegas Valley, Nevada, 1935-63, in Ground-Water Resources--Information Ser., Rept. 5. Nevada Dept. Conservation and Natural Resources, and U.S. Geol. Survey, 10 p.

MARSAL, RAUL J., and MAZARI, MARCOS. 1959. El Subsuelo de la Ciudad de Mexico. Primer Panamericano, Congreso de Mecanica de Suelos y Cimentaciones, 614 p. (2d ed., 1969, is bilingual in Spanish and English.)

MEADE, R. H. 1967. Petrology of sediments underlying areas of land subsidence in central California. U.S. Geol. Survey Prof. Paper 497-C, 83 p.

MINDLING, ANTHONY, 1971. A summary of data relating to land subsidence in Las Vegas Valley. Nevada Univ. System, Desert Research Inst., Center for Water Resources Research, 55 p.

MISKOLCZI, LÁSZLÓ. 1967. A debreceni mozgásvizgálatok geodéziai tanulságai (Geodetic methodology of land subsidence measurements in Debrecen). Geodézia és Kartográfia v. 19, no. 1.

MIYABE, N. 1962. Studies in the ground sinking in Tokyo. Report Tokyo Inst. Civil Eng., p. 1-38.

MURAKAMI, M., and TAKAHASHI, Y. 1969. Land subsidence research and regional water resource planning of the Nanao Basin. IAHS/AISH Pub. No. 121, p. 211-222.

MURAYAMA, S. 1969. Land subsidence in Osaka. IAHA/AISH Pub. No. 88, p. 105-130.

NAKAMACHI, N. 1977. Land subsidence in Osaka, Japan. Society Soil Mechanics and Foundation Eng., v. 25, no. 6, p. 61-67. (In Japanese)

NEWTON, J. G. 1977. Induced sinkholes--a continuing problem along Alabama highways. Internat. Assoc. Hydrological Sci., Pub. 121, p. 453-463.

ORLÓCZI, ISTVAN. 1969. Water balance investigations based upon measurement of land subsidence caused by ground-water withdrawal. IAHS/AISH Pub. No. 88, p. 224-232.

PIANCHAROEN, CHAROEN. 1977. Ground water and land subsidence in Bangkok, Thailand. IAHS/AISH Pub. No. 121, p. 355-364.

POLAND, J. F. 1968. Compressibility and clay minerals of sediments in subsiding ground-water basins, southwestern United States. Geol. Soc. America 81st Ann. Mtg. Prog., Mexico City (1968), p. 241; 1968, Geol. Soc. America Spec. Paper 121, p. 241.

POLAND, J. F. 1977. Land subsidence stopped by artesian-head recovery, Santa Clara Valley, California. IAHS/AISH Pub. No. 121, p. 124-132.

POLAND, J. P., LOFGREN B. E., and RILEY, F. S. 1972. Glossary of selected terms useful in studies of the mechanics of aquifer systems and land subsidence due to fluid withdrawal. U.S. Geological Survey Water-Supply Paper 2025, 9 p.

POLAND, J. F., LOFGREN, B. E., IRELAND, R. L., and PUGH, R. G. 1975. Land subsidence in the San Joaquin Valley as of 1972. U.S. Geol. Survey Prof. Paper 437-H, 78 p.

ROLLO, J. R. 1966. Ground-water resources of the greater New Orleans area, Louisiana. Louisiana Geol. Survey, Water Resources Bull. No. 9, 69 p.

SCHREFLER, B. A., LEWIS, R. W., and NORRIS, V. A. 1977. A case study of the surface subsidence of the Polesine area. Internat. Jour. for Num. and Analytical Methods in Geomechanics, v. 1, no. 4, p. 377-386.

SCHUMANN, H. H. 1974. Land subsidence and earth fissures in alluvial deposits in the Phoenix area, Arizona. U.S. Geol. Survey Misc. Inv. Ser., Map 1-845-H, 1 sheet.

SCHUMANN, H. H., and POLAND, J. F. 1969. Land subsidence, earth fissures, and ground-water withdrawal in south-central Arizona, USA, in Tison, L. J., ed., Land Subsidence, V. 1. IAHS/AISH Pub. No. 88, p. 295-302.

SHANGHAI HYDROGEOLOGICAL TEAM. 1973. On the control of surface subsidence in Shanghai. Acta Geologica Sinica 2, p. 243-254. (In Chinese)

SMITH, C. G., and KAZMANN, R. G. 1978. Subsidence in the capital area ground-water conservation district--an update. Capital Area Ground-Water Conservation Commission, Bull. no. 2, 31 P.

STILWELL, W. B., HALL, W. K., and TAWHAI, JOHN. 1975. Ground movement in New Zealand geothermal fields. Ministry of Works and Development, Wairakei, Private Bag, Taupo. New Zealand. p. 1427-1434.

SZEKELY, FERENC. 1975. Mathematical model for the cone of depression of waterworks in loose sedimentary basins. International Conference of IAH and IAHS, Hydrogeology of Great Sedimentary Basins, Budapest.

TAKEUCHI, S., KIMOTO, S., WADA, M., MUDAI, K., and HINA, H. 1969. Geological and geohydrological properties of land subsided area--case of Niigata lowland. IAHS/AISH Pub. No. 88, p. 232-241.

TOKYO METROPOLITAN GOVERNMENT. 1969. Land subsidence in Tokyo, p. 1-32.

WATER RESOURCES BOARD. 1972. The hydrogeology of the London Basin. Water Resources Board, Reading, 139 p.

WILSON, GUTHLAC, and GRACE, HENRY. 1942. The settlement of London due to underdrainage of the London Clay. Jour. Inst. Civil Eng., v. 19, no. 2, Paper no. 5294, p. 100-127.

WINIKKA, C. C., and WOLD, D. P. 1977. Land subsidence in central Arizona. IAHS/AISH Pub. No. 121, p. 95-103.

WINTZ, W. A., Jr., KAZMANN, R. G., and SMITH, C. G., Jr. 1970. Subsidence and ground-water off take in the Baton Rouge area. Louisiana State Univ., Louisiana Water Resources Research Inst., Bull. 6, 20 p. W. A. Wintz, Jr., Technical Appendix, 70 p.

WU, CHIAN-MIN. 1977. Ground-water depletion and land subsidence in Taipei Basin. IAHS/AISH Pub. No. 121, p. 389-398.

YAMAMOTO, S. 1977. Recent trend of land subsidence in Japan. IAHS/AISH Pub, No, 121, p. 9-15.

ZAMBON, M. 1967. Abbassamenti del suolo per estrazioni di acqua e gas-Deduzioni ed indirizzi logicamente consequenti per la sistemazione del Delta del diume Po. Atti del XXIII Congresso Naz. delle Bonifiche, Rome, 345-370.

2 Field measurement of deformation, by Joseph F. Poland, Soki Yamamoto, and Working Group

2.1 INTRODUCTION

Decline of the water level in wells causes increase in effective stress--that is, increase in the part of the overburden load that is supported by the sediments being stressed. The resulting strain is primarily expressed as a vertical shortening or compaction of the stressed sediments and consequent subsidence of the land surface. Horizontal displacement also occurs but in a lesser amount.

In this chapter we will describe briefly the methods used for measuring vertical displacement of the land surface (subsidence or uplift), vertical displacement of subsurface deposits (compaction or expansion), horizontal displacement of the land surface, and horizontal displacement of subsurface deposits.

2.2 VERTICAL DISPLACEMENT

2.2.1 Precise leveling by spirit leveling

The elevation of bench marks at land surface commonly is determined by precise leveling, using an engineer’s level and a level rod. This is the most practical method for measuring vertical displacement of bench marks in monitoring subsidence. Equipment and procedures are described briefly in most engineer’s handbooks and in detail in "The Manual of Geodetic Leveling" (Rappleye, 1948). Once a network of bench marks has been established and surveyed by precise leveling, a second survey at some later date will show whether vertical movement has occurred, where, and how much.

The bench-mark net should be designed to cover the area known or suspected to be subsiding, and to extend into a broader regional network at two or three reference bench marks assumed to be stable because they are on bedrock or for some other reason. The bench-mark net can be tied to a tidal bench mark if the subsiding area is near the seacoast. Spacing of bench marks in the net is normally in the range of 400 to 1,000 m, but may be much closer in areas of special interest, such-as ties to structures, or a closely spaced set of bench marks to define movement on surface faults. Bench marks should be placed where danger of destruction is minimal. They are installed as permanent marks that in the past usually have consisted of a brass cap, suitably identified, and grouted into a concrete block or post, into bedrock, or attached securely to the top of a pipe or rod. As the need for greater accuracy and for eliminating surficial disturbances has increased, "deep-seated" bench marks are being installed in increasing numbers. They consist of rods 5 to 10 m long, driven into the ground and protected by an outer sleeve through the top 3-4 m, the zone of surficial disturbances (such as frost-heave, dessication, swelling, oxidation, root growth, and animal burrowing). This type of cased-rod bench mark is particularly well suited for use in monitoring areas of present or potential land subsidence where annual elevation changes of a few mm may be of interest if they represent elastic response of an aquifer system, but should be eliminated if they represent surficial disturbance.

To reduce vandalism, a mark that is less obvious than a brass cap should be used. A convex-headed bolt or pin, projecting a few mm above the concrete or pipe-cap, or a carriage bolt with a nut on the embedded end can be used. The bench-mark designation can be scribed in the concrete before it hardens.[1]

---

[1] Detail on installation and protecting of bench marks is available in a publication of the National Oceanic and Atmospheric Administration (NOAA). Rockville, MD, USA 20852. Entitled Geodetic bench marks, by R. P. Floyd, it is NOAA Manual NOS NGS1, 1978, 50 pages.

Near-surface deposits may contain organic materials subject to bacterial decomposition and consequent settlement of the land surface when the water table is lowered in order to grow crops. Such conditions exist in the peat beds of the Fens in England, in the Florida Everglades (Stephens and Johnson, 1951), and in the Sacramento-San Joaquin Delta in California (Weir, 1950). In such areas, bench marks installed to measure change in elevation of subjacent deposits should be rods or pipes driven firmly into the subjacent deposits and preferably protected from change in the thickness of the overlying organic deposits by an outer pipe sleeve. Furthermore, structures that extend down to the subjacent deposits, such as bridge piers or tidal gages, can serve as sites for the establishment of additional bench marks.

Figure 2.1 shows the network of level lines established by the United States Coast and Geodetic Survey (now National Geodetic Survey) in the subsidence area of the Santa Clara Valley in northern California. This network, which is 400 km long, was first leveled in 1934 and has been releveled 11 times since then. Note that three transverse lines extend southwest into consolidated rock and across the well-known San Andreas fault, and three extend east across the Hayward fault. Both faults are active.

In bench-mark surveys of subsiding areas, the leveling may be of first or second order. First order class I leveling is double run and requires that the allowable discrepancy between duplicate lines does not exceed $3\sqrt{K}$ mm where K is the length of the bench-mark line in kilometres. Second order class I leveling requires a closure of not to exceed $6\sqrt{K}$ mm and costs half to two-thirds as much per kilometre as first order class I. Partly because of the difference in cost between first-order leveling and second-order leveling, it is common practice in resurveying a network in a subsiding area to select principal lines for first-order releveling and secondary lines for second-order releveling. It is extremely important that ties to "stable" ground, to consolidated rock, or to tidal gages, should be included in the first-order leveling.

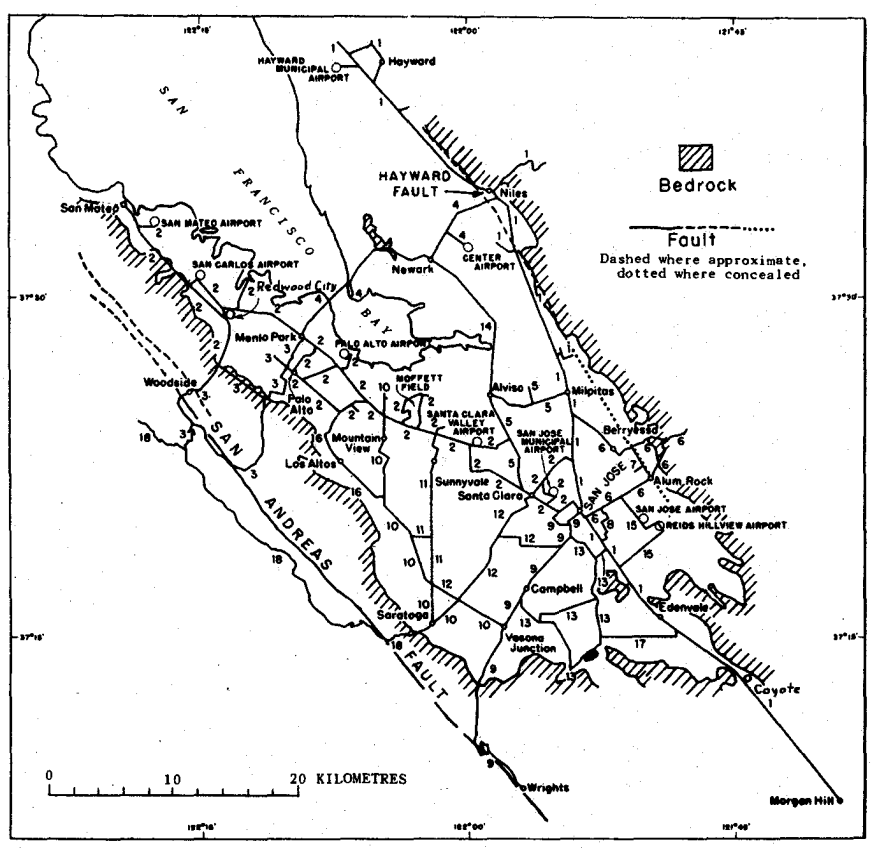

Figure 2.1 Map showing network of level lines in the San Jose subsidence area, Santa Clara Valley, California (modified after National Geodetic Survey; numbers identify level lines).

The releveling pattern at Niigata, Japan, is illustrated in Figure 2.2. The principal first-order leveling lines are identified by the larger circles ("First Class Bench") and those for second-order leveling by the smaller circles. Furthermore, the network is divided into three zones based on rate of subsidence and the economic significance of subsidence: the coastal area northeast of Uchino is releveled every half year, the zone northeast of Yahiko once a year, and the inland zone north of Nagaoka every two years.

Saving time is another reason for using second-order leveling on the secondary lines in a subsiding area. The second-order leveling will cover the distance about twice as fast as first order leveling. In an area that is subsiding 15 to 30 cm per year, a junction point could settle 1 to 3 cm by the time a loop is closed. Any procedures that reduce loop closing time are beneficial. The time of year when the leveling is done is important in a heavily pumped basin, for example, one where the annual fluctuation of artesian head is 10-30 m. Commonly the water level in wells is drawn down in the spring and summer and rises in the autumn and winter when withdrawal is less. Hence, effective stresses are much greater in the summer than in the winter

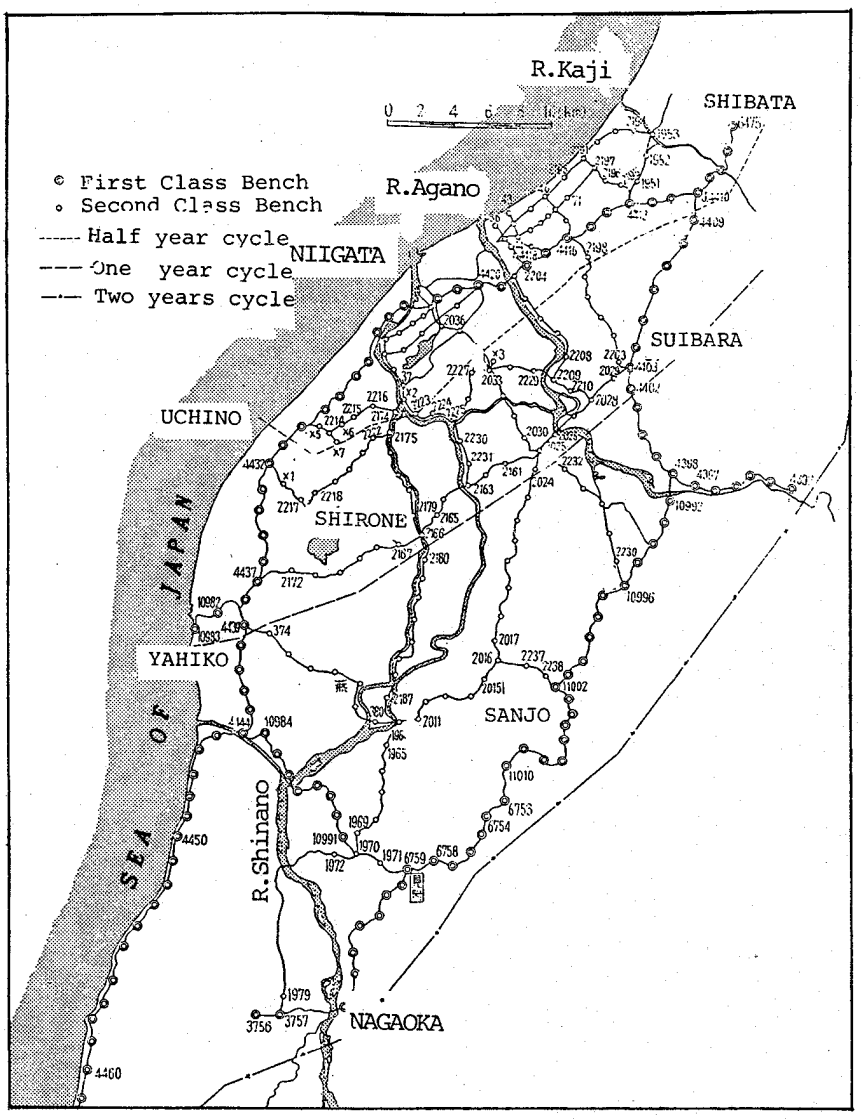

Figure 2.2 Distribution of bench marks in Niigata, Japan.

and the full annual compaction of the aquifer system may occur in 5 to 6 months (see Lofgren, 1968, Figure 3). In such areas, leveling should be accomplished during or immediately following the period of rising water level when compaction and subsidence are minimal.

All the subsidence maps in the case histories of Part II were prepared from change in the elevation of bench marks surveyed at two different times by the leveling procedure. If the bench-mark net has been releveled several times, the magnitude and distribution of subsidence along a line of bench marks can be shown as a series of profiles, one for each releveling, referred to a common base. Figure 9.14.4 is an example of a series of 10 subsidence profiles drawn from surveys from 1919 to 1967, all referred to a 1934 base. 1934 was the first year that the entire line of bench marks was surveyed.

Leveling is a labor-intensive procedure, and as a result the cost has doubled in recent years. The cost of constructing a pipe extensometer that extended to the base of the fresh ground-water reservoir or to the depth tapped by the deepest water wells might well be less than the cost of one releveling of an extensive bench-mark network 300 to 600 km in length. An extensometer placed near the center of a subsidence area could furnish a continuous record of land-surface position and thus would be a subsidence monitor, provided that (1) no compaction of sediments occurred at depths beneath the extensometer footing, and (2) no vertical tectonic movement developed. As a subsidence monitor, it would furnish information needed to decide when to relevel the bench-mark net. Furthermore, under such circumstances, the top of the inner pipe of a pipe extensometer (see Figure 2.5B) would be a reference bench mark of constant elevation and hence a fixed tie for releveling the net. Such a constant reference bench mark near the center of a bench-mark net could eliminate the need for releveling to a regional reference bench mark many kilometres distant.

A guidelines manual for surface monitoring of geothermal areas (Van Til, 1979) was prepared recently to serve as a guide to monitoring the magnitude and direction of land-surface movements prior to, during, and following withdrawal of geothermal fluids from the ground. This manual not only discusses the design of systems and procedures for monitoring subsidence but also describes the capabilities and limitations of instruments available for monitoring purposes. Anyone concerned with the design or operation of a subsidence monitoring system should find the Van Til manual very helpful. Table D-1 from this manual, summarizing instrument capabilities for measuring land-surface displacements, is included as Appendix A in this guidebook.

2.2.2 Other techniques for measuring land-surface displacement

Other instruments utilized in measuring or monitoring differential vertical displacement at land surface are the theodolite with retroreflective targets, capable of measuring vertical angles to 1 second of arc or better, manometers for monitoring settlement of structures or land surface, and tiltmeters for measuring ground tilt. Van Til (1979) has summarized in tabular form the availability, performance characteristics, accuracy, and installation and operating requirements of 8 types of manometers and 6 types of tiltmeters used for monitoring vertical displacements at land surface (see Appendix A). Tide gage records, float measurement on water bodies, and changes in drainage pattern also can be very helpful in defining differential elevation changes or tilting.

2.2.3 Extensometer wells

2.2.3.1 Single and double pipe extensometers

Extensometer wells that have been developed to measure vertical movement or change in thickness of sediments or rocks are similar in principle but vary in detail. Japanese scientists pioneered in the development of this type of observation well. In the early 1930’s they installed the "single pipe well" (also called "single tube well") at several sites in Japan.

The single pipe well (Figure 2.3A), if installed to a shallow depth and passing through soft clay to an aquifer of sand or gravel, may accurately record by increased protrusion of the pipe at land surface the amount of compaction that has occurred in the soft clay. However, at depths greater than 50 to 100 m, the weight of the overlying sediments develops substantial lateral pressure on the pipe. This pressure, which increases with depth, increases the frictional resistance to movement and hence enhances the tendency for the pipe to move vertically in accord with the surrounding sediments. Thus, as the depth to the compacting interval increases, the percentage of the compaction that will appear as increased pipe

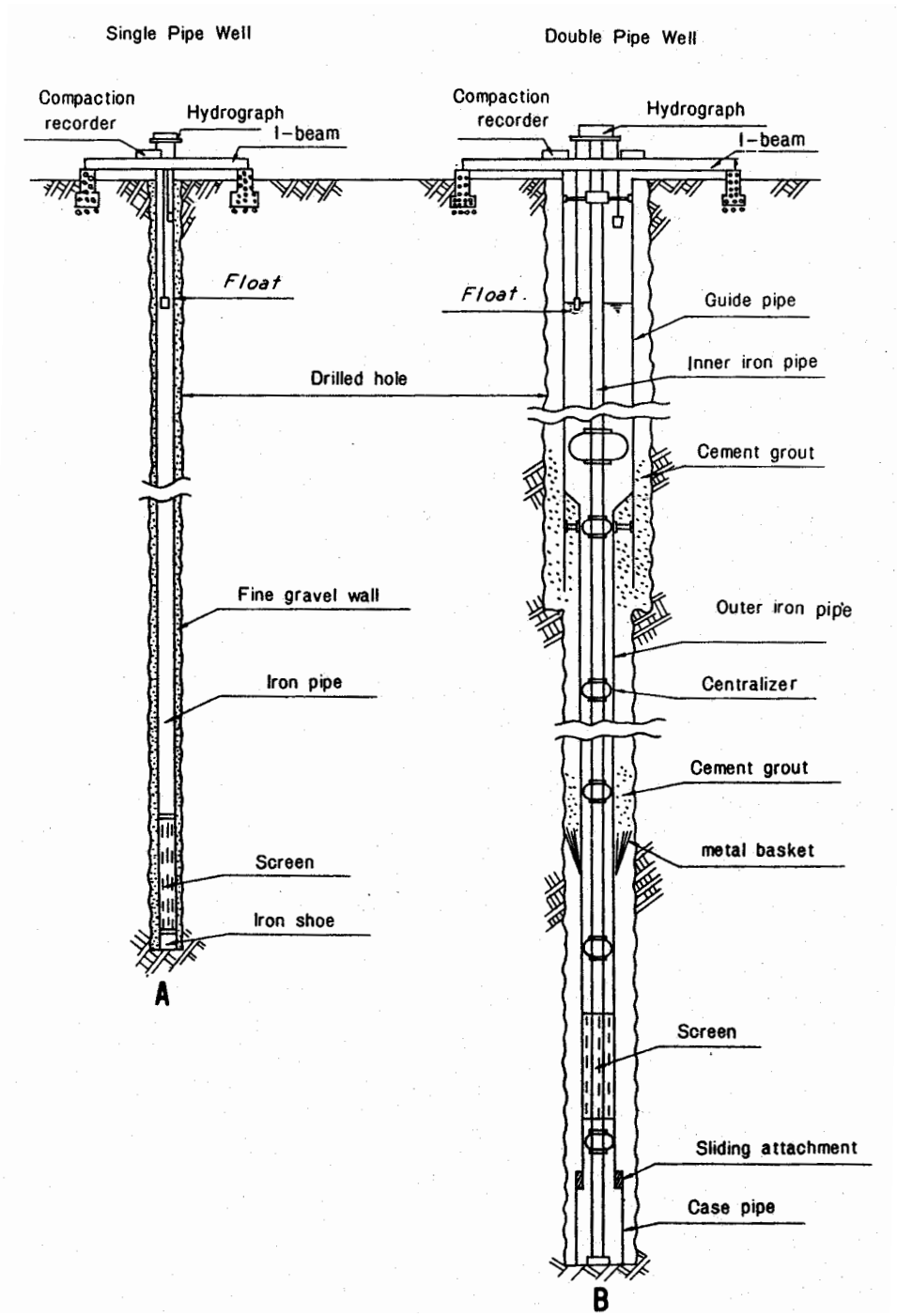

Figure 2.3 Diagram of Japanese extensometers. A, Single pipe well; B, Double pipe well (from Tokyo Metropolitan Gov't, 1969, Fig. 18).

protrusion above land surface decreases and compressional shortening of the pipe at depth increases. Therefore, although increased protrusion of a single pipe well above the land surface is an indicator of subsidence, it should not be considered a reliable measure of the magnitude of compaction for depths greater than 30 to 60 metres.

As demand for ground water increased in Japan and water wells were drilled to greater depths, Japanese scientists designed a "double pipe well" (Figure 2.3B) to measure compaction accurately. A double pipe well was installed at Osaka in 1938. The double pipe well consists

of two concentric iron or steel pipes, inserted into a vertically bored hole. The inner pipe is isolated from the sediments by the outer pipe, and is centered within the outer pipe by centering devices (centralizers). The apparent rising of the inner pipe indicates the relative downward displacement of the I-beam based on the land surface with respect to the top of the inner pipe. Thus, the amount of compaction of the sediments between the land surface and the bottom of the inner pipe can be recorded. The water level in the outer pipe represents the pore-water level or artesian pressure of the aquifer, transmitted through the screen section installed in the outer pipe. This water level is registered by a float-operated water-level recorder when the space between pipes permits.

Note (Figure 2.3B) that the outer pipe is suspended in the well, with a slidable sleeve of oversize casing hanging on the base of the outer pipe and resting on the well bottom. By this means, the weight of the outer pipe is removed from the well bottom and suspended at the land surface.

At the Funabashi-2 well in Chiba (Figure 2.4) the diameter of the outer tube to 60 m depth is 350 mm to accommodate a water-level float, but below that depth is reduced to 200 mm. The diameter of the inner tube is 80 mm. The annulus between the outer tube and the hole wall is cemented at 60 m and 75 m depth. The bottom part of the outer tube has the sliding sleeve ("casing tube") attachment to prevent loading of the well bottom by the weight of the outer tube. The sleeve, closed on the bottom with a bearing plate, is landed on a solid sandy layer and supports the inner tube. Thus, the outer tube can move independently from the inner tube and the sleeve. Figure 2.4 also shows the design of the centralizer--the device centering the inner tube in the outer tube (B)--and details of the instrumentation for recording compaction (or subsidence) and water-level fluctuation (C). If the double tube extensometer well extends through and beneath the base of the compacting sediments, the extensometer records gross compaction, which equals land subsidence if no tectonic movement contributes to the change in land-surface elevation. However, if the bottom of the well is within the compacting interval, the extensometer records compaction--a partial component of the land subsidence.

The validity of the extensometer record depends on the stability of the base of the inner tube with respect to the geologic formation, the stability of the instrument platform with respect to land surface, the degree in which friction between the outer and inner tubes can be minimized, and the accuracy of the measuring apparatus.

The weight of the capped sleeve is composed of its dead weight and the weight of the inner tube. In the Funabashi-2 well, at the bottom plate of the sleeve, the load on the sand-gravel layer is about 2.9 metric tons. Meyerhof (1956) derived a formula to evaluate an ultimate bearing resistance R_u by the number of blows on the sampling spoon during performance of a standard penetration test:

$$R_u = 40\ \bar{N} A_P,$$

where $\bar{N}$ is the average of N blows per foot in a depth interval between 1.0 d downward and 4.0d upward from the base of the tube, A_p is the area of the base of the tube, and d is the diameter of the pile. The diameter of the sliding sleeve (casing tube) in the Funabashi well is 225 mm (Figure 2.4). Thus, $A_p = 0.040\ m^2$. In general, the N value of the sand layer in the Diluvium (Pleistocene) is more than 30. Considering the large factor of safety we can use a reduced formula of

$$R_u = 30\ \bar{N} A_P = 30 \times 30 \times 0.040\ m^2 = 36 \text{ tons}.$$

Then in this case with 0.040 m^2 base area, the steel tube of the well can bear about a 36-ton load. According to the above calculation, the Funabashi-2 well will not sink into the sand-gravel layers. Differences between the results of compaction recorders and dial gauges and also differences between the results of water-level recorders and taped measurement are very small. Hence, it is concluded that extensometer wells having the same construction as the Funabashi-2 well should furnish a good record of compaction or subsidence, provided down hole friction is minimal (the well bore is close to vertical).

2.2.3.2 Anchored-cable and pipe extensometers

The United States Geological Survey (USGS) has developed extensometers (compaction recorders) of two types, anchored-cable and free-pipe, both of which are illustrated in Figure 2.5. The anchored-cable extensometer (A) was first installed in 1955 in an unused irrigation well 620 m deep on the west side of the San Joaquin Valley. The extensometer consists of a heavy anchor

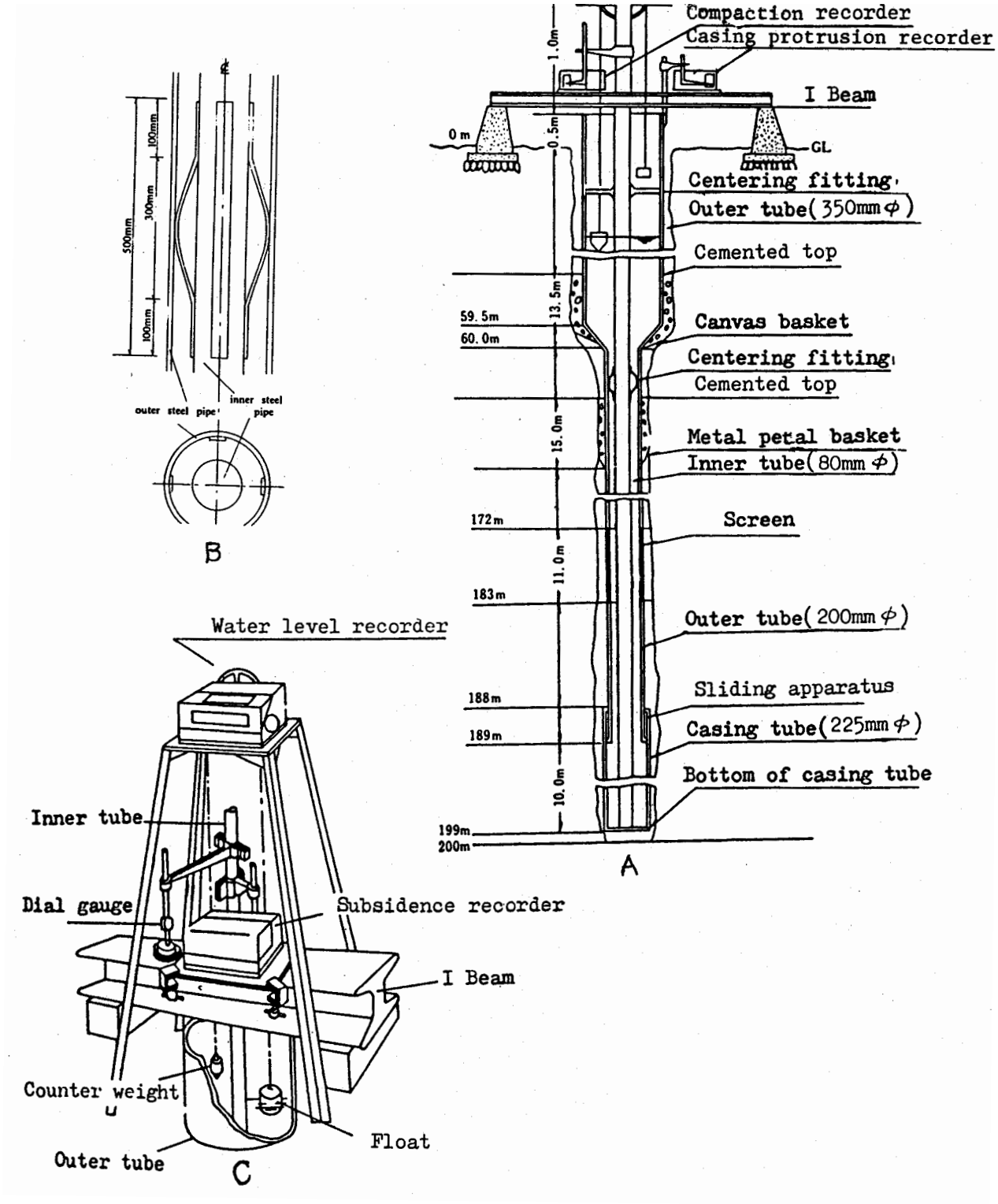

Figure 2.4 Structure of Funabashi observation well (double-tube type). A, Sectional view; B, Centralizer detail; C, Recorder detail.

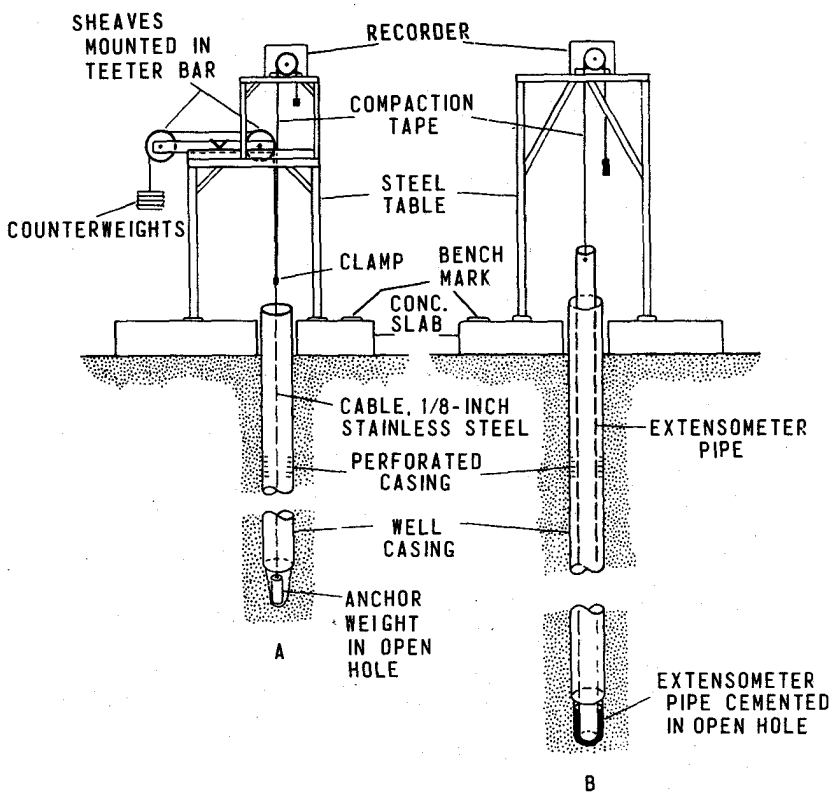

Figure 2.5 Recording extensometer installations. A, Anchored-cable assembly; B, pipe assembly.

(subsurface bench mark) emplaced in the formation beneath the bottom of a well casing; the anchor is attached to a cable that passes over sheaves at the land surface and is counterweighted to maintain constant tension. The cable is connected to a recorder that supplies a time-graph of the movement of the land surface with respect to the anchor--the compaction or expansion of the sediments within that depth range. The inked curve on the recorder chart commonly is amplified 10:1 by suitable gear combinations. The accuracy of the anchored-cable extensometer depends on the plumbness and the straightness of the well casing, the durability and stretch characteristics of the downhole cable, and especially on the success of minimizing cable-casing friction. As pointed out by Lofgren (1969), the cable must remain at constant length during the period of record. If the length changes due to temperature changes, fatigue elongation, or untwisting, the length change is indistinguishable from the record of compaction. The cable now used is a 1/8-inch (3.175 mm) diameter preformed stainless steel, 1 x 19 strand, reverse-lay "aircraft" cable. In order to minimize frictional drag of the surface sheaves, a "teeter bar" on a knife-edge fulcrum (Figure 2.5A and Lofgren, 1969, Figure 8) was designed. Changes as small as 0.1 to 0.2 mm in the thickness of an aquifer system can be recorded with this equipment.

This type of extensometer is being used in California, Nevada, and Arizona in wells as much as 700 m deep. Detailed tests of the accuracy of a similar cable-type extensometer have been made at the Groningen gas field in The Netherlands (de Loos, 1973).

For reasons of economy, most cable extensometers have been installed in unused irrigation wells, after cleaning out the casing and deepening the hole about 10 m below the casing shoe. The anchor weight of roughly 100 kilograms is then lowered into the open hole in the sediments several metres below and independent of the well casing.

To eliminate much of the cable-casing friction problem and thus improve the accuracy of the extensometer record the USGS has installed since 1966 about 30 free-pipe extensometers in California, Arizona, Louisiana, and Texas, to depths as great as 1,000 m. These pipe extensometers (Figure 2.5B) are similar in principle to the Japanese double pipe well. However, they differ in some features. The inside diameter of the well casing (outer pipe) commonly is 4 to 5 inches (10 to 13 cm) and the outside diameter of the couplings on the inner (extensometer)

pipe ranges from 2 to 3.4 inches (5.1 to 8.6 cm). Thus, the space between the casing and the extensometer pipe couplings is only about 2 inches (5 cm); hence, casing centralizers have not been used to center the extensometer pipe. Centralizers have been used, however, in the annulus between the casing and the borehole wall, to center the casing, especially when the law requires cement to be placed in this annulus to protect the ground water of good quality from contamination by water of poor quality at greater depth. Centralizers usually are spaced 15 to 30 m apart.

In about half the installations, a bearing plate on the bottom of the extensometer pipe is landed on the surface of a cement plug (placed in the open hole before the casing is run). In the remainder of the installations, the extensometer pipe is cemented in place in a pocket drilled below the casing shoe. In either case, the top of the cement plug is placed at least three m below the bottom of the casing shoe so that the dead weight of the casing does not stress the extensometer footing. Furthermore, this procedure minimizes the possibility that increasing downward loads, resulting from continuing compaction at shallower depths, will be transmitted through the casing to the extensometer footing. If the cementing of the extensometer footing is accomplished after that pipe has been run into the open-hole pocket, the cement slurry can be pumped into the pocket directly through the extensometer pipe. Care must be exercised, however, in calculating (1) the quantity of cement slurry needed to fill the desired interval of the pocket, and (2) the quantity of followup water needed to displace most of the slurry from the pipe into the pocket without thinning the slurry with water. If the pipe is raised several metres as soon as the followup water has been pumped into the pipe, the water pressure into the pipe and casing can be equalized and the pipe can then be lowered again to rest in the hardening slurry.

Three free-pipe extensometers have been operated since 1975 at a site within a subsiding area in Baton Rouge, Louisiana. These extensometers record compaction of the sediments and water-level change within each of the three depth zones. The extensometer pipes extend to depths of 254, 518, and 914 m. The installations and the record obtained through 1979 have been described by Whiteman (1980). The deepest extensometer indicates an annual land-surface fluctuation of about 4 cm, apparently an elastic response.

The conversion of an abandoned oil-test hole at Westhaven, California, into a dual extensometer and a dual water-level observation well is described in this guidebook because such abandoned oil-test holes are available in many countries, and the cost of conversion is only a small fraction of the cost of drilling and completing one or more new extensometer wells. Figure 2.6 is a diagrammatic sketch of the converted well. This summary of the conversion is condensed chiefly from Poland and Ireland (1965). When the oil-test hole was drilled, a surface string of 11-3/4 inch (29.84 cm) casing was installed from land surface to 611 m. Cement was pumped into the annular space around the casing, from the bottom shoe to land surface, providing a continuous seal to protect the fresh ground water. On abandonment a cement plug was placed in the well between 1930 and 2030 feet (588 and 619 m).

The blank casing was converted to a dual water-level observation well in April 1958. The 11-3/4 inch casing was gun perforated at two depth intervals, near the top and base of the confined aquifer system (see Figure 2.6). To obtain hydraulic separation of the two perforated intervals, a 4-inch diameter pipe with a packer flange at its base was run to a depth of 860 feet (262 m); a cement plug was then placed on top of the packer, thus sealing the annulus between the two casings. Initially, the inner pipe was suspended in tension by a casing hanger resting on the top of the 11-3/4 inch casing. Four months after the inner pipe was installed, the hanger appeared to be rising off the top of the 11-3/4 inch casing, indicating shortening of the casing between land surface and the cemented packer. Beginning in August 1963 the shortening of the full length of casing above the basal cement plug was measured by lowering an anchor weight on top of the cement plug and counterweighting the cable at land surface (see Figure 2.6). Thus the conversion of the oil-test hole provided two water-level observation wells and two extensometers: a pipe-type to 845 feet (258 m) and a cable-type to 1,930 feet (588 m) below land surface.

Monthly measurements from 1964 to the end of 1970, inclusive, indicated compaction from 0-845 ft (0-258 m) was 1.94 ft (0.59 m), and from the land surface to 1,930 ft (0-to-588 m) was 3.57 ft (1.09 m).

These observations at the Westhaven site indicate that even heavy oil-well casing encased in a cement jacket is too weak to resist the compressional force of the compacting sediments. Even in the shallow depth interval from land surface to 845 ft (258 m), the increased protrusion in seven years was only equal to 12 per cent of the subsurface shortening in that interval. It is concluded that in an area subsiding because of sediment compaction due to decrease in fluid pressure, the top of a well casing is not a stable reference bench mark, even if the casing

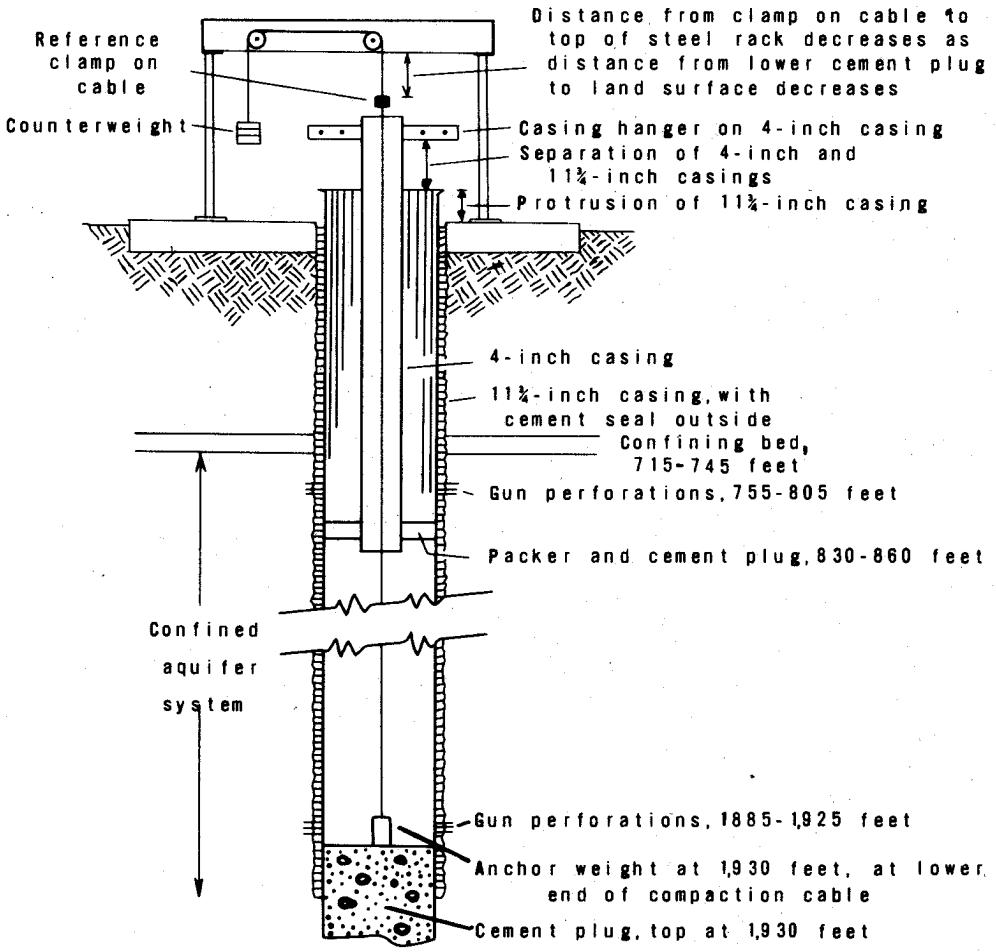

Figure 2.6 Diagrammatic sketch of wells used for measuring water levels and compaction: wells 20/18-1102 and 1103 (from Poland and Ireland, 1965).

extends below the compacting sediments. Also, the evidence is clear that increased protrusion of a casing above the land surface, even though an indicator of land subsidence, is not a reliable measure of either compaction or subsidence. Bull (1975, p. 41-45) cites additional evidence concerning the minor amount of casing protrusion compared to subsurface casing compression in wells on the west side of the San Joaquin Valley.

In Mexico City, however, observed protrusion of some water-well casings has been about the same magnitude as the subsidence. Poland and Davis (1969, p. 225-228 and pl. 6) show graphic pictures taken by Ing. R. Marsal in 1954 of the protrusion of casings of two wells drilled about 1923. They were drilled to a depth of about 100 m but most of the compaction occurs in the highly compressible lake clays in the top 50-60 m. The subsidence at the well sites from 1891 to 1959 was 5.9 m. In 1954, one casing protruded 5.45 m and the second 4.5 m. The protrusion of 5.45 by 1954 is about equal to the subsidence by 1954, proving that essentially all the compaction at the well site is occurring in the top 100 m of sediments, and probably mostly in the top 60 m. The lateral pressure to this depth may not be great enough to compress the outer casing as compaction occurs. However, the excessive protrusion is believed to be due in part to the fact that wells are drilled using more than one casing size.

In evaluating the characteristics of cable and pipe extensometers, the following factors should be considered:

1. If a cased well is available, the cable extensometer costs less to install than the pipe extensometer, chiefly due to the lower unit cost of the cable compared to the pipe.

2. The cable extensometer has minimal cable-casing friction when the well casing is of large diameter (30-40 cm); the friction increases when the well casing is of small diameter (10-15 cm), all other factors being equal.
3. In contrast, the pipe extensometer has minimal pipe-casing friction when the well casing is of small inside diameter (10-15 cm) and the overall space between pipe or pipe couplings and well casing is in the range of 4-6 cm. Alternately, if the well casing is of large diameter, use of pipe centralizers spaced 15 to 30 m apart between casing and pipe, as is done in the Japanese double pipe wells (Figure 2.3B), may produce a record as good as that obtained with the pipe-in-small-casing design. So far as known, no comparative test has been made.
4. The pipe extensometer commonly gives a more accurate record than the cable extensometer, all other conditions being equal.
5. If a well can be drilled so plumb and straight that the departure from verticality at the base does not exceed the inside diameter of the casing, the cable can be positioned to avoid any downhole cable-casing friction. Under such circumstances the cable extensometer is more frictionless than the pipe extensometer. However, a well drilled to a depth of 50 m and with a casing diameter (inside) of 0.3 m would have a departure of 0.3 m from verticality at the bottom if the drift from verticality was 0°20′. For a well 100 m deep, a departure from verticality of 0.3 m at the bottom would require that the drift be held to 0°10′. Thus, it would appear that the chances of drilling a well more than 100 m deep that is sufficiently plumb to eliminate any cable-casing friction are remote. The above discussion does not consider possible cable-casing friction caused by the tendency of rotary-bored holes to develop a spiral pattern.

A cable extensometer at the USGS Cantua site in the San Joaquin Valley, California, installed to a depth of 610 m in a well with 10 cm casing to 595 m, had so much cable-casing friction that the equipment recorded no compaction even when as much as 7.6 cm of compaction had occurred during the prior month. At the time of the monthly visit to service the equipment, the cable was stretched--that is, the counterweight was pushed down about 30 cm and then allowed to rise gently. This operation triggered enough down-hole slippage of the cable at friction points (cable-casing friction) to permit the cable to move upward and record the approximate compaction that had occurred since the last monthly visit. Bull (1975, p. 32 and Figure 25) has discussed the problem and reproduced a part of the stairstepped field record from the extensometer. This extensometer equipment was installed in a corehole. When drilled, the plumbness of the hole was surveyed at 30-metre intervals with a driftmeter. The drift from vertical was 1 degree at 90 m depth and ranged from 5 to 6 degrees between 244 and 580 m depth. In spite of the nonverticality of the hole (and of the casing), an interpolated cumulative compaction curve drawn through the low points of the stepped record produced a reasonably accurate long-term compaction curve for the deep Cantua site extensometer. The compaction plot for well N1 in Figure 9.P.8 is the 13-year record of 3.4 m shortening for sediments between land surface and a depth of 610 m.

At the Terra Bella site on the Friant-Kern Canal in the San Joaquin Valley, casing of 10-5/8 inch (27 cm) diameter was placed in a well to a depth of 377 m and an extensometer pipe of 1-1/2 inch (3.8 cm) diameter was inserted and landed at a depth of 381 m. No centralizers were used. Most of the record in the field compaction charts for this extensometer is composed of a series of stair-step adjustments with individual vertical displacements of 0.15 to 0.3 mm (1-5 to 3 mm at the 10:1 magnification). The overall space between the well casing and the extensometer pipe-couplings is nearly 20 cm, permitting too much flexing of the inner pipe and too many friction points. The compaction record at this site probably could be improved by adding centralizers to center the inner pipe in the casing, by increasing the size of the inner pipe, or by use of a lever and counterweight system at land surface to remove a substantial part of the dead weight of the extensometer pipe. This last procedure should produce the greatest reduction in pipe-casing friction.

Under most favourable conditions, the pipe extensometer as described in this manual will function satisfactorily to depths of 750 to 1,000 m. The most favourable conditions would require straight holes--holes drilled with deviation from the vertical of less than 1/2 degree-and a combination of well casing and extensometer pipe sizes, or use of centralizers, that minimizes pipe-to-casing friction.

The cable extensometer will supply approximate measurements to depths of 600 to 850 m, but the results are less accurate, in general, than with the pipe extensometer.

The depth to which the pipe extensometer equipment is operative--750 to 1,000 m--is adequate for studies of subsidence due to ground-water withdrawal in most of the world. Much ground water is pumped from aquifers less than 300 m deep and most from aquifers less than 600 m deep. However, improvement in the accuracy of compaction measurements at depths greater than 300 m is highly desirable. Furthermore, in connection with the study of subsidence due to other causes, or subsidence due to other types of fluid withdrawal, such as geothermal or oilfield fluids, there is need for improvement of extensometer design to increase the depth of useful measurements. For example, much or nearly all of the dead weight of the inner extensometer pipe can be removed by use of a lever and counterweight system at land surface. Most of the pipe would then be in tension and the frictional stress between pipe and casing should be greatly lessened at the time of compression (or expansion) of the well casing. This method has been applied by Ben E. Lofgren (oral communication, December 1975) to an extensometer 317 m deep in Imperial Valley, California, where more than two-thirds of the pipe weight has been removed by a counterweighted lever designed with a 10-to-1 mechanical advantage. Also, one highly sensitive extensometer was recently constructed in Arizona to a depth of 380 m using this method (F. S. Riley, oral commun., July 1979). In this installation the upper 75 per cent of the extensometer pipe was placed in tension while the lower 25 per cent remained in compression. The neutral point was positioned at a major bend in the casing, as determined by a borehole alignment survey. Before installation of the lever and counterweight this installation had severe friction problems and produced a record characterized by intermittent stair-step movements. After counterweighting the instrument produced a smooth record of continuous compaction.

Research is needed to determine the accuracy of such a lever and counterweight system through a wide span of unloading of the extensometer pipe, say from 25 per cent to 90 per cent. Comparison of simultaneous compaction records from a normally loaded pipe extensometer and a nearby counterweighted extensometer of the same depth and construction, in an area of active subsidence, would be very instructive. Several stages of unloading could be applied to the counterweighted extensometer.

Another way in which the weight of the pipe in a free-pipe extensometer can be reduced is by installing a tapered pipe assembly. For example, the bottom third of the pipe could be 2-1/2 inch, the middle third 2-inch, and the upper third 1-1/2 inch; or the assembly could be 2-inch, 1-1/2 inch, and 1-inch. For an extensometer 750 m deep, a free pipe of 2-1/2 inch constant diameter would weigh 6,580 kg. But if the pipe was installed with equal lengths (250m) of 2-1/2 inch, 2-inch, and 1-1/2 inch pipe, the weight on the bottom joint of the 2-1/2 inch would be decreased about 30 per cent (neglecting buoyancy effects). The decrease in weight should decrease the cost of the installation, and simplify the addition of a lever and counterweight at land surface, if desired.

2.2.3.3 Slip joints

When extensometer or observation wells are being installed in an area that is subsiding at a rapid rate, it is advisable to consider the need for installing a series of slip joints in the casing during construction. When extensometers were being installed on the west side of the San Joaquin Valley of California in 1958-62, the ground-water reservoir was compacting as rapidly as 30 cm per year. Under such circumstances, it was anticipated that the casings of deep extensometers would last longer under severe compressive forces if slip joints were inserted in the well casing. Accordingly, at the Cantua site, for example, eight slip joints were placed at 60-metre intervals in the 4-inch casing 595 metres deep. Figure 2.7 shows details of the slip joint. Each slip joint has about 0.9 m of play between the open and closed position. Since installation in 1958, this extensometer has shortened about 3.5 m. Without slip joints, the elastic compression of the 4-inch (10 cm) casing from full tension when first suspended in the well to the elastic limit in compression would have been about 1.2 m. The additional shortening of 2.3 m beyond the elastic limit of the casing must have resulted from compressional failure of the casing or shortening of the slip joints, or both. Because this equipment is still functioning as an extensometer, we conclude that a major part of the 3.5 m of shortening must have occurred through shortening of slip joints.

2.2.3.4 Telescopic extensometer

An experimental telescopic extensometer, designed by Ignacio Sainz Ortiz, was installed in Mexico City to a depth of 60 m in 1953. Figure 2.8 shows that in the 6-year period 1953-59, 36 cm of shortening occurred in the 60-metre thickness of near-surface deposits. In the first 20-30 m below the land surface lateral stresses against the casing are small. Nevertheless,

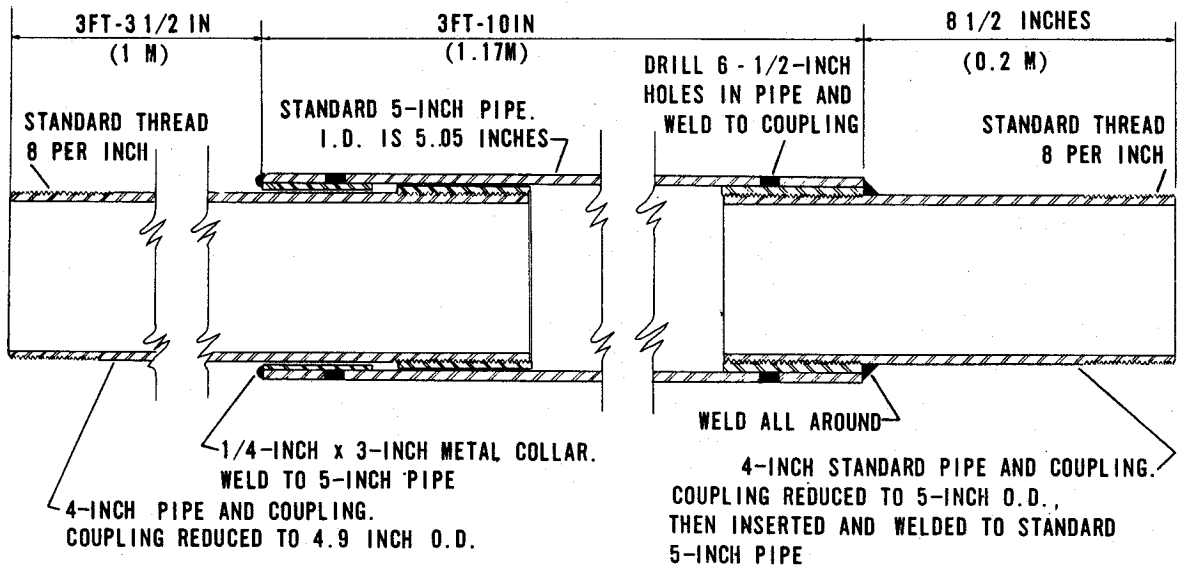

Figure 2.7 Diagram of slip joint.

considering the flexibility of the telescopic construction, the lateral stress should develop enough skin friction to cause the casing to shorten in accord with the surrounding sediments, even at the shallow depth range involved.

2.2.3.5 Extensometer records

Plots of cumulative compaction against time obtained from extensometer records are becoming fairly common in the published record, in connection with field research on land subsidence due to ground-water withdrawal. For example, in Japan, Miyabe (1967, p. 2-3) published compaction plots obtained from extensometers in Tokyo and Hirono (1969) showed plots of compaction from extensometers in Niigata. In the United States, extensometers have been operated for more than 20 years in the San Joaquin and Santa Clara Valleys, California. Computer plots of cumulative compaction through 1970 at 30 sites, together with water-level fluctuations, change in applied stress, and subsidence at most of these sites, have been published (Poland, Lofgren, Ireland, and Pugh, 1975, Figures 53-78).

In the case history for subsidence in the Santa Clara Valley, California, Figure 9.14.5 contains time plots of compaction for 15 years for two depth intervals at the San Jose extensometer site. In Figure 9.14.6 the measured compaction is plotted in annual increments that present a more quantitative picture of the annual change in amount of compaction than does the cumulative plot.

If two or more compaction recorders (extensometers) are installed in adjacent wells of different depths, the record from the multiple-depth installation will indicate the magnitude and rate of compaction (or expansion), not only for total depths of individual extensometers but also for the depth intervals between well bottoms. Figure 9.13.8, discussed in the case history of the San Joaquin Valley, California, is a good example of the record from a multiple-depth installation, and is one of six multiple-depth sites in the valley.

2.2.4 Other techniques of subsurface measurement

2.2.4.1 General

In addition to the pipe-type (double pipe) and anchored-cable extensometers described earlier in this chapter, a number of instruments utilizing similar principles but differing in measurement techniques are being manufactured commercially. O'Rourke and Ranson (1979) have made a summary

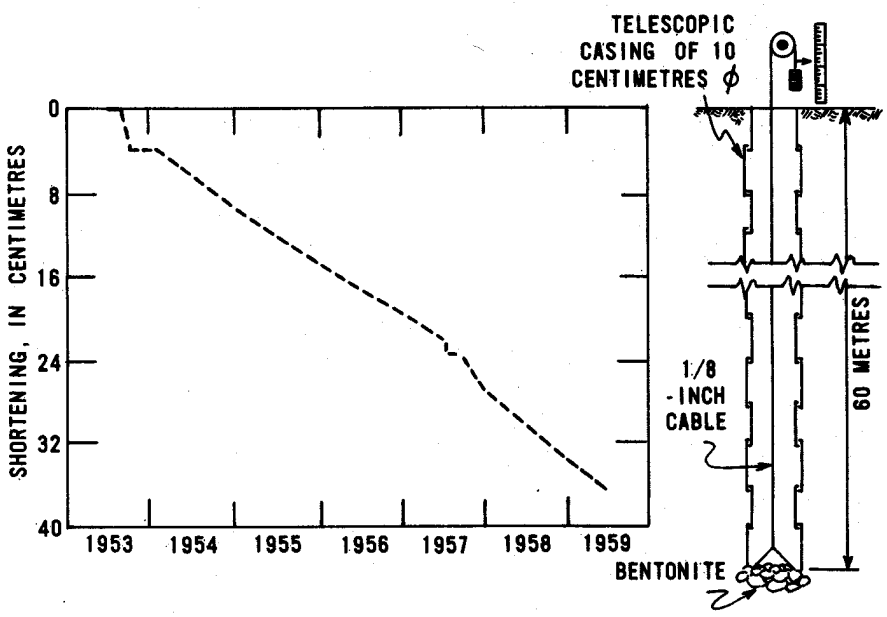

Figure 2.8 Sketch of telescopic extensometer and 6-year record of shortening (compaction of deposits). Redrawn from the Comisión Hydrologica de la Cuenca del Valle de Mexico, 1961, Boletin de Mecanica de Suelos, no. 3, p. 55.

appraisal of the capabilities of existing instruments for monitoring subsurface vertical displacement, examined with respect to availability, performance characteristics, and installation and operating requirements. The summary, reproduced as Appendix B of this guidebook, describes capabilities of 6 wire-type and 6 rod-type extensometers; 1 pipe-type extensometer (the USGS type); 2 multiple base length extensometers with sensors and anchors or magnet markers; 1 chain type extensometer with anchored sensor case; and 6 sonde-type extensometers, including the casing-collar locator and the gamma-ray logger. For details on the various wire-type and rod type extensometers for measuring subsurface vertical displacement, the reader is referred to Appendix B.

The techniques of casing-collar logging and gamma-ray logging with radioactive bullet markers require the use of specialized and expensive equipment. Normally this service would be provided by oil well service companies. In subsidence studies of most ground-water basins, however, the cost of utilizing such expensive equipment on a repeat basis probably would not be economically justified in most cases, when costs were compared with other study techniques. However, because such repeat logging has the decided advantage of indicating the depth range, rate, and magnitude of compaction or expansion of the sediments, a brief statement of the two techniques follows.

2.2.4.2 Casing-collar logging

At Long Beach, California, in the Wilmington oil field, changes in thickness of compacting zones have been measured successfully by running a magnetic collar locator periodically in the same well to determine the change in the distance between casing collars between surveys. According to Allen (1969), the first "collar counting" was in 1949 and more than 200 multiple traverse runs have been made to depths of as much as 1,800 m. These collar logs can be used to measure change in length of individual joints compared to joint length when placed in the well or since a prior logging. They also indicate the depth range, rate, and magnitude of compaction of the sediments if it is assumed that the casing or cement at every point moves in exact accord with contiguous sediments as a result of skin friction produced by lateral stresses. The field evidence at Wilmington from various sources generally supports this assumption for depths greater than 600 m. Collar surveys run five times from 1949 to 1960 in an individual well (Figure 2.9) graphically indicate the depth range, rate, and magnitude of compaction of three

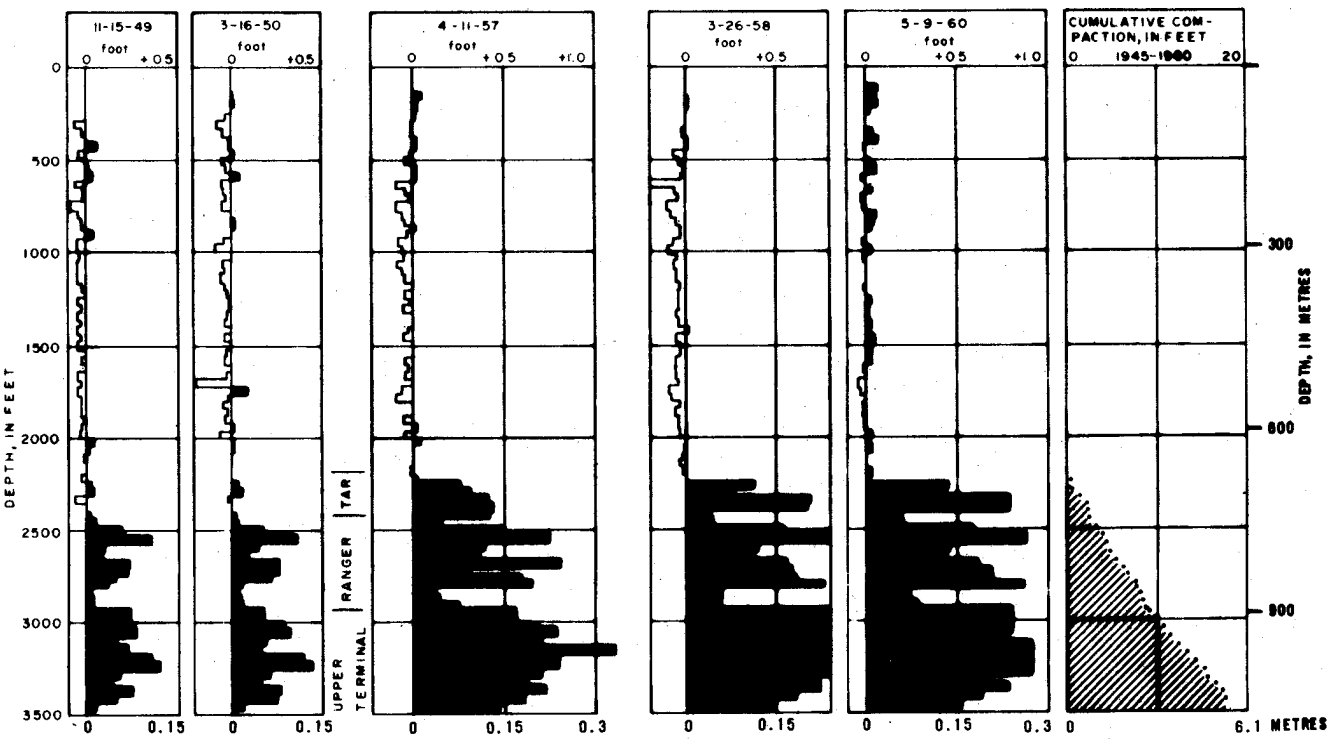

Figure 2.9 Casing collar surveys of a typical well in the Wilmington oil field. Survey on date indicated compared to casing tally of 9-26-45; elongation due to tension shown to left of zero reference, shortening due to compression shown to right (shaded); length of casing joints 12.5 to 13.4 m., in general (data courtesy of Long Beach Harbor Dept.).

oil zones--the Tar, Ranger, and Upper Terminal. The cumulative compaction of these three zones from 1945 to 1960 was 17.6 feet (5.4 m) as summed from the shortening of the casing joints by 1960 compared to their measured length in 1945. Allen and Mayuga (1969, Figure 13) also showed that collar logs can be used to measure oil-zone expansion in an area of rebound by plotting collar-log surveys of wells producing from oil zones that are receiving injection water. According to Allen (oral commun., 1977), recent developments in casing-collar logging at Wilmington provided an accuracy of 9 mm 88.5 per cent of the time for joint lengths of 12.5 to 13.4 m, measured three times. The maximum degree of instrument error is estimated to be 30 mm for each joint length.

Casing-collar logs also have been made in the oil fields on the eastern shore of Lake Maracaibo in Venezuela where maximum subsidence has been about 4 m (Nuñez and Escojido, 1977).

2.2.4.3 Radioactive-bullet logging

At Wilmington, California, at the Lake Maracaibo oil fields in Venezuela, at the methane gas and brine reservoirs of Niigata, Japan, and at the Groningen gas field in The Netherlands, radioactive bullets have been shot into the formation at known depths, and their positions resurveyed later by gamma-ray detectors to measure compaction or expansion. The accuracy of the radioactive-bullet logging equipment used at Wilmington is reported by Allen to be about 3 cm per distance between bullets (at Wilmington 6.1 m) when logging at 7.6 m per minute.

Schoenbeek (1977) reports improvement in the accuracy of measurement at the Groningen gas field. The sandstone reservoir depth is about 2900 m, and the average thickness about 150 m. Radioactive bullets were shot into the formation at 10-m intervals; relative displacement was measured with a gamma-ray sonde containing three detectors. After considerable improvement of technique, the mean error of measurements determined by statistical analysis was reported to be

1 cm in 100 m of measured interval. To achieve this accuracy, however, the logging time had to be slowed to about 20 m per hour. DeLoos (1973) has described in detail the development and testing of logging equipment.

At Niigata, Japan, the radioactive bullet technique was refined by experiments in 1959-60 and the construction of two observation wells (Figure 2.10). According to Sano (1969), the first observation well (Yamanoshita) was completed in 1960 to a depth of 650 m. Four sizes of casing were used, each stage from bottom to top being of larger diameter than the preceding one. The base of each stage was grouted to the contiguous strata and overlapped the head of the stage below it. Sano (1969) states that it was intended that the increase in the overlapped length of each stage should represent the shrinkage between the strata to which the casing was grouted. The system was unsuccessful because the casing contracted with the shrinkage of the formation.

The second well (Uchino) was completed in 1961 to a depth of 950 m. It was constructed with a conductor pipe 100 m long cemented to the surrounding strata through its full length. The main casing 5-1/2 inches in diameter was suspended in the conductor pipe, In effect, this observation well was the single pipe type.

In both observation wells, radioactive bullets were shot into the formation every 40 m and radioactive reference pellets were attached to the casing every 20 m (Figure 2.10). Special logging equipment was designed to improve accuracy. Logging at about 1-year intervals from 1961 to 1966, when the deeper well failed, apparently was reasonably successful in determining location and general magnitude of compaction.

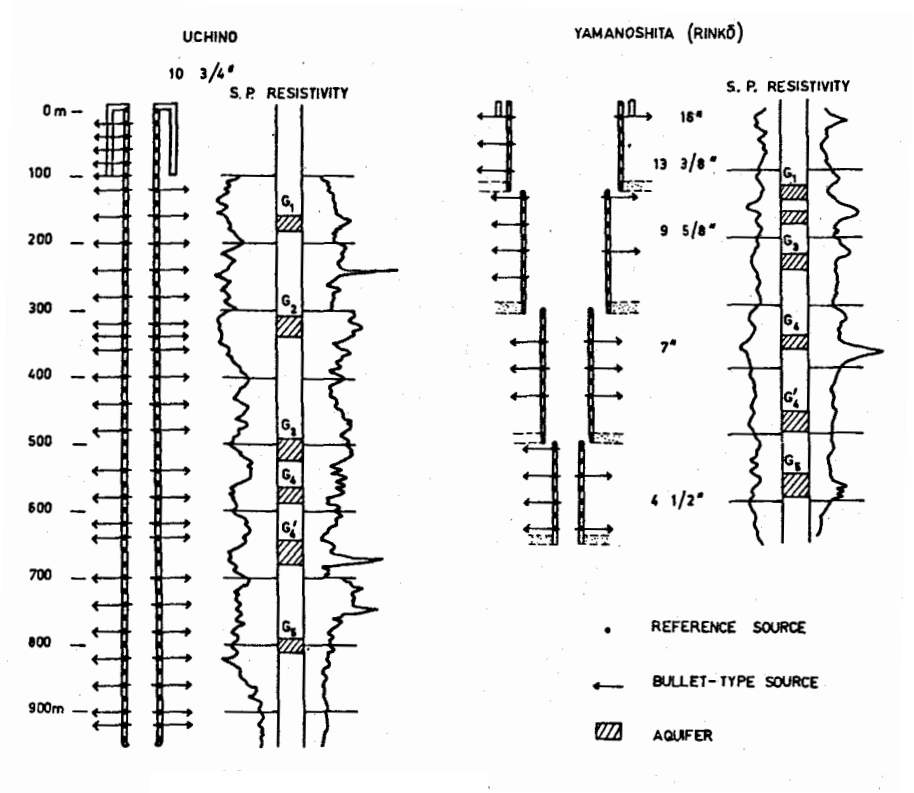

Figure 2.10 Structure of the observation wells in Niigata, Japan (after Sano and Kayana, 1966, Figure 2).

2.3 HORIZONTAL DISPLACEMENT

2.3.1 Land-surface displacement

In areas of subsidence due to fluid withdrawal, horizontal displacement of the land surface has been measured at only a few places. One of those is the Wilmington oil field in Los Angeles County, California, which has experienced as much as nine metres of subsidence. The vertical subsidence has been accompanied by horizontal movement directed inward toward the center of subsidence. This horizontal movement has been measured by surveys of a triangulation network of the Los Angeles County Engineer's office. In 1951, when subsidence at the center was 4.9 m, horizontal movement since 1937 had been as much as 1.9 m (Grant, 1954, Figure 1). By 1962, some points on the east end of Terminal Island had moved as much as 2.7 m, according to the Long Beach Harbor Department.

At Wairakei, New Zealand, Bixley reports that both horizontal and vertical movements have occurred along the steam mains route (see case history 9.9). Maximum movement is near bench mark A97 (Figure 9.9.5), where horizontal movement is about 75 mm/year and vertical movement 130 mm/year.

Until recently, short distances were measured by steel tape and longer distances by triangulation. Triangulation involves the measurement of the angles of a triangle, careful measurement of the length of one side, called the base line, and calculation of the lengths of the other two sides. The process can be extended through angular measurement of many additional triangles.

Within the last decade, however, extremely accurate means have been developed for measuring horizontal distances between points. Electronic Distance Measurement (EDM) equipment permits line-of-sight distance measurement, both rapidly and precisely. Thus, the location of points can now be determined by trilateration, whereby a network of triangles is constructed from one or more known points, with the length of all sides determined directly by use of the EDM equipment. Distance measurements by trilateration have largely replaced measurements by triangulation, especially where extreme accuracy is needed.

The general distance capabilities and accuracy of three types of EDM equipment are as follows:

1. Geodolite, capable of 1 unit in 107 units (laser), 30 km;
2. Electronic EDM, capable of 2 units in 106 (laser), 12 km;
3. Distance meter, capable of 1 unit in 105 (infrared), 3 km.

More information on EDM instruments and other types of equipment to monitor horizontal displacements at land surface are summarized by Van Til (1979, table D-1). Van Til's summary, reproduced in this guidebook as Appendix A, includes a listing of instrument capabilities of steel tapes, EDM instruments, and horizontal extensometers to measure ground strain or crack movement. The appraisal was made with respect to availability, performance characteristics, and installation and operation requirements.

2.3.2 Subsurface displacement

Instruments currently available for the measurement of horizontal displacement at depth are sonde-type borehole inclinometers. Oil-well service companies have equipment to measure both the drift angle (angle of departure from vertical) and the true compass bearing at desired depth intervals to depths as great as 6 km. Most other sonde-type inclinometers have been developed for near-surface geotechnical studies and in general have depth ranges limited to 200-300 m. The availability, operating principles, accuracy, and principal installation and operation features of 10 sonde-type borehole inclinometers and 3 fixed borehole inclinometers are summarized in Appendix B.

2.4 REFERENCES

ALLEN, D. R. 1969. Collar and radioactive bullet logging for subsidence monitoring, Soc. Prof. Well Log Analysts Trans., Paper G, p. 1-19.

ALLEN, D. R., and MAYUGA, M. N. 1969. The mechanics of compaction and rebound, Wilmington oil field, Long Beach, California, USA, in L. J. Tison, ed., Land subsidence, vol. 2, Internat. Assoc. Sci. Hydrology Pub. 89, p. 410-422.

BULL, W. B. 1975. Land subsidence due to ground-water withdrawal in the Los Banos-Kettleman City area, California, Part 2, Subsidence and compaction of deposits, U.S. Geol. Survey Prof. Paper 437-F, 90 p.

FLOYD, R. P. 1978. Geodetic bench marks, National Oceanic and Atmospheric Administration Manual NOS NGS 1, 50 p. NOAA, Rockville, MD, USA 20852

GRANT, U. S. 1954. Subsidence of the Wilmington Oil Field, California, California Division of Mines, Bulletin 170, Chapter X, pp. 19-24.

HIRONO, TAKUZO. 1969. Niigata ground subsidence and ground-water change, in L. J. Tison, ed., Land subsidence, vol. 1, Internat. Assoc. Sci. Hydrology Pub. 88, p. 144-161.

LOFGREN, B. E. 1968. Analysis of stresses causing land subsidence. U.S. Geol. Survey Prof. Paper 600-B, p. 219-225.

LOFGREN, B. E. 1969. Field measurement of aquifer-system compaction, San Joaquin Valley, California, USA, in L. J. Tison, ed., Land subsidence, vol. 1, Internat. Assoc. Sci. Hydrology Pub. 88, p. 272-284.

LOOS de, J. M. 1973. In-situ compaction measurements in Groningen observation wells, Verhandelingen Kon. Ned, Geol. Mijnbouwk. Gen. Volume 28, p. 79-104.

MEYERHOF, G. G. 1965. Penetration test and bearing capacity of cohesionless soils, Proc., American Society of Civil Engineers, Jour. Soil Mech. and Found. Div., vol. 82, SM1 paper no. 866.

MIYABE, NAOMI. 1967. Study of partial compaction of soil layer--in reference to the land subsidence in Tokyo. Tokyo Ins. Civil Eng. Rept. 44, 7 p.

MURAYAMA, S. 1969. Land subsidence in Osaka, in L. J. Tison, ed., Land subsidence, vol. 1, Internat. Assoc. Sci. Hydrology Pub. 88, p. 109-130.

NUÑEZ, 0., and ESCOJIDO, D. 1977. Subsidence in the Bolivar Coast, Internat. Assoc. Sci. Hydrology Pub. 121, p. 257-266.

O'ROURKE, J. E., and RANSON, B. B. 1979. Instruments for subsurface monitoring of geothermal subsidence. Report prepared by Woodward-Clyde Consultants for Lawrence Berkeley Laboratory, Berkeley, Calif., LBL No. 8616, 33 p. and 23 tables.

POLAND, J. P., and DAVIS, G. H. 1969. Land subsidence due to withdrawal of fluids, in Varnes, D. J., and Kiersch, George, eds., Reviews in Engineering Geology, v. 2, Boulder, Colorado, Geol. Soc. America, p. 187-269.

POLAND, J. F., and IRELAND, R. L. 1965. Shortening and protrusion of a well casing due to compaction of sediments in a subsiding area in California, in Geological Survey Research 1965, U.S. Geol. Survey Prof. Paper 525-B, p. B180-B183.

POLAND, J. F., LOFGREN, B. E., IRELAND, R. L., and PUGH, R. G. 1975. Land subsidence in the San Joaquin Valley as of 1972, U.S. Geol Survey Prof. Paper 437-H, 78 p.

RAPPLEYE, H. S. 1948. The manual of geodetic leveling, Special Publication No. 239, NOAA, Rockville, MD, USA. 20852.

SANO, SUN-ICHI. 1969. Observation of compaction of formation in the land subsidence of Niigata City, in L. J. Tison, ed., Land subsidence, vol. 2, Internat. Assoc. Sci. Hydrology Pub. 89, p. 401-409.

SANO, SUN-ICHI, and KANAYA, H. 1966. Observation of partial shrinkage of strata, in Radioisotope instruments in industry and geophysics, Vol. 2, Internat. Atomic Energy Agency, Vienna, p. 279-291.

SCHOONBEEK, J. B. 1977. Land subsidence as a result of gas extraction in Gronigen, The Netherlands, Internat. Assoc. Sci. Hydrology Pub. 121, p. 267-284.

STEPHENS, J. C., and JOHNSON, LAMAR. 1951. Subsidence of organic soils in the Upper Everglades region of Florida, U.S. Dept. Agr., Soil Cons. Service, August, 16 p., 25 figures.

TOKYO METROPOLITAN GOVERNMENT. 1969. Land subsidence in Tokyo, Tokyo, 31 p.

VAN TIL, C. J. 1979. Guidelines manual for surface monitoring of geothermal areas, Report prepared by Woodward-Clyde Consultants for Lawrence Berkeley Laboratory, Berkeley, Calif., LBL report No. 8617, 121 p.

WEIR, W. W. 1950. Subsidence of peat lands of the Sacramento-San Joaquin Delta, California, California Univ. Agr. Exp. Station, Hilgardia, v. 20, no. 3, p. 37-56, June.

WHITEMAN, C. D., Jr. 1980. Measuring local subsidence with extensometers in the Baton Rouge area, Louisiana, 1975-79, Louisiana Department of Transportation and Development, Office of Public Works, Water Resources Technical Report no. 20, 18 p.

3 Mechanics of land subsidence due to fluid withdrawal, by Joseph F. Poland and Working Group

3.1 INTRODUCTION

The three types of fluid withdrawal by man that have caused noticeable subsidence under favorable geologic conditions are (1) the withdrawal of oil, gas, and associated water, (2) the withdrawal of hot water or steam for geothermal power, and (3) the withdrawal of ground water. Each of the three types of withdrawal has produced maximum subsidence of the same order of magnitude. For example, the best known example of oil-field subsidence is the Wilmington oil field in Los Angeles County, California, which has experienced 9 metres of subsidence (Mayuga and Allen, 1969); the withdrawal of hot water for geothermal power at Wairakei, New Zealand, has produced 6-7 metres of subsidence (case history 9.9); and the withdrawal of ground water has produced 9 metres of subsidence in both Mexico City, Mexico, and the San Joaquin Valley of California, USA. (See Table 1.1 and case histories 9.8 and 9.13.) In this guidebook we are concerned with subsidence due to ground-water withdrawal but, regardless of the nature of the fluid removed, the principles involved are the same.

A common understanding of terms is important in discussing the mechanics of land susidence. The reader is referred to three U.S. Geological Survey publications for the definition of many pertinent terms: Water-Supply Paper 494 (Meinzer, 1923) was one of the first comprehensive attempts to define terms used in ground-water studies and has been a much used reference work for the past half century; Water-Supply Paper 1988 (Lohman and others, 1972) contains revised and clarified definitions of selected ground-water terms and stresses the use of consistent units in ground-water flow equations; Water-Supply Paper 2025 (Poland, Lofgren, and Riley, 1972) is a glossary of selected terms useful in studies of the mechanics of aquifer systems and land subsidence due to fluid withdrawal. Principal terms will be defined briefly in this chapter or in an appended glossary, Appendix D.

Figure 3.1 illustrates the terminology for subdivisions of a ground-water reservoir as used in this manual. Case 1, on the left, depicts, from top to bottom, the land surface, a water table, and an unconfined aquifer that functions as an hydraulic unit, a confining bed that functions as a major hydraulic separator; a confined aquifer system that functions approximately as an hydraulic unit; and relatively impermeable bedrock at the base. Case 2 depicts, from top to bottom, the land surface; a water table associated with a semiconfined aquifer system; a confining bed; a confined aquifer system; a second confining bed; a saltwater confined aquifer system; and relatively impermeable bedrock at the base.

Attention is directed to the confined aquifer system that occurs in both cases. Note in particular that aquitards which occur within an hydraulic unit are distinct from a confining bed that serves as an hydraulic separator. For illustrative purposes, the system includes two aquitards (fine-grained compressible interbeds) and three aquifers. Because the aquitards are highly compressible compared to the clastic sand or sand and gravel of the aquifers, they determine by their number and thickness the susceptibility of the aquifer system to compaction in response to increase in stress. In highly compressible confined systems that have experienced several metres of manmade compaction, several tens of aquitards may be interbedded with the aquifers. For example, the microlog of a well drilled through a 400-metre thickness of the confined system on the west side of the San Joaquin Valley, California, displayed 60 aquitards with individual thicknesses ranging from 0.6 m to 15 m and averaging 4.5 m.

In contrast to the large number of aquitards subject to compaction in the San Joaquin Valley, in Mexico City most of the 9 m of compaction has occurred in the top 50 m below land surface, chiefly in two very highly compressible silty clay beds 25-30 and 5-10 m thick. In the upper thicker clay the void ratio averages about 7 and the porosity about 88 per cent; in the lower clay the void ratio averages 4-5 and the porosity about 82 per cent. Figueroa-Vega concludes (case history 9.8, Table 9.8.5) from comparison of casing protrusion and subsidence for 1970-73 that about 75 per cent of the total subsidence was due to compaction of the clayey strata in the top 50 m, and the remainder to compression of the underlying aquifer which is several hundred m thick.

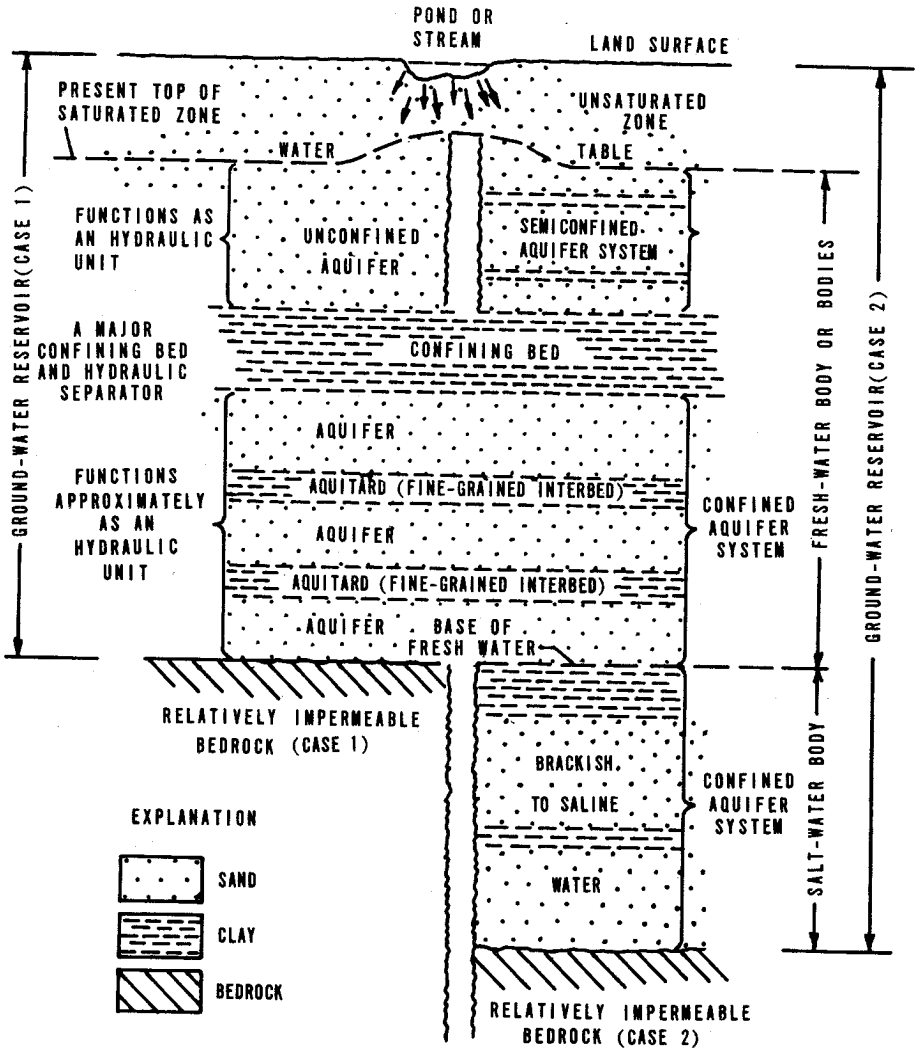

Figure 3.1 Diagram showing terminology for a ground-water reservoir and subdivisions thereof.

In order to count the number and individual thicknesses of the aquitards (or of the aquifers) as displayed in a geophysical bore-hole log, an arbitrary vertical reference, line is drawn on the log. Intervals where the resistivity log lies to the left of the reference line define aquitards; intervals where the resistivity log lies to the right of the reference line define aquifers. Where precisely to draw the reference line becomes a matter of personal judgment. Among the geophysical logs available from oil-field service companies, the microlog of Schlumberger gives considerably more lithologic detail than do the logging devices using a normal electrode configuration. Of these, the short normal with an electrode spacing of about 0.4 metre gives the best detail on thin aquitards.

Figure 9.3.2 is a vertical section of the confined aquifer system beneath Venice, Italy. Using the electric logs and core descriptions from deep test boreholes, the authors of the case history on Venice have divided the confined system into six principal aquifers and a considerable number of aquitards.

3.2 THEORY OF AQUIFER-SYSTEM COMPACTION

In 1925, O. E. Meinzer (Meinzer and Hard, 1925, p. 91) recognized that an artesian aquifer (the Dakota Sandstone) was compressed when the artesian head was decreased. He stated (p. 92) that the overburden pressure of all beds above the confined Dakota aquifer was supported partly by

the fluid pressure at the top of the Dakota and partly by the sandstone itself (grain-to-grain load). He concluded that the grain-to-grain load on the Dakota aquifer at Ellendale, North Dakota, had increased about 50 per cent because of the decline of artesian head.

Meinzer (1928), in a classic paper, discussed the compressibility and elasticity of artesian aquifers in detail. He cited evidence for compressibility and elasticity derived from laboratory tests and from field evidence for confined aquifers and for large artesian basins, notably the Dakota artesian basin. He concluded (p. 289):

> . . . artesian aquifers are apparently all more or less compressible and elastic though they differ widely in the degree and relative importance of these properties. In general the properties of compressibility and elasticity are of the most consequence in aquifers that have low permeability, slow recharge, and high head. In many aquifers these properties are evidently important in supplying water not only by permanent reduction of storage but also by temporary reduction that is replenished when the wells are shut down or during the season of minimum use."

He recognized that water withdrawn from storage was released both by compression of the aquifer and by expansion of the water and that reduction of storage--compression--may be permanent (inelastic) as well as elastic (recoverable).

The next milestone in the understanding of the manner in which artesian aquifers release water from storage was the development by Theis (1935), through analogy with the mathematical theory of heat conduction, of an equation for the non-steady-state flow of ground water to a discharging well. This equation, which for the first time introduced the elements of time and the coefficient of storage (S), subsequently has become the foundation of quantitative ground-water hydrology. Following development of this equation, Theis (1938, p. 894) defined the coefficient of storage as ". . . the volume of water, measured in cubic feet, released from storage in each column of the aquifer having a base one foot square and a height equal to the thickness of the aquifer, when the water table or other piezometric surface is lowered one foot."

Jacob (1940) postulated that when water is removed from and pressure is decreased in an elastic artesian aquifer, stored water is derived from expansion of the confined water, compression of the aquifer, and compression of the adjacent and included clay beds. He concluded that the third source is probably the chief one in the usual case, and he stated (p. 574), ". . . because of the low permeability of the clays (or shales) there is a time lag between the lowering of pressure within the aquifer and the appearance of that part of the water which is derived from storage in those clays (or shales)."

In the field of soil mechanics, Karl Terzaghi (1925; Terzaghi and Peck, 1967) developed the theory of primary one-dimensional consolidation of clays that has served as the basis for solution of most practical soil mechanics and settlement problems in the past half century. This theory commonly is used to estimate the magnitude and rate of settlement or compaction that will occur in fine-grained clayey deposits under a given change in load (stress). According to the theory, compaction results from the slow escape of pore water from the stressed deposits, accompanied by a gradual transfer of stress from the pore water to the granular structure of the deposits. In developing his consolidation theory in 1925, Terzaghi also introduced the basic principle of effective stress that

$$p' = p - u_w, \tag{3.1}$$

where

p' = effective stress (effective overburden pressure or grain-to-grain load),
p = total stress (geostatic pressure), and
u_w = pore pressure (fluid pressure or neutral stress).

This was the same year that 0. E. Meinzer (Meinzer and Hard, 1925) recognized the principle of effective stress in compression of artesian aquifers.

The application of the time-consolidation theory of soil mechanics to explain the theory of aquifer-system compaction has been summarized lucidly by Riley (1969), as follows:

> "The well-known hydrodynamic (Terzaghi) theory of soil consolidation can provide a semi-quantitative explanation for the phenomenon of repeated permanent compaction during successive cycles of loading and unloading through about the same stress range. In the

context of this problem a central tenet of consolidation theory states that an increase in stress applied to a "clay" stratum (aquitard) becomes effective as a compressive grain-to-grain load only as rapidly as the heads (pore pressures) in the aquitard can decay toward equilibrium with the head in the adjacent aquifer(s). Because of the low permeability and relatively high compressibility of the interbedded aquitards, the consolidation (compaction) of a multi-layered aquifer system in response to increased applied stress is a strongly time-dependent process, and complete or "ultimate" consolidation is not attained until a steady-state vertical distribution of head exists throughout the aquifer system. Transient heads in the aquitards higher than those in the adjacent aquifers (termed residual excess pore pressures) are a direct measure of the remaining primary consolidation that will ultimately occur under the existing stress. When pore-pressure equilibrium is attained throughout the aquitard, it is said to be 100 per cent consolidated for the prevailing stress and no further permanent compaction will occur if the same stress is repeatedly removed and reapplied. The possible role of secondary, or nonhydrodynamic, consolidation in aquifer-system compaction is not well-known, but is assumed in this discussion to be minor.)

"For a single homogeneous aquitard, bounded above and below by aquifers in which the head is instantaneously and equally lowered, the time, t, required to attain any specified dissipation of average excess pore pressure is a direct function of: (1) the volume of water that must be squeezed out of the aquitard in order to establish the denser structure required to withstand the increased stress, and (2) the impedance to the escape of this water. The product of these two parameters constitutes the aquitard time constant. For a specified stress increase, the volume of water is determined by the volume compressibility m_v, of the aquitard, the compressibility, β_w, of the water, and the thickness, b′, of the aquitard. The impedance is determined by vertical permeability, K′, and thickness of the aquitard. Thus, the required time, is a function of the time constant, τ, where

$$\tau = \frac{S'_s(b'/2)^2}{K'} \quad (3.2)$$

and where S'_s is the specific storage of the aquitard, defined as

$$S'_s = S'_{sk} + S_{sw} \quad (3.3)$$

in which

$$S'_{sk} = m_v\gamma_w = \frac{\Delta b'}{b'\Delta h_a} \quad (3.4)$$

and

$$S_{sw} = n\beta_w\gamma_w \quad (3.5)$$

S'_{sk} is the component of specific storage due to compressibility of the aquitard, S is the component due to the compressibility of water, h_a is the average head in the aquitard, n is the porosity, and γ_w is the unit weight of water. For consolidating aquitards $S'_{sk} >>> S_{sw}$.

"For convenience, it is customary to define a dimensionless time factor, T, such that

$$T = \frac{t}{\tau'} \quad (3.6)$$

when T equals unity, t equals the time constant. The degree of consolidation U%, at any time, t, is then expressed as a function of T, the form of the functional relation being determined by the initial conditions of the problem. For the commonly used time-consolidation functions, U% is somewhat more than 90 per cent when T is unity. Detailed development of the time-consolidation theory summarized above may be found in Scott (1963, p. 162-197.)"

3.3 ANALYSIS OF STRESSES CAUSING SUBSIDENCE

3.3.1 Types of stresses

As discussed by Lofgren (1968), three types of stresses are involved in the compaction of an aquifer system:

> "These are closely interrelated, yet of such different nature that a clear distinction is of utmost importance. The first of these is a gravitational stress, caused by the effective weight of overlying deposits, which is transmitted downward through the grain-to-grain contacts in the deposits. The second, a hydrostatic stress due to the weight of the interstitial water, is transmitted downward through the water. The third is a dynamic seepage stress exerted on the grains by the viscous drag of vertically moving interstitial water. The first and third are additive in their effect and together comprise the grain-to-grain stress which effectively changes the void ratio and mechanical properties of the deposit; it is commonly known as the "effective stress." The second type of stress, although it tends to compress each individual grain, has virtually no tendency to change the void ratio of the deposit and is referred to as a neutral stress.
> "Of the various methods used in analyzing the effect of these stresses in a compacting aquifer system (Taylor, 1948, p. 203), only two are considered here. Although they vary in their conceptual approach, these methods give the same mathematical results and can be used to check one another. The classical method, the approach most often used in practical soil-mechanics problems, considers the geostatic load, or combined total weight of grains and water in the system, and the neutral, or hydrostatic, stress. The second method considers the static gravitational stress of the grains, which comprises their true weight above the water table and submerged (buoyed) weight below the water table, and the vertical seepage stresses that may exist in the system. Inasmuch as changes in the effective grain-to-grain stress (both gravitational and stress due to seepage) are directly responsible for the compaction of the deposits and are directly related to changes in head in an aquifer system, this second approach has proved the simplest and clearest in our subsidence investigation."

The definition of seepage stress as a net cumulative difference in hydraulic head is a powerful and useful concept, although the interpretation of seepage stress as being caused by viscous drag may be found to be subject to question in the future. For further discussion of this issue, the reader is referred to Helm (1978) and Helm (1980).

The diagram in Figure 3.2 illustrates the stresses acting at the interface between an artesian aquifer and the overlying confining bed. If we assume that the total load, p, exerted on the aquifer is constant and u_w is reduced as a result of pumping, the load borne by the skeleton of the aquifer, p′, is increased by an equal amount. If the artesian head is drawn down to the base of the confining bed (u_w=O), the effective stress, p′, on the aquifer skeleton equals the geostatic pressure p.

The idealized pressure diagram of Figure 3.3 utilizes the classical method to illustrate the stresses that cause subsidence. (Also see Poland and Davis, 1969, Figures 1-3.) For the sake of simplicity, pressure is expressed in terms of the height of an equivalent column of water. The geostatic pressure (total stress), p, of sediments and water at some plane of reference below the water table equals the unit weight of moist sediments above the water table, γ_m, times their thickness, plus the unit weight of saturated sediments below the water table, γ, times their thickness. If we assume an average porosity, n, of 40 per cent, an average specific gravity, G, of 2.70 for the grains, an average specific retention, r_s, of 0.20 for the moisture contained above the water table, and let the unit weight of water be unity, then, γ_m equals 1.8 metres of water per metre of thickness:

$$\gamma_m = [G(l-n) + r_s]\gamma_w, \text{ or } [2.7(1-0.4) + 0.20]1 = 1.8, \tag{3.7}$$

and γ= 2.0 metres of water per metre of thickness:

$$\gamma = [G(l-n) + n]\gamma_w, \text{ or } [2.7(1-0.4) + 0.4]1 = 2.0. \tag{3.8}$$

Thus the geostatic pressure at depth $z_l + z_2$ (figure 3.3) is

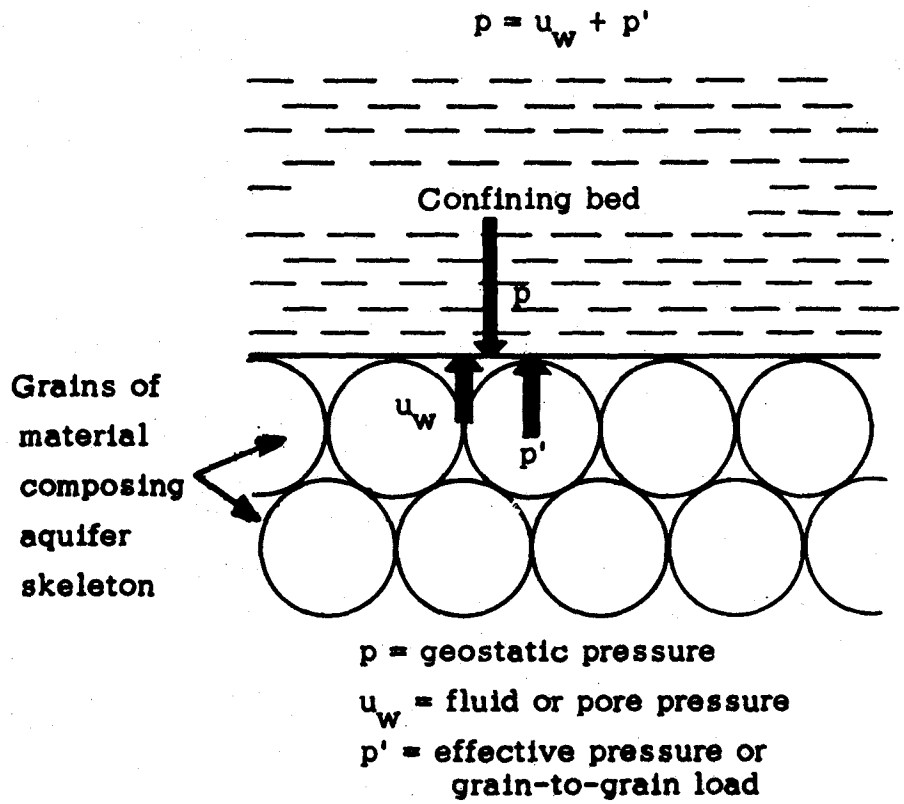

Figure 3.2 Diagrammatic view of stresses acting at interface between artesian aquifer and confining bed (modified from Ferris, Knowles, Brown, and Stallman, 1962, p. 79).

$$p = z_1\gamma_m + z_2\gamma = (50 \times 1.8) + (450 \times 2.0) = 990 \text{ metres of water} \quad (3.9)$$

(a column of water 1 metre high exerts a pressure of 0.1 kg cm^{-2} on its base)

The lowering of artesian head in a confined aquifer system, for example, from depth (Z_1) to (Z_3) in Figure 3.3, does not change the geostatic pressure appreciably. Therefore, the increase in effective stress in the confined aquifers is equal to the decrease in fluid pressure. The compaction in these is immediate and is chiefly recoverable if fluid pressure is restored, but usually it is small.

On the other hand, in the aquitards (fine-grained interbeds) and confining beds, which have low vertical permeability and high specific storage under virgin stressing, the vertical escape of water and the adjustment of pore pressures is slow and time-dependent. Hence, the stress increase applied at the aquifer-aquitard boundaries by the head decline in the confined aquifers becomes effective in these fine-grained beds only as rapidly as pore pressures decay toward equilibrium with those in adjacent aquifers. (See dashed pore-pressure lines of Figure 3.3; where u_t represents the excess pore pressure at time t.) Attainment of pore-pressure equilibrium (dotted lines) may take months or years; the time varies directly as the specific storage and the square of the draining thickness and inversely as the vertical hydraulic conductivity of the aquitard or the confining bed.

Although not illustrated in Figure 3.3, it is readily apparent that increase of fluid pressure from a steady-state condition decreases effective stress and causes expansion of the pressurized sediments (as in subsidence control and underground waste disposal). Fluid pressure cannot exceed geostatic pressures without causing uplift of the overburden.

The stress relations of Figure 3.3 serve to illustrate the principle of effective stress, but do not emphasize the importance of net difference of hydraulic head in causing compaction. Actually, the downward hydraulic gradient developed across the confining bed by the head decline in the confined system induces downward movement of water through the pores that exerts a viscous drag on the clay particles. The stress so exerted on the particles in the confining bed in the direction of flow is a seepage stress.

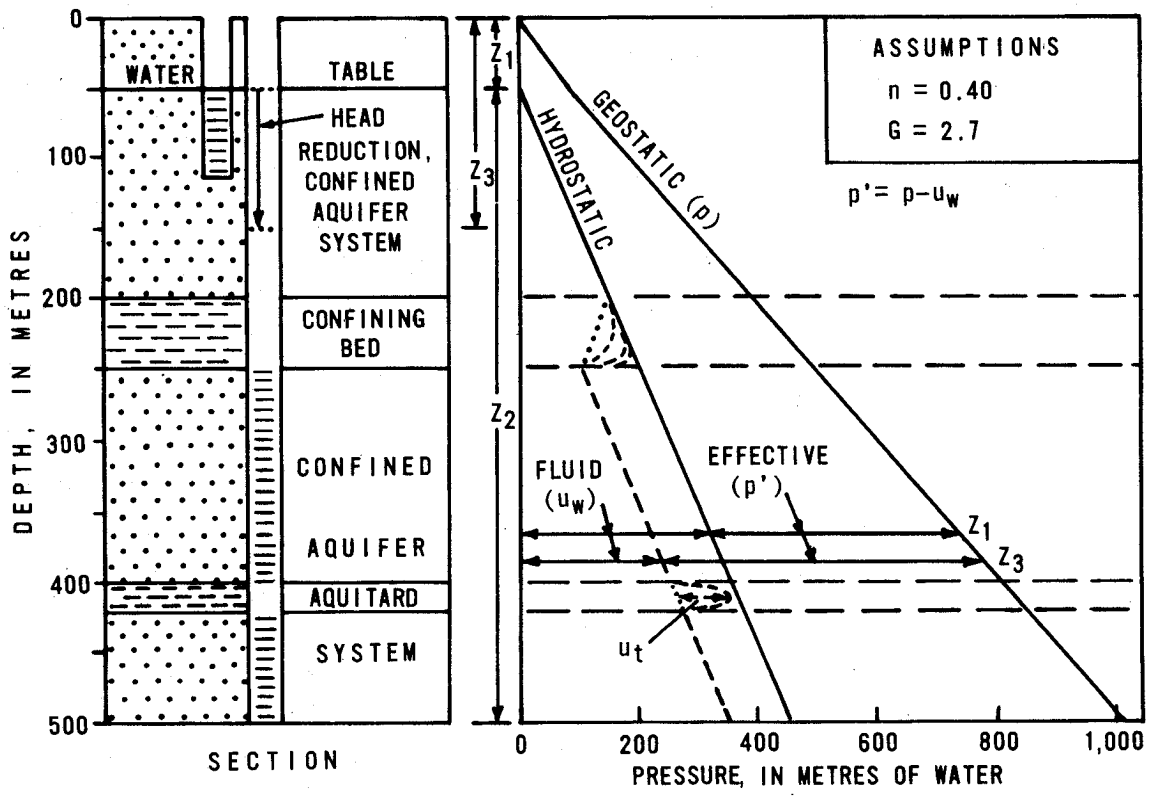

Figure 3.3 Pressure diagram for an unconfined aquifer and a confined aquifer system; head reduction in the confined system only.

3.3.2 Computation of stress change

It is quantitatively convenient in treating complex aquifer systems to compute effective stresses and stress changes in terms of gravitational stress and the vertical normal component of seepage stress, which are algebraically additive. The following brief discussion is summarized from Lofgren (1968) and Poland and others (1975).

Diagram A of Figure 3.4 illustrates part of a confined aquifer system containing an aquitard, overlain by a confining bed and an unconfined aquifer. The water table and the potentiometric surface of the confined system are initially at the same depth; hence, fluid pressure at all depths is hydrostatic. All beds and surfaces within the vertical column are assumed to be horizontal. If we assume the same parameters as for Figure 3.3, and let the unit weight of water be unity, then the effective unit weight of moist deposits above the water table, γ_m, equals 1.8 metres of water per metre of thickness:

$$\gamma_m = [G(1-n) + r_s]\gamma_w, \text{ or } [2.7(1-0.4) + 0.20]l = 1.8 \qquad (3.7)$$

Also, the effective submerged, or buoyant, unit weight of saturated deposits, γ_b, equals one metre of water per metre of thickness:

$$\gamma_b = (1-n)\ (G-1)\gamma_w, \text{ or } (1-0.4)\ (2.7-1)l = 1.0 \qquad (3.10)$$

If these gravitational stresses Are expressed in metres of water (one metre of water is equivalent to 0.1 kg cm^{-2}), they can be added directly to hydraulic stresses.

Vectors to the right of diagram A (Figure 3.4) represent the two components of effective gravitational stress at three depths. At the 400-metre depth, for example, the stress due to the unsaturated deposits, s, equals 200 metres of thickness times 1.8, or 360 metres of water; the stress due to the buoyant weight of submerged deposits, b, equals 200 x 1.0, or 200 metres of water. The sum of s + b, 560 metres of water, is the grain-to-grain stress at this plane of

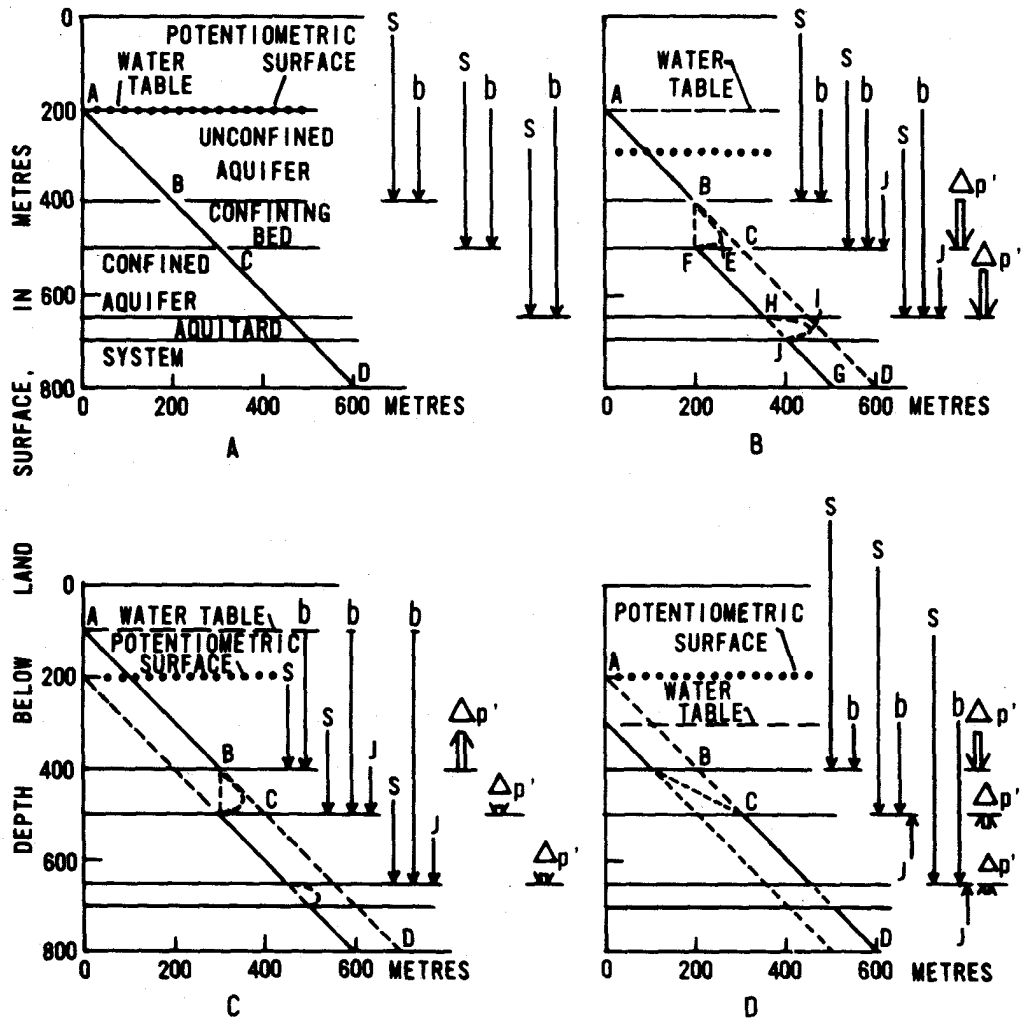

Figure 3.4 Effective stress diagrams for a confined aquifer system overlain by an unconfined aquifer. A, water table and potentiometric surface common. B, water table constant, potentiometric surface lowered. C, water table raised, potentiometric surface constant. D, water table lowered, potentiometric surface constant. Stresses in metres of water; based on assumed porosity = 0.40, specific gravity of solids = 2.7, and specific retention = 0.20. S = effective stress due to weight of unsaturated deposits; b = effective stress due to buoyant weight of submerged deposits; J = seepage stress; Δp′ = change in total effective stress from condition A.

reference. The effective stress of the saturated deposits increases directly with depth below, the water table, as indicated by the increasing vector lengths, b, at the base of the confining bed and the top of the aquitard.

If the potentiometric surface of the confined aquifer system is drawn down 100 metres as in diagram B, gravitational stresses remain as in A because the water table is unchanged. However, a downward component of hydraulic gradient is developed across the confining bed, which induces downward movement of water through the pores and exerts a viscous drag on the grains. The net force transferred to the grains between any two depths is measured by the head loss between those depths. The stress so exerted on the grains is called a seepage stress. This third effective stress component is represented by vector J on a horizontal plane. Its vertical component is algebraically additive to the gravitational stresses and is transmitted downward through the confined aquifer system. The wide arrows to the right of diagram B indicate within a vertical column the net change in the vertical normal component of effective stress at the base of the confining bed and below, from the hydrostatic condition of diagram A.

Because the water table is unchanged the net change is the change in seepage stress, which is equal to the decrease in fluid (neutral) pressure represented by line C-F (base of confining bed).

The increase in effective stress in the permeable aquifers occurs simultaneously with decrease in head, but decrease of pore pressure in the aquitards and confining beds is delayed because of their high compressibility and low vertical permeability. The reduction in head in the permeable aquifers creates a two-directional hydraulic gradient outward from the center of the aquitard and consequently induces two-directional drainage from the aquitard. Thus, although upward and downward seepage forces occur within the aquitard during this adjustment, internal stresses have no net external effect on the rest of the aquifer system. During this period of transient pressures, the effective stress can increase only as rapidly as the excess pore-pressure decreases. The general pattern of decay is illustrated in diagram B of Figure 3.4 in the confining bed by dashed line B-E-F and in the aquitard by dashed line H-I-J. Full dissipation of excess pore pressures to equilibrium (dashed lines B-F and H-J) may require months or years. Note that water drains through both boundaries of the aquitard, but only through the lower boundary of the confining bed under the specified conditions.

If the potentiometric surface of the confined aquifer system remains constant and the water table is raised or lowered, both gravitational and seepage stresses change, but with opposite sign. For example, if the water table is raised 100 m (diagram C) and the parameters are as assumed earlier, the change in gravitational stress is -0.8 metre of water per metre of rise; however, the unit change in seepage stress (differential between water table and potentiometric surface of confined system) is +1.0 metre. Hence, the net unit change in applied stress in the confined system is +0.2 metre of water. Conversely, if the water table is lowered (diagram D), the net change in applied stress is -0.2 metre per metre of decline.

In summary, water-level fluctuations change effective stresses in the following two ways:

1. A rise of the water table provides buoyant support for the grains in the zone of the change, and a decline removes the buoyant support; these changes in gravitational stress are transmitted downward to all underlying deposits.
2. A change in position of either the water table or the potentiometric surface of the confined aquifer system, or both, may induce vertical hydraulic gradients across confining or semiconfining beds and thereby produce a seepage stress. The vertical normal component of this stress is algebraically additive to the gravitational stress. A change in effective stress results if preexisting seepage stresses are altered in direction or magnitude.

The change in applied stress within a confined aquifer system, due to changes in both the water table and the artesian head, may be summarized concisely (Poland and others, 1972, p. 6) as

$$\Delta p_a = -(\Delta hc - \Delta h_u y_s), \qquad (3.11$$

where p_a is the applied stress expressed in metres of water, h_c is the head (assumed uniform) in the confined aquifer system, h_u is the head in the overlying unconfined aquifer, and y_s is the average specific yield (expressed as a decimal fraction) in the interval of water-table fluctuation.

In the San Joaquin Valley, California, the areas in which subsidence has been appreciable coincide generally with the areas in which ground water is withdrawn chiefly from confined aquifer systems. (See Chapter 9.13, Figure 9.13.2.) Furthermore, the great increases in stress applied to the sediments in the ground-water reservoir by the intensive mining of ground water developed chiefly as increased seepage stresses on the confined aquifer systems.

3.4 COMPRESSIBILITY AND STORAGE CHARACTERISTICS

3.4.1 Stress-strain analysis

Field measurements of compaction and correlative change in water level may serve as continuous monitors of subsidence and indicators of the response of the system to change in applied stress. They also can be utilized to construct stress-strain curves from which, under certain favourable conditions, one can derive storage and compressibility parameters of the aquifer system, as first demonstrated by Riley (1969) for the Pixley site in the southern part of the San Joaquin valley, California.

Thirteen years of measured water-level change and compaction at Pixley are shown in Figure 3.5. They have been utilized to derive a computer plot of stress change versus strain (Figure 3.5, E) for a 101-metre thickness of the confined aquifer system. The change in stress (B) applied to all strata within the depth interval is calculated from the hydrographs (A) of wells 16N4 (water table) and 16N3 (confined system). This stress-change graph is plotted with stress increasing downward to emphasize the close correlation with declining artesian head. The compaction within the 131-232-metre depth interval (D) is obtained as the difference between the two extensometer plots on graph C. The stress-strain diagram (E) represents the mechanica1 response (change in thickness) of the 131-232-metre depth interval to change in effective stress. It is plotted from the calculated data of graphs B and D. For convenience, the stress-change plot of graph B is expressed in equivalent units of water head (1 ft of water head is equivalent to 0.4333 lb in^{-2}; 1 m of head is equivalent to 0.1 kg cm^{-2}).

Attention is directed to (1) the annual depth-to-water pattern for the confined aquifer system (see hydrograph for well 16N3) in response to the characteristic seasonal pumping for irrigation--the main seasonal decline occurs in spring to late summer followed by recovery of water level to a peak late in the winter; (2) the reduced rate of compaction during years of small seasonal drawdown of water level in well 16N3, such as 1962, 1963, 1967 and 1969; (3) the small but definite expansion of the deposits (D) in most winters, accompanying the water-level recovery; and (4) the series of annual stress-strain loops (E), formed by the yearly cycles of stress increase and decrease.

As discussed by Riley (1969):

> "The descending segments of the annual loop are of particular interest since the represent the resultant of two opposing tendencies--one toward continuing compaction and one toward elastic expansion in response to decreasing applied stress. Expansion of the more permeable strata of the aquifer system must be essentially concurrent with the observed rise in head in wells. However, the first reduction of stress may produce only a slight reduction in compaction rate. Evidently, initial expansion of the aquifers is concealed by continuing compaction of the interbedded aquitards as water continues to be expelled under the influence of higher pore pressures remaining within the medial regions of the beds.
>
> "Consolidation theory requires that the maximum excess pore pressure, which is in the middle of a doubly-draining aquitard, be related to the same parameters . . . . . that control the time-consolidation function. It is, therefore, inevitable that there be, at the end of a relatively short pumping season, a large range of maximum excess pore pressures in a sequence of aquitards of widely varying thicknesses and physical properties. Thus, as head in the aquifers rises and stress declines, the thinnest and (or) most permeable aquitards, containing the least excess pore pressure, will quickly assume an elastic response; but the thickest and (or) least permeable beds may continue to compact at diminishing rates through most or perhaps all of the period of head recovery and stress relief.
>
> "Evidence for this type of behavior is contained in the continuously curving stress strain line characteristic of much of the descending portions of the annual loops."

If in Figure 3.5E the lower part of the descending curve approximates a straight line with a positive slope, as it does, for instance, in 1968 and 1970, we can assume that essentially all excess pore pressures have been exceeded by the rising heads and that the entire aquifer system is expanding in accordance with its elastic modulus.

The lower parts of the descending segments of the annual loops for the winters of 1968-69 1969-70, and the latter part of 1970 are approximately parallel straight lines, as shown by the upward projection of the dotted lines. The reciprocal of the slope of the dotted lines is realistic estimate of the component of the storage coefficient, S, attributable, to the elastic or recoverable deformation of the aquifer system skeleton, S_{ke}:

$$S_{ke} = \frac{\Delta b}{\Delta h} = 6.4 \times 10^{-4} \qquad (3.12)$$

where b is the thickness of the aquifer-system segment being measured, Δb is compaction, h is applied stress, and Δh is change in applied stress. The component of average specific storage due to elastic deformation is S_{ske}:

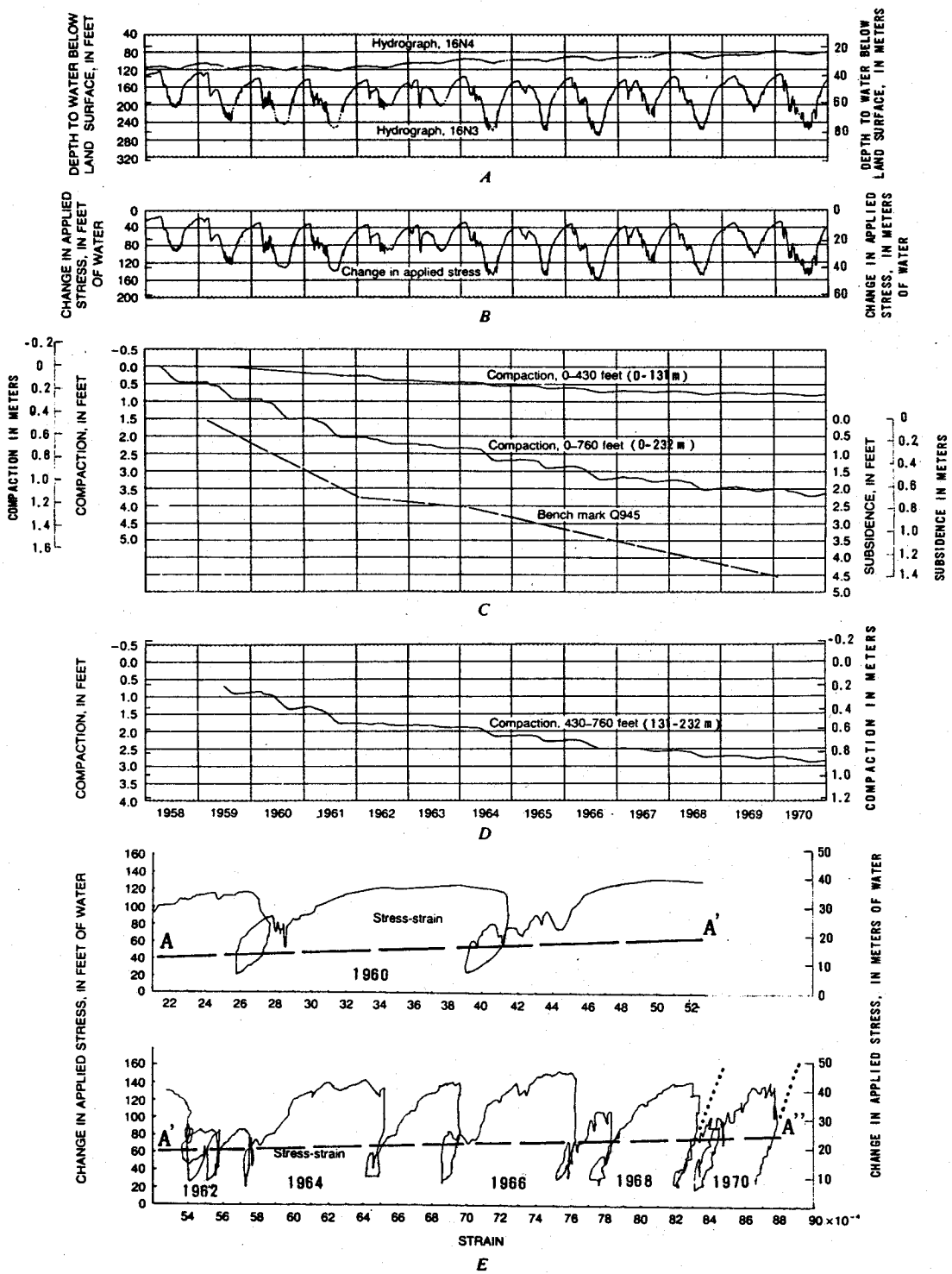

Figure 3.5 Hydrographs, change in applied stress, compaction, subsidence, and stress-strain relationship, 23/25-16N. A, Hydrographs of wells 23/25-16N4, perforated 61-73 m depth, and 23/25-16N3, perforated 110-128 m depth. B, Change in applied stress. C, Compaction to 131-metre depth in well 23/25-16N3 and to 232-metre depth in well 23/25-16N1 and subsidence of bench mark Q945 at well 23/25-16N1. D, Compaction in 131-232-metre depth interval. E, Stress change versus strain (101-metre thickness). (Modified from Poland, Lofgren, Ireland, and Pugh, 1975, Fig. 70.)

$$S_{ske} = \frac{\Delta b}{b} / \Delta h = \frac{S_{ke}}{b} = \frac{6.4 \times 10^{-4}}{101m} = 6.3 \times (10)^{-6} m^{-1}, \tag{3.13}$$

where $\Delta b/b$ represents strain in Figure 3.5E and can be considered a conservative estimate of bulk volume strain, $\Delta V/V$, in the field. The compressibility of the aquifer-system skeleton in the elastic range of stress is α_{ke}:

$$\alpha_{ke} = \frac{S_{ske}}{\gamma_w} = \frac{6.3 \times 10^{-6} m^{-1}}{0.1 kg cm^{-2} m^{-1}} = 6.3 \times 10^{-5} cm^2 kg^{-1}. \tag{3.14}$$

However, if stresses are expressed in metres of water, and if γ_w (the unit weight of water) equals unity, α_{ke} is equal numerically to S_{ske}. It is of interest to note that the compressibility of water, β_w, at 20° C, is 4.7 x 10^{-5} $cm^2 kg^{-1}$. Hence, the average elastic compressibility of the aquifer-system skeleton is about 1.3 times as large as the compressibility of water.

On the other hand,

$$S_{sw} = n\beta_w\gamma_w, \tag{3.5}$$

If the average porosity, n, equals 0.4, then

$$S_{sw} = (0.4)(4.7 \times 10^{-5} cm^2 kg^{-1})(0.1 kg cm^{-2} m^{-l}) = 1.9 \times 10^{-6} m^{-l} \tag{3.15}$$

Therefore, for the 101-metre thickness of the measured interval, the ratio of specific storage values for the elastic deformation of the aquifer system and for the elastic expansion of water is

$$\frac{S_{ske}}{S_{sw}} = \frac{6.3 \times 10^{-6} m^{-1}}{1.9 \times 10^{-6} m^{-1}} = 3.3. \tag{3.16}$$

This means that for each unit of change in head, the volume of water released from or taken into storage per unit volume of the porous medium by elastic (recoverable) deformation of the medium is more than three times the volume released by elastic deformation of the interstitial water

Elastic storage and compressibility parameters have been derived from two other stress-strain plots described in the case histories. One is for a well in western Fresno County, illustrated in Figure 9.13.9. The depth interval measured is 70-176 m below land surface. At this site, S_{ke} = 1.2 x 10^{-3} and S_{ske} = 1.1 x $10^{-5} m^{-1}$. This stress-strain plot (Figure 9.13.9) is of interest also because the lower parts of both the descending and ascending segments of the annual "hysteresis loops" form essentially a common straight line, indicating almost no time delay in adjustment of the aquifer-system skeleton to change in stress in the elastic range of stress.. Of this 106-m thickness of aquifer system, the sum of the aquifers is 71 m or two-thirds of the total and the sum of the aquitards is only one-third of the total. The electric log suggests the aquitards are largely silt and hence relatively permeable compared with clay.

The other plot is for a well in San Jose, California, illustrated in Figure 9.14.7. The depth interval measured is 244 m thick, 61-305 m below the land surface, representing the full thickness of the confined aquifer system. The stress-compaction plot indicates that S_{ke} 1.5 x 10^{-3} and $S_{ske} = S_{ke}/244m$ = 6.15 x $10^{-6} m^{-1}$. In these computations I have assumed that in the range of stresses less than preconsolidation stress, the compressibility of the aquitards and the aquifers is the same. Therefore, the full thickness of the confined aquifer system, 244 m, was used to derive the specific storage component, S_{ske}, in the elastic range of stress.

For stresses exceeding past maximum (preconsolidation) stresses, virgin specific storage and compressibility parameters can be approximated from Figure 3.5. Straight line A-A′-A" is drawn through the annual hysteresis loops approximately at the level at which the rising elastic compaction curve crosses over the descending expansion curve. The reciprocal of the slope of line A-A′-A" is the component of the storage coefficient, S, attributable to the inelastic (nonrecoverable) deformation of the aquifer-system skeleton, S_{kv}:

$$S_{kv} = \frac{\Delta b}{\Delta h} = 6.8 \times 10^{-2} \tag{3.17}$$

The component of specific storage due to inelastic (nonrecoverable) deformation of the aquifer system skeleton is S_{skv}:

$$S_{skv} = \frac{S_{kv}}{b} = \frac{6.8 \times 10^{-2}}{101\text{m}} = 6.7 \times 10^{-4}\text{m}^{-1} \tag{3.18}$$

Relation 3.18 is an average value for the entire system. It is reasonable to assume, however, that only the clay interbeds deform inelastically. To obtain the average nonrecoverable specific storage of the aquitards in accordance with this convention, S_{kv} is divided by the aggregate thickness, b′, of aquitards, which is 70 metres:

$$S'_{skv} = \frac{S_{kv}}{b'} = \frac{6.8 \times 10^{-2}}{70\text{m}} = 9.7 \times 10^{-4}\text{m}^{-1} \tag{3.19}$$

The average aquitard compressibility

$$\frac{S'_{skv}}{w} = \frac{9.7 \times 10^{-4}\text{m}^{-1}}{0.1\text{kgcm}^{-2}\text{m}^{-1}} = 9.7 \times 10^{-3}\text{cm}^{2}\text{kg}^{-1} \tag{3.20}$$

The average compressibility of the aquifer-system skeleton in the virgin range of stressing is α_{kv}:

$$\alpha_{kv} = \frac{S_{skv}}{\gamma_w} = \frac{6.7 \times 10^{-4}\text{m}^{-1}}{0.1\text{kgcm}^{-2}\text{m}^{-1}} = 6.7 \times 10^{-3}\text{cm}^{2}\text{kg}^{-1} \tag{3.21}$$

Thus, from the appraisal of Figure 3.5, and the comparison of α_{ke} of 3.14 to α_{kv} of 3.21, we can conclude that at Pixley, the compressibility of the measured interval of the aquifer system in the virgin range of stressing is about 100 times as great as the compressibility in the elastic range of stressing. Hydrologists should be aware that in multiaquifer systems the values of the compressibility and storage parameters may be 10 to 100 times greater when total applied stresses are in the virgin range of stressing than when they are in the elastic range. This fact must be kept in mind in the interpretation of aquifer tests and when making estimates of the usable storage capacity of a confined-aquifer system.

3.4.2 Soil-mechanics techniques

Compressibility characteristics of fine-grained compressible layers or lenses (aquitards) can be obtained by making one-dimensional consolidation tests of "undisturbed" cores in the laboratory. These tests are described in soil mechanics textbooks and briefly in Chapter, 4 of this manual. The plot of void ratio against the logarithm of load (effective stress) is known as the e-log p plot. Three parameters that can be obtained from this plot are (1) the compression index, C_c, a measure of the nonlinear compressibility of the sample, (2) the coefficient of consolidation, C_v, a measure of the time rate of consolidation, and (3) the approximate value of the preconsolidation load, determined graphically (see Figure 4-9). The preconsolidation load or stress is the maximum prior effective stress to which a deposit has been subjected and which it can withstand without undergoing additional permanent deformation. Most of the compacting deposits in the subsiding areas of Table 1.1 are of late Cenozoic age and before disturbance of equilibrium conditions by man were normally consolidated or slightly overconsolidated (1 to 4 kg cm^{-2}).

For effective stress changes in the stress range less than preconsolidation stress, the compaction or expansion of both aquitards and aquifers is elastic--that is, approximately proportional to change in effective stress over a moderate range in stress, and fully recoverable if the stress reverts to the initial condition.

For increase in effective stress in the range of loading that exceeds preconsolidation stress, the "virgin" compaction of aquitards is chiefly inelastic--that is, not recoverable upon decrease in stress. However, this virgin compaction includes a recoverable elastic component

that is small compared to the nonrecoverable component. The virgin compaction usually is roughly proportional to the logarithm of effective stress.

The compaction of aquifers, in contrast to that of aquitards, is chiefly elastic (recoverable) but it may include an inelastic component. In poorly sorted and angular sands and especially in micaceous sands, the inelastic component may dominate.

A semilogarithmic plot of void ratio, e, versus the logarithm of load (effective stress p′, shown in Figure 3.6, illustrates a graphic method of computing compressibility. The coefficient of volume compressibility, m_v in soil-mechanics terminology,

$$m_v = \frac{e_0 - e_1}{(1 + e_0)\Delta p'}$$

(Terzaghi and Peck, 1967). It represents the compression of the clay, per unit of initia1 thickness, per unit increase in load (for effective stress change in the range exceeding pre-consolidation stress). Utilizing the laboratory virgin compression curve, which is a straight line on the semilogarithmic plot, we see that for a load change Δp′, from 100 to 200 lbs in^{-2}

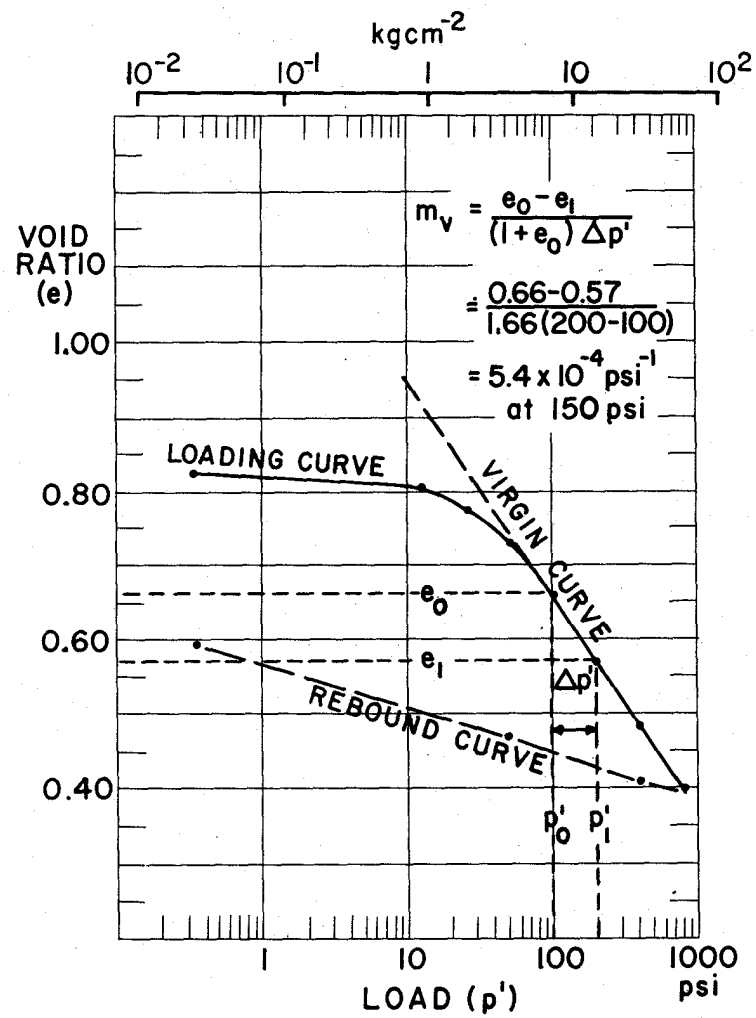

Figure 3.6 Deriving m from e-log p′ plot.

(7 to 14 kg cm^{-2}), the void ratio, e, decreases from 0.66 to 0.57. The decrease in volume or length of the sample, $e_0 - e_l$, divided by the initial volume, $1 + e_0$, and by the change in load for the values given, supplies an approximation of compressibility at the midpoint of $\Delta p'$. Thus, the compressibility at 150 lbs in^{-2} (10.5 kg cm^{-2}) is approximately 5.4×10^{-4} $in^2 lb^{-1}$ (7.7×10^{-3} cm kg^{-1}). The compressibility decreases markedly with increase in effective stress. Repeating the computation, for several increments of load increase furnishes the data for plotting compressibility for the pertinent range in effective stress.

Figure 3.7 is a logarithmic plot showing the principal range in compressibility of tested cores from four core holes tapping alluvial and minor lacustrine deposits in southwestern United States, as well as the compressibility of pure clays made by Chilingar and Knight (1960).

The four core holes are spaced from California to Texas, as follows:

Core hole	Location	Depth (m)
A	Santa Clara Valley, California, in San Jose	305
B	San Joaquin Valley, California, in western Fresno County	610
C	Pinal County, Arizona, near Eloy	592
D	Harris County, Texas, at Clear Lake	294

The graph summarizes the compressibility range for 30 samples from the four core holes for effective stresses between 8 and 100 kg cm^{-2}. If we consider these samples under a common effective stress of 70 kg cm^{-2} (note the vertical dashed line), the range in compressibility of

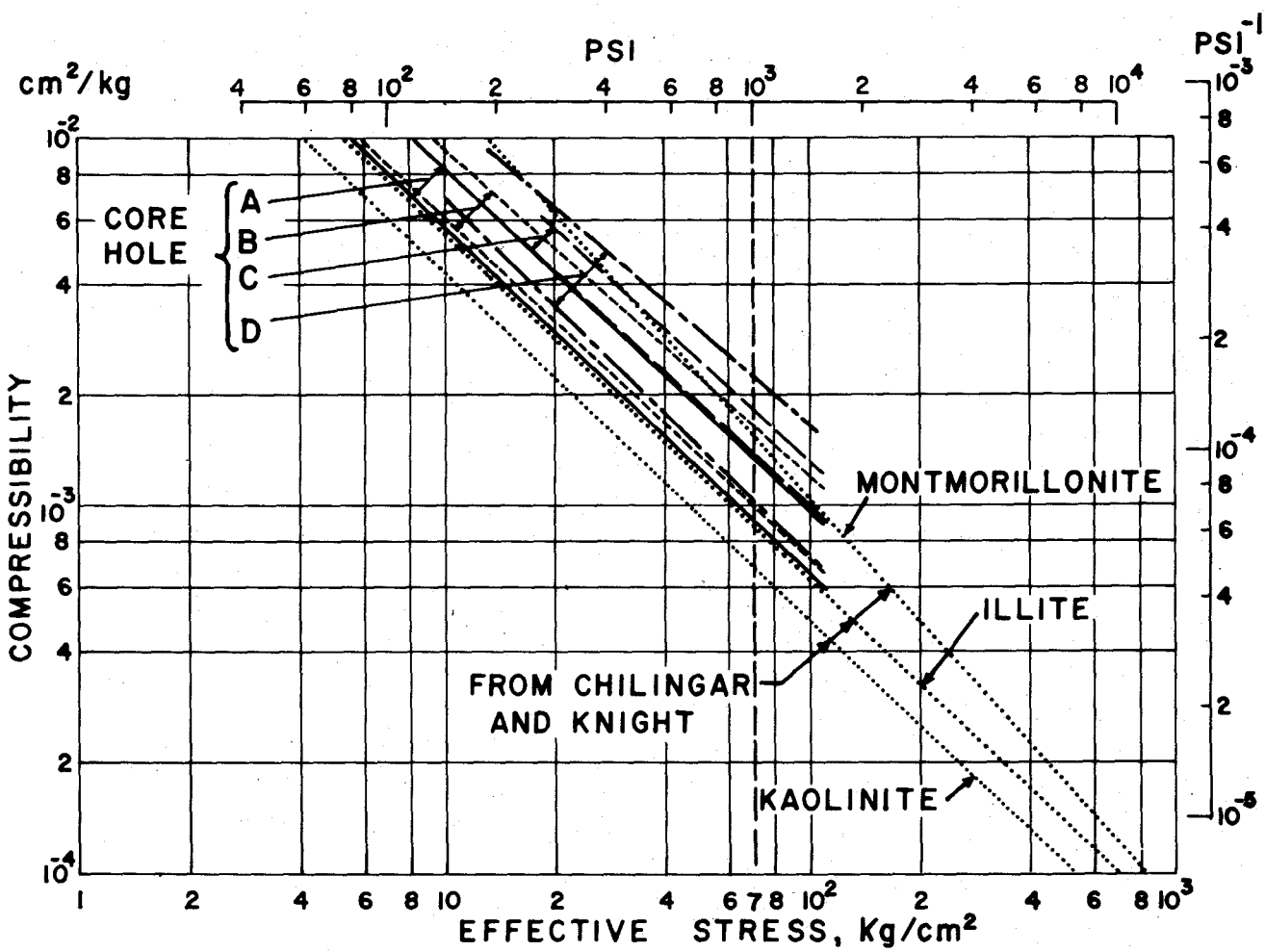

Figure 3.7 Compressibility plots for fine-grained samples from four core holes in southwestern United States and for pure clays tested by Chilingar and Knight (1960).

the 30 cores is about 9 x 10^{-4} to 2.3 x 10^{-3} cm^2 kg^{-l}, a range by a factor of nearly three.

Experimental compaction studies by Chilingar and Knight (1960), made on kaolinite, illite, and montmorillonite clays at pressures from 3 to 14,000 kg cm^{-2} afford an opportunity to compare compressibilities of the fine-grained corehole samples with those of pure clays. The standard clay-mineral samples tested were described by Chilingar and Knight (1960, p. 103) as follows:

Montmorillonite No. 25, Upton, Wyoming
Illite No. 35, Fithian, Illinois
Kaolinite No. 4, Macon, Georgia

The results of their tests, which they expressed in moisture content in per cent (dry weight) versus the logarithm of pressure, have been converted to compressibility versus effective stress and are shown as dotted lines in Figure 3.7. Kaolinite has the lowest compressibility, illite the intermediate, and montmorillonite has the highest. The compressibilities of all 30 corehole samples are higher than those of the standard illite throughout the stress range tested. Furthermore, the compressibilities of all the samples from core holes A and B (central California) fall between the standard illite and montmorillonite curves. X-ray diffraction analysis of the clay-mineral assemblages at all four sites indicated that montmorillonite is the predominant clay mineral, ranging from 6 to 8 parts in 10.

Compressibility tests have been made on many samples of fine-grained sediments taken from a deep (950m) borehole in Venice, Italy, in 1971. Values of m_v versus depth for more than 50 samples are plotted in Figure 9.3.3 of the Venice case history. The compressibilities were computed at the actual "in situ" pressures for both the loading and unloading curves. Ricceri and Butterfield (1974) made a detailed analysis of the compressibility data from the deep borehole. If the compressiblities for samples from 120-220 m depth, computed from the loading curve (m_{vl} points in Figure 9.3.3), are plotted in Figure 3.7, most points fall on or just to the right of the illite curve. Compressibilities average about 3 x 10^{-3} cm^2kg^{-1} for effective stresses in the range of 12 to 22 kg cm^{-2} (120-220 m depth). The highest compressibilities fall within the range of compressibilities for samples from corehole A (Santa Clara Valley, Calif.).

3.4.3 The compressibility environment

Effective stresses, including the increase applied by pumping, are in the range of 10 to 100 kg cm^{-2} for aquifer systems tapped by water wells within depths of 60 to 900 m. This depth range includes about all the stressed sediments of Table 1.1. Within this stress range sands in general are much less compressible than clays. However, at effective stresses of 100 to 200 kg cm^{-2}, evidence is accumulating to show that some sands may be as compressible as clays or siltstones.

Roberts (1969) made a laboratory study of the compressiblity of sands and clays as determined from one-dimensional consolidation tests at stresses up to 700 kg cm^{-2}. The tests showed that in the range of effective stresses from 100 to 200 kg cm^{-2}, some sands were as compressible as typical clays. Roberts noted that sands are relatively incompressible at low pressures (<100 kg cm^{-2})--the compression is due to particle rearrangement. At higher pressures fracturing of the grains develops. He concluded that factors affecting the pressures at which fracturing begins include the initial density of the sample, angularity of the grains, and grain-size distribution.

In a study of subsidence of oil fields bordering Lake Maracaibo in Venezuela, van der Knapp and van der Vlis (1967) made one-dimensional consolidation tests on cores of uncemented sand and clay, taken from depths of 900 to 1050 m. Compressibility was computed from the virgin compression curve of the e-log p’ plot. The composite graphs of compressibility of the sand and clay samples showed that the two materials have comparable compressibilities. For example, at 140 kg cm^{-2} of effective stress, the mean sand compressibility (8 samples) is about 5.7 x 10^{-4} cm kg^{-1} and the mean clay compressibility (11 samples) is about 4.5 x 10^{-4} cm^2kg^{-l}.

The principal oil zones at the Wilmington oil field in Los Angeles and Long Beach, California, that compacted to cause as much as 9 m of subsidence are at depths of 600 to 1200 m. When fluid pressures in the zones were depleted in the late 1950’s prior to repressuring, effective stresses were 100 to 200 kg cm^{-2} According to Allen and Mayuga (1969), axial loading tests on the reservoir sands and siltstones showed the sands to be as compactible, or more so, than the siltstones at the field effective stresses. From the laboratory tests, reservoir calculations, and casing-collar measurements, they concluded that about two-thirds of the compaction

had occurred in the sands and one-third in the siltstones. The sands are composed of about 35-70 per cent quartz, 12-40 per cent feldspar, and 8-12 per cent silt and clay minerals. Above the 1,220 m depth, the sands are uncemented and loose, and they grade in grain size from fine to coarse. Roberts' (1969) findings that some sands fracture appreciably in the stress range of 100-200 kg cm^{-2} suggest that the high compressibility of the feldspathic Wilmington "oil sands" in this same effective-stress range is due chiefly to fracturing.

For additional information on the compressibilities of unconsolidated sands and clays, the reader is referred to Roberts (1969), Meade (1968), Grim (1962), Allen and Chilingarian, in Chilingarian and Wolf (1975, p. 43-77), and Rieke and Chilingarian (1974, p. 173-217).

3.5 REFERENCES

ALLEN, D. R., and MAYUGA, M. N. 1969. The mechanics of compaction and rebound, Wilmington oil field, Long Beach, California, USA, in L. J. Tison, ed., Land Subsidence, v. 2, Internat. Assoc. Sci. Hydrology Pub. 89, p. 410-422.

CHILINGAR, G. V., and KNIGHT, LARRY. 1960. Relationship between pressure and moisture content of kaolinite, illite, and montmorillonite clays. Bull. Am. Assoc. Petroleum Geologists, v. 44, no. 1, p. 101-106.

CHILINGARIAN, G. V., and WOLF, K. H., eds. 1975. Compaction of coarse-grained sediments, I. Elsevier Scientific Publishing Company, Amsterdam, 552 p.

FERRIS, J. G., KNOWLES, D. B., BROWN, R. H., and STALLMAN, R. W. 1962. Theory of aquifer tests. U.S. Geol. Survey Water-Supply Paper 1536-E, p. 69-174.

GRIM, R. E. 1962. Applied clay mineralogy. McGraw-Hill Book Company, Inc. New York, 422 p.

HELM, D. C. 1978. A postulated relation between granular movement and Darcy's law for transient flow. Proceedings of Conference on Evaluation and Prediction of Subsidence, S. K. Saxena, ed., American Soc. Civil Engineers, p. 417-440.

HELM, D. C. 1982. Conceptual aspects of subsidence due to fluid withdrawal, in Recent trends in hydrogeology, Geological Society of America Special Paper in press.

JACOB, C. E. 1940. On the flow of water in an elastic artesian aquifer. Am. Geophys. Union Trans., pt. 2, p. 574-586.

LOFGREN, B. E. 1968. Analysis of stresses causing land subsidence. U.S. Geol. Survey Prof. Paper 600-B, p. B219-B225.

LOHMAN, S. W., and others. 1972. Definitions of selected ground-water terms--Revisions and conceptual refinements. U.S. Geol. Survey Water-supply Paper 1978, 21 p.

MAYUGA, M. N., and ALLEN, D. R. 1969. Subsidence in the Wilmington oil field, Long Beach, Calif., USA, in L. J. Tison, ed., Land subsidence, v. 1. Internat. Assoc. Sci. Hydrology Pub. 88, p. 6C6-79.

MEADE, R. H. 1968. Compaction of sediments underlying areas of land subsidence in central California. U.S. Geol. Survey Prof. Paper 497-D, 39 p.

MEINZER, 0. E. 1923. outline of ground-water hydrology with definitions. U.S. Geol. Survey Water-Supply Paper 494, 71 p.

MEINZER, 0. E. 1928. Compressibility and elasticity of artesian aquifers. Econ. Geology, v. 23, no. 3, p. 263-291.

MEINZER, 0. E., and HARD, H. A. 1925. The artesian-water supply of the Dakota sandstone in North Dakota with special reference to the Edgeley quadrangle. U.S. Geol. Survey Water-Supply Paper 520-E, p. 73-95.

POLAND, J. P. 1972. Subsidence and its control. Am. Assoc. Petroleum Geologists Underground Waste Management and Environmental implications, Memoir No. 18, p. 50-71.

POLAND, J. F., and DAVIS, G. H. 1969. Land subsidence due to withdrawal of fluids, in Varnes, D. J., and Kiersch, G., eds. Reviews in engineering geology, v. 2. Geol. Soc. America, p. 187-269.

POLAND, J. P., LOFGREN, B. E., IRELAND, R. L., and PUGH, R. G., 1975. Land subsidence in the San Joaquin Valley, California, as of 1972. U.S. Geol. Survey Prof. Paper 437-H, 77 p.

POLAND, J. F., LOFGREN, B. E., and RILEY, F. S., 1972. Glossary of selected terms useful in the studies of the mechanics of aquifer systems and land subsidence due to fluid withdrawal. U.S. Geol. Survey Water-Supply Paper 2025, 9 p.

RICCERI, G., and BUTTERFIELD, R. 1974. An analysis of compressibility data from a deep borehole in Venice. Geotechnique, no. 2, p. 175-192.

RIEKE, H. H., III, and CHILINGARIAN, G. V. 1974. Compaction of argillaceous sediments. Elsevier Scientific Publishing Company, Amsterdam, 424 p.

RILEY, F. S. 1969. Analysis of borehole extensometer data from central California, in Tison, L. J., ed., Land subsidence, v. 2. Internat. Assoc. Sci. Hydrology Pub. 89, p. 423-431.

ROBERTS, J. E. 1969. Sand compression as a factor in oil field subsidence, in Tison, L.J., ed., Land subsidence, v. 2. Internat. Assoc. Sci. Hydrology Pub. 89, p. 368-376.

SCOTT, R. F. 1963. Principles of soil mechanics. Addison-Wesley Pub. Co., Palo Alto, California, 550 p.

TAYLOR, D. W. 1948. Fundamentals of soil mechanics. New York, John Wiley and Sons, Inc., 700 p

TERZAGHI, KARL. 1925. Principles of soil mechanics: IV, Settlement and consolidation of clay. Eng. News-Rec., p. 874-878.

TERZAGHI, KARL, and PECK, R. B. 1967. Soil mechanics in engineering practice. New York, John Wiley and Sons, Inc. 2d ed., 729 p.

THEIS, C. V. 1935. The relation between the lowering of the piezometric surface and the rate and duration of discharge of a well using ground-water storage. Am. Geophys. Union Trans., v. 16, p. 519-524.

THEIS, C. V. 1938. The significance and nature of the cone of depression in ground-water bodies. Econ. Geology, v. 33, no. 8, p. 889-902.

VAN DER KNAPP, W., and VAN DER VLIS, A. C. 1967. On the cause of subsidence in oil-producing area, in Drilling and production. Mexico City, 7th World Petroleum Cong. Proc., v. 3, p. 85-95.

4 Laboratory tests for properties of sediments in subsiding areas, by A. I. Johnson and Working Group

4.1 INTRODUCTION

Laboratory tests of core samples are made to determine their physical, hydrologic, and engineering properties and their consolidation and rebound characteristics. The laboratory test results then are utilized, along with the observed changes in artesian head, to compute compaction of the aquifer system on the basis of soil mechanics theory. In addition, the mineralogy and petrography of samples is determined in the laboratory in order to study these properties with special reference to the environment of deposition.

This chapter briefly describes some of the test methods used in the laboratory and presents examples of the tables and graphs summarizing the properties for compacting sediments in the specific study area--primarily the San Joaquin Valley, with some reference to the Santa Clara Valley, both in central California. The physical and geologic characteristics and the subsidence problems for these areas are described in Case Histories 9.13 and 9.14 and all laboratory methods and data are presented in more detail in the report by Johnson, Moston, and Morris (1968). The laboratory analyses that were used directly in this case study were primarily the particle-size distribution, specific gravity and unit weight, porosity and void ratio, and the consolidation and rebound tests. The tests of Atterberg limits and indices were not used quantitatively in the central California study but provided supplementary data that furnish at least a qualitative index to the compressibility characteristics of the sediments. For example, in the Unified Soil Classification system, the liquid limit is used to distinguish between clay of high compressibility and clay of low compressibility. The tests of permeability were useful in related studies. The tests comparing permeability parallel and normal to the stratification gave some data on the relative ease of movement of water in the two directions, and thus were of use in studies of leakage through confining beds.

Applications of laboratory-test data may be found in chapters 3 and 5 and in some case histories in Chapter 9 (such as 9.3, 9.13 and 9.14).

4.2 FIELD SAMPLING

The samples for which test results are discussed later in this chapter were obtained from core holes in the San Joaquin and Santa Clara Valleys, in Central California. Eight core holes were drilled to depths as great as 620 m and samples were collected from these core holes for analysis in the laboratory.

The core holes were drilled by a rotary-drilling rig, utilizing core barrels of the double-tube type, which have an outer rotating barrel and an inner stationary barrel. The inside diameter of the core barrel was nominally 7.6 cm and the average diameter of core recovered was about 7 cm. In most of the work, a core barrel capable of taking a core 3 m long was used. A 6-m core barrel was tried but did not give as good core recovery.

Above the Corcoran Clay Member of the Tulare Formation in the Los Banos-Kettleman City area, (Figure 4.1) a 3-m interval was cored after each 9-m of drilling. Below the top of the Corcoran Clay Member, coring was generally continuous to the bottom of the hole. Core recovery was excellent for unconsolidated to semiconsolidated alluvial deposits of sand, silt, and clay. For example, at core hole 14/13-llDl, the accumulated cored interval was 302 m and the aggregate core footage brought to land surface was 211 m, an average core recovery of 70 per cent. Core recovery was as high as 80 per cent and as low as 30 per cent. The lowest recovery was in the coarse, loose water-bearing material. Hence, the core suite obtained did not contain a representative sampling of the coarser, most permeable layers.

At each of the drilling sites, cores were laid out in sequence in 1.2-m wooden core boxes and properly labelled for future reference. From each 3-m interval cored, the following samples were collected:

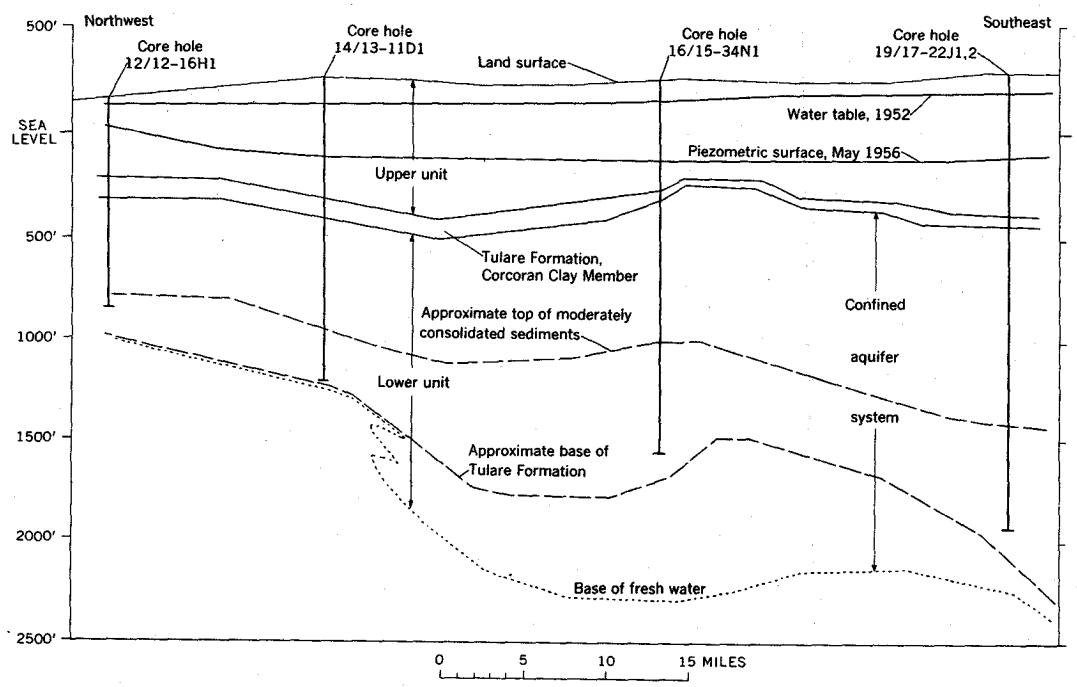

Figure 4.1 Simplified geologic section through core holes in the Los Banos-Kettleman City area, San Joaquin Valley, California.

1. Physical and engineering properties sample.--One litre-sized sample (about 15 cm long), taken from the most representative materials of the cored interval, was sealed in wax in a cardboard container to preserve the natural moisture content insofar as practicable and to prevent disturbance of the core.
2. Petrographic samples.--One or more samples, taken from the same materials and contiguous to the physical characteristic samples, were collected and sealed in wax in a 0.5 litre cardboard container and retained for petrographic examination. For paleontologic examination, samples also were taken of fossiliferous beds encountered in several of the core holes; they were not sealed in wax.
3. General purpose samples.--Two or more 0.25 litre samples were collected for general reference, one representing the fine-textured materials and one representing the coarse-textured layers; they were retained in cardboard cartons but not sealed in wax.

In addition, undisturbed samples of representative fine-grained deposits were collected for consolidation tests. Litre-sized samples were carefully selected and then sealed in wax in metal containers to keep them in an undisturbed condition.

4.3 COMPOSITE LOGS OF CORE HOLES

An electric log was obtained for each core hole after coring was completed. Graphic logs and generalized lithologic descriptions were prepared from the geologists' logs made at the drill site, supplemented by interpretation of the electric log in zones not cored or of poor recovery. These three elements were combined to give a composite log for each core hole. The depths of the samples tested also are plotted on the composite logs. Figure 4. 2 is an example of a composite log for one of the core holes.

The interpretation of electric logs is based on the principle that, in fresh-water-bearing deposits such as those penetrated in this area, high resistivity values are indicative of sand and low resistivity values are indicative of clay and silty clay. Intermediate values are indicative of clayey silt, silt, silty sand, and other sediments classified texturally between sand and clay. Resistivity is indicated by the right-hand curve of the electric log; it increases toward the right. Thus, the Corcoran Clay Member of the Tulare Formation is indicated

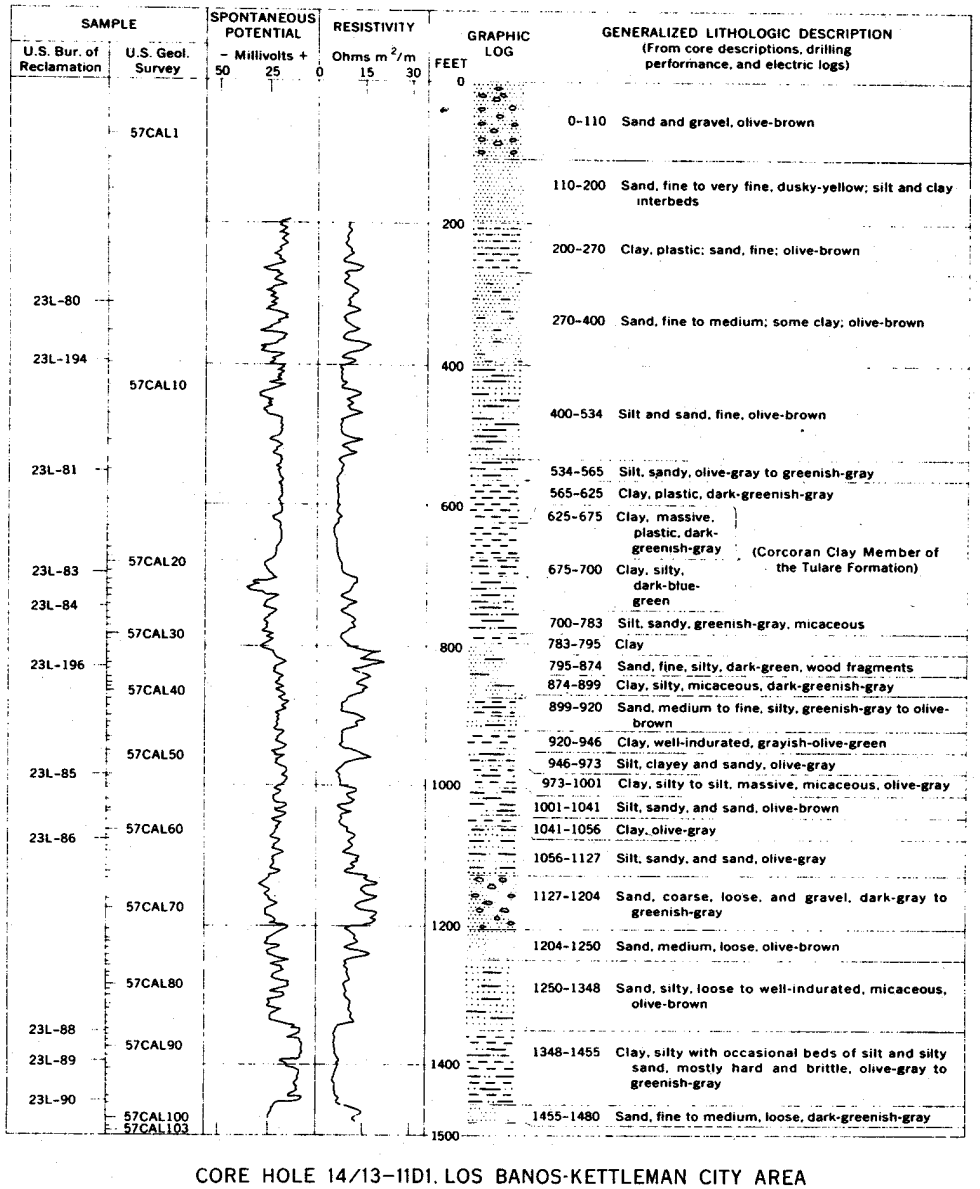

Figure 4.2 Example of a composite log of a core hole.

by a curve segment of uniformly low resistivity (Figure 4.2). The electric logs of the core holes can be compared with the physical and hydrologic properties of the samples plotted according to depth, as in Figures 4.3 and 4.4.

4.4 METHODS OF LABORATORY ANALYSIS

Utilizing a hydraulic-press assembly in the laboratory, cores 5 cm in diameter by 5 cm long were obtained by forcing thin-wall brass cylinders into the larger core--one in a direction at right angles to the bedding (vertical) and the other parallel to the bedding (horizontal). These small cores were used for permeability tests and for determining unit weight and porosity.

The rest of the large core was prepared and used for determination of specific gravity, particle-size distribution, and Atterberg limits and indices. Sample preparation for these analyses began with the air-drying of chunks of the large core. These chunks of material were

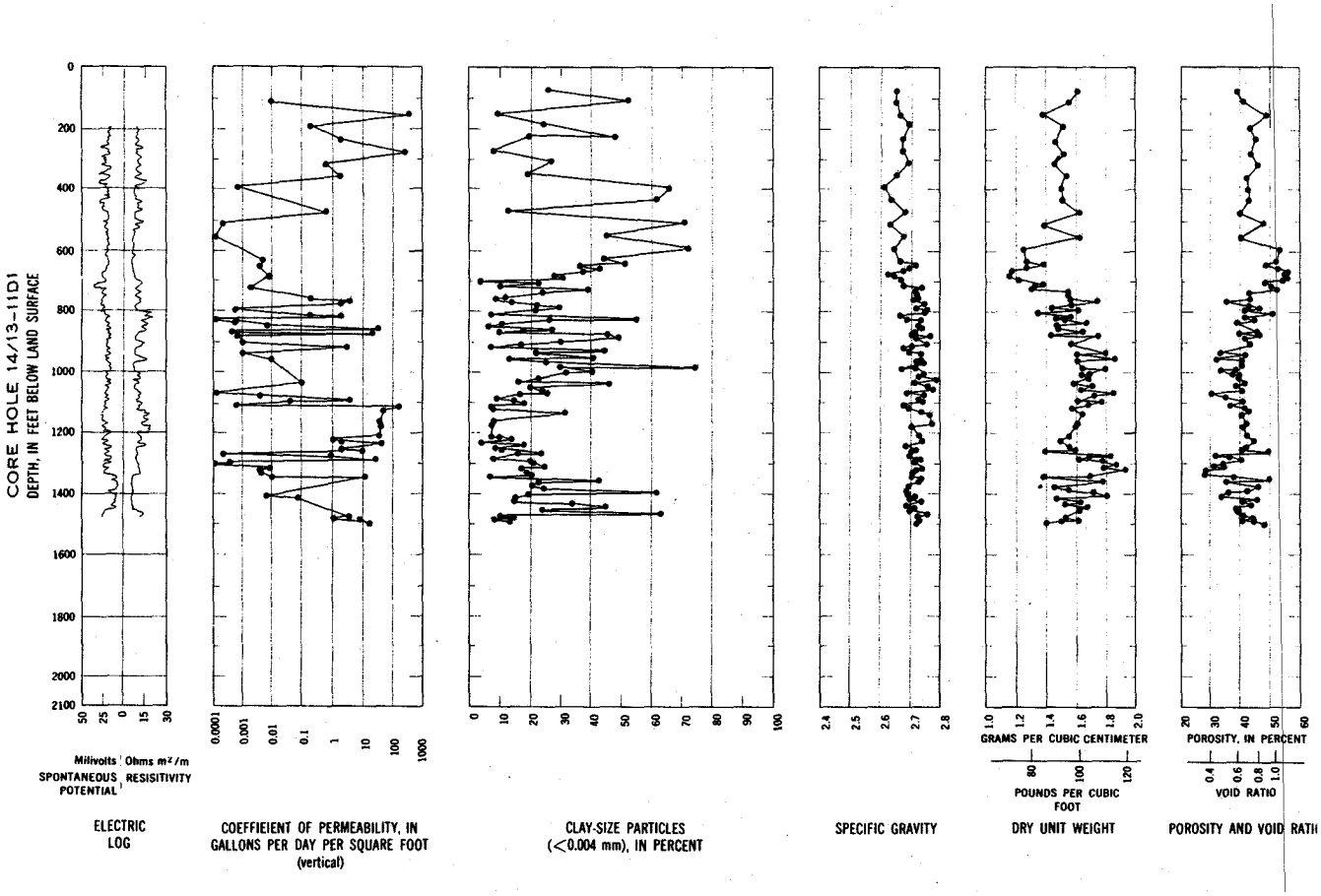

Figure 4.3 A graph of physical properties from core hole 14/13-llDl in the San Joaquin Valley, California.

then gently but thoroughly separated into individual particles in a mortar with a rubber-covered pestle. Care was taken to prevent crushing of the individual particles.

Core samples were analyzed by use of the standard methods described briefly in the following paragraphs. Additional information on the theory and methods of analysis is available in Meinzer (1923, 1949), Wenzel (1942), Taylor (1948), U.S. Bureau of Reclamation (1974, p. 407-508) and the American Society for Testing Materials (1980). Results of the laboratory analyses were reported in tables. The first page of each of the tables is shown as tables 4.1 through 4.5 at the end of this chapter as an example of the format and type of the data reported. The tables were published in inch-pound units, thus readers interested in metric units may refer to the metric conversion table, Appendix E.

4.4.1 Particle-size distribution

Particle-size analysis, also termed a "mechanical analysis," is the determination of the distribution of particle sizes in a sample. Particle sizes smaller than 0.0625 mm were determined by the hydrometer method of sedimentation analysis, and sizes larger than 0.0625 mm were determined by wet-sieve analysis.

The hydrometer method of sedimentation analysis consisted of (1) dispersing a representative part of the prepared sample with a deflocculating agent, sodium hexametaphosphate, in one litre of water and (2) measuring the density of the suspension at increasing intervals of time with a soil hydrometer. At given times, the size of the largest particles remaining in suspension at the level of the hydrometer was computed by use of Stokes' law, and the weight of particles finer than that size was computed from the density of the suspension at the same level.

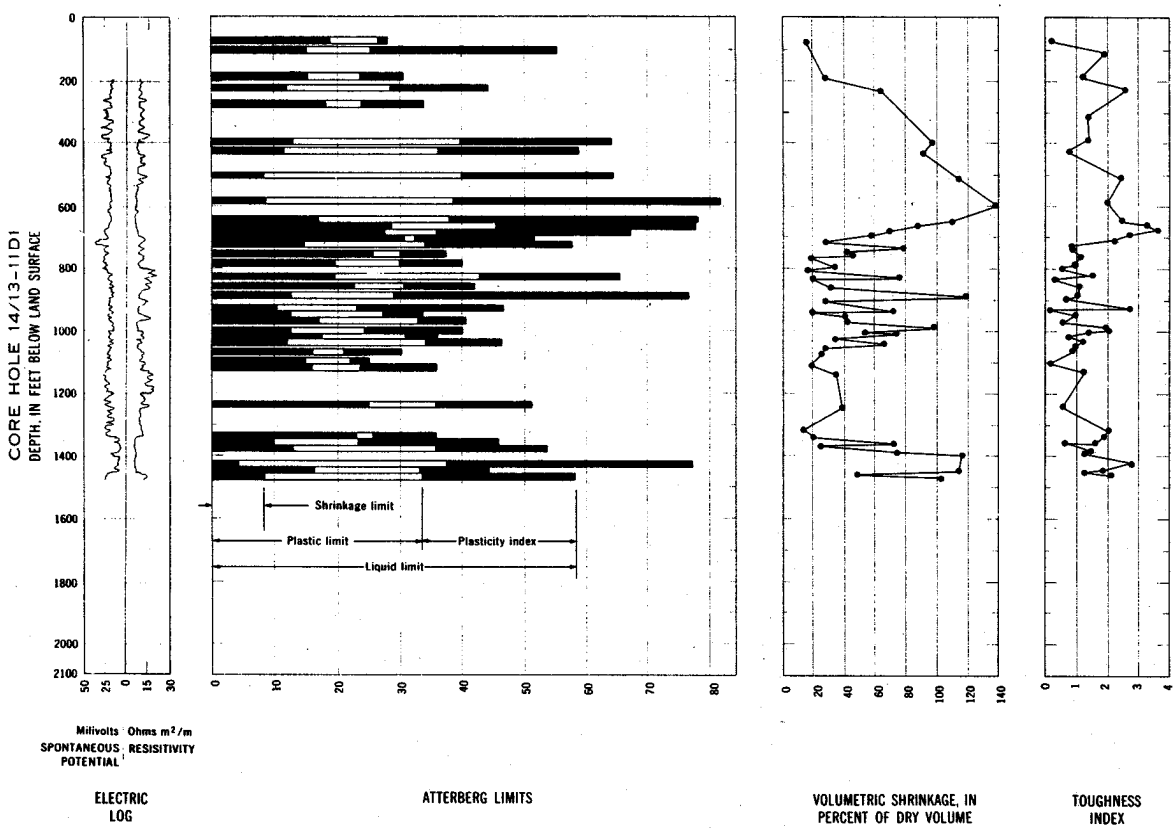

Figure 4.4 Continuation of a graph of properties from core hole 14/13-llDl in the San Joaquin Valley, California.

After the hydrometer analysis, the sample suspension was poured into a sieve which had openings of 0.0625 mm. The sample then was gently agitated and washed over the sieve. The material retained was carefully dried and placed in a set of standard 20-cm sieves which were shaken for a period of 15 minutes on a Ro-tap mechanical shaker. The fraction of the sample remaining on each sieve was weighed on a balance.

From the hydrometer analysis and the sieve analysis, the percentage of the particles smaller than a given size was calculated and plotted as a cumulative distribution curve. The particle sizes, in millimeters, were plotted as abscissas on a logarithmic scale and the cumulative percentages of particles smaller than the size shown, by weight, as ordinates on an arithmetic scale. The percentage in each of several size ranges was then determined from this curve.

The size ranges were identified according to the following particle sizes:

	Diameter (mm)
Gravel	>2.0
Very coarse sand	1.0 -2.0
Coarse sand	.5 -1.0
Medium sand	.25 - .5
Fine sand	.125 - .25
Very fine sand	.0625 - .125
Silt-size	.004 - .0625
Clay-size	<0.004

This size classification system is used by the Water Resources Division, U.S. Geological Survey, and is essentially the same as classifications proposed by Wentworth (1922) and the National Research Council (Lane, 1947), except that those authors proposed further subdivisions of gravel, silt, and clay. Subsequent references to sand, silt, and clay in this report will relate to sand-,silt-, and clay-size particles as specified in the foregoing table.

4.4.2 Permeability

Permeability is the capacity of rock or soil to transmit fluid under the combined action of gravity and pressure. It can be determined in the laboratory by observing the rate of movement of fluid through a sample of known length and cross-sectional area, under a known difference head.

The basic law for flow of fluids through porous materials was established by Darcy who demonstrated experimentally that the rate of flow of water was proportional to the hydraulic gradient. Darcy's law may be expressed as

$$Q = KiA, \tag{4.l}$$

where Q is the quantity of water discharged in a unit of time, A is the total cross-sectiona1 area through which the water flows, i is the hydraulic gradient (the difference in head, h, divided by the length of flow, L), and K is the hydraulic conductivity (occasionally known as the coefficient of permeability) of the material for water, or

$$K = \frac{Q}{iA} = \frac{QL}{hA} \tag{4.2}$$

Because the water is assumed to be relatively pure, density is ignored.

Hydraulic conductivity is determined in the laboratory in constant-head or variable-head permeameters or is computed from consolidation-test results. The permeameters used for the tests discussed in this chapter are described in detail by Johnson, Moston, Morris (1968).

Entrapped air in a sample may cause plugging of pore space and thus reduce the apparent hydraulic conductivity. Therefore, a specially designed vacuum system provided the de-aired tapwater used as the percolation fluid.

The chemical character of the water used for the permeability tests of fine-grained silty or clayey materials should be compatible with the chemical character of the native pore water. If the test water is not compatible, the clay-water system and the permeability values obtained will be affected. The chemical character of the native pore water in the fine-grained sediment was not known at the time of the test and Denver tapwater therefore was used in the permeability tests.

The 5-cm-diameter "undisturbed" cores cut from the larger original core were retained in their cylinders. These cylinders were installed directly in the permeameter to serve as the percolation cylinder of the apparatus. The reported hydraulic conductivity was the maximum value obtained after several test runs and represents saturation permeability.

4.4.3 Unit weight

For reference in developing some of the equations used in following sections of this chapter, it is useful to study the relations found in a unit soil mass, as seen in Figure 4 5. The concepts and symbols shown in that figure will be used in development of equations related to the properties of compacting sediments. Other useful definitions and symbols can be found in the publication of the American Society for Testing and Materials (1980).

The dry unit weight is the weight of solids per unit of total volume of oven-dry rock or soil mass. It normally is reported in grams per cubic centimeter or kilograms per cubic metre. Void space as well as solid particles are included in the volume represented by the dry unit weight. The dry unit weight divided by the unit weight of distilled water at a stated temperature (usually 4° C) is known occasionally as the apparent specific gravity, which is dimensionless.

The volume of the small cores, cut previously from the large cores, was obtained by measurement of the cylinder dimensions. This volume and the ovendry weight of the contained sample were then used to calculate the dry unit weight as follows:

$$\gamma_d = \frac{W_s}{V}, \tag{4.3}$$

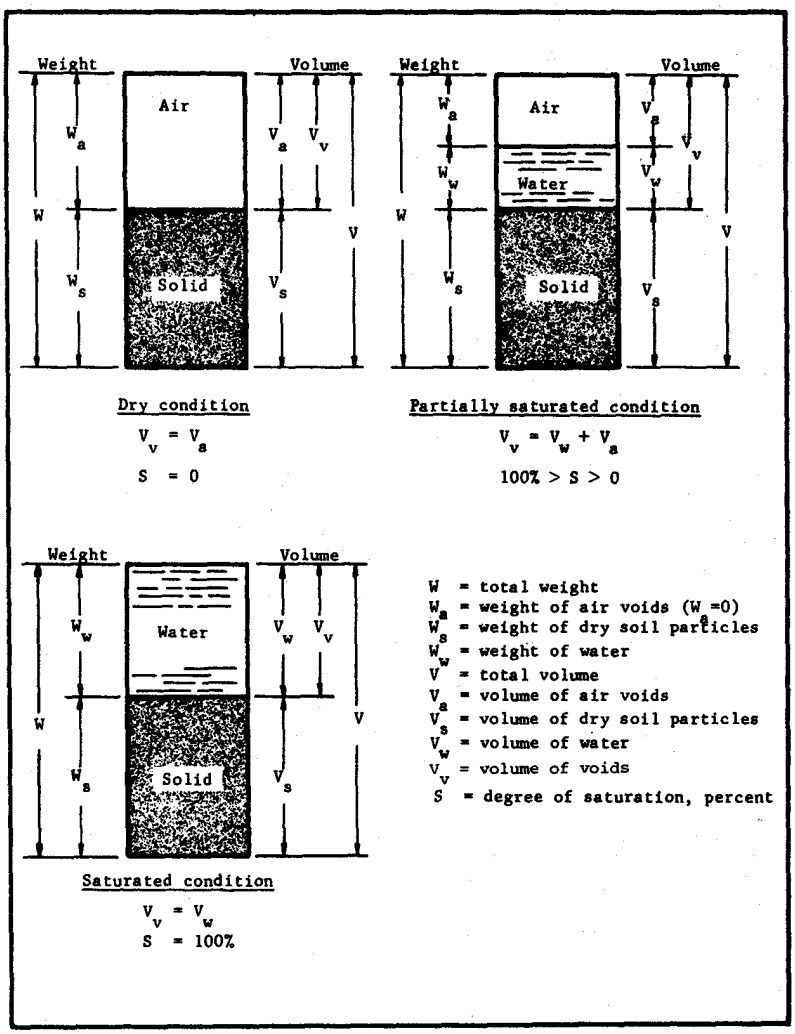

Figure 4.5 Principal phases of a unit soil mass.

where

γ_d = dry unit weight, in grams per cubic centimetre,
W_s = weight of ovendry sample, in grams,
V = total mass volume of sample, in cubic centimetres.

4.4.4 Specific gravity of solids

Specific gravity of solids, G, is the ratio of (1) the weight in air of a given volume of solids at a stated temperature (unit weight of solid particles or particle density) to (2) the weight in air of an equal volume of distilled water at stated temperature (usually 4° C), or

$$\gamma_s = \frac{W_s}{V_s} \quad \text{and} \quad \gamma_w = \frac{W_w}{V_w} ,$$

so

$$G = \frac{\gamma_s}{\gamma_w} \tag{4.4}$$

where

γ_S = unit weight of solids, in grams per cubic centimetre,
V_S = volume of solids, in cubic centimetres,
γ_W = unit weight of water, in grams per cubic centimetre,
W_W = weight of water, in grams,
V_W = volume of water, in cubic centimetres, and
G = specific gravity, a ratio.

The volumetric-flask method was used for determining the specific gravity of solids. A weighed oven-dry part of the sample was dispersed in water in a calibrated volumetric flask. The volume of the particles was equivalent to the volume of displaced water. The unit weight of the solid particles was obtained by dividing the dry weight of the sample by the volume of the solid particles. Because the density of water at 4° C is unity in the metric system, the specific gravity is numerically equivalent to this unit weight.

4.4.5 Porosity and void ratio

Porosity, n, is defined as the ratio of (1) the volume of the void spaces to (2) the tota1 volume of the rock or soil mass. It normally is expressed as a percentage. Therefore,

$$n = \frac{V_v(100)}{V} = \frac{V - V_S(100)}{V}, \tag{4.5}$$

then as

$$\gamma_d = \frac{W_S}{V}$$

and

$$\gamma_s = \frac{W_S}{V_S},$$

$$n = \frac{W_S/\gamma_d - W_S/\gamma_S}{W_S/\gamma_d}(100),$$

or

$$n = \frac{\gamma_S - \gamma_d}{\gamma_S}(100) \tag{4.6}$$

where

n = porosity, in per cent,
V_v = volume of voids, in cubic centimetres,
V = total mass volume, in cubic centimetres,
W_S = weight of oven-dry particles, in grams,
γ_S = unit weight of particles, in grams per cubic centimetre (equal numerically to specific gravity of solids in metric system),
γ_d = dry unit weight of sample, in grams per cubic centimetre, and
V_S = volume of solid particles, in cubic centimetres.

After the dry unit weight and the specific gravity of solids had been determined for the sample, the porosity was calculated from the above equation. The relation among these three properties is illustrated in Figure 4.6.

The void ratio is defined as the ratio of (1) the volume of voids to (2) the volume of solid particles in a soil mass, or

$$e = \frac{V_v}{V_S} \tag{4.7}$$

Its relation to porosity is expressed by

$$e = \frac{n}{1-n}, \tag{4.8}$$

where e = void ratio, and n = porosity, in per cent.

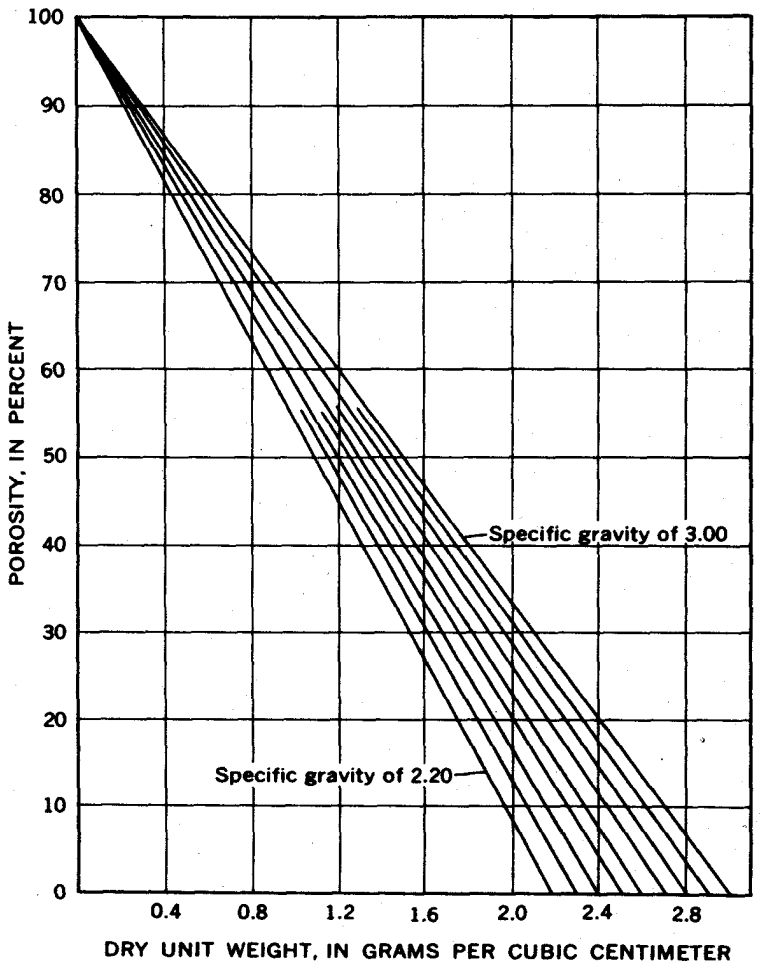

Figure 4.6 Relation of porosity to dry unit weight for various specific gravities of solids.

The relation between void ratio and porosity is illustrated in Figure 4.7.

4.4.6 Moisture content

The moisture content of rock or soil material is the ratio of the weight of water contained in a sample to the oven-dry weight of solid particles, expressed as a percentage, or

$$w = \frac{W_W}{W_S}(100), \tag{4.9}$$

where

w = moisture content, in per cent of dry weight,
W_W = weight of water, in grams, and
W_S = weight of oven-dry sample (dry solids), in grams.

Usually, samples in moisture-proof containers, are weighed to obtain their wet weight. They are oven-dried to constant weight at 110°C and reweighed. The loss of weight (the amount of contained water) divided by the dry weight of the sample equals the moisture content.

4.4.7 Atterberg limits

Atterberg (1911), a Swedish soil scientist, suggested a series of arbitrary limits for indicating the effects of variations of moisture content on the plasticity of soil materials.

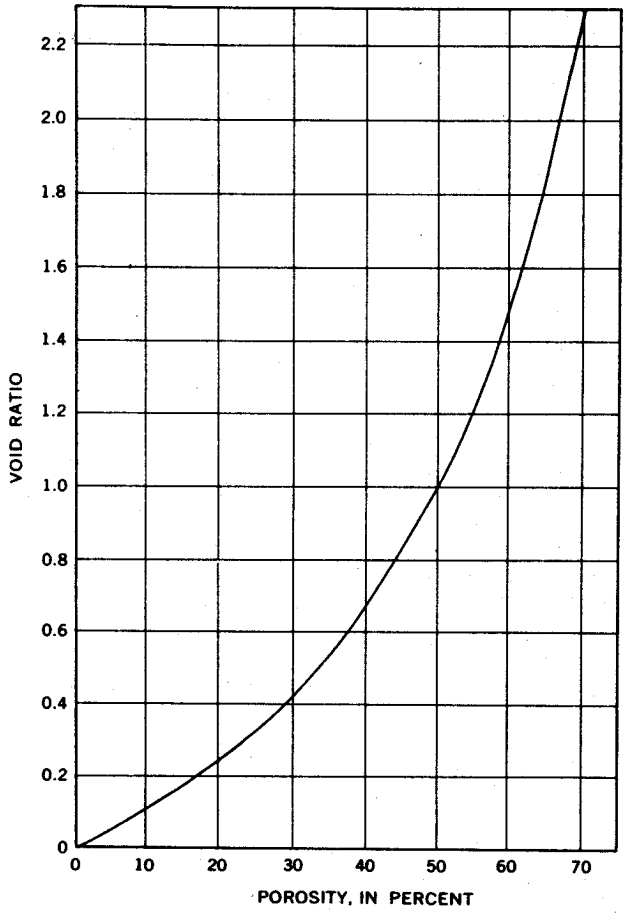

Figure 4.7 Relation of void ratio to porosity.

The most commonly used Atterberg limits, sometimes referred to as limits of consistency, are the liquid and plastic limits. Among a number of indices, the plasticity index is most commonly determined.

The moisture contents at which fine-textured sediments pass from one state of consistency to another are governed by the texture and composition of the sediments. Atterberg (1911), Terzaghi (1926), and Goldschmidt (1926) found that plasticity is a function of the amount of fine platelike particles in a sediment mass. Thus, the Atterberg consistency limits and indices are influenced by the clay content of the sediments tested.

Although the Atterberg limits are somewhat empirical, most soil investigators believe that they are valuable in characterizing the plastic properties of fine-textured sediment, (Casagrande, 1932).

Only the smaller size particles of a given sample, those passing a U.S. Standard No. 40 sieve (finer than 0.42 mm in diameter) are used for Atterberg tests. Although limits and indices are calculated as moisture content, in per cent of dry weight, (W_W/W_S) , all values are usually reported as numbers only.

4.4.7.1 Liquid limit

The liquid limit, w_L, is the moisture content, expressed as a percentage of the oven-dry weight, at which any particular soil material passes from the plastic to the liquid state. It is that moisture content at which a groove of standard dimensions cut in a pat of soil will close for a distance of 1/2 in. (1.3 cm) under the impact of 25 shocks in a standard liquid-limit apparatus. The moist sample was placed in the round-bottomed brass cup of the mechanical liquid-limit device and was divided into two halves by a V-shaped grooving tool. A cam on the device raised the cup and let it drop against the base of the machine until the two edges of the groove flowed

together for the specified half an inch. The number of taps, or shocks, were recorded, and the moisture content of a part of the sample was determined. This process was repeated three times at different moisture contents. These data are plotted as a "flow curve" on a semilogarithmic graph, the number of shocks plotted as abscissa on the logarithmic scale and the moisture content as ordinates on the arithmetic scale. The moisture content corresponding to the intersection of the flow curve with the 25-shock line was taken as the liquid limit of that soil material.

4.4.7.2 Plastic limit

The plastic limit, w_P, is the minimum moisture content, expressed as a percentage of the oven-dry weight, at which soil material can be rolled into 1/8-in. (0.3-cm) diameter threads without the threads breaking into pieces. This moisture content represents the transition point between the plastic and semisolid states of consistency. The moist sample was rolled between the hand and a glass plate until a thread 0.3 cm in diameter was formed. The sample was then kneaded together and again rolled out. This process was continued at slowly decreasing water contents until crumbling prevented the formation of the thread. The pieces of the crumbled sample were then collected together and the moisture content was determined. This moisture content was considered to be the plastic limit.

4.4.8 Consolidation

When a saturated soil sample is subjected to a load, that load initially is carried by the water in the voids of the sample because the water is incompressible in comparison with the sample's structure. If water can escape from the sample voids as a load is continually applied to the sample, an adjustment takes place wherein the load is gradually shifted to the soil structure. This process of load transference is generally slow for clay and is accompanied by a change in volume of the soil mass. Consolidation is defined as that gradual process which involves, simultaneously, a slow escape of water, a gradual compression, and a gradual pressure adjustment. This use of the term should not be confused with the geologists' definition which refers to the processes by which a material becomes firm or coherent (Am. Geol. Inst., 1957, p. 62). The theory of consolidation is discussed in detail by Terzaghi (1943, p. 265-297).

To determine the rate and magnitude of consolidation of sediments, a small-scale laboratory test known as a one-dimensional consolidation test is used. The test and apparatus, described in detail by the U.S. Bureau of Reclamation (1974), are discussed briefly in the following paragraphs for the benefit of the reader. The application of one-dimensional consolidation test data to a foundation-settlement analysis has been described by Gibbs (1953). The apparatus (consolidometer) used by the Bureau of Reclamation (1974) is shown in Figure 4.8. In addition to the unit shown, a means of loading is required--usually a platform scale with a weighing beam attached to the connecting rods of the consolidometer.

Normally, the sample is trimmed to the size of the specimen rings, which are 4-1/4 in. (10.8 cm) in inside diameter and 1-1/4 in. (3.2 cm) high. Samples must be in as near an undisturbed condition as possible. Because of the small size of the cores collected for the subsidence studies, however, consolidation specimens of standard size could not be used, and the core diameter had to be trimmed to fit 2 in. (5-cm) rings.

Loads are applied to the specimen in increments, but the minimum number of increments is usually four-- 12, 25, 50, and 100 per cent of the maximum desired load. Increments are usually selected so that each succeeding load is double that of the previous load. Each load is applied to the consolidometer while dial readings of consolidation are taken and recorded for 4, 10, 20 seconds, and other time intervals up to 24 hours. Additional readings are taken at 24-hour intervals until the consolidation is virtually complete for that load.

The percentage of consolidation of the specimen is computed, and a curve of consolidation versus time is obtained for each load increment. The final stress-strain relations are presented as a curve showing the void ratio versus log of pressure (load), the final condition for each increment of load being a point on the curve (Figure 4.9).

Two important soil properties furnished by a consolidation test are the coefficient of consolidation and the compression index. The coefficient of consolidation, C_V, represents the rate of consolidation for a given load increment. It is determined by use of the 50-percent point on the time consolidation curve in the equation

$$C_v = \frac{T_{50} T_{50}^2}{t_{50}}, \qquad (4.10)$$

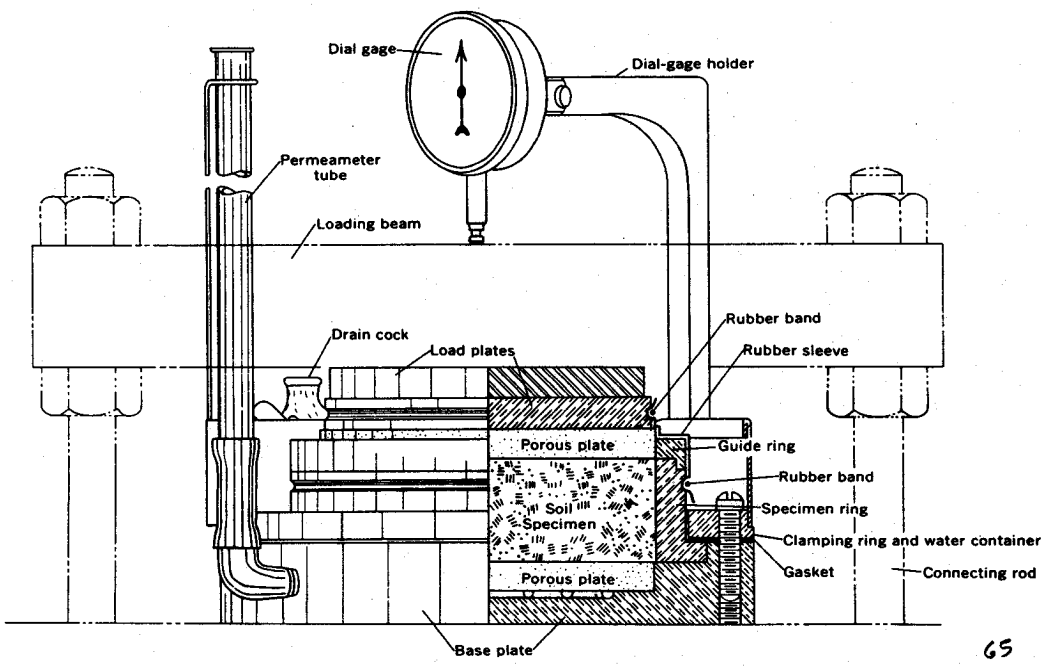

Figure 4.8 One-dimensional consolidometer specimen container (from U.S. Bureau of Reclamation, 1960, p. 495).

where

T_{50} = time factor at 50-per-cent consolidation = 0.20,
H_{50} = one half the specimen thickness at 50-per-cent consolidation, and
t_{50} = time required for specimen to reach 50-per-cent consolidation. The coefficient of consolidation is usually reported in square centimetres per second or in square inches per second.

The compression index, C_C, represents the compressibility of the soil samples. It is the slope of the straight-line portion of the void ratio-log of pressure (load) curve. The compression index can be determined from the equation

$$C_c = \frac{e_o - e}{\log \frac{P_o + \Delta P}{P_o}} \text{ (see Figure 4.9 for symbols).} \qquad (4.11)$$

When the consolidation is complete under maximum loading, the consolidometer can be used as a variable-head permeameter, and the hydraulic conductivity can be determined directly. The mechanical procedure is similar to that described previously (section 4.4.2). The consolidation data also can be used for computing the hydraulic conductivity. The equation utilizing time-consolidation characteristics is

$$K = \frac{C_v(\gamma_w)(e_o - e)}{\Delta_P(1 + e_o)} \qquad (4.12)$$

where

C_V = coefficient of consolidation,
γ_W = unit weight of water,
e_O = void ratio at start of load increment,
e = final void ratio, and
Δ_P = increment of load.

Although the example in Table 4.4 shows feet per year for the permeability (standard inch-pound system units), cm per sec is the commonly reported unit for K.

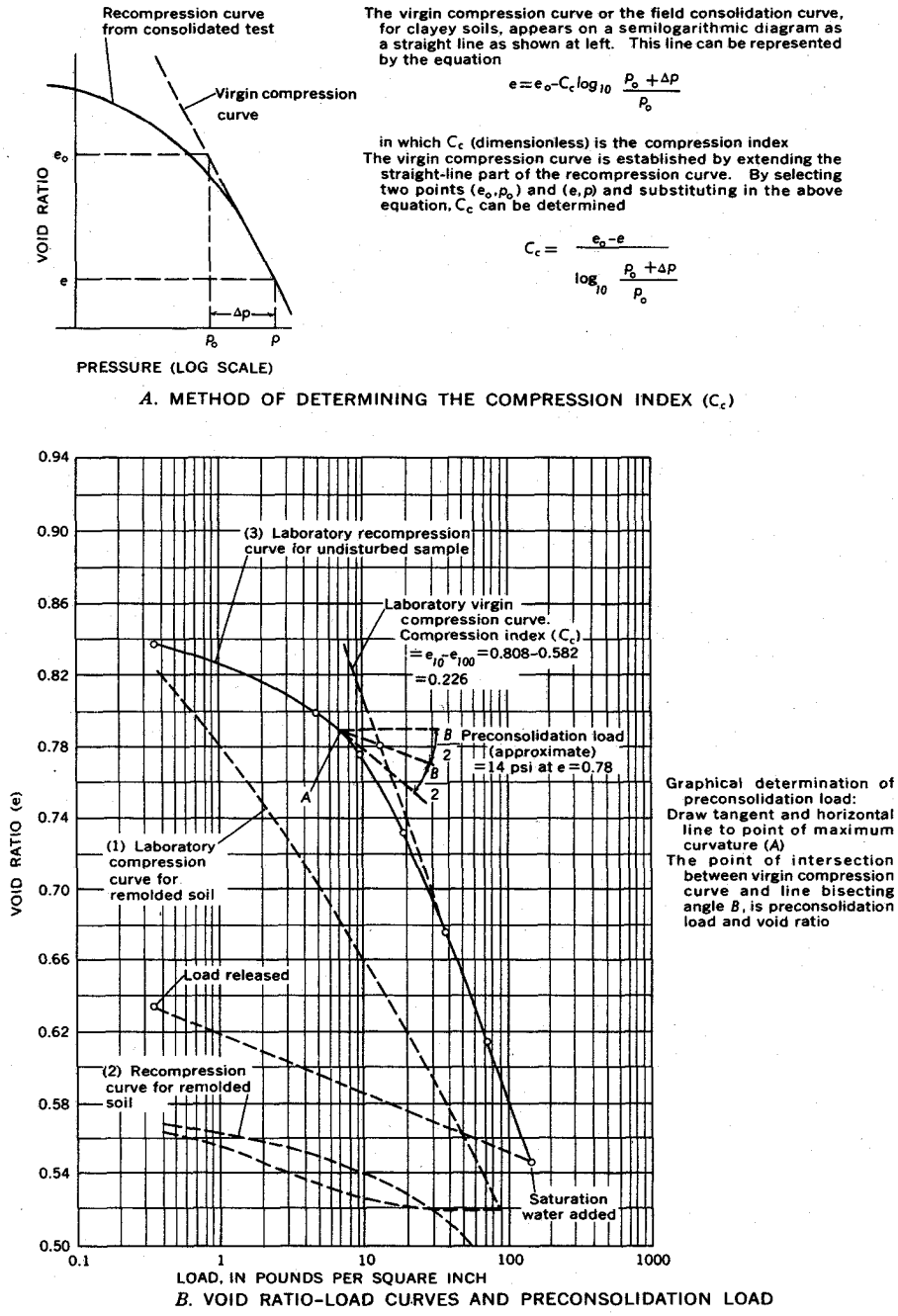

Figure 4.9 Void ratio-load curve, compression index, and preconsolidation load (modified from U.S. Bureau of Reclamation, 1960, p. 58).

4.5 RESULTS OF LABORATORY ANALYSES

4.5.1 Particle-size distribution

An example of particle-size distribution data from central California is presented in Table 4.1. The percentage of gravel-, sand, silt-, and clay-size particles were shown in such tables for each of the 549 samples from seven core holes analyzed in the laboratory. Particle-size distribution curves for all of the samples were plotted on figures similar to Figure 4.10. An example of the size-distribution (gradation) for samples tested for consolidation is given in Table 4.3.

Table 4.1 Physical and hydrologic properties of samples from core holes.

Hydrologic laboratory sample	Sample depth (feet)	Particle analysis, percentage of— Gravel	Sand	Silt	Clay <0.004 mm	Clay <0.002 mm	Median diameter, D_{50} (mm)	Geometrical quartile deviation (sorting coefficient), S_0	Log quartile deviation (log sorting coefficient), $\log_{10} S_0$	Sediment class (Shepard system)	Specific gravity of solids	Dry unit weight G per cc	Lb per cu ft	Total porosity (percent)	Void ratio	Coefficient of permeability (gp per sq ft at 60°F) Vertical	Horizontal
Core hole 14/13-11D1																	
57CAL1	77.0- 77.5		24.8	49.5	25.7	18	0.024	4.04	0.606	Sand-silt-clay	2.66	1.60	99.8	39.9	0.66		
2	110.5- 111.0		10.7	37.3	52.0	44	.0034			Silty clay	2.66	1.56	97.3	41.4	.71	0.01	0.03
3	153.0- 153.5		87.1	3.7	9.2	9	.19	1.46	.164	Sand	2.67	1.37	85.5	48.7	.95	360	
4	191.5- 192.0		29.0	46.8	24.2	20	.028	3.92	.593	Sand-silt-clay	2.70	1.52	94.8	43.7	.78	.2	.2
5a	232.5- 233.0		21.6	30.4	48.0	39	.0045			do	2.68	1.47	91.7	45.1	.82	2	
5b	232.5- 233.0		61.6	18.9	19.5	16	.092	3.16	.500	Clayey sand	2.64	1.64	102.3	37.9	.61	4	
6	277.1- 277.6	1.3	89.0	1.9	7.8	7	.25	1.59	.201	Sand	2.68	1.52	94.8	43.3	.76	270	
7	314.0- 314.5		22.3	51.0	26.7	22	.019	4.12	.615	Sand-silt-clay	2.70	1.46	91.1	45.9	.85	.6	
8	353.0- 353.5		47.0	34.3	18.7	16	.060	3.37	.528	Silty sand	2.66	1.54	96.1	42.1	.73	2	10
9	398.0- 398.5		.6	33.4	66.0	56	.0010			Silty clay	2.62	1.51	94.2	42.4	.74	.0007	.002
10	432.0- 432.5		7.0	31.2	61.8	50	.0020			do	2.64	1.51	94.2	42.8	.75	.00007	
11	471.5- 472.0		47.3	40.0	12.7	11	.059	2.00	.301	Silty sand	2.69	1.63	101.7	39.4	.65	.7	
12	510.3- 510.8	.6	8.9	19.5	71.0	61				Silty clay	2.64	1.39	86.7	47.3	.90	.0002	
13	552.5- 553.0		22.0	33.0	45.0	36	.0062			Sand-silt-clay	2.68	1.63	101.7	39.2	.65	.0001	
14	594.0- 594.5		8.8	19.7	71.5	59	.0012			Silty clay	2.65	1.25	78.0	52.8	1.12		
15	631.0- 631.5		19.2	36.3	44.5	34	.0057	5.68	.754	do	2.67	1.28	79.9	52.1	1.09	.005	
16	646.6- 647.1		1.0	47.5	51.5	40	.0036			do	2.72	1.39	86.7	48.9	.96		
17	652.3- 652.8		23.3	40.1	36.6	26	.0096	5.20	.716	Sand-silt-clay	2.70	1.28	79.9	52.6	1.11	.004	
18	662.1- 662.6		.8	56.2	43.0	30	.0058	3.26	.513	Clayey silt	2.68	1.18	73.6	56.2	1.28		
19	674.0- 674.5		1.0	61.5	37.5	25	.0068	2.61	.417	do	2.63	1.18	73.6	55.1	1.23		
20	682.5- 683.0		26.8	45.2	28.0	20	.013	5.06	.704	Sand-silt-clay	2.65	1.17	73.0	55.8	1.26	.008	
21	697.0- 697.5		.6	68.4	31.0	20	.0082	2.51	.400	Clayey silt	2.67	1.23	76.8	54.1	1.18		
22	707.0- 707.5		80.2	16.1	3.7	3	.26	1.68	.225	Sand	2.67	1.38	86.1	48.3	.94		
23	713.0- 713.5		.2	76.8	23.0	14	.010	2.00	.301	Silt	2.68	1.33	83.0	50.4	1.02		
24	721.5- 722.0		4.0	86.0	10.0	7	.012	1.48	.170	do	2.74	1.31	81.7	52.2	1.09	.002	
25	731.0- 731.5		1.6	59.4	39.0	26	.0067	2.99	.476	Clayey silt	2.72	1.55	96.7	42.8	.75		
26	743.0- 743.5		6.0	70.0	24.0	17	.013	2.57	.410	do	2.72	1.55	96.7	42.9	.75		
27	757.0- 757.5		50.2	38.1	11.7	8	.062	3.06	.486	Silty sand	2.73	1.57	98.0	42.7	.75	.2	
28	764.9- 765.4		77.4	13.9	8.7	7	.34	2.42	.384	Sand	2.71	1.75	109.2	35.4	.55	4	
29	773.0- 773.5		38.2	48.0	13.8	11	.050	2.22	.346	Sandy silt	2.75	1.57	98.0	42.9	.75	2	2
30	784.5- 785.0		16.2	61.8	22.0	14	.020	2.94	.468	Clayey silt	2.72	1.45	90.5	46.7	.88		
31	791.0- 791.5		26.0	44.2	29.8	26	.026	5.89	.770	Sand-silt-clay	2.76	1.62	101.1	41.3	.70	.0006	
32	802.0- 802.5		35.4	43.0	21.6	16	.040	3.56	.551	do	2.75	1.35	84.2	50.9	.04		
33	812.0- 812.5		80.2	11.8	8.0	8	.25	2.36	.373	Sand	2.67	1.57	98.0	41.2	.70	.2	
34	813 - 821	.3	91.7	1.0	7.0	7	.21	1.27	.104	do	2.69	1.47	91.7	45.4	.83	2	
35	826.0- 826.5		1.0	44.0	55.0	38	.0033	2.72	.435	Silty clay	2.74	1.53	95.5	44.2	.80	.0001	
36	831.5- 832.0		12.2	61.3	26.5	20	.020	3.46	.539	Clayey silt	2.74	1.68	104.8	38.7	.63	.0006	
37	843.5- 844.0		69.0	20.0	11.0	9	.12	1.91	.281	Silty sand	2.73	1.48	92.4	45.8	.85	.007	
38	853.0- 853.5		83.2	10.6	6.2	5	.12	1.31	.117	Sand	2.74	1.49	93.0	45.6	.84	33	
39	860.0- 860.5		2.4	70.4	27.2	21	.145	3.01	.479	Clayey silt	2.74	1.62	103.0	39.8	.66		
40	867.0- 867.5		54.2	27.8	18.0	16	.010			Silty sand	2.72	1.64	102.3	39.7	.66	.0005	
41	871.0- 871.5		70.0	19.8	10.2	9	.099	1.73	.238	do	2.71	1.44	89.9	46.9	.88	22	
42	877.0- 877.5		4.5	49.5	46.0	34	.0050	4.24	.627	Clayey silt	2.77	1.76	109.8	36.5	.57	.0007	
43	887.5- 888.0		.8	49.7	49.5	37	.0041	3.16	.500	Silty clay	2.72	1.59	99.2	41.5	.71		
44	901.0- 901.5		8.6	61.2	30.2	19	.011	2.97	.473	Clayey silt	2.76	1.57	98.0	43.1	.76	.001	
45	911.5- 912.0		48.4	34.6	17.0	16	.056	3.52	.547	Silty sand	2.71						
46	917.2- 917.7		80.0	13.0	7.0	7	.22	1.58	.199	Sand	2.68					3	
47	932.0- 932.5		8.0	47.3	44.7	37	.0064			Clayey silt	2.70	1.80	112.3	33.2	.50		
48	936.5- 937.0		12.6	65.4	22.0	14	.016	2.60	.415	do	2.74	1.61	100.5	41.2	.70	.001	
49	951.0- 951.5		4.6	54.4	41.0	33	.0082	5.10	.708	do	2.74	1.87	116.7	31.8	.47		
50	957.5- 958.0		39.4	47.4	13.2	11	.044	2.34	.369	Sandy silt	2.72	1.62	101.1	40.4	.68	.01	
51	968.5- 969.0		6.0	68.8	25.2	20	.016	2.86	.456	Clayey silt	2.75	1.63	101.7	40.7	.69		
52	984.0- 984.5		2.2	23.1	74.7	58	.0015			Silty clay	2.67	1.65	103.0	38.2	.62		
53	987.6- 988.0		27.2	43.0	29.8	26	.026	6.57	.818	Sand-silt-clay	2.72	1.80	112.3	33.8	.51		
54	1,000.5-1,001.0		4.2	54.8	41.0	32	.0068	4.42	.645	Clayey silt	2.75	1.72	107.3	37.5	.60		
55	1,005.1-1,005.6		2.8	65.2	32.0	22	.0090	2.79	.446	do	2.73	1.65	103.0	39.8	.66		
56	1,010.8-1,021.3		11.4	65.8	22.8	16	.024	2.83	.452	do	2.79	1.69	105.5	39.4	.65		
57	1,033.8-1,034.2		52.0	32.0	16.0	13	.070	4.39	.642	Silty sand	2.72	1.58	98.6	41.9	.72	.1	
58	1,039.5-1,040.0		1.8	52.2	46.0	36	.0048			Clayey silt	2.76	1.71	106.7	38.0	.61		
59	1,051.5-1,052.0		12.4	67.6	20.0	15	.025	2.51	.400	do	2.78	1.64	102.3	41.0	.70		
60	1,063.5-1,064.0		35.6	40.4	24.0	20	.026	6.14	.788	Sand-silt-clay	2.69	1.86	116.1	30.9	.45	.0001	
61	1,070.8-1,071.3		19.5	54.5	26.0	21	.020	3.67	.565	Clayey silt	2.75	1.73	108.0	37.1	.59		
62	1,075.0-1,075.5		55.6	27.2	17.2	14	.079	3.02	.480	Silty sand	2.75	1.77	110.4	35.6	.55	.004	
63	1,088.5-1,089.0		81.6	9.4	9.0	8	.18	1.67	.223	Sand	2.73	1.62	101.1	40.7	.69	42	
64	1,092.0-1,092.5		35.4	49.6	15.0	12	.042	3.16	.500	Sandy silt	2.75	1.78	111.1	35.3	.55	.04	
65	1,104.6-1,105.1		38.0	44.0	18.0	15	.037	1.15	.061	do	2.68	1.69	105.5	36.9	.59	.0006	
66	1,113.5-1,114.0		91.2	1.6	7.2	7	.23	1.23	.090	Sand	2.70	1.58	98.6	41.5	.71	174	
67	1,123.5-1,124.0		84.2	7.8	8.0	7	.16	1.38	.140	do	2.74	1.57	98.0	42.7	.75	50	

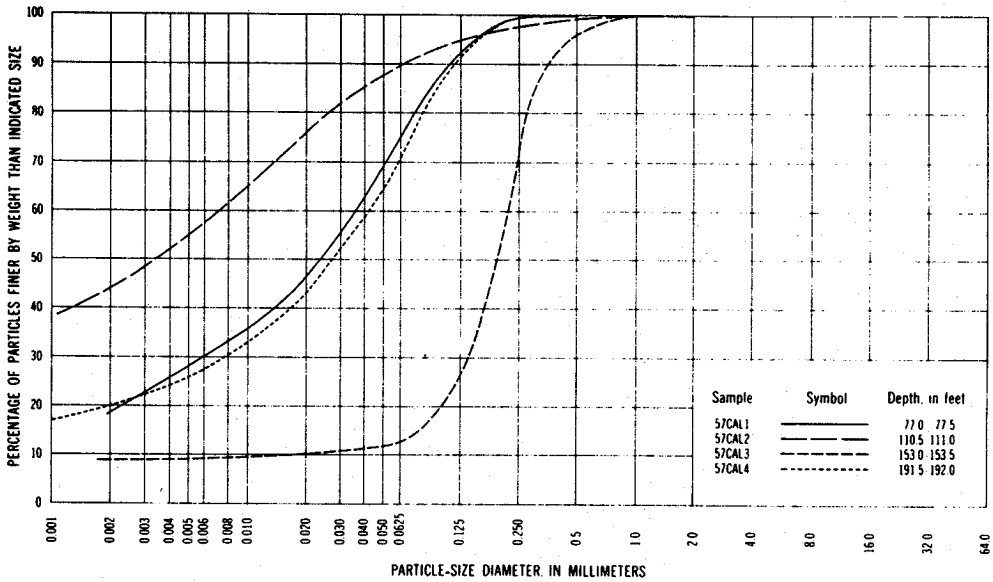

PERCENT OF PARTICLES OF INDICATED SIZE	CLAY 0.004	SILT 0.004-0.0625	SAND: Very fine 0.0625-0.125	SAND: Fine 0.125-0.25	SAND: Medium 0.25-0.5	SAND: Coarse 0.5-1	SAND: Very coarse 1-2	GRAVEL: Very fine 2-4	GRAVEL: Fine 4-8	GRAVEL: Medium 8-16	GRAVEL: Coarse 16-32	GRAVEL: Very coarse 32-64
57CAL1	25.7	49.5	16.6	7.0	1.2							
57CAL2	52.0	37.3	5.5	2.8	1.6	0.7	0.1					
57CAL3	9.2	3.7	13.6	42.6	26.7	4.2						
57CAL4	24.2	46.8	20.6	8.2	0.2							

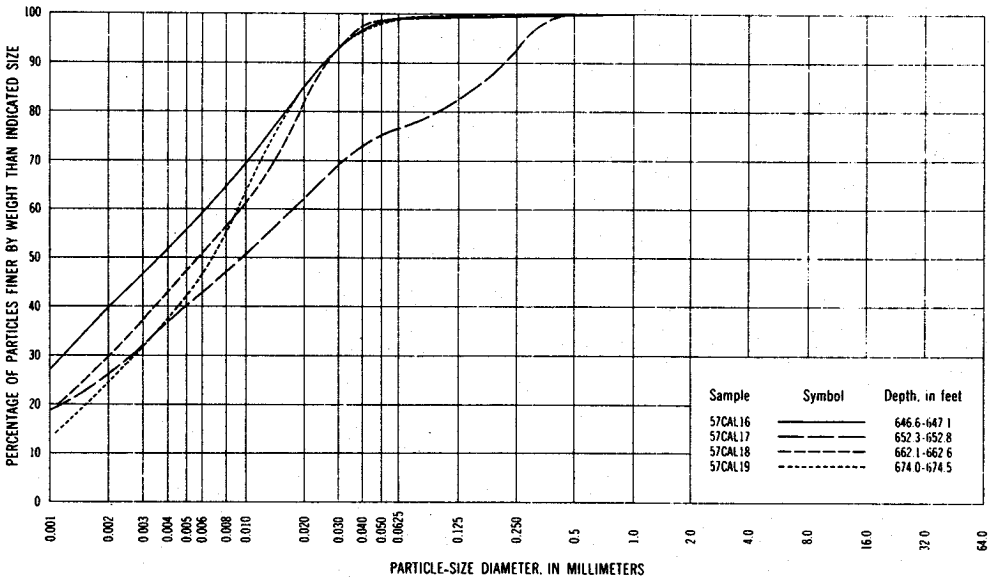

PERCENT OF PARTICLES OF INDICATED SIZE	CLAY 0.004	SILT 0.004-0.0625	SAND: Very fine 0.0625-0.125	SAND: Fine 0.125-0.25	SAND: Medium 0.25-0.5	SAND: Coarse 0.5-1	SAND: Very coarse 1-2	GRAVEL: Very fine 2-4	GRAVEL: Fine 4-8	GRAVEL: Medium 8-16	GRAVEL: Coarse 16-32	GRAVEL: Very coarse 32-64
57CAL16	51.5	47.5	0.2	0.2	0.2	0.4						
57CAL17	36.6	40.1	6.0	9.7	7.6							
57CAL18	43.0	56.2	0.2	0.2	0.4							
57CAL19	37.5	61.5	0.4	0.2	0.2	0.2						

Figure 4.10 Some graphs of particle-size distribution curves for core hole 14/13-llDl in the San Joaquin Valley, California.

Because clay content has an important influence on many of the properties of sediments, the clay content for all the samples was plotted to facilitate comparison with the other properties (see example, Figure 4.3). In Table 4.1, the percentage of particles smaller than 2-µm (0.002-mm) clay, as well as smaller than 4- µm (0.004-mm) clay, has been reported. When the 4-µm rather than the 2-µm size was used as the criterion, 78.5 per cent of the samples showed 1ess than 10 per cent greater clay content. In addition, 20.9 per cent of the samples showed 10-20 per cent greater clay content and 0.6 per cent of the samples showed more than 20 per cent greater clay content for the 4-µm than for 2-µm size criterion.

4.5.2 Sediment classification triangles

Most clastic sediments are a mixture of sand-, silt-, and clay-size particles in varying proportions. A suitable nomenclature for sediments is therefore important to describe the approximate relations among these three main constituents. Because sediment classification is often based on the relative percentages of sand-, silt-, and clay-size particles, it is convenient to plot these three constituents on a triangular chart.

A large number of triangular classification systems have been devised over the years. Some were developed primarily for the use of geologists in relating classification to sedimentation characteristics, and others were developed for the use of soils engineers in relating classification to the engineering properties of the sediments. Shepard (1954) developed a sediment classification triangle based on the needs of sedimentologists for studying mode of transport and environment of deposition of sediments. Shepard’s classification gives equa1 importance to sand-, silt-, and clay-size particles (Figure 4.11).

Because the mode of transport and environment of deposition of the sediments were being studied, as well as the engineering properties, Shepard’s classification was used in the centra1 California study to determine the sediment class name listed for each sample in Table 4.1. For classification of sediments in the lower Mississippi Valley, the U.S. Army Corps of Engineer (Casagrande, 1948) developed a triangle which emphasizes the importance of clay-size particle content. To assist soils engineers in relating the classification of samples to their engineering properties, a transparent overlay of the Mississippi valley classification triangle could be placed over the plots in Figure 4.11 to determine the classification name under that system.

The textural classification used in Table 4.1, based on the Shepard system, is a laboratory classification derived from particle-size distribution graphs. It departs substantially from the field description made from examination of cores and drill cuttings by geologists especially for the fine-textured materials. In the field examination, material containing more than 30-40 per cent of clay-size particles has sufficient clay content to give it the physical properties of clay, such as plasticity. Therefore, the textural description of cores or samples in the field by geologists is not directly comparable to the laboratory textural classification by the Shepard system. Field examination by the geologists results in a textural description much closer to that of the Mississippi Valley classification than to that of the Shepard classification.

4.5.3 Statistical measures

For comparison and statistical analysis, it is convenient to have characteristics of particle-size distribution (mechanical analysis) curves expressed as numbers.

The measure of central tendency is the value (size of particle) about which all other values (sizes) cluster. One such measure is the median diameter, D_{50}, which is defined as that particle diameter which is larger than 50 per cent of the diameters and smaller than the other 50 per cent. It is determined by reading, from the particle-size distribution curve, the particle diameter at the point where the particle-size distribution curve intersects the 50-percent line.

The quartile deviation is a measure of spread of particle sizes. Quartiles are the particle-diameter values read at the intersection of the curve with the 25- (Q_1), 50-(Q_2), and 75- (Q_3) per-cent lines. By convention, the third quartile (Q_3) is always taken as the larger value, regardless of the manner of plotting. The geometrical quartile deviation, or the "sorting coefficient," S_0 of Trask (1932, p. 70-72), is represented by the equation

$$S_0 = \sqrt{Q_3/Q_1} \tag{4.13}$$

An S_0 value of less than 2.5 indicates a well-sorted sediment, of 3 a normally sorted sediment, and of 4.5 a poorly sorted sediment.

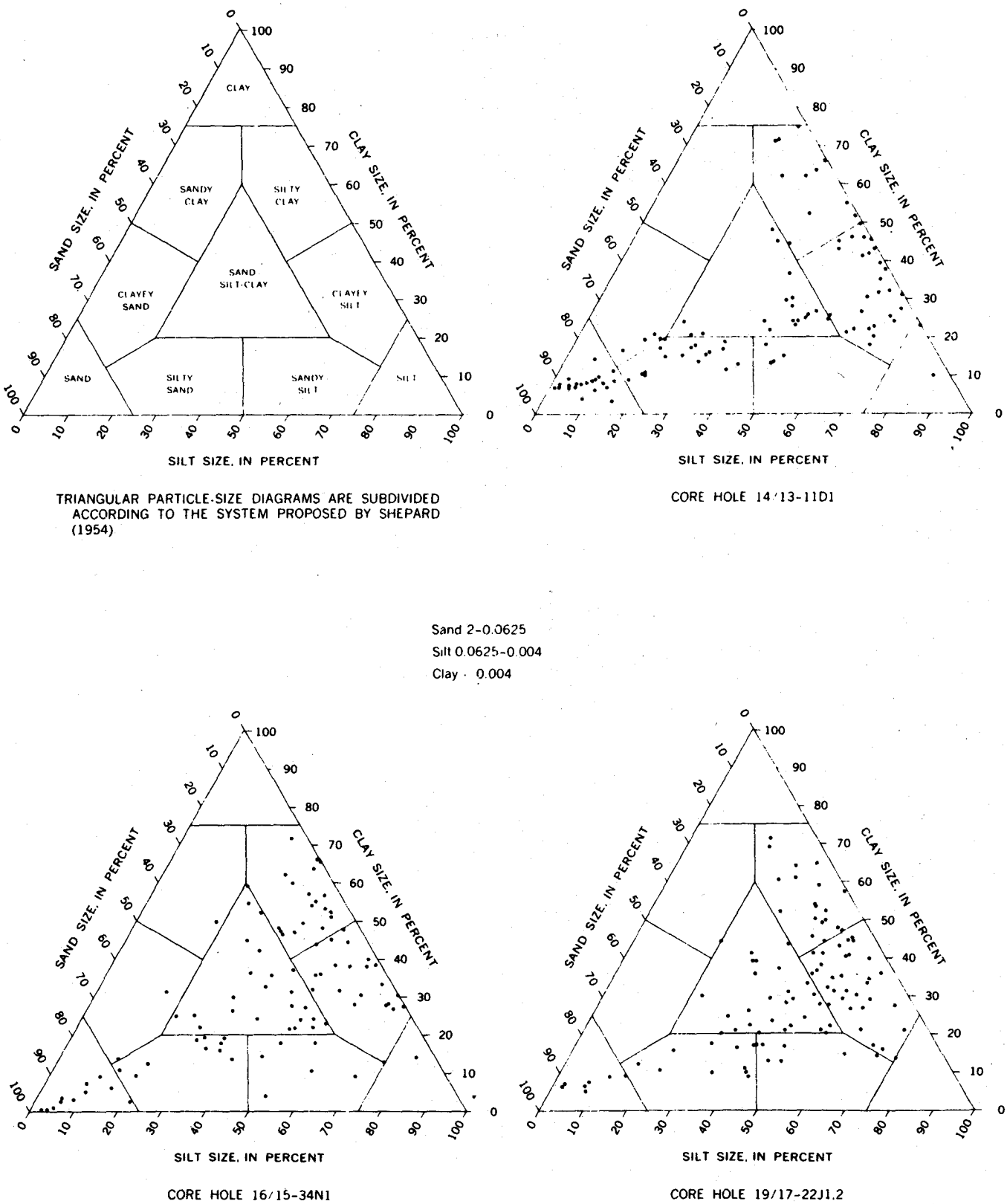

Figure 4.11 Sediment classification triangles for samples from core holes in the Los Banos-Kettleman City area, California.

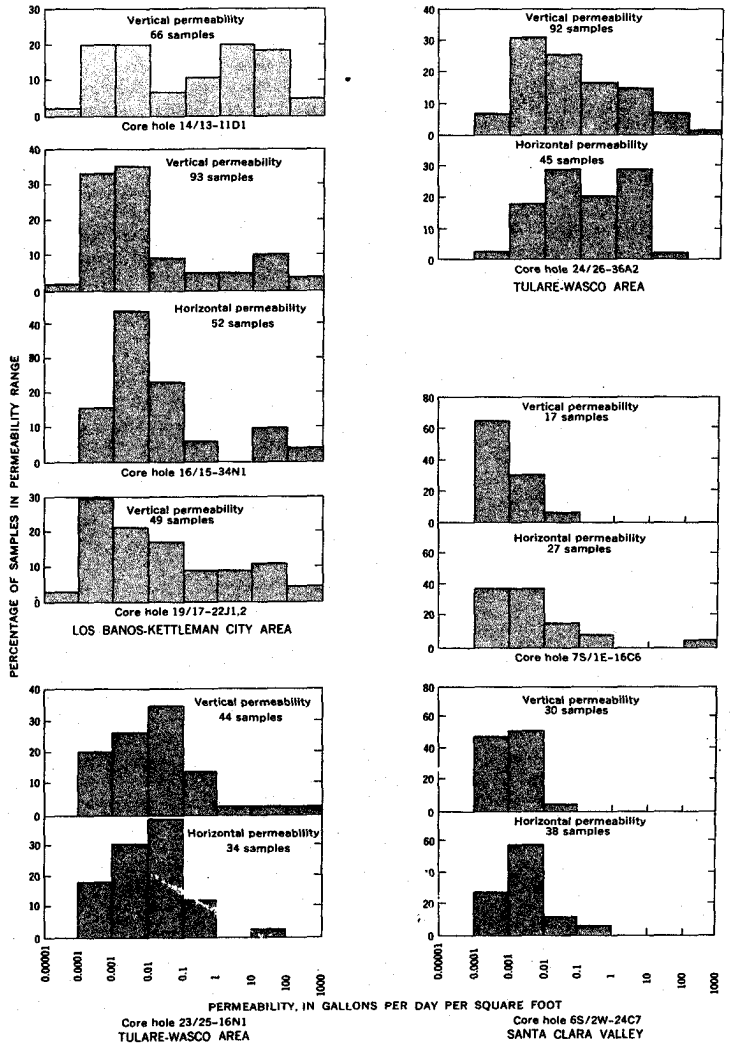

Figure 4.12 Range in permeability of samples from core holes.

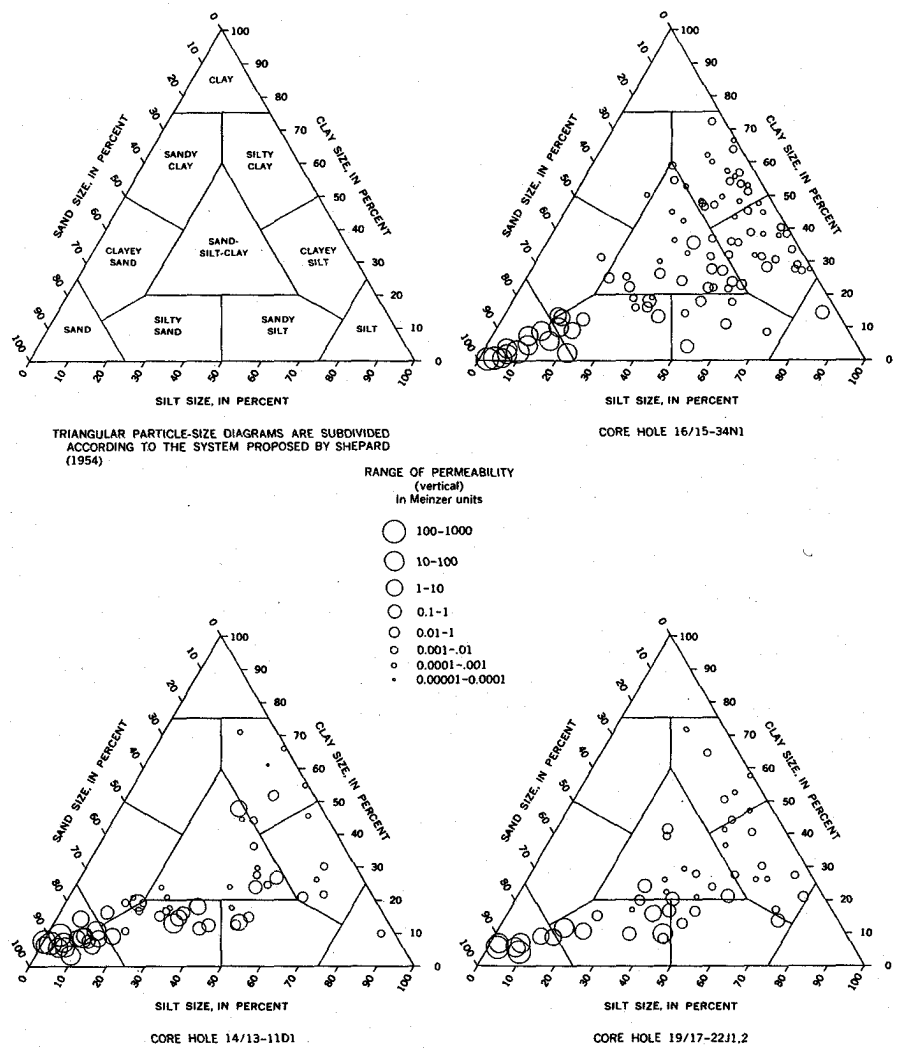

Figure 4.13 Relation between permeability and texture for samples from core holes in the Los Banos-Kettleman City area, California.

The log quartile deviation is the log of the geometrical quartile deviation, or sorting coefficient, S_0, and is represented by the equation

$$\text{Log } S_0 = (\log Q_3 - \log Q_l)/2 \qquad (4.14)$$

The log S_0 can be expressed to the base 10 (Krumbein and Pettijohn, 1938, p. 232) and is so tabulated in this report.

As noted by Krumbein and Pettijohn (1938, p. 232), the geometric quartile measures are ratios between quartiles and thus have an advantage over the arithmetic quartile measures in that they eliminate both the size factor and the unit of measurement. They do not, however, give a direct comparison because the log S_0 (the log quartile deviation) increases arithmetically. Thus, a sediment having log S_0 = 0.402 is twice as widely spread between Q_l and Q_3 as one having log S_0 = 0.201.

Many sedimentologists now use a ∅ scale in which

$$\varnothing = -\log_2 d, \qquad (4.15)$$

in which d is the diameter of the particle in millimetres. This scale has certain advantages over the $\log_{10}$ scale for expressing quartile deviation and other statistical parameters (Krumbein and Pettijohn, 1938, p. 233-235). Therefore, statistical parameters were listed in terms of the ∅ scale in the report by Meade (1967) on the petrology of sediments in subsiding areas of central California.

4.5.4 Permeability

The hydraulic conductivity depends in general on the degree of sorting and upon the arrangement and size of particles. It is usually low for clay and other fine-grained or tightly cemented materials and high for clean coarse gravel. In general, the hydraulic conductivity in a direction parallel to the bedding plane of the sediments (referred to in the data tables as horizontal permeability) is greater than the permeability perpendicular to the bedding plane (referred to as vertical permeability in the tables in this chapter). Most water-bearing materials of any significance as sources of water to wells have hydraulic conductivities above 5×10^{-3} cm per sec.

For central California, the hydraulic conductivities (coefficients of permeability) were presented in tables similar to Table 4.4, and in graphical form such as in Figures 4.12 and 4.13. Figure 4.12 shows the relation of horizontal and vertical hydraulic conductivity for many paired samples. Horizontal hydraulic conductivity was as much as 200 times greater than vertical hydraulic conductivity, with an average ratio of horizontal to vertical permeability of about 3.

Figure 4.14 shows the relation between vertical hydraulic conductivity and texture for samples from core holes in central California. Hydraulic conductivities have been grouped into eight ranges; a symbol representing the proper range for each sample is plotted in the appropriate textural location on the triangle, which is subdivided according to the system proposed by Shepard (1954). Although the highest hydraulic conductivity naturally occurs in the coarse-textured and well-sorted samples, conductivities within each textural classification vary considerably.

The vertical hydraulic conductivities for the clayey sediments tested in the variable-head permeameter under no load (Table 4.1) in general appear to be in a considerably higher range than those in Table 4.4 (ft per yr x 9.7×10^{-7} = cm per sec) which were computed from the consolidation tests for samples of similar texture. There are at least three reasons for this difference:

1. The permeability of a clayey sediment decreases markedly with decrease in void ratio (or porosity). The hydraulic conductivities given in Table 4.4 (in feet per year) are computed from time-consolidation data derived from test loads ranging from 7 to 112 kg per cm^2 and thus represent conditions of substantially reduced void ratios from those of the samples tested in an unloaded condition in the variable-head permeameter. For sample 23L-207 (Table 4.4), the computed coefficient of vertical hydraulic conductivity for the load range 7 to 14 kg per cm^2 is about 50 times as high as that for the load range 56 to 112 kg per cm^2.
2. For a clayey sediment, the water used for testing permeability in the variable-head permeameter, if not chemically compatible with the pore water, may affect the

results substantially. In the water used in the Hydrologic Laboratory for the variable-head tests, calcium was the predominant cation; however, sodium is the predominant cation in the pore water of the sediments beneath the Corcoran Clay Member in the San Joaquin Valley area. The use of water in which the calcium ion is predominant in testing cores of such sediments would tend to increase the value of the hydraulic conductivity obtained in the variable-head tests. The consolidation test, however, did not involve the passage of water through the sample, only the squeezing out of native pore water.

3. For a sample of very low hydraulic conductivity tested under no load in a variable-head permeameter, the disturbed condition of the sample at and near the container wall creates a boundary region which may produce a zone of appreciably higher permeability than that of the undisturbed sample matrix. Tests in a consolidometer, however, create lateral pressure against the container walls and thus tend to reduce the permeability of the disturbed boundary region to approximately that of the sample matrix.

For these three reasons, the coefficients of permeability of the clayey sediments as derived from the unloaded variable-head permeameter tests (Table 4.1) are not directly comparable to those computed from the time-consolidation data (Table 4.4). Coefficients from the consolidation tests are considered more reliable for samples taken as deep as these, but, to be meaningful for field applications, the coefficients would have to be computed at the void ratio or porosity, existing under the overburden (effective) stress conditions in the field.

4.5.5 Specific gravity, unit weight, and porosity

The specific gravity of a sediment is the average of the specific gravities of all the constituent mineral particles. The specific gravity of most clean sands is usually near 2.65, whereas that of clays ranges from 2.5 to 2.9. Organic matter in the sediment will lower its specific gravity.

The dry unit weight of a sediment is dependent upon the shape, arrangement, and mineral composition of the constituent particles, the degree of sorting, the amount of compaction, and the amount of cementation. Dry unit weights of unconsolidated sediments commonly range from 1.3 to 1.8 g per cm^3.

Because porosity is calculated from the dry unit weight and specific gravity of the sediment, it is dependent upon the same factors. Most natural sands have porosities ranging from 25 to 50 per cent, and soft clays from 30 to 60 per cent. Compaction and cementation tend to reduce these values. In general, porosities decrease with depth below land surface, and dry unit weights increase with depth. Athy (1930) described just such a progressive compaction of sediments as the load of overlying material increased with deposition.

The general trends discussed previously are complicated by other factors which affect the unit weight and porosity of individual samples. These factors are (1) differences in particle sizes or in particle-size distribution, (2) differences in type of clay mineral, (3) exposure to atmosphere and pre-consolidation, such as by dessication, during their depositional history (4) differences in intergranular structure as originally deposited, and (5) change in volume and structure of the core during and subsequent to the sampling operations.

The first four factors are natural phenomena, whereas the last one, the change in volume and structure of the core during and subsequent to the sampling operation, is introduced by man in his disturbance of the natural state in order to procure the sample. The sediments cored in the holes of the San Joaquin Valley ranged in depth from 21 to 630 m below the land surface. The effective stress, or grain-to-grain load, of the overburden on these materials in place increased from about 3 to 70 kg per cm^2 in this depth range. While the core was being cut, additional load was placed on the material by the core barrel and drill pipe, especially near the outer edge of the core. As soon as the materials were encased in the core barrel, however, the effective stress of the overburden was removed and they expanded elastically. Thus, the change in volume (porosity and unit weight) from the natural to the laboratory condition is a function of several variables:

1. Compacting effect produced by displacement of the material by the cutting edge, the inside-wall friction, or by overdriving of the core barrel.
2. Expanding effect of removal of the effective stress of the overburden load at the time the core enters the barrel; the magnitude depends on the elasticity of the material and on the amount of the effective stress removed (increasing with depth).

3. Disturbing effects of mechanical rotation of core-barrel teeth and core catcher while cutting the core, removal of core from barrel, packing, shipping, unpacking, and processing.

The net effect of this sampling process is believed to be an expansion of the sediments as tested in the laboratory, thus providing values that are higher for porosity and lower for unit weight than exist in the natural state. On the basis of a study of the consolidation and rebound data, the laboratory-determined porosity of the fine-textured materials from the San Joaquin Valley was estimated to be as much as 2-3 per cent higher than the in-place field porosity (J. F. Poland, written commun., 1963).

4.5.6 Atterberg limits and indices

The Atterberg limits and indices determined for selected fine-textured samples from the core holes are presented in Tables 4.2 and 4.3. Predominantly fine-textured samples to be tested were selected by visual inspection. Because the Atterberg limits describe properties of the fine part of a sample, presenting Atterberg limit data for samples which are predominantly coarse textured could be misleading. When the influence which the limits of consistency have on the behavior of a sample is being judged, the percentage of the sample tested must be considered. Table 4.2 includes a column which lists the per cent (by weight) of the total sample that passed a No. 40 sieve (0.42-mm openings) and was therefore the part of the sample tested for Atterberg limits.

Most of these Atterberg limits and indices are not directly applicable to the study of subsidence and compaction of sediments under increased effective overburden load, but they do furnish a rough comparative measure of the way in which fine-grained sediments respond to a decrease in moisture content as they pass from the liquid to the solid state. Because the values of these indices are related to texture, composition, clay content, and type of clay minerals present, they may be of qualitative use in comparing the fine-textured clayey deposits in different areas to each other and to fine-textured sediments in other areas for which Atterberg indices have been obtained but for which the clay content, the compression index (C_C), and the type of clay minerals present are not known.

The liquid and plastic limits (moisture content, in per cent by weight) for samples from all core holes in the central California subsidence areas are plotted against percentage of clay-size particles in figure 4.14. As shown by the trend lines, both limits tend to increase with an increase in clay content, the liquid limit increasing at a greater rate than the plastic limit.

The trend lines shown in Figure 4.14 were plotted from equations derived by computer. The equations are of the form $y = a + bx$, in which y represents the moisture content (w), x represents the clay content (C), both in per cent, and a and b are constants. In Figure 4.14A the equation of the liquid-limit trend line is w_L - 13.5 + 1.3C and that of the plastic-limit trend line is $w_P = 17.3 + 0.54C$. In Figure 4.14C the equation of the liquid-limit trend line is $w_L = 14.0 + 0.72C$ and that of the plastic-limit trend line is $w_P = 14.7 + 0.22C$. The equations of all these trend lines are for samples having clay content based on the percentage of particles less than 0.004 mm in size.

Figure 4.14D shows trends which are composites of all the samples shown in Figures 4.14A-C. The equation of line 1, the liquid-limit trend line for clay sizes less than 0.002 mm, is $W_L = 27.8 + 0.71C$. The equation of line 2, the liquid-limit trend line for clay sizes less than 0.004 mm, is w_L - 25.8 + 0.60C. The equation of line 3, the plastic-limit trend line for clay sizes less than 0.002 mm is $w_P = 25.6 + 0.21C$. The equation of line 4, the plastic-limit trend line for clay sizes less than 0.004 mm is $w_P = 24.5 + 0.19C$. Lines 1 and 3 are included to show the relation between liquid and plastic limits and per cent of clay-size particles if 0.002 mm is chosen as the upper limit of the clay-size range.

The value of the standard error for each trend line was obtained by computer. The pairs of dashed lines which parallel each trend line designate two standard errors on either side of the trend line. The probability is 19 to 1 that, for a given value of clay content (in per cent), the observed liquid limit or plastic limit will lie within the interval between the dashed lines.

The difference between the liquid and plastic limits, or the plasticity index, represents the range of moisture content within which a sediment mass will remain in the plastic state. The moisture content difference between the liquid-limit trend line and the plastic-limit trend line in each part of Figure 4.14 represents the average plasticity index for different clay contents.

Table 4.2 Atterberg limits and indices of samples from core holes.

Hydrologic Laboratory sample	Depth (feet)	Percent passing No. 40 sieve	Liquid limit	Plastic limit	Shrinkage limit	Plasticity index	Flow index	Toughness index	Shrinkage index	Shrinkage ratio	Volumetric shrinkage	Linear shrinkage
Core hole 14/13-11D1												
57CAL1	77.0- 77.5	100	28	27	19	1	6	0.2	8	1.7	15	4
2	110.5- 111.0	99	56	26		30	16	1.9				
4	191.5- 192.0	100	33	24	15	9	8	1.1	9	1.8	32	8
5a	232.5- 233.0	100	44	29	12	15	6	2.5	17	2.0	64	15
7	314.0- 314.5	100	34	24	18	10	8	1.3	6	1.7	27	8
9	398.0- 398.5	100	64	40	13	24	19	1.3	27	1.9	97	20
10	432.0- 432.5	100	59	36	12	23	28	.8	24	1.9	89	19
12	510.3- 510.8	97	65	40	8	25	11	2.3	32	2.0	114	22
14	594.0- 594.5	100	82	39	9	43	22	2.0	30	1.9	139	25
16	646.6- 647.1	100	78	38	17	40	17	2.4	21	1.8	110	22
18	662.1- 662.6	100	80	44	24	36	11	3.3	20	1.6	90	19
19	674.0- 674.5	100	78	46	28	32	9	3.6	18	1.4	70	16
21	697.0- 697.5	100	67	36	28	31	11	2.8	8	1.5	58	14
23	713.0- 713.5	100	52	33	31	19	9	2.1	2	1.4	29	8
25	731.0- 731.5	100	58	34	15	24	26	.9	19	1.8	77	17
26	743.0- 743.5	100	46	28	21	18	19	.9	7	1.6	40	11
27	757.0- 757.5	98	30		27		11			1.5	4	1
28	764.9- 765.4	65	38	30	26	8	6	1.3	4	1.6	19	5
31	791.0- 791.5	100	40	30	20	10	10	1.0	10	1.7	34	9
32	802.0- 802.5	100	34	26	24	8	13	.6	2	1.7	17	5
35	826.0- 826.5	100	65	43	20	22	14	1.6	23	1.7	77	17
36	831.5- 832.0	100	31	26	19	5	25	.2	7	1.7	20	6
39	860.0- 860.5	100	42	31	23	11	10	1.1	8	1.6	30	8
43	887.5- 888.0	100	76	29	13	47	42	1.1	16	1.9	120	23
44	901.0- 901.5	100	40	30	23	10	15	.7	7	1.6	27	8
47	932.0- 932.5	99	47	23	10	24	9	2.7	13	2.0	74	17
48	936.5- 937.0	100	33	29	20	4	16	.2	9	1.7	22	6
49	951.0- 951.5	100	34	27	13	7	6	1.2	14	1.9	40	11
51	968.5- 969.0	100	41	33	17	8	12	.7	16	1.8	43	11
52	984.0- 984.5	100	59	29	10	30	15	2.0	19	2.0	98	20
54	1,000.5-1,001.0	100	40	24	12	16	8	2.0	12	1.9	53	14
55	1,005.1-1,005.6	100	50	29	11	21	14	1.5	18	2.0	78	17
56	1,020.8-1,021.3	100	36	31	17	5	7	.7	14	1.8	34	9
58	1,039.5-1,040.0	100	47	34	12	13	10	1.3	22	1.9	67	16
59	1,051.5-1,052.0	100	33	24	17	9	10	.9	7	1.8	29	8
61	1,070.8-1,071.3	100	30	21	16	9	11	.8	5	1.8	25	7
65	1,104.6-1,105.1	88	25	22	15	3	15	.2	7	1.8	18	5
68	1,133.0-1,133.5	100	36	24	16	12	10	1.2	8	1.8	36	10
75	1,242.0-1,242.5	100	51	36	25	15	26	.6	11	1.5	39	11
83	1,312.0-1,312.5	98	26	18	18	8	4	2.0	0	1.8	14	4
86	1,339.5-1,340.0	100	36	26	23	10	6	1.7	3	1.6	21	6
88	1,357.0-1,357.5	100	46	23	10	23	14	1.6	13	2.0	72	17
89	1,362.5-1,363.0	100	32	21	18	11	16	.7	3	1.7	24	7
91	1,385.0-1,385.5	100	54	36	13	18	12	1.5	23	1.8	74	17
92	1,397.0-1,397.5	98	61	41	5	20	17	1.2	36	2.1	118	23
96	1,432.5-1,433.0	100	77	38	4	39	14	2.8	34	2.3	168	28
97	1,446.0-1,446.5	100	56	28	5	28	15	1.9	23	2.2	112	22
98	1,454.5-1,455.0	100	44	33	16	11	9	1.2	17	1.7	48	13
99	1,465.0-1,465.5	100	58	34	8	24	11	2.2	26	2.1	105	21
Core hole 16/15-34N1												
58CAL2	298.2- 298.7	98	38	30	13	8	11	0.7	17	1.9	48	13
3	332.4- 332.9	98	40	26	12	14	14	1.0	14	1.9	53	14
5	418.5- 419.0	100	44	30	13	14	11	1.3	17	1.9	59	15
6	454.3- 454.8	99	54	37	8	17	23	.7	29	2.0	92	20
9	509.5- 510.0	100	46	35	15	11	18	.6	20	1.8	56	14
11	532.4- 532.9	97	42	34	12	8	9	.9	22	1.9	57	14
12	552.8- 553.2	100	45	32	11	13	8	1.6	21	1.9	65	16
13	563.7- 564.2	100	56	46	12	10	13	.8	34	1.9	84	18
14	570.7- 571.2	100	70	58	9	12	18	.7	49	2.0	122	23
19	636.4- 636.9	99	61	52	20	9	14	.6	32	1.6	66	16
20	643.2- 643.7	99	31	25	22	6	19	.3	3	1.6	14	4
21	652.6- 653.1	96	32	26	12	6	12	.5	14	1.8	36	10
22	666.0- 666.5	100	55	43	15	12	15	.8	28	1.8	72	17
24	683.7- 684.2	100	36	30	19	6	16	.4	11	1.7	29	8
25	696.6- 697.1	100	59	42	12	17	8	2.1	30	1.8	85	18
26	701.8- 702.4	100	42	32	17	10	18	.6	15	1.7	43	11
27	713.4- 713.9	99	61	40	7	21	16	1.3	33	2.0	108	22
29	732.0- 732.6	100	39	28	18	11	12	.9	10	1.7	36	10
31	753.8- 754.3	100	41	30	14	11	17	.6	16	1.8	49	13
32	762.4- 762.9	100	46	33	7	13	14	.9	26	2.0	78	17
33	773.3- 773.8	100	30	26	19	4	10	.4	7	1.7	19	5
36	806.1- 806.6	100	55	40	12	15	15	1.0	28	1.8	77	17
38	822.1- 822.6	98	60	49	10	11	12	.9	39	1.9	95	20
39	827.8- 828.2	100	47	33	13	14	20	.7	20	1.8	61	15
40	837.7- 838.2	100	58	43	14	15	17	.9	29	1.8	79	18
42	860.1- 860.6	100	31	24	22	7	13	.5	2	1.6	14	4
43	866.7- 867.3	100	30	23	18	7	7	1.0	5	1.7	20	6
45	891.6- 892.1	100	53	41	11	12	15	.8	30	1.9	80	18
48	922.6- 923.1	100	46	35	13	11	14	.8	22	1.8	59	15
49	931.2- 931.7	100	35	28	15	7	12	.6	13	1.8	36	10
50	940.6- 941.1	100	46	36	9	10	8	1.2	27	2.0	74	17
51	946.3- 946.8	100	63	43	7	20	22	.9	36	2.0	112	22
52	963.7- 964.2	100	37	28	16	9	14	.6	12	1.8	38	10
53	971.5- 972.0	100	57	46	16	11	20	.6	30	1.7	70	16
54	980.6- 981.1	100	35		27		14			1.5	12	3
58	1,042.8-1,043.3	100	51	45	14	6	13	.5	31	1.8	67	16
61	1,189.5-1,190.0	100	47	34	16	13	24	.5	18	1.8	56	14
63	1,225.0-1,225.5	100	38	34	25	4	14	.3	9	1.6	21	6
64	1,238.1-1,238.6	100	47	36	17	11	16	.7	19	1.7	51	13
66	1,254.9-1,255.4	100	41	36	30	5	7	.7	6	1.4	15	4

Table 4.3 Visual classification, Atterberg limits, and specific gravities of samples tested for consolidation.

[Data from Earth Laboratory, U.S. Bureau of Reclamation, Denver, Colo.]

Earth Laboratory sample	Depth (feet)	Gradation (estimated)				Color (wet)	Soil classification and description	Unified Soil Classification symbol	Atterberg limits			Specific gravity of solids
		Maximum size (U.S. Standard sieve No.)	Gravel >4.76 mm (percent)	Sand, 4.76–0.074 mm (percent)	Silt and clay <0.074 mm (percent)				Liquid limit (percent)	Plastic limit (percent)	Plasticity index	
Core hole 12/12-16H1												
23L91	84.3– 84.6	30	0	10	90	Brown	Clay, containing some fine sand; medium plasticity; slight dilatancy; medium dry strength; no reaction to HCl; trace of gypsum.	CL	31	14	17	2.80
92	159.4– 159.8	100	0	10	90	do	Clay, containing some fine sand; medium to high plasticity; slow dilatancy; medium reaction to HCl.	CL-CH	50	19	31	2.74
93	230.8– 231.2	50	0	10	90	Tan to brown	Clay, lean; low plasticity; slight dilatancy; low dry strength; slight reaction to HCl.	CL	33	11	22	2.73
94	324.5– 324.9	100	0	20	80	Gray	Clay, containing fine sand; low plasticity; medium dilatancy; ome micaceous material present; no reaction to HCl.	CL	29	19	10	2.68
95	374.0– 374.5	200	0	0	100	do	Clay, fat; high plasticity; no dilatancy; no reaction to HCl	CH	54	23	31	2.73
96	425.0– 425.3	100	0	10	90	do	Clay, fat, containing fine sand lenses; high plasticity; no dilatancy; no reaction to HCl; moist, and firm.	CH	76	27	49	2.67
97	471.2– 471.5	100	0	5	95	do	Clay, fat; high plasticity; no dilatancy; lensed with fine sand	CH	58	20	38	2.68
98	516.5– 516.9	50	0	75	25	Gray to black	Sand, fine, no plasticity; fast dilatancy; strong organic odor present; soft and loosely cemented.	SM				2.70
99	579.0– 579.3	100	0	35	65	Tan	Clay, silty containing fine sand; medium plasticity; slight dilatancy.	CL	32	14	18	2.69
100	625.0– 625.4	200	0	0	100	Gray	Clay, fat; high plasticity; no dilatancy; firm; numerous planes containing some silt.	CH	59	19	40	2.79
101	675.9– 676.2	50	0	45	55	do	Clay, silty containing fine sand, medium plasticity, slow dilatancy; clay on outer surface; sand in center, angular.	CL	45	14	31	2.72
102	722.0– 722.3	100	0	5	95	do	Clay, fat; high plasticity; no dilatancy, blocky structure; fractures contain silt.	CH	70	20	50	2.69
103	773.0– 773.4	50	0	60	40	Brown to gray	Sand, fine containing silt; no plasticity; fast dilatancy; lensed with clay and silt; medium cementation; no reaction to HCl.	SM				2.77
104	821.4– 821.8	50	0	55	45	Gray	Sand, fine containing silt; no plasticity; fast dilatancy; organic odor present; no reaction to HCl.	SM				2.74
105	877.4– 877.8	30	0	65	35	Brown	Sand, fine, uniform; no plasticity; fast dilatancy; free water present; no reaction to HCl.	SM				2.71
106	926.8– 927.2	50	0	20	80	Gray	Clay, silty; medium plasticity; slow dilatancy; no reaction to HCl; top of sample contained sand of No. 30 size; rest of sample was silt and clay lensed.	CL	47	32	15	2.72
107	972.0– 972.4	30	0	75	25	do	Sand, fine: no plasticity; fast dilatancy; slight binder	SM				2.70
108	998.6– 999.0	50	0	40	60	Brown	Clay containing fine sand; medium plasticity, slow dilatancy; sample lensed with clay and fine sand.	CL	37	20	17	2.68

Casagrande (1948, P. 919) devised a chart on which the liquid limit is plotted against the plasticity index and used it for rough classification of soils. Points representing different samples from the same stratum or fine-grained deposit plot as a straight line that is rough1y parallel to an "A" line, an empirical boundary between typically inorganic clays above and plastic organic soils below the line. The higher a sample plots on this chart at a given liquid limit, the greater its toughness and dry strength and the lower its permeability and rate of volume change. Figure 4.15 shows plasticity charts of the Casagrande type on which the data for all samples tested from the central California subsidence areas have been plotted.

4.5.7 Consolidation

As one phase of the research on subsidence and compaction of aquifer systems in central California, laboratory consolidation tests were made on representative cores from eight core holes. The results of these consolidation tests were utilized in interpretive reports of the Geological Survey to compute compaction in the confined aquifer system in response to the known decline in artesian head. The method has been described by Miller (1961); it is a refinement of a technique outlined by Gibbs (1959, p. 4-5) based upon Terzaghi's (1943) theory of consolidation and the use of one-dimensional consolidation tests. The consolidation test results are summarized as in Table 4.4.

Consolidation-test curves representative of samples from various depths in one of the San Joaquin valley core holes are shown in Figure 4.16. The curves show, in general, that the Corcoran Clay Member has a greater unit consolidation potential than any of the other sediments. The compaction of the Corcoran Clay Member, however, has contributed very little to the total subsidence to date (Miller, 1961, p. B57) because, where the Corcoran is thick, water moves out very slowly, owing to the formation's low vertical permeability. Where the Corcoran is thin and more permeable, it forms only a small percentage of the water-bearing section. Consolidation curves for the Corcoran Clay Member are generally steep in the load range 14-70 kg per cm^2 and indicate that the clay is normally loaded and has not been precompressed. Therefore the clay has only partly completed its potential consolidation at the present time and at the present artesian pressure.

4.5.7.1 Estimating the compression index

Terzaghi and Peck (1948, p. 66), in a continuation of work begun by Skempton (1944, p. 126), state that the compression indices for clays in a remolded state (C'_C) increase consistently with increasing liquid limit (w_L). Using data from approximately 30 samples selected at random from different parts of the world and representing both ordinary and extra-sensitive clays, Terzaghi and Peck (1948) state that the data on compression indices and liquid limits for these clays plot on a graph within ± 30 per cent of a line representing the equation

$$C'_C = 0.007\ (w_L - 10 \text{ per cent}). \tag{4.16}$$

They state further that for an ordinary clay of medium or low sensitivity tested in the undisturbed state, the value of C_C corresponding to field consolidation is approximately equal to 1.30 C'_C; thus,

$$C_C = 0.009\ (w_L - 10 \text{ per cent}). \tag{4.17}$$

Hence, these authors conclude that for normally loaded clays with low or moderate sensitivity the compression index, C_C can be estimated approximately from knowledge of the liquid limit and use of equation 4.17. However, Terzaghi and Peck do caution that this approximate method of computation may furnish merely a lower limiting value for the compression index of an extra-sensitive clay. Later papers by Nishida (1956), and Roberts and Darragh (1963), showed exceptions to the compression index-liquid limit relationships described by Terzaghi and Peck (1948) and indicated a wide scattering of data. Furthermore, they found no simple correlation between these factors for the sample data they studied.

Figure 4.17 shows the relationship between liquid limit and compression index for core samples from test holes in subsiding areas of central California. Although the liquid limit is calculated as moisture content in per cent of dry weight, values usually are reported as numbers only and are reported thus in Figure 4.17 and henceforth in this section. The compression indices used in these graphs were obtained from consolidation tests, not by calculation from the

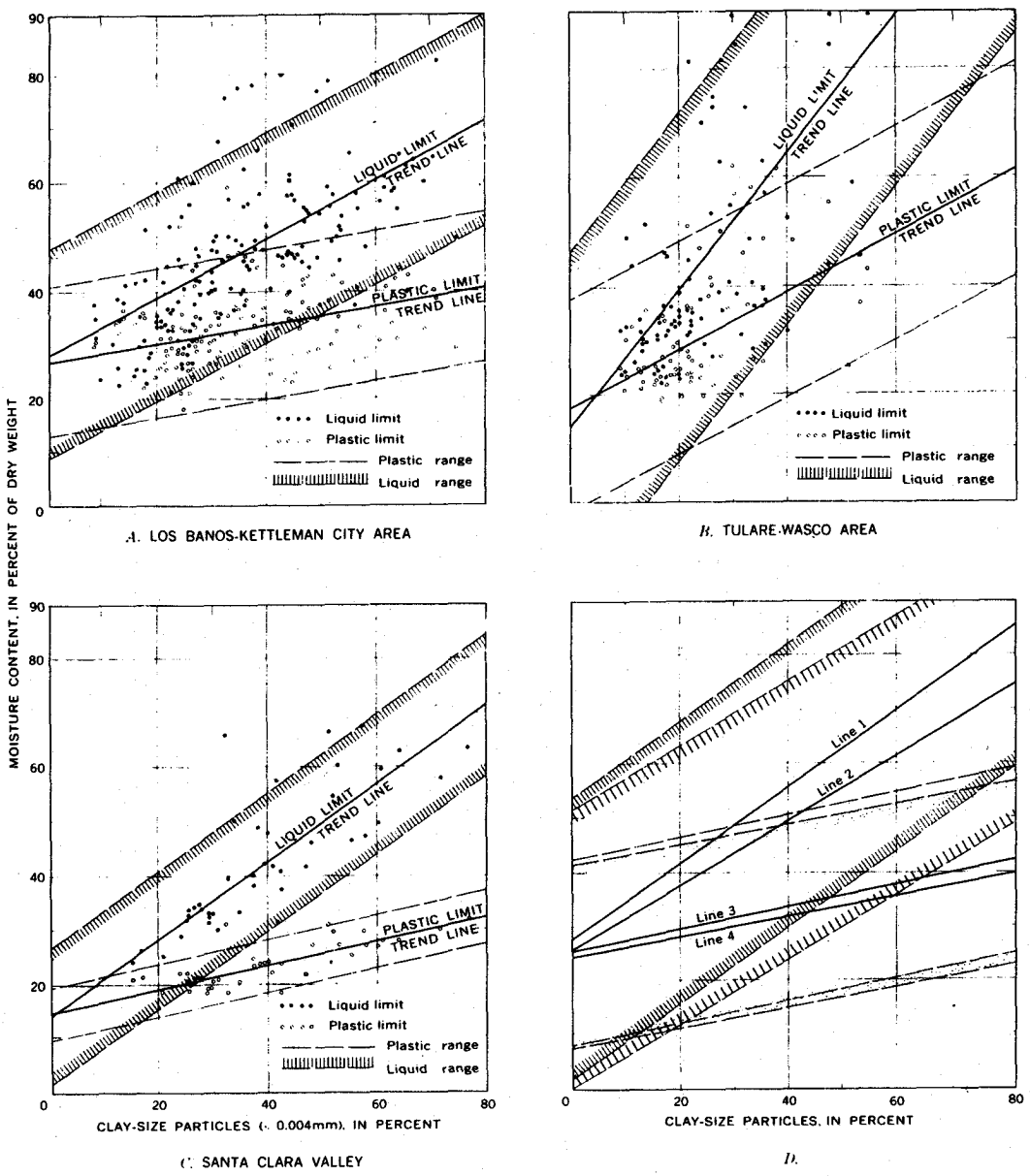

Figure 4.14 Effect of clay content on liquid limit; D, composite of all samples tested.

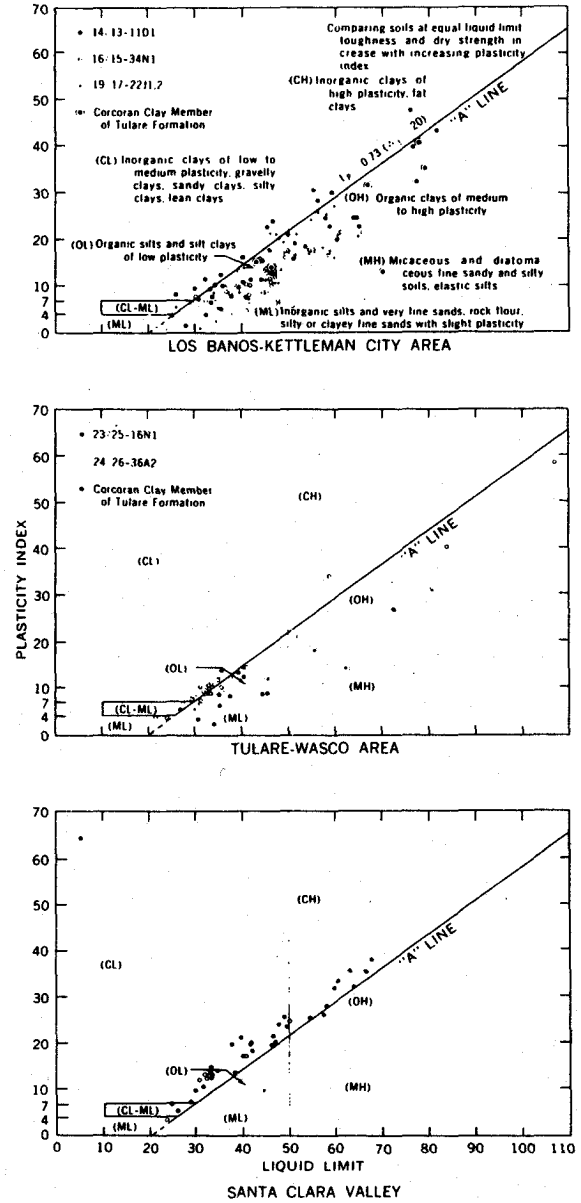

Figure 4.15 Unified soil classification for core-hole samples (ASTM, 1980).

Table 4.4 Consolidation test summaries.

[Data from Earth Laboratory, U.S. Bureau of Reclamation, Denver, Colo.]

Earth laboratory sample	Depth (feet)	Compression index, C_c: From consolidation curve	Compression index, C_c: From Atterberg test	Time-consolidation data: Load range (psi)	Coefficient of consolidation, C_v: Sq in. per sec	Coefficient of consolidation, C_v: Sq ft per yr	Coefficient of permeability: Calculated (ft per yr)	Coefficient of permeability: From test (ft per yr)	Unified soil classification symbol
Core hole 12/12-16H1									
23L91	84.3- 84.6	0.12	0.19	100- 200	3.3×10^{-4}	72.5	8.5×10^{-3}		CL
				200- 400	1.5×10^{-4}	31.8	2.0×10^{-3}		
92	159.4- 159.8	.22	.36	100- 200	9.2×10^{-5}	20.1	2.8×10^{-3}		CL-CH
				200- 400	5.1×10^{-5}	11.2	1.3×10^{-3}		
93	230.8- 231.2	.21	.21	200- 400	1.7×10^{-4}	37.2	4.0×10^{-3}		CL
94	324.5- 324.9	.11	.17						CL
95	374.0- 374.5	.32	.39	200- 400	1.5×10^{-5}	3.3	2.9×10^{-4}		CH
				400- 800	1.0×10^{-5}	2.2	1.5×10^{-4}		
96	425.0- 425.3	1.13	.59	200- 400	4.2×10^{-6}	0.92	3.2×10^{-4}		CH
				400- 800	3.2×10^{-6}	.70	1.2×10^{-4}		
97	471.2- 471.5	.90	.43	200- 400	1.3×10^{-4}	28.5	8.0×10^{-3}		CH
				400- 800	1.3×10^{-4}	28.5	3.6×10^{-3}		
98	516.5- 516.9	.41						5.7	SM
99	579.0- 579.3	.23	.20	200- 400	5.6×10^{-4}	122.0	7.2×10^{-3}		CL
				400- 800	3.8×10^{-4}	83.2	4.4×10^{-3}		
				800-1, 600	2.5×10^{-4}	54.8	1.5×10^{-3}		
100	625.0- 625.4	.34	.44	400- 800	1.7×10^{-5}	3.7	2.6×10^{-4}		CH
				800-1, 600	8.0×10^{-6}	1.8	6.0×10^{-5}		
101	675.9- 676.2	.27	.32	400- 800	1.1×10^{-3}	232.1	1.2×10^{-2}		CL
				800-1, 600	6.9×10^{-4}	151.1	4.8×10^{-3}		
102	722.0- 722.3	.34	.54	400- 800	2.7×10^{-5}	5.9	3.3×10^{-4}		CH
				800-1, 600	6.0×10^{-6}	1.3	5.0×10^{-5}		
103	773.0- 773.4	.33		800-1, 600	4.3×10^{-5}	9.4	3.5×10^{-4}		SM
104	821.4- 821.8	.20						14.2	SM
105	877.4- 877.8	.18						33.9	SM
106	926.8- 927.2	.68	.34	400- 800	1.6×10^{-4}	35.0	3.7×10^{-3}		CL
				800-1, 600	8.5×10^{-5}	18.6	1.2×10^{-3}		
107	972.0- 972.4	.33						38.4	SM
108	998.6- 999.0	.30	.24					1.4	CL
Core hole 14/13-11D1									
23L80	315.0- 315.3							25.3	SP
194	397.0- 397.3	0.36		200- 400	1.8×10^{-4}	39.4	4.0×10^{-3}		CL
				400- 800	5.1×10^{-5}	11.2	8.1×10^{-4}		
				800-1, 600	1.2×10^{-5}	2.6	9.0×10^{-5}		
81	554.0- 554.4	.22		200- 400	6.8×10^{-5}	15.0	9.5×10^{-4}		CL
				400- 800	2.2×10^{-5}	4.9	2.2×10^{-4}		
				800-1, 600	4.1×10^{-5}	9.0	1.8×10^{-4}		
83	699.0- 699.4	.97		400- 800	5.8×10^{-5}	12.8	2.1×10^{-3}		CL
				800-1, 600	3.2×10^{-5}	7.1	5.0×10^{-4}		
84	746.0- 746.4	.30		200- 400	1.7×10^{-4}	37.4	2.6×10^{-3}		
				400- 800	1.2×10^{-4}	26.9	1.5×10^{-3}		
				800-1, 600	6.6×10^{-5}	14.5	5.5×10^{-4}		
196	832.2- 832.7	.36		200- 400	2.0×10^{-4}	43.8	3.6×10^{-3}		CL
				400- 800	6.7×10^{-5}	14.7	9.4×10^{-4}		
				800-1, 600	4.5×10^{-5}	9.9	3.7×10^{-4}		
85	983.6- 984.0	0.35		200- 400	1.2×10^{-5}	2.6	2.1×10^{-4}		CL
				400- 800	1.0×10^{-5}	2.2	1.1×10^{-4}		
				800-1, 600	1.2×10^{-5}	2.6	1.2×10^{-4}		
86	1,076.0-1,076.4							1.7	SM
88	1,350.5-1,350.8							19.3	SP
89	1,395.0-1,395.3			200- 400	1.0×10^{-4}	21.8	1.2×10^{-3}		CL
				400- 800	1.7×10^{-5}	3.6	1.5×10^{-4}		
				800-1, 600	1.1×10^{-5}	2.4	8.0×10^{-5}		
90	1,450.0-1,450.3	.29		800-1, 600	3.9×10^{-5}	8.4	2.4×10^{-4}		CL
Core hole 16/15-34N1									
23L197	299.1- 299.5	0.34	0.38	200- 400	3.4×10^{-4}	74.9	1.1×10^{-2}		CH
198	418.1- 418.5	.32	.31	100- 200	1.7×10^{-3}	361.4	6.3×10^{-2}		CL
				200- 400	5.0×10^{-4}	109.5	1.3×10^{-2}		
				400- 800	1.4×10^{-4}	30.7	2.1×10^{-3}		
200	538.9- 539.2	.30	.42	200- 400	3.4×10^{-4}	74.5	6.3×10^{-3}		CH
				400- 800	1.3×10^{-4}	28.5	2.1×10^{-3}		
201	571.2- 571.6		.65						CH
202	636.9- 637.3	.70	.63	400- 800	1.8×10^{-5}	3.9	4.0×10^{-4}		CH
				800-1, 600	8.1×10^{-6}	1.8	1.3×10^{-4}		
204	713.1- 713.4	.31	.46	200- 400	3.3×10^{-4}	72.3	3.6×10^{-3}		CH
				400- 800	7.0×10^{-5}	15.3	8.9×10^{-4}		
				800-1, 600	5.0×10^{-5}	11.0	4.1×10^{-4}		
206	859.7- 860.1		.19	800-1, 600	5.6×10^{-4}	122.6	4.6×10^{-3}		SC
207	901.7- 902.1	.29	.55	100- 200	1.4×10^{-4}	30.7	3.0×10^{-3}		CH
				200- 400	3.1×10^{-5}	6.6	4.9×10^{-4}		
				400- 800	1.6×10^{-5}	3.5	2.0×10^{-4}		
				800-1, 600	7.5×10^{-6}	1.6	6.1×10^{-5}		
208	972.0- 972.4	.42	.53	200- 400	2.3×10^{-4}	50.4	3.1×10^{-3}		CH
				400- 800	2.2×10^{-5}	4.8	3.6×10^{-4}		
				800-1, 600	6.5×10^{-6}	1.4	7.0×10^{-5}		
210	1,153.6-1,154.0	.21	.23	400- 800	6.2×10^{-4}	135.8	5.1×10^{-3}		CL
				800-1, 600	3.2×10^{-4}	70.0	2.2×10^{-3}		
212	1,237.7-1,238.1			400- 800	3.7×10^{-5}	8.1	2.7×10^{-4}		CH

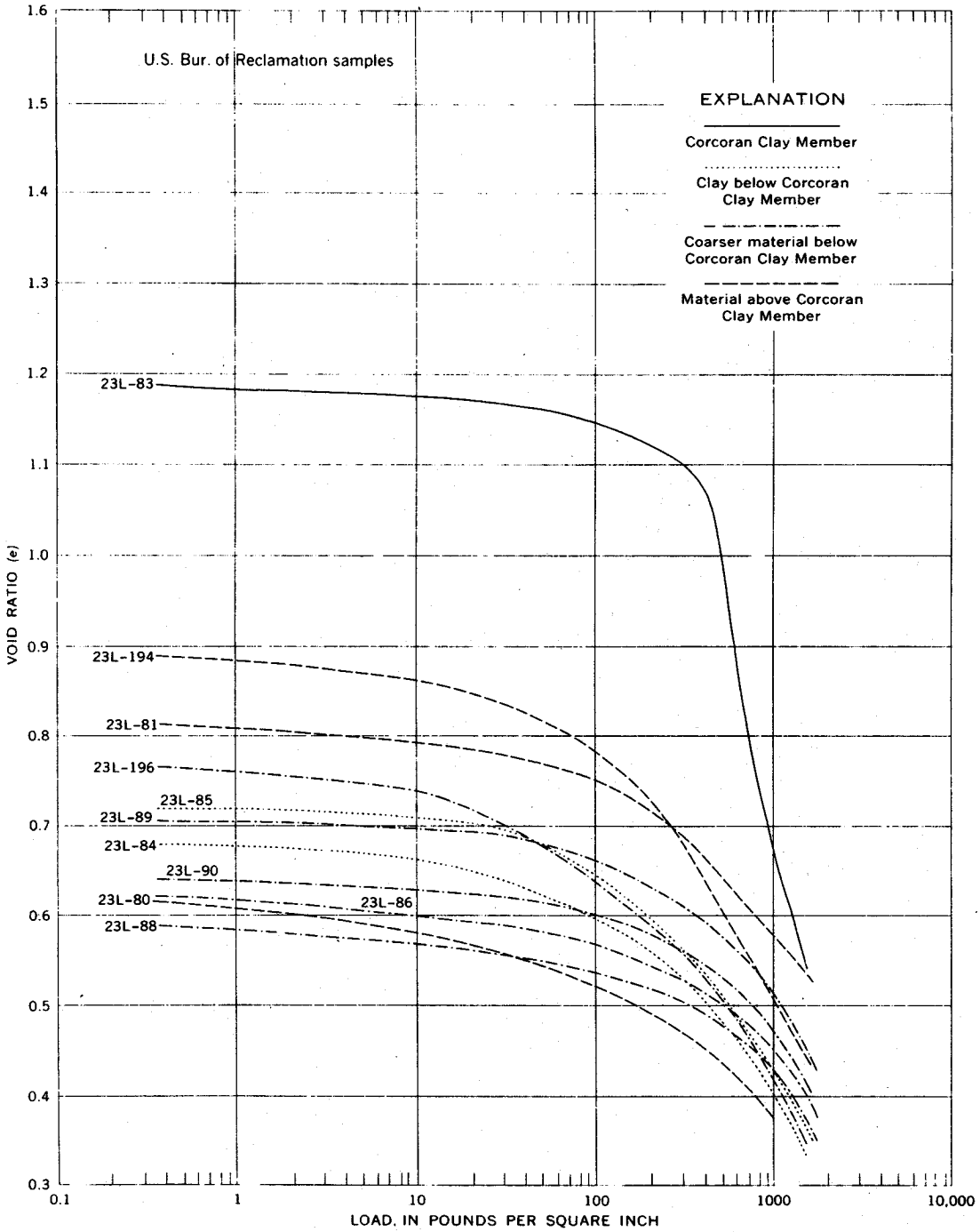

Figure 4.16 Void ratio/load curves for selected samples from core hole 14/13-llDl in the San Joaquin Valley, California.

Terzaghi and Peck equation. The solid line in each of the parts of Figure 4.17 represents the regression line for the Terzaghi and Peck equation, $C_C = 0.0009\ (w_L - 10)$.

The data in Figure 4.17 show that 10 of the 22 samples from the Los Banos-Kettleman City area, 11 of the 12 samples from the Tulare-Wasco area, and 4 of the 21 samples, from the Santa Clara Valley, lie outside the ±30 per-cent limits of scatter about the regression line for the Terzaghi and Peck equation, $C_C = 0.0009\ (w_L - 10)$. Three samples of clay in the Los Banos-

Kettleman City area have compression indices approximately twice as large as would be predicted from the Terzaghi-Peck equation. The void ratio-load curves for these three samples suggest that they are extrasensitive clays and, if so, they would be expected to plot well above the equation line. However, even if these samples are excluded, the data of Figure 4.17 show that the relationship between liquid limit and compression index for fine-textured sediments on the west side of the San Joaquin Valley does not fit the Terzaghi-Peck equation as closely as might be expected from the discussion by those authors (Terzaghi and Peck, 1948), p. 66).

Regression lines were determined by computer for the liquid limit-compression index relationship for samples from core holes in the San Joaquin and Santa Clara Valleys. Table 4.5 presents the equations of the regression lines for data from the central California area so they can be compared with the regression line for the Terzaghi and Peck equations, $C'_C = 0.0007\ (w_L - 10)$ and $C_C = 0.0009\ (w_L - 10)$. The table shows that only the equation for core hole 16/15-34N1 is approximately equivalent to either equation discussed by Terzaghi and Peck. Figure 4.17, part D, and Table 4.5 show that the equation of the regression line for 11 samples from the San Joaquin Valley (except the three samples with the exceptionally high compression indices) is $C_C = 0.014\ (w_L - 22)$ and the equation for the Santa Clara Valley is $C_C = 0.003\ (w_L + 35)$.

4.5.7.2 Correlation of compression indices

Figure 4.18 demonstrates the correlation between compression indices estimated from liquid-limit tests and those determined from consolidation curves such as are shown in Figure 4.16. In Figure 4.18 the heavy line passing through the origin at an angle of 45 degrees to the x and y axes represents absolute correlation between the values represented by the two axes. The compression indices estimated from liquid limits for the Los Banos-Kettleman City area and Santa Clara Valley generally are higher than those determined from consolidation curves and those for the Tulare-Wasco area are lower.

The data in Figure 4.18 also show that the sediments of marine origin have much higher compression indices when determined from consolidation curves than when estimated from liquid limits. Furthermore, sediments of lacustrine origin have somewhat lower compression indices when determined from consolidation curves than when estimated from liquid limits. Again, the explanation may be due to the difference in load conditions, the marine sediments being the deepest and the alluvial sediments being the shallowest.

4.5.7.3 Estimating coefficients of consolidation

Figure 4.19 shows the computed coefficient of consolidation for 1 to 4 different load ranges plotted against liquid limit for samples from the central California areas. Although the coefficient of consolidation shows a general decrease for increasing values of liquid limit, Figure 4.17 indicates that the coefficient of consolidation for any particular load range can vary through more than one order of magnitude for any given liquid limit. Terzaghi and Peck (1948, pp. 76-77) described a similar relationship for data from about 30 samples and noted that the relationship is different for each core hole as well as for each area.

4.5.7.4 Effect of soil classification

Information in Figures 4.17 and 4.18 indicates the effect of particle size and texture on the consolidation characteristics and the liquid limit. The Unified Soil Classification (Am. Soc. Testing Materials, 1964, pp. 208-220) designation, which is based on texture, is indicated at the top of Figure 4.17.

In general, those samples with a classification of CH-MH have the largest liquid limits and compression indices, and the smallest coefficients of consolidation. Samples with a classification of SC and SM have the smallest liquid limits and compression indices, and the largest coefficient of consolidation. Samples with a classification of ML, CL and CH have values somewhere between these two extremes. Samples of sediments of alluvial origin tended to be classified as CL and CH; and those of marine origin were classified primarily as CH-MH.

4.5.7.5 Relationship of consolidation characteristics and liquid limits

Data presented in this chapter show that the equations presented by Terzaghi and Peck (1948) (equations 4.16 and 4.17) do not apply to the relationship between compression index and liquid limit for sedimentary deposits tested from the central California subsidence areas.

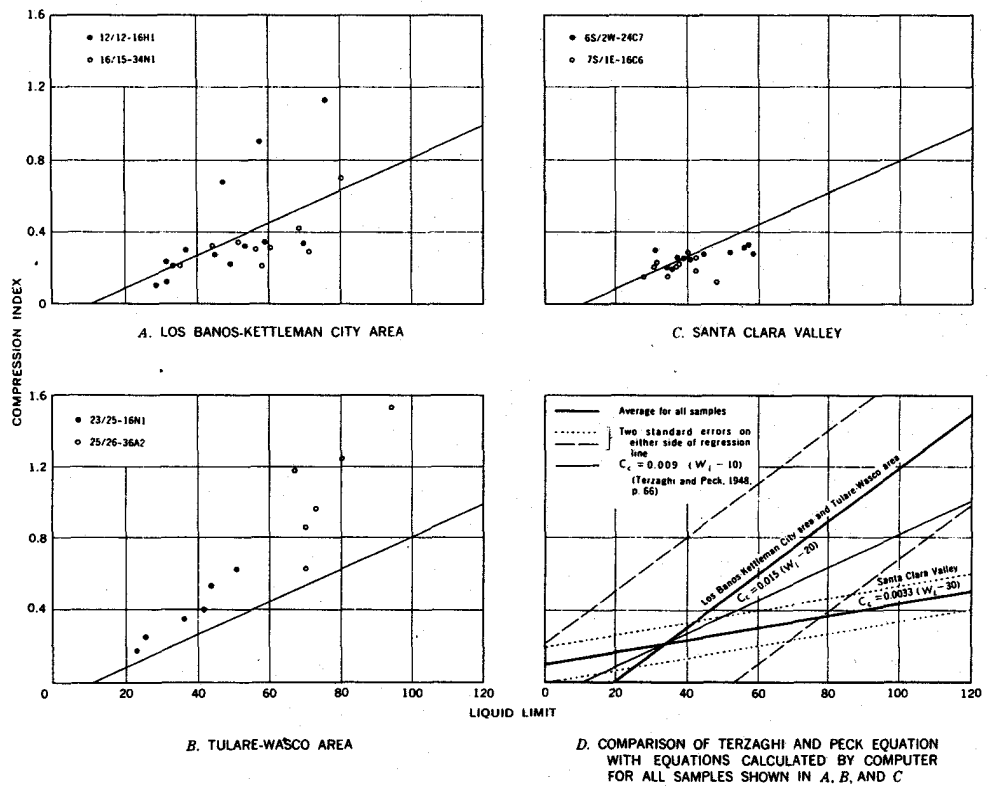

Figure 4.17 Relation between liquid limit and compression index for selected samples from core holes in San Joaquin and Santa Clara Valleys, California.

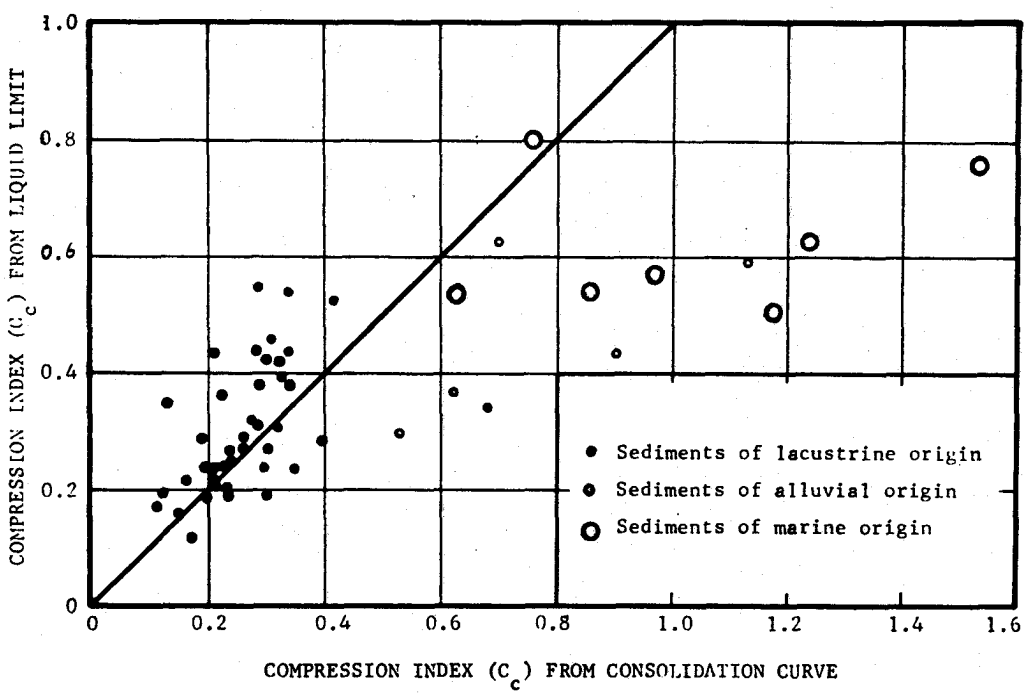

Figure 4.18 Comparison of two methods for determination of compression index for all samples from subsidence areas in the San Joaquin and Santa Clara Valleys, California.

Table 4.5 Equations for regression lines for various groups of data from subsiding areas in central California

Data used	Equation
Los Banos-Kettleman City area	
Core hole 12/12-16Hl, exclusive of the 3 samples with exceptionally high compression indices	$C_C = 0.005\ (w_L=6)$
Core hole 16/15-34N1	$C_C = 0.007\ (w_L-12)$
All samples in area, exclusive of 3 samples with exceptionally high compression indices	$C_C = 0.006\ (w_L-3)$
Tulare-Wasco area	
Core hole 23/25-16Nl	$C_C = 0.015\ (w_L-l$
Core hole 24/26-36A2	$C_C = 0.024\ (w_L-32)$
All samples in area	$C_C = 0.018\ (w_L-16)$
San Joaquin Valley, exclusive of 3 samples with exceptionally high compression indices	$C_C = 0.014\ (w_L-22)$
Santa Clara Valley	
Core hole 6S/2W-24C7	$C_C = 0.003\ (w_L-47)$
Core hole 7S/lE-16C6	$C_C = 0.0005\ (W_L+370)$
All samples in area	$C_C = 0.003\ (w_L+35)$

Furthermore, the data show that no single equation applies to the relationship for all areas studied, with the following equations being obtained for the two valleys:

San Joaquin Valley: $C_C = 0.014\ (w_L - 22);$ (4.18)

Santa Clara Valley: $C_C = 0.003\ (w_L + 35).$ (4.19)

In essentially every case, the equations of the regression lines represent only general trends because there is considerable scatter of data for all core holes. The trend line for data from the Santa Clara Valley is so nearly horizontal that a rather narrow range of compression indices could be obtained over a wide range of liquid limits. Compression indices estimated from liquid limits, however, showed better correlation with indices determined from consolidation curves when the sediments were of alluvial or lacustrine origin than when they were of marine origin.

All coefficients of consolidation showed a general decrease for increasing values of liquid limit. However, because the coefficients for any particular load range could vary through more than one order of magnitude for any given liquid limit, the relationship could not be estimated with reasonable accuracy. In fact, the general trend for the relationship even varies, for each subsidence area and for each core hole.

At least for the areas studied in central California, the consolidation characteristics of the undisturbed sediments in the field cannot be closely approximated by liquid limits, which are made on disturbed samples of those sediments. The studies also indicate that the equations reported by Terzaghi and Peck (1948) must be used with extreme caution to estimate the consolidation characteristics of sediments in areas of subsidence--especially if the compacting sediments are at considerable depth.

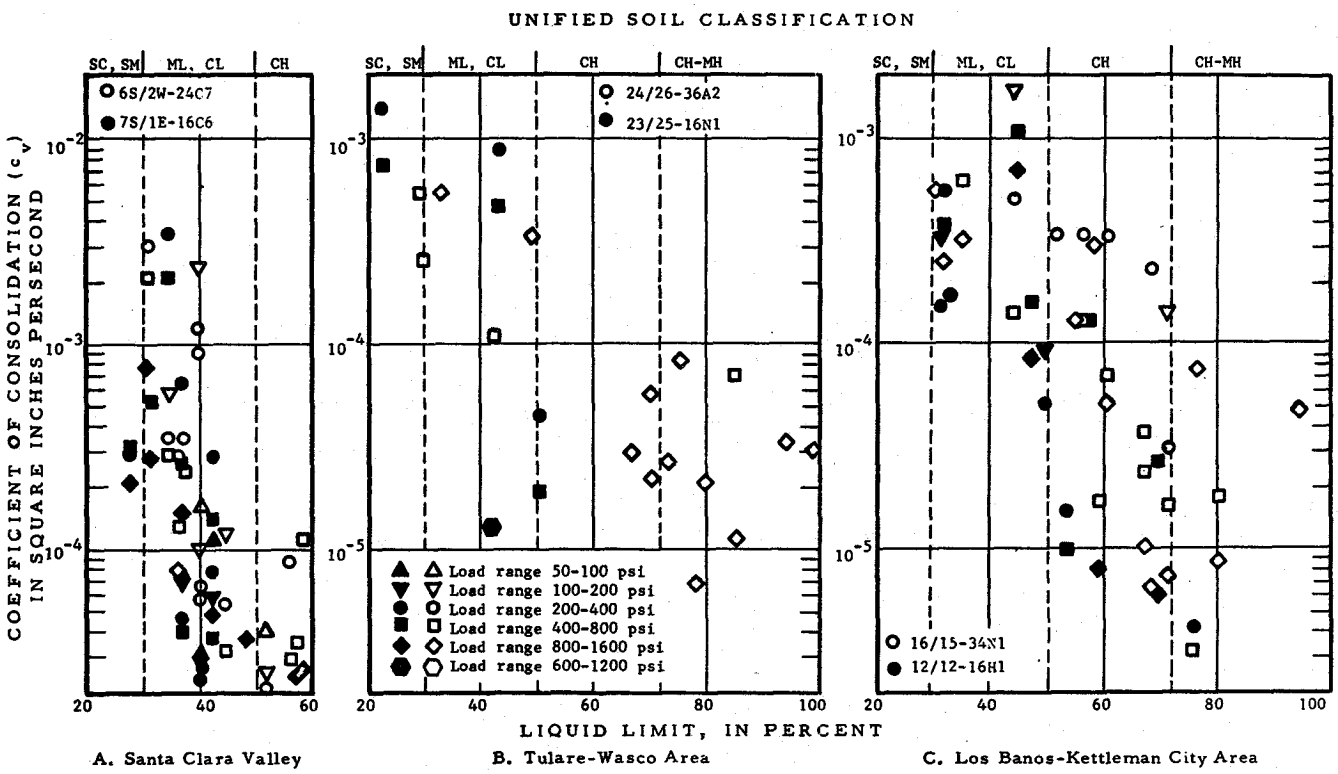

Figure 4.19 Relation of coefficient of consolidation to liquid limit for samples from core holes in the San Joaquin and Santa Clara Valleys, California.

4.6 REFERENCES

AMERICAN GEOLOGICAL INSTITUTE. 1960. Glossary of geology and related sciences, 2d ed. Washington, 397 p.

AMERICAN SOCIETY FOR TESTING MATERIALS. 1980. Annual Book of Standards, Part 19. Philadelphia, 654 p.

ATHY, L. P. 1930. Density, porosity, and compaction of sedimentary rocks. Am. Assoc. Petroleum Geologists Bull., v. 14, pt. 1, no. 1, p. 1-24.

ATTERBERG, A. 1911. Über die physikalische bodenuntersuchung, und Über die plastizitat der tone. Internat. Mitt. Bodenkunde, v. 1, p. 10-43.

BULL, W. B. 1961. Causes and mechanics of near-surface subsidence in western Fresno County, California, in Short papers in the geologic and hydrologic sciences. U.S. Geol. Survey Prof. Paper 424-B, p. B187-B189.

BULL, W. B. 1964. Alluvial fans and near-surface subsidence, western Fresno County, California. U.S. Geol. Survey Prof. Paper 437-A, p. Al-A71.

CALIFORNIA STATE WATER RESOURCES BOARD. 1955. Santa Clara Valley investigation, Sacramento, Bull., 7, 154 p.

CASAGRANDE, ARTHUR. 1932. Research on the Atterberg limits of soils. Public Roads, v. 13, no. 9, p. 121-136.

CASAGRANDE, ARTHUR. 1948. Classification and identification of soils. Am. Soc. Civil Engineers Trans., v. 113, p. 901-930.

CLARK, W. 0. 1924. Ground water in Santa Clara Valley, California. U.S. Geol. Survey Water Supply Paper 519, 209 p.

DAVIS, G. H., and POLAND, J. F. 1957. Ground-water conditions in the Mendota-Huron are Fresno and Kings Counties, California. U.S. Geol. Survey water-Supply Paper 1360-G, 409-588.

GIBBS, H. J. 1953. Estimating foundation settlements by one-dimensional consolidation test Denver, Colo. U.S. Bureau of Reclamation Eng. Mon. 13, 24 p.

GIBBS, H. J. 1959. A laboratory testing study of land subsidence. Pan-Am. Conf. Soil Mech Found. Eng., lst, Mexico City, 1959, Proc., p. 3-36.

GOLDSCHMIDT, V. M. 1926. Undersokelser over lersedimenter. Beretning om Nordiske Jordbrugs forskeres Kongress i Osla, Copenhagen Nordisk Jordsbrugsforskning, v. 4, no. 7, p. 434-445.

INTER-AGENCY COMMITTEE ON LAND SUBSIDENCE IN THE SAN JOAQUIN VALLEY. 1955. Proposed program for investigating land subsidence in the San Joaquin Valley, California. Sacramento, Calif., 60 P.

INTER-AGENCY COMMITTEE ON LAND SUBSIDENCE IN THE SAN JOAQUIN VALLEY. 1958, Progress report on land-subsidence investigations in the San Joaquin Valley, California, through 1957. Sacramento, Calif., 160 p. 45 p1s., 5 tables.

JOHNSON, A. I., and MORRIS, D. A. 1962a. Physical and hydrologic properties of water-bearing deposits from core holes in the Los Banos-Kettleman City area, California. U. S. Geological Survey open file report, 182 p.

JOHNSON, A. I., and MORRIS, D. A. 1962b. Relation of volumetric shrinkage to clay. content of sediments from the San Joaquin Valley, California, in Short papers in geology, hydrology, an topography. U.S. Geol. Survey Prof. Paper 450-B, p. B43-B44.

JOHNSON, A. I., and MOSTON, R. P. 1969. Relationship of consolidation characteristics an Atterberg limits for subsiding sediments in Central California, U.S.A. Internat. Symposium on Land Subsidence, Tokyo, IAHS, p. 579-587.

JOHNSON, A. I., MOSTON, R. P., and MORRIS, D. A. 1968. Physical and hydrologic properties of water-bearing deposits in subsiding areas in central California. U.S. Geol. Survey Prof. Paper 497-A, 71 p., 14 p1s.

KRUMBEIN, W. C., and PETTIJOHN, F. J. 1938. Manual of sedimentary petrography. New York, Appleton-Century-Crofts, Inc., 549 p.

LANE, E. W., Chairman. 1947. Report of the Subcommittee on Sediment Terminology. Am. Geophys. Union Trans., v. 28, p. 936-938.

LOFGREN, B. E. 1960. Near-surface land subsidence in western San Joaquin Valley, California. Jour. Geophys. Research, v. 65, no. 3, p. 1053-1062.

LOFGREN, B. E. 1963. Land subsidence in the Arvin-Maricopa area, San Joaquin Valley, California, in Short papers in geology and hydrology. U.S. Geol. Survey Prof. Paper 475-B, p. B171-175.

LOFGREN, B. E. 1969. Field measurement of aquifer-system compaction, San Joaquin Valley, California.Internat. Symposium on Land Subsidence, Tokyo--1969, I.A.S.H. Pub. 88, p. 272-284.

MEADE, R. H. 1964. Removal of water and rearrangement of particles during the compaction of clayey sediments--review. U.S. Geol. Survey Prof. Paper 497-B. 23 p.

MEADE, R. H. 1967. Petrology of sediments underlying areas of land subsidence in central California. U.S. Geol. Survey Prof. Paper 497-C, 83 p.

MEINZER, 0. E. 1923. The occurrence of ground water in the United States, with a discussion of principles. U.S. Geol. Survey Water-Supply Paper 489, 321 p.

MEINZER, 0. E., ed. 1949. Hydrology, in Physics of the Earth. New York, Dover Pubs., Inc., 712 p.

MILLER, R. E. 1961. Compaction of an aquifer system computed from consolidation tests and decline in artesian head, in Short papers in the geologic and hydrologic sciences. U.S. Geol. Survey Prof. Paper 424-B, p. B54-58.

MORRIS, D. A., and JOHNSON, A. I. 1959. Correlation of Atterberg limits with geology of deep cores from subsidence areas in California. Am. Soc. Testing Materials Spec. Tech. Pub. 254, p. 183-187.

NISHIDA, YOSHICHIKA. 1956. A brief note on compression index of soil. Am. Soc. Civil Engineers, Soil Mech. Found. Div. Jour., vol. 82, SM 3, Paper 1027, 14 p.

POLAND, J. P. 1960. Land subsidence in the San Joaquin Valley, California, and its effect on estimates of ground-water resources, in International Association of Scientific Hydrology Commission of Subterranean Waters. I.A.S.H. pub. 52, p. 324-335.

POLAND, J. P. 1969. Land subsidence and aquifer system compaction, Santa Clara Valley, Calif. Internat. Symposium on Land Subsidence, Tokyo 1969, I.A.S.H. pub. 88, p. 285-294.

POLAND, J. F., and DAVIS, G. H. 1956. Subsidence of the land surface in the Tulare-Wasco (Delano) and Los Banos-Kettleman City areas, San Joaquin Valley, California. Am. Geophys. Union Trans., v. 37, no. 3, p. 287-296.

POLAND, J. F., and GREEN, J. H. 1962. Subsidence in the Santa Clara Valley, California--A progress report. U.S. Geol. Survey Water-Supply Paper 1619-C, 16 p.

REITEMEIER, R. F. 1946. Effect of moisture content on the dissolved and exchangeable ions of soils of arid regions. Soil Sci., v. 61, p. 195-214.

RILEY, F. S. 1969. Analysis of bore-hole extensometer data from Central California. Internat. Symposium on Land Subsidence, Tokyo 1969, I.A.S.H. pub. 89, p. 423-431.

ROBERTS, D. V., and DARRAGH, R. D. 1962. Areal fill settlements and building foundation behavior at the San Francisco airport, in Field testing of soils. Am. Soc. Testing materials Spec. Tech. Pub. 322, p. 211-230.

SHEPARD, F. P. 1954. Nomenclature based on sand-silt-clay ratios. Jour. Sed. Petrology, v. 24, no. 3, p. 151-158.

SKEMPTON, A. W. 1944. Notes on the compressibility of clays. Geol. Soc.--London Quart. Jour., vol. C, p. 119-135.

TAYLOR, D. W. 1948. Fundamentals of soil mechanics. New York, John Wiley & Sons, Inc., 700 p.

TERZAGHI, KARL. 1926. Simplified soil tests for subgrades and their physical significance. Public Roads, v. 7, p. 153-162.

TERZAGHI, KARL. 1943. Theoretical soil mechanics. New York, John Wiley & Sons, Inc., 510 p.

TERZAGHI, KARL, and PECK, R. B. 1,948. Soil mechanics in engineering practice. New York, John Wiley & Sons, Inc. 566 p.

TRASK, P. D. .1932. Origin and environment of source sediments of petroleum, Houston. Gulf Publishing Co., 323 p.

TWENHOFEL, W. H., and TYLER, S. A. 1941. Methods of study of sediments. New York, McGraw-Hill Book Co., Inc., 183 p.

U.S. BUREAU OF RECLAMATION. 1974. Earth manual. Denver, 751 p.

WENTWORTH, C. K. 1922. A scale of grade and class terms for elastic sediments. Jour. Geology, v. 30, p. 377-392.

WENZEL, L. K. 1942. Methods for determining permeability of water-bearing materials. U.S Geol. Survey Water-Supply Paper 887, 192 p.

5 Techniques for prediction of subsidence, by Germán Figueroa Vega, Soki Yamamoto, and Working Group (Section 5.3.6 by Donald C. Helm)

It is very important to predict the amount of subsidence and to estimate the subsidence rate in the near future. There are many methods for predicting the amount of land subsidence due to the overdraft of fluids from aquifers. Some methods are simple and others are complex. It is preferable to use several methods whenever possible and to reach a conclusion based on the overall judgment.

Both adequate and accurate data are required to obtain useful results, although these depend on the purpose, time length of the forecast, and cost. The methods used may be classified into the following categories: (1) Empirical methods; (2) semi-theoretical approach; (3) theoretical approach.

5.1 EMPIRICAL METHODS

This is the method of extrapolating available data to derive the future trend. It is a time series model. The amount of subsidence, the amount of compaction, and sometimes tidal height near the sea coast, are available to plot against time. In this method, the amount of subsidence is considered a function of time, ignoring causality of land subsidence.

5.1.1 Extrapolation of data by naked eye

No explanation of this procedure is needed except that a smooth curve with a natural trend should be obtained.

5.1.2 Application of some suitable curve: Nonlinear extrapolation

1. Fitting of quadratic function (Figure 5.1):
   The following function is used and the least squares method is applied:

   $s = ax^2 + bx + c$, or $s = ax + b$, (5.1)

   where
   s = subsidence amount,
   x = time, and
   a, b, and c are constants.

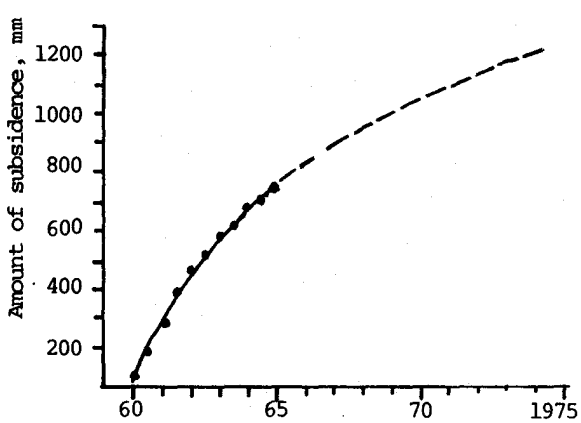

Figure 5.1 Fitting of quadratic curve (bench mark no. 2179, Niigata).

2. Fitting of exponential or logarithmic function (Figures 5.2 and 5.3):
   The following function is applied and the least squares method is used:

   $s = ax^b$, $\log s = \log a + b \log x$, or(5.2)

   $s = ae^{bx}$,

   where
   s = amount of subsidence,
   x = time, and
   a and b are constants.

Many data correlating land subsidence and water level have been published. Figures 5.4 through 5.7 are four examples of such correlations.

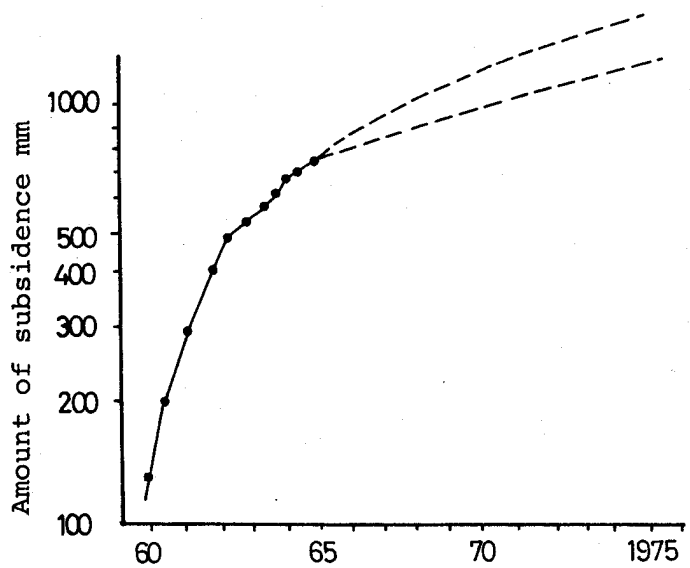

Figure 5.2 Fitting of exponential curve (bench mark no. 2179, Niigata)

.

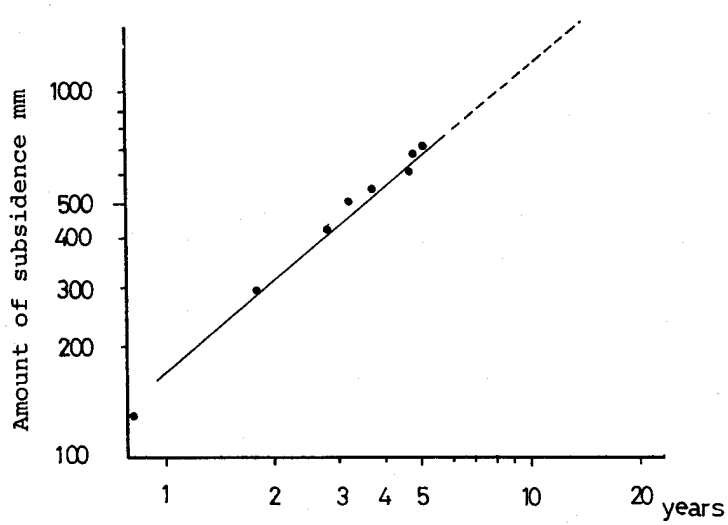

Figure 5.3 Log-log relation between subsidence and years.

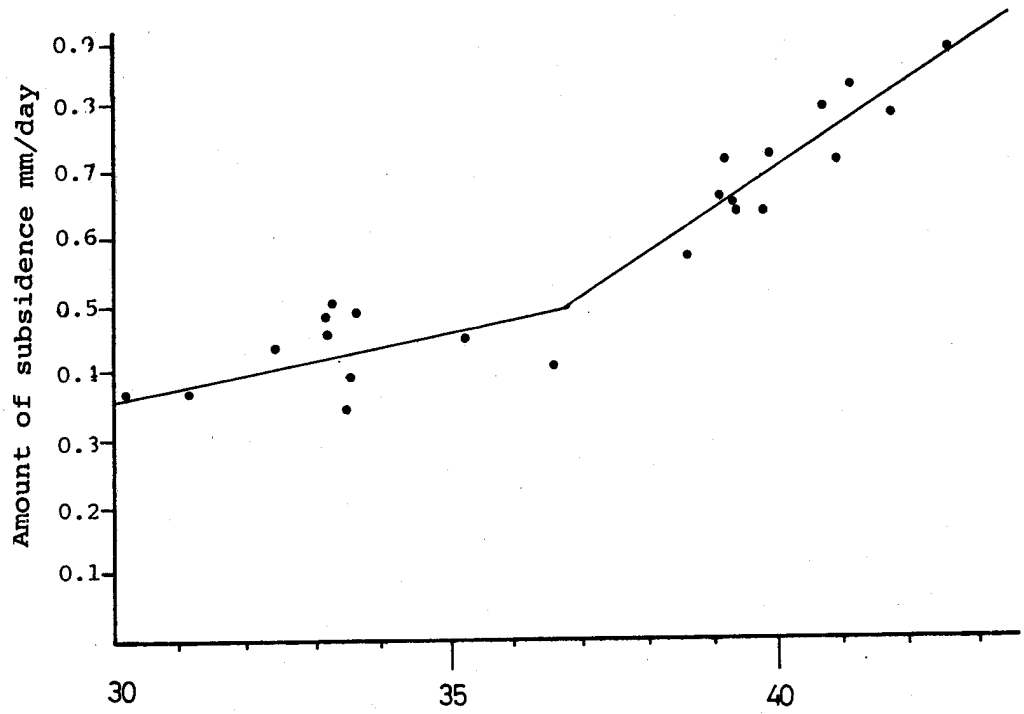

Figure 5.4 Correlation of land subsidence and water level in well 610 metres deep, Tokyo, Japan.

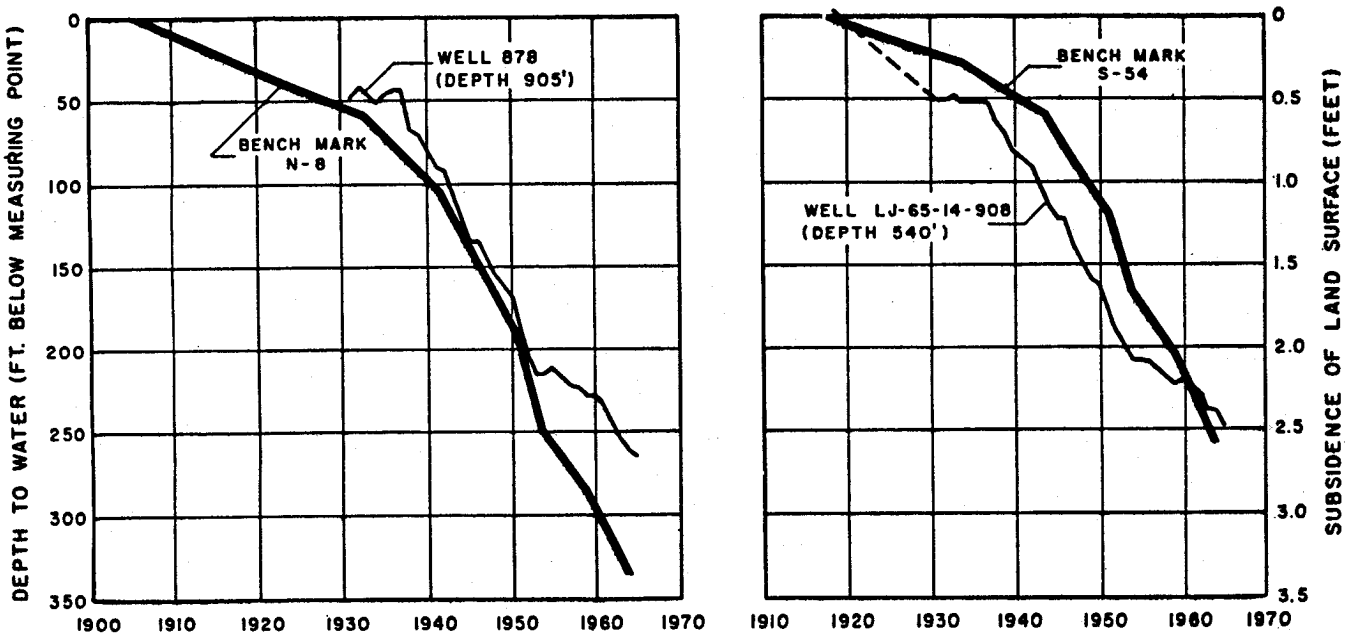

Figure 5.5 The relation between water-level declines and land-surface subsidence in the Houston area, Texas (Gabrysch, 1969).

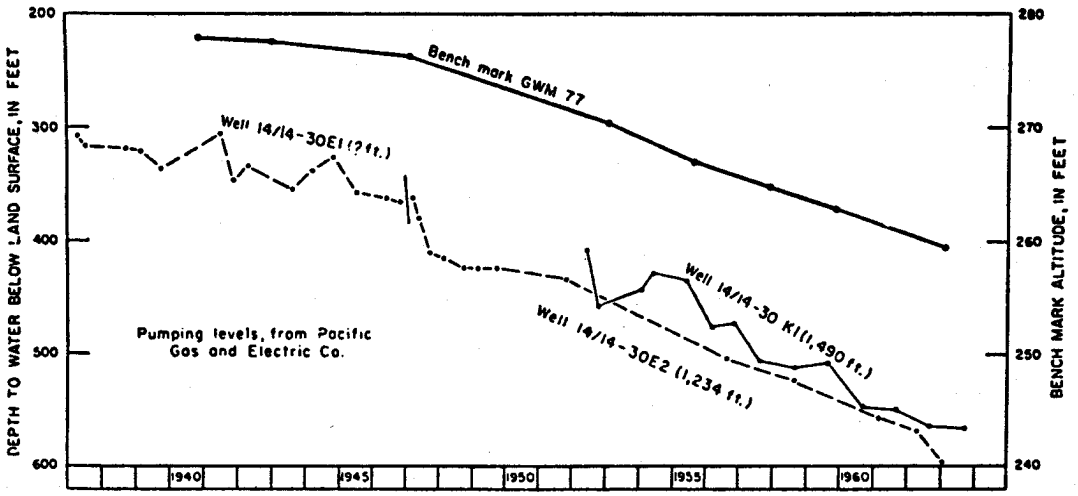

Figure 5.6 Correlation between subsidence and change in artesian head near center of subsidence west of Fresno, California (Lofgren, 1969).

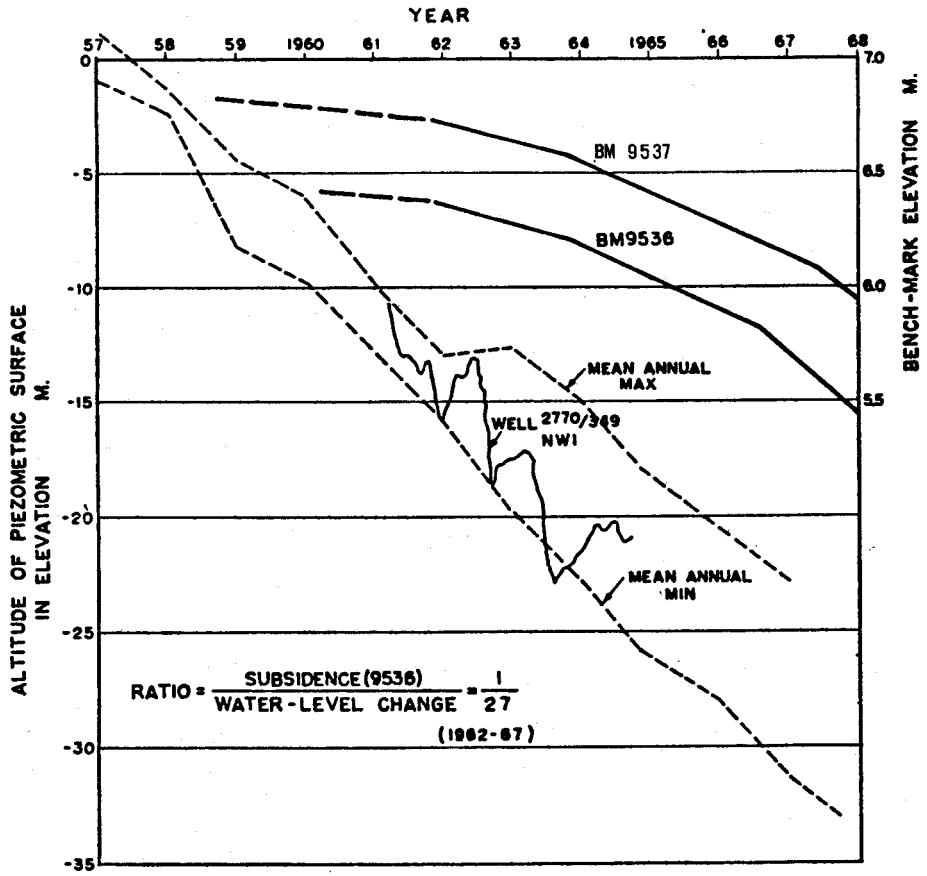

Figure 5.7 Change in altitude at BM9536, -37 and change in artesian head in nearby wells (Hwang and Wu, 1969).

5.2 SEMI-THEORETICAL APPROACH

This method utilizes the relation between subsidence and related phenomena. Although the relation is not strictly theoretical but rather an apparent one, still it can be used to estimate future trend.

5.2.1 Wadachi's (1939) model

Wadachi (1940) pointed out that the rate of subsidence, not the amount of subsidence itself, is proportional to the water-level change (Figure 5.8) and proposed the following equation:

$$\frac{dH}{dt} = k(p_0 - p) \tag{5.3}$$

where

$\frac{dH}{dt}$ = of subsidence,
p_0 = reference water level,
p = water level, and
k = a constant

This suggests that there exists a reference water level. That is to say, if the water level p recovers to the reference water level p_0, no subsidence occurs. But according to Yamaguchi's recent study (1969) there is no such reference water level. In place of Wadachi's equation, he proposed the following one:

$$\frac{ds}{dt} = ks_c\left\{(p_0 - p)t - \frac{dp}{dt}\right\}\exp\{-k(p_0 - p)t\}, \tag{5.4}$$

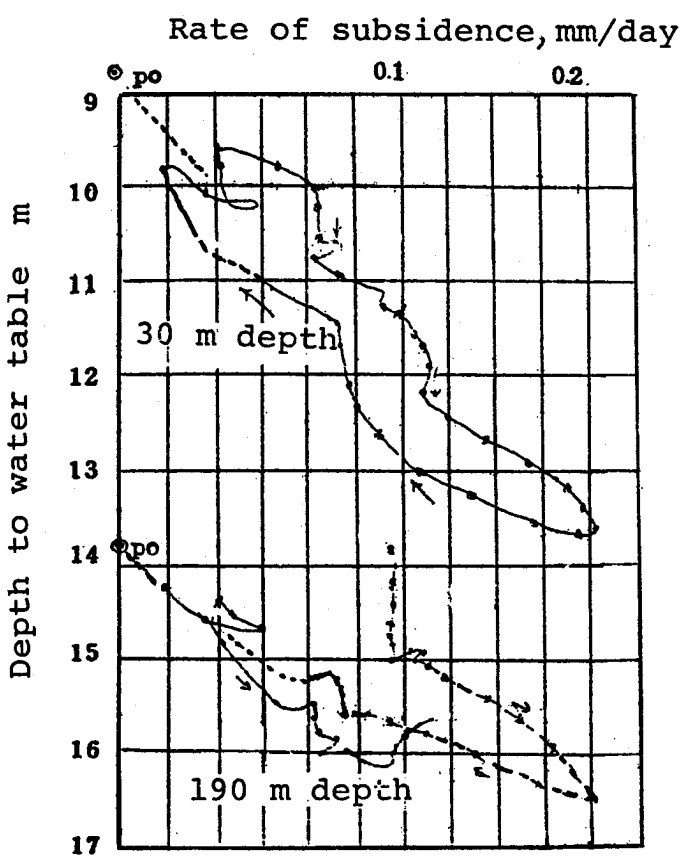

Figure 5.8 Relation between water level and rate of subsidence.

where

$\frac{ds}{dt}$ = rate of subsidence,
s_c = final subsidence amount,
P_0 = initial water level,
p = water level,
k = constant, and
t = time.

On solving this equation, the quantities

$$Y = \log\left[\frac{ds}{dt} \Big/ \left\{(p_0 - p)t - \frac{dp}{dt}\right\}\right] \text{ and } x = (p_0 - p)$$

are plotted on the respective axes as in Figures 5.9a and 5.9b and s_c can be obtained.

5.2.2 Ratio of subsidence volume to liquid withdrawal

According to Yamamoto (personal communication), the relation between liquid production and subsidence in the Niigata gas field (case history 9.7) has been expressed by the following equations, with fair results:

$$s = aQ + b, \text{ or } s = a\sqrt{Q} + b, \tag{5.5}$$

where

s = subsidence,
Q = amount of liquid production, and
a and b are constants.

Castle, Yerkes, and Riley (1969) stated that direct comparisons between the various measures of liquid production and subsidence in six oil fields showed a close relation. Correlation between production and subsidence has varied approximately linearly with net production (Figure 5.10).

The following relation has also been established but not yet published (Yamamoto, personal communication):

$$s = C/m_V \tag{5.6}$$

where

s = subsidence,
m_V = coefficient of volume compressibility, and
C = $\Delta H/\Delta Q$, where ΔH and ΔQ are the change of bench-mark elevation and the amount of production per unit area, respectively.

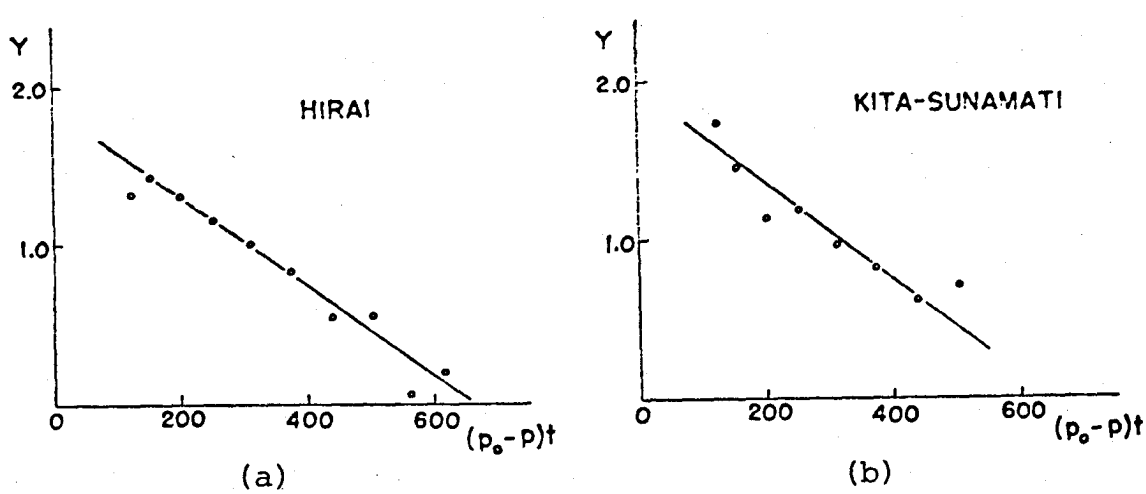

Figure 5.9 Relation between Y and $(p_0 - p)t$.

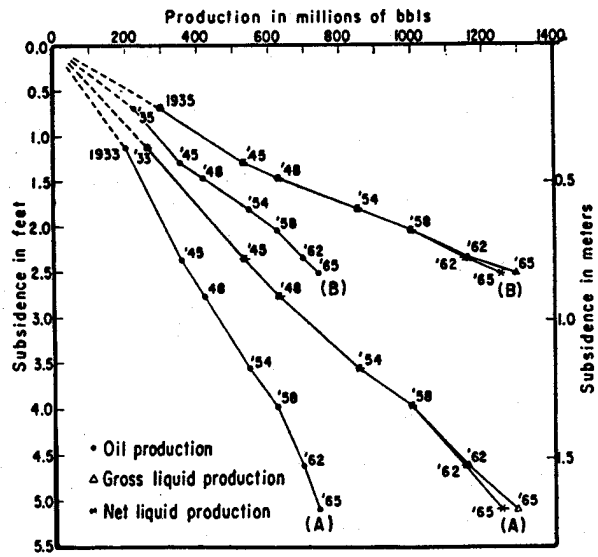

Figure 5.10 Cumulative oil, gross-liquid, and net-liquid production from the Huntington Beach oil field plotted against subsidence at bench marks located (A) near the center of subsidence and (B) midway up the southeast limb of the subsidence bowl. Prepared from production statistics of the California Division of Oil and Gas and elevation data of the U.S. Coast and Geodetic Survey and the Orange County Office of County Surveyor and Road Commissioner. Easily related elevation measurements have been available only since 1933; estimates of subsidence since 1920 shown by dashed lines (Castle, Yerkes, and Riley, 1969).

In one region in Japan, the change of the computed leakage rate, L, plotted against the measured volumetric land-subsidence rate, V_S, showed a close correlation (Figure 5.11).

On the Shiroishi Plain, Kyushu, Japan, Shibasaki et al (1969) proposed the following simple relationship for the data in the three-year period 1963 to 1966:

$$V_S = 0.27\ L + 0.25, \tag{5.7}$$

where each unit is expressed in $10^6 m^3$/mo (cubic metres per month) (Figure 5.12).

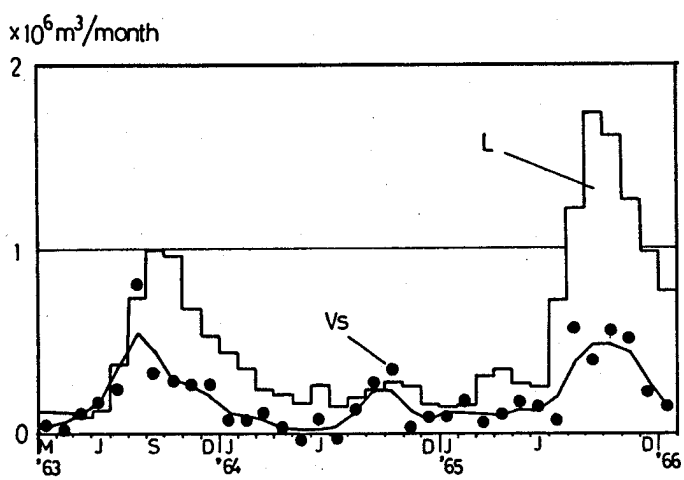

Figure 5.11 Changes of leakage rate, L, and volumetric land subsidence rate, V_S, both in m^3/month, over Shiroishi basin (Shibasaki, Kamata, and Shindo, 1960).

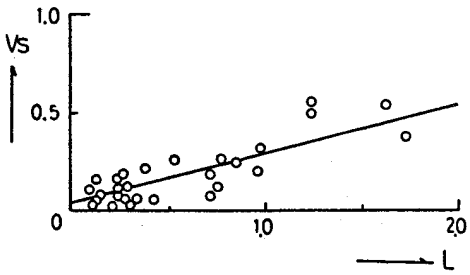

Figure 5.12 Simple relationship between leakage rate and volumetric subsidence rate over Shiroshi basin (Shibasaki, et al., 1969).

Although Castle, Yerkes, and Riley (1969) found that subsidence in six oil fields varied approximately linearly with net liquid production, the correlation between reservoir-pressure decline and subsidence was poor. Their explanation for this is as follows:

> "The general theory advanced in explanation of reservoir compaction and resultant oil-field subsidence (Gilluly and Grant, 1949) is, in its broad outlines, beyond challenge. Thus Terzaghi's principle, which relates increased effective stress directly to fluid pressure decline, probably is validly applied to the multifluid-phase system. Yet in seeming opposition to this generalization, measured reservoir pressure decline within the Vickers zone was disproportionately high with respect to surface subsidence during the early production years (Figure 2a and d); a similar situation is believed to have prevailed in the Wilmington field (City of Long Beach, 1967, unpublished data). Whatever the relationship, then, between measured reservoir pressure decline and compaction, the two are certainly not directly proportional.
> "The most likely explanation for the poor correlation between reservoir-pressure decline and subsidence (or compaction) is that pressure decline as measured at individual producing wells is generally non-representative of the average or systemic decline over the field as a whole. Thus in examining this problem in the Wilmington field, Miller and Somerton (1955, p. 70) observed that 'reductions in average pressure in the reservoir are virtually impossible to determine with a satisfactory degree of accuracy.' This deduction, coupled with the observed linearity between net-liquid production and subsidence, suggests that the liquid production may constitute a better index of average reservoir-pressure decline than that obtained through down-hole measurements."

Figures 5.13, 5.14, and 5.15 present additional examples illustrating the relation between fluid withdrawal and subsidence. Figure 5.13 shows the relation between land subsidence in mm/year and annual discharge in 106m3/year on the Shiroishi Plain in Japan (From Kumai, et al., 1969). Figure 5.14 illustrates the stress-strain relation obtained by plotting discharge in $10^3 m^3$/month against land subsidence in mm/month in Osaka, Japan, for the five years 1954-1958. Figure 5.15 shows the consistent relationship between the cumulative volumes of subsidence and ground-water pumpage in the Los Banos-Kettleman City area, California, from 1926 to 1968. The volume of subsidence was equal to one-third the volume of pumpage consistently through the 42-year period.

5.2.3 Ratio of subsidence to head decline

The subsidence/head-decline ratio is the ratio between land subsidence and the head decline in the coarse-grained permeable beds of the compacting aquifer system, for a common time interval. It represents the change in thickness per unit change in effective stress ($\Delta b/\Delta p'$). This ratio is useful for predicting a lower limit for the magnitude of subsidence in response to a step increase in virgin stress (stress exceeding past maximum). If pore pressures in the compacting aquitards reach equilibrium with those in adjacent aquifers, then compaction stops and the subsidence/head-decline ratio is a true measure of the virgin compressibility of the system. Until or unless equilibrium of pore pressures is attained, the ratio of subsidence to head decline is a transient value.

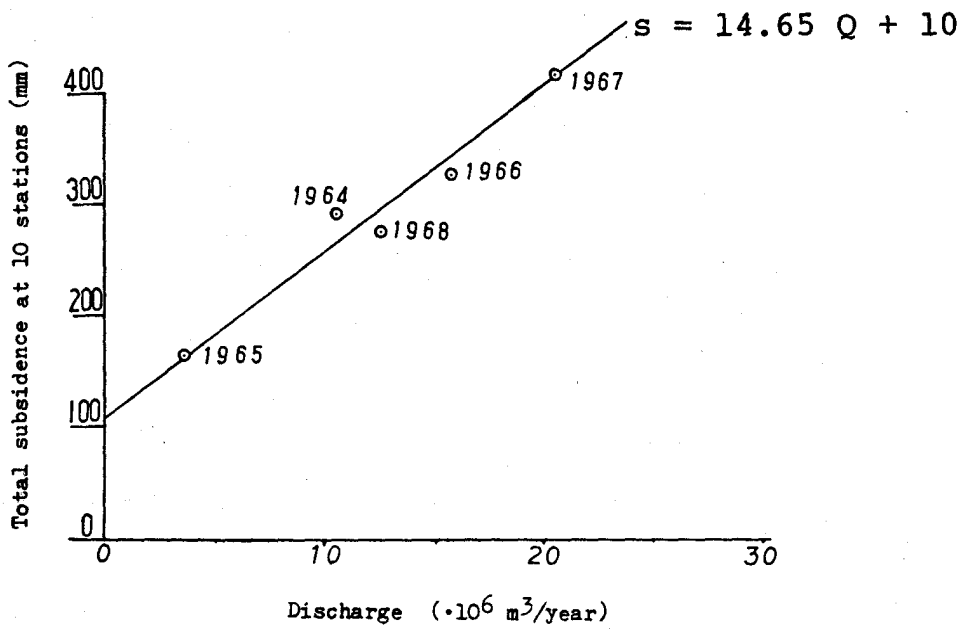

Figure 5.13 Simple relationship between annual land subsidence and corresponding discharge (Kumai, et al., 1969).

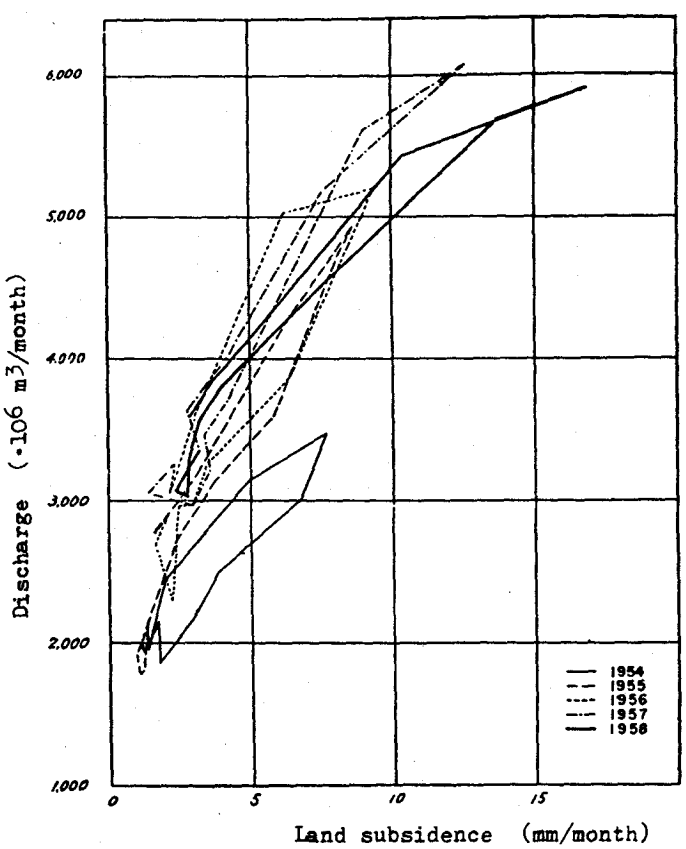

Figure 5.14 Correlation between subsidence and discharge of ground water (Editorial Committee for Land Subsidence in Osaka, 1969).

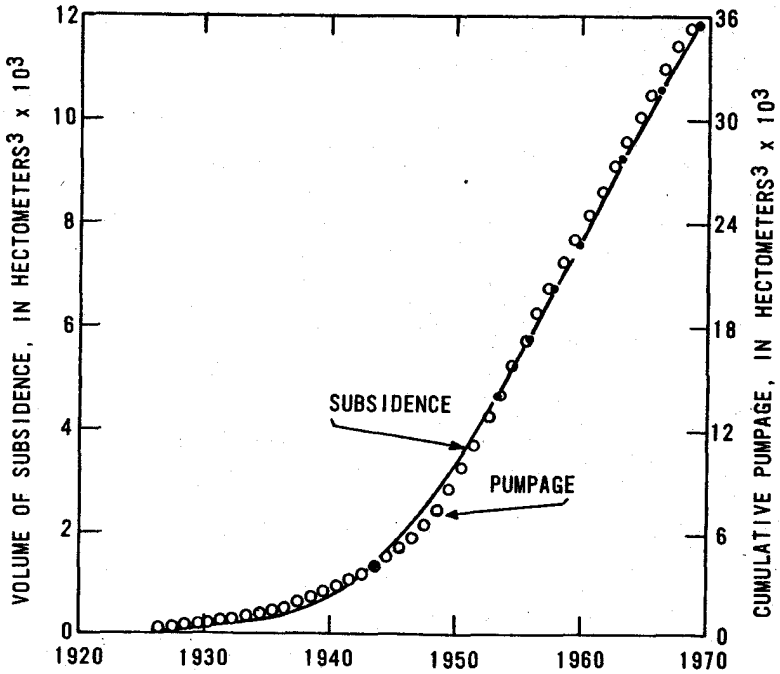

Figure 5.15 Cumulative volumes of subsidence and pumpage, Los Banos-Kettleman City area, California. Points on subsidence curve indicate times of leveling control (from Poland, et al., 1975).

Subsidence/head-decline ratios can be derived at a point if the water-level change for the compacting system and the periodic surveys of the elevation of a nearby bench mark are available for a common time period. For example, Figure 5.5 illustrates the subsidence and head-decline records for a pair of bench marks and nearby wells in Houston, Texas. At plotting scales of 1 (subsidence) to 100 (water level), the plots are roughly coincident. The indicated subsidence/ head-decline ratio is approximately 1/100.

Figure 5.6 is another example of close correlation between subsidence and head decline. The intensive pumping of ground water for more than two decades caused an artesian-head decline of about 300 ft (90m), producing a subsidence of about 18 ft (5.5 m). The indicated subsidence/ head-decline ratio is 1/16 (Lofgren, 1969). Although the ordinate scales in figures 5.5 and 5.6 are in feet, the ratio is dimensionless and hence would be identical in the metric system.

From the subsidence and head-decline record for Figure 5.7, Hwang and Wu (1969) derived a subsidence/head-decline ratio of 1/27 for the period 1962-67. Note, however, that although the mean annual minimum water-level trend is approximately a straight line, the rate of subsidence accelerated sharply in 1967. Hence, a ratio derived from the subsidence rate and water-level change in 1967 would be much larger, roughly about 1/12.

For all three of the examples discussed (Figures 5.5-5.7) it should be emphasized that the ratios are reliable only if the water levels are representative of the average artesian head in the aquifers (coarse-grained beds) of the compacting system.

If maps of subsidence and head decline are available for a common period of time during which both subsidence and head decline continued without interruption, the ratio of subsidence to head decline can be plotted on a map as lines of equal ratio. Figure 5.16 is such a ratio map, plotted from maps showing subsidence and head decline from 1943 to 1959 in an area of 4000 km^2 on the west side of the San Joaquin Valley, California (after Bull and Poland, 1975, Figure 32). The ratios on this map range from 0.08 to 0.01, indicating that the head decline required to produce 1 m of subsidence has ranged from 12 to 100 m, depending on the location. In addition to their use in prediction, the ratios in Figure 5.16 represent a minimum value of the storage coefficient component for virgin compaction of the aquifer-system skeleton.

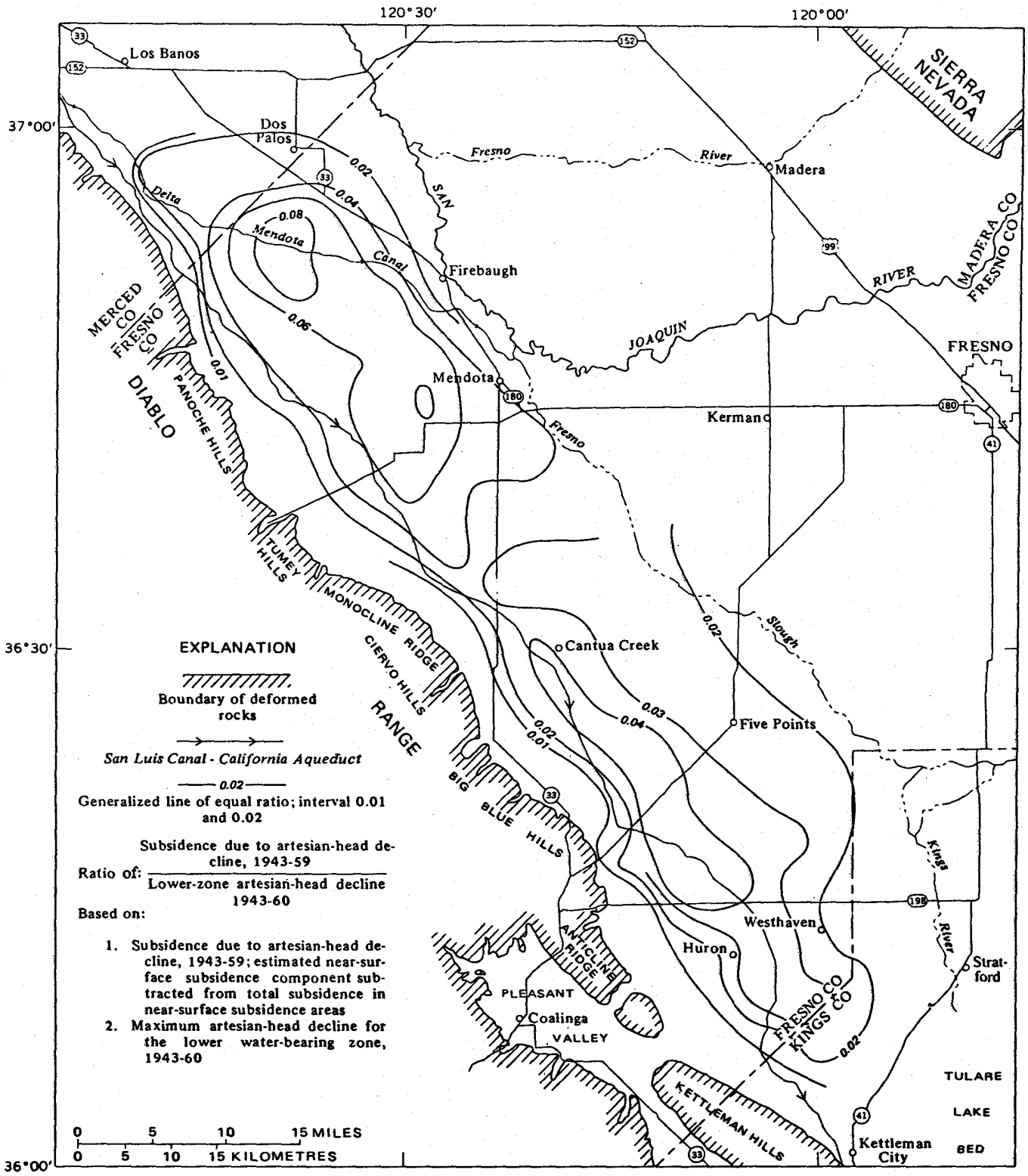

Figure 5.16 Ratio of subsidence to head decline, west side of San Joaquin Valley, California, 1943-59 (Bull and Poland, 1975, Figure 32).

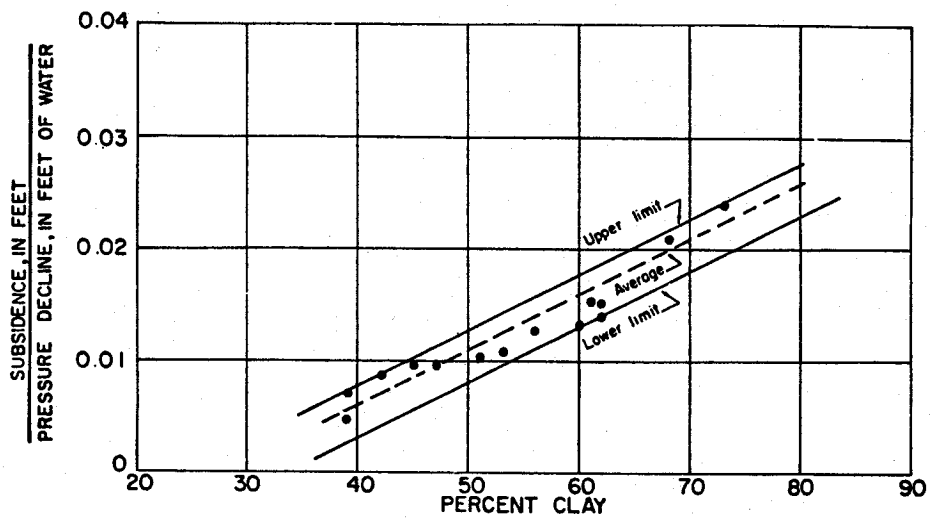

Figure 5.17 Relation between per cent clay and subsidence due to pressure decline (Gabrysch, 1969).

5.2.4 Clay content-subsidence relation

Figure 5.17 shows the general relationship in the Houston-Galveston area, Texas, between the percentage of clay beds and the subsidence head-decline ratio. According to Gabrysch (1969), the percentage of clay beds was determined from interpretation of electrical logs; the pressure-head decline was determined from measured water levels in wells; and subsidence values were taken from changes in nearby bench-mark elevations.

5.3 THEORETICAL APPROACH

5.3.1 General remarks

Regional subsidence due to ground-water extraction is a complex phenomenon which may be roughly "felt" in an intuitive fashion very difficult to explain quantitatively, due to the complexities of the materials involved.

Basically, the extraction of ground water reduces the interstitial water pressure (neutral pressure) which, according to the well-known "effective-pressure principle" of Terzaghi, means a transference of load to the soil skeleton (effective pressure) and its subsequent volume reduction (i.e., surface subsidence).

From a qualitative standpoint there is no "mystery" at all. However, in trying to explain the phenomenon both qualitatively and quantitatively, a series of unsuspected problems arise originating mainly from the elusive mechanical properties of soils.

Soils are complex multiple-phase systems constituted by solids, liquids, gases, and other substances like organic matter, ions, etc., which form, from a mechanical standpoint, a highly hyperstatic system whose properties must be inferred, at best, through statistical averages or "representative" tests.

As a result, soils incorporate into their mechanical properties all the behavioral aspects of their components, i.e. elasticity and plasticity of solids; viscosity of liquids; compressibility of gases; decay properties of organic matter; attraction and repulsion of ionic charges, etc., in a much more involved fashion.

This type of material has non-linear elastic, plastic, and viscous properties whose mechanical parameters are anisotropic and are history-, stress-, and time-dependent.

Such material is very difficult--if not impossible--to handle in any kind of a theoretical model of subsidence and this explains why the different approaches described in the scientific literature for that purpose, resort to many simplifications and idealizations in order to obtain some kind of a model that allows a more or less correct interpretation of past events, prediction of future ones, and decisions to be made about them. The questions are: What to simplify? How to idealize soils?

Unfortunately, there is no general rule, because the dominant feature in one case may be negligible in another and therefore, judgment and expertise must be exercised for best results. As general information, the more common simplifications regarding soil properties are listed here:

1. No organic matter present;
2. Only two phases present (solid-liquid);
3. No viscous properties;
4. No plastic properties;
5. Newtonian behavior of liquid phase;
6. No anisotropy;
7. Linear elastic properties of soil structure;
B. Constant parameters or, at least, one set for virgin compression and another for expansion and recompression.

Additionally, other simplifications regarding the system of aquifers and aquitards may be introduced, such as

9. Horizontal strata;
10. Horizontal flow in aquifers and vertical flow in aquitards;
11. Subsidence due mainly to aquitard consolidation;
12. No free surface of flow in the aquifers.

and so on.

As might be expected, the larger the number of simplifications made, the more restricted the nature of the resultant model and the more specific its applicability.

However, it should be remembered that, in practice, simplifications must be made according to the nature and volume of the available information and that the best way of modeling a given case may be to begin with the simpler models first, advancing later to the more involved ones, up to the highest level justified by the existing data.

In the remainder of this chapter an insight will be given on the details of several types of subsidence models (Figueroa Vega, 1973, 1977).

5.3.2 Compressibility relationships and total potential subsidence

The traditional laboratory test employed to disclose the compressibility relationships of soils is the consolidation test (odometer test) developed by Karl Terzaghi. The test is discussed in Chapter 4.

In this test, soils exhibit a more or less linear relationship between e (void ratio) and log p'/p_0', effective intergranular pressure) of the type

$$e = e_0 - C_C \log \frac{p'}{p_0'}, \tag{5.8}$$

(a slightly modified form of equation 4.14 shown in Chapter 4), where Cc is the "compression index" and eo and pol are initial reference values. This relationship is valid for increasing values greater than the maximum intergranular pressure the soil has supported in the past (pol, preconsolidation pressure). For discharge or recharge at pressures lower than the preconsolidation pressure (i.e.: within preconsolidation range) the relationship is similar, with a lower Cc value (Cc), which means that only part of the total deformation of a soil is recoverable and also that the compressibility parameters of a soil are history dependent.

In the soil mechanics field, it is customary to define the "coefficient of volume compressibility," m_V, as

$$m_V = \frac{\frac{de}{dp'}}{1+e_0} = \frac{a_V}{1+e_0}, \tag{5.9}$$

where a_V stands for the coefficient of compressibility, such that, within a small increment of pressure, the total settlement of a column of soil of thickness, H_0, may be computed as

$$\Delta H = m_V \, \Delta p' H_0. \tag{5.10}$$

As may be noted in equation (5.9), m_v, is stress dependent and therefore its value must be estimated for the proper e_0 and $\Delta p'$ values. Otherwise, equation (5-10) may lead to serious errors.

Equation (5.10) may be applied directly--as in the soil mechanics field--as a first approximation, whenever the strata thickness sequence is known (H_{01}, H_{02}, ..., H_{0i}) as well as the corresponding neutral pressure reductions due to water extraction (taken initially as the effective pressure increments) and their estimated coefficients of volume compressibility (m_{v1}, m_{v2},....,m_{vi}). The total subsidence in this case would be approximately

$$\overline{\Delta H} \approx \sum_{1}^{i} m_{vi} \Delta P_i' H_{oi} . \tag{5.11}$$

When all the involved strata remain saturated and the total relative shortening of the column is small, the foregoing calculations may be accepted as sufficiently good for practical purposes. In other cases, they must be taken only as giving approximate values and subsequent calculations must be made utilizing these values to estimate the total initial and final column loads at each level, the initial and final effective pressures (vertical pressure due to total load) and applying again equation (5.11) and repeating the process iteratively, until final results take account properly of both effects.

5.3.3 Differential equations of ground-water flow in an aquifer-aquitard system

Steady laminar flow of interstitial water within any portion of saturated soil obeys two basic laws--the mass conservation law:

$$\mathrm{div}(\gamma \bar{v}) = 0 , \tag{5.12}$$

where "div" stands for the divergence operator, "γ" for density of water, "v" for flow velocity vector, and Darcy's Law:

$$\bar{v} = -K \ \mathrm{grad}\ h, \tag{5.13}$$

where K is the hydraulic conductivity of the soil and "h" the hydraulic head.

Combining these laws into a single equation and neglecting the variability of γ and K gives

$$\nabla^2 h = \frac{\partial^2 h}{\partial x^2} + \frac{\partial^2 h}{\partial y^2} + \frac{\partial^2 h}{\partial z^2} = 0 , \tag{5.14}$$

the well-known Laplace equation. Therefore, h must be an harmonic variable satisfying the existing boundary conditions.

Equation (5.12) simply states that the mass of water within the portion of saturated soil remains constant. When the flow is unsteady, this does not hold anymore and some water is stored in or extracted from a specified elemental volume of soil and equation (5.14) must be modified accordingly, resulting in

$$K\nabla^2 h = S_s \frac{\partial h}{\partial t} , \tag{5.15}$$

where "S_S" is the specific storage and a linear compressibility relationship is assumed both for water and soil structureo.

In a homogeneous horizontal aquifer of constant thickness "b" with horizontal flow, equation (5.15) reduces to

$$\frac{\partial^2 h}{\partial x^2} + \frac{\partial^2 h}{\partial y^2} = \frac{S_s}{K}\frac{\partial h}{\partial t} = \frac{S}{T}\frac{\partial h}{\partial t} = \frac{1}{\nu}\frac{\partial h}{\partial t} , \tag{5.16}$$

where

$$S = bS_S;\ T = bK;\ \text{and}\ \nu = \frac{T}{S} \tag{5.17}$$

are the storage coefficient, transmissivity and hydraulic diffusivity respectively. In a compressible aquitard with vertical flow, equation (5.15) reduces simply to

$$\frac{\partial^2 h}{\partial z^2} = \frac{1}{\nu}\frac{\partial h}{\partial t} . \tag{5.18}$$

These equations may also be written in terms of "s" (drawdown) instead of "h" (hydraulic head).

Equation (5.16) is the classical aquifer differential equation due to Theis (Theis, 1935) and equation (5.18) is the classical consolidation equation due to Terzaghi (Terzaghi, 1923). Both equations must be solved subject to their proper initial and boundary conditions.

In a system with aquifer(s) and aquitard(s), the mathematical problem to solve is made up of one equation of the type (5.16) for each aquifer including some additional terms to take account of vertical inflows or outflows, if any, and one equation of the type (5-18) for each aquitard, plus the adequate initial and boundary conditions and additional conditions stating equality of hydraulic heads in any plane of contact of any two of the existing aquifer(s) and aquitard(s). This is referred to as a "quasi three-dimensional model." The final result is a complex coupled system which may be solved with the help of numerical methods (finite differences or finite elements). The assumption of vertical flow in aquitards and horizontal flow in aquifers is only justified when the permeability of the latter is much higher than that of the former (say tenfold or more). Otherwise, it is necessary to resort to a truly three dimensional model, where all the second order partial derivatives are kept for all the strata.

The solution of the coupled system implies advancing numerically and simultaneously the solution for all the involved strata through each time increment, and this may represent a large number of calculations which might eventually overflow the working capability of the available computer. Models of this kind have been developed and published elsewhere (Carrillo, 1950; Gambolati, 1972).

An interesting alternative solution, for quasi three dimensional models, as applied to the Mexico City case (Figueroa V, 1973), is to depart from a coupled system to reduce the problem’s complexity via integrodifferential equations. This will be outlined in the next section.

5.3.4 Uncoupling the system and solving a simpler problem

For a system made up of one aquifer underlain and overlain by consolidating aquitards, several mathematical formulations are possible in accordance with the upper and lower boundary conditions type (constant head or null flow). In any case, the mathematical formulation is made up, in terms of drawdowns, as explained before, by one equation of the type (5.16), including in its left side two terms of the form

$$\mp\frac{K_i}{T}\frac{\partial}{\partial z}s_i(x, y, 0, t) \tag{5.19}$$

to take account of vertical flow into the main aquifer, through the aquifer-aquitard common boundaries, plus two equations of the type (5.18) also in terms of drawdowns, plus the corresponding initial and boundary conditions.

For all the resulting cases of this system it has been shown (Herrera and Figueroa, 1969) that the problem was equivalent to

$$\frac{\partial^2 s}{\partial x^2} + \frac{\partial^2 s}{\partial y^2} + \int_0^t \frac{\partial}{\partial t}s(x, y, \beta)G(t-\beta)\partial\beta = \frac{1}{\nu}\frac{\partial s}{\partial t} , \tag{5.20}$$

where the convolution term includes the vertical inflows to the aquifer, and

$$G(t) = \frac{K_1}{T}\frac{\partial}{\partial z}A_1(0, t) - \frac{K_2}{T}\frac{\partial}{\partial z}A_2(0, t) \tag{5.21}$$

in which G(t) is the zero elevation at the aquifer-aquitard contacts and A_l and A_2 the basic

solutions of classical consolidation theory corresponding to the particular boundary conditions present in each case. Additionally, in general

$$G(t) = -C - F(t) \tag{5.22}$$

where "C" is a constant depending on the system's parameters which incorporates the vertical inflows coming from the exterior boundaries of the system in the cases of constant head boundary conditions, and the function F (t) incorporates the vertical inflows released from aquitards by consolidation.

Equation (5.20) may be reduced to

$$\frac{\partial^2 s}{\partial x^2} + \frac{\partial^2 s}{\partial y^2} - C_s - \int_0^t \frac{\partial}{\partial \beta} s(x, y, \beta) \bullet F(t-\beta)\partial\beta = \frac{1}{\nu}\frac{\partial s}{\partial t}. \tag{5.23}$$

Furthermore, the integral term may be approximated by

$$\int_0^t \frac{\partial}{\partial \beta} s(x, y, \beta) \bullet F(t-\beta)\partial\beta = I\frac{\partial}{\partial t} s(x, y, t) \tag{5.24}$$

when $\partial s/(\partial\beta)$ has a slow variation, being

$$I = \int_0^\infty F(\beta)\partial\beta, \tag{5.25}$$

a constant. Under these conditions, the problem further reduces to

$$\frac{\partial^2 S_c}{\partial x^2} + \frac{\partial^2 S_c}{\partial y^2} = \frac{1}{\nu_c}\frac{\partial S_c}{\partial t}, \tag{5.26}$$

where

$$S_c = s e^{c\nu_c t} \tag{5.27}$$

and

$$\nu_c = \frac{\nu}{1 + I_\nu}. \tag{5.28}$$

This is the "correspondence principle" (Herrera and Figueroa, 1969). It means that the original coupled system is equivalent, under the already stated conditions, to an equivalent confined aquifer system.

For the case of a single aquifer and a single aquitard, the applicable expressions are

$$G(t) = -\frac{K_1}{Tb_1} 1 + 2 \sum_{n=1}^{\infty} \exp - \frac{n^2 \pi^2 \nu_1}{b_1^2} t, \tag{5.29}$$

$$I = \frac{S_1}{3T}; C = \frac{K_1}{Tb_i}; \nu_c = \frac{3T}{3S + S_1} \tag{5.30}$$

for the constant head external boundary condition and

$$G(t) = -\frac{2K_1}{Tb_1} \sum_{n=0}^{\infty} \exp\left(-\frac{\left(n+\frac{1}{2}\right)^2 \pi^2 \nu_1}{b_1^{\,2}} t\right), \tag{5.31}$$

$$I = \frac{S_1}{T}; C = 0; \nu_c = \frac{T}{S+S_1}, \tag{5.32}$$

for the zero gradient external boundary condition. In all these formulas, the index 1 refers to the aquitard.

Both the integrodifferential equation and the correspondence principle have been applied to the Mexico City case, with some additional considerations which will be mentioned later, with reasonably good results. As a general comment, the applicability of the above-mentioned simplifications of the correspondence principle is much greater than it seems, for the following reasons.

Apparently, the correspondence principle would be applicable whenever $\partial s/\partial t$ "has a slow variation" as stated before. However in the extreme case of constant drawdown the right part of equation (5.24) equals zero for $t \neq 0$, which means that there is no consolidation except at $t = 0$, where the subsidence cause is concentrated. So, the former condition should read "has a slow variation everywhere."

It must be noted that equation (5.24) simply removes the lag-effects of the consolidation process and therefore it may work only if the drawdown is gradual. The more $\partial s/\partial t$ departs from a constant value the more the results depart from reality.

However, the consolidation process compensates this situation somehow, because while at any time increment, the subsidence increment includes some subsidence due to the preceding drawdowns, also part of the subsidence due to its own drawdown increment is transferred to future time increments. In any case, a short consolidation time may improve the results.

It is possible that an integration by parts of the memory term could lead to a better approximation, and this is a question which must be explored.

Another reason which supports the correspondence principle is the remarkably good correlation found between total drawdown and total subsidence.

According to the experience gained in the Mexico City case, from a practical standpoint there seems to be no strong reason to use equation (5.26) instead of equation (5.23) as there is not a big difference in computing time or computer memory requirements. So, its use seems to be more practical in non-computer modeling, as described in the next section.

In applying equation (5.23), some aspects must be considered:

1. Additional terms must be included to take into account infiltration or pumpage.
2. Compressibility parameters must distinguish between virgin compression and elastic recompression.
3. The storage coefficient in the main aquifer must be changed in those cells of the model where drawdowns are such that ground-water flow changes from confined to unconfined.
4. The aquifer compaction itself, if considered relatively important, may be added, computing it as an instant response to drawdown, thus taking care of point (b), above.

The procedures described herein may be incorporated in any of the existing types of ground-water models.

5.3.5 Simplified subsidence modeling

In some cases it may be desirable to have a fast estimate of the probable order of magnitude of subsidence versus time due to regional pumpage in some selected site(s) and this may be done through (1) estimating future drawdowns in the site(s) and (2) estimating future subsidence in the site(s).

The first part may be achieved by simple superposition of the Theis equation or by the application of the Influence Diagram (Figueroa Vega, 1971), together with the application of the aforementioned Correspondence Principle (equations 5.26, 5.27 and 5.28).

The superposition of the Theis equation needs no further comment. It may be advisable when the number of wells is not too large.

When there are many wells and their distribution is fairly uniform with an average pumpage of "q" units of volume per unit of time, it is much more practical to apply the influence diagram mentioned before, which is a diagram similar to that developed by Newmark (1942) in the soil mechanics field to integrate vertical stresses due to a distributed surcharge.

By means of it, drawdown "s" at the site and at time "t," due to a distributed pumpage of intensity "q" in any area is simply

$$s = \frac{qt}{S}(0.0025N_i + 0.001N_e), \tag{5.33}$$

where "S" is the storage coefficient and "N_i" and "N_e" are the internal and external "squares" covered by the pumping area drawn at a proper scale.

The application of equation (5.33) for several times makes it possible to plot estimated future drawdowns versus time.

The next step is to estimate the future subsidence, the time derivative of which is T (transmissibility) times the convolution term of the left side of equation (5.23), i.e.:

$$\frac{\partial h}{\partial t} = T\int_0^t \frac{\partial}{\partial \beta} s(x, y, \beta) \bullet F(t-\beta)\partial\beta\ . \tag{5.34}$$

This expression may be easily approximated by numerical methods with the help of a pocket programmable calculator and the total subsidence for each time is the area under the curve versus t.

Equation (5.34) takes only into account the consolidation of the clay strata. Compression of the aquifer may be included, as an instant response for each increment of time, using equation (5.11).

The former procedure, though simple and lacking precision, may be used as a basis for preliminary decision-making in many cases of regional subsidence due to ground-water extraction, while a more precise digital computer model is elaborated and validated.

5.3.6 Other types of subsidence models, by Donald C. Helm[2]

A variety of prediction techniques have been discussed--empirical, semi-theoretical, and theoretical. The empirical and semi-theoretical techniques require induced subsidence to have already begun. Empirical and semi-theoretical methods offer reasonable parameters that link subsidence to some other measurable phenomenon in the field. The theoretical techniques which have been discussed to this point require the results of laboratory tests in order to predict subsidence.

Two other techniques for subsidence prediction will now be discussed. This will be followed by a discussion of the role of the unpumped overburden. One technique, which uses a depth-porosity model, is too primitive to require induced subsidence to have already begun. This is its power; it can give a rough approximation of potential ultimate subsidence of an area where the local confined aquifer system has not yet been stressed. The second technique that will be discussed uses an aquitard drainage model. In contrast to the depth-porosity model, this second technique requires compressible beds to be stressed in the field. It is sufficiently sophisticated not to require laboratory tests on soil specimens. Neither the depth-porosity model nor the aquitard-drainage model requires laboratory tests; each uses its own independent field-based method for parameter evaluation. They are both useful techniques.

The parameter found by using the depth-porosity model is a generalized depth-dependent approximation for a coefficient of volume change, m_v, of equation 5.10 which corresponds to nonrecoverable specific storage, S'_{skv}, of equations 3.4 and 3.19. This parameter controls the ultimate response to stress of a specified bed. The parameters found by using the aquitard drainage model are site-specific average values of specific storage, S'_{skv}, and the vertical component of hydraulic conductivity, K′. These parameters control the time-delayed response to

---

[2] Work performed under auspices of the U.S. Department of Energy by the Lawrence Livermore National Laboratory under contract No. W-7405-ENG-48.

stress of compressible interbeds within a confined system. They appear directly in equation 3.2 and indirectly in equation 5.15.

5.3.6.1 Depth-porosity model

Porosity of sedimentary materials is known to decrease in general with depth (Figure 5.18). Based on empirical data for shale and mudstone, Athy (1930) and Magara (1978) suggest that a relation between porosity and depth can be found from an exponential expression

$$n + n_0 e^{-cz} \tag{5.35}$$

for conditions of compaction equilibrium where n is porosity at a specified depth z, n_0 is an extrapolation of n to land surface (z = 0), and c is an empirically determined constant. For Athy's data of shale porosities from Oklahoma, n_0 equals 0.48 and c equals 0.0014 when z is expressed in metres. Schatz, Kasameyer, and Cheney (1978) suggest using equation 5.35 for site-specific values for n_0 and c as a means of approximating S'_{skv} as a function of depth, z, for all compressible sedimentary material including shale, mudstone, sandstone, and clay. They tacitly argue that decreasing fluid pressure due to producing an artesian aquifer system has an

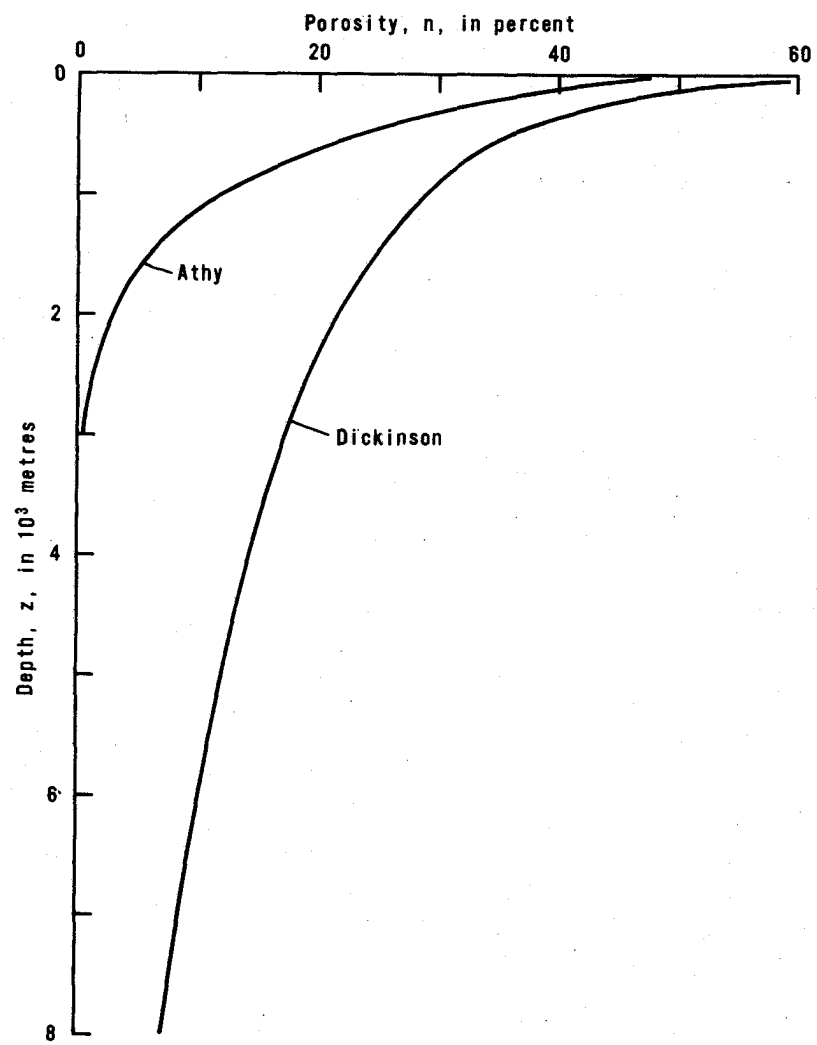

Figure 5.18 Two examples of decrease of porosity with depth.

equivalent effect on porosity that lowering the bed to a greater depth would have. Hence the curves in Figure 5.18 are treated by them to represent a type of ultimate stress/strain relation for equilibrium compaction.

Unfortunately, not all empirical depth-porosity curves follow an exponential relation as expressed by equation 5.35. A notable exception (Magara, 1978, p. 93) is Dickinson's (1953) data for shale porosities from the Gulf of Mexico coast. Helm (1980, unpublished manuscript) has found that Dickinson's shale porosities follow a logarithmic relation with depth, namely

$$\Delta n = -a\ \Delta \ln x, \tag{5.36}$$

$$n = n_{ref} - a\ \ln(z/z_{ref}), \tag{5.37}$$

where n_{ref} and z_{ref} are reference values for porosity and depth and a is an empirical constant. If a is interpreted as a type of compression index, equations 5.36 and 5.37 approximate the type of stress-strain relation one would anticipate from standard soil mechanics interpretation of laboratory consolidation data. For Dickinson's field data from the Gulf Coast, a equals 0.103 and n_{ref} is found to equal 0.05 for an arbitrary reference depth z_{ref} of 10^4 m.

It is now possible to get two depth-dependent theoretical values of S'_{skv} based on equations 5.35 and 5.37. Recalling equation 3.10, we can express how lithostatic effective stress, p', due to submerged weight of overlying material changes with depth, z, by the gradient

$$\frac{dp'}{dz} = (1-n)(G-1)\gamma_W = \frac{G-1}{1+e}\gamma_W\ . \tag{5.38}$$

According to the left-hand equality of equation 3.4 and equation 5.9, we write

$$S'_{skv} = -\frac{1}{1+e}\frac{de}{dp'}\gamma_W = -(1-n)\frac{de}{dp'}\gamma_W. \tag{5.39}$$

Equation 5.39 can be written

$$S'_{skv} = -(1-n)\frac{de}{dn}\frac{dn}{dz}\frac{dz}{dp'}\gamma_W = -\frac{\gamma_W}{1-n}\frac{dn}{dz}\frac{dz}{dp'}, \tag{5.40}$$

which, in accordance with equation 5.38, becomes

$$S'_{skv} = -\frac{1}{(1-n)^2(G-1)}\frac{dn}{dz}\ . \tag{5.41}$$

It now becomes necessary to determine dn/dz from Figure 5.18. For Athy's curve, equation 5.41 becomes

$$S'_{skv} = \frac{c}{(G-1)}\frac{n}{(1-n)^2}, \tag{5.42}$$

where we have used equation 5.35. For Dickinson's curve, however, equation 5.41 becomes

$$S'_{skv} = \frac{a}{(G-1)z(1-n)^2} \quad (5\text{-}43)$$

where we have used equation 5.37.

Figure 5.19 shows the relation of S'_{skv} and depth z in accordance with Athy's data (dashed line) and Dickinson's data (solid line). The dashed line in Figure 5.19 was found by substituting equation 5.35 into the right-hand side of equation 5.42 and assuming n_0 to equal 0.48 and c to equal 0.0014. The solid line in Figure 5.19 was similarly found by substituting equation 5.37 into the right-hand side of equation 5.43 and assuming n_{ref} to equal 0.05, Z_{ref} to equal 10^4 m, and a to equal 0.103.

The marks on Figure 5.19 indicate a selection of S'_{skv} values determined by other methods. The X's in the upper right-hand corner of Figure 5.19 represent values of S'_{skv} calculated from results (Marsal and Graue, 1969, Table 5, p. 190) of standard laboratory consolidation tests on soil samples near Mexico City. The symbols X_{SC}, X_T, and X_W represent values of S'_{skv} calculated from results of standard laboratory consolidation tests on soil samples taken respectively from the Santa Clara Valley, California (Poland, written communication, 1978), from near Seabrook,

Texas (Gabrysch and Bonnet, 1976, Table 3), and a composite of values from the Wilmington Oil Field, California (Allen and Mayuga, 1969). Subsidence is known to have occurred at all these sites. The circles represent values of S_{skv} determined from simulating observed compaction and expansion in California by means of a digital computer code. This computer simulation technique uses the aquitard-drainage model and is discussed in the next section.

It is evident from Figure 5.19 that within 1000 metres of land surface, Dickinson's curve gives a high, but reasonable, estimate of S'_{skv}. Helm (1980, unpublished manuscript) suggests the use of the solid curve in Figure 5.19 as a first approximation of S'_{skv}, For example, assume a confined aquifer has not been developed and hence no field-based compaction records are available. However, suppose one knows that an areally extensive confined aquifer system lies at a depth between roughly 100 and 300 metres. Within this 200-metre interval there is found to exist about 100 metres of fine-grained compressible interbeds. Hence the thickness of compressible beds, b′, is about 100 m, the average depth is about 200 m, and in accordance with Dickinson's curve in Figure 5.19 we can estimate S'_{skv} to approximate $10^{-3}m^{-1}$. Using equation 3.4, we find

$$\Delta b'/\Delta h_a = S'_{skv}b' \cong 10^{-3} \times 10^{2} = 10^{-1}. \qquad (5.44)$$

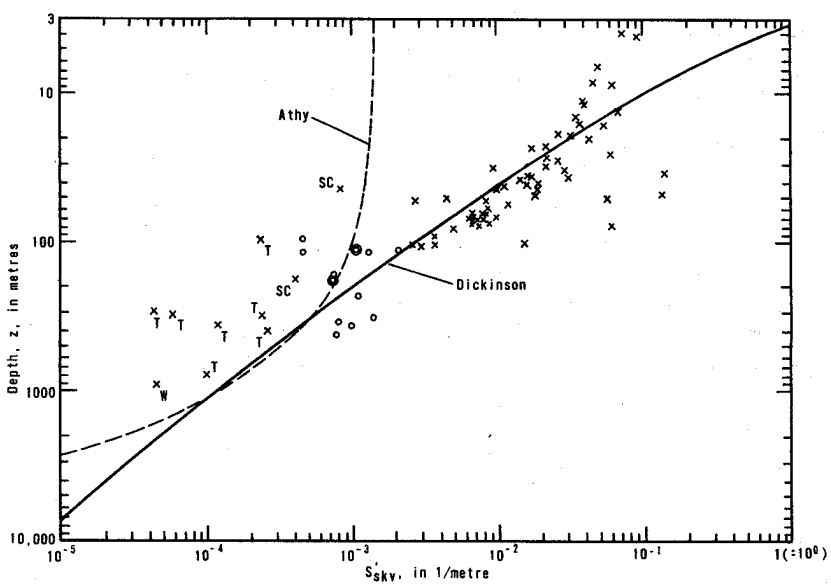

Figure 5.19 Specific storage for nonrecoverable compaction, S'_{skv}, as a function of depth, z.

Equation 5.44 tells us, as a first approximation, that for every foot of long-term drawdown, one can expect about one-tenth of a foot of ultimate compaction.

Let us interpret equation 5.44 in a somewhat broader time frame. One would expect a time lag of decades before compaction in the field would reach its ultimate value (equation 5.44) even under conditions of no recovery of artesian head. If at any time artesian head recovers above a transient critical elevation, ongoing residual subsidence will stop.

Predicting this critical elevation of head is discussed in the next section. Equation 5.44 and use of Dickinson's curve in Figure 5.19 tacitly requires sedimentary material within a con-

fined system initially to be normally consolidated. Another tacit assumption of equation 5.44 is that volume strain expresses itself entirely in vertical compression. For a confined aquifer system whose volume strain is isotropic, the vertical component of strain is one-third the volume strain. Whenever in situ strain is actually isotropic, use of Dickinson's curve (Figure 5.19) in equation 5.44 would thereby automatically give an estimate of vertical compression three times too large.

Methods for approximating a regional distribution of Δh_a, which appears in the left-hand side of equation 5.44, are available (e.g., Figueroa Vega, 1971). Discussion of these methods is beyond the scope of the present section.

5.3.6.2 Aquitard-drainage model

Tolman and Poland (1940) suggested that subsidence in the Santa Clara Valley, California, is caused not simply by declining artesian heads and the resulting compaction of permeable sands, but primarily by the nonrecoverable compaction of slow-draining clay layers within the confined system. This marks the conceptual birth of the aquitard-drainage model (Figure 5.20). Riley (1969) applied Terzaghi's (1925) theory of one-dimensional consolidation quantitatively to the aquitard-drainage model. Helm (1972, 1975, 1976) borrowed Riley's insights to develop a

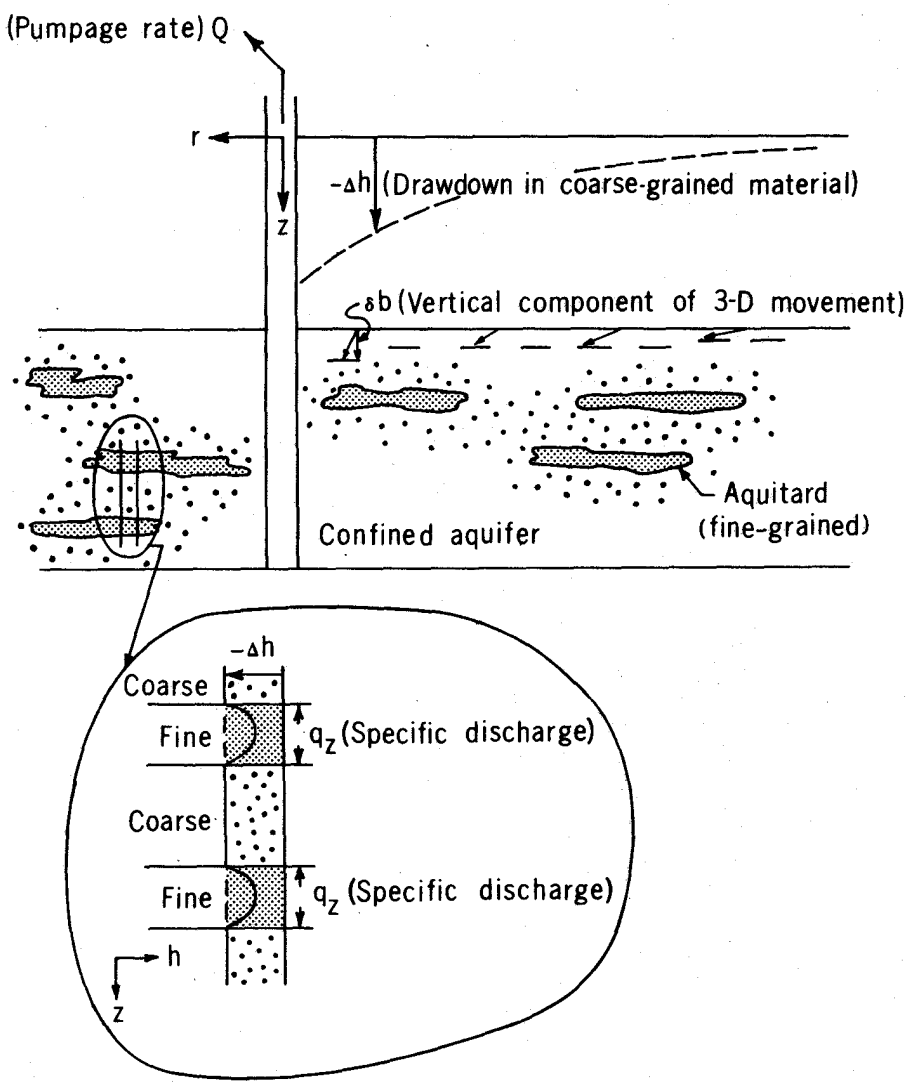

Figure 5.20 Aquitard-drainage model (modified from Helm, 1980, Figure 4).

one-dimensional computer code to simulate time-delayed aquitard compression and expansion in response to arbitrary fluctuations of hydraulic head within the coarse-grained portion of a confined aquifer system. In turn, Freeze (Witherspoon and Freeze, 1972; Gambolati and Freeze, 1973) and Narasimhan (Narasimhan and Witherspoon, 1977) borrowed Helm's insights for developing their own one-dimensional computer codes for aquifer-system compaction and expansion. Digitalizing the aquitard-drainage model led directly to a powerful predictive technique (Helm, 1978; Pollard and others, 1979) for land subsidence caused by water-level fluctuations within a confined aquifer system.

The aquitard-drainage model (Figure 5.20) represents the confined aquifer system as containing two basic types of porous material: a group of (i) fine-grained interbeds each of which is completely surrounded by a hydraulically connected system of (ii) coarse-grained material. The fine-grained interbeds (aquitards) are considered much less permeable than the interconnected coarse-grained portion of the confined aquifer system. Because slow-draining aquitards are interbedded within an aquifer, they are conceptually distinct from caprock, confining bed, or semi-confining bed that serves as a confined aquifer's upper boundary. The aquitard-drainage model conceptually attributes the observed time-lag (of compaction response to stress change) to the vertical component of fluid flow from one idealized material (aquitard) to another (aquifer) within the two-material system itself. The slow vertical drainage, q_z, from highly compressible aquitards to the less compressible aquifer material serves a somewhat similar rheological function in this model that a viscous "dashpot" serves in a viscoelastic reservoir model that has only one idealized undifferentiated material (Corapcioglu and Burtsaert, 1977).

In conjunction with appropriate field data, the model predicts (1) residual nonrecoverable compaction within a system, (2) time-dependent in situ preconsolidation pressure (a critical depth to water at which non-recoverable compaction is stopped during the unloading phase and is triggered during the reloading phase of a specified unloading-reloading cycle), and (3) a timeconstant, τ, for a confined system at a site of interest. According to Terzaghi's theory of consolidation, τ can be interpreted to represent the length of time required for initially unstressed aquitards to reach a 93 per-cent nonrecoverable compaction if water levels in adjacent aquifers (of a confined system) are instantaneously lowered a specified amount and then held constant.

By simulating field compaction and expansion at 8 sites in the Santa Clara Valley and 7 sites in the San Joaquin Valley, California, Helm (1978, Table 2) estimated that in 1978 residual compaction in the Santa Clara Valley ranged from a minimum of 0.52 m at one site to a maximum of 2.53 m at another. Among the analyzed sets of field data collected in the San Joaquin Valley, calculated residual compaction ranged from a minimum of 0.85 m at one site to a maximum of 9.75 m at another. In the early 1970's the critical depth to water was calculated site by site to range from a few to several tens of metres above a local past maximum depth to water. Time constants also were estimated from site-specific field data. In the Santa Clara Valley, τ was calculated to range from a minimum of 13 years at one site to 125 years at another. In the San Joaquin Valley τ was calculated to range from 5 years at one site to 1350 years at another.

Figures 5.21 and 5.22 illustrate the use of a one-dimensional computer simulation based on the aquitard-drainage model. Using the stress curve shown in the upper graph of Figure 5.21 as input values, parameter values within the mathematical model are calibrated in order to make calculated compaction (dotted line in the lower graph of Figure 5.21) be as close an approximation to observed compaction (solid line in the lower graph of Figure 5.21) as possible. Using these parameter values and the input stress curve shown in the upper graph of Figure 5.22, a predicted compaction curve is calculated for the period 1921-74. This prediction is shown by the solid line in the lower graph of Figure 5.22. Actual compaction is estimated as a portion of subsidence measured at bench mark J111 and is plotted as solid circles in the lower graph of Figure 5.22. The excellent agreement between predicted and observed compaction in Figure 5.22 confirms the parameter values found during the calibration process (Figure 5.21). This result increases one's confidence in the residual compaction, preconsolidation stress, and time constants that are estimated from this procedure.

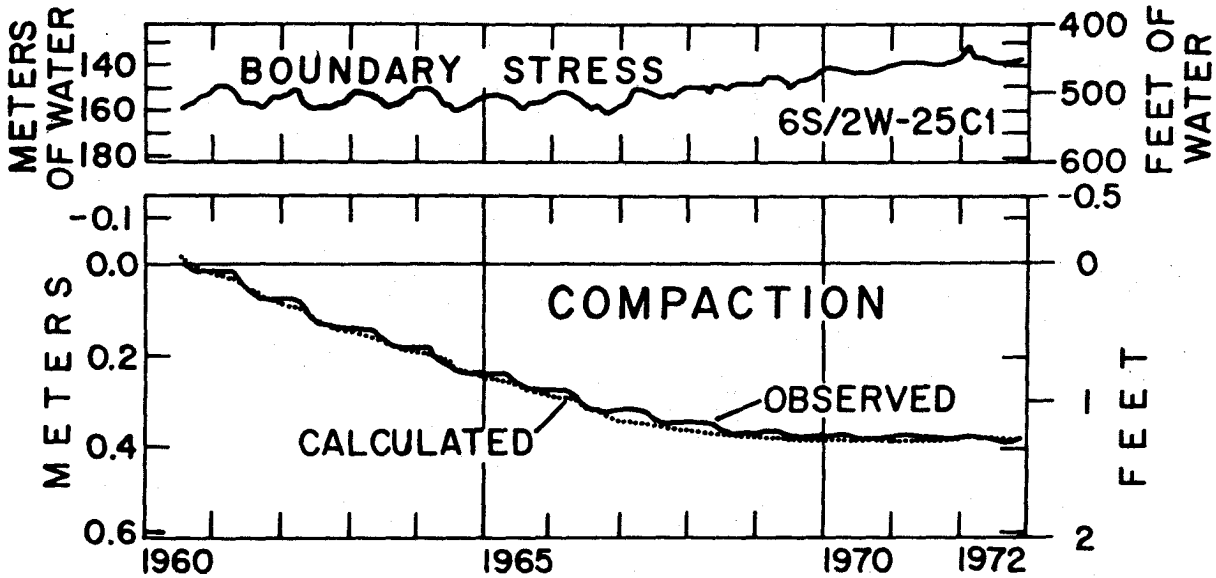

Figure 5.21 Simulation of compaction based on water-level data for well 6S/2W-25Cl (1960-72) and compaction data observed in well 24C3.

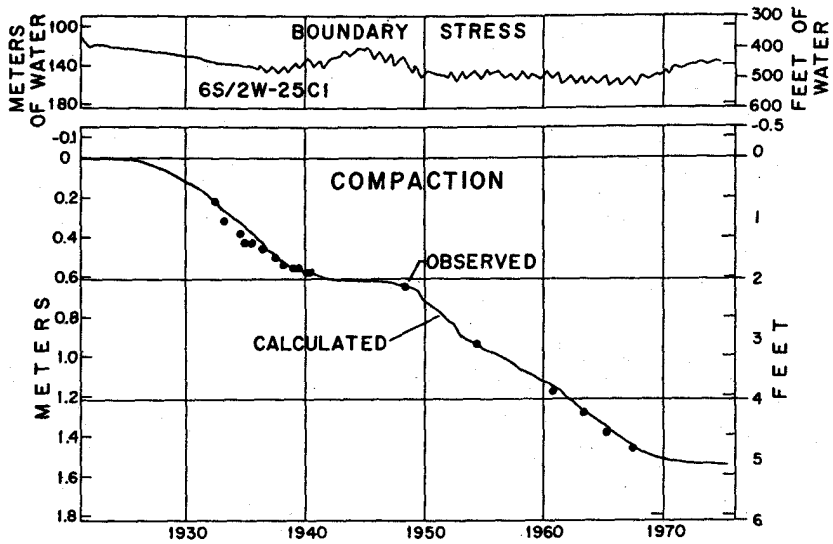

Figure 5.22 Simulation of compaction based on water-level data for well 6S/2W-25Cl (1921-74) and on compaction estimated as a portion of subsidence measured at bench mark

5.3.6.3 Influence of material within the unpumped overburden

Subsidence due to fluid withdrawal is the expression at land surface of the compression at depth of a stressed artesian aquifer system. Material within the intervening unpumped overburden may possibly play a role in mitigating land surface effects. Geertsma (1957, 1973) has in effect discussed quantitatively the role of the overburden. His equation for ultimate vertical displacement, U_z, directly over the center of an axially symmetric confined aquifer system (Figure 5.23) is

$$U_z(0,\ 0) = -\ 2((1-\nu)c_m b\Delta p\ \{l-[C/(1+C)^2]\}, \qquad (5.45)$$

where

ν is Poisson's ratio,
b is thickness of compressing bed(s),
p is pressure change,
C is D/R,
D is depth to compressing bed(s), and
R is radius of stressed system.

For highly compressible poro-elastic bulk material, Geertsma's coefficient of uniaxial compaction, c_m, becomes

$$C_m = (l-2\nu)(l+\nu)/E(1-\nu), \tag{5.46}$$

where E is Young's modulus.

Equation 5.45 should be used with caution for the following reasons. Due to gravitational body forces on submerged solids, it is reasonable to assume that the base of a depressured aquifer system does not move upward. Unfortunately, Geertsma neglects such body forces in his analysis with the unrealistic result that under some circumstances the base of his idealized reservoir (confined aquifer system) mathematically moves upward a significant amount. This physically unlikely upward movement can mathematically nearly equal the total compaction of the stressed system. Hence there may mathematically be no downward movement of the top of the idealized reservoir. Correspondingly under these circumstances there would mathematically be no subsidence at land surface whatsoever. This questionable aspect of Geertsma's analysis reflects itself in equation 5.45.

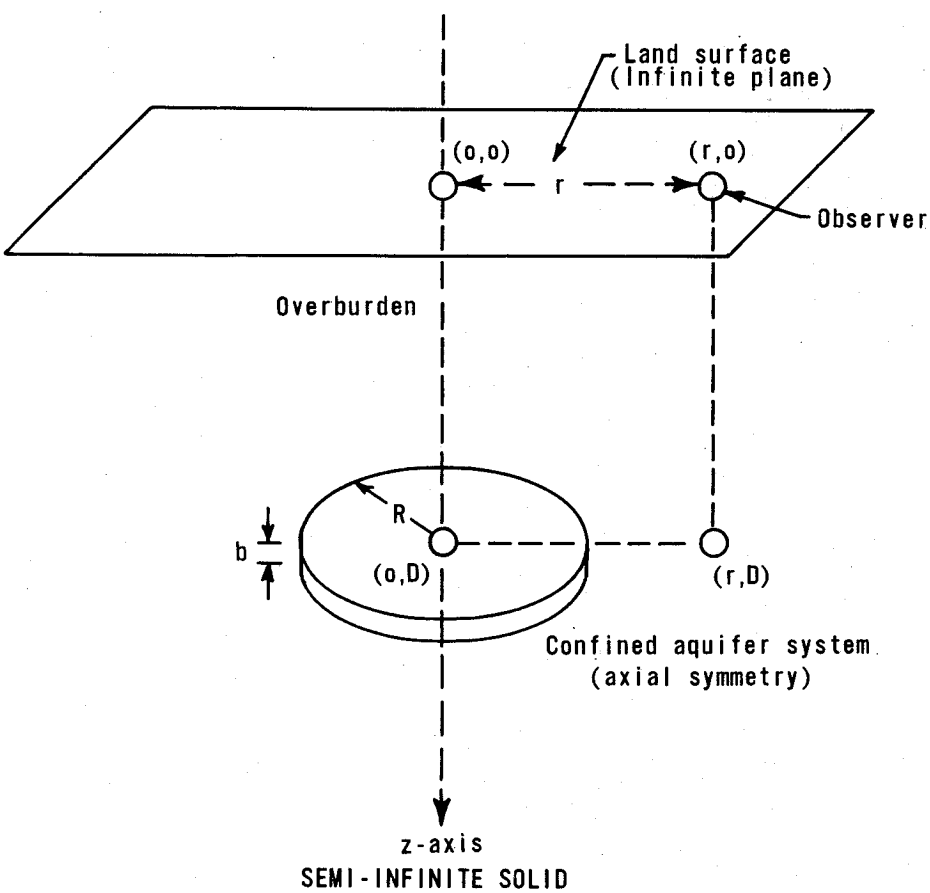

Figure 5.23 Half-space model (modified from Helm, 1980, Figure 2).

It is more reasonable to assume that the volume of compaction of a compressible aquifer system expresses itself eventually by an equal volume of subsidence at land surface. Whenever the upper boundary of a compacting aquifer system moves downward in response to compression of underlying sediments, Geertsma (1973) himself points out that the volume which this upper surface moves is preserved at land surface. When the vertical movement of the base of a confined aquifer system can realistically be considered negligible, land subsidence, according to Geertsma, equals volumetrically the total compaction of the confined aquifer system.

The areal distribution of subsidence is somewhat influenced, however, by the ratio of depth D to radius R (Figure 5.23) of the depressured confined aquifer system. The effect of compaction of an aquifer system with a large D/R ratio may be spread over a large area at land surface and hence minimize the vertical component of volumetric subsidence. The limit, however, would not be zero (which is erroneously implied by equation 5.45) but some finite fraction of b′, of equation (5.44). For most ground-water systems the D/R ratio is sufficiently small that the overburden's spreading effect can be completely ignored. This implies the direct applicability of a depth-porosity model (Section 5.3.6.1).

The conceptual model used by many investigators, including Geertsma, will now be described. It is a variation of what can more generally be called a half-space model (Figure 5.23). The earth is represented as a homogeneous, isotropic, semi-infinite elastic (or poro-elastic) medium. Land surface is represented as a flat upper surface that is free to move. Neither calculated surface movement nor topographic relief affects the essential flatness of the idealized surface. Although a depressured zone at depth D below land surface with a center at radial distance r from an observer on land surface is represented by an idealized spherical tension center by Carrillo (1949), by vertical pincers by McCann and Wilts (1951), and by a radially symmetric group of strain nuclei by Geertsma (1957), the various representations are conceptually similar. Gambolati (1972) has discussed the major conceptual distinctions between the tension-center representation (Carrillo, 1949; McCann and Wilts, 1951) and the strain-nucleus representation (Mindlin and Cheng, 1950; Sen, 1950; Geertsma, 1957, 1966, 1973; Finol and Farouq Ali, 1975). Briefly, a tension center model tacitly requires an infinitely compressible reservoir within an elastic half-space. The strain-nucleus model requires the confined aquifer system's compressibility to equal the compressibility of the surrounding elastic halfspace. Finite heterogeneity between the compressing system and the surrounding half-space was introduced to the model by Gambolati (1972).

The question of finite heterogeneity deserves some comment. A confined aquifer system by definition yields fluid to a discharging well and experiences a pressure loss. The surrounding material by definition does not yield fluid. Hence porosity within a compressible confined aquifer system decreases. Porosity does not necessarily decrease within the surrounding halfspace. This distinction is analogous to the distinction in soil mechanics between drained and undrained compression. Decrease in porosity as a source for fluid discharge inherently introduces an extra component into a compressibility term for a confined aquifer system. This extra component does not appear in a corresponding compressibility term for the undrained surrounding half-space. Specifically, only S_{SW} of equation 3.3 is appropriate to use for the surrounding half-space whose individual grains are considered incompressible,, whereas the sum of S'_{SK} and S_{SW} is appropriate to use for the aquifer system itself. S'_{SK} is a function of porosity loss whereas S_{SW} is a function of the expansion of interstitial water. Hence, the hydraulics of underground fluid flow alone helps dictate the apparent heterogeneity of compressibilities between a compressing aquifer system and the surrounding half-space. This apparent or in situ hydraulic heterogeneity is distinct from standard differences in material properties which are tested and recorded in the laboratory.

5.4 REFERENCES

ALLEN, D. R., and MAYUGA, M. N. 1969. The mechanics of compaction and rebound, Wilmington oil field, Long Beach, California, USA, in Tison, L. J. (ed.), Land subsidence, Vol. 2. Internat. Assoc. Sci. Hydrology, Pub. 89, p. 4710-423.

ATHY, L. F. 1930. Density porosity, and compaction of sedimentary rocks. Bull. American Assoc. Petroleum Geologists, v. 14, p. 1-24.

BULL, W. B., and POLAND, J. F. 1975. Land subsidence due to ground-water withdrawal in the Los Banos-Kettleman City area, California, Part 3. Interrelations of water-level change, change in aquifer-system thickness, and subsidence. U. S. Geological Survey Professional Paper 437-G, 62 p.

CARRILLO, NABOR. 1949. Subsidence in the Long Beach-San Pedro area. Stanford Research Institute, p. 67-69.

CASTLE, R. 0., YERKES, R. F., and RILEY, F. S. 1969. A linear relationship between liquid production and oil-field subsidence, in Tison, L. J. (ed.), Land subsidence, Vol. 1. Internat. Assoc. Sci. Hydrology Pub. 88, p. 162-173.

CORAPCIOGLU, M. Y., and BRUTSAERT, W. 1977. Viscoelastic aquifer model applied to subsidence due to pumping. Water Resources Research, v. 13, p. 597-604.

DICKINSON, G. 1953. Geological aspects of abnormal reservoir pressures in Gulf Coast Louisiana. Bull. American Assoc. Petroleum Geologists, v. 37, no. 2, p. 410-432.

FIGUEROA VEGA, GERMÁN E. 1971. Influence chart for regional pumping effects. Water Resources Research, v. 7, no. 1, p. 209.

FIGUEROA VEGA, GERMÁN E. 1973. Aquifer and subsidence model for Mexico City. 85th Annual Meeting of The Geological Society of America, v. 5, no. 7, p. 620.

FIGUEROA VEGA, GERMÁN E. 1977. Subsidence of the City of Mexico; a historical review. Second Internat. Symposium on Land Subsidence Proc., IAHS-AISH Pub. 121, p. 35.

FINOL, A., and FAROUQ ALI, S. M. 1975. Numerical simulation of oil production with simultaneous ground subsidence. Jour. Soc. Petroleum Eng., p. 411-422.

GABRYSCH, R. K. 1969. Land surface subsidence in the Houston-Galveston region, Texas, in Tison, L. J., ed., Land subsidence, Vol. 1. Internat. Assoc. Sci. Hydrology, Pub. 88, p. 43-54.

GABRYSCH, R. K., and BONNET, C. W. 1976. Land-surface subsidence at Seabrook, Texas. U.S. Geological Survey Water-Resources Investigation 76-31, 53 p.

GAMBOLATI, G. 1972. A three dimensional model to compute land subsidence. Bull. Internat. Assoc. Hydrol. Sci., v. 17, no. 2, p. 219-226.

GAMBOLATI, G., and FREEZE, R. A. 1973. Mathematical simulation of the subsidence of Venice, 1, Theory. Water Resources Research, v. 9, no. 3, p. 721-733.

GEERTSMA, J. 1957. The effect of fluid pressure decline on volumetric changes of porous rocks. Trans. Amer. Soc. Mech. Engrs., AIME v. 210, p. 331-340.

GEERTSMA, J. 1966. Problems of rock mechanics in petroleum production engineering. Proc. First Cong. of the Internat. Soc. of Rock Mech., Lisbon, v. 1, p. 585-594.

GEERTSMA,J. 1973. A basic theory of subsidence due to reservoir compaction: the homogeneous case. Verhandeliger Kon. Ned. Geol. Mijhbouwk, v. 28, p. 43-62.

HELM, D. C. 1972. Simulation of aquitard compaction due to changes in stress [abs.]. EOS Trans. American Geophys. Union, v. 53, no. 11, p. 979.

HELM, D. C. 1975. One-dimensional simulation of aquifer system compaction near Pixley, Calif. 1, Constant parameters. Water Resources Research, v. 11, no. 3, p. 465-478.

HELM, D. C. 1976. One-dimensional simulation of aquifer system compaction near Pixley, Calif. 2, Stress-dependent parameters. Water Resources Research, v. 1, no. 3, p. 375-391.

HELM, D. C. 1978. Field verification of a one-dimensional mathematical model for transient compaction and expansion of a confined aquifer system, in Verification of mathematical and physical models in hydraulic engineering. Proc. 26th Hydraul. Div. Specialty Conf., College Park, Maryland, American Soc. Civil Eng., p. 189-196.

HERRERA, I., and FIGUEROA, G. E. 1969. A correspondence principle for the theory of leaky aquifers. Water Resources Research, v. 5, no. 4, p. 900-904.

HWANG, JUI-MING, and WU, CHIAU-MIN. 1969. Land subsidence problems in Taipei Basin, in Tison, L. J., ed., Land Subsidence, Vol. 1. Internat. Assoc. Sci. Hydrology, Pub. 88, p. 21-734.

IIDA, K. 1976. Land subsidence in Nobi Plain and change of water level. Rept. Commission on Environmental Protection, Nobi Area (Japan).

KUMAI, H., SAYAMA, M., SHIBASAKI, T., and UNO, K. 1969. Land subsidence in the Shiroishi Plain Kyushu, Japan, in Land Subsidence, Vol. 2. Internat. Assoc. Sci. Hydrology, Pub. 89, p. 645-657.

LOFGREN, B. E. 1969. Field measurement of aquifer-system compaction, San Joaquin Valley, California, USA, in Land Subsidence, Vol. 1. Internat. Assoc. Sci. Hydrology, Pub. 88, p. 272-284.

McCANN, G. D., and WILTS, C. H. 1951. A mathematical analysis of the subsidence in the Long Beach-San Pedro area. Calif. Inst. Technology, Tech. Rept., 117 p.

MAGARA, KINJI. 1978. Compaction and fluid migration. Elsevier Scientific Pub. Co., New York, 319 p.

MARSAL, R. J., and GRAUE, R. 1969. The subsoil of Lake Texcoco, in Carillo, Nabor, The subsidence of Mexico City and Texcoco Project. Secretaria de hacienda y credito publico fiduciarie, Mexico, p. 167-202.

MINDLIN, R. D., and CHENG, D. H. 1950. Thermoelastic stress in the semi-infinite solid. Jour. of Appl. Phys., v. 21, p. 931.

NARASIMHAN, T.N., and WITHERSPOON, P. A. 1977. Numerical model for land subsidence in shallow ground-water systems, Internat. Assoc. Sci. Hydrology Pub. 121, p. 133-144.

NEWMARK, N. M. 1942. Influence charts for computation of stresses in elastic foundations. University of Illinois, Bull. 40(12).

POLAND, J. F., LOFGREN, B. E., IRELAND, R. L., and PUGH, R. G. 1975. Land subsidence in the San Joaquin Valley, California, as of 1972. U.S. Geological Survey Professional Paper 437-H, 77 p.

POLLARD, W. S., HOLCOMBE, R. F., and MARSHALL, A. P. 1979. Subsidence cause and effect. Harris-Galveston Coastal Subsidence District Phase 1-A study, McClelland Engineers, Inc., Houston, Texas, 2 vols.

RILEY F. S. 1969. Analysis of borehole extensometer data from central California, in Tison, L. J., ed., Land subsidence, Vol. 2. Internat. Assoc. Sci. Hydrology, Pub. 89, p. 423-431.

SCHATZ, J. F., KASAMEYER, P. W. and CHENEY, J. A. 1978. A method of using in situ porosity measurements to place an upper bound on geothermal reservoir compaction, in Proc. Second Invit. Well Testing Symp., Berkeley, Calif. Lawrence Berkeley Laboratory.

SEN, B. 1950. Note on the stresses produced by nuclei of thermoelastic strain in a semi-infinite elastic solid. Quart. Appl. Math., v. 8, p. 635.

SHIBASAKI, T., KAMATA, A., and SHINTO, S. 1969. Hydrologic balance in the land subsidence phenomena, in Tison, L. J., ed., Land Subsidence, Vol. 2. Internat. Assoc. Sci. Hydrol. Pub. 88, p. 201-214.

TERZAGHI, KARL. 1923. Die Berechnung der Durchlassigkeitsziffer des Tones aus dem Verlauf der hydrodinamischen Spannungserscheinungen. Sitzber, Akad. Wiss. Wien, Abt. IIa, v. 132.

TERZAGHI, KARL. 1925. Settlement and consolidation of clay. Eng. News-Rec., McGraw-Hill, New York, p. 874-878, Nov. 26

THEIS, C. V. 1935. The relation between the lowering of piezometric surface and the rate and duration of discharge of a well using ground-water storage. Trans. American Geophys. Union, v. 16, p. 519-524.

TOLMAN, C. F., and POLAND, J. F. 1940. Ground-water, salt-water infiltration, and groundsurface recession in Santa Clara Valley, Santa Clara County, California. Trans., American Geophys. Union, pt. 1, p. 23-34.

WADACHI, K. 1940. Ground sinking in west Osaka (second rept.) Rept. Disaster Prevention Research Institute, No. 3.

WITHERSPOON, P. A., and FREEZE, R. A. 1972. The role of aquitards in a multiple-aquifer system. Penrose Conf. of the Geological Society of America, 1971, Geotimes, v. 17, no. 4, p. 22-24.

YAMAGUCHI, R. 1969. Water level change in the deep well of the University of Tokyo. Bull. Earthquake Research Institute, No. 47.

6 Economic and social impacts and legal considerations, by Joseph F. Poland, Laura Carbognin, Soki Yamamoto, and Working Group

6.1 GENERAL COMMENTS

Land subsidence induces very serious economic and social problems, which unfortunately appear later than the commencement of the subsidence event and when most damages are irreversible.

Because intensive ground-water withdrawals often occur in urbanized and/or industrial areas, the subsidence effects are widespread and affect not only the natural structures but also the man-made ones. In general, and sad to say, damages may be recorded but it is nearly impossible to establish their actual cost.

The physical environment is a principal determining factor in the severity of economic and social impacts as a result of land subsidence due to ground-water withdrawal. Coastal-plain areas, initially 1 to 5 metres above mean sea level, are susceptible to severe impact if appreciable subsidence develops. The severity of the damage and the social problems to be anticipated are greatly increased if the subsiding area lies in a region subject to typhoons or hurricanes. Furthermore, the greater or more calamitous is the actual, anticipated, or potential damage, the greater is the likelihood that legal decisions may develop to modify the doctrine of absolute ownership or the doctrine of "correlative rights," with respect to liability for subsidence of the lands of others due to pumping of ground water.

Table 1.1 lists 42 subsidence areas worldwide. Of these, at least 19 border the ocean or a bay and 2 others are crossed by tidal rivers. In this casebook it is not practicable to discuss economic problems and legal considerations for all the subsiding areas. Therefore, in this chapter we will limit the discussion to a few significant socioeconomic problems and legal developments in Italy, Japan, and the United States.

6.2 ITALY

Reported cases of subsidence in Italy due to ground-water withdrawal are few because not all the occurrences have been identified and classified as of yet.

Venice and Ravenna cases (case histories 9.3 and 9.15) must be included among the more serious; the former for its precarious environmental setting in which the phenomenon occurs even if at low rates, the latter for its areal extent and intensity.

Both cases were brought about by the intensive exploitation of underground fluids, occurring with the Italian post-war industrial boom during the 50’s and the 60’s. in both cases exploitation occurred without taking into account possible consequences to the subsoil equilibrium.

After 20 years of continuous ground-water withdrawal, subsidence has by now greatly affected the environment and its consequences are dramatic and even more serious for the irreversible effects.

Both Ravenna and Venice are located in shallow coastal zones so that the well-known subsidence effects are worsened because the land-sea interaction is considerably reduced.

Ravenna, about 7 km from the coast, is periodically flooded because its defences are no Longer sufficient against seasonal stormy seas. Venice, built in a lagoonal environment, has a close relationship with its waters and even with just normal tidal events the city becomes partially submerged and socioeconomic activity nearly stops.

Whereas Ravenna’s historical center is somewhat protected from marine aggression, Venice is continually exposed to sea domination, thus assuming a dismal appearance which naturally conflicts with the goal of the picturesque tourist attraction. Damages are enormous for both the artistic patrimony and the normal life activity (ruined merchandise, failures in heating systems, short circuits in electrical systems, etc.).

These inconveniences are a menace to the increasingly unstable socioeconomic life because of the frequently occurring flooding paralyzing the city, for health reasons (a very humid environment), for sanitary purposes (faulty sewage system), etc.

All this and other social reasons contribute to the Venetian exodus. For this reason, the city is witnessing a rapid decline in population, especially of its poorer working classes which suffer more than the others for their ghetto-like living conditions.

Depopulation occurs even in the islands and in the least defended littorals (ex. Pellestrina). The closer and more modern industrial area (Marchera) is the greatest attraction for more modern living conditions even if there are more psychosociological stresses.

At Ravenna subsidence affects especially the littoral zones (beach regression) where the largest resorts are located, and the widespread land fills where the usable soil thickness for cultivation is reduced and the types of cultivation must be diversified. Moreover subsidence causes considerable hydraulic problems in river flow in the delta zone, facilitates salt-water intrusion at the river's mouth, and produces problems to inland navigation, in the sewage system, etc.

Although at Ravenna, the damages are very serious and economically severe they are not as dramatic as at Venice where subsidence becomes a factor of survival.

At Ravenna the hydraulic problem would almost be permanently resolved after constructing suitable sea defences and restoring older hydraulic structures. The irreversible sinking of the area greatly affects only the littorals which are diminished in their width.

In Venice the sluice gates proposed to be constructed at the inlets to control the lagoon's water level would only partially resolve Venice's complex problem; resulting changes in the lagoon ecosystem would necessitate heavy commitments for a solution.

Even if subsidence is not the main factor responsible for the slow death of Venice, without a doubt its effects have indirectly determined this evolution. This leads to the necessity of concrete interventions.

The two worst Italian cases of subsidence just described involve two very important cities because of their unusual environments and artistic patrimonies. In these cases, as well as in many other Italian cases, the cause should be sought in the haphazard territorial planning in overestimating the possibility of utilizing ground-water resources.

Strict legislation for control and regulation of environmental use plus an efficient supervising organ for the development of underground waters would have safe-guarded the areas. Unfortunately, in Italy, public institutions and laws for territorial protection against subsidence effects due to ground-water withdrawal do not exist. Underground water management is still governed by an old law of 1933, which is only effective in a few municipalities. Furthermore, such legislation deals only with the authorization to search for water and, then, the declaration of finding it.

After the 1933 law, there has been no legislation which establishes any control on artesian pumping for the defense of the territory against subsidence. Only in recent years has government's attitude changed mainly due to the alarming situations which arose in Venice and Ravenna.

So far no specific norms or restrictions have been adopted: Italian government policy leaves preventive measures restricting ground-water exploitation to the local authorities.

6.3 JAPAN

6.3.1 Socioeconomic impacts

Land subsidence has been reported in more than 40 areas in Japan; most of these areas are subsiding because of excessive ground-water withdrawal and consequent declining artesian head. Many of the large cities in Japan are built on low flat alluvial plains underlain by unconsolidated water-bearing deposits of Quaternary age. The 10 chief subsidence areas due to ground-water withdrawal (shown in Figure 1.1 and described in Table 1.1) all border the ocean; in several of these areas subsidence has lowered the land surface below sea level, creating a hazardous situation. Yamamoto (1977) reports that as of 1975 the areas of land subsidence in Japan totaled 7,380 km^2, of which about 1,200 km^2 was below mean sea level.

The prolonged subsidence since 1920 in the Koto district in the eastern part of Tokyo developed the most serious environmental subsidence problem in Japan and probably in the entire world. The artesian head in the confined aquifers, initially above sea level, declined to as much as 60 m below sea level by 1965. The long-continued head decline, due to excessive withdrawal of ground water for industrial plants, caused the subsidence. As a result, 80 km^2 of land in eastern Tokyo had sunk below mean high-tide level by 1969; the lowest ground was about 2.3 m below mean sea level (Shimizu, 1969, Table 3). Two million people live in this area bordering Tokyo Bay. To prevent flooding and loss of life many protective measures have been taken. These have been described in part by Yamamoto in Case History 9.4. Banks of through-flowing rivers have been raised several metres, a wall has been built to surround the entire area that is below

high-tide level, and many water gates have been built to prevent high water from entering the depressed area.

During the early 1960's, restrictions were established on pumping from certain depth zones and drilling of new wells, and extraction of ground water for industry in the Koto district began decreasing. By 1965 pumpage had decreased by one-half (Aihara, et al., 1969, Fig. 1). As a result the artesian head subsequently has recovered 10 to 30 m or more since the 1965 low level, and the land surface has almost completely stopped subsiding. In fact, a few centimetres of land-surface rebound has been observed. However, the rebound never will amount to more than a few per cent of the subsidence. Consequently this area and its resident population of two million people are faced with the fact that all water originating in the area below sea level, or introduced into the area for domestic or industrial supply or by flooding, will have to be pumped out as long as people live there or possibly until the land surface might be raised above sea level by a long-term project of importing a massive landfill. Despite the protective measures taken, the danger of major flooding due to typhoons or to failure of dikes or pumps caused by a violent earthquake is ever present.

Two other subsidence areas in Japan have extensive areas that have sunk below high-tide level. They are Osaka (100 km^2 below high tide) and the Nobi Plain (363 km^2 below high tide). Together with Tokyo they contain about half of the land that has subsided below hightide level in Japan. More than one million people lived in the two areas in 1969. Beginning in the early 1960's the use of ground water in Osaka has been regulated as an alternate supply of surface water became available. As a result a sharp recovery of artesian head occurred in Osaka, beginning in 1962 (see Case History 9.5, Figure 9.5.4); by 1965 the rate of subsidence had decreased markedly. Protective measures taken are similar to those adopted in eastern Tokyo. All areas below sea level are faced with the problem of how to minimize damage from a typhoon.

6.3.2 Ground-water law in Japan

Japan has two laws which regulate and or prohibit ground-water utilization. One is the "Industrial Water Law" and the other is the "Building Water Law." Japan has no law regulating ground-water withdrawal for irrigation (agricultural use).

The Industrial Water Law (law No. 146 CF 1956) is aimed at making contributions to the sound development of industries and the prevention of subsidence of the ground by ensuring a rational supply of industrial water and achieving the conservation of ground-water resources.

The areas where drawing of industrial ground water is controlled are designated by Cabinet Order out of areas where drawing of ground water is causing an abnormal drop in the ground-water level, salinization or contamination of ground water, or subsidence of ground, and water services for industrial use are already installed or the installation work is expected to be commenced within a year.

Prefectural governors issue pumping licenses mentioned if the position of the strainer for the well and the sectional area of the discharge port of the pump fulfill certain technical criteria.

The Building Water Law (law No. 100 CF, 1962) is aimed at protecting the lives and properties of the people by exercising necessary control in order to prevent the subsidence of ground as a result of drawing ground water for buildings at the specified area.

Areas where drawing of ground-water for buildings is controlled are designated by Cabinet Order out of areas where drawing of ground-water for buildings is liable to cause the subsidence of ground and resultant damage due to the high tide and flood.

Prefectural governors or mayors of the designated cities issue licenses upon request from interested individuals provided the position of the strainer for the pumping facilities and the sectional area of the discharge port of the pump fulfill certain technical criteria.

Those who are already drawing ground water for buildings when the area concerned is designated shall be considered to have obtained the license, if their methods of drawing ground water for buildings fulfill the technical criteria, and even in the case of failure to fulfill the technical criteria, they shall be treated as having a license, in principle, for a certain limited term exceeding two years.

The pumping of ground water without a license is punishable with a prison term of less than one year or a fine of less than ¥100,000.

In Case History 9.4 for Tokyo, Yamamoto describes in chronologic order the application of restrictions under the "Industrial Water Law," beginning in 1961, and restrictions under the "Building Water Law," beginning in 1963. The restrictions under the "Industrial Water Law" are designed to reduce ground-water withdrawals by supplying substitute water. The restrictions

under the "Building Water Law" are designed to limit the pumping of ground water for air conditioning and other non-drinking purposes in medium and high-rise buildings (see also Figure 9.4.9).

The local Metropolitan Environmental Pollution Control ordinance restricted the drilling of new wells in areas not covered by the two National laws described above. Also, in 1972 the Tokyo Metropolitan Government bought the mining rights to ground water containing natural gas, thereby stopping the pumping of gas-bearing water from wells 800-2,000 m deep tapping the Kagusa Group of Pliocene age.

The case history of the Nobi Plain (ch. 9.6) contains, two pages of detailed regulations for the withdrawal of ground water. Two small areas (see Figure 9.6.7) designated by the Industrial Water Law are supplied by industrial water from surface sources. Ground-water withdrawal in the remainder of the area is covered through regulation by ordinances of prefectures or of cities (by regulation zone determined by rate of subsidence per year). These ordinances specify depth of well or strainer, inside area of discharge pipe, the power of the pump motor, and the total daily discharge of the well. These complex regulations doubtless are related to the fact that 248 km^2 of the Nobi Plain were below mean sea level in 1976. The regulations have been established in an attempt to minimize the decline of artesian head, the compaction of sediments, and the rate of land subsidence.

6.4 UNITED STATES

6.4.1 Economic and social impacts

Table 1.1 lists 18 areas of land subsidence in United States due to ground-water withdrawal and Figure 1.2 shows the geographic location of 17 (not including the Alabama sinkhole area). Four of these areas border the ocean or bays but two--Savannah and New Orleans--have relatively minor subsidence problems compared to the Houston-Galveston area, Texas, and the Santa Clara Valley at the south end of San Francisco Bay in California. Ranked in terms of the severity of socio-economic problems the three principal subsidence areas in the United States due to ground-water withdrawal are (1) the Houston-Galveston area in Texas, (2) the San Joaquin Valley in California and (3) the Santa Clara Valley in California. Environmental and economic effects of subsidence in these three areas are discussed briefly in following pages. For an expanded analysis of economic effects in these and several other subsiding areas, the reader is referred to a report by Viets, Vaughan, and Harding (1979).

6.4.1.1 Houston-Galveston area, Texas

The principal detrimental effects of land-surface subsidence in the Houston-Galveston area are (1) structural damage, probably due to faulting, that has cracked buildings and disrupted pavements; (2) damage to well casings as a result of compressional stresses; (3) lessened efficiency of storm-drainage facilities and (4) submergence of coastal lowlands. According to Gabrysch (Case History 9.12), most of the damage is related to the lowering of land-surface elevations in the vicinity of Galveston Bay and the subsequent inundation by tidal waters. Several roadways have been rebuilt at higher elevations; ferry landings have been rebuilt; and levees have been constructed to protect some areas. Jones and Larson (1975) estimated the annual cost of subsidence in terms of property value losses during 1969-74 to be about $32 million in 2,450 km^2 of the area most severely affected by subsidence.

The Brownwood subdivision on the west side of Baytown is an outstanding example of both the social and economic impacts of subsidence. The subdivision has subsided about 2.8 m since 1915; some homes are permanently flooded with bay water. After a feasibility study including eight alternative plans, the U.S. Army Corps of Engineers has proposed that the entire subdivision, including 456 homes and 1,550 residents be relocated above the 50-year flood plain, at an estimated cost of about $40 million (using May 1979 price data).

Although no detailed appraisal has been made of overall costs of subsidence in the Houston-Galveston area, partial estimates, including the costs just cited, indicate that total costs to date have been several $100 million.

The most critical socioeconmic hazard to the Houston-Galveston area is the threat of catastrophic flooding by hurricane tides. The severity of the hazard will increase as long as subsidence of the coastal areas continues. Gabrysch reports (Case History 9.12) that hurricanes resulting in tides of 3.0-4.6 metres above sea level strike the Texas coast on the average of once every 10 years. This problem is discussed in more detail by Teutsch (1977).

6.4.1.2 San Joaquin and Santa Clara Valleys, California

San Joaquin Valley.--As discussed in Case History 9.13, the extensive major subsidence in the San Joaquin Valley has caused several problems, primarily economic rather than social. (1) The differential change in elevation of the land surface has created problems in the construction and maintenance of water-transport structures, including canals, irrigation and drainage systems, and stream channels. Three major canals have required remedial work because of subsidence. (2) Many hundreds of irrigation wells 200-900 m deep failed between 1945 and 1970 due to compressive rupture of casings caused by the compaction of the aquifer systems. Costs of well repair or of replacement attributable to subsidence have been many millions of dollars. (3) The need for preconsolidation of deposits susceptible to hydrocompaction increased the construction costs of the California Aqueduct by an estimated $25 million. (4) Increased cost and number of surveys made by governmental agencies and by private engineering firms to determine the elevations of bench marks to establish grades on construction sites, for revision of topographic maps, for construction of subsidence maps, and for land leveling to compensate for effects of subsidence.

No overall estimate has been made of the costs attributable to subsidence in the San Joaquin Valley but if partial estimates are correct, total costs must be in excess of $50 million.

Santa Clara Valley.--As described in Case History 9.14, the subsidence in the Santa Clara Valley has created several major problems, primarily economic. They include: (1) Land adjacent to San Francisco Bay has sunk 2-3 m since 1912, requiring construction and repeated raising of levees to restrain landward movement of bay waters onto lands now below sea level; and also requiring continued maintenance of 60 km of subsiding salt-pond levees. Also, Santa Clara County has built and maintained flood-control levees to correct for subsidence effects at a cost of $9 million. (2) Many hundreds of water-well casings have failed in vertical compression due to compaction of the confined-aquifer system. The estimated cost of repair or replacement is at least $5 million. (3) construction and maintenance of a pump station at the regional sewage treatment plant, needed because of subsidence, at a cost of $10 million (Viets and others, 1979). (4) Costs involved in repair of railroads, roads, and bridges; replacing or increasing the size of storm and sanitary sewers because of change in grade due to subsidence; establishing and resurveying the bench-mark net, and making private engineering surveys; and finally the reduction in value of 44 km^2 of land standing below high-tide level as of 1967 compared to its value if it all still stood above sea level.

No overall estimate has been made of the costs attributable to subsidence in the Santa Clara Valley but the partial relatively firm estimates suggest that total costs must have been at least $35 million.

6.4.2 Legal developments in California and Texas

In California, until the start of the 20th century, the English common law rule of absolute ownership of percolating waters prevailed. According to this doctrine: in the absence of any malice or any contractual or statutory restriction, the owner has the absolute right to intercept the water before it leaves his property and make whatever use of it he pleases, regardless of the effect that such use may have on an adjoining or lower proprietor through whose land the water infiltrates, percolates, or flows (Kooper and Finlayson, 1979).

In 1903, however, the California Supreme Court in Katz v. Walkinshaw (141 Cal. 116) spelled out a set of rules for ground water known as the "correlative rights" doctrine. Owners of land overlying a ground-water basin who used the water on the overlying land were recognized as holding the paramount right. Such owners among themselves were to share the water on a correlative basis, similar to the sharing of surface waters by riparians. Any water surplus to the needs of these overlying owners remained available for appropriation by others (Governor’s Commission to review California water rights law, 1978).

According to Koopman and Finlayson (1979), the rule of law governing liability for subsidence caused by the removal of ground water is not settled in most jurisdictions although the trend appears to be toward greater liability. This change in the law is reflected by a reversal of the position of the American Law Institute in the Restatement of Torts II compared to the Restatement of Torts I.

The Restatement of Torts I stated the rule: "to the extent that a person is not liable for withdrawing subterranean water from the land of another, he is not liable for subsidence of the other’s land which is caused by the withdrawal." Restatement of Torts, Section 318 (1938). The

position stated in the restatement of Torts II is: "One who is privileged to withdraw subterranean water, oil, minerals or other substances from under the land of another is not for that reason privileged to cause the subsidence of the other's land by such withdrawal." Restatement of Torts II, Section 318 (1969).

In 1958, the United States of America sued all the oil and gas producers in the Wilmington oil field in southern California, claiming that their operations had withdrawn undergound support from its Naval Base on Terminal Island and other properties, thereby causing subsidence which seriously damaged the government property. This case was the largest damage suit in United States history for subsidence caused by pumping fluids from the ground. The case was settled out of court. The government was assured of the control of subsidence by passage of the Anti-Subsidence Act of 1958, which compelled the oil producers in the Wilmington field to unitize and undertake to repressurize the depleted reservoir.

Again, according to Koopman and Finlayson (1979), "the statute clearly reflects a desire to retain the economic benefits of the Wilmington oil production, while relying on technology to prevent damage to private property rights. . . The Act shows the intent of the California Legislature to prevent further subsidence, but not to set liability."

As summarized by the Governor's Commission to review California water rights law (1978) "there have been two main approaches in California to instituting successful ground-water management. One has been by formation of a water district with powers to carry out a ground-water management program. The second has been management by a court-appointed watermaster with powers similar to those of a management district, after an adjudication of substantially all rights to extract ground water in the management area.

"The orange County Water District has been the leader in the water district non-adjudication approach to ground-water management. The district has a wide range of management powers, including the power to require pumpers to file periodic 'water production statements' with the district.

"The district's financing powers are extensive. It was the first district to levy a pump tax ('replenishment assessment'). The pump tax applies to all ground-water extraction, so there is no advantage to being an overlying landowner or an early appropriator. The district uses 'basin equity assessments' either to increase or decrease the cost of ground water in order to influence the relative amounts of ground water and surface water that are used, and to regulate pumping patterns.

"A central function of the Orange County Water District is to use imported water to replenish the ground-water supply. The district's replenishment operations include 'spreading' the water in areas chosen because they allow the water to percolate rapidly into the ground-water basin, and 'in-lieu' replenishment. In-lieu replenishment involves substituting a surface water supply for ground-water pumping in a particular area to allow the ground-water level to recover as a result of natural recharge.

"The San Gabriel adjudication watermaster program indicates the direction that the adjudication-watermaster approach to ground-water management is taking. The San Gabriel watermaster has a much more sophisticated range of powers and authority than the California Department of Water Resources has as watermaster for the court in four areas in Southern California. The San Gabriel watermaster, composed of nine members appointed by the court pursuant to an agreement among ground-water users in the adjudicated area, is a policy maker. It can levy a 'replacement water assessment,' which is a charge on pumping in excess of a pumper's adjudicated share of the basin's yield, can conduct a ground-water replenishment program, and has authority to control storage in the basin."

The Santa Clara Valley Water District in Santa Clara County, California, was formed by a special act of the California Legislature that was approved by the voters in 1929. A principal goal of the district in its subsequent management of all available water supplies, to balance supply and demand and hence to stop the land subsidence, has been the reduction in pumpage of ground water. (See Case History 9.14) The annual pumpage of ground water decreased about 20 per cent from 1960-65 to 1970-75. A principal reason for the decrease in pumpage was a use tax levied on a ground-water pumpage since 1964. The enactment of the 1929 legislation providing for the local management of ground-water resources, including the taxing power, represented a major departure from the early rule of absolute ownership.

Historically Texas has followed the English common law rule of absolute ownership to withdraw water from beneath his property with no liability for damage to other lands. In the past five years, however, the trend has clearly been toward holding pumpers of ground water responsible for damage from subsidence. First came the creation of the Harris-Galveston Coastal Subsidence District in 1975, followed by two major legal decisions involving subsidence and liability.

The Harris-Galveston Coastal Subsidence District was created by the Texas Legislature in May 1975 "to provide for the regulation of the withdrawal of ground water within the boundaries of the district for the purpose of ending subsidence which contributes to or precipitates flooding, inundation, or overflow of any area within the district, including without limitation rising waters resulting from storms or hurricanes" (Neighbors, 1979).

The act creating the district provides that water wells located within the district, with casing diameter in excess of five inches, are required to have a permit to withdraw a specified amount of water for a period of not less than one year nor more than five years. The district is supported financially by the permit fees. The current permit fee rate is $4.50 per million gallons (3,785 m^3).

A major court decision in Coastal Industrial Water Authority v. W. B. York (1976) involved the submergence of York's land in the Houston Ship Canal due to the subsidence. The court held that the property owner did not lose title to the land due to the fact that it had become submerged from subsidence as a result of pumping of ground water.

In 1978, according to Neighbors (1979), the Texas Supreme Court reinforced the Legislature's authority to regulate ground-water withdrawal for the purpose of controlling subsidence. In Smith-Southwest Industries, Inc. v. Friendswood Development Co. (1978) the Court referred to the creation of the Subsidence District and other legislative acts in establishing the intent of the Legislature to limit the common-law rule of absolute ownership of ground water. The Court held that ground-water users were not liable for subsidence damages caused by past actions, but could be held responsible for damages due to future pumpage if such were conducted in a negligent or malicious manner. The opinion concludes "Therefore, if the landowner's manner of withdrawing water (in the future) is negligent, willfully wasteful or for the purpose of malicious injury, and such conduct is a proximate cause of the subsidence of the land of others, he will be liable for the consequences of his conduct."

6.5 REFERENCES

AIHARA, SHIGERU, et al. 1969. Problems of groundwater control in Tokyo, in L. J. Tison, ed., Land subsidence, v. 2, IASH/AISH Pub. 89, p. 635-644. Coastal Industrial water Authority v. W. B. York, 532, S.W. 2d 949 (1976). Governor's Commission to Review California Water Rights Law. 1978. Final Report, Sacramento, California, 264 p.

JONES, L. L., and LARSON, JAMES. 1975. Economic effects of land subsidence due to excessive ground-water withdrawal in the Texas Gulf Coast area. Texas Water Resources Institute, Texas A and M Univ., Tech. Report-67, 33 p.

KOOPER,W., and FINLAYSON, D. J. 1979. Legal aspects of subsidence due to well pumping. Am. Soc. Civil Engineers Annual Meeting, Atlanta, Georgia, Oct., preprint no. 3748, 24 p.

NEIGHBORS, R. J. 1979. Subsidence in Harris and Galveston Counties, Texas. Am. Soc. Civil Engineers Annual Meeting, Atlanta, Georgia, Oct., no. 3663, 23 p., also ASCE Jour. Irrig. and Drainage, v. 107, no. IR2, June 1981, p. 161-174.

SHIMIZU, RYOSAKU. 1969. Land subsidence in Japan. Booklet prepared for 1969 Internat. Symposium on Land Subsidence, Tokyo, Japan.

SMITH-SOUTHWEST INDUSTRIES, INC., et al v. FRIENDSWOOD DEVELOPMENT CO., et al. @@ Tex Sup. Ct. J. 105 (Nov. 29, 1978).

TEUTSCH, J. S. 1977. Subsidence in the Houston-Galveston region, A comprehensive analysis. Master's thesis, Rice University, Houston, Texas.

VIETS, V. F., VAUGHAN, C. K. and HARDING, R. C. 1979. Environmental and economic effects of subsidence. Report prepared by EDAW, Inc. and Earth Sciences Associates for Lawrence Berkeley Laboratory, Berkeley, California, under LBL Contract No. 300-3902, 232 p.

YAMAMOTO, SOKI. 1977. Recent trend of land subsidence in Japan. 1AHS/AISH Pub. No. 121, p. 9-15.

7 Review of methods to control or arrest subsidence, by Joseph F. Poland and Working Group

7.1 SUMMARY OF AVAILABLE METHODS

7.1.1 General statement

Methods to control or arrest subsidence include reduction of pumping draft, artificial recharge of aquifers from the land surface, and repressuring of aquifers through wells, or any combination of these methods. The goal is to manage the overall water supply and distribution in such a way that the water levels in wells tapping the compacting aquifer system, or systems, are stabilized or raised to some degree. In other words, at least manage the overall supply in such a way that effective stress in the aquifer system is not increased beyond the stress experienced to date.

The local geologic conditions determine whether artificial recharge can be accomplished by regulated application at the land surface or by repressuring of aquifers by means of injection through wells.

Both the artificial recharge of aquifers from the land surface and the repressuring of aquifers through wells normally require a supply of potable surface water. The question may be asked: "Why not use the supplementary surface supply directly at land surface and thereby reduce ground-water draft, instead of recharging the ground-water supply?" The answer may be that it is impracticable to deliver all the supplementary supply direct to users so part of the supply is recharged to the water table. The ground-water reservoir then acts as the distribution system. Such is the case in the Santa Clara Valley in California (Case History 9.14).

7.1.2 Reduction of pumping draft

Reduction of pumping draft may be accomplished to some degree by one or more of the following methods:

1. Import of substitute surface water.
2. Conservation in application and use of water:
   a. through improvement of irrigation methods, such as change from ditch and furrow or flood irrigation to overhead sprinkler irrigation or to drip irrigation.
   b. through change from crops requiring heavy duty or demand to crops requiring less duty, such as from cotton to orchards.
3. For overdrawn ground-water basins, adjudication (equitable distribution) of available supply.
4. In urban areas, by recirculation and reuse of treated water by industrial plants.
5. By decreasing irrigated area or industrial plants using large quantities of water.
6. By moving the well fields to tap more permeable (less compressible) deposits.
7. By changing the depth range of perforated intervals in well casings or screens to tap less compressible deposits.
8. By legal control.

Whether any one of these remedies is economically justified depends on its cost compared with the costs of continued subsidence. The first requirement for estimating costs is an estimate of the magnitude of subsidence that would occur (1) if the artesian head was maintained at the present level, and (2) in response to an assumed additional decline in head.

7.1.3 Artificial recharge of aquifers from the land surface

Land subsidence usually results from compaction of compressible confined aquifer systems due to intensive withdrawal of ground water and consequent decline of artesian head. Because confining beds restrict the vertical downward movement of water from the land surface, artificial recharge of confined system(s) by application of water at the land surface directly overhead ordinarily

is not practicable. However, the geology of the system may be such that the confined aquifer system may crop out at or near the margins of the ground-water basin; this outcrop area may be near enough to the subsiding area so that artificial recharge on the outcrop area will raise the local water table and also the artesian head in the confined system.

7.1.4 Repressuring of aquifers through wells

Repressuring of confined aquifer systems by artificial recharge directly through wells, although expensive, may prove to be the only practical way to slow down or stop land subsidence in a particular area. The Wilmington oil field in southern California is a classic example of subsidence control by injection of water through wells. Repressuring of the oil zones to increase oil production and to control subsidence began on a major scale in 1958. By 1969, when 175 x $10^3 m^3$ (1.1 x 10^6 barrels) of water per day was being injected into the oil zones, the subsiding area had been reduced from 58 to 8 km^2, and locally the land surface had rebounded as much as 0.3 m (Mayuga and Allen, 1969). In 1975 about 80 x 106 m^3 (500 x 10^6 bbls) of water was injected into the oil zones to (1) control subsidence, (2) produce 10 x 10^6 m^3 of oil and (3) utilize 67 x 10^6 m^3 of water produced with the oil. According to Gates, Caraway, and Lechtenberg (1977), the injection of this great quantity of water from diverse sources created many problems which were controlled by various chemical and physical treatments.

Replenishinq ground-water supplies by artificial recharge through wells and pits has been practiced in many areas, including many sites in California and more than a thousand recharge wells on Long Island, New York. The results of such practices have been summarized to 1967 in two annotated bibliographies on artificial recharge of ground water (Todd, 1959; Signor, Growitz, and Kam, 1970). In general, results were satisfactory when the water was clear; most of the problems of recharge through wells involved clogging of the well and aquifer. In a study of problems in artificial recharge through wells in the Grand Prairie region of Arkansas, Sniegocki (1963) found that the principal causes of clogging were air entrainment, suspended particles in the recharge water, and micro-organisms. He concluded that wells should be recharged with treated water and that water-treatment cost and contemplated use of the recharged water are the principal factors involved in determining the economic feasibility of artificial recharge. The availability of water suitable for injection would be another important factor.

Injection of treated fresh water into a confined aquifer system to create an hydraulic barrier (pressure ridge) to sea-water intrusion has been practiced successfully in southern California for 25 years. The operating agency, the Los Angeles County Flood Control District, had 180 injection wells in operation in 1976. According to Rancilio (1977), during two decades of operating experience the District never has had to cease operation of an injection well permanently because of loss of operating efficiency. Because of the continuing success of this massive injection operation for a quarter century, the reader interested in injection wells is referred to the paper by Rancilio (1977) which describes in detail the typical design of a successful injection well, operating conditions and costs, injection rates and heads, clogging problems, and redevelopment of injection wells. Both the cable-tool and reverse-rotary methods were used in construction of the injection wells but at least two-thirds of the wells are reverse-rotary, with asbestos-cement casing and gravel pack. The operational injection heads ranged from 9 to 61 metres and injection rates ranged from 6 to 28 l/s.

7.2 REVIEW OF METHODS USED

7.2.1 Summary statement

Table 1.1 lists 42 areas of land subsidence due to ground-water withdrawal. Methods used to control or arrest subsidence in these areas may be summarized as follows:

In 15 areas, ground-water draft has been reduced as a result of substituting imported or locally treated surface water.
In 4 areas, ground-water draft has been reduced by regulation but surface water import not reported.
In one area, pumping of gas-bearing water was stopped by legal action (Po Delta, Italy); in another area (Niigata, Japan) reinjection of all gas-bearing water has been required since 1973.
In one area, ground-water pumped from mines has been led outside rock compartments or injected into a leached dolomite aquifer through 10 boreholes since 1973.
In 20 areas no methods for control have been reported.

7.2.2 Shanghai, China

Land subsidence in Shanghai, China, was first reported in 1921. By 1965 the maximum cumulative subsidence in the city was 2.63 m (Case History 9.2). Injection of river water through wells to recharge the principal aquifers began about 1964. By 1966, more than 100 industrial plants operating more than 200 wells had joined in the recharge operation to build up pressure in the confined aquifer system. As shown by the record from typical bench marks in the urban area of Shanghai (Figure 9.2.1), the cessation of subsidence was virtually instantaneous. Within a year or two, bench marks apparently were rising and from 1966 to 1976, as much as 34 mm of rebound occurred.

The injection of river water through production wells is undertaken chiefly in the winter months when many factories are not operating and when the river water is coldest. Because much of the ground water withdrawn is used for cooling purposes in the factories in the summer, any decrease in water temperature in the aquifers is beneficial. As a result of careful monitoring of river-water temperature to obtain water of minimum temperature for injection, the ground-water temperature at one site reportedly has been lowered 6° C.

7.2.3 Venice, Italy

After studying by mathematical model the physical mechanism and the quantitative relationship linking the pumping rate to the resulting subsidence of Venice, the behavior of the aquifer system and ground surface became well understood. (See Case History 9.3.) Because land subsidence was caused by pressure drawdown in the aquifer system, it was apparent that the only remedy consisted of raising the pressure surface beneath Venice.

Injection of water through injection wells was suggested as a possible measure by a number of experts. However this solution would have required water with chemical properties similar to those of the underground water. Moreover the effectiveness of this remedy could not be scientifically proven.

An uplift experiment on a small island near Venice was successfully carried out by pressure grouting using special cement mortars (Marchini and Tomiolo, 1977). Unfortunately, the experiment could not be transferred to uplift such an extensive area as Venice.

Other proposed solutions, including the construction of a deep wall acting as a hydraulic barrier for the city, were soon abandoned on the grounds of impracticability.

The recognition of the physical mechanism underlying the subsidence of Venice and the results provided by theoretical and experimental patterns showed that the most effective and cheapest solution consisted of reducing the withdrawal rate in the Venetian area. The recovery of the flow field was shown to be rather fast and the arrest of the settlement was proven to be almost instantaneous.

Accordingly, the Venice Municipality prompted the completion of the planned aqueduct and the construction of a new one to supply the industrial area with water taken from the Sile and the Brentella Rivers, which flow in the vicinity of the Venetial Lagoon. More that 90 per cent of the water used for industrial purposes now is supplied by surface water from the local rivers. Furthermore, as soon as the aqueducts became operative, the Magistrato alle Acque (Civil Engineers Branch) of Venice issued a prohibition against opening new wells and an injunction to close the existing wells.

To date, more than 70 per cent of the artesian wells that were active in 1969 have been gradually shut down; this trend still continues and a constant improvement of the subsidence situation in Venice has been observed (see Case History 9.3)

7.2.4 Japan

The ten principal subsidence areas in Japan, due to excessive ground-water withdrawal, are listed in Table 1.1. In all of these areas ground-water withdrawal has been reduced by regulation; in parts of Tokyo withdrawal of ground water from wells has been prohibited completely. (See Case History 9.4). In seven areas surface water has been imported as a replacement for ground water. In several areas, industrial waste water is being treated and reused.

In Niigata (Case History 9.7) experiments of water injection into the confined aquifers containing methane gas were carried out from 1960 to 1963 (Ishiwada, 1969). The purpose of the injection was the maintenance of reservoir pressures and reduction of the rate of subsidence. Both degassed formation water and river water were used as the injection fluids. According to

Ishiwada, the permeability of the main reservoirs ranges from 10 to 50 darcys, the injection rate is less than one-quarter of the production rate, and back-washing at adequate time intervals is necessary to continue long-term injection.

Since 1973, all degassed formation water has been reinjected into the gas-bearing reservoirs by law.

7.2.5 United States

Table 1.1 describes 18 areas of land subsidence in the United States. Of these, six have imported surface water to satisfy water demands. This has led to the reduction of pumping draft and the local stabilizing or raising of artesian pressures. They include the Santa Clara Valley and three areas in the San Joaquin Valley in California, as well as Las Vegas Valley in Nevada and the Houston-Galveston area in Texas. A major aqueduct to import Colorado River water to south-central Arizona now (1980) is under construction.

Repressuring through injection wells has not been used in any of these areas and artificial recharge of a substantial part of the imported surface water has been practiced only in the Santa Clara Valley. In the other five areas, imported surface water has been used as a direct replacement or substitute for ground-water pumpage.

7.3 REFERENCES

GATES, G. L., CARAWAY, W. H., and LECHTENBERG, H. J. 1977. Problems in injection of waters in Wilmington oil field, California. IAHS-AISH Pub. 121, p. 319-324.

ISHIWADA, YASUFUMI. 1969. Experiments on water injection in the Niigata gas field. IAHS-AISH Pub. 89, p. 629-634.

MARCHINI, S., and TOMIOLO, A. 1977. The use of mud-jacking for the upheaving of urban zones. Computer control of the works. Experimental application to the problem of Venice. IAHS-AISH Pub. 121, p. 63-94.

MAYUGA, M. N., and ALLEN, D. R. 1969. Subsidence in the Wilmington oil field, Long Beach, Calif., USA. IAHS-AISH Pub. 88, p. 66-79.

RANCILIO, J. A. 1977. Injection well operation and maintenance. IAHS-AISH Pub. 121, p. 325-333.

SIGNOR, D. C., GROWITZ, D. J., and KAM, WILLIAM. 1970. Annotated bibliography on artificial recharge of ground water, 1955-1967. U.S. Geological Survey Water-Supply Paper 1990, 141 p.

SNIEGOCKI, R. T. 1963. Problems in artificial recharge through wells in the Grand Prairie region, Arkansas. U.S. Geological Survey Water-Supply Paper 1615-F, 25 p.

TODD, D. K. 1959. Annotated bibliography on artificial recharge of ground water through 1954. U.S. Geological Survey Water-Supply Paper 1477, 115 p.

Part II
Case histories of land subsidence due to ground-water withdrawal

8 Types of land subsidence, by Alice S. Allen, Bureau of Mines, U.S. Department of the Interior, Washington, D. C.

8.1 INTRODUCTION

Land subsidence is merely the surface symptom, and the last step, of a variety of subsurface displacement mechanisms. Not all of these mechanisms are well understood. Subsidence processes are concealed below ground; their development to the point of surface deformation may involve long periods of time; and for at least some mechanisms, significant evidence may lie outside the area directly beneath the surface subsidence. Furthermore, at some sites more than one condition favourable to subsidence occurrence may be present and require consideration in analyzing causal mechanisms and devising remedial procedures.

Subsidence is a familiar accompaniment of a variety of natural events that comprise the geologic history of many areas. For practical reasons geologic processes that are accompanied by subsidence have been examined for evidence that the range in their rates of progress extends into a time frame that may produce damaging effects in terms of man’s time scale. The processes investigated are those that remove or rearrange subsurface materials to produce void space or significant volume reduction--solution, underground erosion, lateral flow, and compaction--or, in the case of tectonic activity, deep-seated downward displacement. For all of these naturally occurring geologic processes, examples of related surface subsidence have been found, though some are rare (Allen, 1969). The incidence of subsidence is greater where some of these geologic processes are set in motion or accelerated by man’s engineering activities that involve excavation, loading, or changes in the ground-water regime.

The term "subsidence" is used in this discussion in a broad sense to include both gentle downwarping and the collapse of discrete segments of the ground surface. Displacement is principally downward, although the associated small horizontal components have significant damaging effects. The term is not restricted on the basis of size of area affected, rate of displacement, or causal mechanism.

An overview of favorable geologic settings and engineering operations that may contribute to land subsidence is presented as background for the specialized treatment of subsidence caused by ground-water withdrawal, which is the subject of this guidebook. Topics on which information is widely available are mentioned briefly. More space is given to topics for which published information is less readily available for most readers. Mining subsidence is not reviewed, but several examples of interaction between mining and natural geologic processes are cited. Subsidence in regions underlain by permafrost and in areas of active volcanism is not discussed.

8.2 THE ROLE OF SUBSURFACE SOLUTION IN SUBSIDENCE

Common soluble components of earth materials that may be associated with subsidence include salt, gypsum, and the carbonate rocks--limestone and dolomite. The roles that these soluble materials play in the development of surface subsidence depends in part on the degree of their solubility, and in part on other physical characteristics.

8.2.1 Salt

Although rock salt (sodium chloride) is one of the most soluble of the common earth materials, the presence of underlying salt deposits has only rarely been associated with surface subsidence under natural conditions in recent times. This is in part because the original occurrence of salt deposits is limited geographically, and in part because salt deposits have already been removed to considerable depths except in arid climates by the leaching action of ground water. Collapse breccias found in strata overlying salt-bearing horizons constitute geologic evidence that subsidence has taken place under natural conditions in the geologic past. Collapse breccias due to solution along the margins of underlying salt deposits have been reported from the Michigan Basin (Landes, 1963), the Delaware basin of West Texas and southeastern New Mexico (Maley and Huffington, 1953), and in the western Canadian area underlain by evaporites of the Prairie Formation (DeMille and others, 1964).

In south-central Kansas where salt deposits still exist at depths between 90 and 120 m, a dramatic example of natural subsidence in historic time was documented in photographs in 1879 (Johnson, 1901, Pls. 136-138). A deep crater about 60 m in diameter was discovered disrupting a cattle trail. The interrupted tracks of a wagon that had passed 3 weeks earlier were clearly seen on both sides of the sinkhole. Another sinkhole about 130 km to the northeast carried away a railroad station overnight (Johnson, 1901, p. 713, footnote).

Indirect evidence of natural subsidence is the presence of surface depressions occupied by lakes or swamps in areas where underlying salt deposits have been undergoing dissolution. The eastern boundary of the Kansas salt deposits is fairly abrupt where salt deposits 60 m thick are missing in wells a few miles to the east. Above, the blunt edge of the salt is a narrow belt of marshes, swamps, and lakes, many of which contain salty water (Bass, 1926). Lakes also occur overlying salt domes in Louisiana (Barton, 1936, O'Donnell, 1935). At an oil-producing operation at Sour Lake dome in Texas, Sellards (1930) described one lake that had formed under natural conditions, and a large sinkhole that appeared in 1929 which was attributed to removal of salt in the saturated water that had been produced along with the oil over a long period of time.

The incidence of subsidence in some areas underlain by salt deposits has been stimulated by salt mining operations. In Cheshire, England, where salt has been mined since pre-Roman times, the effects of solution subsidence on the topography and on structures have been spectacular (Calvert, 1915; Howell and Jenkins, 1977; Wallwork, 1973). Early mining was by the room-and-pillar method in which pillars were left to support the surface. As unsaturated ground water gained access to old mine workings, the dissolution of pillar salt led to surface subsidence, though it was limited as the ground water in contact with the salt became saturated. When methods of salt production changed to pumping the so-called "wild" brines, surface subsidence was greatly accelerated. Water levels were lowered by continued pumping, and additional under-saturated ground water circulated randomly through the cavernous saltbeds, continually removing any protective envelope of saturated brine that may have developed. The topography, previously modified by natural solution subsidence, was further changed by the development of craterlike depressions 10 to 200 m in diameter, and linear hollows over 200 m wide and 8 km long. Streets and railroad tracks were distorted. In Northwich, very few pre-1900 buildings survived the subsidence damage. In the 1970's, natural brine pumping is being phased out, and most salt production is by controlled solution mining. Fresh water or undersaturated brine is injected through boreholes into deeper deposits of massive salt, creating regularly spaced solution cavities about 90 m in diameter. Mature cavities are maintained in stable condition by flooding with saturated brine.

A recent investigation of subsidence related to salt dissolution in Kansas found only five subsidence events due to salt mining over an 88-year period, and eight subsidences related to oil and gas operations (Walters, 1977). The rare subsidence occurrences were attributed to aquifers above the salt not being adequately isolated by surface casing or, in the case of salt-water disposal wells, casing failures which permitted flow of unsaturated brine across the salt.

8.2.2 Gypsum

Gypsum ($CaSO_4 \cdot 2H_20$) is a soluble rock-forming mineral which, with its anhydrous counterpart, anhydrite, occurs abundantly in marine evaporite basin deposits. Evidence that surface subsidence was caused by dissolution of gypsum in past geologic times includes collapse features in rocks overlying gypsum deposits in the Roswell basin, New Mexico (Bean, 1949), and in the southern Black Hills of South Dakota and Wyoming (Bowles and Braddock, 1960), and solution-subsidence troughs in the gypsum plain of west Texas and southeastern New Mexico (Olive, 1957).

Sinkholes on the present-day land surface have been reported in areas underlain by gypsum-bearing rocks in New Mexico (Bean, 1949; Morgan, 1942) and Oklahoma (Fay, 1959) in the United States and at various localities in Europe (International Association of Engineering Geology, 1973).

In addition to collapse and sinkholes that overlie deposits of relatively pure gypsum, subsidence may also be associated with rocks and soils that contain minor amounts of gypsum. Klein (1966) described several types of gypsum occurrence in a very arid part of the San Joaquin Valley, California, which were investigated by the Bureau of Reclamation in connection with locating and designing a large water-transfer, pump-storage, and irrigation project. Along margins of periodic shallow lakes, efflorescent accumulations of gypsum contained solution cavities that were believed responsible for damages to canals and embankments. Weathered-shale bedrock contained secondary gypsum in veinlets and seams, which made up from 2 to 5 per cent of the rock mass. Similar veinlets and seams of gypsum characterized the weak, clayey gravel in

one of the abutments of the St. Francis dam near Los Angeles, which failed disastrously in 1928 soon after the reservoir had been filled. Solution of gypsum was cited as a likely contributor to disintegration of the weak foundation material (Ransome, 1928).

The presence of small quantities of gypsum (1 to 3 per cent of dry weight) appears to be a general indicator of soils in the San Joaquin Valley that are susceptible to subsidence on wetting, but the role played by the gypsum is conjectural. Bull (1964) concluded that the gypsum content cannot be used exclusively as an indicator of potential subsidence, and he did not consider solution of gypsum to be a major cause of the subsidence. Differences in gypsum content of subsiding and nonsubsiding soils reflects compositional differences in their source areas, and possibly the removal of gypsum from nonsubsiding soils by water percolating from streams. Klein (1966) believed that the presence of gypsum contributed to the flocculation of clay particles influencing the size and amount of pore space, and shared responsibility for the low density of these deposits with the presence of trapped air inherited from their mudflow origin. Noting that much of the gypsum occurred as minute efflorescent crystals coating the small voids characteristic of the subsiding soils before hydrocompaction, he suggested that gypsum supplemented the clay minerals as a weak and easily soluble cementing agent.

8.2.3 Carbonate rocks

The carbonate rocks, limestone and dolomite, are responsible for the most widespread incidence of subsidence related to solution, not because of a high degree of solubility, but because of wide geographic distribution. A great deal of information is available on solution features in carbonate rocks (Internat. Assoc. of Engineering Geology, 1973; Tolson and Doyle; 1977, Transportation Research Board, 1976). LaMoreaux, LeGrand, and Stringfield (1975, p. 45-47) list more than 50 symposia and conferences on hydrology of carbonate rocks held throughout the world in the past 30 years.

The incidence of sinkhole development may be greatly increased when equilibrium conditions are disturbed by man’s construction projects or mining operations, particularly those that alter ground-water levels or increase surface infiltration. Newton (1976) reported that more than 4,000 induced sinkholes, areas of subsidence, or other-related features have occurred in Alabama since 1900, most of them since 1950. In Missouri, 97 catastrophic surface failures have been recorded since the 1930’s, of which 46 were attributed to man’s activity (Williams and Vineyard, 1976). Subsidence accelerated by dewatering of underground mines in carbonate terrain has been described by Foose (1968).

Collapse at the ground surface may appear suddenly, but is the culmination of a sequence of processes starting with the development of solution openings in bedrock. Interconnecting systems of solution passageways develop over geologic time and persist, owing to a combination of the slow rate of dissolution of carbonate rocks and their high compressive strength, which maintains the integrity of the cavity systems. Subsequently, unconsolidated overburden materials may be slowly washed down into bedrock cavity systems. The resulting voids in the overburden may become enlarged until the remaining cover is too thin to support the surface and collapse takes place.

8.3 THE ROLE OF SUBSURFACE MECHANICAL EROSION IN SUBSIDENCE

Subsurface mechanical erosion is the term used for an infrequently recognized phenomenon in which temporary subsurface flow channels are developed in unconsolidated or friable materials that may lead to surface collapse. The term "piping" has also been used for this process. Water percolating through pervious surficial materials becomes diverted to a more or less horizontal path on reaching the water table or a less pervious stratum. The water, which transports grains of silt and sand, finds an outlet along a nearby valley wall or cliff face or internally in caves, mine openings, or boreholes. Erosion tends to work headward from the outlet, creating and enlarging a tunnel that intersects the vertical flow channel of concentrated percolation water. As tunnel enlargement and upward propagation of the roof reduce the support capacity of the surface materials, the ground surface collapses to produce sinkholes.

In order to produce surface subsidence, the subsurface erosion mechanism is believed to require three conditions (Allen, 1969): (1) A pervious, easily erodible material must be overlain by material sufficiently competent, at least temporarily, to form a roof above the developing tunnel; (2) water must have access to the erodible material with sufficient head to transport grains of silt or sand; and (3) some sort of outlet must be available for disposal of the flowing water and the sediment grains that it transports. Examples of subsidence attributed to subsurface erosion in a variety of geologic materials are summarized in Table 8.1.

Table 8.1. Occurrences of subsidence due to subsurface erosion.

Location (Reference)	Surface expression	Erodible material	Roof	Channel development	Outlet
Kanus, China (Fuller, 1922)	Circular holes 1.5-6 m diam.; vertical walls	Loess	Dry loess	Tunnels up to 1 m wide, 3 m high	Ravine walls; plateau rims
Kamloops, B.C., Canada (Buckham and Cockfield, 1950)	Circlar sinkholes 15-30 m diam; funnel shaped	Pleistocene "White Silts" on Thompson River Terraces	Dry silt	Nearly horizontal passageways up to 1 m high; at temporary water table	Gulleys; terrace front
Eastern Oregon (Parker and other, 1964)	"Pseudokarst" (resembles karst topography in limestone areas)	Altered tuff and volcanic ash	Dry tuff and ash	Eroded cavern complex 200 m long with 4 levels	Hanging valley walls
Chuska Mountains NW New Mexico (Wright, 1964)	Pleistocene depressions containing intermittent lakes	Uncemented eolian sandstone	Cemented sandstone strata	Inferred but not observed; process inactive at present	Steep mountain escarpments
Zuni Dam, New Mexico (Eckel, 1939)	Cracking and subsidence of abutments, 1909, 1936	Sand bed 1-2.5 m thick; underlain by clay	Basalt flow, jointed	Through joints in basalt, water under head flushed out sand, creating large voids	Cliff below dam
Memphis, Tennessee (Terzaghi, 1931)	Subsidence of building and strip of land 200 m long; bluff subsided 18 m over 2 1/2 month period	Bed of uniform, rounded, fine quartz sand, 14 m thick	Fairly stiff clay	Inferred channel eroded along under side of sand, leaving cavity which collapsed	Mississippi River bluff
Minneapolis-St. Paul, Minnesota (Schwartz, 1936; Soper, 1915)	A few sinkholes; not all tunnels broken through to surface	Poorly cemented St. Peter sandstone (Ordovician)	Platteville limestone	Caves developed in friable sandstone, probably more than a kilometre long in places	River gorges
Attala County, Mississippi (Parks, 1963)	Caves and sinkholes near hilltops and heads of gullies	Thin deposits of leached silt	Quartzitic sandstone, fractured	Through cracks in quartzitic bed, water washes out silt forming tunnels 6+ m long and caves 1+ m high	Heads of gullies

The material that forms the roof of tunnels at some localities is a different, and more competent, material than that in the eroded horizon. In other localities, the material forming the roof and the eroded horizon are the same (i.e. loess, altered volcanics), but the competency of the roof is dependent on cohesion in a dry condition provided by montmorillonitic clay bonding. Such cohesion is lost upon saturation as the component particles become disaggregated when wet.

Cases of underground mechanical erosion are difficult to identify. At least part of the process must be inferred in the absence of direct observation. Tunnel development is concealed below ground and may only be disclosed by the apparently sudden collapse at the surface. The collapse is the last step in a long continued process in which sediments are eroded grain by grain and transported to the outlet. Accumulations of transported sediments are rarely observed because the silt and sand grains either become incorporated in the colluvium below the outlet on a valley wall, or are washed down into cavities or excavations in the bedrock.

8.4 LATERAL FLOW AS A SUBSIDENCE MECHANISM

Lateral flow of subsurface materials as a cause of subsidence is uncommon but not unknown. Examples have been reported both under natural geologic conditions and under loading by man’s activities (Allen, 1969). Common earth materials susceptible to plastic flow are salt, gypsum, clay, and clay shale.

Geologic examples of subsidence by salt flowage are rim synclines surrounding salt domes in coastal Texas and Louisiana (Nettleton, 1934; Ritz, 1936) and broad synclines associated with salt tectonics in the Paradox Basin in Utah and Colorado (Cater, 1954). Where the Green and Colorado Rivers have cut deep canyons well down into the formation overlying salt and gypsum in Utah, the removal of load has permitted salt and gypsum to flow laterally, resulting in very local folds and graben (Baker, 1933).

Flowage of shale has produced a geologic subsidence feature termed "cambering" in the Jurassic iron ore locality in east-central England (Hollingworth and Taylor, 1951). Cambering occurs in deeply dissected areas in which a competent rock such as ironstone or limestone overlies Lower Jurassic clay shale. Lateral flowage of clay shale toward the valley axes has lowered the overlying competent rock as much as 30 m; in places the lowering has been intensified by subsurface erosion along the shale-ironstone contact and by sliding of the ironstone on the shale surface.

On thick glacial clay deposits in the Great Lakes region of North America, lateral flowage has been induced beneath stockpiles of ore, resulting in slight-lowering of the ground surface and increasing the distance between ore-retaining walls over a few decades by nearly 2 m (Terzaghi, 1953).

8.5 COMPACTION AS A CAUSE OF SUBSIDENCE

A common cause of ground-surface subsidence is reduction in the volume of low-density sedimentary deposits that accompanies the process of compaction, in which particles become more closely packed and the amount of pore space is reduced. Compaction may be induced by loading, by drainage, by vibration, by extraction of pore fluids, and under certain conditions by the application of water. Compaction occurs both naturally and by man’s manipulation.

The amount of subsidence effected by compaction is a function of the relative amount of pore space in the material as originally deposited, the effectiveness of the compacting mechanism, and the thickness of the deposit undergoing compaction. Natural deposits of unusually high initial porosity include modern delta deposits, terrigenous mudflows, undisturbed loess, and peat.

8.5.1 Loading

The effects of natural loading are most apparent where great thicknesses of fine-grained sediments accumulate rapidly. The process of compaction is accompanied by contemporary subsidence. On the modern Mississippi River delta, 300 to 500 million tons of sediment is deposited each year. Fisk and others (1954) found that levee deposits on the lower delta had subsided 6 m and interdistributary marsh deposits, 8.5m.

At New York’s La Guardia Airport, the natural compaction of an 18-m thickness of saturated organic silt and clay deposits was accelerated by artificial loading (Engineering News Record, 1949; Kyle, 1951). Half the airport was reclaimed from Flushing Bay by placing 7.5 m of fill over the saturated sediments. After 25 years of operation, parts of the filled area had subsided

2.5 m, with further subsidence anticipated (Halmos, 1962). Protection from tide waters is furnished by a dike around three sides of the airport, which was built on soil stabilized by sand drains that extend 20 m below sea level.

8.5.2 Drainage

In low-lying areas, lowering of the water table by artificial drainage stimulates compaction of sediments with accompanying subsidence of the surface. Compaction rates have much more than academic significance in areas such as the polders of the Netherlands where vast regions have been reclaimed from the sea by building dikes and installing pumps. Bennema and others (1954) found that clay deposits containing 30 to 35 per cent of a minus 2-micrometre fraction compressed to about half their original thickness after reclamation over a 100-year period. Sediments with about 20 per cent fine fraction compressed about 25 per cent; compaction of sand layers was negligible.

Drainage of peat areas can be expected to result in subsidence for two reasons. Peat is commonly underlain by, and frequently interbedded with, fine sediments that are susceptible to compaction when drained. In addition, peat has certain physical and chemical characteristics that lead to extreme volume changes upon drying (Highway Research Board, 1954; MacFarlane, 1959; Stephens and Speir, 1969). Peat has a water-holding capacity ranging from 300 to 3,000 per cent.

Its bulk density is extremely low--about 960 kg/m^3 when wet and 64 kg/m^3 when dry. Particle specific gravity is also low--between 1.0 and 2.0. Furthermore, peat undergoes irreversible biochemical changes on drying that reduce volume. The largest peat areas in the United States that have been subsiding following reclamation for agricultural development are the Florida Everglades (Stephens and Speir, 1969) and the delta area at the confluence of the Sacramento and San Joaquin Rivers in California (Weir, 1950). In the Chikuho coalfield in Japan, subsidence in areas underlain by thick peat and organic clay deposits was attributed to their compaction in response to the lowering of ground-water levels during mining operations (Noguchi, Takahashi, and Tokumitsu, 1969).

8.5.3 Vibration

Sedimentary materials may be compacted by vibration under natural conditions during earthquakes. Buildings on saturated alluvium or uncompacted fill may subside or settle differentially in response to earthquake vibrations or, if the foundations are tied to a lower stable stratum, the buildings may appear to rise as the surrounding sediments subside by compaction.

A variety of manmade sources of vibration have been cited by Terzaghi and Peck (1967) as having produced subsidence by compaction of underlying earth materials. These sources of vibration include heavy rock-crushing equipment, turbogenerators, truck traffic, an elevated railway, pile driving and blasting. At sites of structures to be built on saturated sand, future subsidence may be forestalled by the vibroflotation process of foundation treatment. Giant vibrators fitted with jets are lowered to the desired depth and withdrawn slowly, resulting in cylinders of compacted sand (Sowers and Sowers, 1961). Loose foundation materials may also be densified by buried charges of explosives (Lyman, 1942). Underground nuclear explosions in unconsolidated materials are characterized by craters on the ground surface (Drell, 1978).

8.5.4 Extraction of pore fluids

Of all causes of land subsidence, both natural and those induced by man’s activities, subsidence associated with extracting fluids from subsurface formations is best understood. Many areas of subsidence caused by pumping of artesian water, oil, and gas have been identified, surface and subsurface changes have been monitored, and corrective measures have been devised. A decade ago the topic of "Land Subsidence Due to Fluid Withdrawal" was reviewed by Poland and Davis (1969). Current progress in identifying and coping with subsidence caused by withdrawing ground water in many parts of the world is reported in the case histories comprising Chapter 9 of this volume.

8.5.5 Hydrocompaction

Certain materials of unusually low density deposited in areas of low rainfall undergo significant compaction when they become thoroughly wetted. The process, termed "hydrocompaction,"

produces rapid and irregular subsidence of the ground surface, ranging from 1 to nearly 5 m. Reclamation projects that import and distribute irrigation water in dry areas underlain by loess and by mudflow deposits have encountered subsidence problems. It is thought that clay bonding of the particles is responsible for maintaining open textures while the deposits are in a dry condition, and for rapid disaggregation and volume loss when immersed in water (Bull, 1964). Surface subsidence resulted from wetting without the addition of surcharge load at many sites; at others, a combination of water infiltration and surface loading was required. A review of the phenomenon of hydrocompaction by Lofgren (1969) describes the process and associated subsidence occurrences in the United States, Europe, and Asia.

8.6 TECTONIC SUBSIDENCE

Large areas of measurable downward displacement have been associated with a few earthquakes of large magnitude. The 1959 Hegben Lake earthquake in Montana produced an asymmetrical subsided area 69 by 22 km, in which the maximum subsidence was 6.6 m (Myers and Hamilton, 1964). During the 1960 series of earthquakes in Chile, subsidence of 1 to 1.5 m was reported to have affected a coastal area 600 by 30 km (Weishcet, 1963). The 1964 Alaska earthquake produced an asymmetrical downwarped area 800 by 160 km. Tectonic subsidence, which ranged up to 2.3 m, was augmented in many places by compaction of unconsolidated materials (Plafker, 1965).

8.6.1 Discussion

The state-of-the-art in land-subsidence analysis progresses unevenly because the degree of understanding of various subsidence mechanisms varies. Most study has been directed to subsidence related to man’s engineering activities. This is facilitated by availability of data on quantities of subsurface material removed (or injected), on rates and duration of extraction operations, and on changes in ground-water levels. Natural processes are not as easily quantified.

A case of land subsidence is necessarily the integrated surface expression of whatever processes may be active at that site, whether natural or manmade, or both. A working hypothesis as to the mechanism or combination of mechanisms operative at the specific site is requisite for designing control measures. The complexity of subsidence mechanisms and their interaction requires cooperative effort among different disciplines, both in collecting physical evidence and in developing the rationale for the processes involved. The hydrologic sciences have been, and will continue to be, significant contributors to land subsidence investigations.

8.7 REFERENCES

ALLEN, ALICE S. 1969. Geologic settings of subsidence, in Reviews in Engineering Geology, Volume II. Geol. Soc. America, P. 305-342.

BAKER, A. A. 1933. Geology and oil possibilities of the Moab district, Grand and San Juan Counties, Utah. U.S. Geol. Survey Bull. 841, 95 p.

BARTON, D. C. 1936. Late recent history of the Côte Blanche salt dome, St. Mary Parish, Louisiana. Am. Assoc. Petroleum Geologists Bull., v. 20, no. 2, p. 179-185.

BASS, N. W. 1926. Structure and limits of the Kansas salt beds. Kansas Geol. Survey Bull. 11, P. 90-95.

BEAN, R. T. 1949. Geology of the Roswell Artesian Basin, New Mexico, and its relation to the Hondo Reservoir. New Mex. State Engineer Office Tech. Rept., no. 9, p. 1-31.

BENNEMA, J., GEUZE, E. C. W. A., SKITS, H., and WIGGERS, A. J. 1954. Soil compaction in relation to Quaternary movements of sea-level and subsidence of the land especially in the Netherlands. Geologie en Mijnbouw, new ser., v. 16, no. 6, p. 173-178.

BOWLES, C. G., and BRADDOCK, W. A. 1960. Solution breccias in the upper part of the Minnelusa sandstone, South Dakota and Wyoming (Abstract). Geol. Soc. America Bull., v. 71, p. 2032.

BULL, W. B. 1964. Alluvial fans and near-surface subsidence in western Fresno County, California. U.S. Geological Survey Professional Paper 437-A, 71 p.

BUCKHAM, A F., and COCKFIELD, W. E. 1950. Gullies formed by sinking of the ground (British Columbia). Am. Jour. Sci., v. 248, no. 2, p. 137-141.

CALVERT, A. F. 1915. Salt in Cheshire. London, E. and F. N. Spon, Ltd.; New York, Spon and Chamberlain, 1,206 p.

CATER, F. W., Jr. 1954. Geology of the Bull Canyon Quadrangle, Colorado. U.S. Geol. Survey Geol. Quad. Map (GQ-33).

DeMILLE, G., SHOULDICE, J. R., and NELSON, H. W. 1964. Collapse structures related to evaporites of the Prairie Formation, Saskatchewan. Geol. Soc. America Bull., v. 75, p. 307-316.

DRELL, S. D. 1978. The case for the test ban. Washington Post, July 4, p. A17.

ECKEL, E. B. 1939. Abutment problems at Zuni Dam, New Mexico. Civil Eng., v. 9, no. 8, p. 490-492.

ENGINEERING NEWS-RECORD. 1949. Saving LaGuardia Airport. Eng. News-Rec., v. 143, no. 24, p. 35-37.

FAY, R. 0. 1959. Guide to Roman Nose State Park, Blaine County, Oklahoma. Oklahoma Geol. Survey Guidebook 9, 31 p.

FISK, H. N., McFARLAN, EDWARD, Jr., KOLB, C. R., and WILBERT, L. J. 1954. Sedimentary framework of the modern Mississippi delta. Jour. Sed. Petrology, v. 24, no. 2, p. 76-99.

FOOSE, R. M. 1968. Surface subsidence and collapse caused by ground-water withdrawal in carbonate rock areas. 23d Internat. Geological Congress, Proceedings, v. 12, p. 155-166.

FULLER, M. L. 1922. Some unusual erosion features in the loess of China. Geog. Rev., v. 12, p. 570-584.

HALMOS, E. E. 1962. Face lift for a busy airport. Excavating Engineer, v. 56, no. 6, p. 18-22.

HIGHWAY RESEARCH BOARD. 1954. Survey and treatment of marsh deposits. Natl. Research Council, Highway Research Board Bibliography 15, Pub. 314, 95 p.

HOLLINGWORTH, S. E., and TAYLOR, J. H. 1951. The Northampton Sand Ironstone; stratigraphy, structure and reserves. Great Britain, Geol. Survey Memoir, 211 p.

HOWELL, F. T., and JENKINS, P. L. 1970. Some aspects of the subsidences in the rocksalt districts of Cheshire, England, in Proceedings, 2d International Symposium on Land Subsidence. Anaheim, Calif., 1976; Internat. Assoc. Sci. Hydrologists Pub. No. 121, pp. 507-520.

INTERNATIONAL ASSOCIATION OF ENGINEERING GEOLOGY. 1973. Symposium--sinkholes and subsidence-engineering-geological problems related to soluble rocks. Proceedings published by Deutsche Gesellschaft für Erd und Grundbau, Essen.

JOHNSON, W. D. 1901. The High Plains and their utilization. U.S. Geol. Survey 21st Ann. Rept., pt. 4, 601-741.

KLEIN, IRA E. 1966. Foundation and ground-water problems related to the occurrence of gypsum in hydraulic engineering works of the United States Bureau of Reclamation in the San Luis Unit of the Central Valley Project in California, in International Symposium on Public Works Construction in Gypsiferous Terrains, Madrid, 1962. Servicio Geologico de Obras Publicas, Madrid, Paper C.2-7, 38 p.

KYLE, J. M. 1951. Settlement correction at La Guardia Field. Am. Soc. Civil Engineers Trans., v. 116, p. 1343-1348.

LaMOREAUX, P. E., LeGRAND, H. E., and STRINGFIELD, V. T. 1975. Progress of knowledge about hydrology of carbonate terrains, in Burger, A., and Debertret, L., Hydrogeology of karstic terrains. Internat. Assoc. of Hydrogeologists, Internat. Union of Geological Sciences, Ser. B., no. 3, Paris, p. 41-52.

LANDES, K. K. 1963. Effects of solution of bedrock salt in the earth's crust, p. 64-73 in Bersticker, A. C., and others, eds., Symposium on salt. Cleveland, Northern Ohio Geol. Soc., 661 p.

LOFGREN, B. E. 1969. Land subsidence due to the application of water, in Reviews in Engineering Geology, Volume II. Geol. Soc. of America, p. 271-303.

LYMAN, A. K. B. 1942. Compaction of cohesionless foundation soils by explosives. Am. Soc. Civil Engineers Trans., v. 107, Paper no. 2160, p. 1330-1341.

MacFARLANE, I. C. 1959. A review of the engineering characteristics of peat. Am. Soc. Civil Engineers Proc., Jour. Soil Mechanics and Found. Div., V. 85, no. SMI, pt. 1, p. 21-35.

MALEY, V. C., and HUFFINGTON, R. M. 1953. Cenozoic fill and evaporite solution in the Delaware Basin, Texas and New Mexico. Geol. Soc. America Bull., v. 64, p. 539-546.

MORGAN, A. M. 1942. Solution phenomena in the Pecos Basin in New Mexico. Am. Geophys. Union Trans., v. 23, pt. 1, p. 27-35.

MYERS, W. B., and HAMILTON, WARREN. 1964. Deformation accompanying the Hebgen Lake earthquake of August 17, 1959. U.S. Geol. Survey Prof. Paper 435-1, p. 55-98.

NETTLETON, L. L. 1934. Fluid Mechanics of salt domes. Am. Assoc. Petroleum Geologists Bull., v. 18, no. 9. p. 1175-1204.

NEWTON, J. G. 1976. Induced and natural sinkholes in Alabama--a continuing problem along highway corridors. Natl. Acad. Sci. Transportation Research Record 612, Part 1, pi 9-16.

NOGUCHI, T., TAKAHASHI, R., and TOKIMITSU, Y. 1969. On the compression subsidence of peat and humic layers in the Kami-Shinbashi area, Kurate-Machi, Kurate-Gun, Fukuoka Prefecture, in Tison, L. J., ed., Land Subsidence, v. II. Internat. Assoc. Sci. Hydrology, Pub. 89, p. 458-466.

O'DONNELL, LAWRENCE. 1935. Jefferson Island salt dome, Iberia Parish, Louisiana. Am. Assoc. Petroleum Geologists Bull,. v. 68, p, 351-358.

OLIVE, W. W. 1957. Solution-subsidence troughs, Castile formation of Gypsum Plain, Texas and New Mexico. Geol. Soc. America Bull., v. 68, p. 351-358.

PARKER, G. G., SHOWN, L. M., and RATZLAFF, K. W. 1964. Officer's Cave, a pseudokarst feature in altered tuff and volcanic ash of the John Day Formation in eastern Oregon. Geol. Soc. America Bull., v. 75, p. 393-402.

PARKS, W. S. 1963. Attala County mineral resources. Mississippi Geol. Econ. and Topog. Survey Bull. 99, 191 p.

PLAFKER, GEORGE. 1965. Tectonic deformation associated with the 1964 Alaska earthquake of March 27, 1964. Science, v. 148, no. 3678, p. 1675-1687.

POLAND, J. F., and DAVIS, G. H. 1969. Land subsidence due to withdrawal, of fluids, in Reviews in Engineering Geology, Volume II. Geol. Soc. America, p. 187-269.

RANSOME, F. L. 1928. Geology of the St. Francis damsite. Economic Geology, v. 23, p. 553-563.

RITZ, C. H. 1936. Geomorphology of Gulf Coast salt structures and its economic application. Am. Assoc. Petroleum Geologists Bull., v. 20, no. 11, p. 1413-1438.

SCHWARTZ, G. M. 1936. The geology of the Minneapolis-St. Paul metropolitan area. Minnesota Geol. Survey Bull. 27, 267 p.

SELLARDS, E. H. 1930. Subsidence in Gulf coastal plain salt domes. Texas Univ. Bull. 3001, p. 9-36.

SOPER, E. K. 1915. The buried rock surface and pre-glacial river valleys of Minneapolis and vicinity. Jour. Geology, v. 23, p. 444-460.

SOWERS, G. B., and SOWERS, G. F. 1961. Introductory soil mechanics and foundations (2d ed.). New York Macmillan, 386 p.

STEPHENS, J. C., and SPEIR, W. H. 1969. Subsidence of organic soils in the U. S. A., in Tison, L. J., ed., Land subsidence, v. 1. Internat. Assoc. Sci. Hydrology, Pub. No. 89, p. 523-534.

TERZAGHI, KARL. 1931. Earth slips and subsidences from underground erosion. Eng. News-Rec., v. 107, no. 3, p. 90-92.

TERZAGHI, KARL. 1953. Foundation of buildings and dams, bearing capacity, settlement observations, regional subsidences. Zurich, 3d Internat. Conf. on Soil Mechanics and Foundation Eng., 3rd, Proc., v. 3, p. 158-159.

TERZAGHI, KARL, and PECK, R. B. 1967. Soil mechanics in engineering practice (2d ed.). New York, John, Wiley, 729 p.

TOLSON, J. S., and DOYLE, F. L., eds. 1977. Karst hydrology. Internat. Assoc. of Hydrogeologists, 12th Internat. Congress, Huntsville, Alabama, 1975, Proceedings, 578 p.

TRANSPORTATION RESEARCH BOARD. 1976. Subsidence over mines and caverns, moisture and frost actions, and classification. Nat. Acad. Sci., Transportation Research Record 612, 83 p.

WALLWORK, K. L. 1973. Salt and environmental planning: an historical perspective to a contemporary land-use problem, in Fourth Symp. on Salt. Northern Ohio Geol. Soc., v. 1, pp. 435-441.

WALTERS, R. F. 1977. Land subsidence in central Kansas related to salt dissolution. Kansas Geol. Survey Bull. 214, Univ. of Kansas Pub., Lawrence, Kans., 82 p.

WEIR, W. W. 1950. Subsidence of peat lands of the Sacramento-San Joaquin delta, California. Hilgardia (California Agr. Expt. Sta. Jour.), v. 20, no. 3, p. 37-56.

WEISCHET, WOLFGANG. 1963. Further observations of geologic and geomorphic changes resulting from the catastrophic earthquakes of May 1960, in Chile. Seismol. Soc. America Bull., v. 53, no. 6, p. 1237-1257 (trans. by R. Von Huene).

WILLIAMS, J. H., and VINEYARD, J. D. 1976. Geologic indicators of catastrophic collapse in karst terrain in Missouri. Natl. Acad Sci. Transportation Research Record 612, pt. 1, p. 31-37.

WRIGHT, H. E., Jr. 1964. Origin of the lakes in the Chuska Mountains, northwestern New Mexico. Geol. Soc. America Bull., v. 75, p. 589-598.

9 Case Histories

Case History No. 9.1. Latrobe Valley, Victoria, Australia, by C. S. Gloe, State Electricity Commission of Victoria, Victoria, Australia

9.1.1 INTRODUCTION

The Gippsland Basin covers an area of some 40,000 km^2. Four-fifths of this area is located off-shore and the remaining fifth in the Gippsland Region of south-eastern Victoria. The offshore area contains a number of oil and gas fields, while the on-shore portion includes an area of some 800 km^2 known as the Latrobe Valley Depression where major deposits of brown coal occur beneath a thin cover of overburden.

The excavation of brown coal for the generation of electricity and production of briquettes commenced in the Latrobe Valley some 50 years ago. The coal is won from open cuts, the development of which has been accompanied by significant vertical and horizontal movements, both within the excavation as well as in surrounding areas. To enable the coal from the second major open cut to be excavated under safe operating conditions, it has been necessary to reduce the artesian pressures of underlying aquifers. The resulting increased effective stresses have induced consolidation of strata and cause subsidence which is now regional in extent.

9.1.2 GEOLOGY

The Gippsland Basin developed in the off-shore area in Upper Cretaceous times with the deposition of lacustrine and fluviatile sands and clays and a number of brown coal seams. The basin gradually developed westwards and lithologically similar sediments were deposited in the onshore area in Lower Tertiary times (Figure 9.1.1).

Within the Latrobe Valley Depression some 700 m of Tertiary sediments named the Latrobe Valley Coal Measures, and including some volcanics towards the base, were deposited mainly on Lower Cretaceous arkoses and shales. The coal measures include three groups of major coal seams, separated and underlain by clays and sands (Gloe, 1975).

In late Tertiary times the coal measures were tilted, folded and faulted. Extensive erosion followed, virtually to the stage of peneplanation. Subsequently, a thin cover of clays, silts and sands was deposited on the eroded surface. As a result of the peneplanation, considerable thicknesses of sediments were removed from uplifted blocks. In the areas of the Yallourn and Morwell open cuts, the two major open cuts in the Latrobe Valley, up to 150 m and 300 m respectively of clays, sands and brown coals were removed (Figure 9.1.2).

In the Yallourn open cut the Yallourn seam averages 60 m in thickness and underlies 10 to 15 m of younger overburden. Beneath the Yallourn seam are some 120 to 150 m of sands and clays overlying a further thick coal seam.

The Morwell 1 (Ml) seam being excavated in the Morwell open cut ranges from about 90 to 135 m in thickness beneath 12 to 15 m of overburden. Underlying the coal seam are 15 to 23 m of sands and clays followed by the Morwell 2 (M2) coal seam which is up to 50 m thick in this area. A further sequence of clays and sands, including an almost completely weathered layer of basalt and a thick basal silty gravel, totalling some 140 m in thickness, underlies the M2 seam.

9.1.3 HYDROLOGY

Unconfined ground waters are present over most of the area, but quantities are mainly small. The water occurs in the overburden sands as well as in the joint system of the uppermost coal seam.

Confined waters are found in the sands underlying coal seams, and in some fresh basalt flows. Prior to the development of the Morwell open cut, water struck in bores in low-lying areas flowed at the surface, sometimes under considerable head (Gloe, 1967).

In the area of the Morwell open cut some 8 to 9 m of medium to coarse grained, poorly sorted and highly permeable sands, known as the M1 aquifer, occur beneath the Ml seam. The sands are irregular and typical sheet deposits (Barton, 1971). Along the northern edge of the open cut the original piezometric level stood at +60 AHD, a height some 150 m above the level of the aquifer in that area.

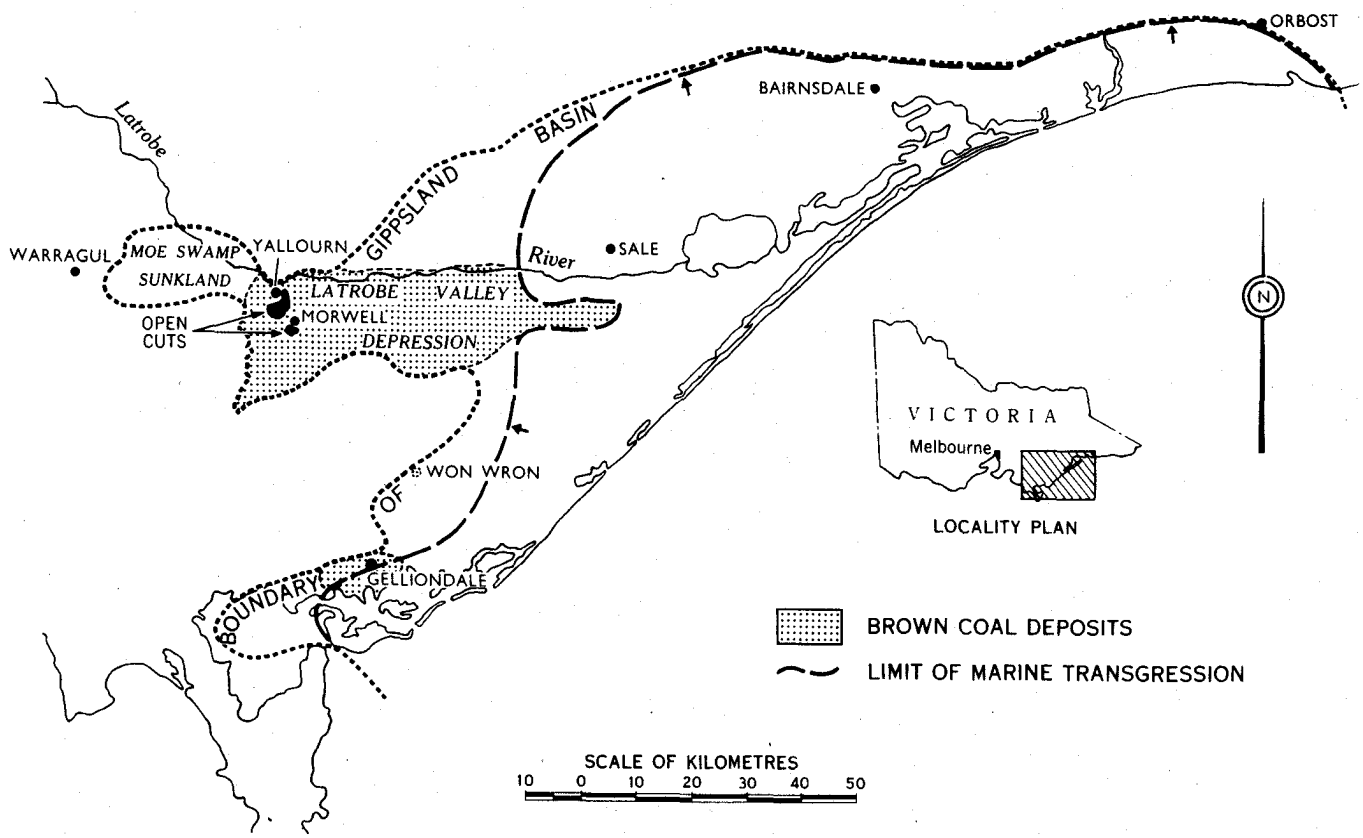

Figure 9.1.1 Gippsland Basin.

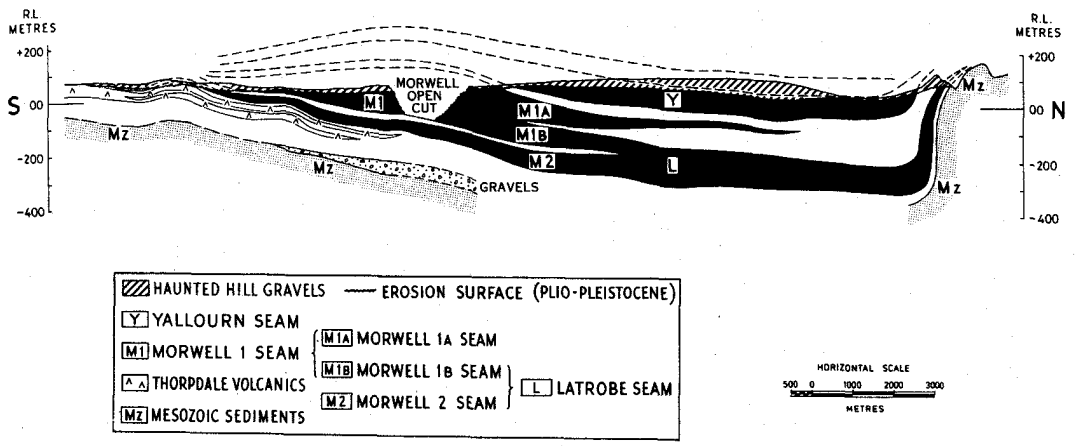

Figure 9.1.2 Reconstruction of pre-erosional stratigraphy

The M2 aquifer consists of several irregular sand beds occurring between 3 and 50 m below the M2 seam. There is evidence of vertical leakage between the M1 and M2 aquifers--partly due to numerous boreholes, partly to the fracturing which accompanied heaving of the floor of the open cut as new levels were established, but also naturally as part of a leaky aquifer system.

In the Yallourn open cut the weight of the clays underlying the Yallourn seam is sufficient to withstand the hydrostatic pressure of the artesian waters present in that area. However, at Morwell it had been calculated that the weight of coal and clay would be unable to withstand the artesian pressures once a working level had been established to an area 300 m across at a depth of some 65 m below the original surface. As this still left some 50 m of coal above the base of the seam, it was clear that the M1 aquifer pressures would need to be progressively reduced as the open cut was developed in depth (Gloe, 1967).

The main program of pressure reduction, frequently called dewatering, commenced in 1960 as the first coal cut was excavated. Initially, free-flow bores were used, new bores being established as new levels were opened up. By 1967 it was found necessary to construct pumping bores in the M1 aquifer. Subsequent investigations established that the pressures from the M2 aquifer, although already substantially reduced through leakage, would require further lowering to ensure safe operating conditions. This reduction was achieved initially through free-flow bores and subsequently using pumping bores with yields of up to 160 l/s.

The maximum rate of pumping from the M2 aquifers was 1160 l/s at which time the total pumping rate was 1320 1/s. Piezometric levels were lowered to safe operational levels and have been maintained for two years with yields of 925 1/s from M2 aquifer and 130 1/s from M1 aquifer. Total artesian water pumped from Morwell open cut to June 1977 was 250,000 x 10^6 1.

Contours of the M1 aquifer piezometric surface as at July 1977 are shown in Figure 9.1.3. The M2 aquifer levels have a generally similar pattern. The original levels were of a gently sloping surface with values of +60 AHD at Morwell open cut and rising to +65 AHD in the west.

Investigations of recharge and intake areas have included carbon dating of water samples. The youngest water from near the western edge of the basin was 2200 years old, while the water pumped from the Morwell open cut gave values of 23 500 years for the M1 and 13 800 years for the M2 aquifer waters. These ages conform with the concept of a multi-aquifer and aquitard, or leaky aquifer system, with a large volume of water in storage, but in which the upper aquifers at least are not replenished by rapid infiltration of rainwater in intake areas. It is considered that much of the water pumped from the M1 aquifer has been derived through leakage from lower aquifers and from compaction of aquitards.

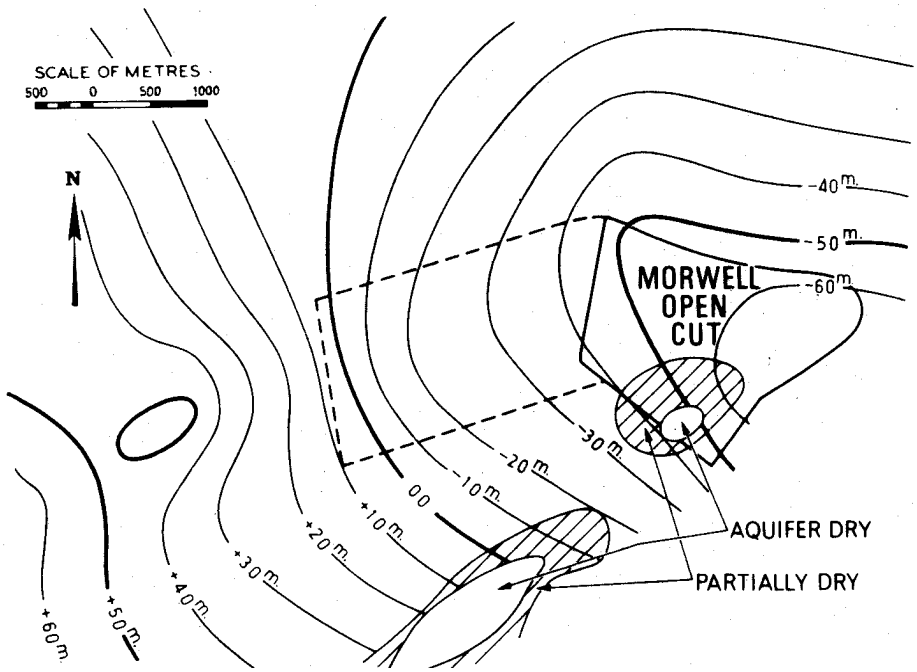

Figure 9.1.3 Piezometric surface of Morwell 1 aquifer.

9.1.4 MECHANICAL PROPERTIES OF BROWN COAL AND ASSOCIATED STRATA

9.1.4.1 Brown coal

Properties of brown coal have been described by Gloe, James and McKenzie (1973). Brown coal was shown to be a highly preconsolidated organic material with a low bulk density (1.13 g/cm^3) and very high moisture content (up to 200 per cent as expressed on an engineering basis).

Average values of preconsolidation pressures assigned to M1 and M2 coals in the vicinity of the Morwell open cut based on estimates made using Casagrande's method were 2300 kPa and 2900 kPa respectively.

The coefficient of volume decrease (mv) depends both on the consolidation pressure and initial moisture content, but for purposes of calculating consolidation settlements where the consolidation pressure is less than 1300 kPa the following values of (mv) were assigned:

M1 coal--0.2 cm^2/kN at top of seam to 0.1 cm^2/kN at base of seam;

M2 coal--0.1 cm^2/kN.

9.1.4.2 M1 aquiclude

Beneath the M1 seam there is a 3 to 13 m layer of stiff grey preconsolidated silty clay. The clay is composed of kaolinite and a-quartz with a plasticity index around 20 to 25 per cent and a liquid limit of about 60 per cent.

Average properties for the clay are

Clay fraction, 44 per cent
Bulk density, 1.8 8/cm^3
Compression index (C_C), 0.5
Coefficient of volume decrease (mv), 0.2 cm^2/kN
Consolidation pressures, 1300 kPa

9.1.4.3 M1 and M2 aquifer sands

The gradation of the M1 sand is highly variable ranging from coarse sand with fine gravel and fine sand to silty fine sand. The sand is dense to very dense and relatively incompressible. In the area of the open cut the M2 sands are generally thicker and hence have a higher transmissibility than those of the M1 aquifer. In other respects the sands are similar.

9.1.4.4 M2 aquicludes and aquitards

The M2 aquicludes and aquitards range from clays to silts with properties generally similar to those of the M1 aquiclude.

9.1.5 EXTENT OF MOVEMENTS

Surface movements, both inside and outside the Yallourn and Morwell open cuts have occurred ever since excavation commenced. Regular surveys are carried out to determine the amounts of these movements.

The movements at Morwell open cut exceed those at Yallourn open cut, mainly because of the dewatering operations and greater depth of the open cut. The surveys at Morwell which were initiated prior to the commencement of open cut operations are based on a datum line remote from the open cut with survey beacons around the open cut being located by triangulation. The beacons form the control for precise traverses of pin lines established in and around the open cut.

By 1977 when the open cut had reached its full depth and was being developed to the west, horizontal movements had reached as much as 2.25 m and vertical movement 1.68 m at the top of the northern and eastern batters. These movements decrease outwards from the edge of the open

cut.

Contours of horizontal movement in the Morwell area and of subsidence in the Yallourn-Morwell area are shown on Figures 9.1.4 and 9.1.5 respectively. The pattern of horizontal movement is roughly concentric about the floor of the open cut with the major movement occurring within 400 m of the edge of the open cut. The 20 cm contour is at present stationary and approximately 1000 m north and east of the open cut. On the other hand, subsidence is far more regional in extent--now affecting the whole of the Yallourn-Morwe11 area and extending eastwards into Loy Yang, some 20 km east of Morwell. By 1977 the 20 cm and 50 cm subsidence contours were located some 7.2 km and 4.5 km respectively north of the open cut with the 50 cm contour embracing an area of 47 km^2 and including much of Morwell township.

The C line of survey marks passes through the southern portion of Morwell township at right angles to the northern edge of the open cut. Horizontal movement and subsidence profiles along the C line are shown in Figure 9.1.6. By 1977 the total southerly displacement of a point adjacent to the open cut was 2.01 m, but at a distance of 400 m from the open cut was only 0.39 m. Similar patterns of movement are found on other pin lines extending outwards from the open cut. In the vicinity of the open cut subsidence commenced at a slower rate, and at one stage was little more than half that of horizontal movement. However, a steady rate of subsidence has been maintained while horizontal movements have decreased after deepening of the open cut ceased and development extended westwards. At 200 m from the northern edge of the open cut, vertical and horizontal movements are now roughly equal, while at 800 m vertical movements exceed horizontal by 0.95 m (Figure 9.1.6).

Evidence of subsidence such as protrusion of casing above ground surface is visible at Morwell. Figure 9.1.7 shows clamps on an observation bore casing set in the M1 aquifer now standing 1.0 m above the shallow surface casing on which they originally rested.

9.1.6 CAUSES OF MOVEMENT

Factors contributing to movement were discussed by Gloe, James and Barton (1971), Gloe (1976) and Hutchings, Fajdiga and Raisbeck (1977). Apart from the geometry of the cut and the

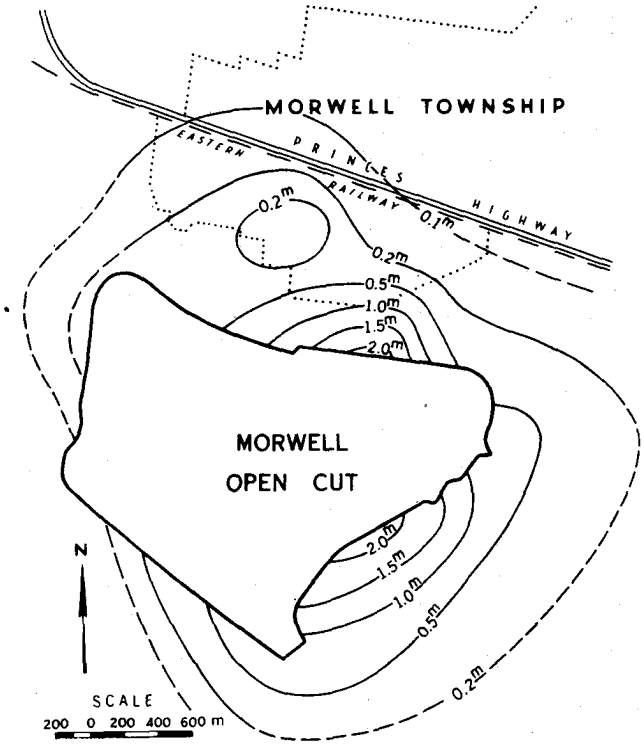

Figure 9.1.4 Horizontal movement adjacent to Morwell open cut

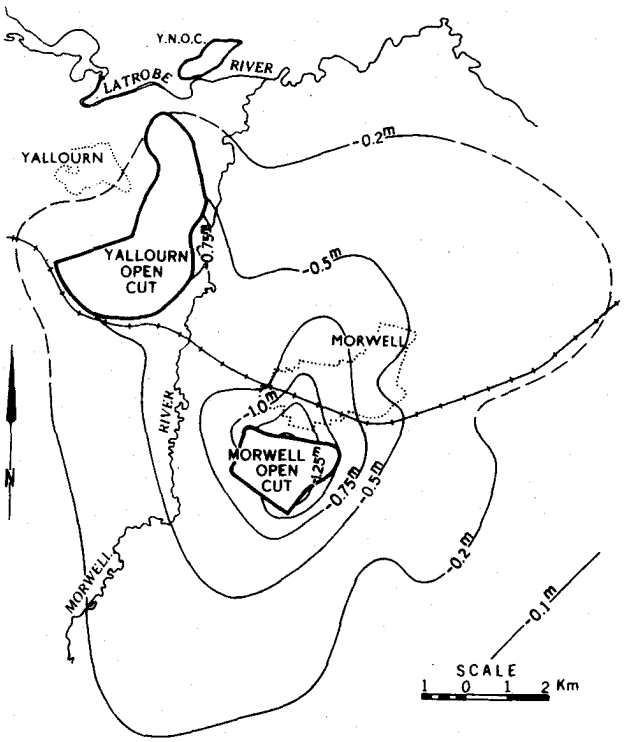

Figure 9.1.5 Regional subsidence in the Yallourn-Morwell area.

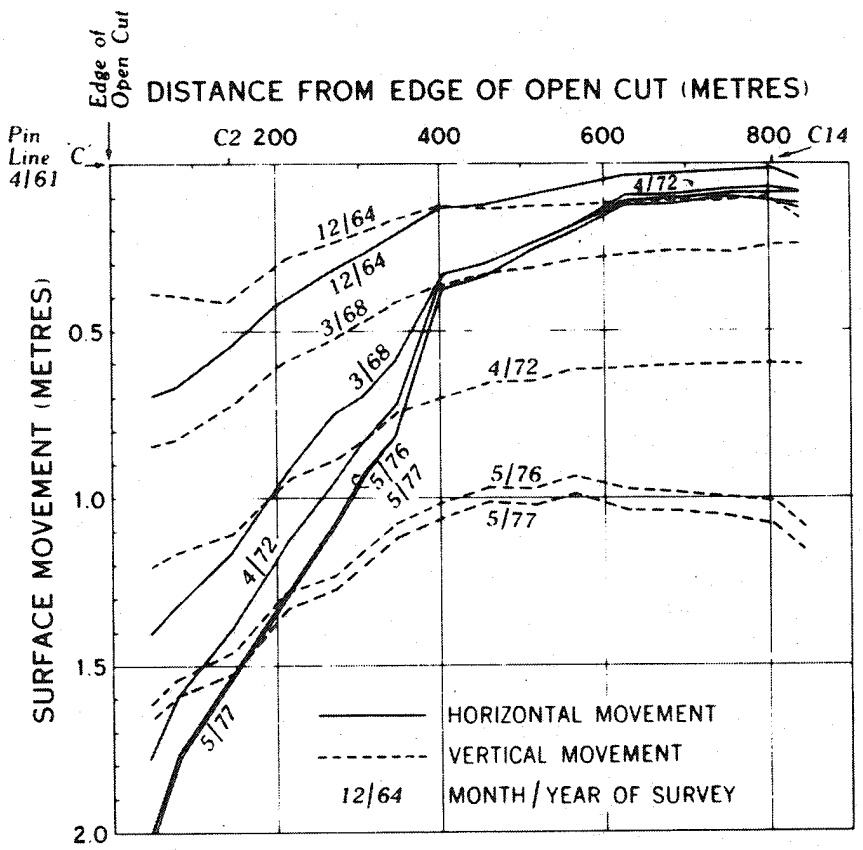

Figure 9.1.6 Horizontal movement and subsidence profiles on C line.

.

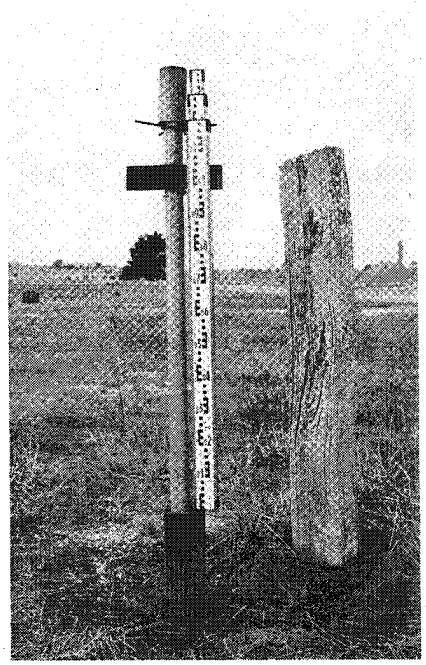

Figure 9.1.7 Protruding bore casing north of Morwell open cut.

geological structure, the significant factors influencing movements in the area around Morwell open cut are pressure relief and reduction in artesian and ground-water pressures.

As stated above, the major horizontal movements occur within a distance of some 400 m from the edge of the open cut and are considered to be due to pressure relief as well as to response to differential subsidence.

Subsidence near the open cut is influenced by pressure relief (inward and downward movement of batters), but regional subsidence is attributed mainly to consolidation of strata through increase of effective stresses resulting from the lowering of artesian water pressures. The lowering of the ground-water table by natural drainage through joints or horizontal bores drilled at toes of batters for lengths of up to 250 m also results in consolidation. However, such effects are not considered to extend beyond distances of 600 m from the open cut.

The relationships between subsidence, piezometric levels and flow rates are shown on Figure 9.1.8. Since 1960 the M1 and M2 aquifer pressure levels have been lowered by some 125 m and 120 m respectively in the area of the floor of the open cut. Dewatering of M2 aquifer was not commenced until 1970 and hence the 50 m reduction in piezometric level of this aquifer must have been achieved through upward leakage.

Although no significant horizontal movements have occurred at C14 (800 m north of open cut) this survey mark is subsiding at a rate similar to that at C2 (150 m north) where substantial horizontal movements have taken place. The regional character of subsidence is further illustrated by the steady lowering of Pin M158, located 5 km north of open cut, but where no horizontal movements have been recorded.

9.1.7 PREDICTED FUTURE MOVEMENTS

Future vertical movements in areas beyond the perimeter of the open cut have been estimated from consolidation theory on the assumption that drainage of batters and reduction of artesian pressures are the major factors contributing to subsidence. Fortuitously the effective stresses resulting from the dewatering will be lower than preconsolidation pressures. Hence, future subsidence will occur as a result of consolidation on the recompression portion of the field consolidation curves.

With the full development of Morwell open cut, ultimate settlement values are predicted to reach approximately double those which have occurred to 1977 in the main Morwell township area. Values of up to 3 m are expected at the southern edge of the town and 1 m at the northern boundary. Present subsidence contours will increase towards the west and the 3 m contour will be located west of the Morwell River (about 3.5 km west of the present floor of the open cut).

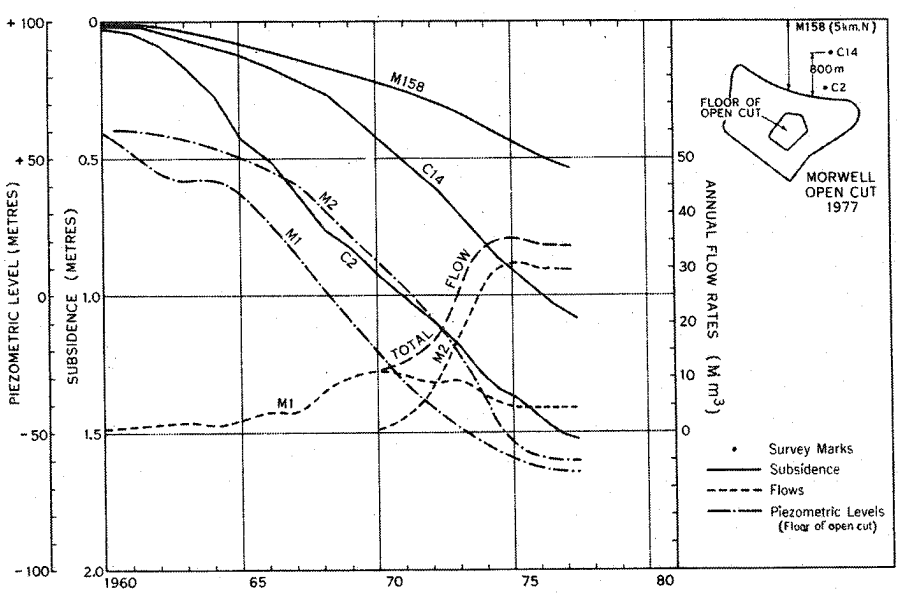

Figure 9.1.8 Relationship of piezometric levels and subsidence

Regional subsidence within the Latrobe Valley depression is likely to extend, both into the Moe Basin, a probable intake area, as well as to the east. The new major open cut at Loy Yang has a designed depth of 200 m and the required lowering of piezometric levels in this area is likely to result in even greater settlements than will occur at Morwell. Ultimately, the settlement "basins" at Morwell and Loy Yang are expected to coalesce.

9.1.8 SIGNIFICANCE OF MOVEMENTS

Structural damage due to earth movements is related more to the degree of horizontal strain and differential subsidence than to absolute values of movements. The strain values are determined from precise surveys of survey pins generally 60 m apart and, therefore, abrupt discontinuities which may have developed could be masked. One such feature has been detected on the ground and can be traced from the open cut for some 200 m into the southern limits of the township.

9.1.8.1 Effects on Morwell Township

Morwell township of 16 000 inhabitants extends to within 300 m of the northern edge of the open cut (Figure 9.1.5). Houses are mainly single storey and of timber or brick veneer construction with fibrous plaster lining. The commercial centre is located 1 km from the open cut and contains brick buildings of one or two stories. The recorded maximum value of north-south horizontal strain is less than 0.8 per cent. Strains are negligible over the northern portion of the township. Future strains in the southern township fringe are predicted to be about 0.5 per cent. Larger strains could occur in some localized areas and could affect houses and services.

Differential subsidence has rarely exceeded 0.3 per cent in Morwell township, and values are commonly less than 0.1 per cent over most of the area. With the predicted doubling of total subsidence in the township area, and the general differential subsidence values unlikely to exceed 0.3 per cent, it is concluded that differential subsidence will not significantly affect buildings and services within the township.

All relevant authorities in the township and district are fully aware of the history and amounts of movement occurring. Each receives copies of the annually revised earth movement survey data and the information is available to the public. A technical panel, consisting of two experienced geotechnical personnel from the State Electricity Commission, and a representative from the Commonwealth Scientific and Industrial Research Organization, Division of Applied Geomechanics, has been established to review claims for damage from owners of private property, and to assess whether the damage was due to open cut operations or to some other cause. A six-year period of surveillance has resulted in the detection of some minor cracking in concrete pavements and brickwork; however, to date no claims have been proved. It has also been shown that grades on drainage and sewage lines have not been significantly affected by earth movements.

9.1.8.2 Effects on engineering structures

Important engineering structures associated with the mining operations and power generation are located within the open cut and beyond the perimeter. These structures include dredgers, conveyor systems, pipelines, power stations, storage bunkers, cooling towers and water storages. Risks of damage within the open cut are reduced by the designed geometry of the excavation, and by the design of equipment to minimize the effect of movements. Beyond the perimeter of the open cut, power stations and associated structures are generally located 500 to 700 m from the edge of the open cut where future ground strains are estimated to be within acceptable limits.

9.1.9 CONCLUSIONS

Large vertical and horizontal movements have resulted from the development of deep and extensive open cuts in the brown coal deposits of the Latrobe valley.

Regional subsidence has been due to the reduction of artesian water pressures in aquifers underlying the coal seams, while horizontal movements are due mainly to pressure relief within the open cuts and are localized around each excavation.

Total, movements are expected to double as development of the Morwell open cut continues. Although the southern fringe of Morwell township could be affected by horizontal strain, serious problems are not anticipated. The regional subsidence is likely to be relatively uniform and the resulting low differential subsidence values should not affect buildings and services in Morwell township, nor major engineering structures outside the perimeter of the open cut.

Regular survey and surveillance programs will be continued in collaboration with the various authorities involved in the area, but no special measures to control or ameliorate subsidence are planned, other than to limit the reduction of artesian pressures to the minimum value consistent with safety of operations.

9.1.10 ACKNOWLEDGEMENTS

The material in this case history is published with the permission of the State Electricity Commission of Victoria. The investigations described were carried out in collaboration with Golder Brawner and Associates Ltd of Vancouver.

9.1.11 REFERENCES

BARTON, C. M. 1971. The Morwell interseam sands. J. Geol. Soc. Aust., 17, pp. 191-204.

GLOE, C. S. 1967. The lowering of the artesian water pressure surface in the vicinity of the Morwell Open Cut. Inter. Assoc. Hydrogeol. Cong. Hannover, 1965, vii, pp. 193-196.

GLOE, C. S., JAMES, J. P., and BARTON, C. M. 1971. Geotechnical investigations for slope stability studies in brown coal open cuts. Proc. Ist Aust-N.Z. Conf, Geomech. 1, pp. 329-336.

GLOE, C. S., JAMES, J. P., and McKENZIE, R. J. 1973. Earth movements resulting from brown coal open cut mining--Latrobe Valley, Victoria. Subsidence in Mines, 4th Ann Symp. Illawarra Branch, Australias. Inst. Min. Metall., 8 pp. 1-9.

GLOE, C. S. 1975. Latrobe Valley Coalfield, in Economic geology of Australia and Papua-New Guinea. 2. Coal. Australias. Inst. Min. Metall., pp. 345-359.

GLOE, C. S. 1977. Land subsidence related to brown coal open cut operations, Latrobe Valley, Victoria, Australia. Second International Symposium on Land Subsidence. Proc. Anaheim Symp. 1976, IASH-Unesco, pp. 399-407

HUTCHINGS, R., FAJDIGA, M., and RAISBECK, D. 1977. The effects of large ground movements resulting from brown coal open cut excavations in the Latrobe Valley, Victoria. Large ground movements and structures. Conf. Cardiff, 1977 (in print).

Case History No. 9.2. Shanghai, China, by Shi Luxiang and Bao Manfang, Shanghai Geological Department, Shanghai, China

9.2.1 INTRODUCTION

Shanghai is the largest industrial city in China, standing on the coast of the East China Sea and situated at the front edge of the Yangtze Delta. The elevation[1] of the flat-lying city area is 3-4 metres above sea level. The summer-winter temperature variation is very large. The Whangpoo River and Soochow Creek, both being the outlets of Taihu Lake, are the chief tide waterways of the city.

Land subsidence was first reported in 1921. After liberation, with the rapid development of industrial production, the exploitation of ground water increased, and subsidence continued. The greatest subsidence occurred from 1956 to 1959, at an annual rate of 98 mm. Up to 1965, the maximum cumulative subsidence, as indicated by one of the bench marks in the city area, was as high as 2.63 m (Figure 9.2.1). The area of cumulative subsidence exceeding 500 mm was 121 km^2, forming two plate-shaped depressions in the urban district and affecting the suburban districts, too.

[1]"Elevation" in this paper is based upon the Wusong datum.

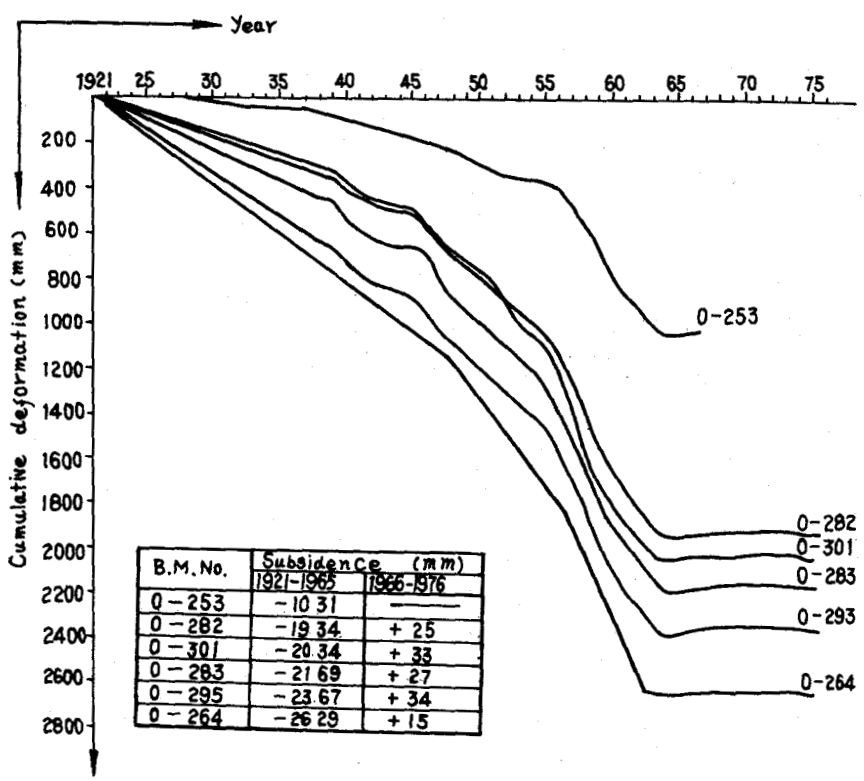

Figure 9.2.1 Cumulative deformation shown by some typical bench marks in the urban area of Shanghai. +, rebound; -, subsidence

After 1963, antimeasures were taken against land subsidence. In 1965, the annual rate of subsidence in the urban area was reduced to 23 mm. From the research results of the preceding period, calculations for the relations among pumpage, water level, and subsidence for the year of 1966 were made in 1965, and the scheme for planning exploitation for the year of 1966 was drawn up. The exploitation of factories followed the plan, and therefore, in 1966, annual rebounding of 6.3 mm occurred in the urban area.

9.2.2 GENERAL GEOLOGICAL CONDITION OF THE OVERBURDEN

In the Shanghai area, unconsolidated materials, about 300 metres thick, of alternating marine and continental facies were deposited on the bedrock during the Quaternary Period. The upper portion of 150 m is composed of clayey soil and sand of littoral and fluvial delta facies; the lower portion of 150 m consists of alternating sand layers of fluvial and variegated clays of lacustrine facies.

Based on the hydrogeological characteristics of the overburden, one water-bearing layer and five aquifers may be identified (hereinafter called aquifers, Figure 9.2.2). The general features of these aquifers are: flat-lying, thick, fine-grained, with small hydraulic gradient and low velocity of ground-water flow. These aquifers are marked by a distinct regularity of lithological changes, finer grained with decreasing thickness from northeast to southwest. Aquitards are widely distributed, only absent in the eastern part, or in local areas along the Whangpoo River, thus bringing about direct hydraulic interconnections between the first, second and third aquifers.

According to its engineering-geological character, the overburden may be divided into 13 layers. Among them are three stiff clay layers below the second aquifer, with fairly high compressive strength; their void ratio is less than 0.70, and their coefficient of compressibility less than 0.025 cm^2/kg. The amount of compression of the layers is comparatively small, as shown in the surveys made over the years. Above the second aquifer are three compressible layers (soft clay layers) with low compressive strength and one dark-green stiff clay layer with fairly high compressive strength. The void ratio of these layers, their water content, coefficient of permeability, coefficient of compressibility, and other principal physical mechanical indices decrease as the depth of the layers increases (Figure 9.2.3).

9.2.3 RELATIONSHIP BETWEEN GEOLOGICAL STRUCTURE AND LAND SUBSIDENCE

According to geological surveys and analytical studies of the observation data, land subsidence principally occurred in the upper layers of the overburden. To present in full the factors causing subsidence, the urban area of Shanghai may be divided into four geological structure areas of land subsidence, based on the different combinations, from the depth of 70 m upward, of three compressible layers and one dark-green stiff clay layer, and based on their relationship with the lst and 2nd aquifers (Figure 9.2.4).

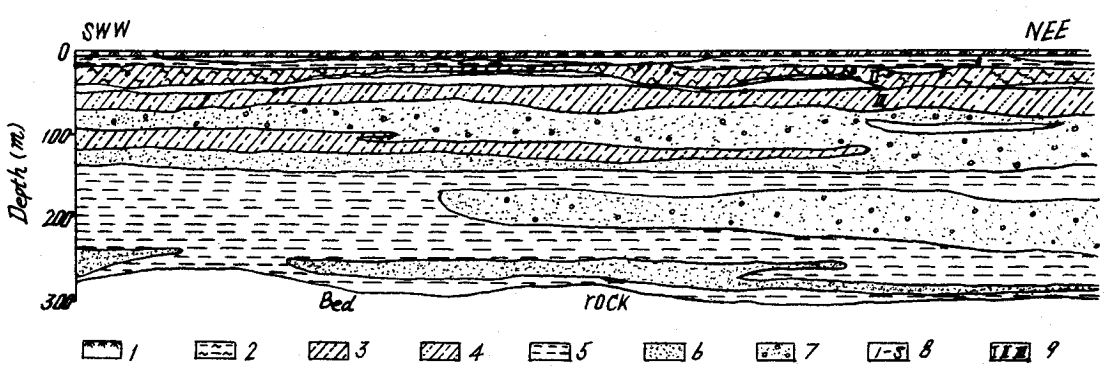

Figure 9.2.2. Geological profile of the urban area of Shanghai. 1, surface soil; 2, muddy clay; 3, muddy clayey loam; 4, clayey loam with sand; 5, stiff clay; 6, sand; 7, sand with gravel; 8, confined aquifer; 9, compressible layer.

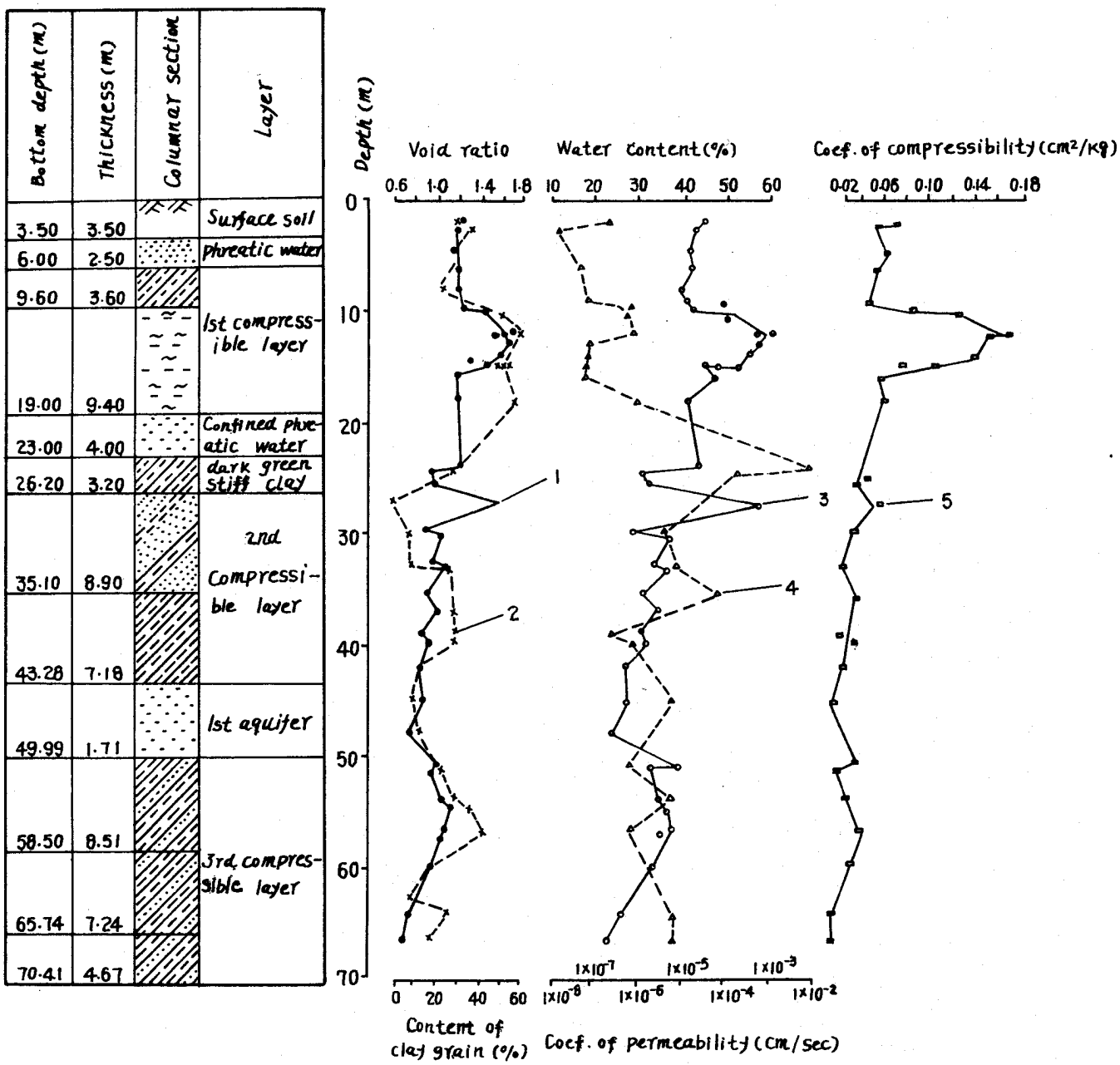

Figure 9.2.3 Variations of main physical-mechanical properties of soil layers with depth. 1, void ratio; 2, content of clay particle; 3, water content; 4, coefficient of permeability; 5, coefficient of compressibility. Legend of columnar section as shown in Figure 9.2.2.

Area No. l(I). Consisting of the lst compressible layer, the dark-green stiff clay layer and the lst and 2nd aquifers. Due to the thin compressible layers and the thick sand layers in addition to the dark-green stiff clay layer, the rebound of land surface was comparatively great after measures were taken.

Area No. 2(II). Consisting of the lst and 3rd compressible layers, the dark-green stiff clay layer and the lst and 2nd aquifers. Owing to the fact that the 3rd compressible layer is comparatively thick, the cumulative subsidence was relatively greater than that in Area No. 1 before measures were taken. However, this is also an area in which the rebound is comparatively great after taking the measures.

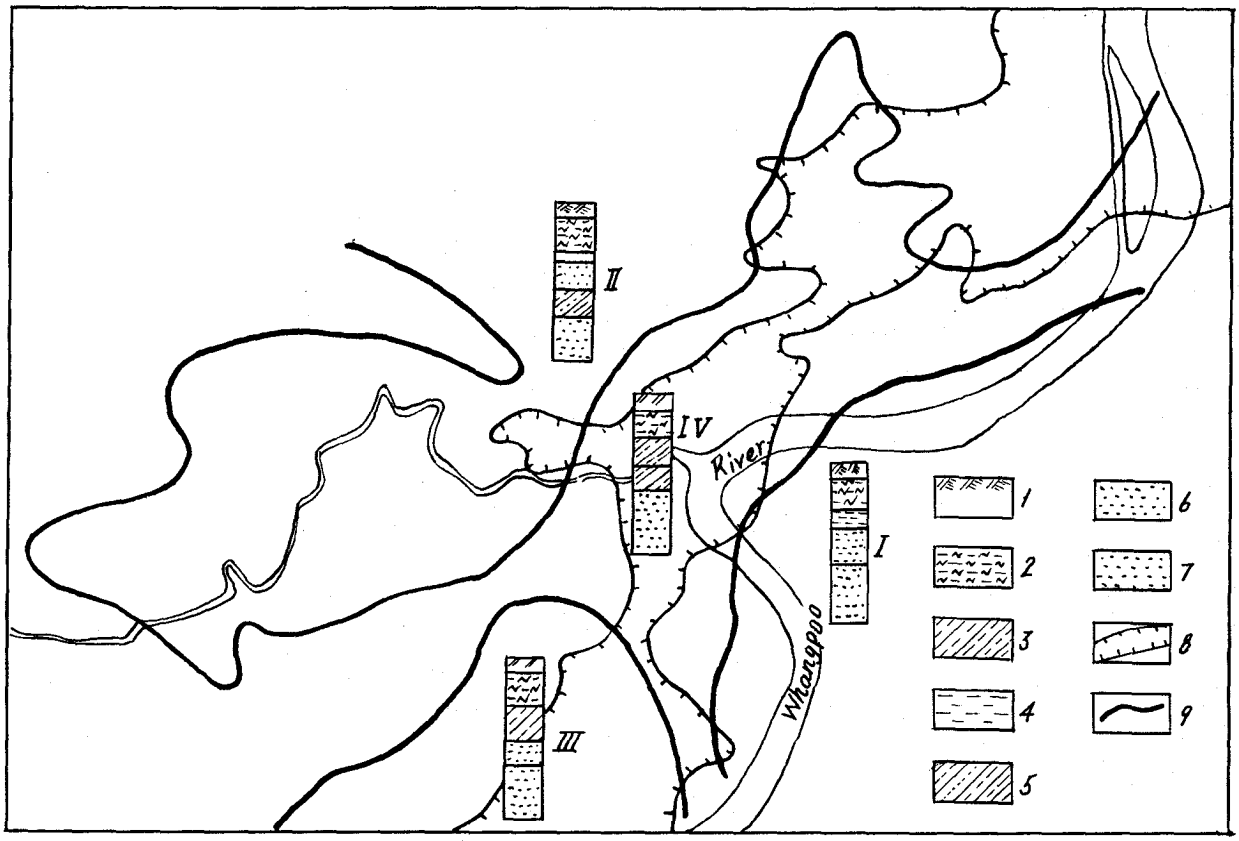

Figure 9.2.4 Relationship between the geological structure and land subsidence in urban area of Shanghai. 1, surface soil; 2, lst compressible layer; 3, 2nd compressible layer; 4, dark-green stiff clay layer; 5, 3rd compressible layer; 6, lst aquifer; 7, 2nd aquifer; 8, slight subsidence within the boundary line, rebound area outside the boundary line; 9, geological structure area and boundary line.

Area No. 3 (III). Consisting of the lst and 2nd compressible layers and the lst and 2nd aquifers. Due to the absence of the dark-green stiff clay layer and the existence of the direct hydraulic interconnection between the lst and 2nd aquifers, the cumulative subsidence was comparatively great before we adopted the methods for improvement. Since the measures were taken, the rate of subsidence has slowed down, though there is still slight subsidence in the lst and 2nd compressible layers.

Area No. 4 (IV). Lying in the central part of the city in a NE-SW direction. This is largely an unexploited and unrecharged area. It comprises the lst, 2nd and 3rd compressible layers and the 2nd aquifer. Since the three compressible layers are thick and there is no dark-green stiff clay layer, the cumulative subsidence had been comparatively great before remedial measures were applied. After we had taken these measures, with the recovery of the ground-water level, the third compressible layer was no longer under compression and began to swell. However, continuation of slight compression of the first two compressible layers has been observed. The geological structure of this area is generally weak.

From the exploration data, we recognized as follows:

1. In areas with the same geological conditions of ground-water exploitation, the amplitude of subsidence varies with the thickness and the compressibility of the compressible layers. Generally, the greater the thickness and the compressibility, the greater the subsidence.

2. The amount of compression of the lst compressible layer depends upon whether the dark-green stiff clay layer is present in the lower part. The subsidence in Areas Nos. 3 and 4, where there is no dark-green stiff clay layer, is greater than that in Areas Nos. 1 and 2 where the dark-green stiff clay layer is present.

3. The rate of compression of the lst and 2nd compressible layers depends upon whether hydraulic interconnection exists between the lst and 2nd aquifers. Therefore, the rate is greater in Area No. 3 where the hydraulic interconnection exists than in Area No. 2 where it does not.

It may be understood that in the course of history, the soil layers have been under the action of fairly low water head. From the relation of preconsolidation pressure of the various soil layers, we know it is equivalent to the action of preloading. Therefore, each layer has its own preconsolidation pressure p_C and preconsolidation ratio $c_r = P_C/P_O$, in which P_O is the overburden pressure). From the depth of the soil layers above 70 m, p_C values are worked out by laboratory tests. We know that the average preconsolidation pressure p_C of the lst and 2nd compressible layers approaches the overburden pressure p_0 of the overlying soil layers. It may be the normal consolidation layer. The 3rd compressible layer is 40-70 m below the surface, and its p_C and c_r increase with depth. The compression of the 3rd compressible layer (over-consolidated) will not occur if the average $(p_C\text{-}p_O) \approx 1$ kg/cm^2, i.e., if the drawdown of the ground-water level in the 2nd aquifer does not exceed the average $(p_C\text{-}p_0)$ value while the measures controlling land subsidence are being taken.

9.2.4 CALCULATION

According to the mechanism of deformation of the soil layers under the pumping drawdown, it is suitable to apply a one-dimensional equation to calculate the compressive deformation of the soil layers. The drain path of the lst, 2nd and 3rd compressible layers is mainly upward and downward toward the sand layers. Although the ground-water cone exists, yet it has a wider range and small hydraulic gradient. The difference of horizontal water pressure is not great, so the transverse drainage may not be considered.

This principle has been applied to the annual calculation since 1965, and the results have been checked the next year in order to make a comparison with the practice to correct the calculated indices year by year. The calculated value and practice would gradually correlate with each other.

In 1972, according to the elastic-plastic characteristics of deformation of soil layers and the principles of soil mechanics, a physical model was developed. Then through the statistical analysis of a large amount of observed data of deformation, which were influenced by the variation in elevation of the ground-water level under a certain pumping and recharging condition, a simplified mathematical model was developed, in order to get the optimizing numerical solution with computer. Consequently, the forecast and prediction of land subsidence can be made.

Accuracy of calculation has been checked through practice. The period of prediction for scheme calculation is one year. The calculation has been made since 1972. The practice has demonstrated that the maximum error of predicting elevation of water head was ± 0.5 m, when the annual amplitude of water head was less than 6-8 m; the average error of predicting absolute deformation was below 1.7 mm, when the annual average amplitude of deformation was less than 14.3 mm.

9.2.5 MEASURES

The purpose of land subsidence research is to solve the problem of land subsidence; therefore, it is the key of the question to take measures.

The main cause of land subsidence in Shanghai is intensive exploitation of ground water and corresponding drawdown of water level. In order to control land subsidence and to rationalize the exploitation of ground water, the measures for recovering and raising up the ground-water level have been taken on the basis of analysing and researching the laws of land subsidence, according to Shanghai's specific conditions. Preliminary control of subsidence of the urban area has been achieved. The measures taken are chiefly as follows:

1. Restricting and rational usage of ground water.

   Owing to the great disaster made by the land subsidence, in 1963 it was resolved that measures for restricting ground-water exploitation were to be taken by Shanghai Municipal Government. Ground water in Shanghai is mainly utilized to reguate the air and lower the temperature, so the paper, iron and steel industries which do not need cooling energy from the ground water, have changed to using surface water. In addition, some factories have installed refrigeration equipment instead of

using ground water. Cooling energy from this equipment may be equivalent to the cooling energy provided by 200 deep wells. Since 1965, the calculation of land subsidence has been made annually, thus giving the planning exploitation scheme for the next year. And the factories, according to the plan for rational usage of ground water, have taken measures for multiple and comprehensive utilization of ground water.

2. Artificial recharge of ground water.

   The "measures of recharging in winter for summer use and recharging in summer for winter use" have been employed since 1965. The textile mills which need cooling energy can use lower temperatures in summer. From the practice over years, it was proved that after recharging, the temperature of ground water of the 2nd and 3rd aquifers gradually decreased by 6-10° C in comparison with the original, and that of the 4th and 5th aquifers also decreased by 9-10° C. Besides, recharging in winter for summer use and recharging in summer for winter use had the function of raising the ground-water level in order to diminish land subsidence.

3. Adjustments of exploited aquifers.

   Before the measures had been taken, ground water was mainly pumped from the 2nd and 3rd aquifers in the urban area. Although the 4th aquifer contains abundant ground water of fairly good quality, the original temperature is high, so it is not suitable for cooling. Hence the pumpage from the 4th aquifer is small. Due to the irregular distribution of the 5th aquifer and the high temperature of its ground water, pumpage from this aquifer also is small. However, after recharging cool water in winter to these aquifers, the temperature of ground water in them decreases and the water can be used for cooling purposes. Therefore, pumpage from the 2nd and 3rd aquifers has been decreased, and the use of ground water from the 4th and 5th aquifers has been increased. On the other hand, the strength of the soil layer underneath the 3rd aquifer is fairly high, and deformation is not obvious after the exploitation of the 4th and 5th aquifers. This will decrease the rate of land subsidence.

9.2.6 REFERENCES

SHANGHAI HYDROGEOLOGICAL TEAM. 1973. On the control of surface subsidence in Shanghai. Acta Geologica Sinica 1973, No. 2.

SHANGHAI HYDROGEOLOGICAL TEAM. 1976. Preliminary studies on land subsidence of the urban area of Shanghai, China. Not published.

Case History No. 9.3. Venice, Italy, by Laura Carbognin, Paolo Gatto, and Giuseppe Mozzi, National Research Council, S. Polo 1364, Venice, Italy; Giuseppe Gambolati, IBM Scientific Center, S. Polo 1364, Venice, Italy; Giuseppe Ricceri, Department of Soil Mechanics, University of Padua, Italy

Reprinted from IAHS-AISH Publication No. 121, 1977, p. 65-81, by permission.

9.3.1 INTRODUCTION

Many areas of Italy are affected by land subsidence. Among these, the area of Venice (Figure 9.3.1) has caused the greatest concern. Its sinking in fact, in spite of the relatively small rate, could be fatal, due to the low level of the city in relation to the sea. The well-known floods (or "acque alte," a local idiom meaning high waters), essentially caused by weather and astronomical factors, are indirectly enhanced by subsidence both in amplitude and in frequency. When the studies were started, it became quite clear that, out of the various factors responsible for the sinking, the withdrawal of underground water was the main one. Thus, after a preliminary analysis, the research effort was mainly directed to hydrogeology.

In 1969, the Italian Consiglio Nazionale delle Ricerche (CNR, National Research Council) constituted a working group for the Venice problem. Starting that year an accurate inventory was made of the data already available but widely scattered. They were filed according to

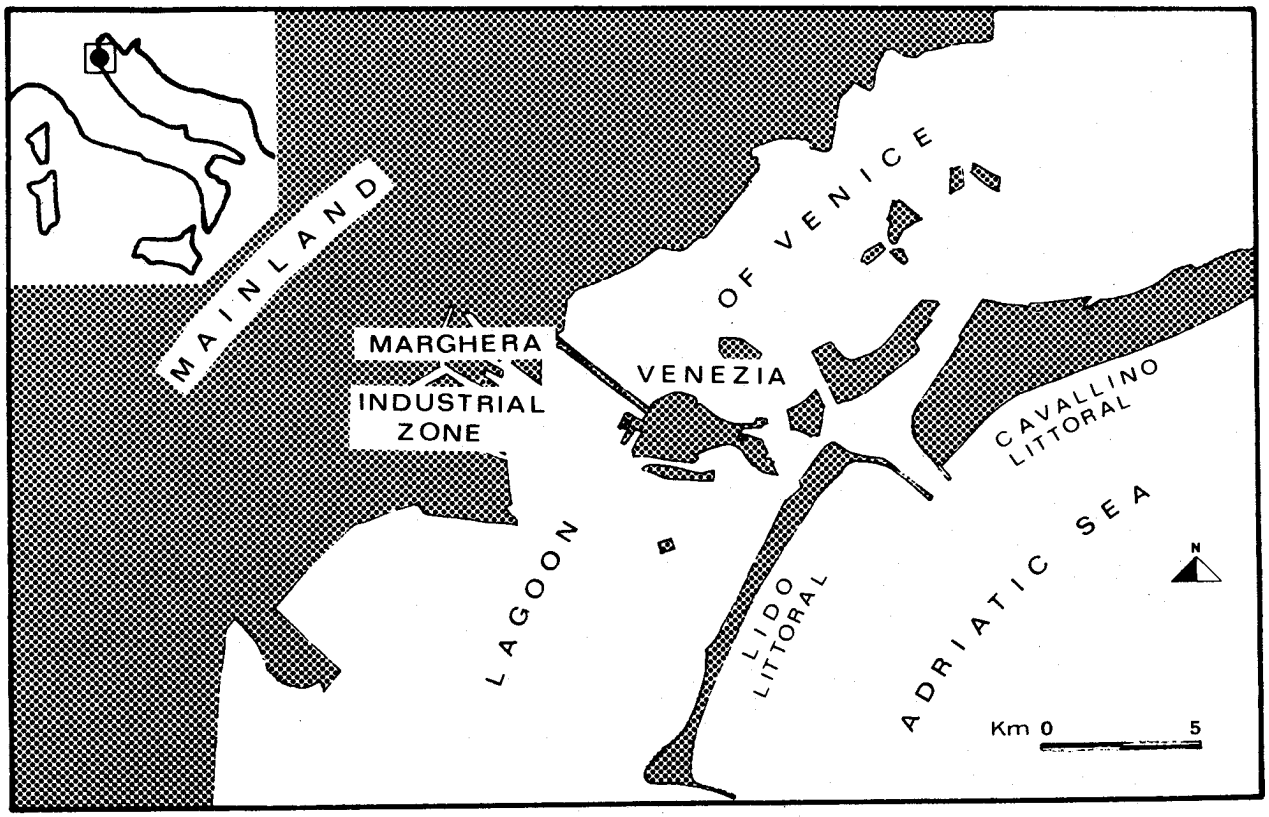

Figure 9.3.1 Map of the Venetian area under investigation.

lithostratigraphy, hydrology, geotechnique, and geodesy. During their processing, specific experimental tests were performed, to validate and supplement the preliminary reconstructions.

The analysis was given two major aims: first, to describe the physical environment where the phenomena under study occur; next, to describe their evolution, to investigate their mechanism, and to make predictions with numerical models. The final results of the research confirm the dependence of the subsidence on the artesian withdrawals, the possibility of stopping the settlement of the city, and even of obtaining a slight rebound by naturally recharging the depleted aquifer system.

9.3.2 THE PHYSICAL ENVIRONMENT

The Venice confined system, down to 1000 m depth (Quarternary basement), is constituted by sand layers (aquifers) bounded by silt and clay layers (aquitards). Moving northwest, towards the foothills of the Alps, the sedimental structure tends to change. Materials are more and more coarse, while the aquitards become thinner, and, at a certain point, they disappear. In the foothill belt the unconsolidated mantle is a whole homogeneous system of sand and gravel. For the hydrologist, it represents the reservoir supplying the aquifer-aquitard system extending beneath Venice and even further.

The Venetian aquifer system has been investigated in detail by taking information from both the existing artesian wells (Alberotanza, et al., 1972) and a new deep test borehole, VE 1 CNR, where continuous samples of the Quarternary series were taken (Consiglio Nazionale Ricerche, 1971). Thousands of analyses were performed on the borehole samples, and a complete physiography of the local subsurface formations was obtained. From this drilling more complete interpretation of the scattered information was made possible. Moreover, the starting point was available for the definition of the hydrogeological stereogram of the region. Figure 9.3.2 is a map of the upper 350 m, where the aquifers are pumped (after Gambolati, et al., 1974, slightly modified). Six aquifers appear, four of which are extensively exploited (2nd, 4th, 5th and 6th).

Permeability, grain-size and clay chemistry of aquifers and aquitards are reported in tables 1, 2 and 3, whose values were obtained by analyzing the cores of the VE 1 CNR and two other test boreholes LIDO 1 and MARGHERA 1.

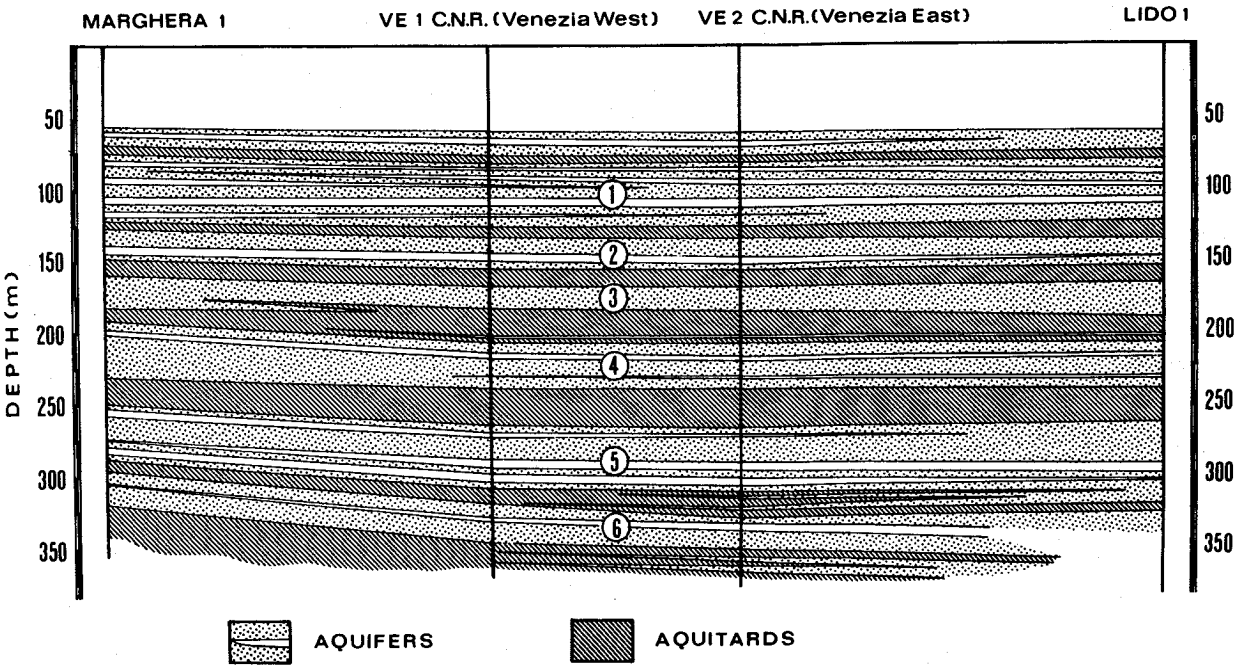

Figure 9.3.2 Hydrogeological map of the confined aquifer system updated using the electric logs recorded in deep test boreholes.

Table 9.3.1 Average permeability of samples taken from VE 1 CNR Borehole (placed in Venice), from laboratory tests.

Depth (metres)	Aquifers (average horizontal permeability)	Aquitards (average vertical permeability)
74- 81		3×10^{-5} cm/sec
81-124	1×10^{-3} cm/sec	
124-132		7×10^{-8} cm/sec
132-153	1×10^{-3} cm/sec	
153-163		3×10^{-6} cm/sec
163-181	4×10^{-5} cm/sec	
181-203		5×10^{-7} cm/sec
203-235	6×10^{-4} cm/sec	
235-260		6×10^{-7} cm/sec
260-302	2×10^{-4} cm/sec	
302-318		6×10^{-6} cm/sec
318-340	10^{-6} cm/sec[1]	

[1] The 6th aquifer is exploited only at Marghera, since at Venice its permeability is too low.

Table 9.3.2 Summary of grain size analysis as measured in the laboratory on samples taken from the VE 1 CNR borehole (after Gambolati, et al., 1974).

Depth (metres)	Lithotypes			
	Coarse fraction	Sands	Silts	Clays
0- 50	0.3	38.0	41.7	20.0
51-100	0.7	50.0	35.0	14.3
101-150	---	46.2	42.2	11.6
151-200	0.4	33.6	48.2	17.8
201-250	---	26.0	54.0	20.0
251-300	5.6	38.4	34.8	21.2
301-350	---	13.5	61.6	24.9
Average	1.0	35.1	45.4	18.5

Permeability (Table 9.3.1) was defined by laboratory tests performed only on clean sand for aquifers and silt clay for aquitards.

The prevailing fraction (Table 9.3.2) is silt, followed by sand and clay.

The illite is dominant (Table 9.3.3); instead the most plastic one, montmorillonite, is in general rather scarce, and its relative abundancy grows towards the historical center and Lido.

Some details of the mechanical properties of these soils are given here (see a recent and more complete paper by Ricceri and Butterfield, 1974). The values of the compressibility coefficient ($m_V=(\Delta e/\Delta P)(l/l+e_o)$) versus depth (Figure 9.3.3) have been computed by oedometric tests at the actual "in situ" pressure (p_o) in the loading (m_{v1}) and unloading (m_{v2}) curves. The maximum load attained in these tests was $5 \div 20 p_o$ for the samples coming from the upper 100 metres and twice the values of p_o for the others, In Figure 9.3.3, solid lines connect the values m_{v1}, and m_{v2} for each sample; dashed lines refer to oedometric tests where loads were increased slightly above p_o and then gradually reduced to zero. The two coefficients decrease with increasing depth. In particular, m_{v2} seems rather insensitive to the maximum load applied in the test, and its average value is about 20 per cent of M_{V1}.

The reader is referred to the bibliography for further information about the physical aspects of the Venetian formations.

Table 9.3.3 Percentages of various clay-types in the core samples taken from MARGHERA 1, VE 1 CNR, and LIDO 1 test boreholes (after Mozzi et al., 1975).

Clay Minerals	Test boreholes			Average
	MARGHERA	VENICE	LIDO	
Illite	48.75	48.45	48.00	48.40
Chlorite	33.75	28.00	30.00	30.58
Kaolinite	11.25	12.80	9.00	11.02
Montmorillonite	6.25	10.75	13.00	10.00

9.3.3 HISTORY OF THE PHENOMENA

By comparing the development of the artesian exploitation and of subsidence, three periods appear distinguishable: the first before 1952, the second from 1952 to 1969 and the last afterwards.

In Figure 9.3.4 the average piezometric level in different places of the Venetian area is plotted versus time.

9.3.3.1 Period before 1952

When the artesian exploitation was not very intensive, subsidence was due only to natural causes; its rate was about one millimetre per year (Leonardi, 1960; Fontes and Bortolami, 1972).

The extraction of the artesian water began about in 1930 when the first factories were established in Marghera. The piezometric level remained above the ground level, except in Venice, where it became lower since the time of World War II. The average decrease was slow all over the area, up to the fifties, when an intensive exploitation started, due to the strong industrial development (Figure 9.3.4).

9.3.3.2 Period between 1952 and 1969

After 1950 the changes became more evident. Artesian water was very actively withdrawn (Serandrei Barbero, 1972) and in the fifties all the hydraulic heads declined below the surface. In the industrial area the average rate reached 0.70 m/y, which is definitely higher than in any other part of the area (Figure 9.3.4). The observed minima were attained in 1969; in Marghera the fourth and fifth aquifers went down to 16 m below surface and in Venice the third and fifth went to 7 m below. From 1952 to 1969, as an average in the industrial zone, a hydraulic head loss of more than 12 m was recorded. In Marghera the withdrawal occurred in about 50 wells, and it was about 460 l/s in 1969; in Venice there were about 10 active wells, but in fact only one (10 l/s) represented the whole extraction of the city. A significant ratio of 1 to 50 existed between the exploitation in the historical center and in Marghera.

In the period 1952-1968 geodetic surveys showed an average subsidence of 6.5 mm/y in the industrial area and 5 mm/y in the city. The most alarming figures appeared between 1968 and 1969, where maxima were observed of more than 17 mm in Marghera and 14 mm in Venice (Caputo et al., 1971) (Figure 5). Overall between 1952 and 1969 the local average subsidence was over 11 cm in the industrial zone and about 9 cm in the city, with local maxima of 14 and 10 cm respectively (Figure 9.3.5)

9.3.3 Years between 1969 and 1975

These years are characterized by a great number of experimental data and theoretical studies worth describing.

After drilling the deep test hole, VE 1 CNR, previously mentioned, two important steps were carried out: the annual repetition of the geodetic survey for controlling the ground movement in the area and the installation of a network of 112 piezometers (24 of which were continuously recording) for controlling the six exploited aquifers (Figure 9.3.6). Therefore it was possible

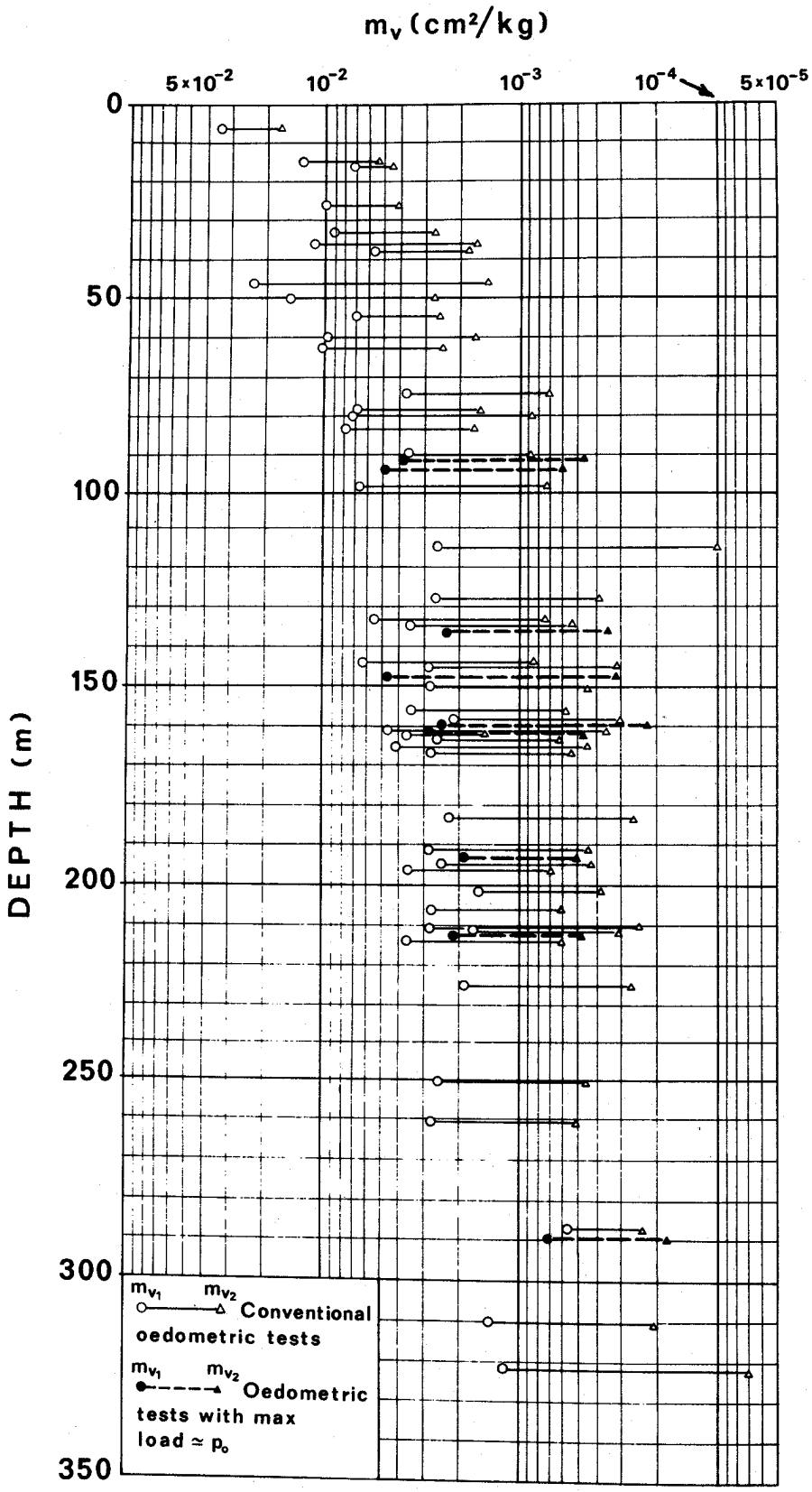

Figure 9.3.3 Coefficients of compressibility m_{v1} and m_{v2} versus depth.

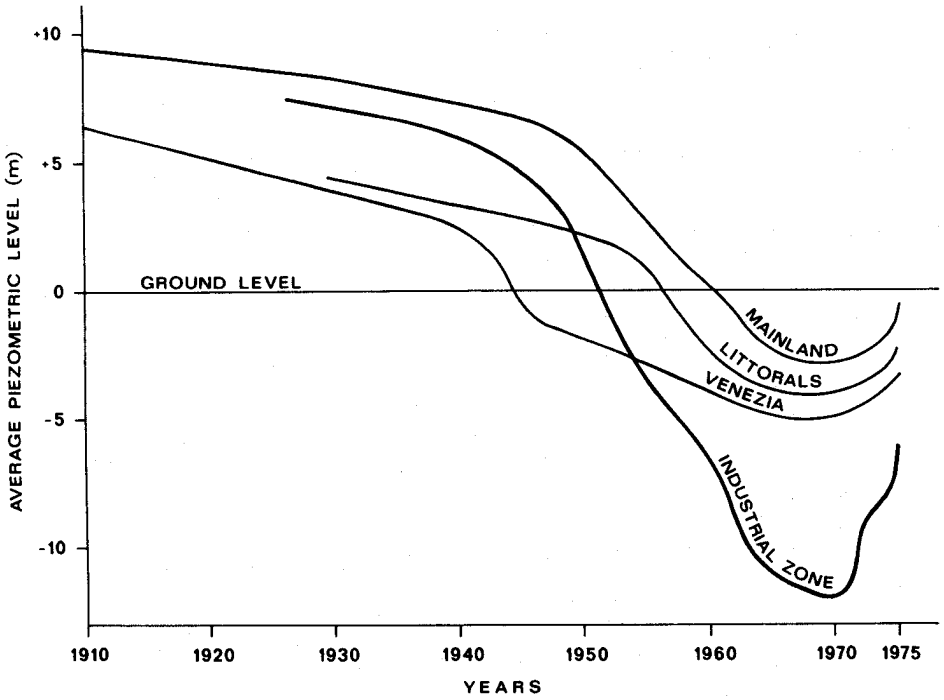

Figure 9.3.4 Average piezometric levels from 1910 to 1975

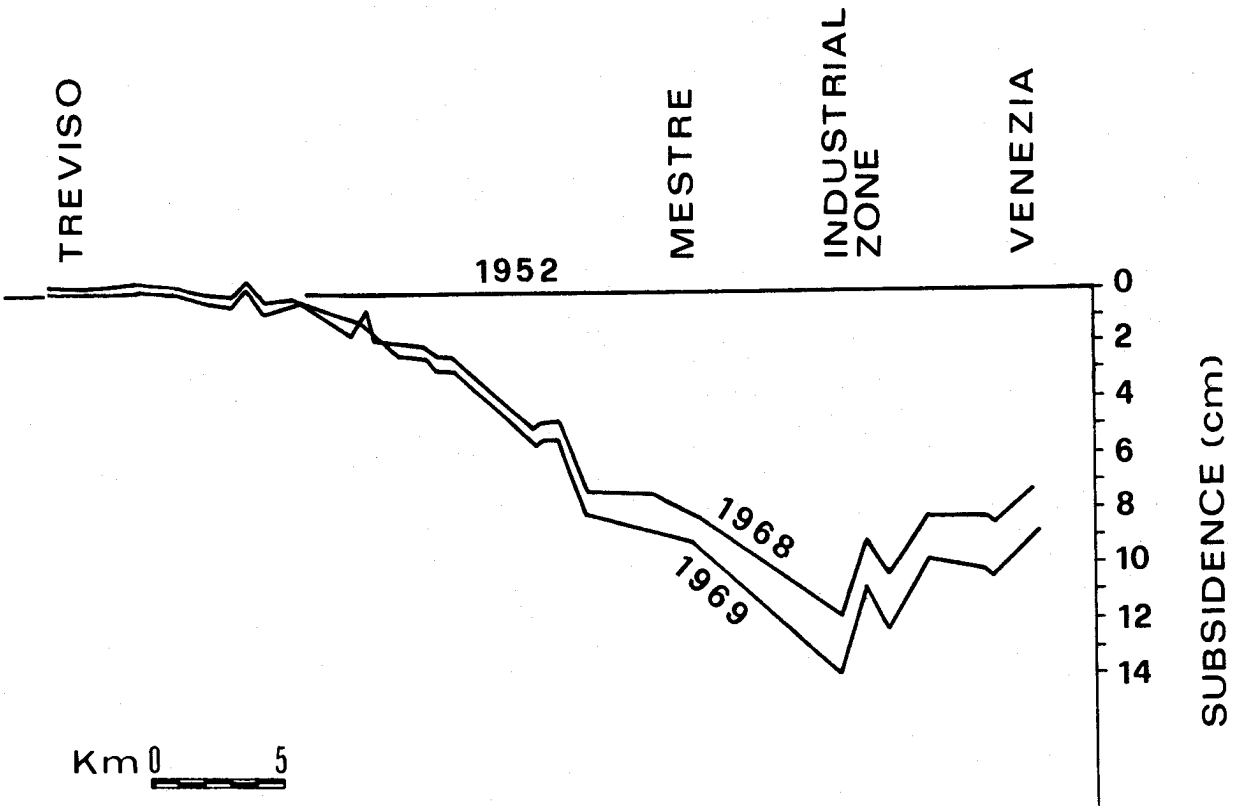

Figure 9.3.5 Comparative plot of the levellings in 1968 and 1969 as referred to 1952

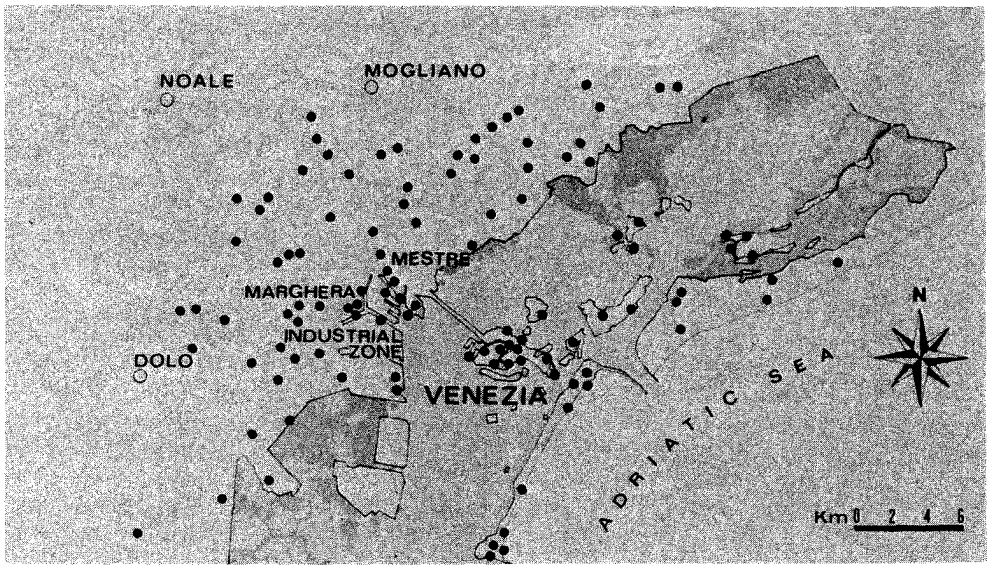

Figure 9.3.6 Map of the 112 piezometers

to annually reconstruct the altimetric profiles and the maps of the equipotential lines (e.g., see Figure 9.3.7 which refers to the 5th aquifer for 1975. Similar behaviour holds true for the previous years).

In general, after the minima recorded in 1969, one can observe a gradual and remarkable, improvement in the piezometric surfaces. In 1975, the average recovery in the industrial area reached a maximum of over 8 m, and in Venice more than 3 m. This new behaviour can be seen in Figure 9.3.4 and it is also well shown in Figure 9.3.8, where the progressive reduction of the depressurized area in recent years is evident.

Similarly to what happened when piezometric levels were declining, a ground-surface rebound is now accompanying the piezometric recovery. After a stability period, which is evident from the 1973 survey (Folloni et al., 1974), the 1975 levelling shows a rebound of the land which, in the historical center, is more than 2 cm with respect to 1969 (Figure 9.3.9). Even taking into account the range of the errors affecting the altimetric curve (Gubellini and DeSanctis Recciardone, 1972), the variation of the ground level in this area remains positive. This is consistent with what appears in the tidal records in Rovinj and Bakar (on the Yugoslavian coast, which is taken to be stable) and those in Venice. Until 1969, the average annual sea level recorded at Venice was apparently increasing with respect to that of the other two stations. In recent years this did not occur any more (Tomasin A., private communication based on official data).

9.3.4 DISCUSSION

9.3.4.1 Analysis of experimental data

We will now analyze the most recent data, i.e., those from the period when the phenomena show a reverse trend.

Looking at the isopiezometric maps, we noted that

1. the piezometric surfaces of the aquifers in the Venetian area show strong depression, assuming the shape of an inverted asymmetrical cone typical of localized pumpage (Mozzi et al., 1975);
2. the maximum drawdown in all the aquifers occurs in the Marghera area, which appears as the main withdrawal center. Minor discrepancies are seen in the islands of Murano, Burano, Le Vignole and Lido:
3. the greatest depressurization is found in the 4th and 5th aquifers;

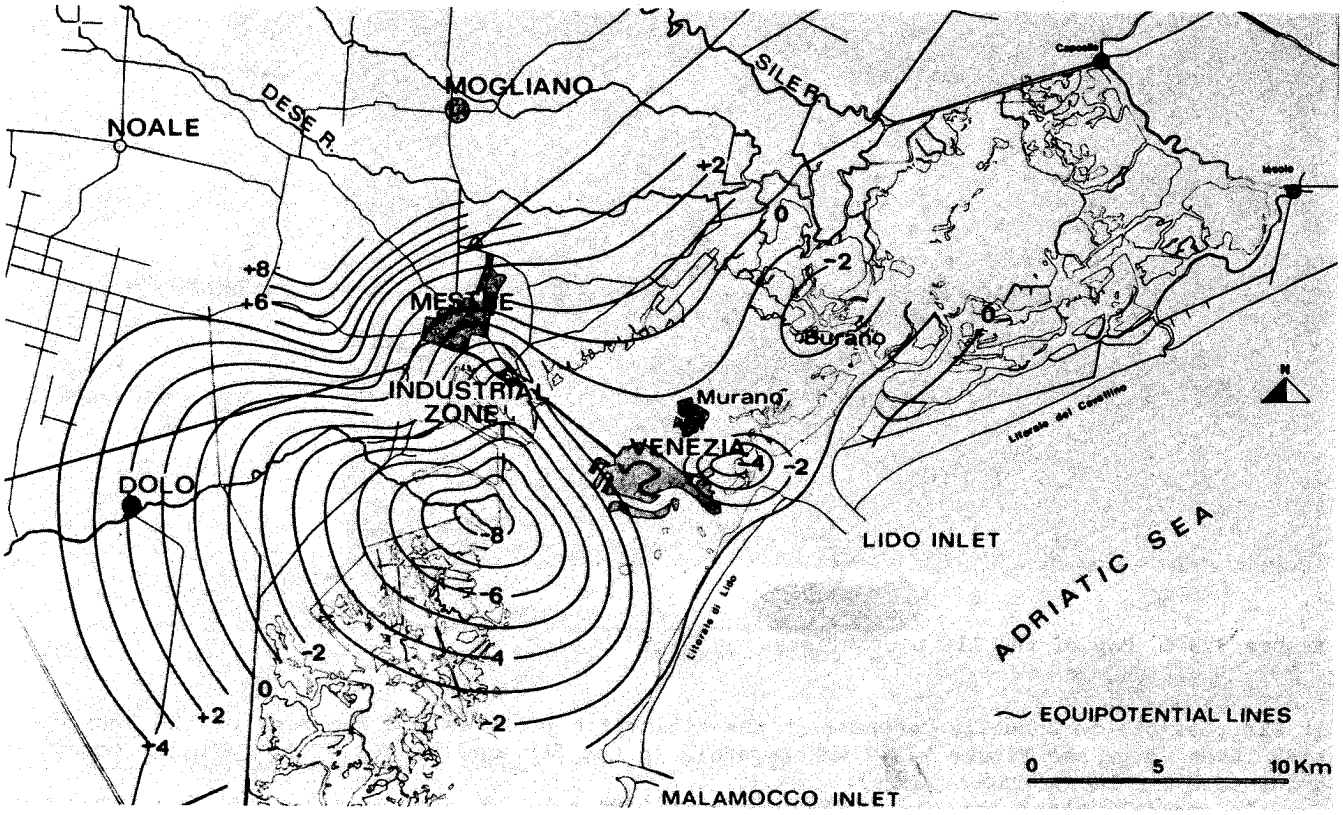

Figure 9.3.7 Piezometric surface of the 5th aquifer in 1975. Equipotential lines are given in metres a.s.l.

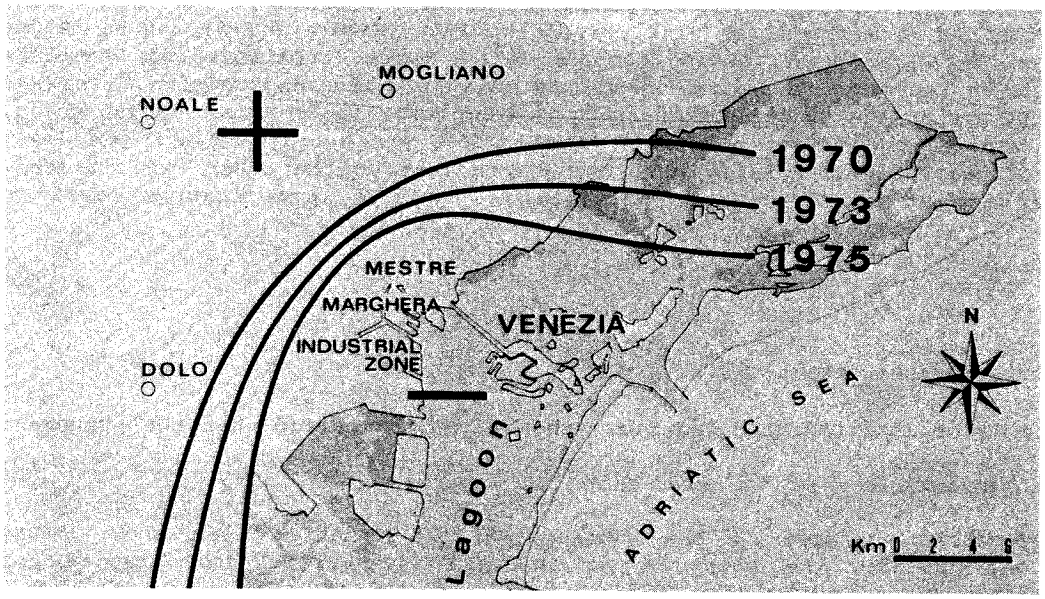

Figure 9.3.8 Boundary of the areas where average piezometric level is above (+) or below (-) the ground level in 1970, 1973 and 1975.

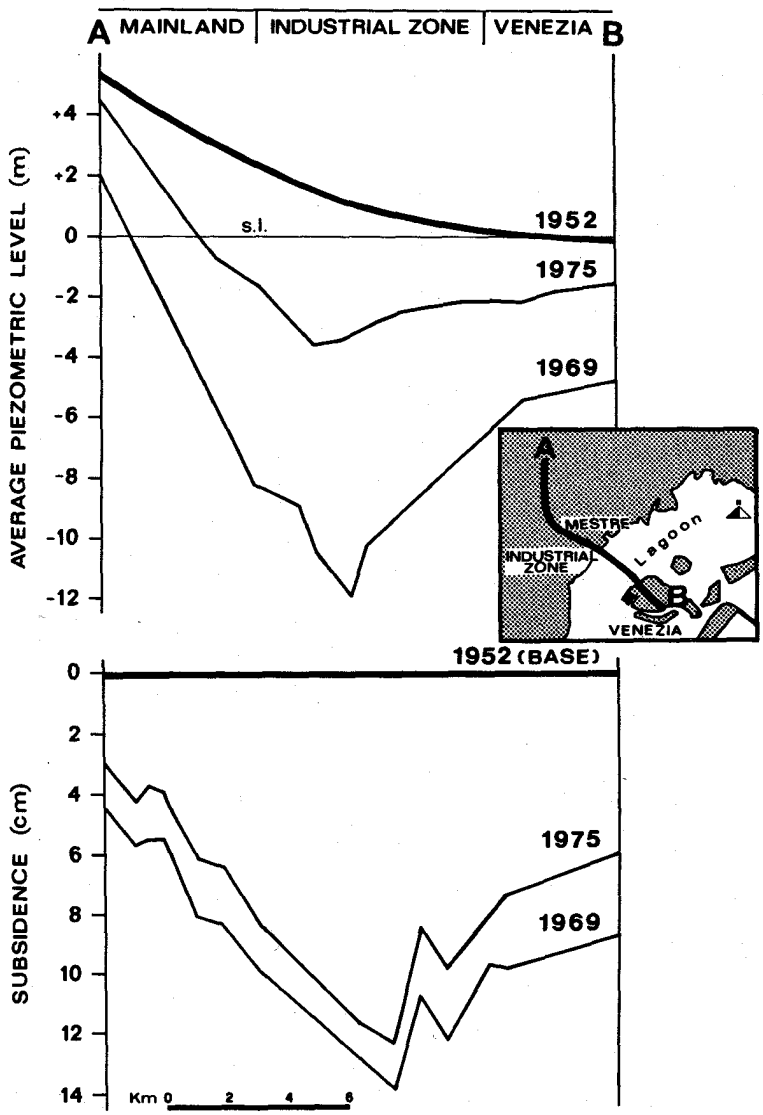

Figure 9.3.9 Comparison of the average piezometric levels and ground levels over mainland (A) and Venice (B).

4. the development of the equipotential lines shows that pumpage at Marghera affects the natural hydraulic balance of the aquifers also in the historical center, where the local withdrawals do not account for the observed drawdown;
5. the distance between equipotential lines gets smaller landward. Figure 9.3.7 also suggests that a no-flux boundary condition exists seaward. This is in keeping with the reconstructed geology.

The aquifer recovery is due to a decrease in the water exploitation. Since 1970, some areas in the district have been supplied by the public aqueduct. The industrial activity of Marghera has been reduced. Above all, well drilling was prohibited in the Venetian plain. In January 1975, the new industrial aqueduct, supplied by the Sile River, was put into operation (a 60 per cent reduction in the number of active wells was observed in Marghera from 1969 to 1975, when the withdrawal was estimated to be about 200 l/s).

The raising of the hydraulic levels is certainly not due to the increased recharge of the aquifers, since in the last decade the natural water supply in the recharge area is diminishing (Carbognin et al., in press).

The levellings, as already stated, show the cessation of the subsidence and a certain rebound. The close connection between withdrawal and subsidence is evident in Figure 9.3.9, where the altimetrical variations and the average piezometric level variations are given for the periods 1952-69 and 1969-75, along the same section from the mainland to Venice. Graphical comparison visualizes the presence of minima in the industrial zone, and similar behaviour of the processes during exploitation and recovery. In the rebound phase, however, we notice that while at Marghera a strong recovery determines a slight altimetrical rebound, at Venice a minor piezometric recovery causes a greater rebound. This can be ascribed to the diverse nature of the cohesive soils at Marghera and Venice.

The assumption of the interdependence between the piezometric and the altimetric variations was statistically verified. In fact, the linear correlation coefficient, with a 95 per cent probability, is between 0.70 and 0.92. The connection between the two variables is therefore expected to be extremely high. Consequently, the coefficient of determination indicates that the piezometric variations account for 70 per cent of the altimetric ones, in terms of variance and in the limiting hypothesis of linear behaviour. The residual variance must be explained by other factors, such as natural subsidence and loading by buildings, but also errors in measurements and deviation from the linear hypothesis.

The interpretation of the subsidence to piezometric variations ratio ($R = \eta/\Delta h$) is also interesting. Its trend in the years 1952-69 (Figure 9.3.10-A) is progressively rising from the industrial zone (1/109) towards the historical center (1/54). This variation can be attributed to the already noted gradual increase towards Venice of the more compressible soils. It explains why in Venice, where less water was pumped than in Marghera, a subsidence of the same magnitude was observed. A similar behaviour is found in the rebound phase (Figure 9.3.10-B) between 1969 and 1975. However in this period, the curve lies definitely below the other one, thus confirming that the elasticity of the system is very limited.

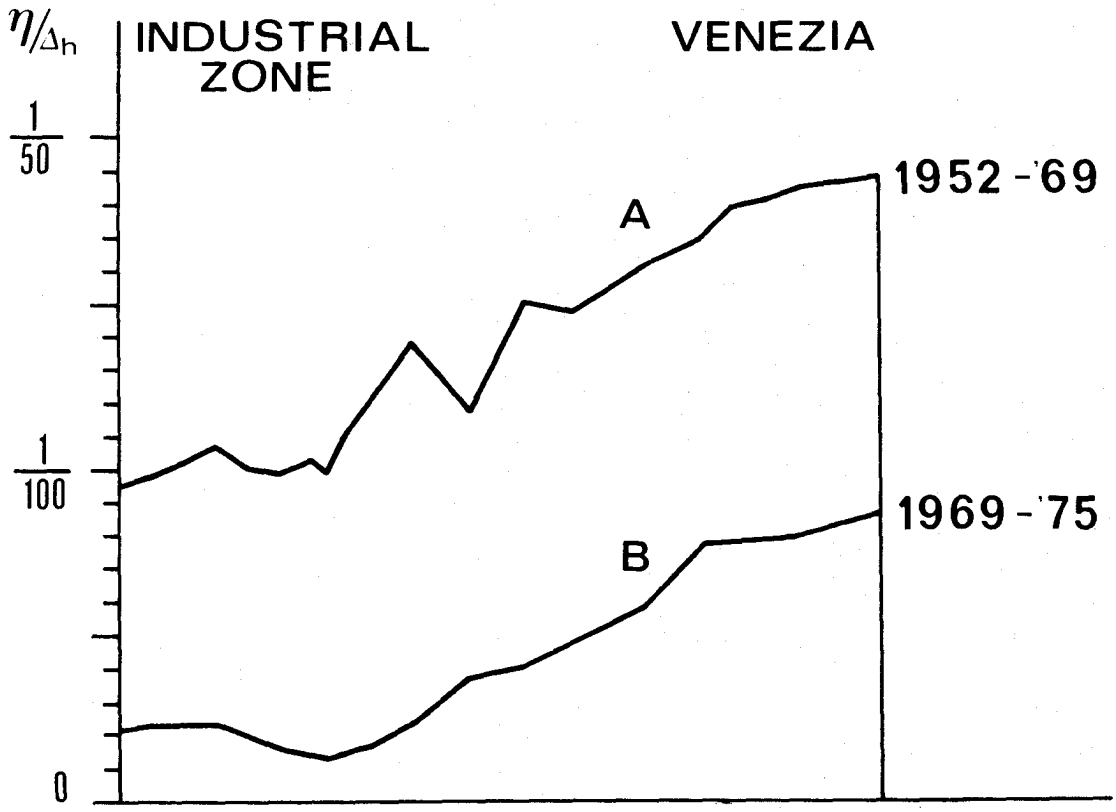

Figure 9.3.10 The ratio of subsidence to piezometric variations from the industrial zone to Venice; A, settlement and B, rebound.

9.3.4.2 Predictive simulations with the new records

Recently, a numerical model based on the classical diffusion equation and one-dimensional vertical consolidation has been used to simulate the past behaviour of the Venice subsidence and to predict the future settlement of the city (Gambolati and Freeze, 1973; Gambolati et al, 1974; Gambolati et al., 1975). A complete description of the approach together with an extensive discussion of the underlying assumptions may be found in the works cited.

The model has been applied again by using the new records to check its ability to reproduce the complex event at hand and to verify "a posteriori" its predictive capacity.

To date the pumpage at Marghera has been reduced to 40 per cent of its maximum value (460 l/s in 1969) and this change in the withdrawal rate has been assumed to have occurred in 1970, for it is apparent from Figure 9.3.4 that the flow field recovery in Marghera started in 1970. Permeability distribution is the same as that used in the previous simulation (Gambolati et al., 1974) while the soil compressibility in rebound has been increased to 20 per cent of the corresponding values in compression, as is evidenced by the most recent laboratory tests summarized in Figure 9.3.3. Therefore, the new results are slightly different from the early predictions given in figures 21 and 22 of the paper by Gambolati et al., 1974.

Figure 9.3.11 and Figure 9.3.12 show the piezometric decline in the first aquifer (where the largest amount of data is available) and the Venice subsidence respectively versus time as provided by the mathematical model using the updated records. For the benefit of the reader the behaviour during the calibration period has been reported as well. The comparison with the experimental observations indicate a fairly good agreement, and especially so, if one considers the degree of uncertainty which is inevitably related to physical events of such a great complexity. This is further evidence of the adequacy of the above model to reliably predict the settlement of Venice. At the same time the results allow the conclusion that the numerical models can be useful tools to investigate and keep under control land subsidence caused by subsurface fluid removal.

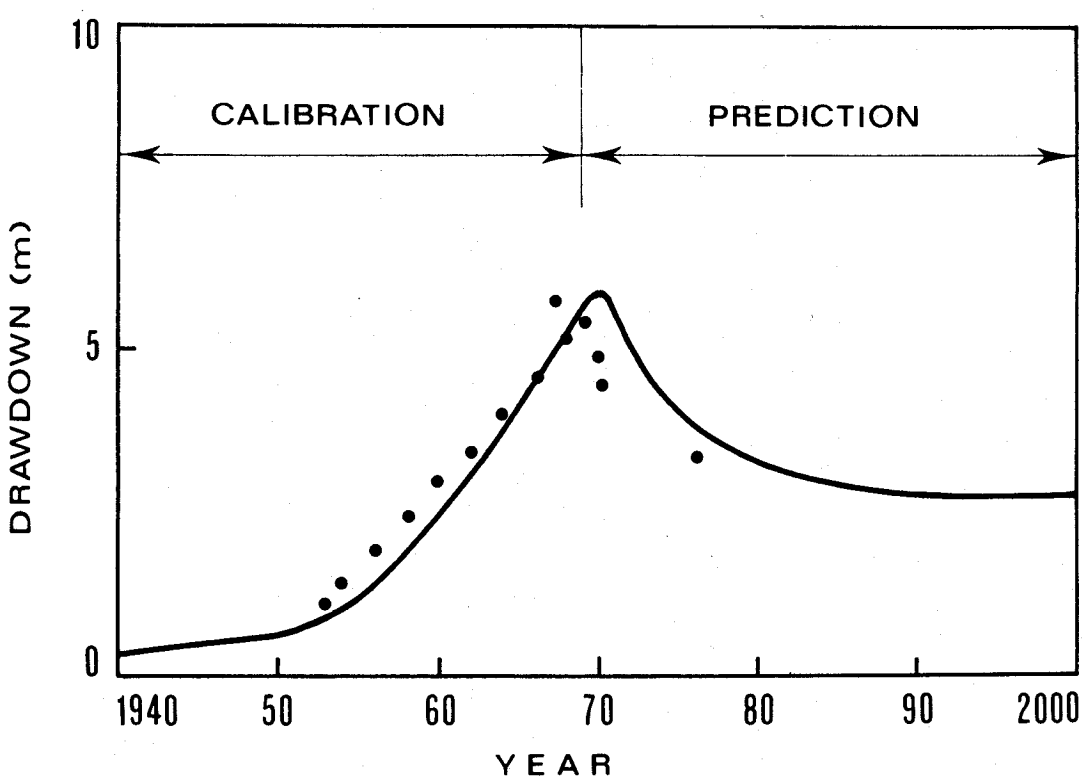

Figure 9.3.11 Piezometric decline versus time in the first aquifer. The closed circles represent experimental records and the solid line gives the response of the model using the new data in our possession.

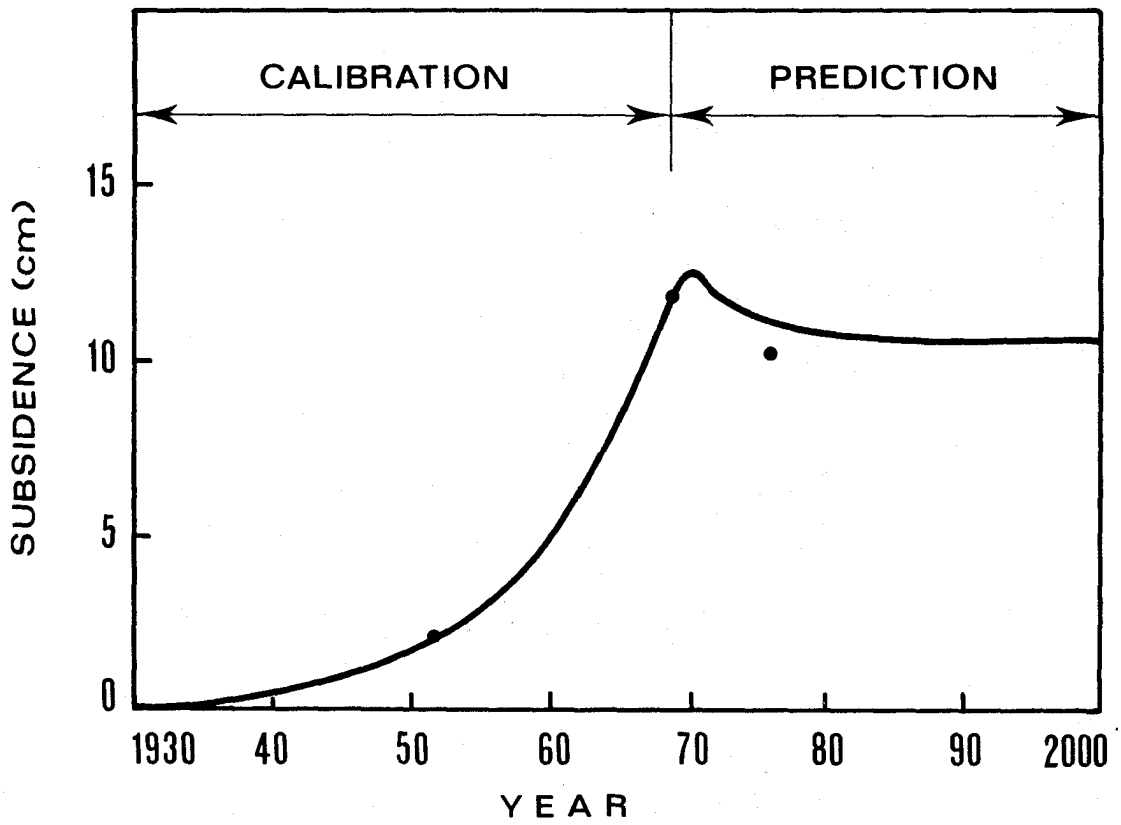

Figure 9.3.12 Subsidence in Venice versus time as provided by the model using the new data in our possession. The experimental records (o) are indicated.

9.3.5 CONCLUSIONS

The results of the experimental research have confirmed that also in the case of Venice, the sinking was caused by the artesian withdrawals. Also statistical analysis attributes 70 per cent of land subsidence occurring between 1952-1969 to the withdrawal of the underground water.

The experimental data showed that the pumpage performed at Marghera has greatly altered the natural flow field under the historical center and that the effects of the resulting subsidence are not uniformly distributed. In fact, for every metre of piezometric decline, the subsidence in the industrial area and in Venice was respectively 1 and 2 centimetres. This is connected to the relative increment towards Venice of the clay-type soils, which are more compressible, making the level of the city more dependent on the piezometric situation.

Soil deformations related to hydraulic head variations occur in a relatively short time due to the fact that aquitards are mainly silty and each of them is interrupted by thin sandy layers which facilitate the drainage.

But the most significant fact that arises from our investigation remains in any case the sudden rise of the piezometric levels recorded in the whole area since 1970, and related to a significant reduction of the artesian withdrawals in the last years. It is also important that there is a parallel surface rebound (2 cm in Venice), that ensures that land subsidence has been arrested. This result is in agreement with the predictions from the mathematical model.

Since a more careful use of the underground waters gives a very quick recovery, one can trust that a complete re-establishment of the natural hydraulic balance can be obtained, maybe with further intervention against wasting water (which can be estimated to be about 4.5 m^3/s due to the spontaneous spilling in the adjacent areas which influence the Venetian aquifer system).

Recovery will not, however, bring back the land to the original position, as it has been demonstrated that the reversibility of the compaction of the aquitards is possible for only 20 per cent (which would correspond to a rebound of about 3 cm).

Although the drawdown of the piezometric levels due to the intensive extractions of 1952-69

was the principal cause of the subsidence, we do not see a need for stopping the residual extractions.

Because of the unstable situation of Venice, it is necessary to continue the control of the piezometric levels of the aquifers and the ground altimetry. This is the only system by which we can evidence possible future variations from the present trend.

9.3.6 REFERENCES

ALBEROTANZA, L., FAVERO, V., GATTO, P., MASUTTI, M., MOZZI, G., PIANETTI, F., and R. SERANDREI. 1972. Catasto pozzi del Comune di Venezia. Cons. Naz. Ric., Lab. Din. Gr. Mas., Tech. Rep. 23, 5 vols., Venezia, 1,168 p.

BENINI, G. 1971. Relazione fra emungimenti ed abbassamenti del suolo. Ministero Lavori Pubblici, Comitato Difesa Venezia, III Gruppo, Padova, 97 p.

CAPUTO, M., FOLLONI, G., GUBELLINI, A., PIERI, L., and M, UNGUENDOLI. 1972. Survey and geometric analysis of the phenomena of subsidence in the region of Venice and its hinterland. Riv. Ital. di Geofisica, Milano, v. XXI, n.1/2, pp. 19-26.

CARBOGNIN, L., GATTO, P., and G. MOZZI. 1974. Situazione idrogeologica nel sottosuolo di Venezia. Cons. Naz. Ric., Lab. Din. Gr- Mas., Tech. Rep. 32, Venezia, 29 p.

CARBOGNIN, L., and P. GATTO. 1976. A methodology for hydrogeological data collection in the Venetian Plain. IBM Seminar on "Regional Groundwater Hydrology and Modeling," Venezia, 24 p.

CARBOGNIN, L., GATTO, P., and G. MOZZI. 1976. Movimenti del suolo a Venezia e variazioni piezometriche negli acquiferi artesiani. Cons. Naz. Ric., Lab. Din. Gr. Mas., Tech. Rep. 67, Venezia, in press.

CONSIGLIO NAZIONALE DELLE RICERCHE. 1971. Relazione sul Pozzo VE 1 CNR. Cons. Naz. Ric., Lab. Din. Gr. Mas., Tech. Rep. 14-21, Venezia.

CONSIGLIO NAZIONALE DELLE RICERCHER. 1975. Livellazione geometrica di precisione rua di Feletto-Venezia. Unpublished report of the Lab. Din. Gr. Mas., Venezia.

FAVERO, V., ALBEROTANZA, L., and R. SERANDREI BARBERO. 1973. Aspetti paleoecologici, sedimentologici e geochimici dei sedimenti attraversati dal pozzo VE, 1 bis CNR. Cons. Naz. Ric., Lab. Din. Gr. Mas., Tech. Rep. 63, Venezia, 51 p.

FOLLONI, G., DE SANCTIS RICCIARDONE, and A. GUBELLINI. 1974. Evoluzione recente del fenomeno di subsidenza nella zone di Venezia e del suo entroterra. ist. di Topografia e Geodesia, Universita di Bologna, 16 p.

FONTES, J. CH., and G. BORTOLAMI., 1972. Subsidence of the area of Venice during the past 40,000 years. Cons. Naz. Ric., Lab. Din. Gr. Mas., Tech. Rep. 54, Venezia, 11 p.

GAMBOLATI, G., and FREEZE, R. A., 1973. Mathematicam simulation of the subsidence of Venice, lst Theory, Water Resource Research, v. 9, no. 3, pp, 721-733,

GAMBOLATI, G., GATTO, P., and FREEZE, R. A., 1974. Mathematical simulation of subsidence of Venice, 2nd results. Water Resource Research, v. 10, no. 3, pp. 563-567.

GAMBOLATI, G., GATTO, P., and FREEZE, R. A., 1974. Predictive simulation of the subsidence of Venice. Scienze, v. 183, pp. 849-851.

GUBELLINI, A., and G. DESANCTIS RICCIARDONE., 1972. Analisi dei risultati di due livellazioni esequite nella zona di Venezia nel 1970 e nel 1971. Cons. Naz. Ric., Lab. Din. Gr., Mas., Tech. Rep. 41, Venezia, 18 p.

LEONARDI, P., 1960. Cause geologiche del graduale sprofondamento di Venezia e della sua Laguna. Ist. Ven. Sc. Lett. e Arti, Venezia, 21 p.

MINISTERO DEI LAVORI PUBBLICI. 1973. Pozzi LIDO 1 e MARGHERA 1. Comitato Difesa Venezia, III Gruppo, Relazione AGIP, S.Donato Milanese.

MINISTERO DEI LAVORI PUBBLICI. 1974. Catasto dei pozzi artesiani. Comitato Difesa Venezia, IV Gruppo, no. 1, Fasc. no. 18, 35 p.

MOZZI, G., BENINI, G., CARBOGNIN, L., GATTO, P., and M. MASUTTI. 1975. Evoluzione delle pressioni di strato negli acquiferi artesiani. Cons. Naz. Ric., Lab. Din. Gr. Mas., Tech. Rep. 66, Venezia, 38 p.

NEGLIA, S. 1972. Pozzi VE 1 e VE 1 bis CNR, Analisi geochimiche sulle carote argillose. Cons. Naz. Ric., Lab. Din.,Gr. Mas., Tech. Rep. 56, Venezia, 16 p.

POLAND, J. F., and MOSTERTMAN, L. J. 1969. Reconnaissance investigation of the subsidence of Venice and suggested steps toward its control. UNESCO report, Paris, 24 p.

RICCERI, G., and BUTTERFIELD, R. 1974. An analysis of compressibiility data from a deep borehole in Venice. Geotechnique, v. 24, no. 2, London, pp. 175-192.

ROWE, P. W. 1973. Soil mechanics aspects of the cores of the deep borehole VE 1 CNR in Venice. Cons. Naz. Ric., Lab. Din. Gr. Mas., Tech. Rep. 57, Venezia, 53 p.

SERANDREI BARBERO R. 1972. Indagine sullo sfruttamento artesiano nel Comune di Venezia, 1846-1970. Cons. Naz. Ric., Lab. Din. Gr. Mas., Tech. Rep. 31, Venezia, 97 p.

Note by the authors:

After 1975, both piezometric and geodetic surveys were continued on the studied area. The 1978 situation shows that the natural repressuring of the aquifers has continued and today artesian heads are coming back to the value recorded before the over-pumpage in 1952. At the same time precise leveling shows that the land has stabilized after the 1975 rebound.

Case History No. 9.4. Tokyo, Japan, by Soki Yamamoto, Rissho University, Tokyo, Japan

9.4.1 TOPOGRAPHY AND GEOLOGY OF TOKYO

Tokyo is situated at the bottom of the Kwanto structural basin, the biggest plain in Japan. Kwanto Plain is surrounded by mountains and hills on the north, west, and south where basement rocks of Tertiary and Pre-Tertiary age are exposed. The overlying new strata dip to the center of the basin.

All the rivers, such as the R. Tone, the R. Ara, and the R. Tama, start from this divide, transporting their sediments into Old Tokyo Bay. They developed fans at the foot of the mountain and a deltaic plan at their mouths in Tokyo Bay.

After the intermittent uplift, broad terraces were formed on this basin (Figure 9.4.1); on the surface of the terraces, thin volcanic ashes (Tephra) of different origins and deposited at different times are found. The maximum thickness of sedimentary rocks above the basement complex is about 300 m at the center of the basin.

The metropolis of Tokyo is located on the upland and lowland. The stratigraphic succession and schematic cross section in the Tokyo area are shown in Table 9.4.1 and Figure 9.4.2. There are many buried valleys in the lowland where an alternation of fairly thick sand and gravel layers are deposited, underlain by the Tokyo Group (Figure 9.4.3).

9.4.2 HYDROLOGY

The areas in Tokyo where land subsidence has taken place are tile Musashino upland and the alluvial lowland. There are two groups of aquifers, shallow and deep ones. The main shallow aquifer on the lowland (Koto) is Holocene sand and gravels and that on the upland area is Musashino gravel which is extensively distributed. In addition, deep artesian water is obtained from the Tokyo Group in the lowland and the Tokyo and Kazusa Groups in the upland. The Kazusa Group in the lowland contains natural methane gas which was produced for municipal supply in the Koto district. The large scale ground water development started in 1914 in Tokyo. After that time, the number of deep wells with large diameters increased rapidly. In an area extending from the northern part of the alluvial lowland to the southern part of Saitama Prefecture, there was artesian flow of ground water until the latter half of the 1920’s. At that time the ground-water level in the Koto district had fallen to about 10 m below the ground surface. The ground-water level continued to fall year after year, but toward the end of World War II it rose again temporarily. After the War, as the quantity of ground-water withdrawals increased, the ground-water level again went down until August, 1971, when it reached a low of minus 63-94 m from the mean sea level of Tokyo Bay (Tokyo Peil) in the northern part of the alluvial lowland.

Figure 9.4.4 shows the annual change of the ground-water level in selected observation wells.

The annual amounts of ground-water withdrawal in Tokyo from 1964 to 1975 are shown in Table 9.4.2. In the 23 wards, 1,160,000 m^3/day of ground water was withdrawn in 1964, but the quantity began to decrease by 1966, and it fell to 128,000 m^3/day, or about a tenth, in 1975. This decline is attributed to the withdrawal restrictions imposed to control land subsidence. Figure 9.4.5A shows the distribution of withdrawals by ward in 1967, and Figure 9.4.5B shows the annual total, 1950-1967.

In the northern part of Tokyo, the drilling of wells to a depth of up to 160 m had been banned by December, 1971; by May, 1974 drilling of wells with a depth exceeding 160 m was also banned. As a result, the quantity of ground-water withdrawals, which amounted to 80,000-90,000 M^3/day in the period from May, 1972 to 1973, decreased to 7,000-8,000 m^3/day after May 1974. Furthermore, the ground-water level, which was lowest (T.P.* minus 48.9 m) in July, 1971, rose again gradually, as the quantity of ground-water withdrawals decreased.

---

* T. P. = Tokyo Bay datum

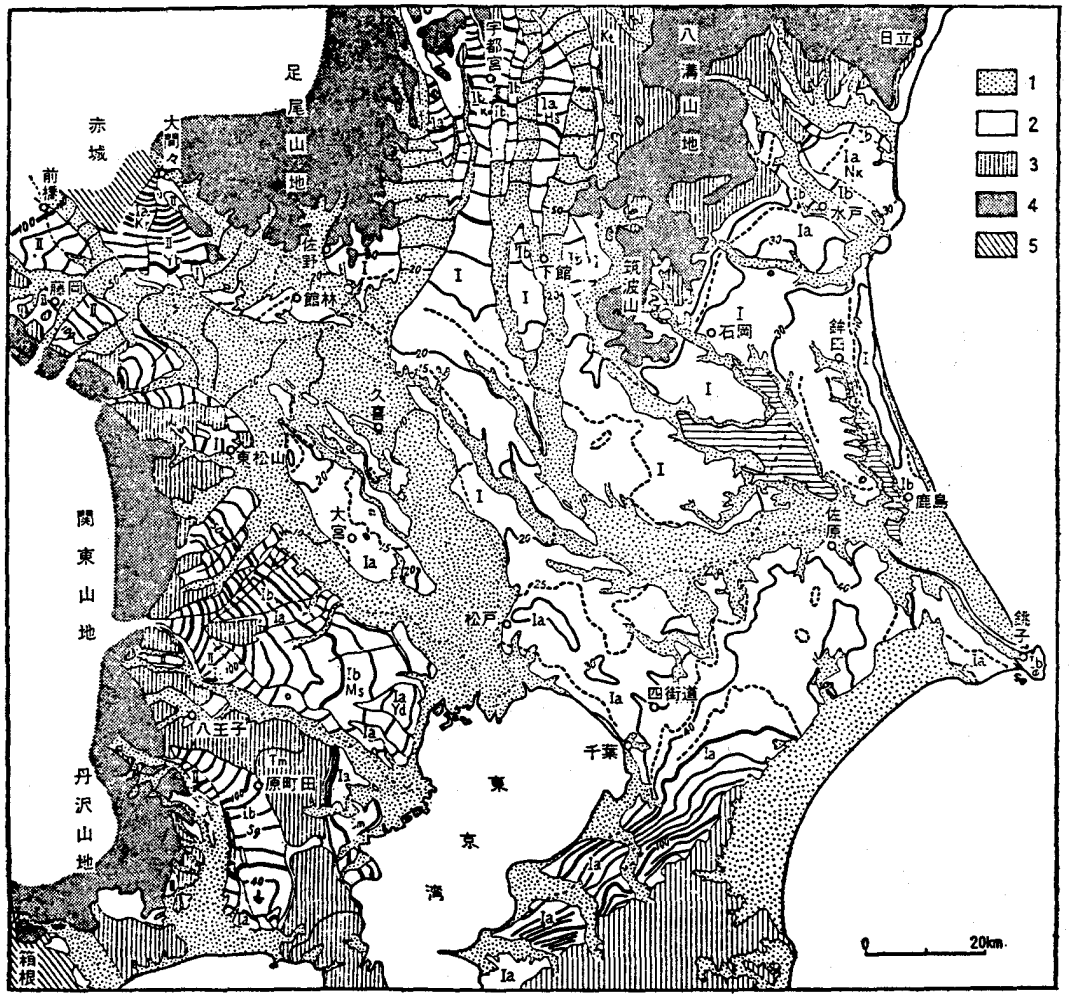

Figure 9.4.1 Geomorphological map of Kwanto District (after Kaizuka). 1, Alluvial lowland; 2, Diluvial upland; 3, Tertiary hill; 4, mountain; 5, volcano.

9.4.3 LAND SUBSIDENCE

In 1923, a severe earthquake occurred near Tokyo, causing widespread damage in the Koto region, east of the city of Tokyo. In order to study the crustal disturbance which might have accompanied this severe earthquake, a precise leveling was rerun in this region. As a result, it was found that the land subsidence was as a whole increasing gradually year by year. It was also found that the extent of the region where the land subsidence was then advancing occupied an area of about 100 km^2, situated between the Sumida and the Arakawa rivers, which flow through the region from north to south.

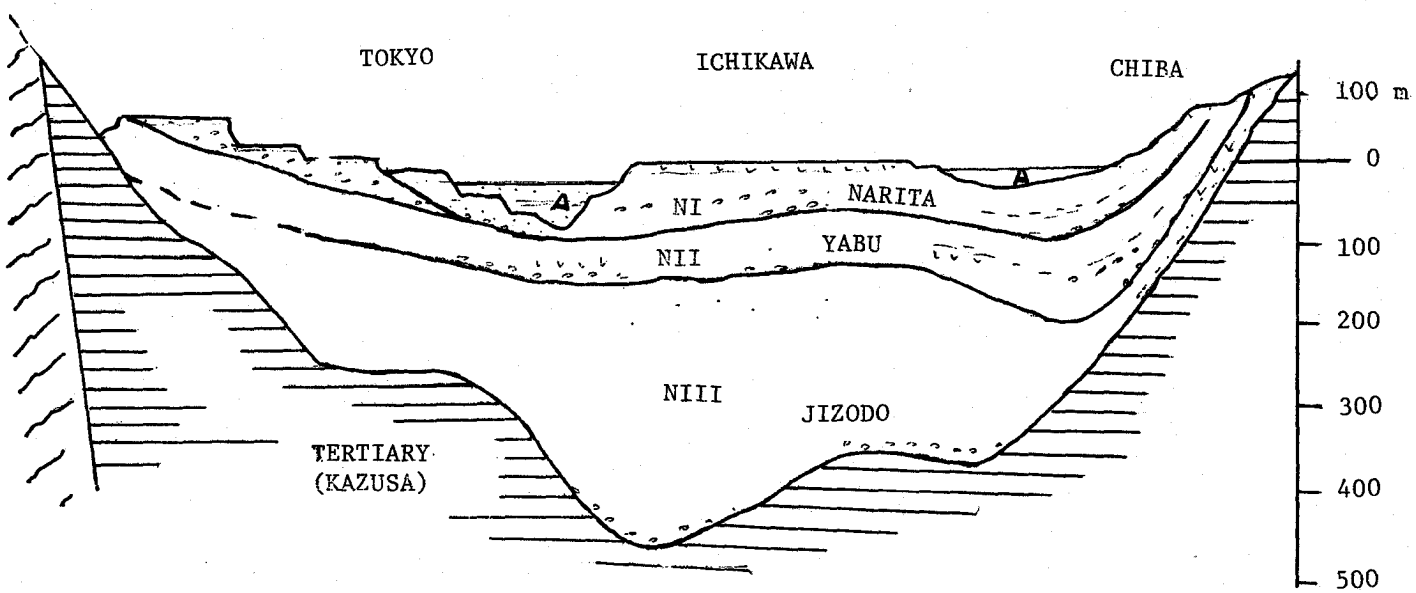

Figure 9.4.2 Schematic geologic cross section of Kwanto Basin.

Table 9.4.1 Stratigraphic succession in Tokyo

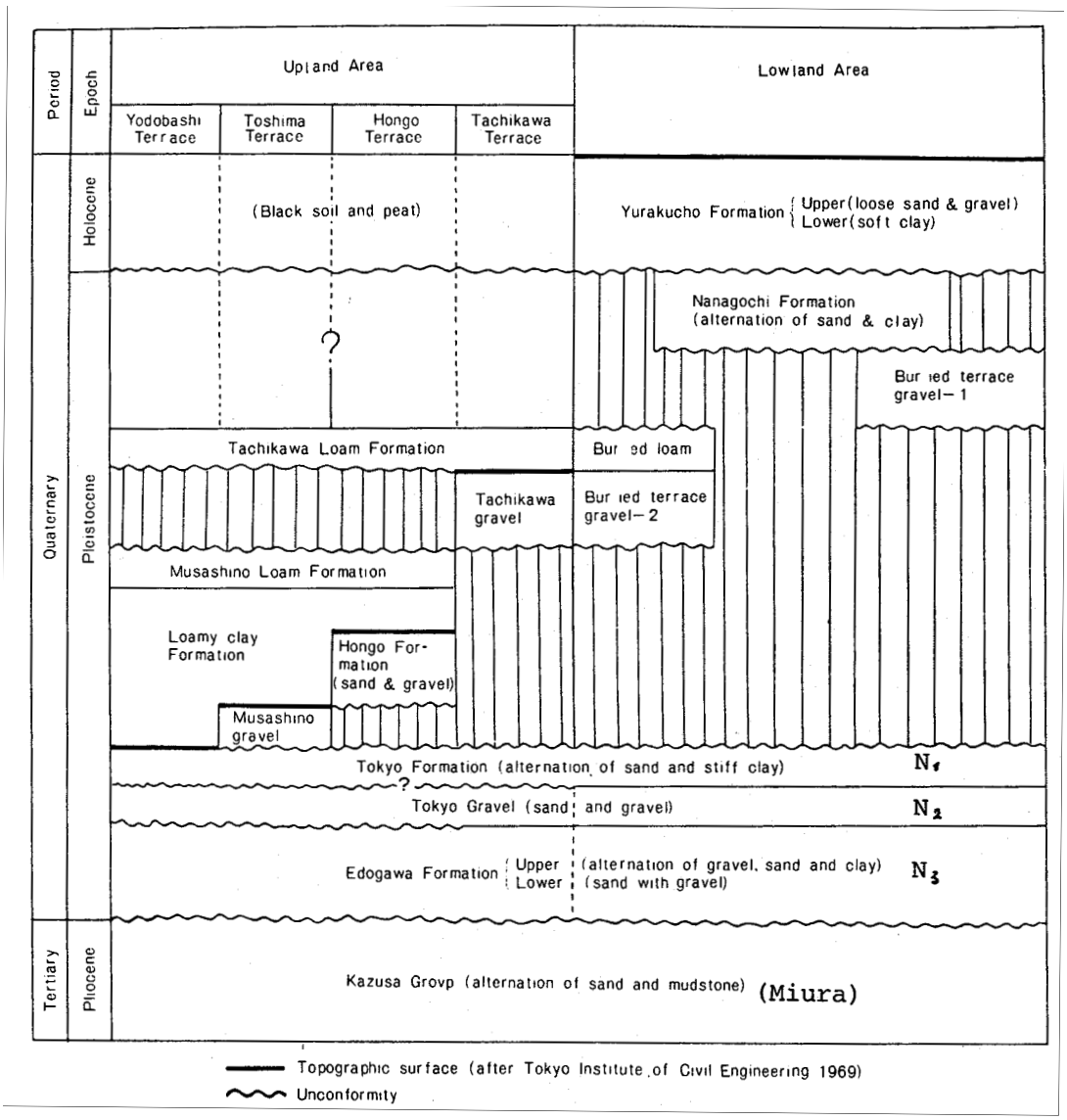

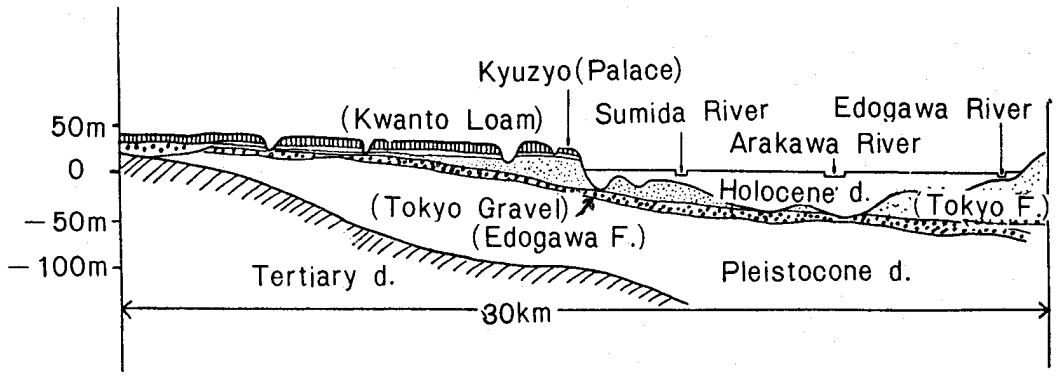

Figure 9.4.3 Geologic cross section.

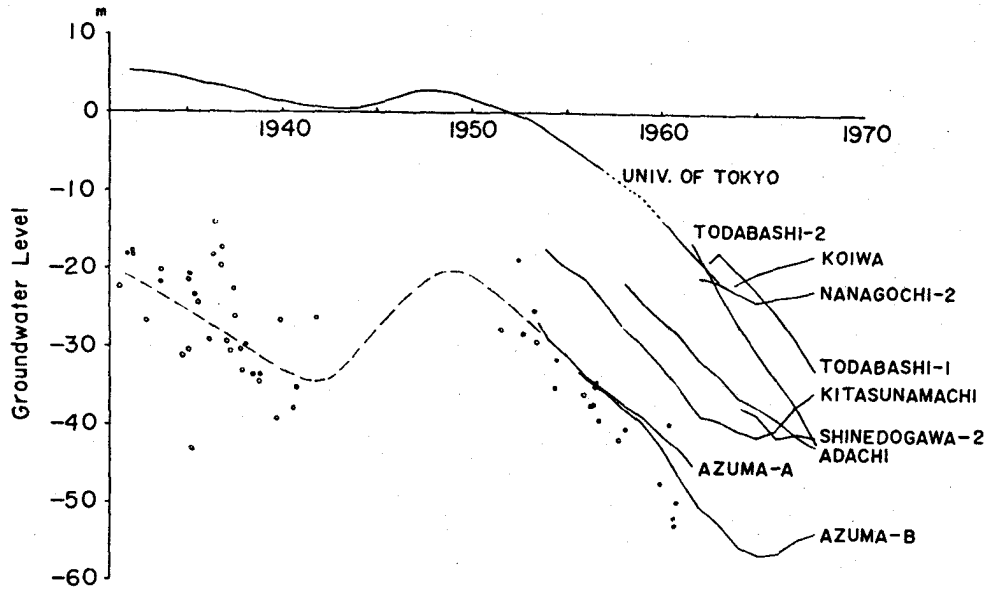

Figure 9.4.4 Secular trend of ground-water levels. Small circles indicate ground-water levels at the time of bore drilling near AZUMA-A and B (node 4)

Table 9.4.2 Amounts of ground-water withdrawal in Tokyo.

Unit: $1000m^3/day$

Year / Area	1964	1965	1966	1967	1968	1969	1970	1971	1972	1973	1974	1975
23 wards	1162	1017	805	732	679	674	747	550	324	283	195	128
Tama	353	480	536	594	626	765	953	891	853	861	818	790
Total	1515	1497	1341	1326	1305	1439	1700	1441	1177	1144	1013	918

Data from Bureau of Environmental Protection, Tokyo Metropolitan Government

In association with the advancement of such a local subsidence, several remarkable phenomena occurred, such as "lift up" of masonry buildings and well pumps and inundation by rivers and sea tide.

In order to make clear the general features of the subsidence, precise leveling along the network of the leveling routes in Tokyo was started. It takes, however, considerable time to carry out the leveling survey on the network, including all bench-marks in Tokyo. Therefore, the leveling survey has been repeated frequently on the network of bench-marks in the region where the land subsidence is greatest.

In the first stage of study of the subsidence, the leveling was repeated at irregular intervals. Afterwards, it was thought to be inconvenient to work out vertical displacements based on the data of precise levels repeated at irregular intervals, since the amounts of the subsidence became larger and the rates of the subsidence were different from place to place. Therefore, in the Koto region, i.e., the region east of the Sumida river, where the subsidence was greatest, the leveling was repeated every two years, during the period from 1938 to 1946. Since then, leveling has been repeated every year in this region.

First order leveling and observations of the compaction of soil layers and the ground-water levels by means of observation wells were also carried out. As of January, 1976, the area Surveyed by leveling extended to 900 km^2, using 632 bench-marks where the levelings are made

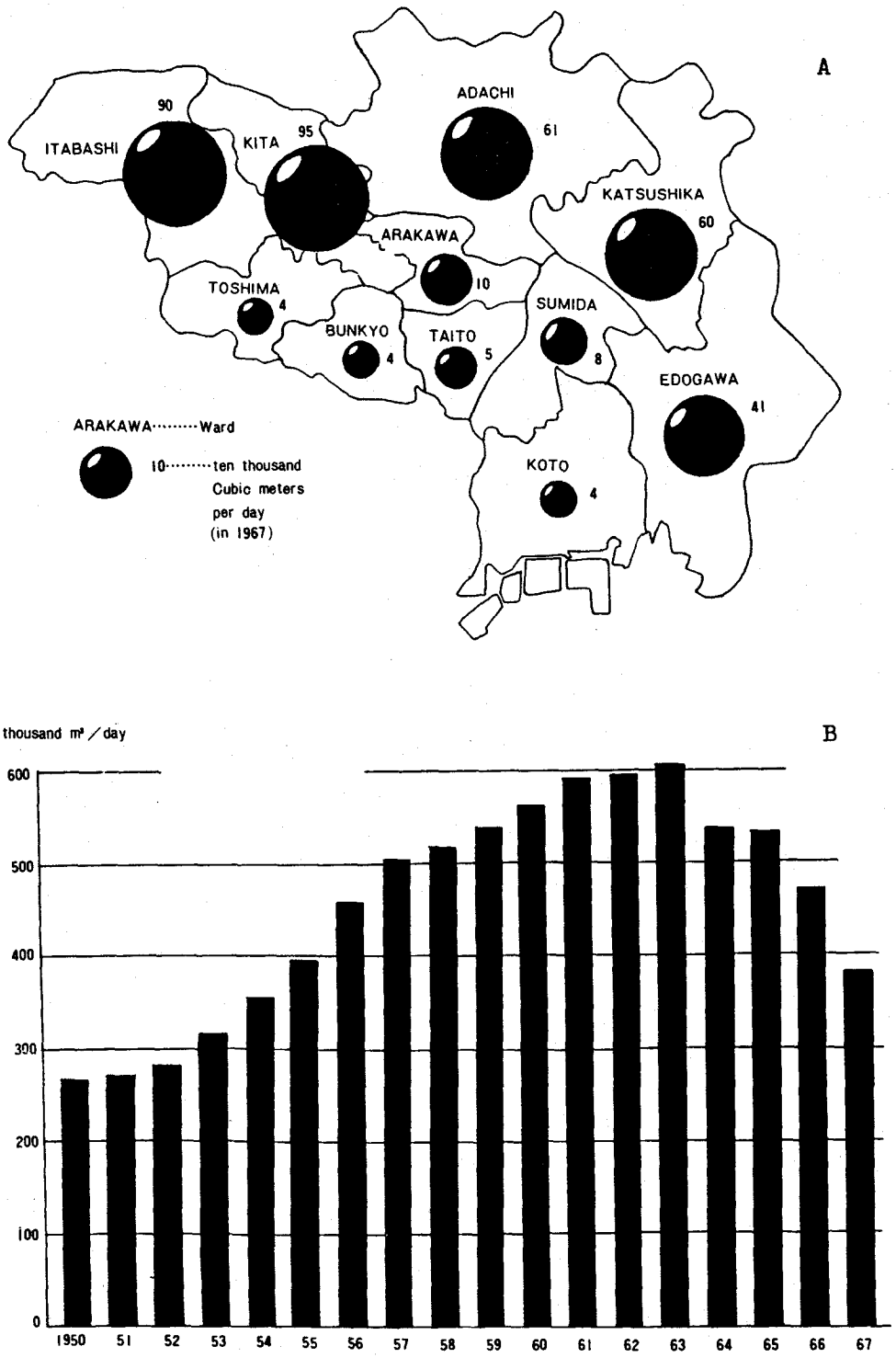

Figure 9.4.5 Amounts of ground-water withdrawal; A, by ward; B, by year.

every year. The compaction of soil layers and the changes of ground-water levels are observed at 68 observation wells located at 34 sites (Figure 9.4.6). The water-level plots are dashed.

Land subsidence has occurred in the Koto district since around 1900 and in the eastern part of the alluvial lowland (Edogawa Ward) since 1920. On the other hand, in the Musashino upland, land subsidence began to occur in the latter half of the 1950's.

The maximum subsidence in Tokyo is about 4.6 m and the maximum rate is 27 cm/yr (Figure 9.4.7). The total subsiding area in Kwanto (Tokyo, Chaiba, Kanagawa, and Saitama) amounts to 2420 km^2 and the area where the subsidence amounts to more than 10 cm/yr is still about 100 km^2.

In order to prevent or abate such a rate of subsidence, the pumping of ground water was restricted as stated above, and thus the rate has dropped year after year since 1972.

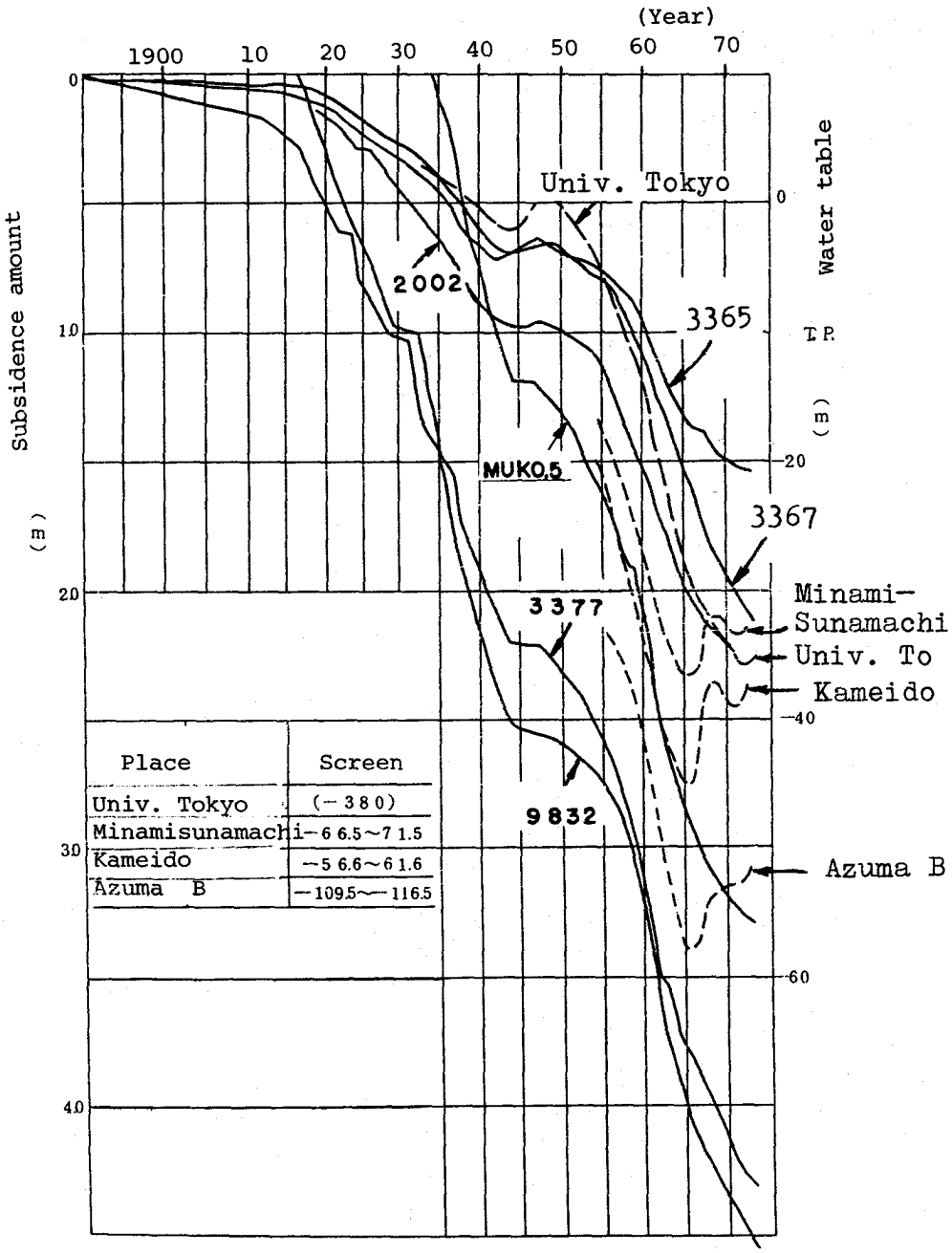

Figure 9.4.6 Secular changes of land subsidence and ground-water levels in Tokyo.

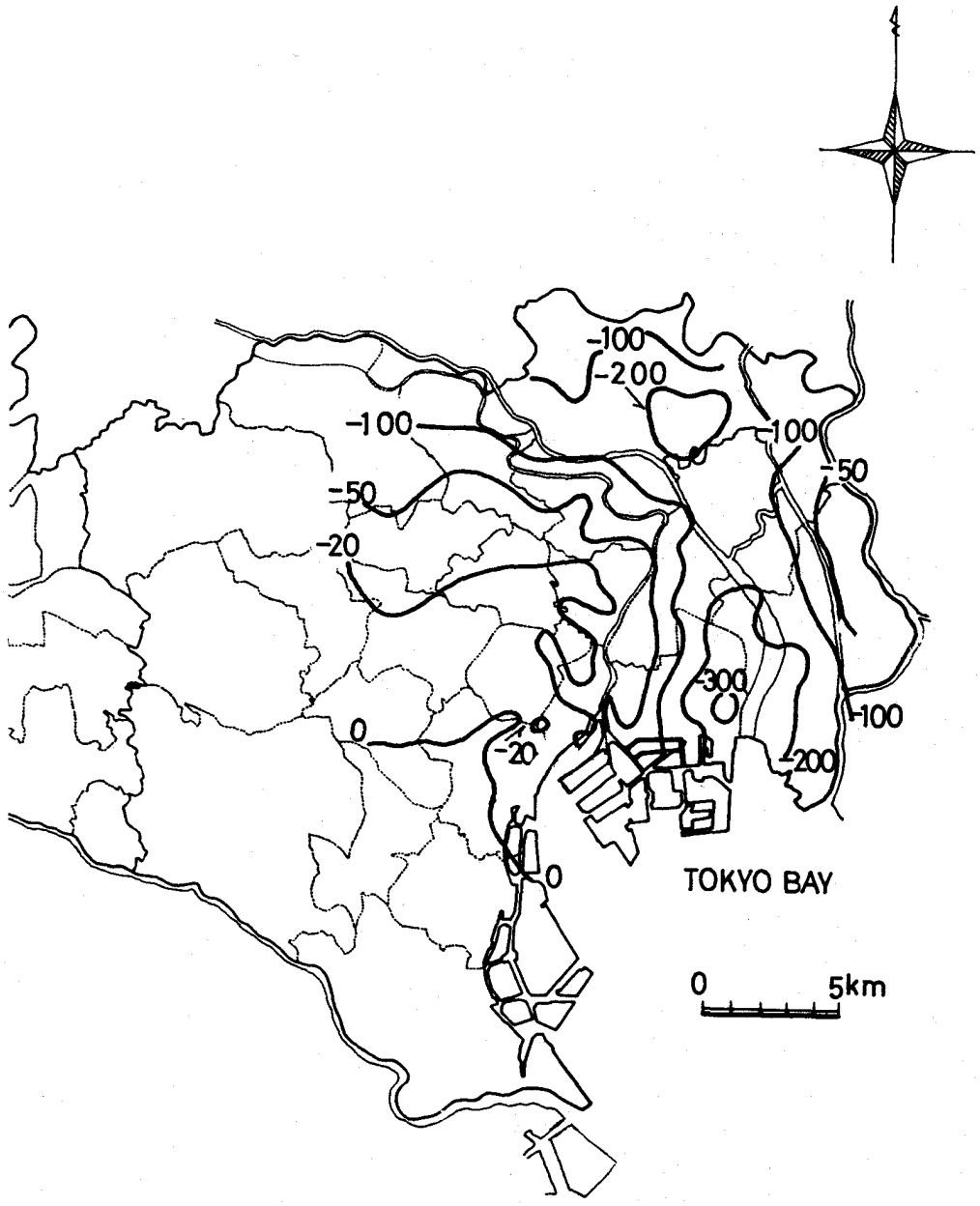

Figure 9.4.7 Total subsidence in Tokyo from 1938 to 1975.

9.4.4 PARAMETERS

Soil tests were carried out on undisturbed core samples. Consolidation tests were made by applying one-directional pressure. C_c value ranged from 0.2 to 1.2 and has the tendency of increasing with increasing water content. The M_v value varies as follows:

Alluvial clay	$2 - 3 \times 10^{-2}$ cm^2/kg
Diluvial clay	$2 - 6 \times 10^{-3}$
Tertiary clay	$1 \times 10^{-3} - 4 \times 10^{-4}$.

K: hydraulic conductivity

Tokyo Group 2.1×10^{-2} cm/sec

Kazusa Group 1.3×10^{-2}

9.4.5 COUNTERMEASURES

In Tokyo, the local government legislated a Metropolitan Ground-Water Law, superposed on the "Industrial Ground-Water Law" and "Building Ground-Water Law." Moreover, they constructed dikes for floods and high tides, pumping installations for drainage, water-supply works for industry, and polder systems. The estimated cost for the countermeasures for the period 1957 through 1970 is about 225 million U.S. dollars.

The regulations for ground-water withdrawal are as follows:

1. Restrictions under the Industrial Water Law.
   The restrictions are designed to reduce the ground-water withdrawals by supplying substitute waters. The main restrictions are described chronologically in the following:

   January 1961: A ban on drilling a new well in the southern part of the alluvial lowland (the Koto district).
   July 1963: A ban on drilling a new well in the northern part of the alluvial lowland (the Johoku district).
   June 1966: Pumping of ground water in the southern part of the alluvial lowland (the Koto district) was restricted.
   December 1971: Pumping of ground water in the northern part of the alluvial lowland (the Johoku district) was restricted.
   April 1975: Pumping of ground water in the eastern part of the alluvial lowland (the Edogawa district) was restricted.

2. Restrictions under the Law Controlling Pumping of Ground Water for Use in Buildings
   The law aims at holding in check the pumping of ground water for air conditioning and other non-drinking purposes in medium- and highrise buildings. The progress of restrictions under the law is described chronologically in the following:

   July 1963: A ban on the drilling of new wells in the alluvial lowland.
   July 1965 and July 1966: Restrictions on the pumping of ground water in the alluvial lowland.
   May 1973: The restriction was extended to the whole area of the 23 wards, and the control of ground-water withdrawals was strengthened.

3. Restrictions under the Tokyo Metropolitan Environmental Pollution Control Ordinance.
   The ordinance restricted the drilling of new wells in areas not covered by the two laws mentioned above.

4. Suspension of drawing ground water containing natural gas
   The Tokyo Metropolitan Government in December 1972 bought the mining rights for water-soluble natural gas extracted in the neighborhood of the Ara River estuary, and thereby suspended the pumping of gas-water (3,000 M^3/day) from the Kazusa Group.
   On the other hand, in the Tama district, the drilling of new wells for industrial water and water for non-drinking purposes (for example, the supply of bath water) is restricted under the Metropolitan Ordinance mentioned in (3) above, but with an increase in population in the district, the demand for ground water climbed from 350,000 m^3/day in 1964 to some 900,000 M^3 /day in 1971.

The replacement drinking water and building water are supplied from the River Tone through the Musashi aqueduct and the industrial water is supplied from the Metropolitan industrial water works on the Tone which is provided by the construction of high dams on the upper part of this river.

9.4.6 SELECTED REFERENCES

MIYABE, N. 1962. Studies in the ground sinking in Tokyo, Rept. Tokyo Institute of Civil Engineering, p. 1-38.

INABA, Y., AOKI, S., ENDO, T., and R. KAIDO. 1969. Reviews of land subsidence researches in Tokyo, IAHS Pub. No. 88, p. 87-98.

ISHI, M., KURAMOCHI, F., and T. ENDO. 1977. Recent tendencies of the land subsidence in Tokyo, IAHS Pub. No. 121, p. 25-34.

Case History No. 9.5. Osaka, Japan, by Soki Yamamoto, Rissho University, Tokyo, Japan

9.5.1 GEOLOGY OF OSAKA

The Osaka basin surrounded by the Rokko and Ikoma Ranges is one of the typical Quaternary basins in the Kinki Triangle. The Rokko elevation reaches more than 900 m in the highest part and the sinking Osaka basin has been filled by the Pleistocene Osaka group and the later sediments which are certainly over 600 m in thickness in the central part of the basin. The horizon belonging to the lower Pleistocene which is the same one recognized at a depth of more than 500 m by boring in the Osaka basin can be confirmed at the height of 500 m in the Rokko Range. The amplitude of the folding of the basement represented by the Osaka basin and the Rokko Range is considered to reach more than 1,000 m since the early Pleistocene (Figure 9.5.1 and 9.5.2).

Complex thrust systems have developed especially along the boundary zones between uplifts and subsidences. The beds older than the middle Pleistocene are divided by thin tuff beds of Ma_0, Ma_l, Ma_2, --- , Ma_{l2}, and have been strongly disturbed by faulting everywhere around the Osaka basin. Terrace deposits have been confirmed to be displaced by faulting at many places. For example, the granite mass of Rokko has thrust up against the higher terrace deposit.

A wide terrace developed in the northern part of the Osaka basin; it is named the Itami terrace, and is the lowest one in this area. The Itami gravels composing this terrace surface gently dip to the center of the Osaka basin. A radiocarbon age determination made on a wood fragment contained in the Itami clay which is overlain by the Itami gravels is 29,800±1,200 years B.P.

The distribution of the "Alluvial deposits" in Osaka has been revealed by boring and the sonic Sparker survey. The deposits indicate the curvature of the surface of the basement and may suggest the shape of basin-forming recent subsidence of the Osaka basin (Table 9.5.1).

9.5.2 HYDROLOGY AND SUBSIDENCE

The first layer below the ground surface is an alluvial layer except on the Uemachi upland running south from the vicinity of Osaka Castle. The average thickness of this alluvial clay layer is about 15 m. The thickness becomes greater as it approaches the coastal zone. Below the Alluvium are very thick Diluvial deposits of Pleistocene age, which consist of alternations of sand and clay layers. Both alluvium and diluvium layers form an excellent aquifer in this district (Figure 9.5.3).

The ground water head was very high in the city until about 50 years ago. It is reported that even flowing artesian wells could be seen at some parts of the city. With the development of industry, however, the use of ground water gradually increased and land subsidence due to the withdrawal of ground water began to appear. Before 1928, the land subsidence in the city was very slight, being at a rate of 6-13 mm/yr. This slight subsidence is considered to be the result of the natural movement of the earth crust and of the natural consolidation of the newly deposited alluvial clay.

After that time, however, a remarkable increase in use of ground water caused an increase in the rate of subsidence (Table 9.5-2).

Since that time, precise leveling for the wider part in the city has been carried out every year by the Osaka Municipal office following the suggestion of M. Imamura. Besides the leveling, the amount of consolidation of soil layer and the artesian heads of various aquifers (O.P.* -33 m, O.P. -62 m, O.P. -176 m) were observed by self-recording apparatus by K. Wadachi at Kujoh Park in 1938. Figure 9.5.4 shows the total amount of subsidence of various bench marks in

---

* O.P. (Osaka Peil) means the lowest low-water level observed in Osaka Port in 1885 and this level is used as the standard datum in Osaka area.

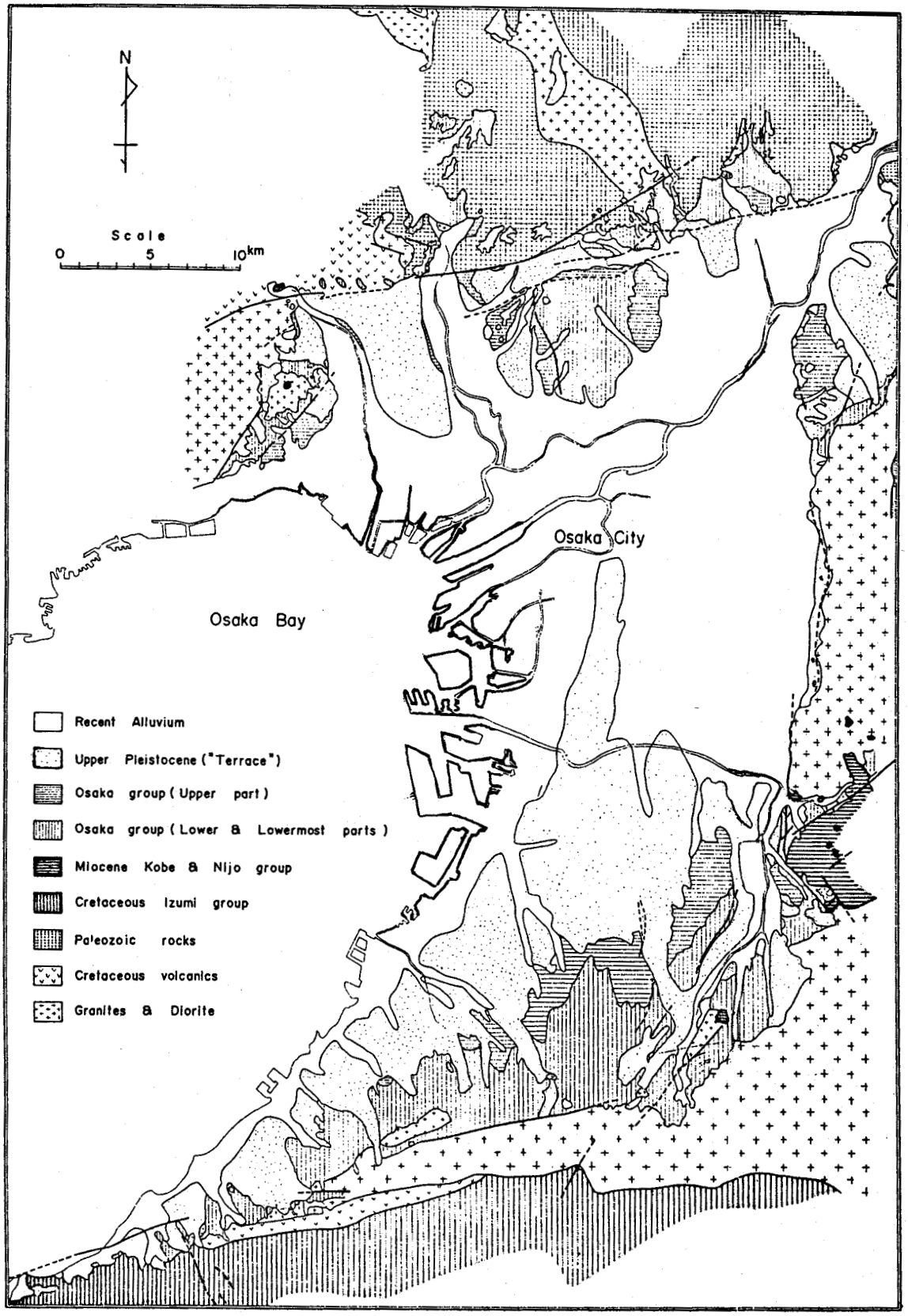

Figure 9.5.1 General geologic map.

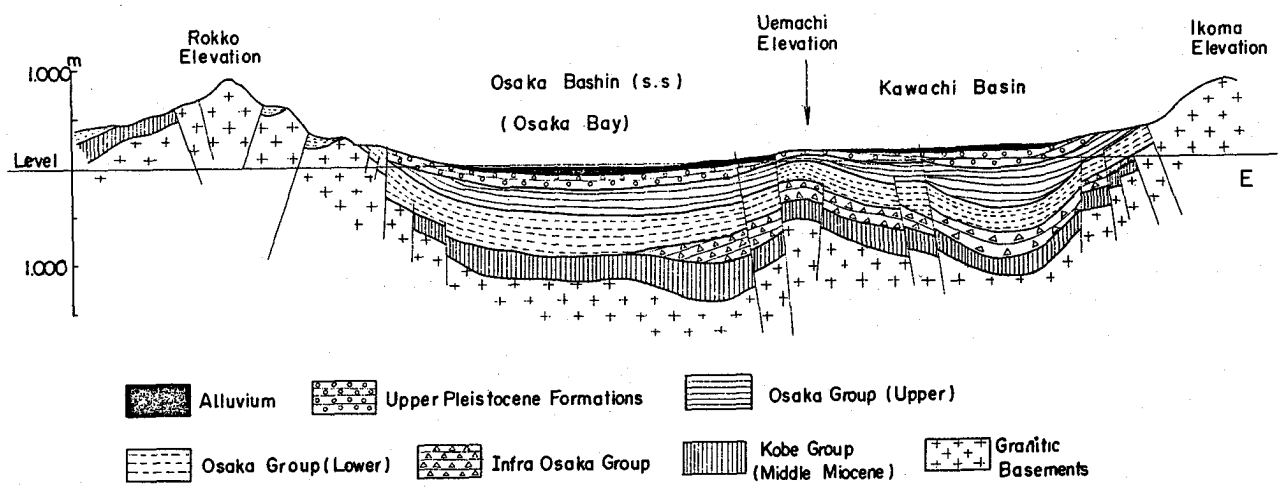

Figure 9.5.2 Diagrammatic profile of the Osaka basin (Ikebe & Takenaka).

western Osaka and secular variation of the artesian head at the Kujoh well 176 m deep. As seen in this figure, the rate of subsidence seems to be classified into four phases. In the first period from 1935 to 1943 the land subsidence was very rapid as the industry in the city developed. In the second period from 1944 to 1951, land subsidence was very slight or sometimes stopped. At that time, industrial activity was greatly depressed by the war disaster and the use of ground water decreased. It began to increase again in the third period from 1952 to 1964 because of the remarkable increase of industrial water use. From 1964 to the present, it has decreased because of the regulations against ground water use. The variation of ground water head is almost similar to that of land subsidence.

The artesian head and rate of subsidence are closely correlated at the Kujoh well. In spite of some unconformity of peak years, however, the general features of the variation in the artesian water head and in the rate of subsidence show a close correspondence and suggest a causal connection between these phenomena. The period when land subsidence stopped corresponds to the period of recovery of the ground water head (Figure 9.5.4).

The total subsidence during 34 years from 1935 to 1968 in Osaka is shown by the isopleths in Figure 9.5.5. In this figure, it can be noticed that the subsidence is larger nearer to the coastal zone, and a zone of little subsidence is left in the upland in the middle of Osaka where no alluvial covering exists. The subsidence area covers about 570 km^2 at present, but is successfully decreasing.

In spite of the success in preventing land subsidence in Osaka City, the subsidence in eastern and northern Osaka has increased remarkably during the recent few years. These regions have been developed lately and many factories which demand much ground water have been built.

9.5.3 PARAMETERS

The compression index C_c was obtained by the standard oedometer test. The value varies from 0.2 to -1.8 and is proportional to the liquid limit w_L. The equation of the regression line is $C_c = 0.017\ (w_L - 37)$. The preconsolidation pressure varies from 2 to 50 (kg/cm^2). It increases proportionally to the depth and is generally larger than the present effective overburden pressure.

9.5.4 ECONOMIC AND SOCIAL IMPACT

This can be seen from Figure 9.5.6 easily. Total amounts of industrial products are presented in yen deflated in economic appraisal of 1965.

Table 9.5.1 Stratigraphic correlation of geology in Osaka.

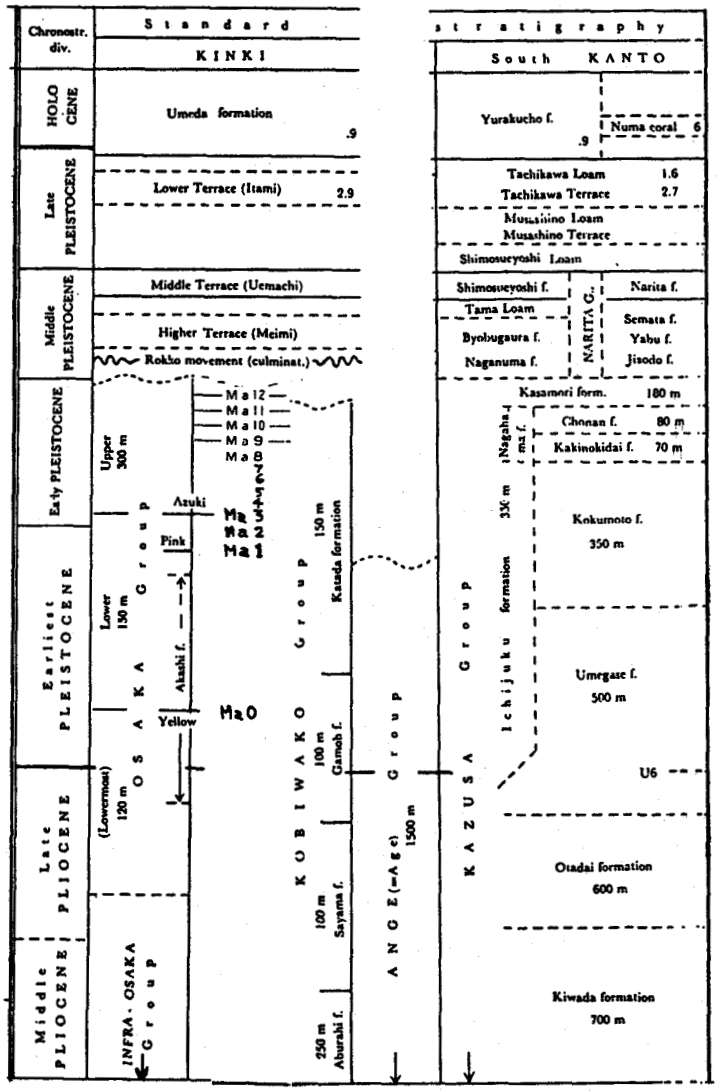

9.5.5 COUNTERMEASURES WITH LEGAL REGULATION

Due to land subsidence, the ground surface of a part of western Osaka has sunk below sea level and the city is exposed to the danger of floods caused by storm surges in Osaka Bay. Subsidence areas below high tide have extended to about 100 km^2.

In 1934 a very large flood occurred, caused by the Muroto Typhoon, the biggest typhoon that ever attacked Osaka. An area of about 49 km^2 was flooded by the storm surge of O.P. + 4.20 m. In order to prevent further disasters, the dikes have been repaired and built more satisfactorily.

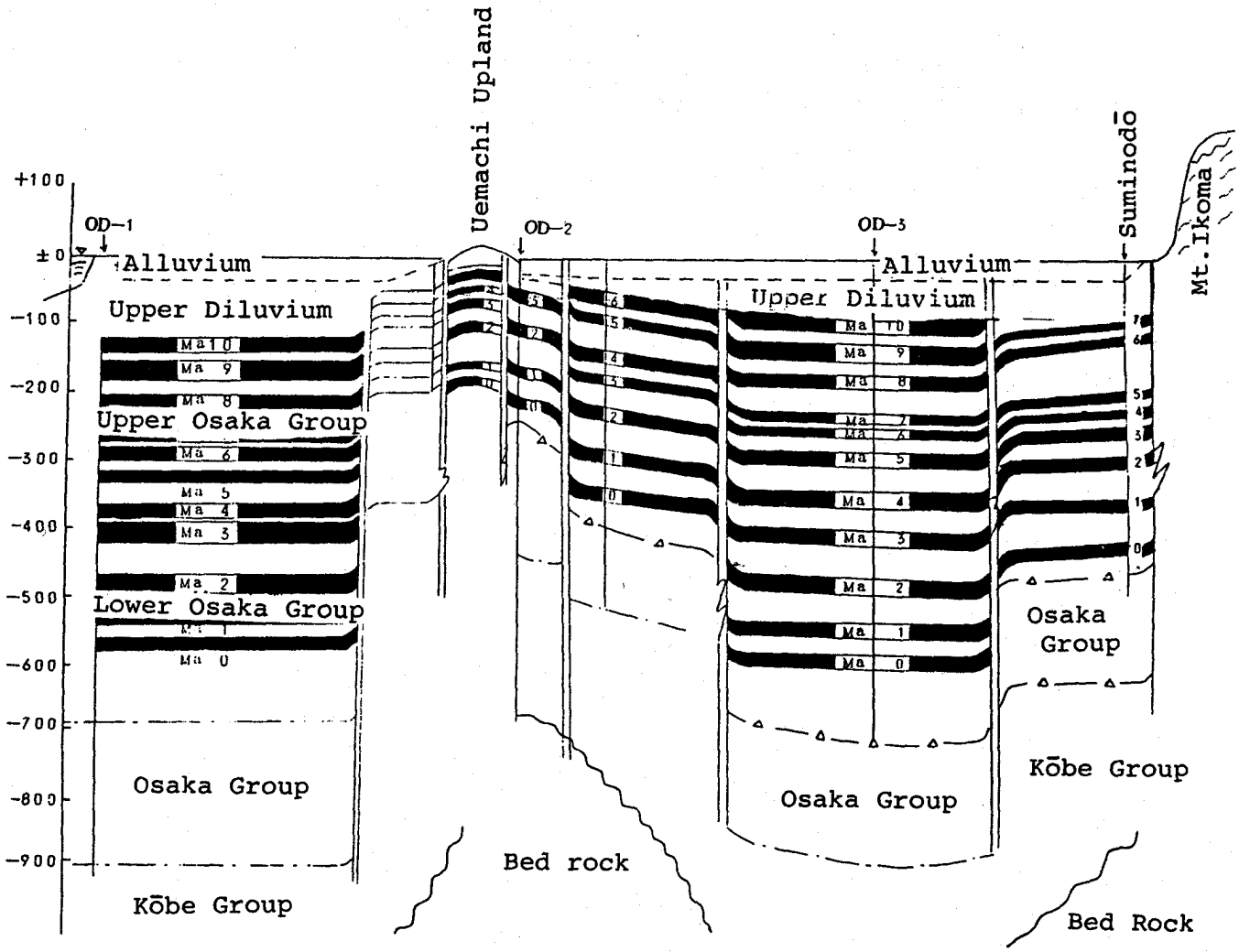

Figure 9.5.3 Geologic cross section of Osaka.

Table 9.5.2. Change of ground water withdrawal in Osaka

Year	Discharge amount x 10^3 m^3/year	Year	Discharge amount x 10^3 m^3/year	Year	Discharge amount x 10^3 m^3/year
1920	956	1956	65060	1963	94780
1930	6386	1957	93120	1964	79190
1940	18997	1958	110720	1965	56120
1945	19309	1959	130420	1966	34410
1953	30000	1960	144100	1967	15400
1954	37440	1961	130420	1968	4660
1955	57440	1962	123680	1974	42

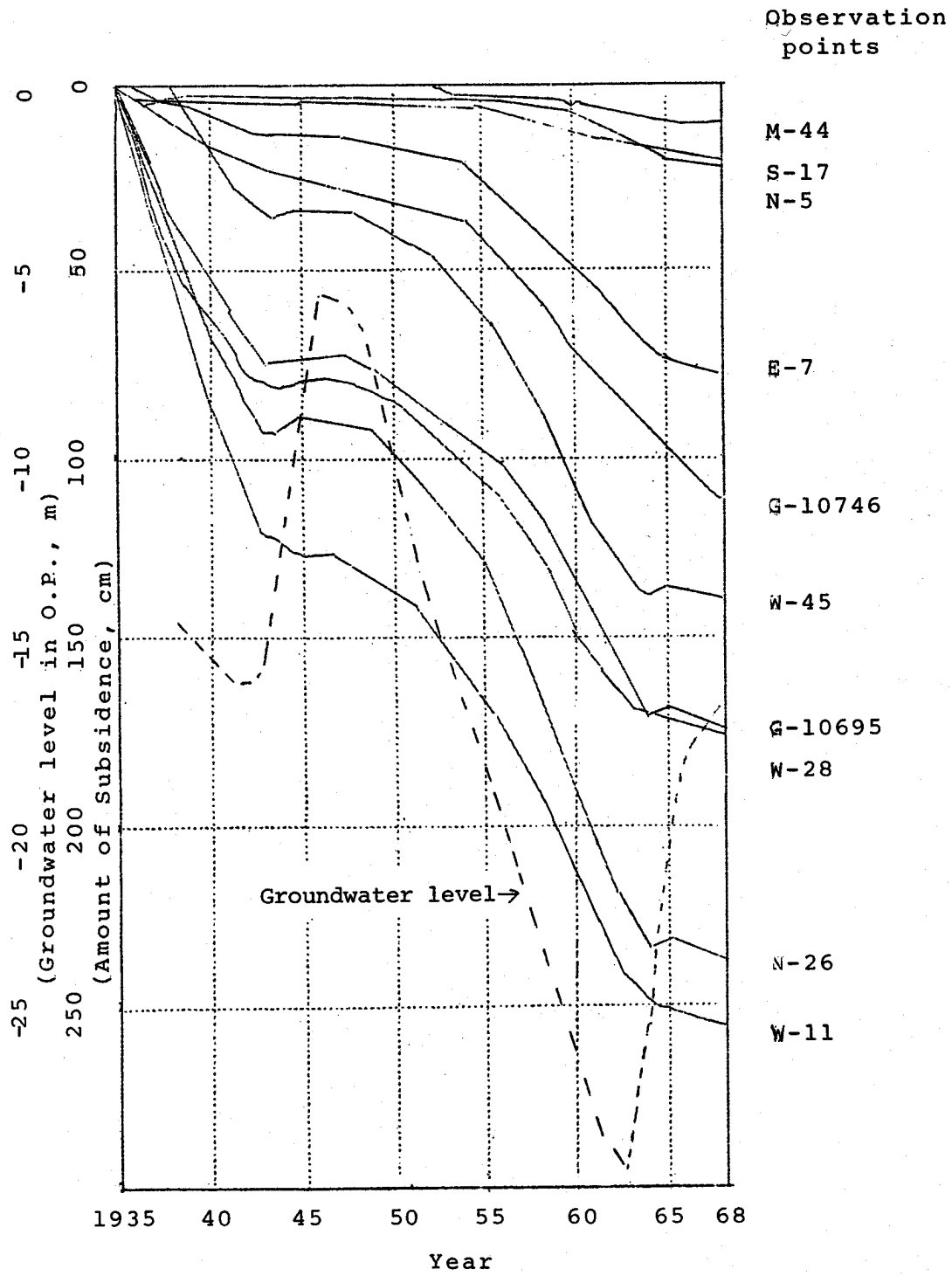

Figure 9.5.4 Secular changes of land subsidence and ground-water level in Osaka.

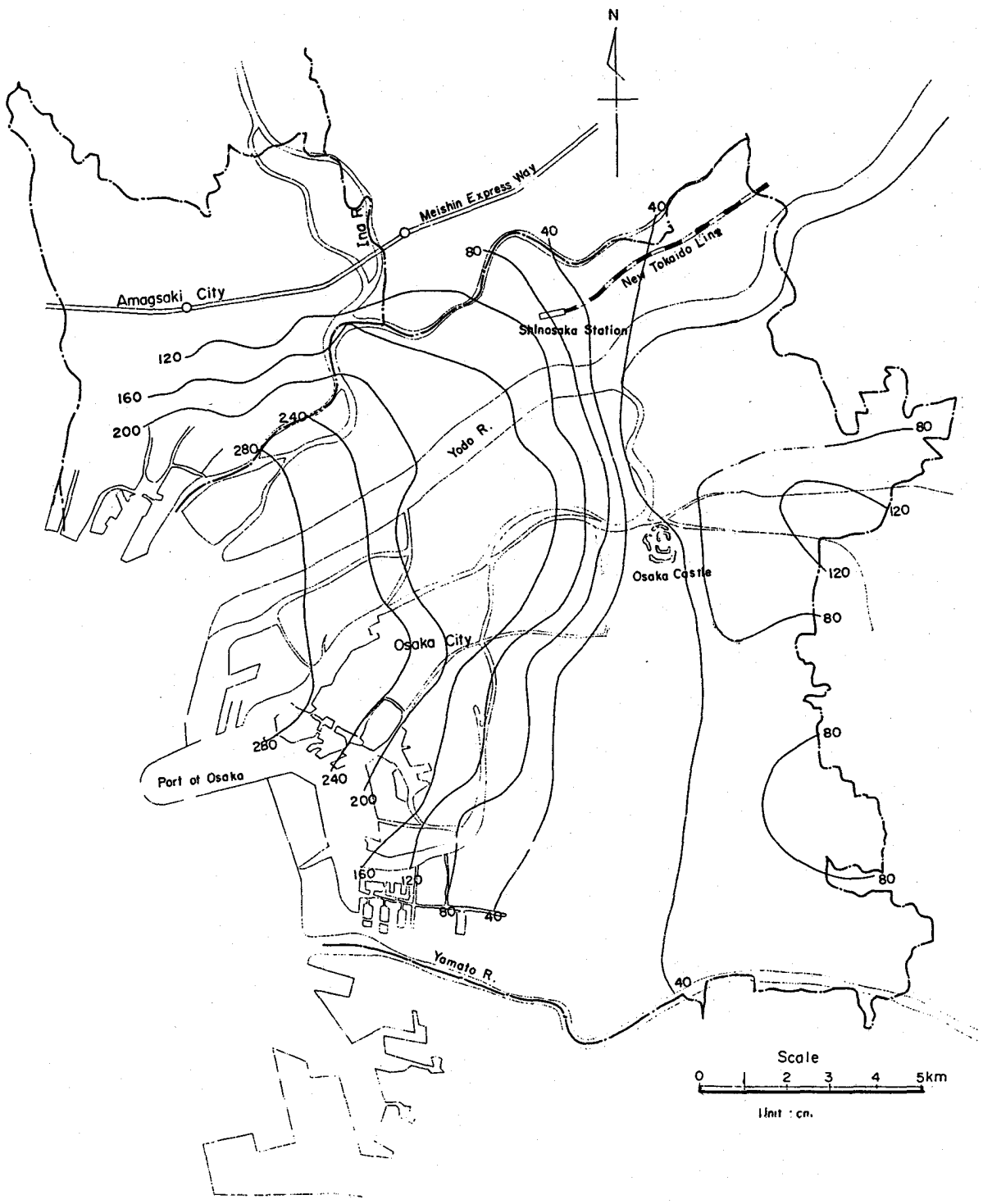

Figure 9.5.5 Isopleths of amount of land subsidence in Osaka area from 1935 to 1968

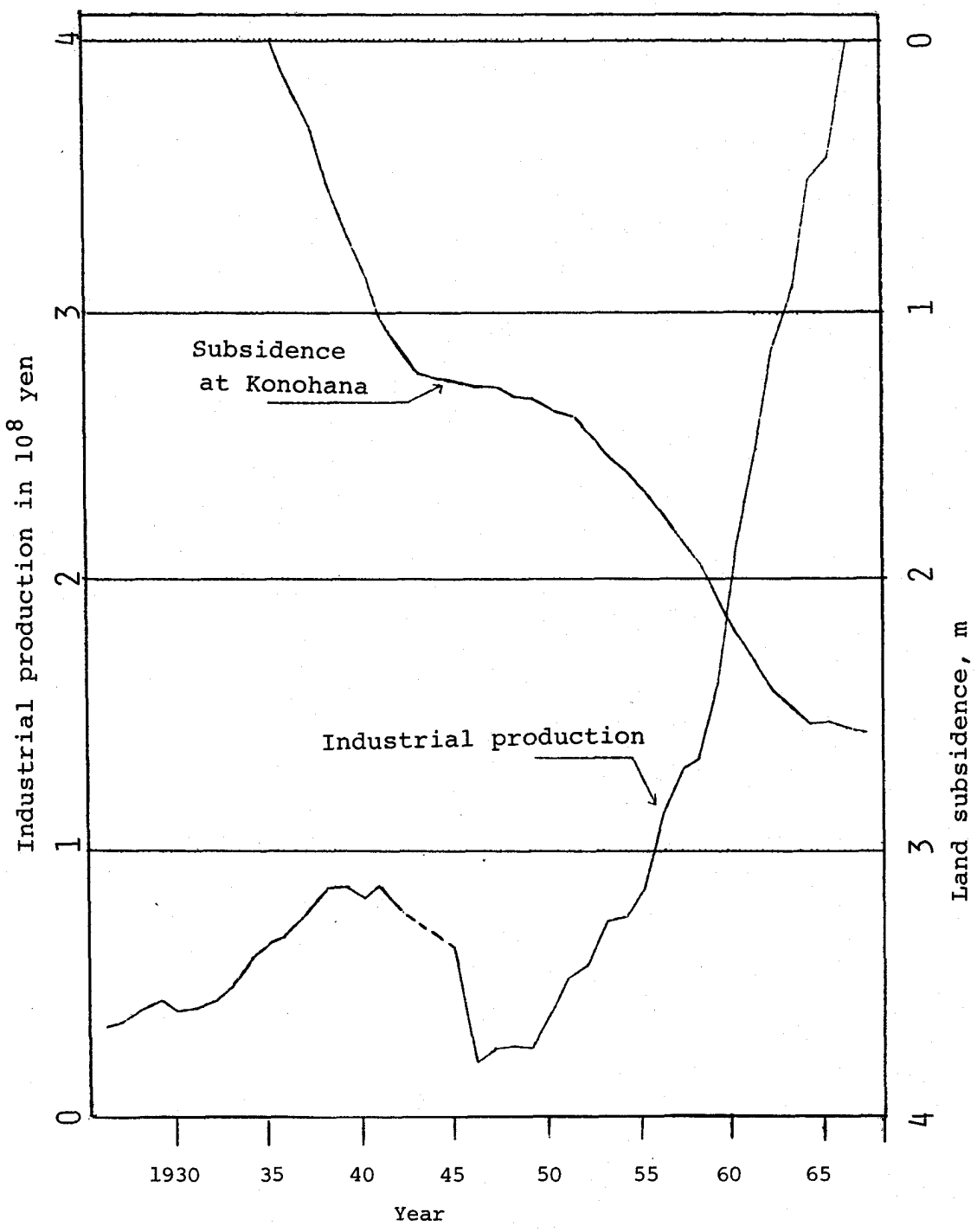

Figure 9.5.6 Land subsidence and industrial production in Osaka Prefecture. (Industrial production is inflated to the value of 1965.)

Besides these prevention works, the use of ground water has been gradually regulated in accordance with the progress of the industrial water supply works for delivering surface water, which was planned as the substitute for ground water. In 1962, Osaka City constructed industrial water supply works and in 1970, the Osaka prefectural government also constructed industrial water supply works introducing water from the River Yodo which started from Lake Biwa, the biggest lake in Japan.

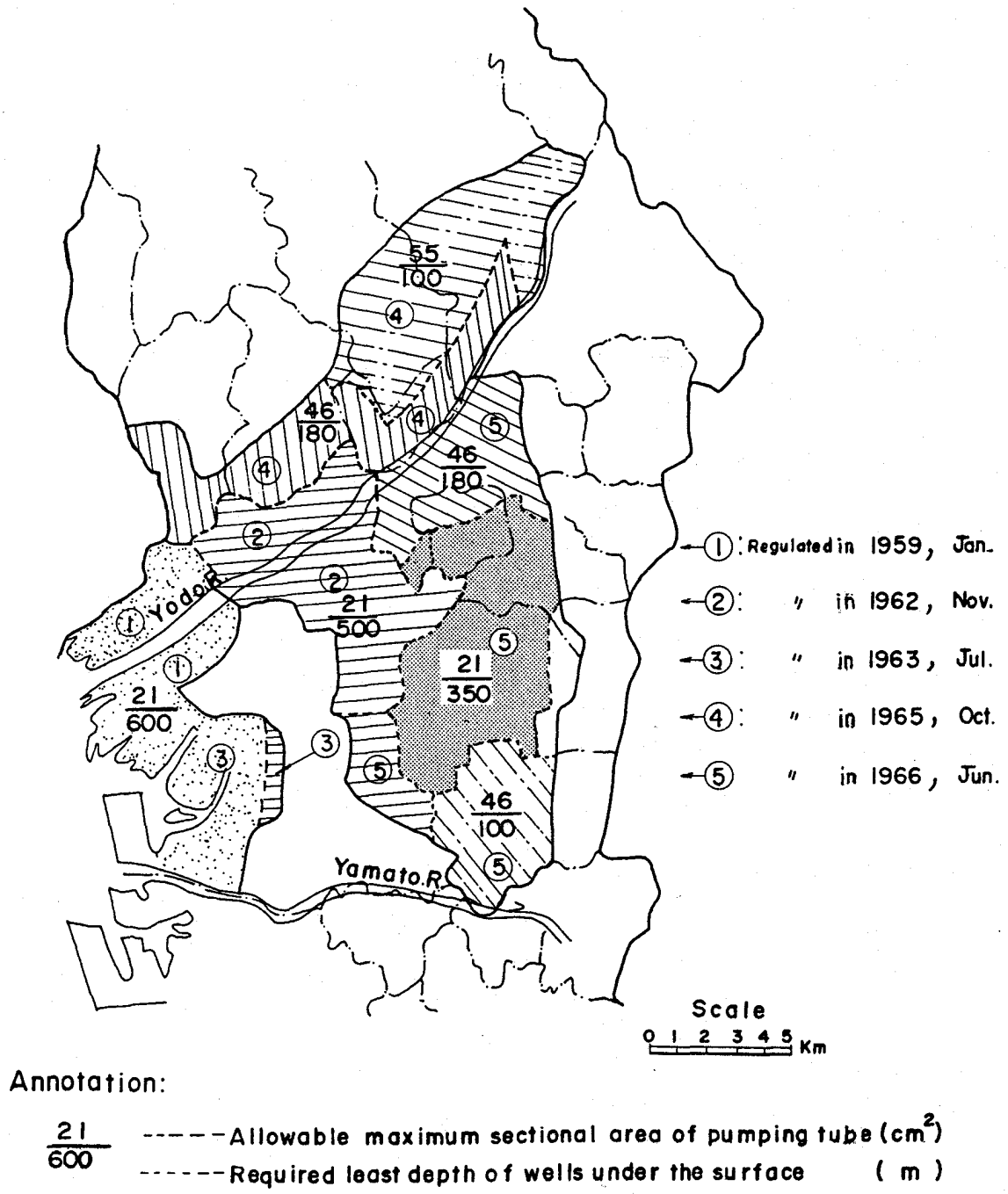

Figure 9.5.7 Regulated areas against use of ground water for industry.

Because of the regulation against the use of ground water in Osaka City land subsidence in the city gradually decreased and has almost stopped at present (Figures 9.5.7 and 9.5.8).

9.5.6 SELECTED REFERENCES

MURAYAMA, S. 1969. Land subsidence in Osaka, IASH Pub. No. 88, p. 105-130

NAKAMACHI, H. 1977.Land subsidence in Osaka, Soil and Foundation, 25-6, p. 61-67.

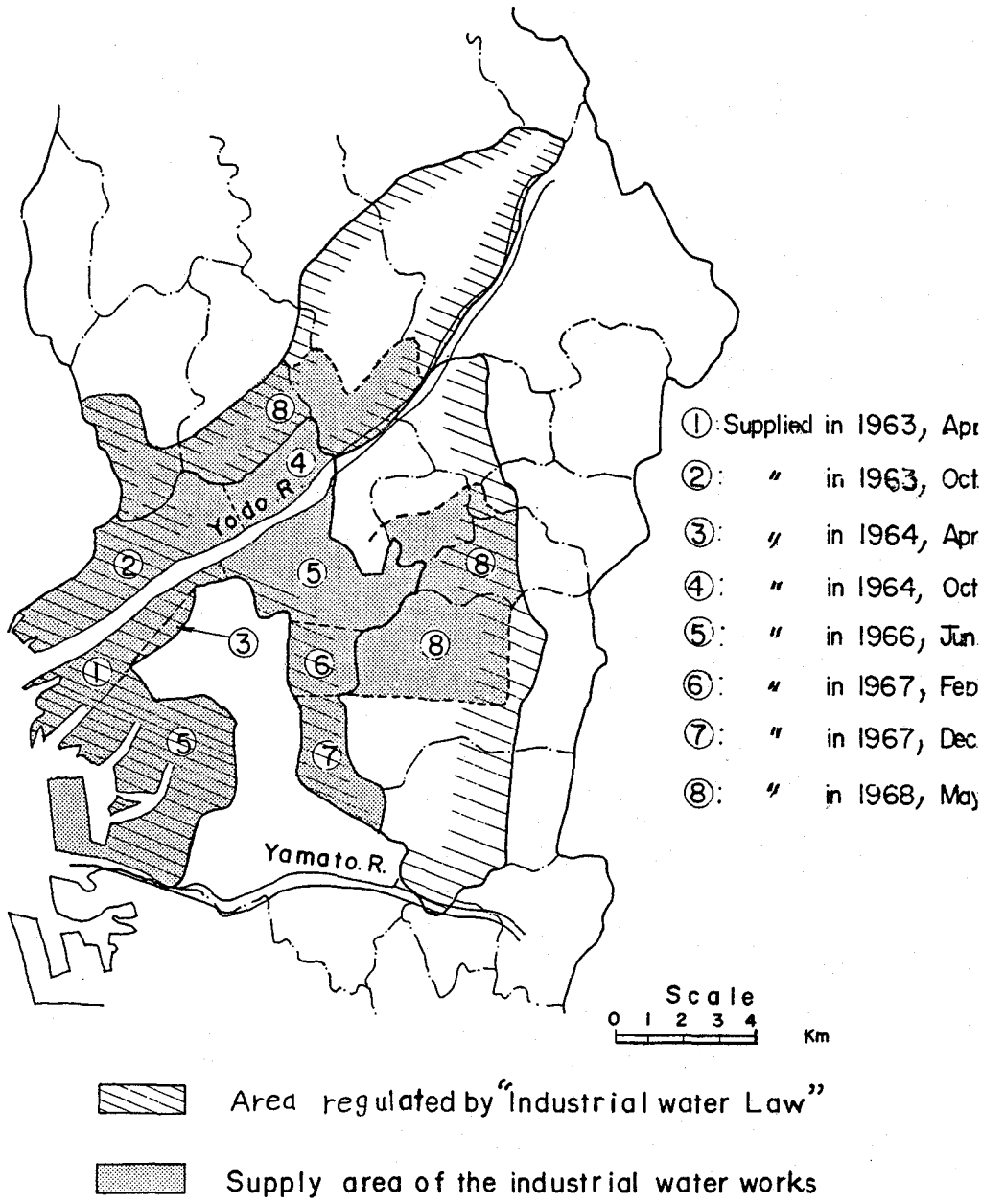

Figure 9.5.8 Supply area of industrial waterworks.

Case History No. 9.6. Nobi Plain, Japan, by Soki Yamamoto, Rissho University, Tokyo, Japan

9.6.1 TOPOGRAPHY AND GEOLOGY OF NOBI PLAIN

The Nobi Plain underlain by young sediments is situated in the central part of Japan and is about 1800 km^2 in area. This plain faces Ise Bay, where the Ibi, Nagara, Kiso, and Shonai rivers discharge, and is composed of alluvial fans, flood plains, deltaic plains, terraces, reclaimed lands, and filled-up ground (Figure 9.6.1).

The west-east profile of the southern part of this area is illustrated in Figure 9.6.2. The basement block in the Nobi Plain area bounded by the Yoro fault has tilted and is covered with sediments dipping westward. The depth of strata is about 2,000 m to the basement rocks.

The subsurface stratigraphy of these sediments in the plain has been explored on the basis of borehole material obtained from several thousands of water wells and test borings. The

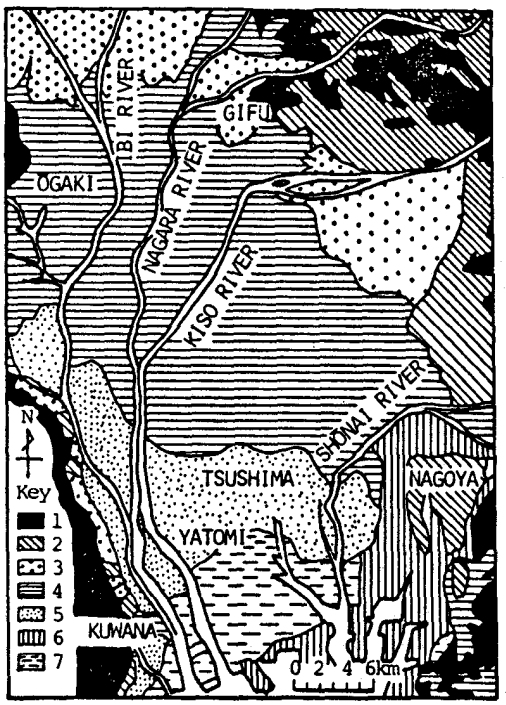

1. Mountain and Hill 2. Terrace
3. Alluvial Fan and Cone
4. Flood Plain 5. Deltaic Plain
6. Filled-up Ground
7. Reclaimed Land

Figure 9.6.1 Topographic features of the Nobi Plain.

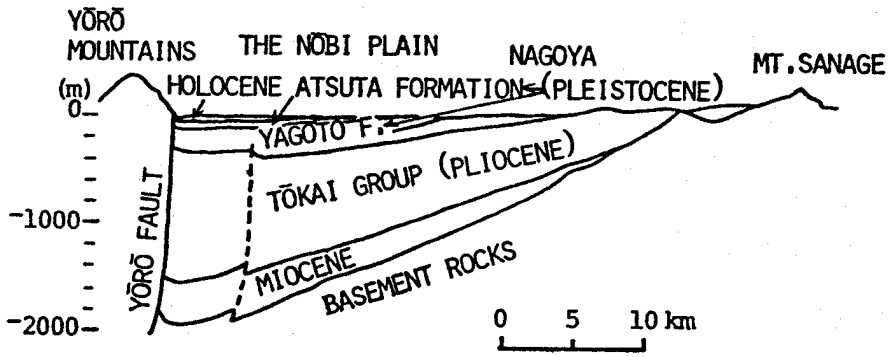

Figure 9.6.2 West-east profile of the Nobi plain.

Table 9.6.1 The Subsurface Stratigraphy in the Nobi Plain

		(Thickness)
HOLOCENE	NANYO FORMATION (H) (loose upper sand bed and very soft marine clay bed)	10-60 m
PLEISTOCENE	NOBI FORMATION (N) (alternation of sand and silt bed)	10-20 m
	DAICHI GRAVEL BED (G1)	10-30 m
	ATSUTA FORMATION (D3) (upper sand and clay beds and unconsolidated lower marine clay bed)	10-100 m
	DAINI GRAVEL BED (G2)	5-30 m
	AMA FORMATION GROUP (alternations of semiconsolidated sand, clay and gravel beds)	30-100 m
	PRE-AMA FORMATION GROUPS (alternations of semiconsolidated sand, clay and gravel beds)	30-70 m
PLIOCENE	TOKAI GROUP (alternations of semiconsolidated clay, sand and gravel beds)	200-1000 m
	M I O C E N E S E R I E S	
P R E - T E R T I A R Y B A S E M E N T R O C K S		

geological succession of these sediments is shown in Table 9.6.1, and a geologic cross section in Figure 9.6.3.

The middle Pleistocene and younger sediments are composed of an alternation of clay, sand and gravel beds. Changes in sedimentary environments and climatic fluctuations of these sediments have been studied by means of microfossil analyses of numerous core samples (Nobi Plain Quaternary Research Group, 1976).

Semiconsolidated fresh-water lacustrine clay beds and fluvial sand and gravel beds are interbedded in the lower horizon of the Pleistocene sediments, the so-called Pre-Ama Formation Groups. The Ama Formation Group and the younger sediments are composed of alternations of fluvial sand or gravel beds and unconsolidated marine clay beds, deposited under inner bay conditions. Each of these marine clay beds shows a sedimentary cycle from transgressive to regressive phase, and represents a relatively warm period, interglacial epoch or interstadial. In colder periods, the gravel beds have been deposited as either terrace or river-bed gravels

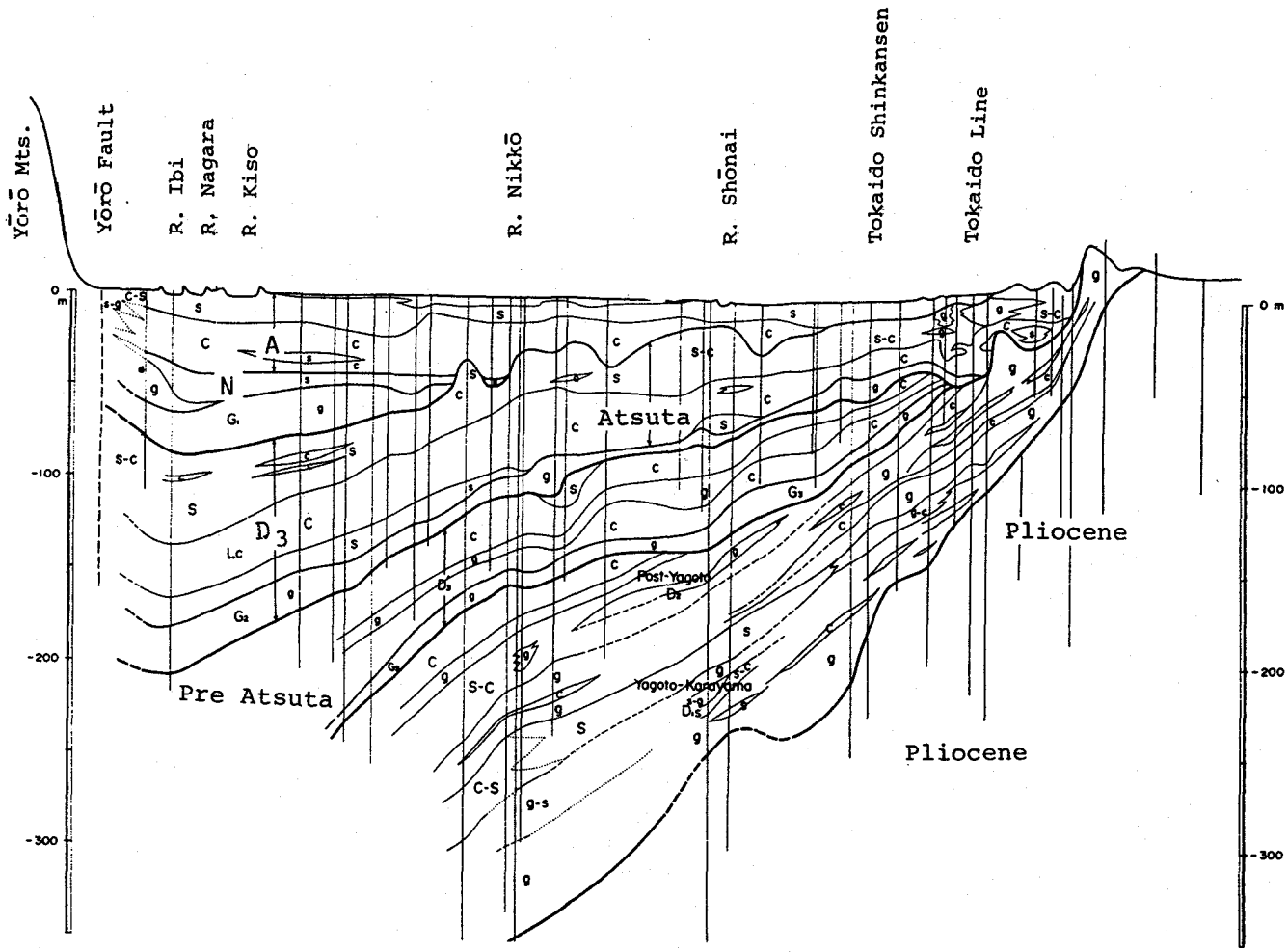

Figure 9.6.3 Geologic cross sectiopn of Nobi Plain.

in the valleys formed during the period of low sea level falling. The river-bed gravel deposited in the bottom of the valleys during a maximum stage of sea level falling reaches 20 m or more in thickness. The terrace gravel beds are generally thinner than the valley bottom gravel beds. These two types of gravel beds are distributed under almost the whole area of the Nobi Plain. Buried topography such as hills, terrace, and valleys formed in the process of sea-level lowering is depicted in the base contour map of these gravel beds. The buried topography and types of gravel beds affect ground-water yield in this plain. The marine clay beds overlying the gravel beds have attained more than 30 m in thickness in the valleys, and spread far and wide under the plain area except for the alluvial fan area, where the clay beds thin out and grade into sand or gravel beds (Figure 9.6.3).

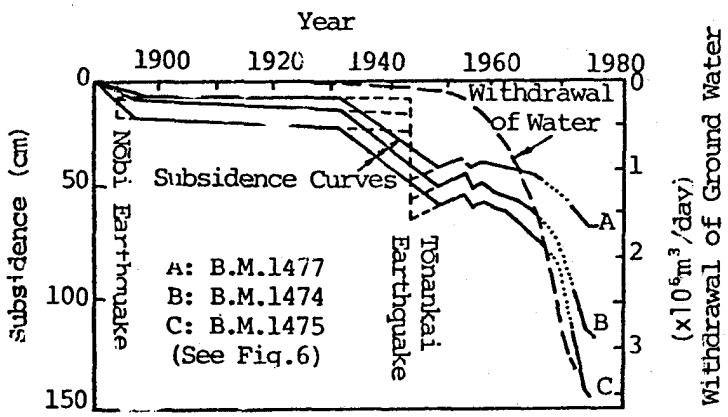

Figure 9.6.4 Subsidence of bench marks and withdrawal of ground water in the Nobi Plain.

Table 9.6.2 Withdrawal of ground water in the Nobi Plain.

Year	m^3/day
1925	1638
1945	129088
1950	154040
1955	360301
1960	849338
1965	1552764
1970	3002128
1973	3514195

9.6.2 HYDROLOGY

In the alluvial fan area, precipitation and surface water percolate downward through these permeable sand and gravel beds, and recharge ground water in the Nobi Plain. A superficial sand bed, the upper member of the Nanyo Formation, as much as 15 m thick, contains unconfined ground water which is recharged directly from precipitation and infiltration of irrigated water. The gravel beds, Gl, G2, and others interbedded in clay beds, are artesian aquifers and supply a large quantity of ground water. Before the pumping was largely developed, many flowing wells tapped these gravel beds in most of the Nobi Plain.

The increasing withdrawal of ground water in the Nobi Plain is shown in Tables 9.6.2 and 9.6.3. The use for industry amounts to 60 per cent of the total.

Recent annual withdrawals of ground water in the Nobi Plain equal 32 per cent of the annual rainfall on this plain. This volume is much larger than the natural recharge of ground water.

In the 1920's, the piezometric levels of confined aquifers were above the ground surface in most of this plain. In the 1940's, flowing wells were still observed in Ogaki, Kanie, and Kasugai districts. But since then, the piezometric levels have declined due to the increase in the number of artesian wells.

Table 9.6.3 Use of ground water for each purpose in the Nobi Plain (1973).

Item	Total	Industry	Buildings	Water Supply	Agriculture
Withdrawal of Ground Water (m^3/day)	3,802,293	2,290,015	343,025	477,028	692,225
Percentage	100	60	9	13	18

9.6.3 LAND SUBSIDENCE

The records of three bench marks depicted in Figure 9.6.4 show the evolution of land subsidence in this area. During the period from 1950 to 1973, the subsidence increased exponentially and some areas subsided more than 20 cm in 1973.

Figure 9.6.5 shows a comparison between the areas subsiding more than 2 cm/yr from Feb., 1961 to February, 1962, and from November, 1972 to November, 1973. This figure illustrates how the subsiding area in this plain enlarged from 1961 to 1973.

The subsidence of this plain during about 15 years from February, 1961 to November, 1975 is shown in Figure 9.6.6. The southern part of Nagashima facing the Ise Bay settled 147 cm during these 15 years. The total subsiding area is 1140 km^2 (Environment Agency, Japan, 1976). By 1973, 363 km^2 had become lower than the mean high-sea level (1.1 m higher than the mean sea level), 248 km^2 lower than the mean sea level, and 37 km^2 lower than the mean low-sea level (1. 4 m lower than the mean sea level). The area below mean sea level enlarged from 186 km^2 in 1961 to 248 km^2 in 1973.

Regulations for withdrawal of ground water in the Nobi Plain are as follows:

1. The Industrial Water Law (established in 1956)
   The areas designated by the Industrial Water Law are supplied with industrial water from surface sources instead of restriction on pumping of ground water. The regulations for these areas are shown in Table 9.6.4.

2. Regulations by Ordinance of Aichi Prefecture
   Aichi Regulation Zone I (enforced on 30 September 1974)
   This regulation zone was decided considering the rate of subsidence greater than 5 cm/year in 1972 and/or 1973. In this zone, a newly bored well must meet the following conditions;
   a. The depth of strainer should not be greater than 10 m.
   b. The inside area of discharge pipe should be less than 19 cm^2.
   c. The power of motor should be less than 2.2 kw.
   d. Total discharge should be less than 350 m^3/day.

   Concerning the wells that existed before the regulation, flow meters were installed in them and the discharge records are reported to the Prefectural office every year. Since the lst of January, 1976, the withdrawal of ground water from existing wells was restricted within 80 per cent of the discharge in the past (Figure 9.6.7).
   Aichi Regulation Zones II and III (enforced on 1 April 1976)
   The regulations for newly bored wells and existing wells are the same as those for Zone I, except that for the existing wells in Zone II, the withdrawal from the lst of April, 1977 is going to be restricted within 80 per cent of the discharge in the past, and for the existing wells in Zone III, the withdrawal in future is going to be restricted within the discharge in the past.

3. Regulations by Ordinance of Mie Prefecture (enforced on 1 April 1975)
   The regulations for newly bored wells and existing wells are the same as those explained for Aichi Regulation Zones II and III, where Mie

Table 9.6.4 Regulations for the Areas Designated by the Industrial Water Law

Area	Zone (See Fig. 9.6.7)	Allowed Depth of Strainer	Inside Area of Discharge Pipe
Southern Industrial Area of Nagoya designated in 1960	N_1	deeper than 80 m	less than 46 cm^2
		deeper than 300 m	greater than 46 cm^2
	N_2	deeper than 90 m	less than 46 cm^2
		deeper than 180 m	greater than 46 cm^2
Industrial Area of Yokkaichi designated in 1957 and 1963	Y_1	deeper than 100 m	less than 21 cm^2
		deeper than 230 m	from 21 cm^2 to 46 cm^2
	Y_2	deeper than 50 m	less than 21 cm^2
		deeper than 150 m	from 21 cm^2 to 46 cm^2

Table 9.6.5 Dealing with existing wells in the case where the strainers are deeper than 10 m in Nagoya

Zone	Wells for Buildings	Wells for Industry
I	Changed to use city water since 16 Nov. 1975	Change to the industrial water supply as soon as possible
II	Changed to use city water since 16 Nov. 1976	
III	Increasing withdrawal is forbidden	

Regulation Zones I and II correspond to Aichi Regulation Zones II and III, respectively.

4. Regulation by Ordinance of Nagoya City (enforced on 16 November 1974) According to the ordinance of Nagoya City, a new well can be allowed only in the case where the strainer is not deeper than 10 m and the inside area of discharge pipe is less than 19 cm^2. Existing deep wells are being treated as shown in Table 9.6.5. The regulation zones of Nagoya City are overlapped by the regulation zones of Aichi Prefecture. Therefore, the withdrawal of ground water in Nagoya is controlled by ordinances of Nagoya City and Aichi Prefecture.

Figure 9.6.8 shows the subsidence of Nagashima during the recent ten years and piezometric levels of the lst confined aquifer (G_l) and the 2nd confined aquifer (G_2) measured at Matsunaka observation well during the recent five years. The confined aquifers G_1 and G_2 are located at depths between 40 m to 60 m and 100 m to 115 m respectively at the observation site. Concerning the piezometric levels, seasonal changes are superposed on total trends of ground water levels. The seasonal drops of piezometric levels are caused by the increase of pumpage for cooling and

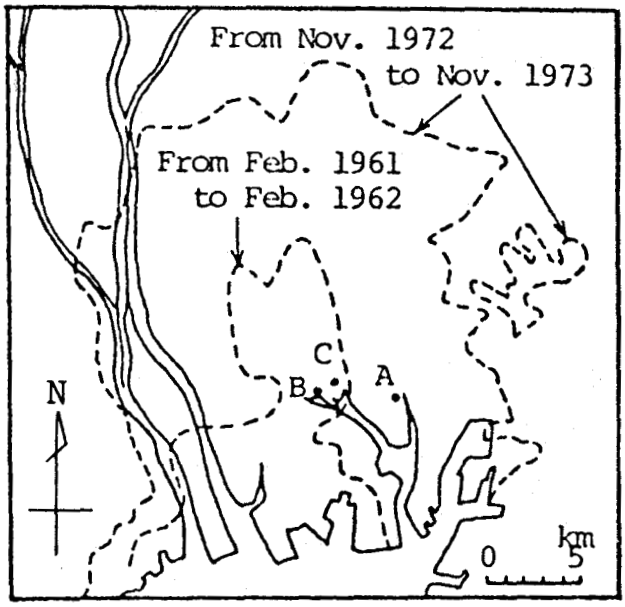

Figure 9.6.5 Enlargement of the area subsiding more than 2 cm/yr.

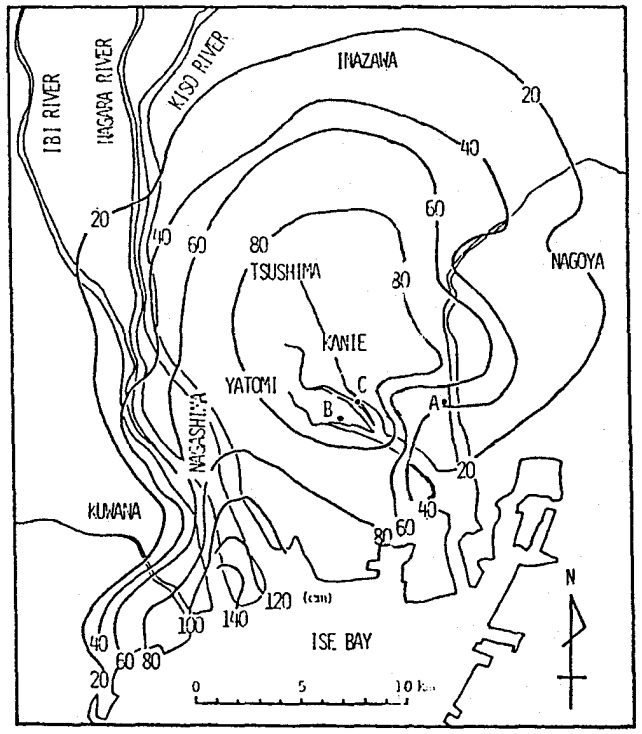

Figure 9.6.6 Subsidence for 15 years from February 1961 to November 1975 in the Nobi Plain.

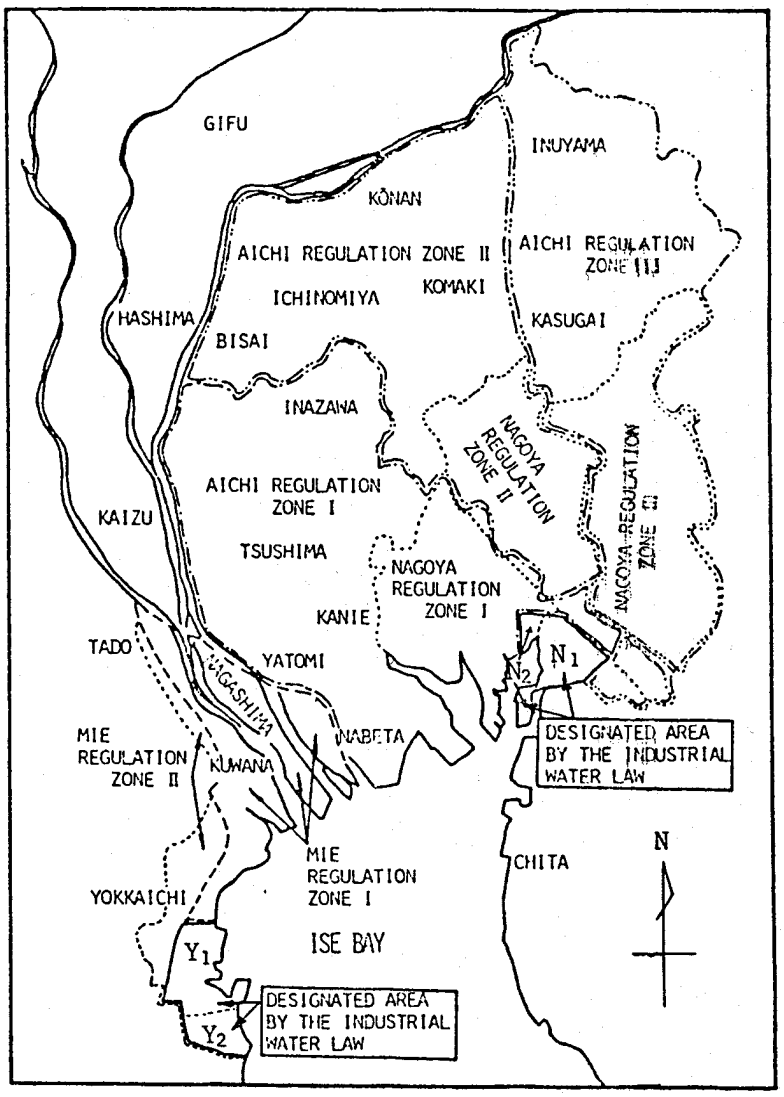

Figure 9.6.7 Restriction of withdrawal of ground water in the Nobi Plain.

irrigation in summer. The piezometric level of the deeper confined aquifer is lower than the one of the shallower confined aquifer, because ground water of better quality is pumped up in plenty from the deep aquifer.

The piezometric levels of aquifers show, recovering trends since 1974. Reflecting this favorable turn in the ground water situation, the subsiding area became smaller and the rate of subsidence decreased.

Moreover, several rebounding areas appeared around the area having reduced subsidence. (See Figure 9.6.9.)

9.6.4 PARAMETERS

The compression index C_c varies vertically and horizontally in clay layers and the values are closely related to the sedimentary facies. The value is the largest in the middle horizon of finer materials. Lateral distribution of the mean C_c value calculated by averaging vertical

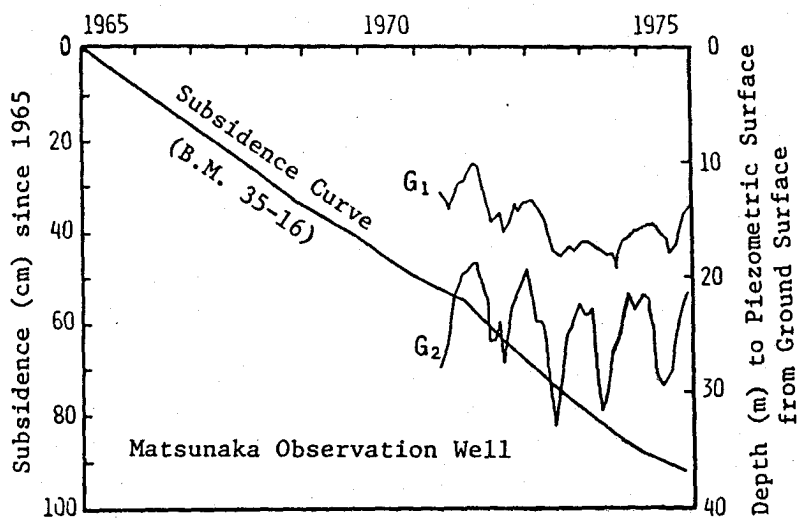

Figure 9.6.8 Subsidence and ground water conditions at Nagashima during recent years.

variations reflects the sedimentary environment of the clay bed. It varies from 0.3 to 0.8 from the margin of this plain to the central area. There is a good correlation between e_o and C_c which can be expressed as follows:

$$C_c = 0.5\ (e_o - 0.5)$$

where e_o is the natural void ratio of clay.

9.6.5 SELECTED REFERENCES

IIDA, K., SAZANAMI, T., KUWAHARA, T., and K. UESHITA. 1977. Subsidence of the Nobi Plain, IAHS Pub. No. 121, p. 47-54.

KUWAHARA, T., UESHITA, K., and K. IIDA. 1977. Analysis of land subsidence in the Nobi Plain, IAHS Pub. No. 121, p. 55-64.

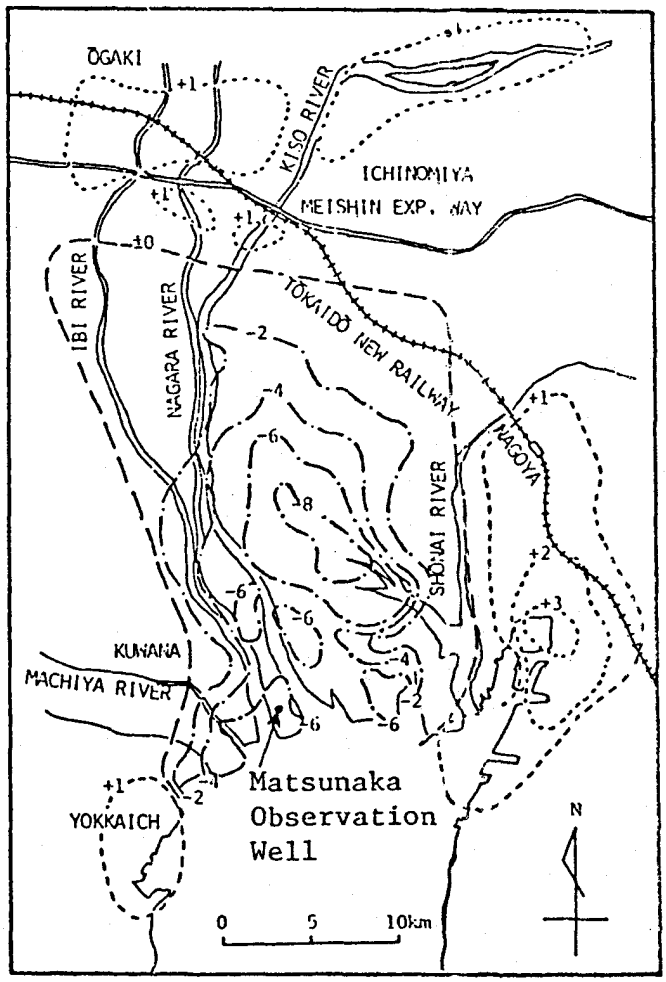

Figure 9.6.9 Subsidence and rebound of the Nobi Plain from November 1974 to November 1975 (unit: cm/yr).

Case History No. 9.7. Niigata, Japan, by Soki Yamamoto, Rissho University, Tokyo, Japan

9.7.1 TOPOGRAPHY AND GEOLOGY

Niigata Plain is the largest coastal plain along the Japan seacoast. It is bounded on the east by mountains, on the south and west by hills and on the north by the Japan Sea, with coastal sand dunes. Through the center of this plain the R. Shinano, the R. Agano and their branches flow down from south to north into the Japan Sea. Along these rivers, especially on down reaches, there are many back marshes, swamps, and lakes (Figure 9.7.1.).

This area is a typical synclinal basin with deposits of Cenozoic age underlain by a basement complex (Figure 9.7.2.). The subsurface geology of this area consists of Holocene, Pleistocene and Neocene deposits. The stratigraphic correlation is as shown in Table 9.7.1.

9.7.2 HYDROLOGY

It had been well known that there was abundant methane gas in this area. The major gas reservoirs in the Niigata gas field belong to the Uonuma Group of Pleistocene age which is characterized by the alternation of clay, sand and gravel beds. Gas reservoirs, i.e., confined aquifers consisting of sand and gravel, are filled with brackish to saline water.

Large quantities of saline ground water containing dissolved gas are pumped up from wells as much as 1000 metres deep, tapping relatively unconsolidated segments of the G_l, G_2,....G_7 layers of Cenozoic age (Figure 9.7.3.). Shallow aquifer G_1 is exploited for domestic use, but the others are exploited for industrial uses (Figures 9.7.4. and 9.7.5.). About 200 million cubic metres of methane was produced in 1958, 60 per cent of the methane gas production in Japan.

The producing wells increased rapidly to 1959 near the mouth of the R. Shinano along the coast of the Japan Sea. With increase of the amount of ground-water withdrawal from gas wells, the rapid lowering of the groundwater level was recognized. The permeability of the gas reservoirs varies from 50 to 200 millidarcys.

9.7.3 SUBSIDENCE

Although no attention had been paid, about 1930 the land subsidence in Niigata was indicated by geologists as "Pseudo-sinking" of sea coast. Subsidence of the Niigata area, especially the harbor district, became noticeable by 1955 (Figure 9.7.6.). Most of the harbor area which initially was only 1-2 m above mean sea level had been damaged by inundation from the sea.

The results of first-order leveling over this area were reexamined and extraordinary subsidence was recognized. Another area of surface subsidence had occurred in the inland part of the Niigata Plain, in the southern part of Niigata city. In 1959, the center of the subsidence was located near Shirone town, and the subsidence rate was about 14 cm in ten months. Based on the data of compaction meters, it was concluded that the compaction was located in the zone shallower than 120 m depth, which is correlated with the Holocene and younger Pleistocene deposits. As shown in Figure 9.7.7, about 10,000 wells producing natural gas for domestic use are located in this area. The amount of the ground-water withdrawal from these wells in 1960 was estimated to be approximately 60,000 m^3/day.

First-order level surveys have been made in Niigata and its vicinity by the Japan Geographical Survey Institute in 1898, 1930, 1951, 1955 and 1957, and leveling has been conducted at 6-month intervals since 1957. (See Figure 2.2.) The subsidence of 20 cm at the harbor mouth in 6 months indicates an annual rate of 40 cm. By 1959, the annual rate had increased to 54 cm a year.

Long-term graphs of elevation change for five bench marks which are representative of the subsidence trend are shown in Figure 9.7.8. They show a slow subsidence of about one half a centimetre per year from 1898 to 1952 and a rapid acceleration since 1955. The cause of the slow

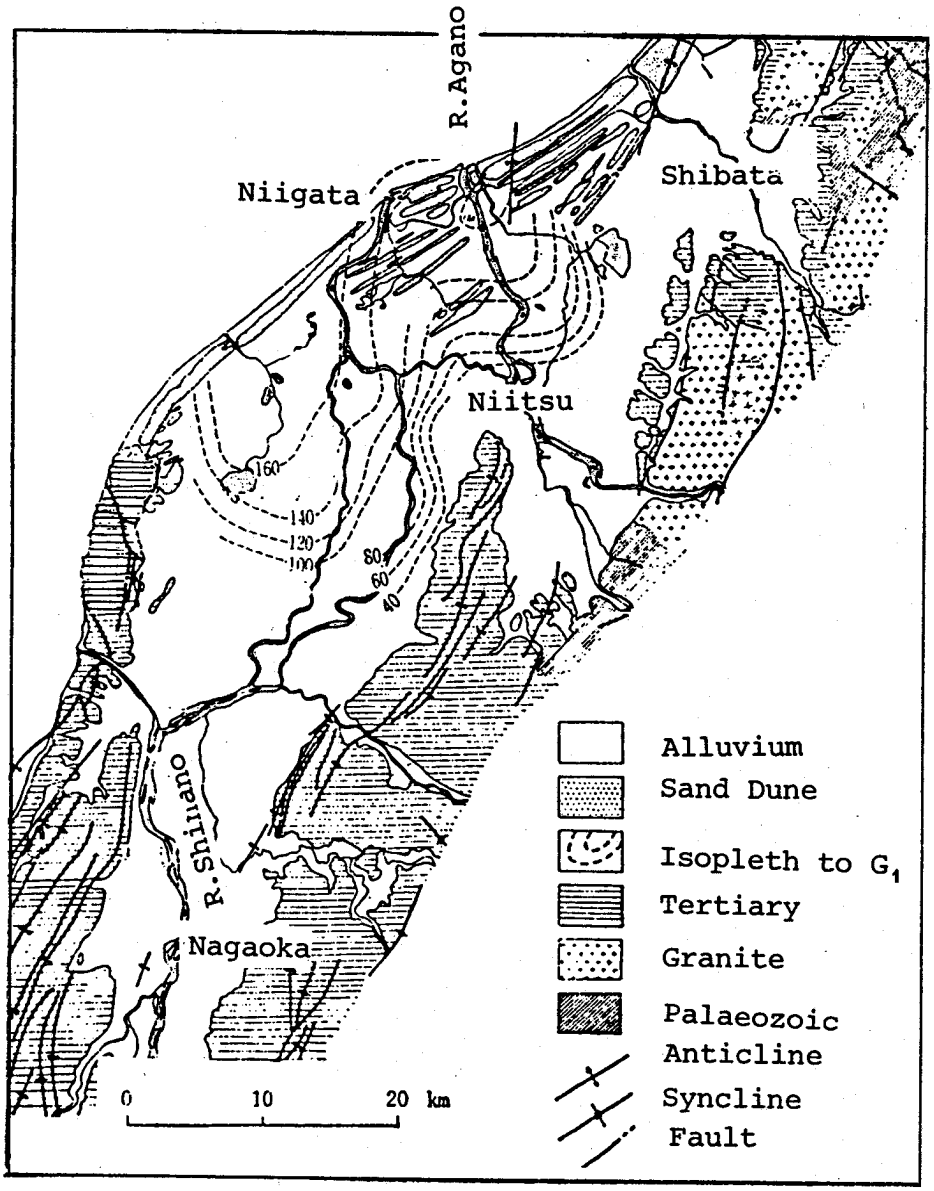

Figure 9.7.1 Physiographic map of Niigata area.

subsidence prior to 1952 has not been explained. Natural gas production, shown in Figures 9.7.4 and 9.7.5, began about 1947 and increased rapidly in the fifties. The volume of gas-bearing water pumped reportedly has been about equal to the volume of gas recovered. Because of the coincidence in time and place of the increase in rate of subsidence and of fluid withdrawal, we concluded that the cause of the accelerated subsidence is the withdrawal of the water and gas. This withdrawal has decreased the fluid pressure in the gas-bearing zones and has caused the compaction of sediments.

The rate and distribution of compaction in depth is being observed by means of 12 novel compaction recording wells, installed in 1958-1959, and ranging in depth from 20 to 1190 m. When the results obtained from these observation wells were analyzed, they showed a remarkable contraction of the layer from 380 to 610 m depth. The subsiding area of Niigata districts is about 430 km^2.

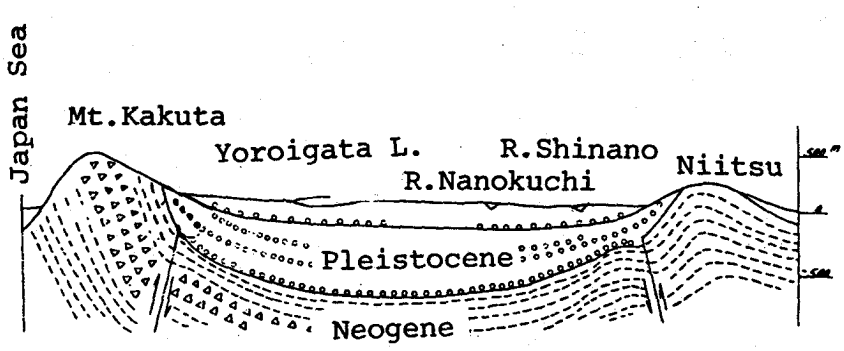

Figure 9.7.2 Diagrammatic cross section of Niigata.

9.7.4 PARAMETERS

M_V	$1x10^{-2}$	-	$5x10^{-2}$	CM^2/kg
C_V	$1x10^{-1}$	-	$1x10^{0}$	$CM^2/min.$

9.7.5 LEGAL ASPECTS AND COUNTERMEASURES

Since 1960, control of ground-water withdrawal has been undertaken by putting area "A" completely under the ban of gas production (Figure 9.7.9). They also established area "B," where extraction of gas from shallower reservoirs than G_6 is prohibited, and "C," where gas production is permitted within the limit of the past production record. Over all this area, new drilling is prohibited.

Besides legal restrictions, hydrogeologists had carried on experiments of water injection into gas reservoirs since 1966 or so. The injectivity index is usually less than a quarter of the productivity index. After 1965, the gas company started to inject saline water into four reservoirs (G_{4-1}, G_5, G_{5-1}, G_6). The change of ground-water level and compaction of these layers has been observed in this area (Figures 9.7.10, 9.7.11, 9.7.12, and 9.7.13). Since 1973, all the pumped water, about 110,000 cubic metres per day, after gas separation, has been injected into the gas reservoirs through injection wells, with no surface drainage.

The total estimated cost of countermeasures over the whole Niigata area is difficult to estimate but the direct cost is estimated as $12 million for the period 1957 to 1974.

9.7.6 SELECTED REFERENCES

AOKI, S. 1977. Land subsidence in Niigata. IAHS Pub. No. 121, p. 629-634.

HOKURIKU AGRICULTURAL BUREAU. 1965. Land subsidence of agricultural land in Niigata, pp. 1-485.

ISHIWADA, Y. 1969. Experiments on water injection in the Niigata gas field. IASH Pub. No. 88, pp. 629-634.

Table 9.7.1 Geological correlation and gas reservoir.

Age	Division	Lithology	Thickness
HOLOCENE	I	Silt & clay alternation	120 - 160 m
	II	Silty clay	
	III	Silt, clay and sand	
	IV	Peat, clay & sand alternation	
	V	Clay-silt, Gravel, sand and silt G_1	
PLEISTOCENE (Uonuma - Kanbara)	upper	G_2 Sand & gravel G_3	310 - 660 m
	middle	G_4 Mudstone,Conglomerate and sandstone	
	lower	G_{4-1} Mudstone G_5 sandstone & conglomerate	
NEOGENE	Hai zume	G_{5-1} Conglomerate G_{5-2} Conglomerate G_6 Conglomerate	500 - 700 m
	Nishiyama	G_7 Sandstone G_8 Sand & gravel	

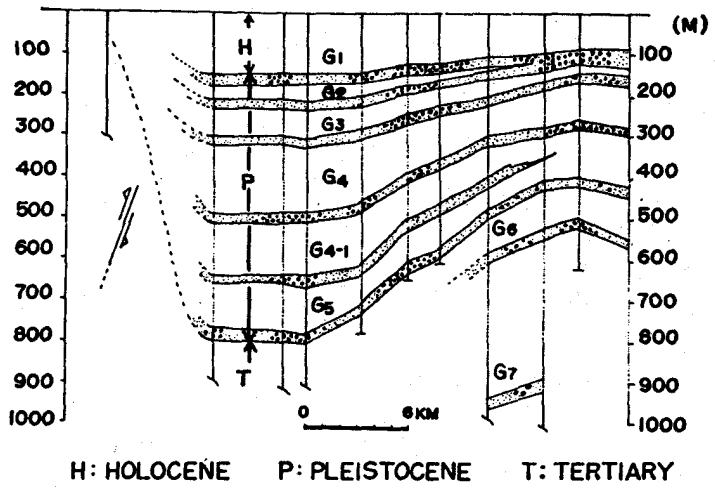

Figure 9.7.3 Geologic profile.

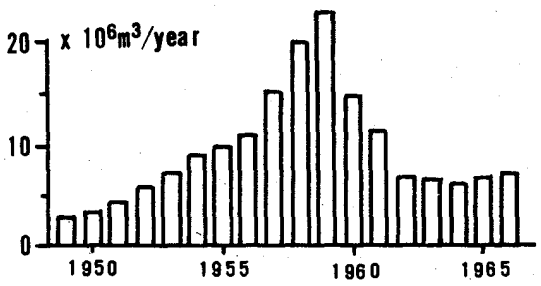

Figure 9.7.4 Annual amount of withdrawal of gas water for industrial use.

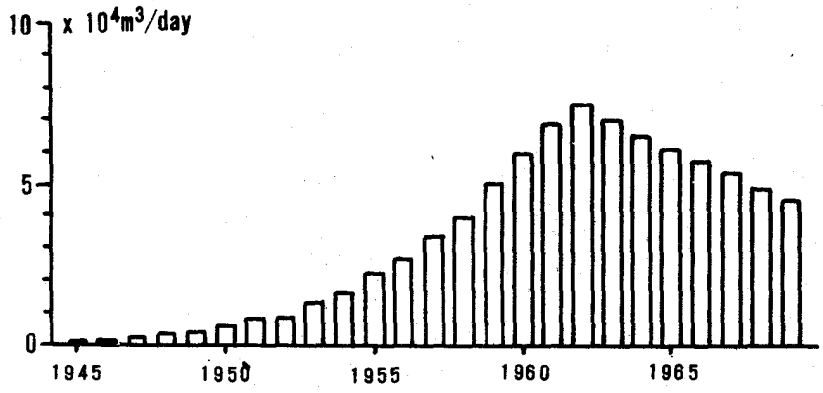

Figure 9.7.5 Daily amount of withdrawal of gas water for domestic use.

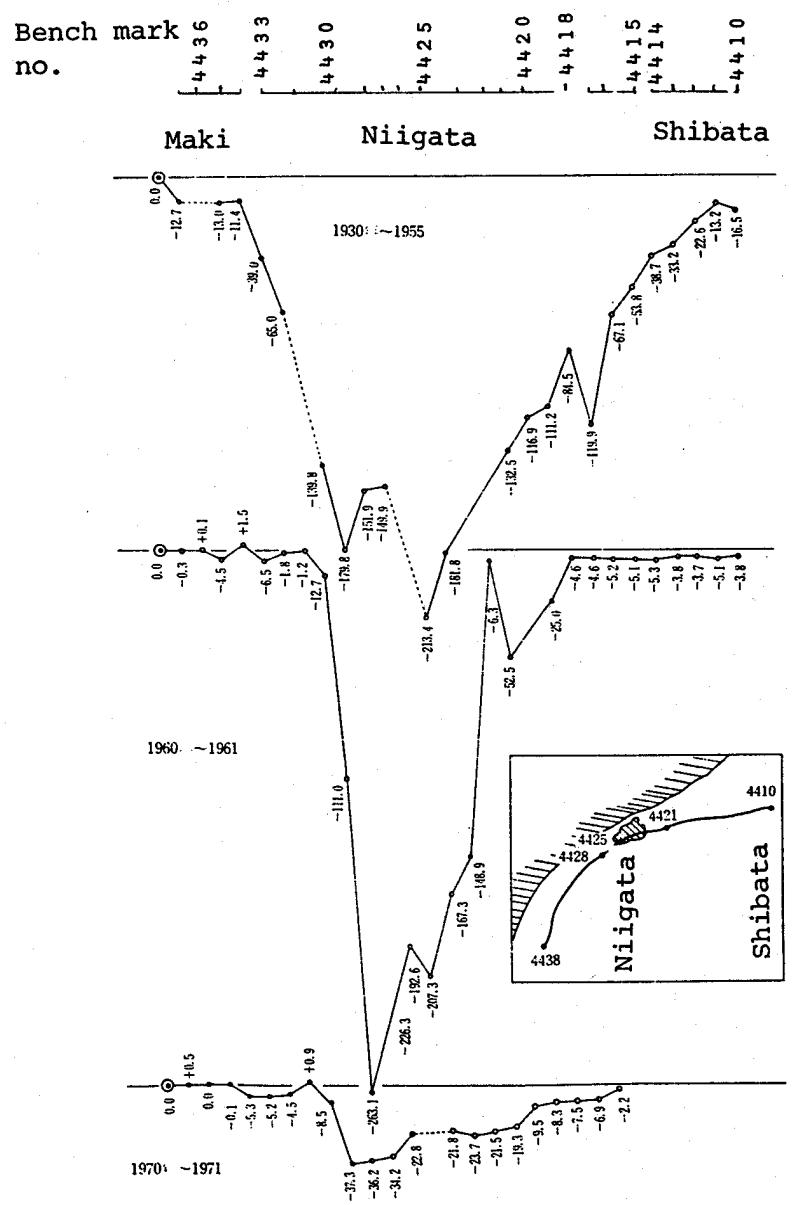

Figure 9.7.6 Subsidence of bench marks on selected points in Niigata and vicinity, in millimetres.

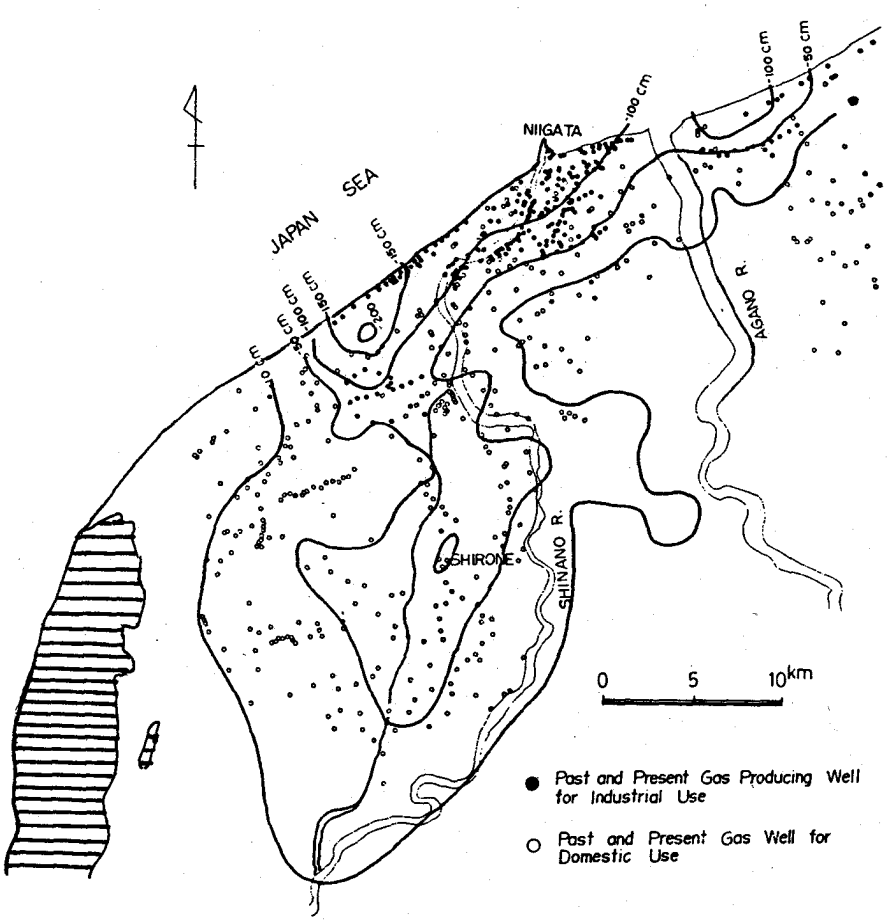

Figure 9.7.7 Distribution of gas wells and total amount of land subsidence during the period 1959-74.

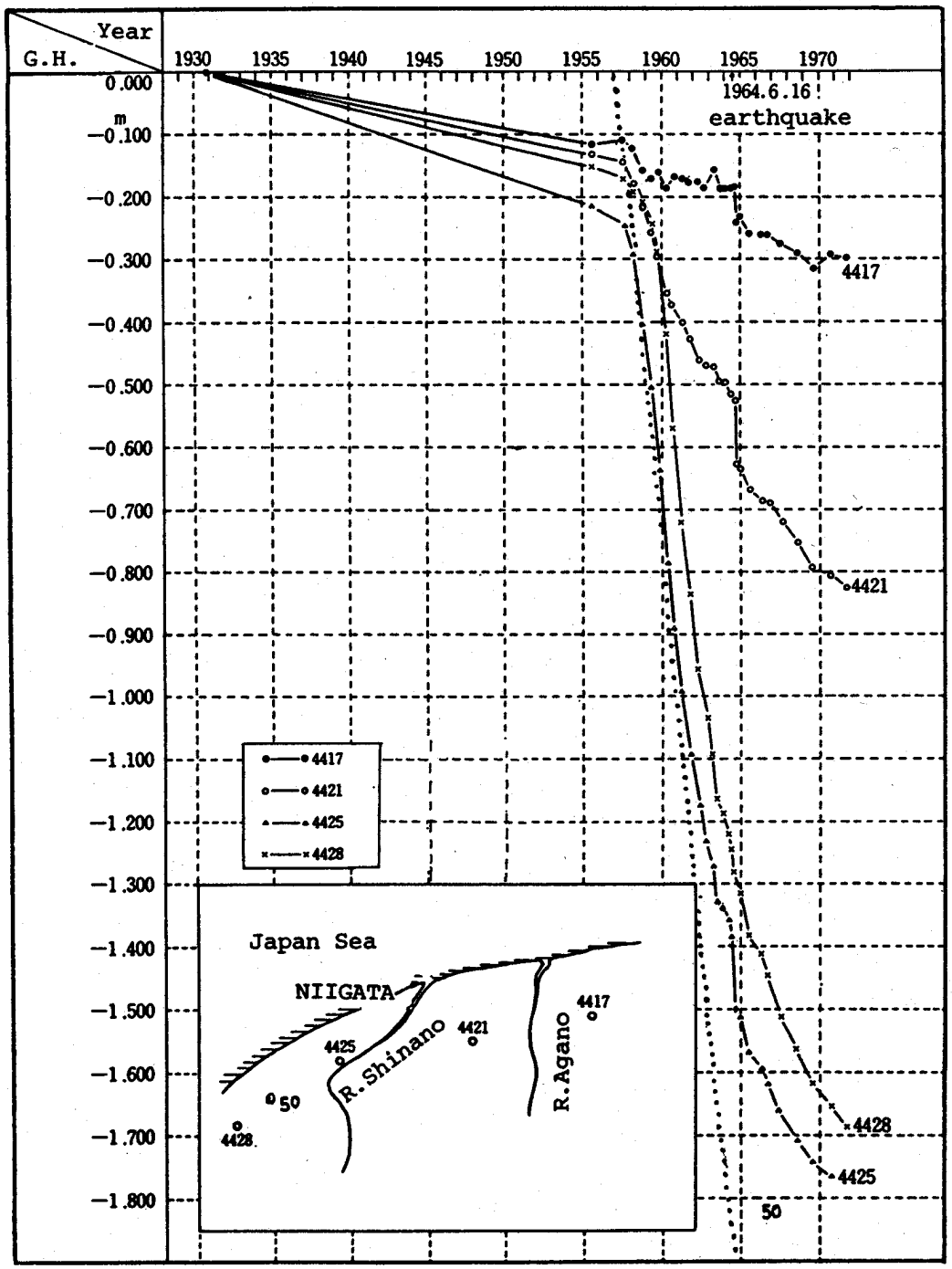

Figure 9.7.8 Change of ground height in Niigata (m).

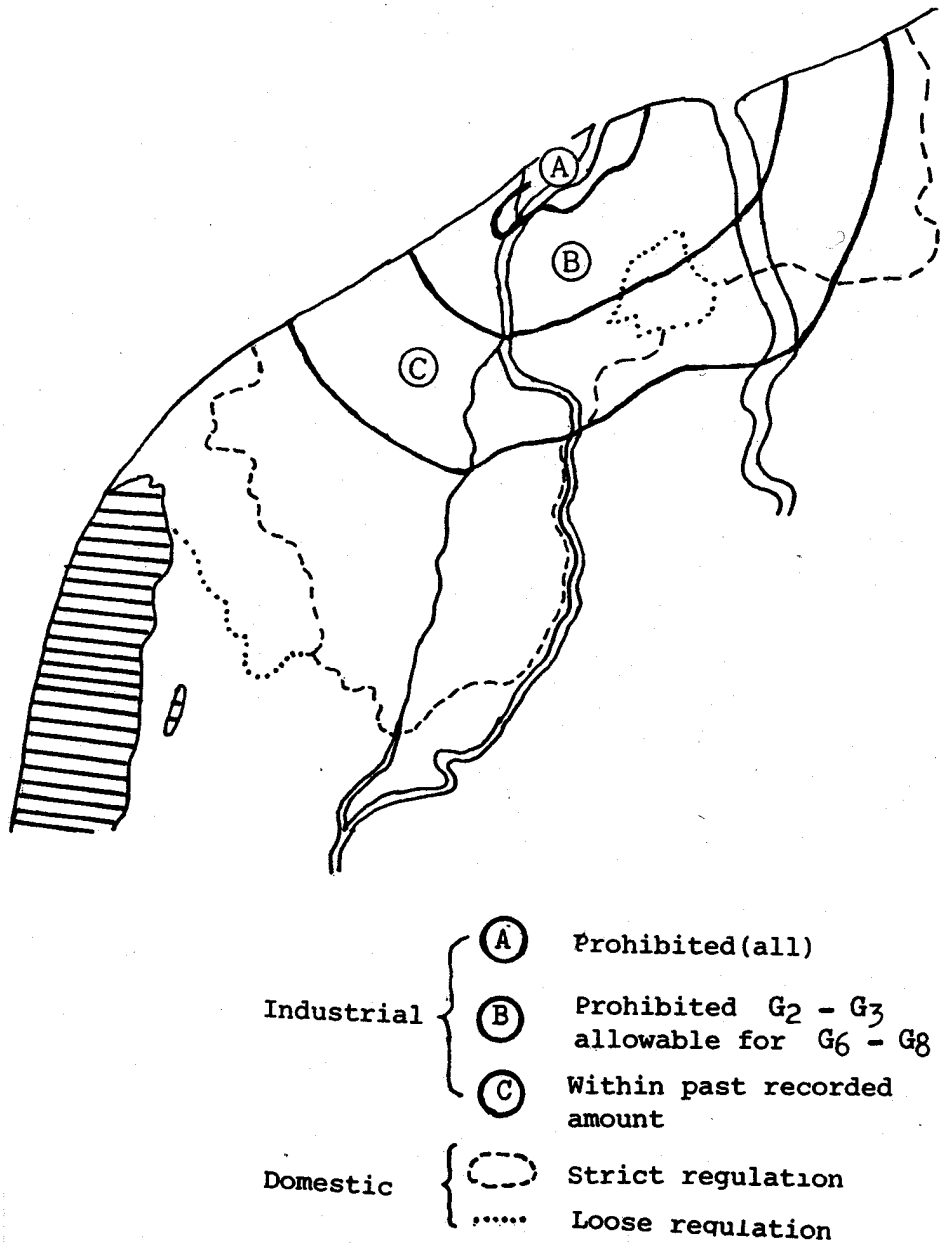

Figure 9.7.9 Regulation by law in Niigata area.

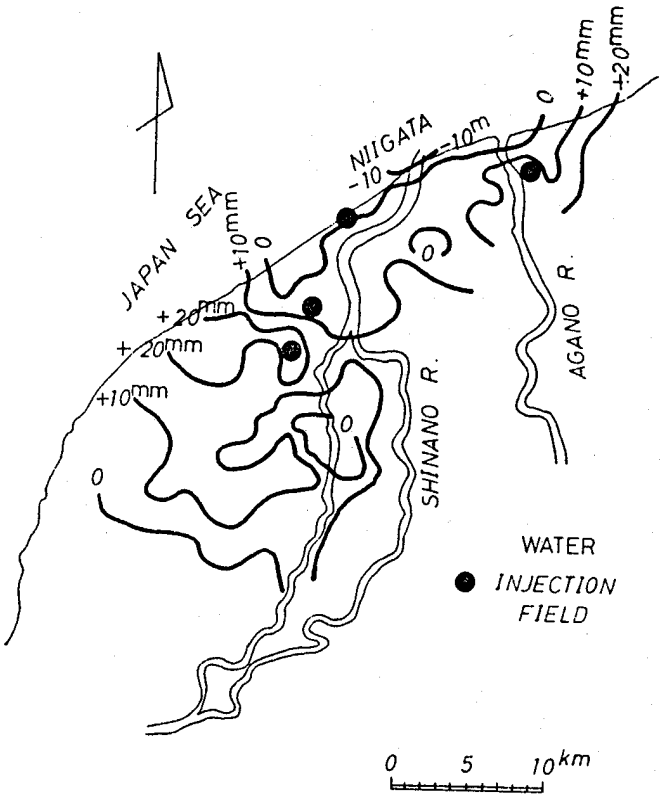

Figure 9.7.10 Land subsidence during 1973-74.

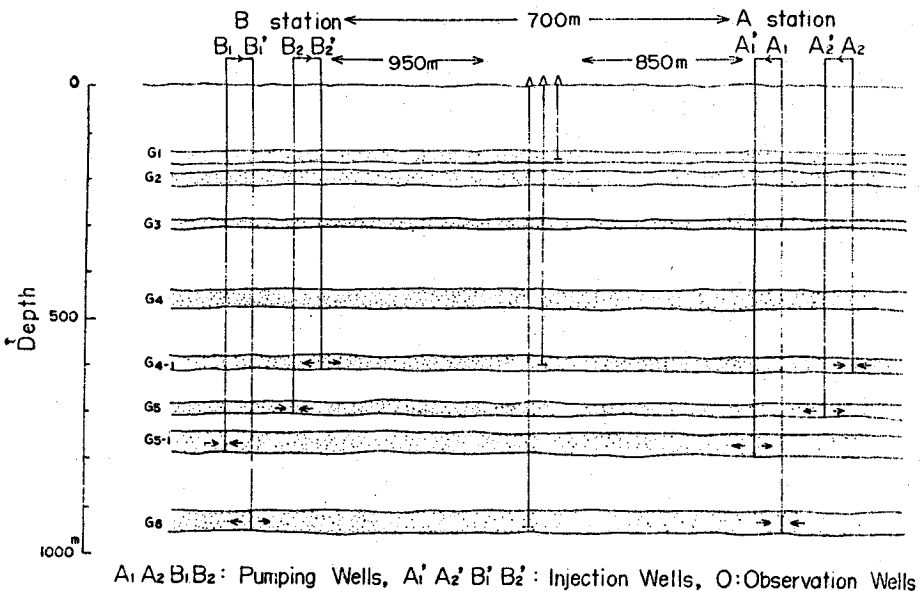

Figure 9.7.11 Profile of water injection experimental station (at Kurosaki).

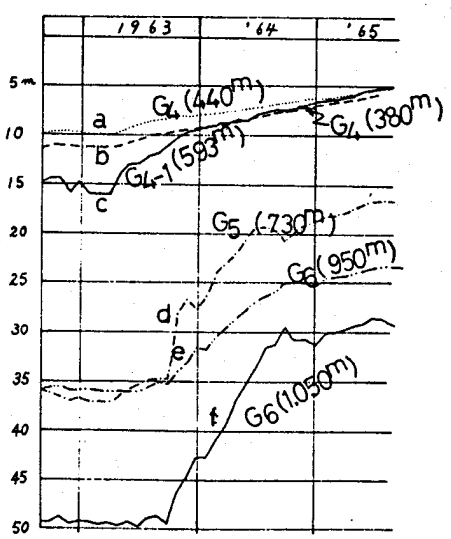

Figure 9.7.12 Change in ground-water levels at observation wells (Kurosaki).

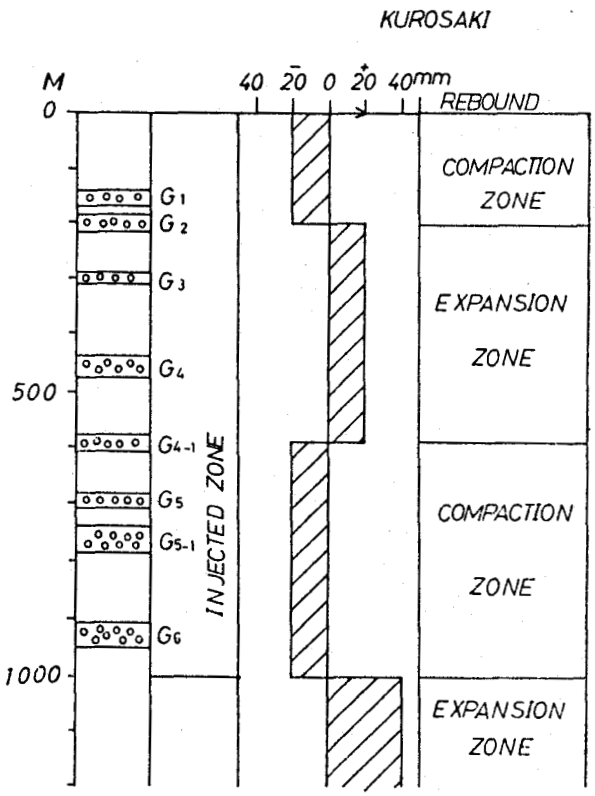

Figure 9.7.13 Columnar section showing the position of expansion and compaction layers at Kurosaki.

Case History No. 9.8. Mexico., D. F., Mexico, by Germán E. Figueroa Vega, Comisión de Aguas del Valle de México, Mexico, D., F.

9.8.1 GEOLOGY

Mexico City is located in the southwestern portion of the Valley of Mexico. The general geological features of the zone are shown in Figure 9.8.1. in which it may be seen that the most ancient outcrops, in the upper part of the western and northern ranges of the zone, are andesitic and dacitic formations of the middle Tertiary, overlain on their slopes by volcanic and alluvial formations of the upper Tertiary and Quaternary (Comisión Hydrológica de la Cuenca del Valle de México, 1961b).

The southern range is almost completely covered by Quaternary basaltic emissions and the flatter portion of the city is constituted by Quaternary lacustrine clays. These clays overlie Quaternary clastics that constitute the aquifer whose overdraft has caused the subsidence. The definition of the symbols which appear in Figure 9.8.1. is given in Table 9.8.1.

The clayey formation has a variable thickness from 0 to 50 m. with some intercalations of fine sands and silts, void ratios up to 15 and water contents up to 650 per cent. As a consequence, its shearing strength is very low and its compressibility very high.

The aquifer contains thick strata of gravel and sand of good permeability. Wells are generally of high yield (180 to 360 m^3/hr or more) with specific capacities ranging between 18 and 36 m^3/hr/m and more.

The mechanical properties of Mexico city clays, especially their low shearing strength, make it necessary to carry out special soil mechanics studies practically in all types of foundations.

In general, foundations by continuous slabs are possible only in buildings with no more than 4 or 5 stories. in any building higher than this, it is necessary to resort to the use of compensated foundations which present difficulties due to stability problems in slopes and in bottoms of excavations. An easier alternative is the use of friction or point piles. In this way it has been possible to construct buildings up to 42 stories high.

Because of similar problems in the construction of sewage tunnels and their shafts, it has been necessary to use shields and compressed air and, in some cases, very special construction methods.

The Mexico City clays have been studied from a mineralogical standpoint by nuclear spectrography, electronic microscopy, and interchange of cations and thermic differential analysis to determine their composition. Their approximate composition is 80 per cent montmorillonite and 15 per cent kaolinite, with some beidellite, illite, and halloysite. The clayey materials are mixed with 2 to 20 per cent of the total weight of solids (mixtures of sands and fossils) to which some investigators attribute the elastic properties of clays (Marsal and Mazari, 1959).

9.8.2 HYDROLOGY

The portion of the valley which contains the City of Mexico has an area of approximately 958 km^2. The annual precipitation ranges from 60 mm in the lower zone to 1300 mm in the higher zone, with an average on the order of 890 mm per year.

The potential evaporation ranges between 1900 mm per year for the lower zone and 900 mm for the higher zone, with an average of the order of 1300 mm.

The mean runoff of the period 1948-60, within the 958 km^2, including the urban area of the city, was 20.5 per cent and in the nonurbanized area (238 km^2), 14.6 per cent (Comisión Hydrológica de la Cuenca del Valle de México, 1963).

Figure 9.8.2, which shows a north-south stratigraphic profile of the city, and Figure 9.8.3, which shows an east-west stratigraphic profile (Marsal and Mazari, 1959), allow us to appreciate that the permeable outcrops are in the slopes of the mountains. This is why those zones are the main recharge areas of the aquifer under exploitation. In spite of this, infiltration may occur in the clayey zone as happens in the northern part of the city which has

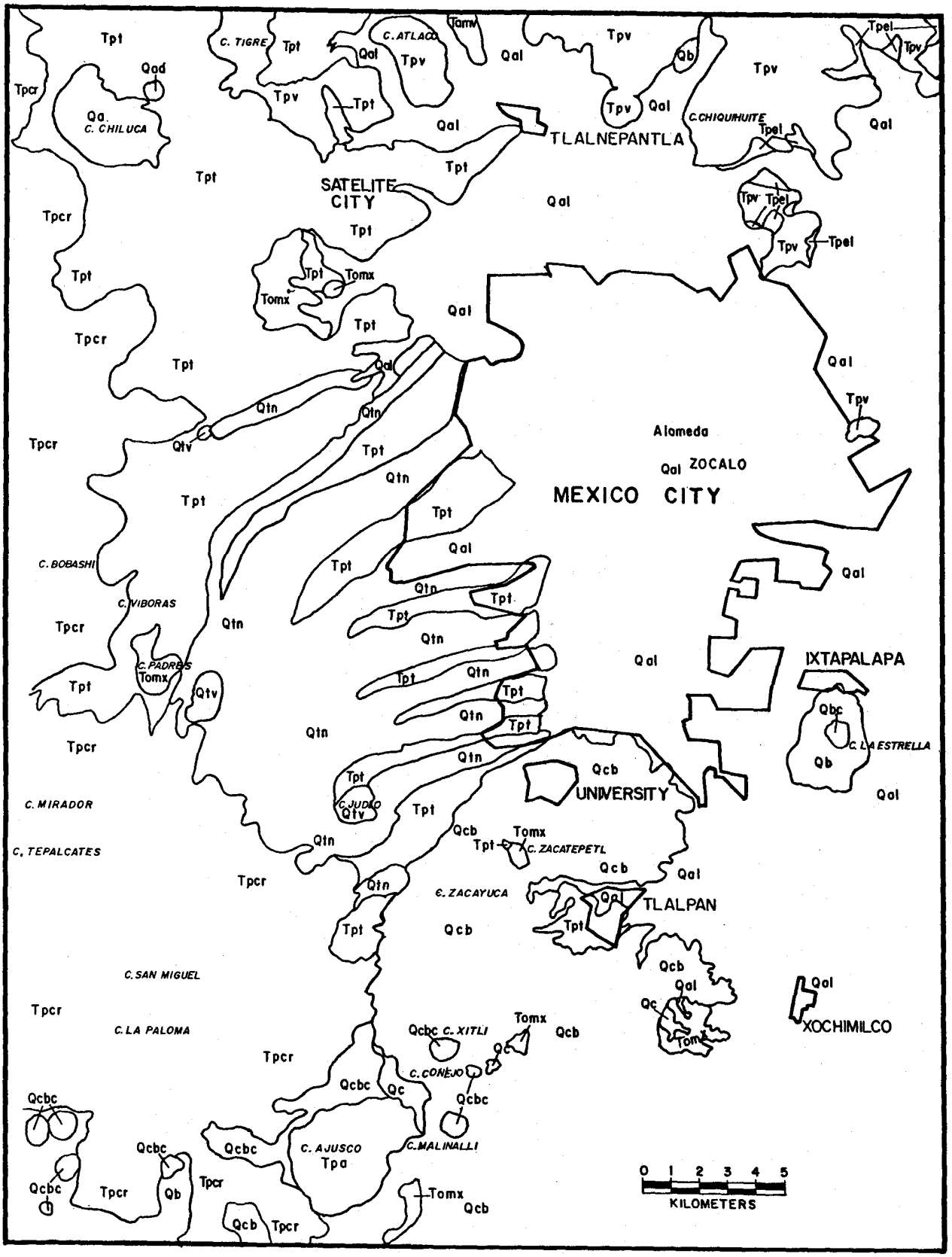

Figure 9.8.1 Geologic map (after Comisión Hydrológica de la Cuenca del Valle de México, 1961).

Table 9.8.1 Geological symbols and units.

Qal	Alluvials, lacustrine and clastic deposits	
Qb	Interstratification of lavas and tuffs	
Qbc	Ash cones	Quaternary basalt-andesite
Qad	Andesite lava domes	volcanic series
Qa	Andesite lava	
Qcb	Interstratification of lavas and basalt tuffs	Quaternary Chichinautzin
Qcbc	Ash cones	volcanic series
Qtn	Nuees ardents, peleans, lahars,	
Qtv	Fluvial conglomerates, pumice horizons, soils and tuffs	Quaternary Upper Tarango formation
Tpt	Nuees ardents of ashlar stone type, pumice horizons, soils and tuffs	Tertiary Lower Tarango
Tpel	Eluvial deposits	formation
TpV	Undifferentiated volcanic rocks Tepozotlan range andesite. Guadalupe range dacites. Range deposits.	Tertiary volcanic rocks
Tpa	Ajusco andesite	
Tpcr	Andesite series of the Cruces range.	
Tomx	Undifferentiated volcanic series of the Xonchitepec range.	

a similar stratigraphy. Here there is a solar evaporator for the industrial exploitation of brines. Water remains all year on the surface and it has been determined by careful balances that the yearly infiltration loss is 20 cm. As it is estimated that in the city the fresh water loss in the net leakage is almost 30 per cent, there may be a local infiltration on the order of 2 m^3/s or more.

It is rather difficult to estimate the historical development of local pumpage because, even now, no flow measurements are made in most of the wells.

Taking into consideration the existent fractional information and the reported population at different dates, it has been estimated that the extraction, which began around 1850, is presently on the order of 12 m^3/s. The approximate development is shown in Table 9.8.2 (Figueroa Vega, 1973a and 1977).

In regard to deep piezometric developments, there are similar problems, since their detailed measurement has been made only during the last 10 years. Notwithstanding, from existent data in the Well Register it has been possible to reconstruct partially the evolution as shown in Figures 9.8.4 and 9.8.5. Evolutions prior to 1948 may be estimated only by the fact that, according to old local drillers, many wells within the Lake zone of the city were still flowing wells at the beginning of this century. The water table has remained nearly constant 1 to 2 m below the land surface throughout the period of ground-water development.

9.8.3 LAND SUBSIDENCE

The subsidence of Mexico City is one of the most remarkable cases in all the world.

The phenomenon, which began during the past century, was discovered casually as a result of a polemic about the subsidence of the gates of San Lazaro, at the beginning of the main sewage channel of the city.

In February 1925, Roberto Gayol, author of the project of the sewage net of the city and director of its construction, demonstrated before the Association of Engineers and Architects of Mexico that the problem was just the result of the general subsidence of the bottom of the valley, presenting as evidence two precision levelings, made in 1877 and 1924, of a monument located near the Cathedral (Gayol, 1925). Gayol attributed the phenomenon to the effect of the recently built drainage system.

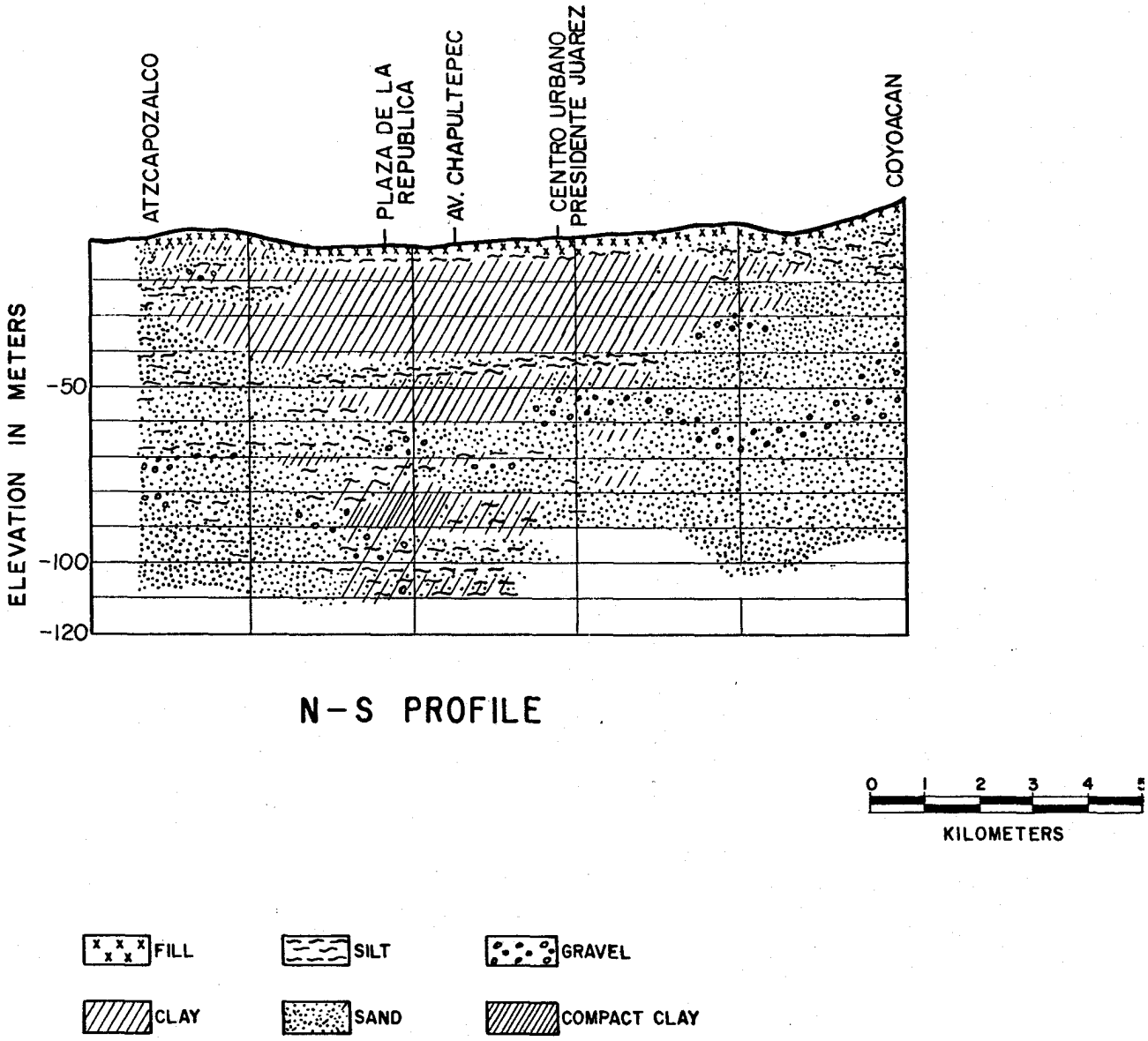

Figure 9.8.2 North-south geological profile (after Marsal and Mazari, 1959).

In spite of the importance of the discovery, 23 years elapsed before Nabor Carrillo demonstrated that the main cause of the subsidence was the extraction of ground-water by wells for municipal use (Carrillo, 1948).

Carrillo, using a profile consisting of an aquifer overlain by clayey strata and assuming a lineal distribution within the clays for the neutral pressures at the beginning and end of the process of consolidation, found the evolution of neutral pressures in the aquifer, corresponding to a constant subsidence velocity of the surface of the clay (Carrillo, 1948).

After that, other investigators continued developing these ideas (Marsal, Hiriart, and Sandoval, 1951). By collecting all the available information regarding precision levelings and mechanical properties of the local clays, they reconstructed the history of the subsidence and made a first prediction about its probable future total magnitude, as shown in Figure 9.8.6 (Marsal, 1952).

At the same time, bench marks and piezometric stations were installed for the observation of subsidence and the evolution of the neutral pressures at different depths. In accordance with the consolidation theory, the neutral pressures are directly related with the phenomenon,

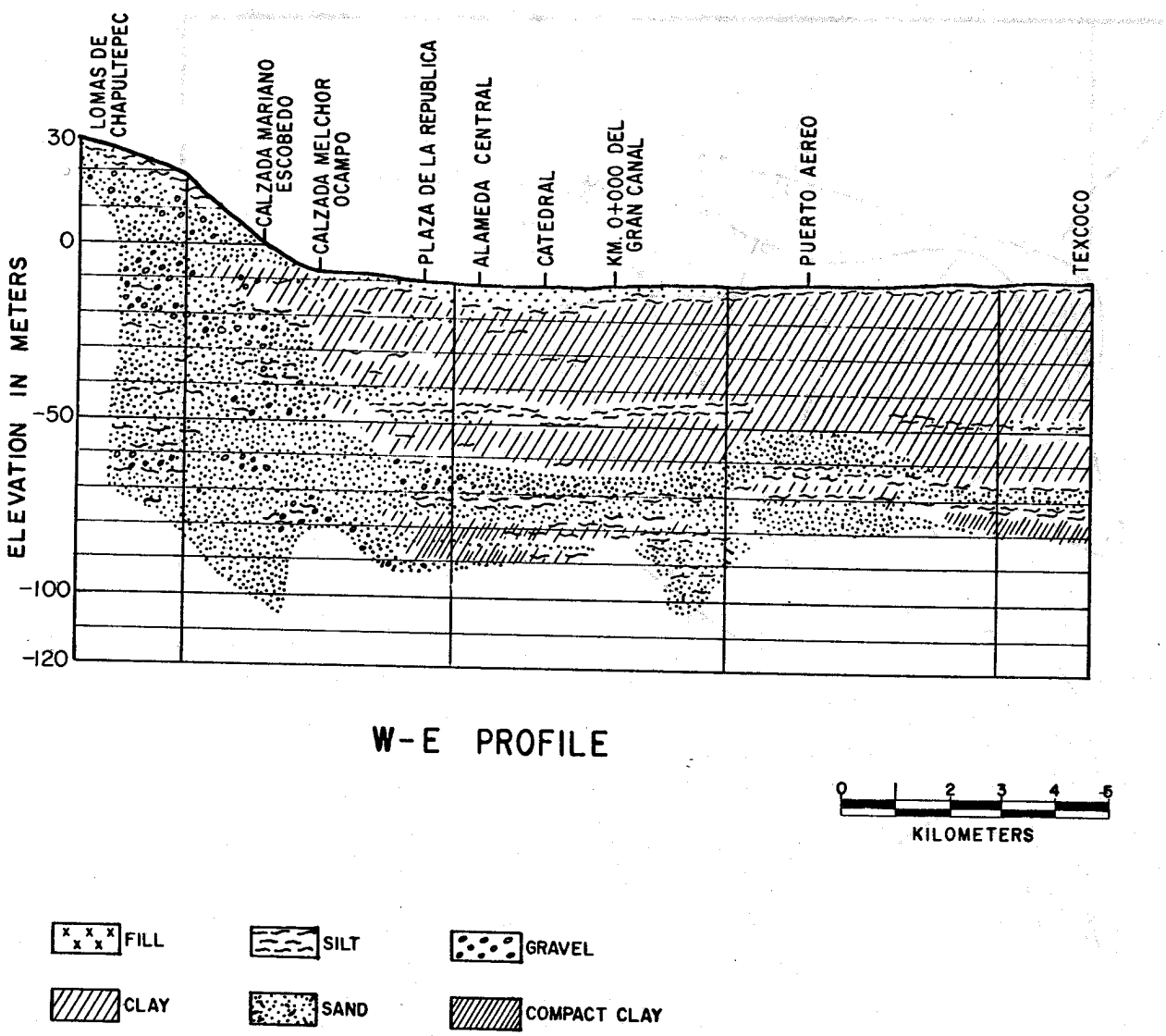

Figure 9.8.3 East-west geological profile (after Marsal and Mazari, 1959).

Table 9.8.2. Orders of magnitude of ground water pumpage in Mexico City.

Year	Pumping Rate (m3/s)
1860	0.0
1910	0.5
1930	1.5
1940	6.0
1950	9.0
1960	9.0
1970	9.0
1974	12.0

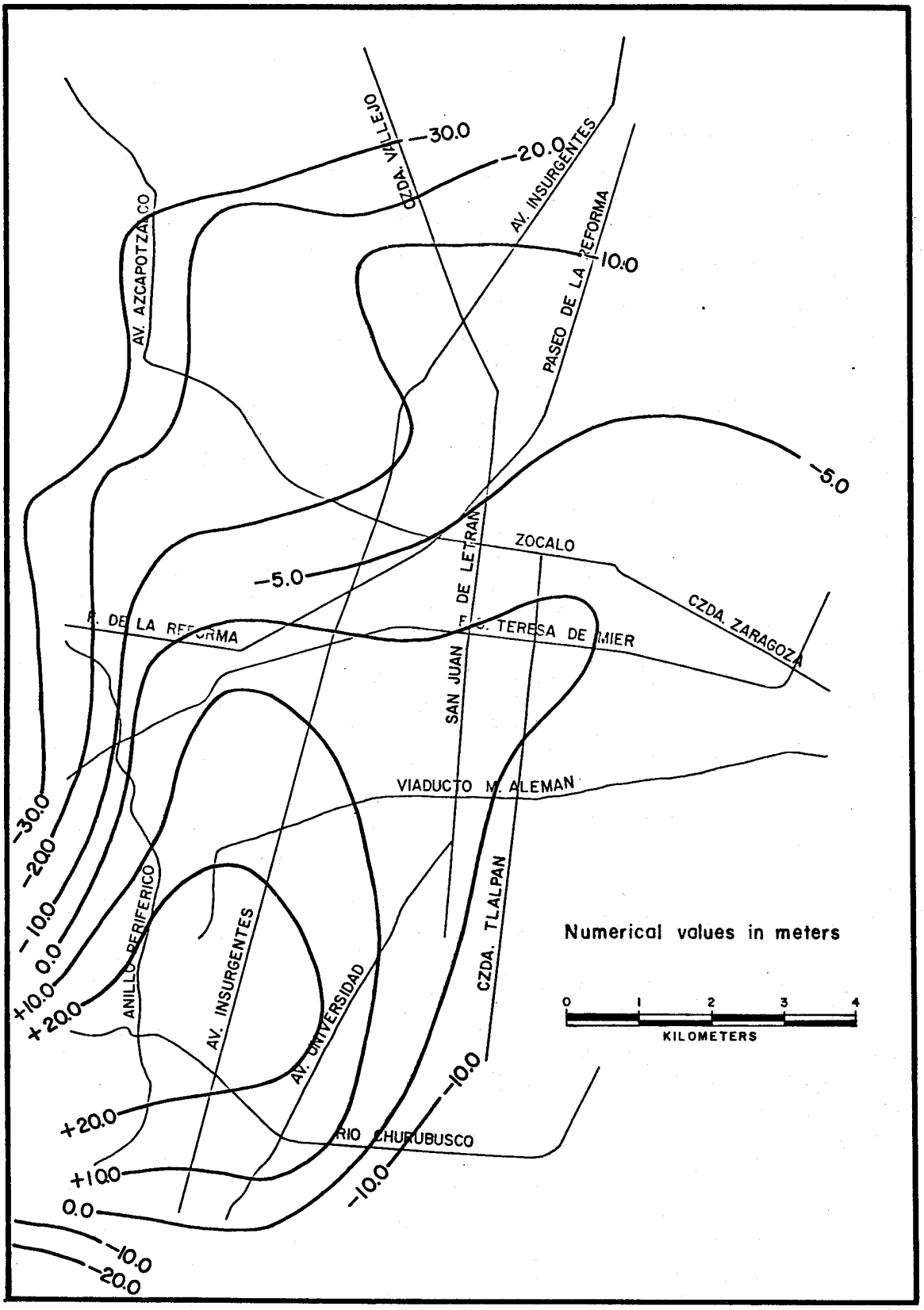

Figure 9.8.4 Change in ground-water level, 1948-1975.

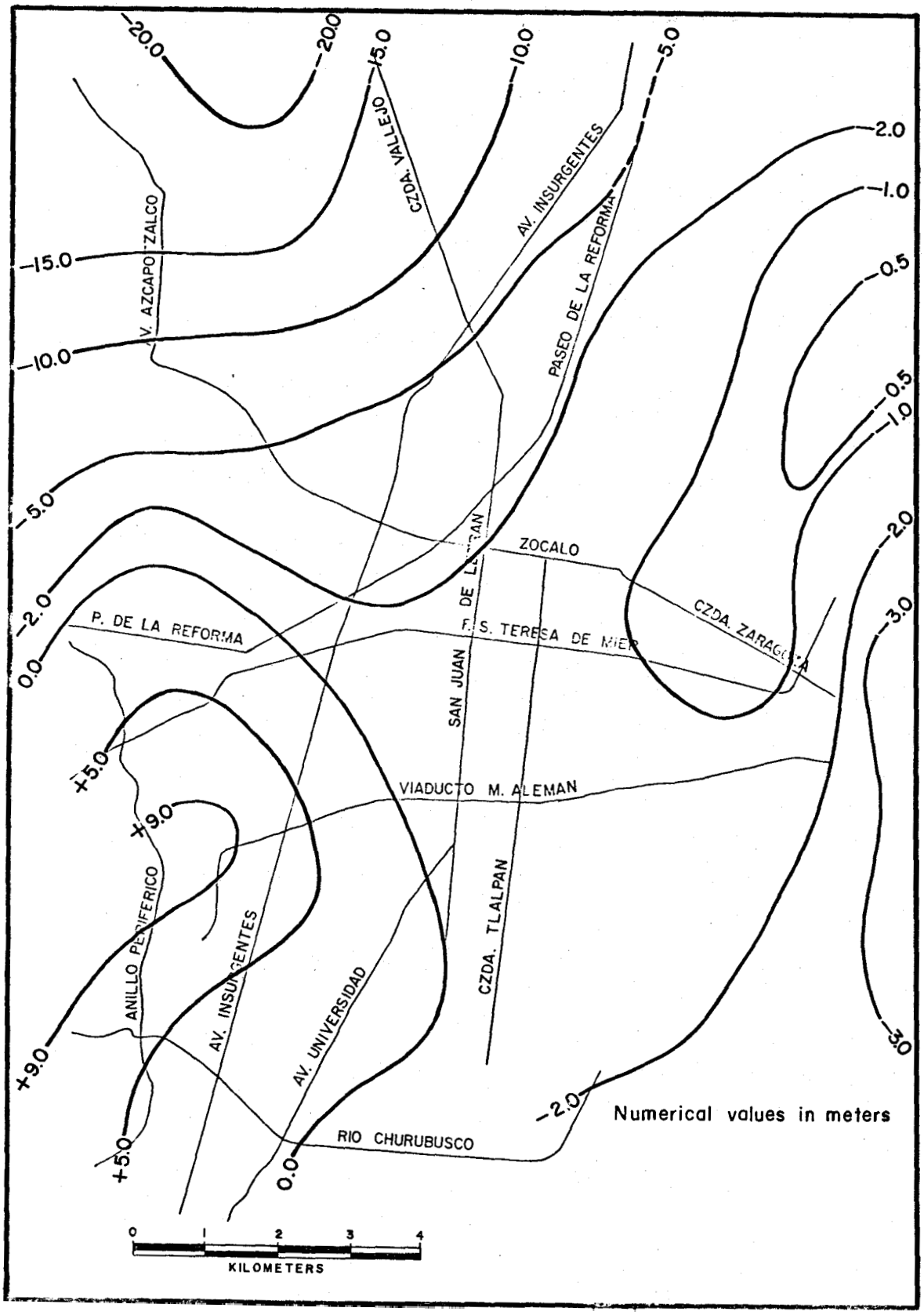

Figure 9.8.5 Change in ground-water level, 1969-1975.

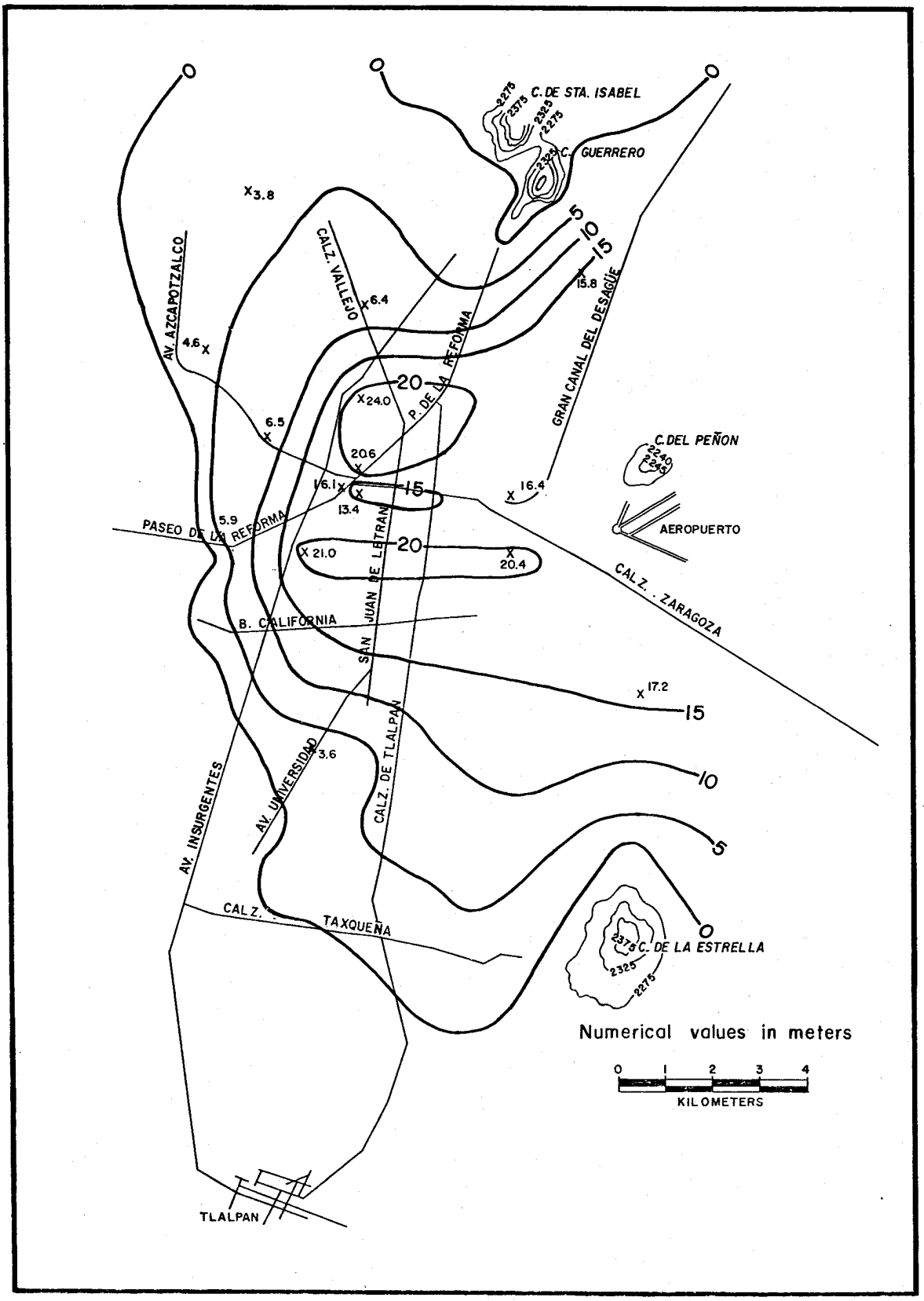

Figure 9.8.6 Potential upper limits of subsidence (after Marsal, 1952).

since their reduction causes a load transfer to the soil structure, with its consequent reduction of volume and resulting subsidence of its surface.

As for the mechanical properties of the clays in the city, a huge quantity of information has been collected, giving rise to a statistical presentation of the existing data and to a stratigraphic zoning of the city, which may be seen in Figure 9.8.7 (Marsal and Mazari, 1959).

Here, in the presence of three main zones, may be noticed: the Hills Zone, located over tuffs of low compressibility, the Transition Zone, and the Lake Zone, located over clays of high compressibility.

In 1954 the Hydrological Commission of the Valley of Mexico, which is now the Water Commission of the Valley of Mexico, took charge of the observation of the subsidence, adopting for this the already established practices. Since then more piezometric stations have been installed, and new precision levellings performed, as well as other observations to be mentioned later in this paper.

The data relative to the above have been published previously (Comisión Hydrológica de la Cuenca del Valle de México, Boletín de Mecánica de Suelos Num. 1, 1953; 2, 1958; 3, 1961a; 4, 1965; 5, 1967; 6, 1970; and 7, 1975).

Accordingly, the subsidence of Mexico City has been known since 1891 for the old part of the city and since 1952 for the total city area.

For the purposes of the present paper, some other figures have been selected (Figures 9.8.8 through 9.8.11) showing, for the old part of the city, the subsidence during the periods 1891-1952, 1952-1973, and 1891-1973, and for all the city during the period 1952-1973. In the same way, Figure 9.8.12 shows the observed subsidence through time of several selected points.

On the other hand, Tables 9.8.3 and 9.8.4 show the mean velocity of subsidence in the old part of the city and in the total area for different periods. The general evolution of subsidence in Mexico City can be visualized through the maps, graphs, and tables included herein. It may be seen that at some places it has almost reached 9 metres. Figure 9.8.12 shows the general trend of subsidence, which has evolved as an inverted "S" of asymptotic nature, with a remarkable diminution in recent years.

In addition to the subsidence, superficial cracks have been observed in two zones: along Paseo de la Reforma and a parallel street, within the clayey zone, and in the northwestern part of the City, in the tuffaceous zone. Those of the first zone have brought about the demolition of several houses and a part of a school and also caused serious damage to the abutments of a recently built bridge. The latter are even more impressive.

The subsidence of the city has also been noticed through the protrusion of well casings. Table 9.8.5 shows a comparison between observed protrusions and measured subsidences in several wells.

It has been shown by correlation studies that for the period 1970 - 1973, approximately 75 per cent of the total subsidence was due to consolidation of the clayey strata and the remaining 25 per cent to the compression of the materials of the deep strata that constitute the aquifer.

There is no doubt about the main cause of Mexico City's subsidence: the overdraft of the aquifer. As a rough estimate the weight of the buildings contribute only 10 to 15 per cent of the total subsidence.

Since 1972 a digital model has been developed to simulate the subsidence of Mexico City. The central idea is to reduce the system of partial differential equations which represent the behavior of the coupled system aquifer-consolidating strata to an integrodifferential equation for the aquifer alone, including the inputs by consolidation through a convolution or memory term (Figueroa Vega, 1973b and 1977).

Some preliminary results show that the simulation is possible, within the limitations imposed by the employed simplifications.

The model is presently in its calibration stage, which has been impaired because data pertaining to the aquifer are relatively scarce (Figueroa Vega, 1977).

9.8.4 ECONOMIC AND SOCIAL IMPACT OF SUBSIDENCE

It is difficult to estimate the economic and social impact of the subsidence of Mexico City. Among the main resulting damages are those to buildings, sidewalks, and pavements, not to mention the continuous dislocation of the freshwater and sewage nets.

On the other hand, the sewage of the city, which originally drained by gravity, has been eliminated by pumping since the flood which occurred during 1951.

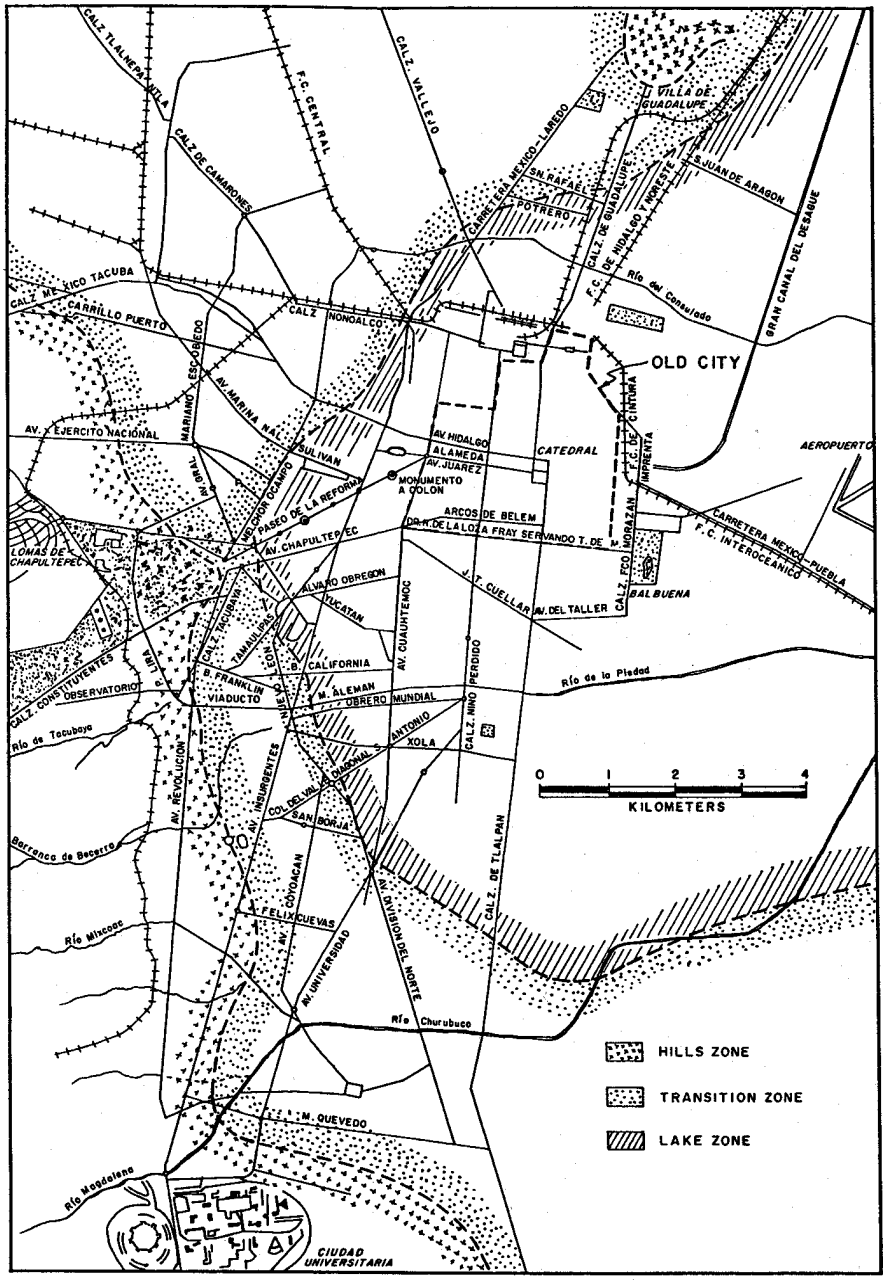

Figure 9.8.7 Zonification of the city (after Marsal and Mazari, 1959).

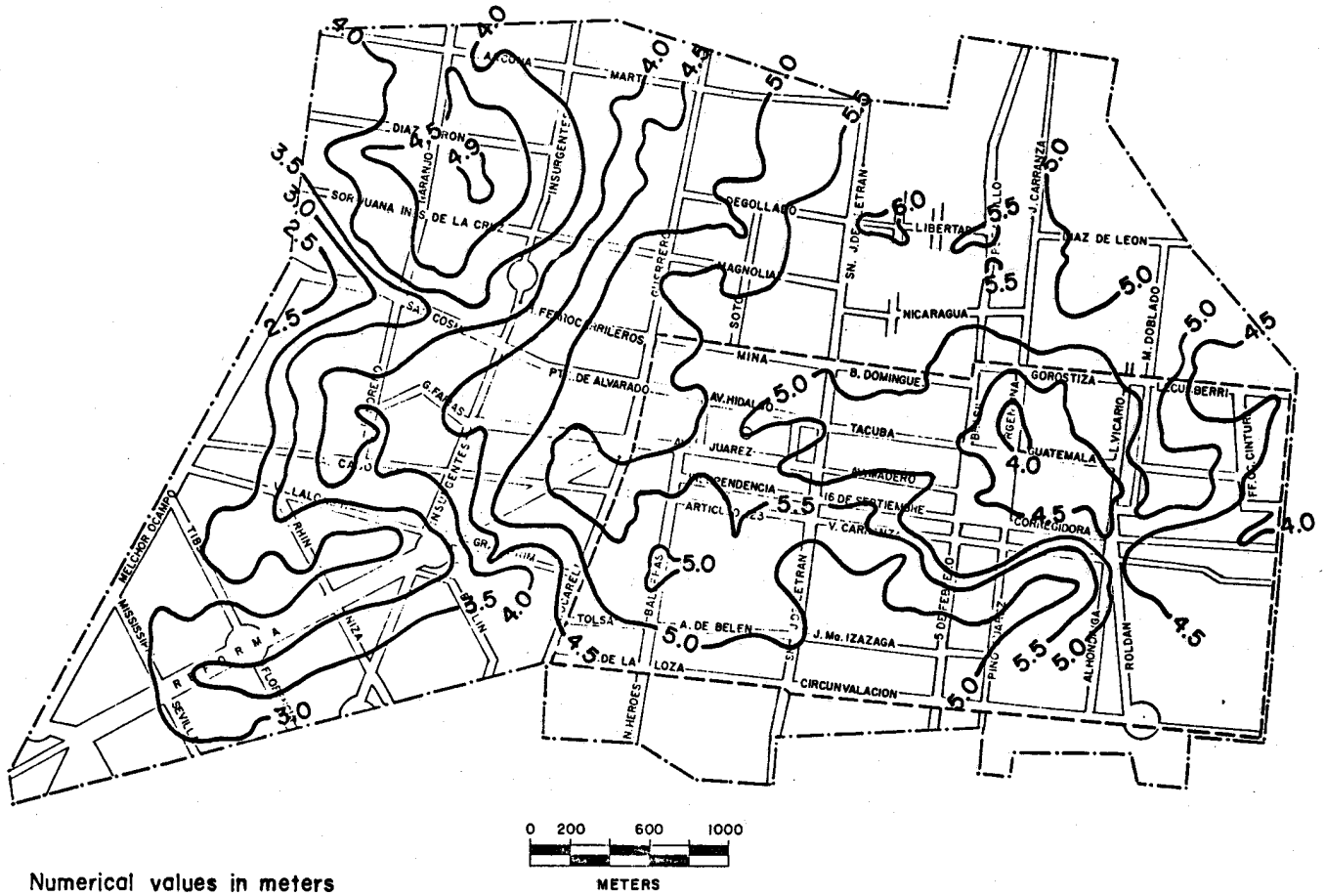

Figure 9.8.8 Subsidence (Old City), 1891-1952 (after Comisión Hidrológica de la Cuenca del Valle de México, 1953).

The constant danger of new floods in case of an electric system, failure, compelled the city authorities to build a Deep Sewage System, with a capacity of 200 m^3/s and a length on the order of 60 km. Complementary collectors are presently under construction.

The total cost of the project would have been much less, if it had been possible to eliminate the sewage by gravity. On the other hand, the overexploitation and the consequent ground-water declines have raised the cost of ground-water extraction, and the loss of water due to dislocation of the distribution net has been estimated up to 15 m^3/s.

Because of above-mentioned factors, the subsidence of Mexico City could conceivably be more expensive than bringing water from other watersheds to avoid the overexploitation of the local aquifer.

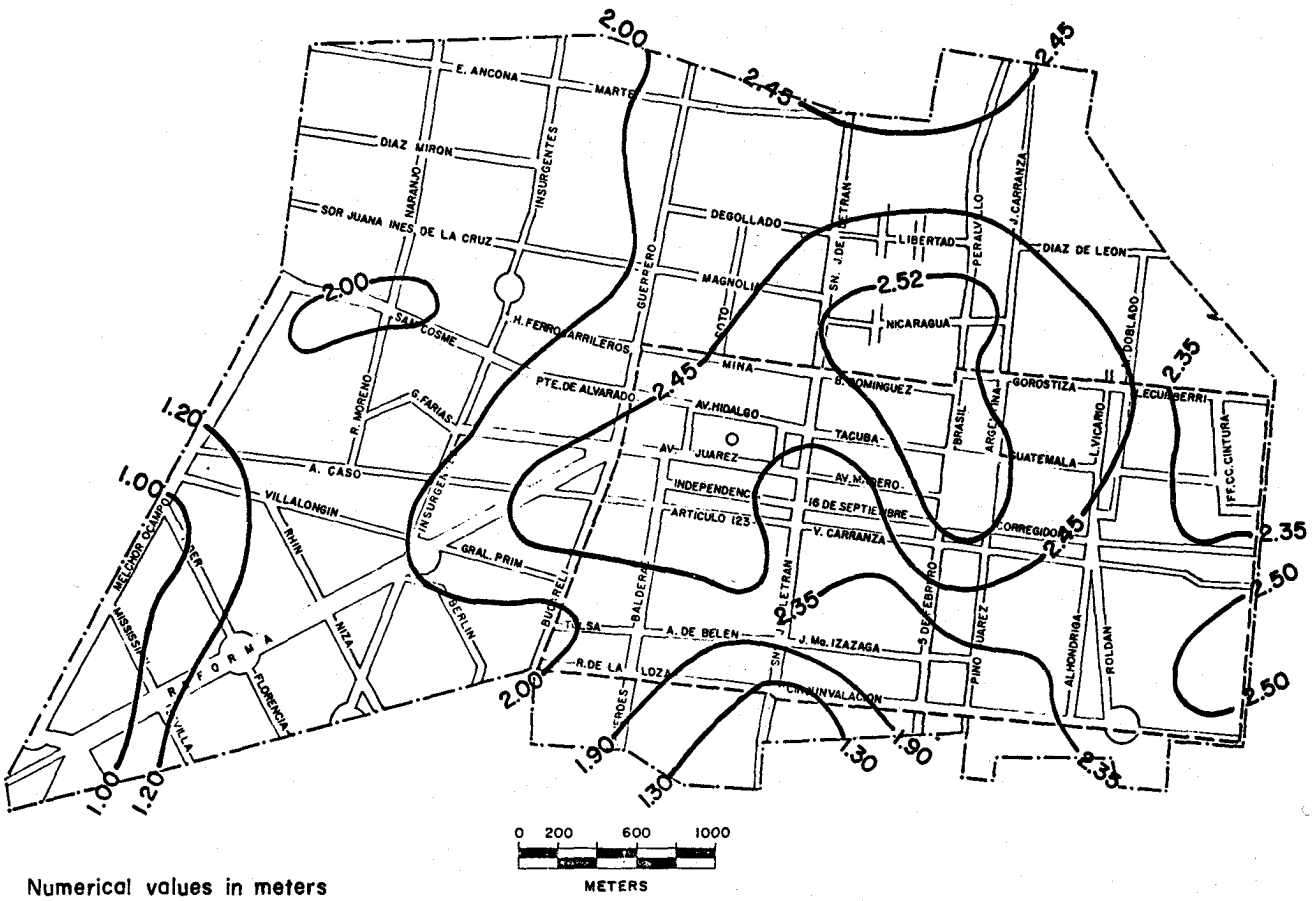

Numerical values in meters

0 200 600 1000
METERS

Figure 9.8.9 Subsidence (Old City), 1952-1973 (after Comisión de Aguas del Valle de México, 1975).

9.8.5 LEGAL ASPECTS

From a legal standpoint, the ground water in Mexico belongs to the nation and for this reason no legal action is taken against its overexploitation. As a result, social costs originating from overdraft are normally covered through taxation and water rates.

9.8.6 MEASURES TAKEN TO CONTROL OR AMELIORATE SUBSIDENCE

Soon after the floods of 1951, the City authorities began bringing water from other sources outside the Basin and managed to keep the local extraction constant for many years, as shown in Table 9.8.2. The effect of this may be appreciated in the final portion of the curves of Figure 9.8.12.

The accelerated growth of the city in the last years, which has been an average on the order of 5 per cent annually, has made it necessary to increase slightly the local extractions, as

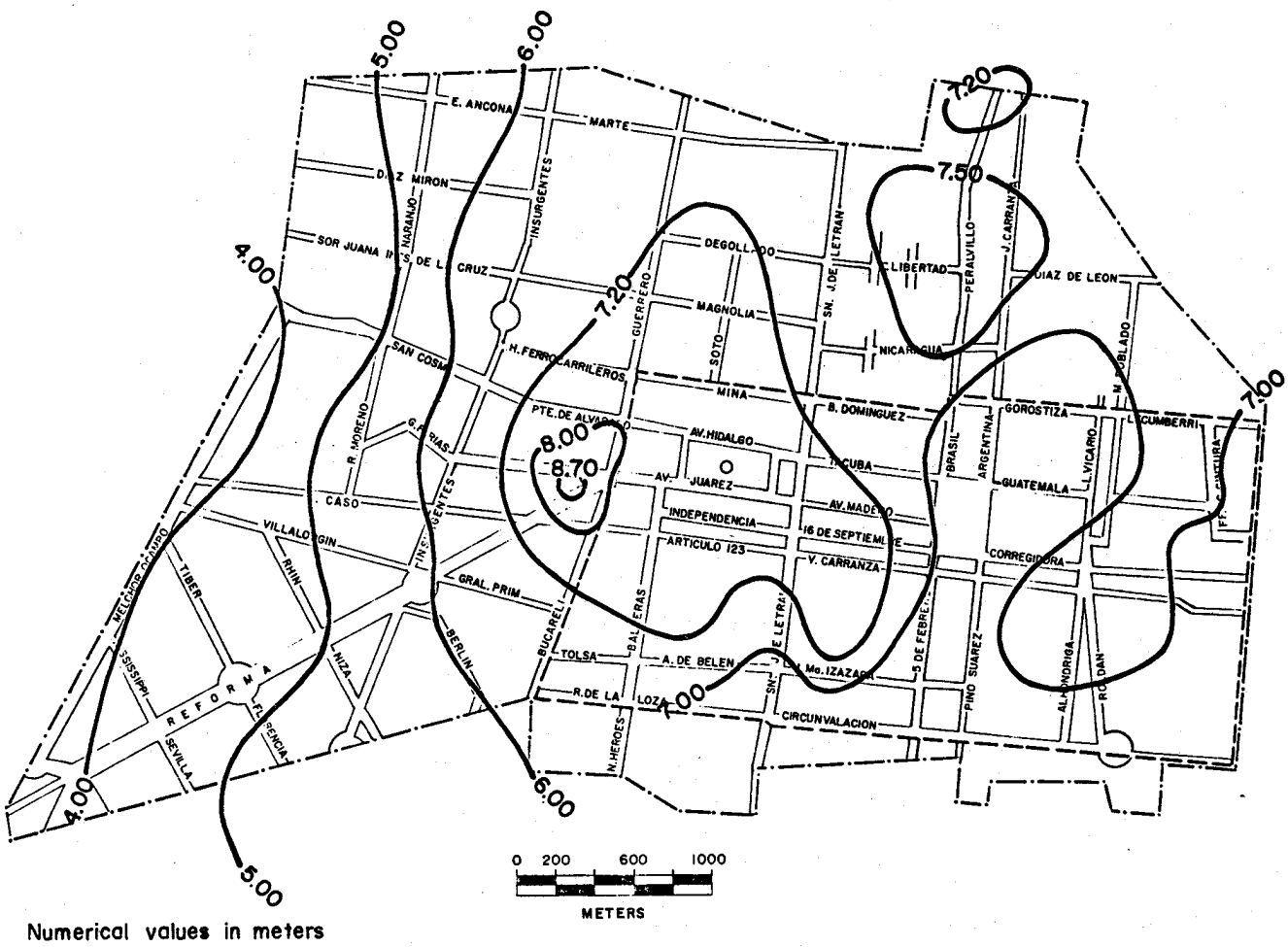

Figure 9.8.10 Subsidence (Old City), 1891-1973 (after Comisión de Aguas del Valle de México, 1975).

shown in the same table. Nevertheless, large projects to bring water from other watersheds are now under way in order to satisfy the future demands and, if possible, to be able to diminish the local extraction in order to solve the subsidence problem. Additionally, the construction of sewage treatment plants for industrial use is now under way and recirculation of water in industries is being made mandatory in order to shut down some of the wells employed by the industries, as these consume almost 30 per cent of the water used by the city. It is estimated that in the near future the substitution of treated sewage water for ground water for industrial use could be of the order of 5 to 7 m^3/s.

The effect of these measures will undoubtedly reduce or cancel the subsidence of the City of Mexico. The schedule for this depends now on political decisions and on availability of funds.

9.8.7 REFERENCES

CARILLO, N. 1948. Influence of artesian wells on the sinking of Mexico City: Proc. of the Int. Conf. on Soil Mechanics, Holland.

COMISION HIDROLOGICA DE LA CUENCA DEL VALLE DE MEXICO. 1953. Boletín de Mecánica de Suelos Num. 1, México, D.F.

_____. 1958. Boletín de Mecinica de Suelos Num. 2, México, D.P.

_____. 1961a. Boletín de Mecánica de Suelos Num. 3, México, D.F.

_____. 1961b. Informe sobre la geologia de la Cuenca del Valle de México y zonas colindantes.

_____. 1963. Hidrologia de la Cuenca del Valle de México, Tomos II y V.

_____. 965. Boletín de Mecánica de Suelos Num. 4, México, D.F.

_____. 1967. Boletín de Mecánica de Suelos Num. 5, México, D.F.

_____. 1970. Boletín de Mecánica de Suelos Num. 6, México, D.F.

COMISION DE AGUAS DEL VALLE DE MEXICO. 1975. Boletín de Mecánica de Suelos Num. 7, Mexico, D.F.

FIGUEROA VEGA, G. E. 1973a. El Hundimiento de la Ciudad de México. Breve Descripción; Recursos Hidráulicos. Vol. II, num. 4; pp. 525-534.

_____. 1973b. Aquifer and subsidence model for Mexico City. 85th annual meeting of The Geological Society of America; v. 5, no. 7, p. 620.

_____. 1977. Subsidence of the City of Mexico, A Historical Review; Publication No. 121 of The International Association of Hydrological Sciences, pp. 35-38.

GAYOL, R. 1925. Estudio de las pertubaciones que en el fondo, de la Ciudad de México ha producido el drenaje de las aquas del subsuelo, por las obras del desaque y rectificación de los errores a que ha dado lugar una incorrecta interpretación de los efectos producidos. Revista Mexicana de Ingeniería y Arquitectura, Vol. III, Num. 2. pp. 96-132.

MARSAL, R. J. 1952. Estudios relativos al comportamiento del subsuelo de la Ciudad de México. Instituto Nacional de Investigacion Cientifical México, D-F,

MARSAL, R. J., HIRIART, F., and SANDOVAL, R. 1951. Hundimiento de la Ciudad de México. Congreso Cientifico Mexicano. México, D.P.

MARSAL, R. J., and MAZARI, M. .1959. El Subsuelo de la Ciudad de México. Primer Congreso Panamericano de Mecánica de Suelos y Cimentaciones, México, D.F. Republished in 1969 with English translation.

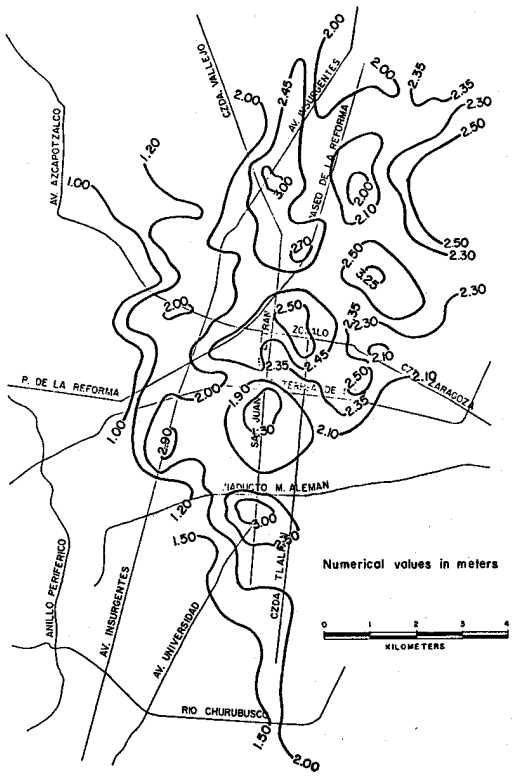

Figure 9.8.11 Subsidence (total area), 1952-1973 (after Comisión de Aguas del Valle de México).

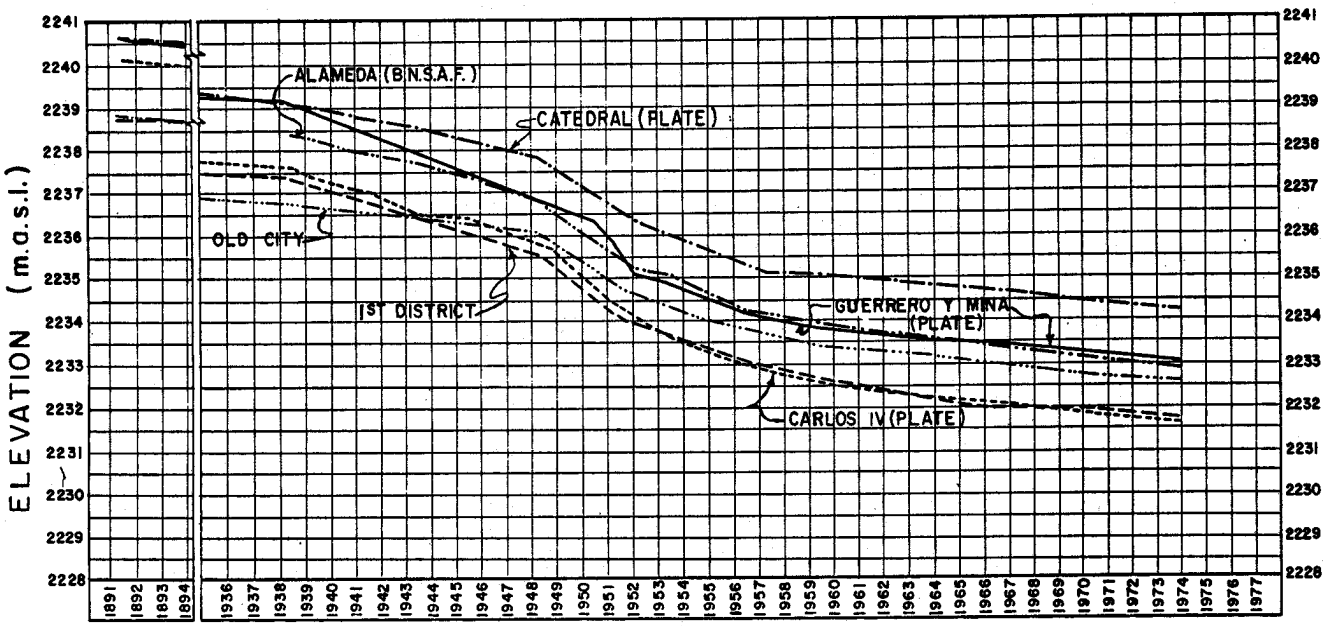

Figure 9.8.12 Subsidence evolution at selected sites (after Comisión de Aguas del Valle de México).

Table 9.8.3 Mexico City subsidence (older part) (from Figueroa Vega, 1977, Table 2).

From - to	Total subsidence (m)	Average (m/year)
1891 - 1938	2.12	0.045
1938 - 1948	0.76	0.076
1948 - 1950	0.88	0.440
1950 - 1951	0.46	0.460
1951 - 1952	0.15	0.150
1952 - 1953	0.26	0.260
1953 - 1957	0.68	0.170
1957 - 1959	0.24	0.120
1959 - 1963	0.22	0.055
1963 - 1966	0.21	0.070
1966 - 1970	0.28	0.070
1970 - 1973	0.17	0.051

Table 9.8.4 Mexico City subsidence (total area) (from Figueroa Vega, 1977, Table 3).

From - to	Total Subsidence (m)	Average (m/year)
1952 - 1959	1.014	0.140
1959 - 1963	0.440	0.110
1963 - 1966	0.254	0.080
1966 - 1970	0.260	0.065
1970 - 1973	0.203	0.059

Table 9.8.5 Well casings protrusion (from Figueroa Vega, 1977, Table 4).

Well	Protrusion 1970 - 1973 (m)	Subsidence 1970 - 1973 (m)
San Juan de Aragón Campamento	0.304	0.440
Czda. Guadalupe	0.130	0.172
Sta. Isabel Tola	0.259	0.320
Monumento de la Revolución Frontón México	0.179	0.200
Jardin de los Angeles No. 2	0.076	0.145
Insurgentes Norte 1407	0.199	0.283
Penitenciaria Jardin	0.233	-
Gómez Farías No. 61	0.113	0.140
Monumento de la Revolución Procuraduría	0.323	-
Jardin de los Angeles No. 3	0.100	0.145
Jardin de los Angeles No. 1	0.146	0.150

Case History No. 9.9. The Wairakei Geothermal Field, New Zealand, by Paul F. Bixley, Ministry of Works and Development, Wairakei, New Zealand

9.9.1 INTRODUCTION

The Wairakei geothermal area is located 8 km north of Lake Taupo in the center of the North Island of New Zealand (Figure 9.9.1). Geothermal investigations at Wairakei began in 1950 and culminated with the commissioning of the first stage of the power station in 1958 and the second stage in 1964 bringing the installed capacity to 192 MWe. Steam is supplied to the power station by 64 wells, most of which produce a steam-water mixture at the wellhead. The mixture is separated, the steam piped to the power station and waste water dumped into the Waikato River. The 64 production wells cover an area of 2 km^2 referred to in this paper as the "production field."

The first indication of ground movement came in 1956 when discrepancies were found in the levels of several benchmarks since the previous survey in 1950 (Hatton, 1970). One benchmark had subsided 76 mm. A levelling network was established and gradually expanded until by 1971, the most recent comprehensive survey, the area of subsiding ground was found to exceed 30 km^2. Within this area were two zones of relatively rapid subsidence; one immediately north of the eastern production field and the other at Karapiti, a region of natural thermal activity about 3 km south of the production field. Economic interest has centered on the zone of rapid subsidence northeast of the production field, as steam mains to the power house, and channels carrying separated water pass across this zone. Benchmarks in this zone are levelled to third order standards annually (third order accuracy is within 12 $mm\sqrt{km}$, where km is kilometres of line traversed).

9.9.2 GEOLOGY

The geology of the Wairakei geothermal field has been discussed in detail by Grindley (1965). The production field is underlain by a near flat sequence of acid volcanics, consisting of six basic units down to 1.2 km (most wells are drilled to 600-1200 m, one well is drilled to 2.5 km). These units are: Recent Pumice, Wairakei Breccia, Huka Falls Formation, Haparangi Rhyolite, Waiora Formation and Wairakei Ignimbrites. Almost all production comes from within the Waiora Formation where active faults have been intercepted by drillholes (Grindley, 1965). There is also evidence for a permeable zone in the Waiora Breccia just above the Wairakei Ignimbrite contact (Bolton, 1970).

WAIRAKEI IGNIMBRITES: Hard welded ash flow tuff, thickness 950 m in the single hole penetrating this formation.

WAIORA FORMATION: Pumice sandstone, pumice breccia and thin (up to 70 m) ignimbrite sheets. Total thickness 400 m in the western section of the production field, thickening rapidly to the east to greater than 750 m.

HAPARANGI RHYOLITE: An extensive rhyolite sill, intruded into the Waiora Formation to the west of the production area. Maximum thickness 450 m.

HUKA FALLS FORMATION: Bedded mudstone and tuffaceous sandstone; thickness 60-220 m.

WAIRAKEI BRECCIA: Chalazoidite and vitric tuff conformably overlying the Huka Falls Formation; differentiated from the Huka Falls Formation by the incoming of chalazoidites. Maximum thickness 170 m.

RECENT PUMICE: Superficial deposits up to 30 m thick, consisting of alluvium derived from the dissection of underlying formations together with ash and pumice/lapilli shower material.

The relationship between these units is shown on the cross section ABC (Figure 9.9.2).

The age of the above sequence ranges from lower-mid Pleistocene for the Wairakei Ignimbrites to possibly as young as 20,000 years BP for the Wairakei Breccia (Browne,1973).

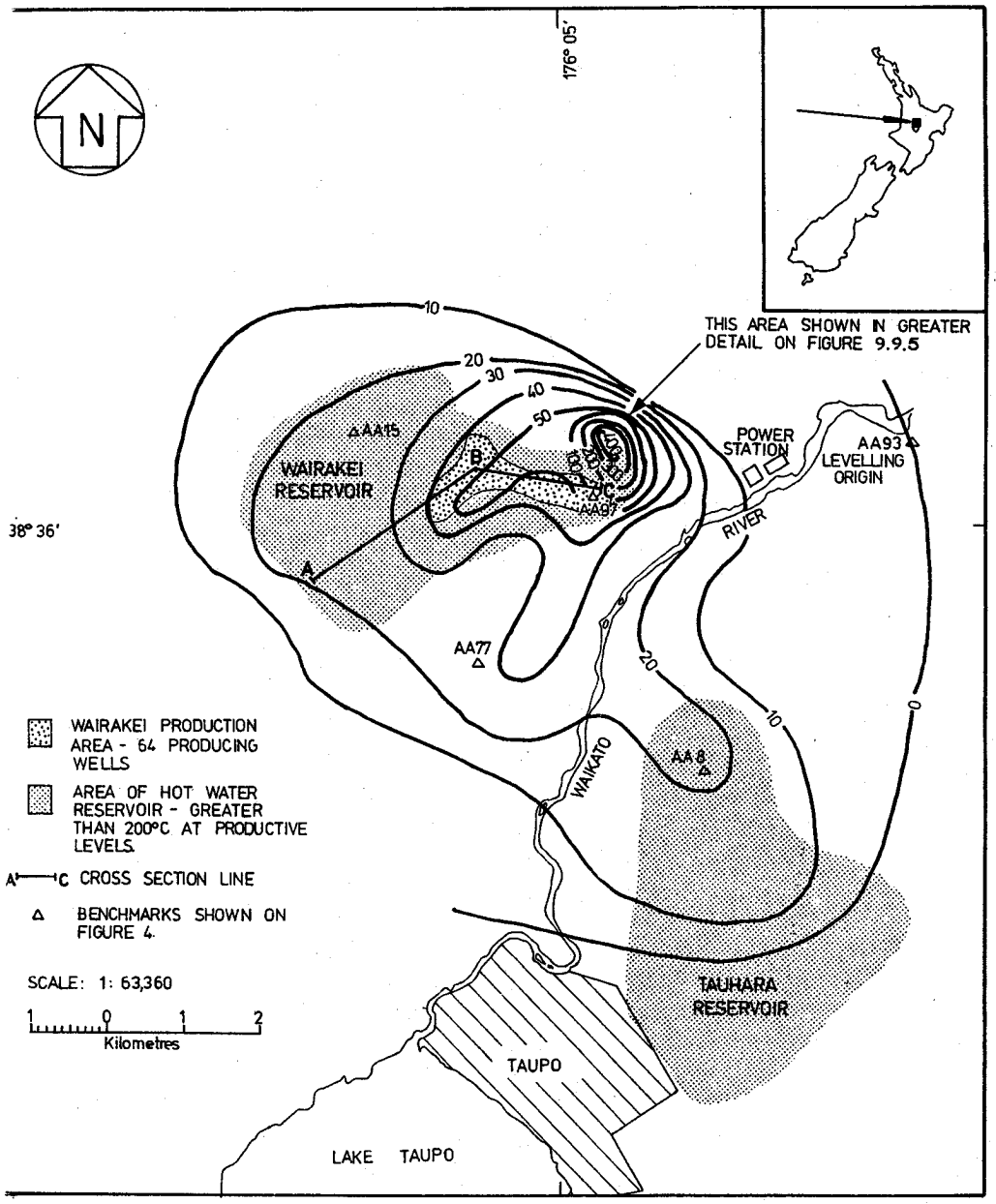

Figure 9.9.1 Land subsidence 1956 to 1971, of Wairakei-Tauhara geothermal areas, New Zealand. Lines of equal subsidence in millimetres per year. Reservoir boundaries are taken as the estimated 2000 temperature contour at the production level, based on surface resistivity measurements and downhole temperature profiles.

The Haparangi Rhyolite at Wairakei is considered tentatively to be an intrusive rhyolite of late Huka age (Grindley 1965).

9.9.3 STRUCTURE

The Wairakei production field is located on a structural high situated between the major Taupo-Reporoa Basin to the east and a series of smaller block and basin structures to the west. Structure is largely controlled by a series of normal faults which strike northeast, parallel to the trend of the Taupo Volcanic Zone. Most of these faults are still active.

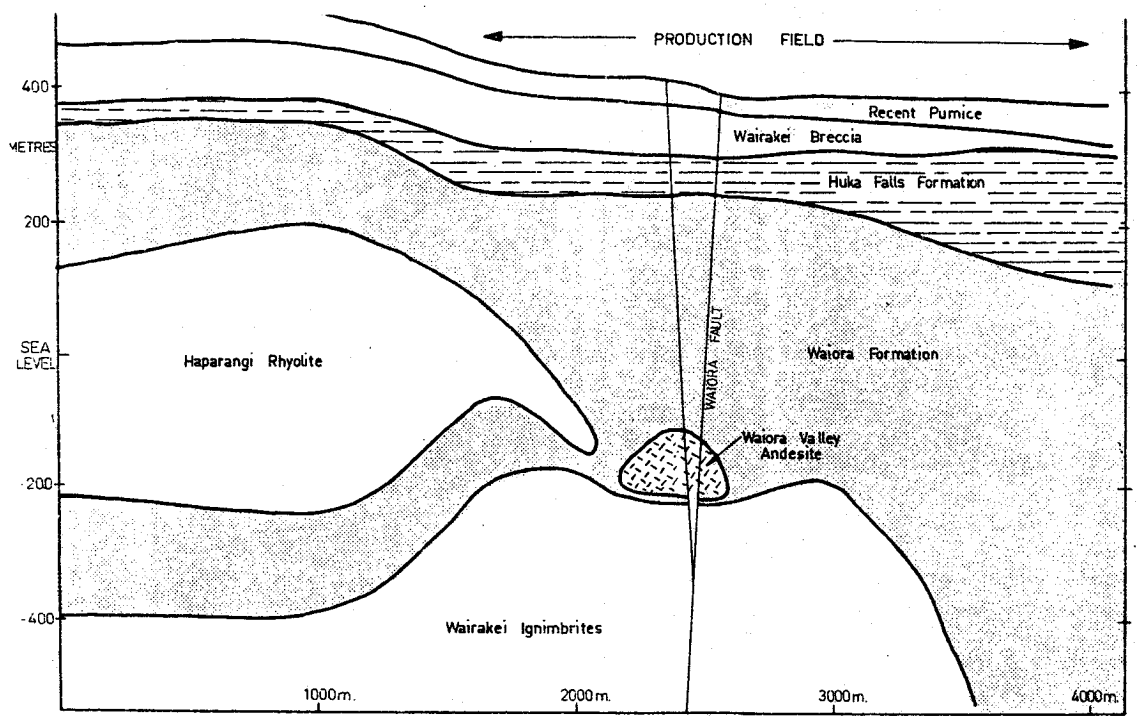

Figure 9.9.2 Cross section ABC through Wairakei geothermal reservoir showing geological structure. Vertical scale twice the horizontal scale.

9.9.4 ROCK PROPERTIES

Cores taken from investigation wells drilled into the hot water reservoir at Wairakei have been extensively tested for wet and dry bulk densities, particle density and porosity.

In 1975 Terra Tek Inc. conducted a series of comprehensive tests on selected cores from Wairakei for Systems Science and Software Inc. (Pritchett, 1977). Cores used for these tests had remained drying in the core shed for ten years before testing. Bulk density and particle density measurements agreed with those previously done on fresh cores. Results of these tests are tabulated below:

Table 9.9.1. Properties for Wairakei Hot Water Reservoir Rocks. Densities are tonnes/m^3 and effective porosity per cent by volume.

Formation	Bulk density wet	Bulk density dry	Effective porosity	Grain density
Surface Pumice	1.88	1.39	49	2.71
Huka Falls Formation	1.99	1.59	40	2.70
Waiora Formation	2.02	1.64	39	2.72
Wairakei Ignimbrite	2.36	2.22	14	2.69

The linear coefficient of expansion for the Waiora Formation was found to be 8.2×10^{-6} m/m/°C and the dry specific heat 0.71 to 0.75 J/g°C. Thermal conductivity increased with increasing stratigraphic depth of the formation: measured values (saturated) were: Surface Pumice 1.03, Huka Falls Formation 1.28, Waiora Formation 1.56, and Wairakei Ignimbrite 2.11 W/m°c.

9.9.5 HYDROLOGY

The production field covers an area of 2 km^2 but this is only part of a much larger reservoir, as shown on Figure 9.9.1. Down to depths explored by drilling (1.2 km, and one well to 2.5 km) the Waiora Formation, a heterogeneous mixture of acid volcanic pyroclastics, vitric tuffs, sediments, and a rhyolite sill, forms the aquifer system from which geothermal fluids are withdrawn. A hot water reservoir (over 200°C) covering an area of 11 km^2 has been delineated by drilling and geophysical exploration.

At Wairakei 100 wells have been completed in the production area, 16 deep exploration wells in the hot water reservoir outside the production area and four deep and two shallower wells completed in the "cold" area outside the hot water reservoir.

Exploratory wells drilled outside the hot water reservoir have shown that there are hydrological connections between these "cold" wells and the hot water reservoir. Well 223, a "cold" well 5 km west of the production area, reacts almost immediately to changes in drawoff rate in the production field (Bolton, 1970). Bolton used the steep pressure gradients between cold wells and the hot water reservoir as evidence for some kind of low permeability barrier between the hot water reservoir and the surrounding cold water, down to depths of at least 1 km.

The Wairakei hot water reservoir is connected hydrologically to another hot water reservoir of about the same size located 8 km to the SE at Tauhara (Figure 9.9.1). This reservoir has not been exploited.

The intensive pattern of active, northeast-striking faults through the Wairakei reservoir is the major control on fluid flow. These faults penetrate the Huka Falls Formation "caprock" allowing the escape of hot fluids to feed natural thermal features, and when pressure conditions are suitable they may allow cold water from the surface water table to penetrate the hot water system. The faults also provide channels for vertical inflow of hot water into the aquifer system from below. Within the hot water filled aquifer system faults allow rapid propagation of pressure changes.

Thus the hot water aquifer system at Wairakei is unconfined, in that the "caprock" is penetrated by active faults and the same faults provide channels for inflow of hot water into the system from below. In addition, although there seem to be impermeable barriers around the hot water systems down to depths of at least 1 km, the cold wells located outside the hot water reservoir are affected by pressure change within the reservoir.

9.9.6 HISTORIC DEVELOPMENT OF MASS WITHDRAWAL

The withdrawal history from the Wairakei reservoir is shown in Figure 9.9.3. Output from the "western" wells includes all investigation wells located outside the production field and well 204 which blew out in 1960 and continued to discharge uncontrolled until 1973 when discharge ceased. Heat withdrawal from the production field is currently 1570 MW, and natural heat discharge is of the order of 400 MW (both relative to 12°C) - Current mass withdrawal rate is about 5500 t/h.

9.9.7 CHANGE OF PRESSURE IN THE AQUIFER SYSTEM

Average pressures at 152 m below sea level in the production field are plotted on Figure 9.9.3. Pressure changes due to withdrawal of mass and heat are discussed in detail by Bolton (1970) and Pritchett (1977). Bolton pointed out that the behavior of the Wairakei reservoir is primarily governed by the saturation pressure-temperature relation for water. Hydrostatic pressures throughout the reservoir have followed the trends shown on Figure 9.9.3. However, in the upper parts of the aquifer system below the production field a zone filled with saturated steam has developed. Pressure drop in this zone depends on changes in steam temperature.

9.9.8 LAND SUBSIDENCE

Surveys show an area of over 30 km^2 is subsiding at more than 10 mm/year (Figure 9.9.1). Within this area are two smaller zones each of about 1 km^2 which have subsided comparatively rapidly. The zone at Karapiti, 3 km south of the production field, was the most rapidly subsiding part of the survey network until about 1963, when the subsidence rate decreased to the same rate as for the surrounding ground surface. Subsidence at bench mark AA77 within this zone is plotted on Figure 9.9.4.

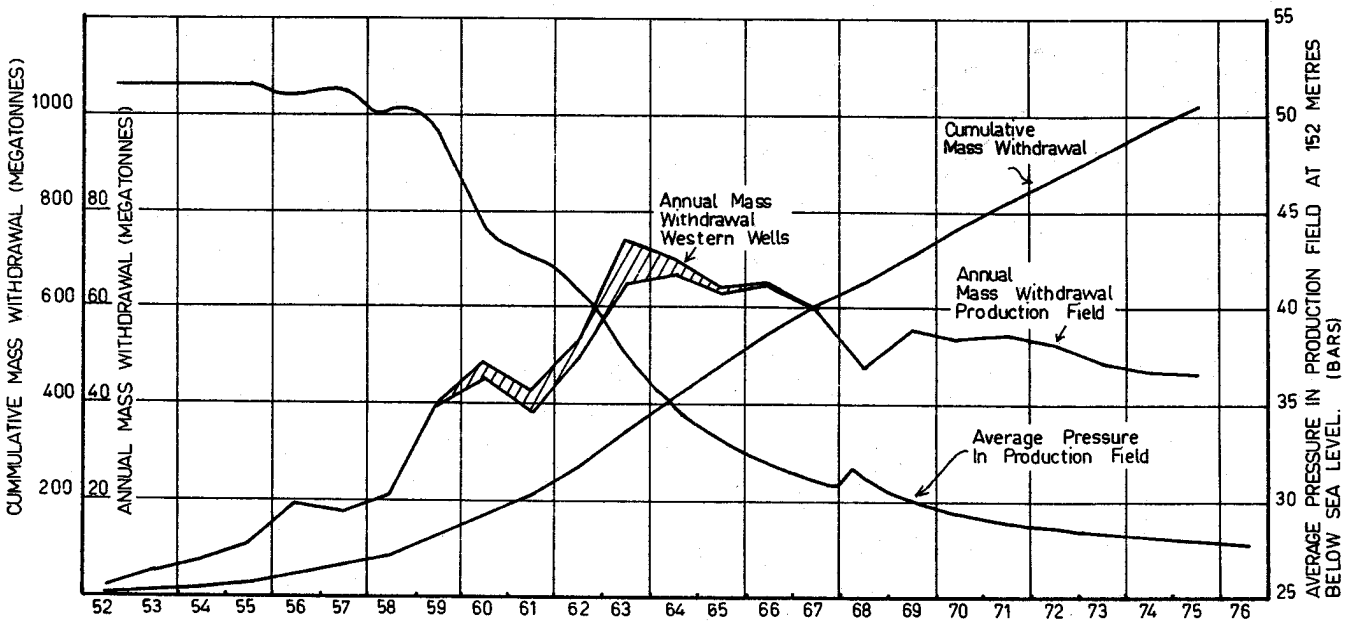

Figure 9.9.3 Wairakei hot water reservoir: mass withdrawal and aquifer pressure, 1952-1976. (Pre-1962 pressures after Bolton, 1970.)

About 1960 the subsidence rate at bench mark A97 began to increase and over the next few years the zone of rapid subsidence immediately north of the eastern production field shown on Figure 9.9.5 was delineated. Subsidence at bench mark A97 in this zone is shown on Figure 9.9.4. Subsidence of A97 between 1971 and 76 continued at 135 mm/year compared with 138 mm/year between 1966 and 71 as shown on Figure 9.9.4. Economic interest centres on this zone of subsidence as both the steam and waste water channels from the production field cross the subsiding basin. Bench marks in this zone are surveyed annually to third order standards.

Subsidence at bench marks AA8, at Tauhara, and AA15 to the west of the Wairakei production field are also shown on Figure 9.9.4.

9.9.9 HORIZONTAL MOVEMENT

The network which has been set up to measure horizontal movement at Wairakei has been described by Stilwell (1975), and Hatton (1970) showed the calculated and measured horizontal strain along the steam mains due to subsidence. The horizontal control network was re-surveyed in 1977 and vector directions shown by Stilwell were confirmed. Vector movement is generally toward the center of subsidence. Annual horizontal movement between 1968 and 77 was about 110 mm/year at a radius of 250 m from the centre of subsidence, decreasing to about 15 mm/year at 750 m radius.

9.9.10 CAUSE OF SUBSIDENCE

Subsidence in the area shown on Figure 9.9.5 must be related to the withdrawal of geothermal fluids. However, the more widespread subsidence as shown on Figure 9.9.1, although probably related to the underground hot water system, may be the result of natural events rather than withdrawal of fluids in the production area. Browne (1973) pointed out that at the Broadlands geothermal area (20 km NE of Wairakei) a natural rate of subsidence of 3.6 mm/year may have been occurring for the last 3400 years. Withdrawal of fluid at Wairakei has resulted in a number of continuing changes. The most significant of these is the overall lowering of hydrostatic pressures in the aquifer and the creation of a steam zone in the upper part of the aquifer in the production field. Computer modelling by Pritchett (1977) suggests that the gradual lowering of temperatures in this zone of saturated steam has been a major factor in controlling the

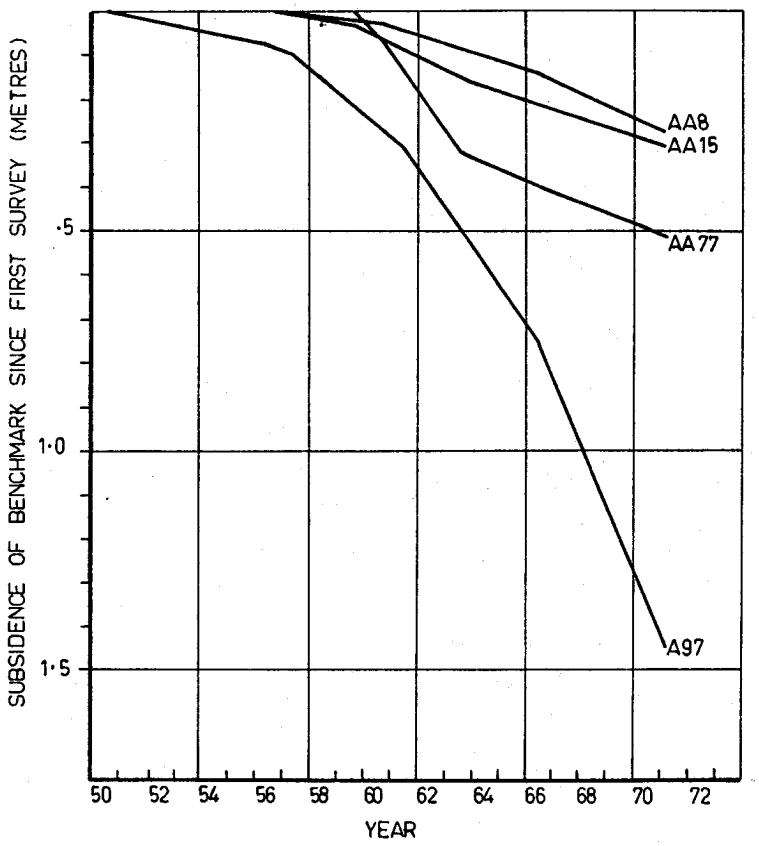

Figure 9.9.4 Subsidence at selected bench marks. For locations see Figure 9.9.1. Benchmark A97 first surveyed 1950, AA8 and AA15 1956, and A77 1959.

location and magnitude of subsidence. McNabb (1977) has suggested that pressure changes in the aquifer allowing cool surface water to penetrate fissures in the "caprock" and cool thick sections of underlying formations could account for the observed subsidence.

It is probable that the observed subsidence is the result of falling hydrostatic pressure in the deeper part of the aquifer system, falling steam pressure in the upper part of the aquifer and possibly the intrusion of cold water from the surface water table into the aquifer system. There has been no evidence of subsidence causing casing protrusion. Most casing strings are cemented into the Huka Falls Formation, thus the formation causing subsidence must lie below the Huka "caprock."

Hatton and Stilwell drew a correlation between the thickness of the producing aquifer (Waiora Formation) and the amount of subsidence.

9.9.11 ECONOMIC IMPACT OF SUBSIDENCE

The major structures affected by subsidence are the steam pipelines from the production field to the power house and the channels carrying separated geothermal water to waste. Differential subsidence has had no observed effect either on the power house or on ancillary buildings around the production field.

Both horizontal and vertical movement have occurred along the steam mains route. Maximum movement is near bench mark A97 (Figure 9.9.5), where horizontal movement is about 75 mm/year and vertical movement 130 mm/year. As the steam mains cross the edge of the subsiding basin, different sections are put in tension and compression (Hatton, 1970). Movement is accommodated to some extent by expansion loops which were built into the pipelines to allow for thermal

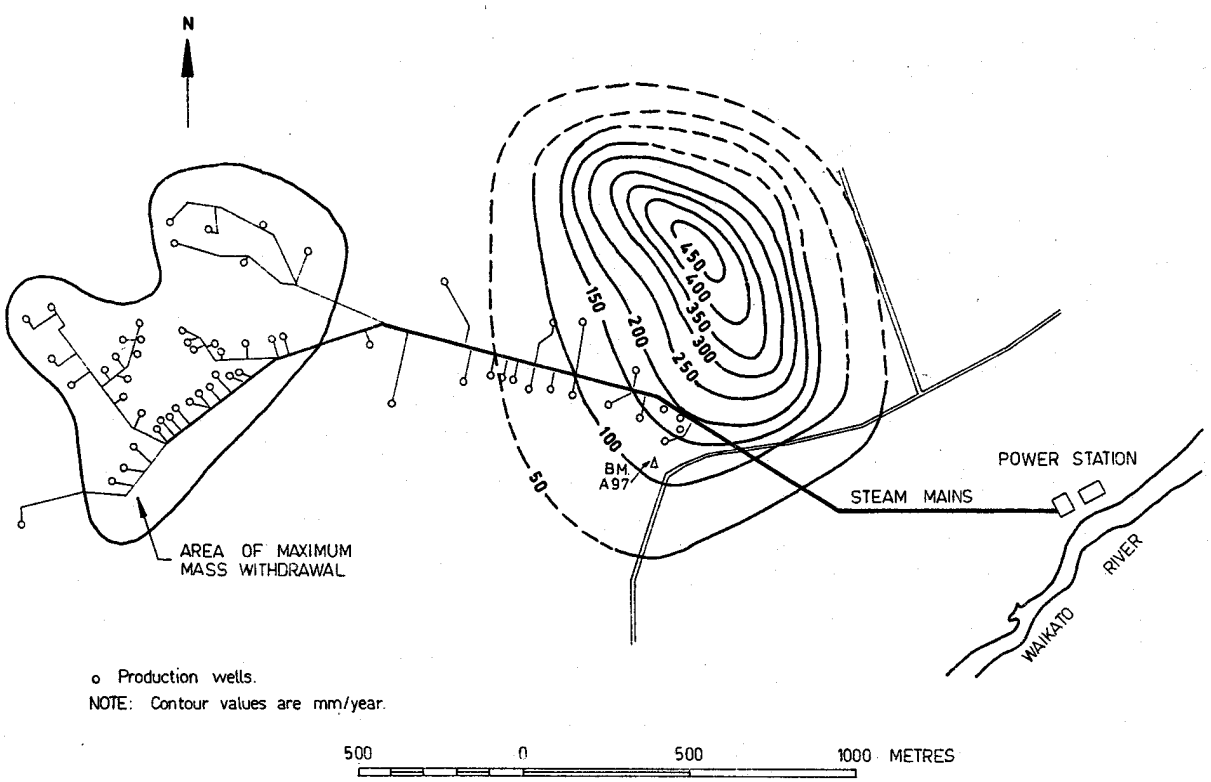

Figure 9.9.5 Subsidence rate in Wairakei production field, 1964-74. Redrawn from Figure 1, in Stilwell, Hall, and Tawhai, 1975, "Ground Movement in New Zealand Geothermal Fields," in Proceedings of Second U.N. Symposium on the Development and Use of Geothermal Resources: San Francisco, May 1975.

expansion. When these loops reach the limit of the travel, sections are either added or removed from the pipeline to restore the loops to their proper operating positions.

The waste water channels have a special sliding joint to allow movement between different sections of the reinforced concrete lining.

No measures are taken to control the rate or location of subsidence. Instead, the amount of subsidence and its effects are closely monitored in areas of economic interest and remedial action taken when installations are endangered.

9.9.12 ACKNOWLEDGMENT

The permission of Mr. N. C. McLeod, Commissioner of Works, to publish this paper is acknowledged.

9.9.13 REFERENCES

BOLTON, R. S. 1970. The behaviour of the Wairakei geothermal field during exploitation. Geothermics, Special Issue 2, pp. 1426-1439.

BROWNE, P. R. L. 1973. Geology, mineralogy and geothermometry of the Broadlands geothermal field, Taupo volcanic zone, New Zealand. Submitted for Ph.D. thesis at Victoria University of Wellington.

GRINDLEY, G. W. 1965. The geology, structure and exploitation of the Wairakei geothermal field, Taupo, New Zealand. Bulletin, N.Z. Geological Survey, 75.

HATTON, J. W. 1970. Ground subsidence of a geothermal field during exploitation. Geothermics, Special Issue 2, pp. 1294-1296.

MCNABB, A. 1977. Ground subsidence and reinjection. Internal report, Applied Maths Division, Department of Scientific and Industrial Research.

PRITCHETT, J. W. 1977. Geohydrological environmental effects of geothermal power production, phase IIA. Systems, Science and Software Report SSS-R-77-2998.

STILWELL, W. B., HALL, W. K., and J. TAWAHAI. 1975. Ground movement in New Zealand geothermal fields. Proceedings of second United Nations symposium on the development and use of geothermal resources.

Table 9.10.1 Aquifer characteristics

Aquifer	Location of tested well	Coefficient of transmissibility [m^2/hr]	Permeability [m/hr	Storage coefficient
Bangkok	Bang Pun	160	3.40	1.00×10^{-4}
Phra Pradaeng	Pom Phra	110	3.74	-
	Chun Navy Base			
	Phra Pradaeng	70	2.38	-
	Wat Phai Ngoen	120	2.38	1.00×10^{-4}
Nakhon Luang	Wat Phai Ngoen	65	2.21	1.00×10^{-4}
	Lum Phini Park	100	3.40	2.00×10^{-4}
	Pak Kret	110	2.55	-
	Bang Bua	125	3.45	2.2×10^{-4}
	Dept. of Mineral Resources	50	2.65	2.60×10^{-4}

Table 9.10.2.Ground water pumpage for public water supply in Bangkok[1]

Year	Pumping rate (m^3/day)	Year	Pumping rate (m^3/day)
1965	84,314	1971	331,966
1966	199,170	1972	318,276
1967	316,963	1973	362,738
1968	342,963	1974	370,032
1969	310,027	1975	350,000
1970	307,540	1976	345,000

[1]Source of data: Bangkok Metropolitan Water Works Authority.

Case History No. 9. 10. Bangkok, Thailand, compiled by Soki Yamamoto, Rissho University, Tokyo, Japan

9.10.1 GEOLOGIC FORMATIONS AND GROUND WATER

The Lower Central Plain, approximately 120 kilometres in width and 200 kilometres in length, was originally formed by the accumulation of clastic sediments more than 2,000 metres thick in the fault/flexure depression since Tertiary time (Figure 9.10.1).

The ground surface of Bangkok is entirely underlain by blue to gray marine clay up to 30 metres thick, known as the Bangkok Clay. The upper 15 metres of the Bangkok Clay, generally called the Bangkok Soft Clay, is very soft and highly compressible. The lower part, referred to as the Bangkok Stiff Clay, which is rather stiff and less compressible, extends to an average depth of 25-30 metres. The water in these clays is very saline and salty.

The water-bearing formations of Bangkok consist mainly of sands and gravels with minor clay lenses. They are similar in occurrence and composition but can be zoned according to the geoelectrical properties (Figure 9.10.2) into 8 principal artesian aquifers, separated by thick confining clay or sandy clay layers; namely:

Bangkok Aquifer (50 m zone),	Sam Khok Aquifer (300 m zone),
Phra Pradaeng Aquifer (100 m zone),	Phaya Thai Aquifer (350 m zone),
Nakhon Luang Aquifer (150 m zone),	Thon Buri Aquifer (450 m zone),
Nonthaburi Aquifer (200 m zone),	Pak Nam Aquifer (550 m zone).

Aquifer characteristics of three aquifers are listed in Table 9.10.1. These aquifers generally extend the full width and length of the Plain. Most wells in Bangkok penetrate the second, third and fourth aquifers because they are highly productive, with a Coefficient of Transmissibility of 40-130 m^2hr (150,000-250,000 gallons per day per foot), and yield water of relatively excellent quality. The first aquifer, immediately beneath the Bangkok Clay, gives saline water whereas the fifth and sixth aquifers are not popular due to their greater depths and water of inferior quality. The seventh and the eighth have been proved to yield fresh water but have been tapped by only few wells. The sediments at depths from 650 metres to the metamorphic basement rocks at about 2,000-3,000 metres have been indicated by electric well logging to yield brackish to saline water. In the northern part of the Lower Central Plain, however, fresh ground water could be obtained from the first aquifer.

Ground water has been exploited for domestic supply in Bangkok for the past six or seven decades, but heavy utilization began in 1957 when the surface water for domestic and industrial use could not meet demand. For many years, about one third of the total public water supply in Bangkok has come from the aquifers (Table 9.10.2.).

It is estimated that the present total pumpage for domestic and industrial use is as high as 700,000 m^3/day. This pumping rate exceeds the safe yield and brings about an acute problem of water level decline. At an early stage of development, the water level was about at the ground surface but it gradually fell until cones of depression developed in many areas. In 1958-1959 the water level in the center of Bangkok was about 8-9 metres from the ground surface while that in the suburbs was 4.5-6 metres. Since 1967 a remarkable change of water level could be observed. During 1968-1969 the depth to water level in heavily pumped area was 22-25 metres, and 10-12 metres in the suburbs. At present the general depth to water level is 30 metres while that at the center of the cone of depression is in excess of 33 metres (Figure 9.10.3). The annual rate of decline in the water level is now as high as 3-4 metres for the 100-metre, 150-metre and 200-metre aquifers. In the 50-metre aquifer the water level is also falling about 1 metre a year due to the interception of recharging water at the northern part of the Plain. The consequences of heavy pumpage are not only the over-draft of aquifers but also the salt water encroachment into the southern part of the Bangkok Metropolis and the possibility of land subsidence.

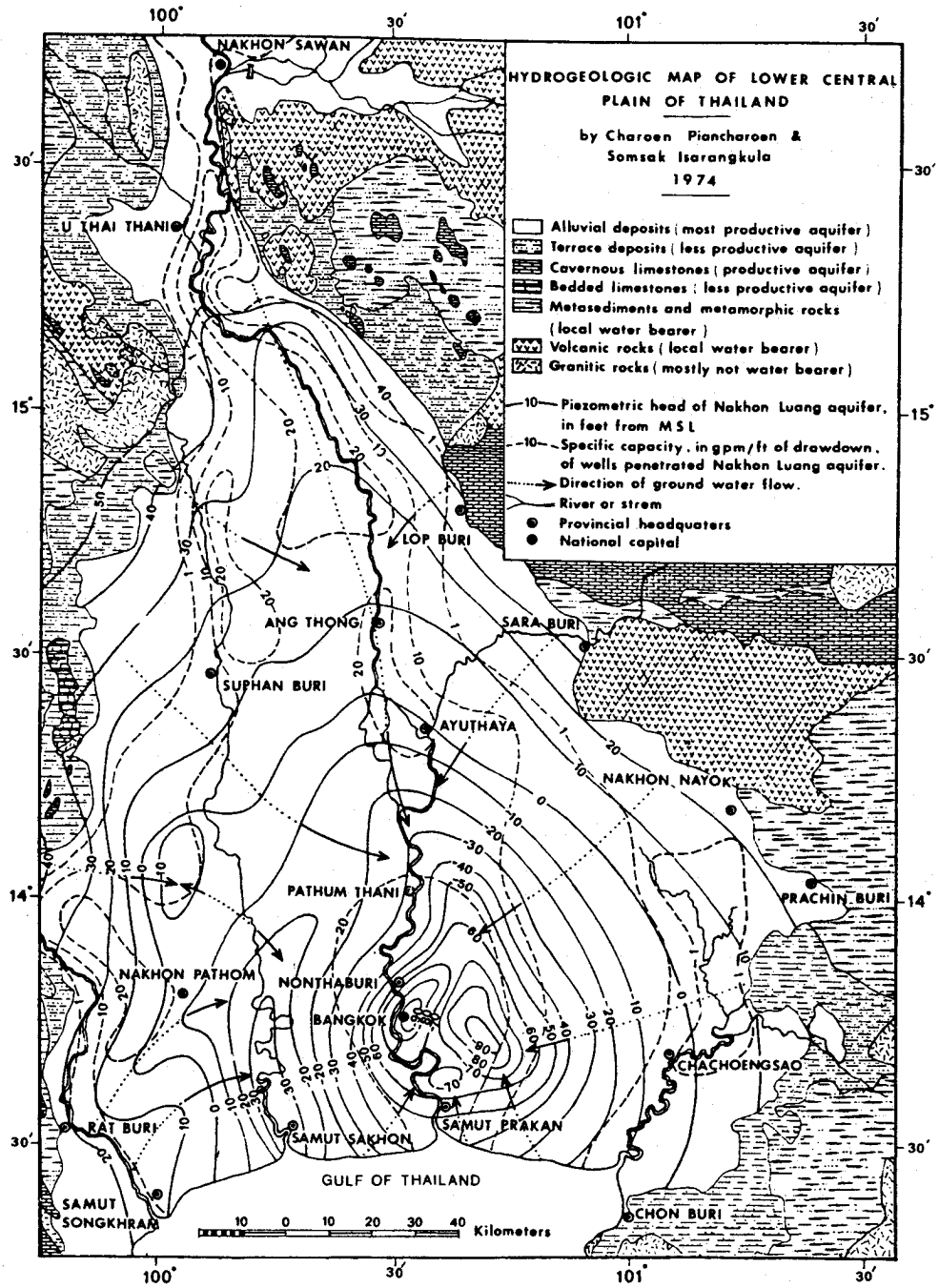

Figure 9.10.1 Hydrogeologic map of the Lower Central Plain of Thailand (after Piancharoen, 1977, Figure 1).

9.10.2 PROBLEMS OF LAND SUBSIDENCE

There is no serious damage due to land subsidence in Bangkok at the present time although flooding in localized areas is believed to be a result of a reduction in the altitude of the ground surface. However, the possibility of land subsidence due to the effect of deep well pumping has been spoken of by soil scientists for many years but no definite scientific proofs could be issued. No systematic investigation or observation leading to a reliable quantitative expression of subsidence behavior has been made to date.

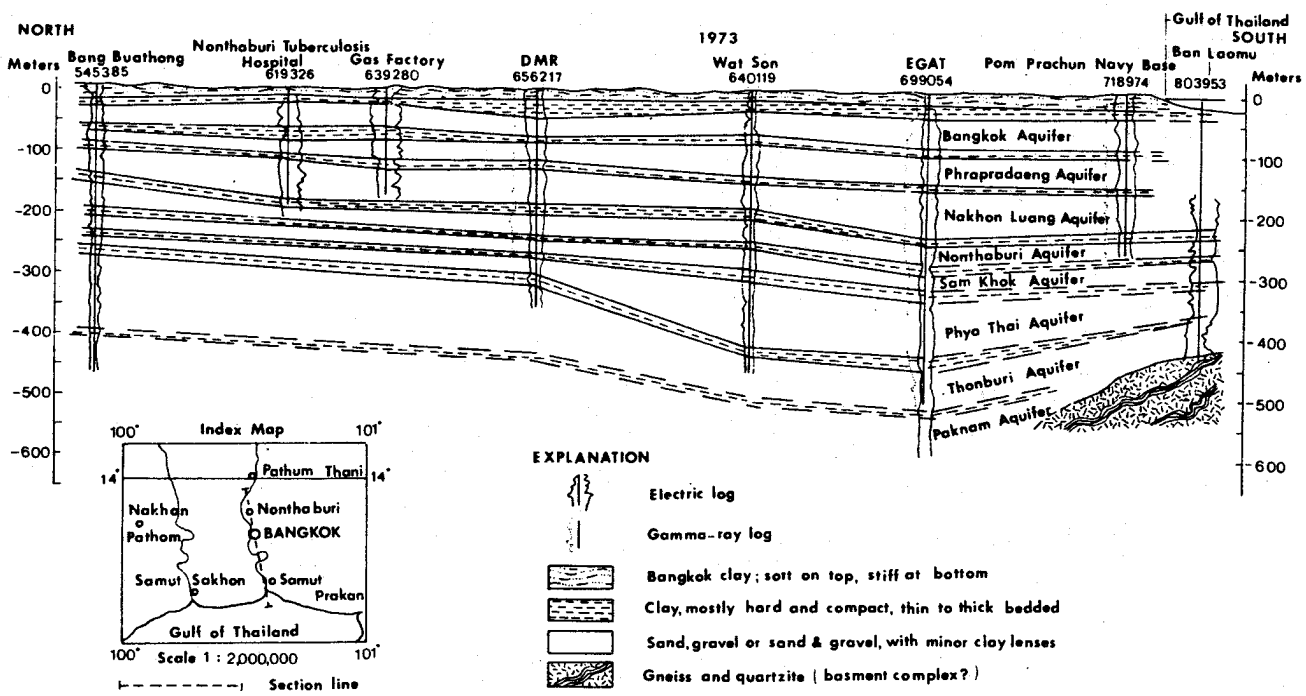

Figure 9.10.2 Hydrogeologic north-south section of the Lower Chao Phraya Delta showing principal aquifers of Bangkok Metropolis (correlated by electric and gamma-ray logs) (after Piancharoen, 1977, Figure 2).

9.10.3 INVESTIGATION PROGRAMS

Since the tests and accompanying evidence are far from conclusive, the problem of land subsidence and whether Bangkok is sinking is still debatable. Many geologists and hydrologists believe that the present deep well pumpage, mostly below 150 metres, has no effect on land subsidence, and if there is any subsidence external loads are to blame. Local flooding is also believed to be due to poor drainage in Bangkok. Three projects are now being submitted for consideration; namely, the leveling in the Bangkok Metropolitan Area for the investigation of land subsidence, the investigation of land subsidence caused by deep well pumping, and the development and management studies of ground water resources in the Bangkok area. These programs will be interrelated and aimed for completion within four years with a total budget of about 1.5 million U.S. dollars.*

9.10.4 SELECTED REFERENCES

PIANCHAROEN, C. 1977. Ground water and land subsidence in Bangkok, Thailand. IAHS. Pub. No. 121, pp. 355-364.

PIANCHAROEN, C., and C. CHUAMTHATSONG. 1978. Ground water of Bangkok Metropolis, Thailand. IAH Memoire, Vol. XI (Budapest), pp. 510-528.

---

* According to Dr. Prinya Nutalaya of the Asian Institute of Technology, progressive protrusion of water-well casings has been noted in Bangkok (oral communication to Joseph F. Poland, September 1978). This would suggest the beginnings of sediment compaction and land subsidence.

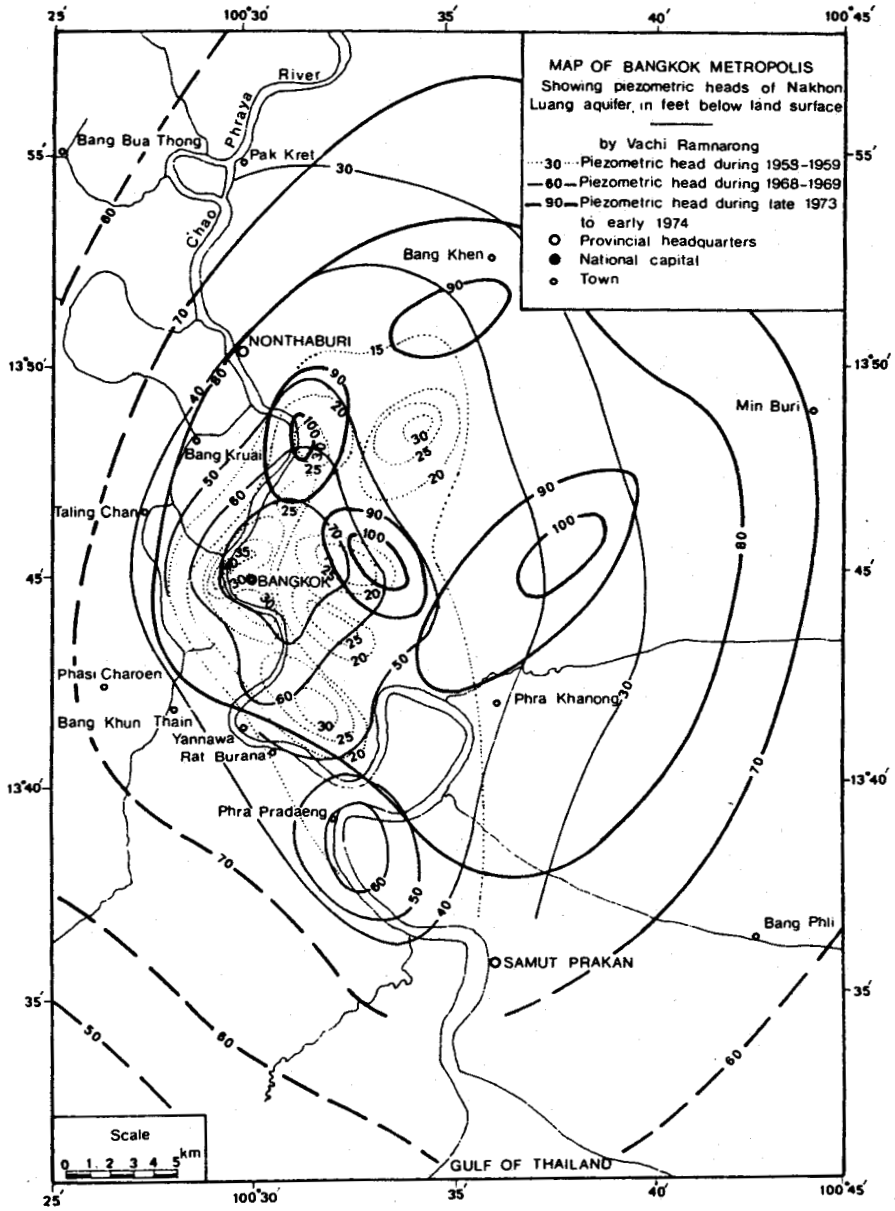

Figure 9.10.3 Water level map of the Nakhon Luang Aquifer (after Piancharoen, 1977, Figure 3).

Case History No. 9.11. Alabama, U.S.A., by J. G. Newton, U.S. Geological Survey, Tuscaloosa, Alabama

9.11.1 INTRODUCTION

Sinkholes in Alabama are divided into two categories defined as "induced" and "natural." Induced sinkholes are those related to man’s activities whereas natural sinkholes are not. Induced sinkholes are further divided into two types: those resulting from a decline in the water table due to ground-water withdrawals and those resulting from construction. Those resulting from a decline in the water table, the subject of this case history, far outnumber those resulting from all other causes. Information presented here consists of excerpts taken from five reports by the author. These reports, approved for publication by the Director, U.S. Geological Survey, are listed with the references cited in this case history. They resulted from investigations by the U.S. Geological Survey made in cooperation with the Geological Survey of Alabama and/or the Alabama Highway Department.

9.11.2 GEOLOGIC AND HYDROLOGIC SETTING

The terrane used to illustrate sinkhole development is a youthful basin underlain by carbonate rocks such as limestone and dolomite (Figure 9.11.1). The basin contains a perennial or near-perennial stream. This particular terrane is used because it is very similar to that of 10 active areas of sinkhole development in Alabama that have been examined by the author. Factors related to the development of sinkholes that have been observed in these areas are generally applicable to other carbonate terranes. The terrane illustrated differs from those examined only in the inclination of beds, which is shown as horizontal for ease of illustration.

The development of sinkholes is primarily dependent on past and present relationships between carbonate rocks and water, climatic conditions, vegetation, and topography, and on the presence or absence of residual or other unconsolidated deposits overlying bedrock. The source of water associated with the development of sinkholes is precipitation which, in Alabama, generally exceeds 1,270 mm annually. Part of the water runs off directly into streams, part replenishes soil moisture but is returned to the atmosphere by evaporation and transpiration, and the remainder percolates downward below the soil zone to ground-water reservoirs.

Water is stored in and moves through interconnected openings in carbonate rocks. Most of the openings were created, or existing openings along bedding planes, joints, fractures, and faults were enlarged by the solvent action of slighly acidic water coming in contact with the rocks. Water in the interconnected openings moves in response to gravity from higher to lower altitudes, generally toward a stream channel where it discharges and becomes a part of the streamflow.

Water in openings in carbonate rocks occurs under both water-table and artesian conditions; however, this study is concerned primarily with that occurring under water-table conditions. The water table is the unconfined upper surface of a zone in which all openings are filled with water. The configuration of the water table conforms somewhat to that of the overlying topography but is influenced by geologic structure, withdrawal of water, and variations in rainfall. The lowest altitude of the water level in a drainage basin containing a perennial stream occurs where the water level intersects the stream channel (Figure 9.11-1). Openings in bedrock underlying lower parts of the basin are water filled. This condition is maintained by recharge from precipitation in the basin. The water table underlying adjacent highland areas within the basin occurs at higher altitudes than the water table near the perennial stream. Openings in bedrock between the land surface and the underlying water table in highland areas are air filled (Figure 9.11.1).

The general movement of water through openings in bedrock underlying the basin, even though the route may be circuitous, is toward the stream channel and downstream under a gentle gradient approximating that of the stream. Some water moving from higher to lower altitudes is discharged through springs along flanks of the basin because of the intersection of the land surface and the water table. The velocity of movement of water in openings underlying most of the lowland

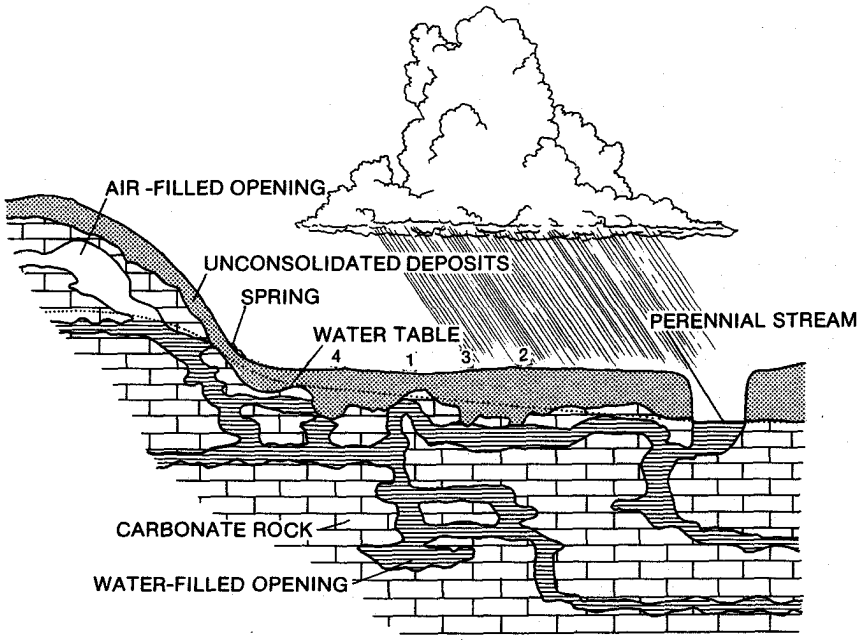

Figure 9.11.1 Schematic cross-sectional diagram of basin showing geologic and hydrologic conditions. (Numbers apply to sites described in report.)

area is probably sluggish when compared to that in openings at higher altitudes.

A mantle of unconsolidated deposits consisting chiefly of residual clay (residuum), that has resulted from the solution of the underlying carbonate rocks, generally covers most of the bedrock in the typical basin described. Alluvial or other unconsolidated deposits often overlie the residual clay. The residuum commonly contains varying amounts of chert debris that are insoluble remnants of the underlying bedrock. Some unconsolidated deposits are carried by water into openings in bedrock. These deposits commonly fill joints, fractures, or other openings enlarged by solution that underlie the lowland areas. The buried contact between the residuum and the underlying bedrock, because of differential solution, can be highly irregular (Figure 9.11.1).

9.11.3 CAUSE

A relationship between the formation of sinkholes and high pumpage of water from new wells was recognized in Alabama as early as 1933 (Johnston, 1933). Subsequent studies in Alabama (Robinson and others, 1953; Powell and LaMoreaux, 1969; Newton and Hyde, 1971; Newton and others, 1973; and Newton, 1976) have verified this relationship. Dewatering or the continuous withdrawal of large quantities of water from carbonate rocks by wells, quarries, and mines in numerous areas in Alabama is associated with extremely active sinkhole development. Numerous collapses in these areas contrast sharply with their lack of occurrence elsewhere.

Two areas in Alabama in which intensive sinkhole development has occurred and is occurring have been studied in detail. Both areas were made prone to the development of sinkholes by major declines of the water table due to the withdrawal of ground water. The formation of sinkholes in both areas resulted from the creation and collapse of cavities in unconsolidated deposits caused by the declines (Newton and Hyde, 1971; Newton and others, 1973). The growth of one such cavity in Birmingham has been photographed through a small adjoining opening (Newton, 1976).

Previous reports have described only indirectly or in part the hydrologic forces resulting from a decline in the water table that create or accelerate the growth of activities that collapse and form sinkholes. These forces, based on studies in Alabama (Newton and Hyde, 1971; Newton and others, 1973), are (a) a loss of support to roofs of cavities in bedrock previously filled with water and to residual clay or other unconsolidated deposits overlying openings in bedrock, (b) an increase in the velocity of movement of ground water, (c) an increase in the

amplitude of water-table fluctuations, and (d) the movement of water from the land surface to openings in underlying bedrock where recharge had previously been rejected because the openings were water filled. The same forces creating cavities and subsequent collapses also result in subsidence. The movement of unconsolidated deposits into bedrock where the strength of the overlying material is not sufficient to maintain a cavity roof, will result in subsidence at the surface (Donaldson, 1963).

To demonstrate forces that result in the development of cavities and their eventual collapse, a schematic diagram is shown in Figure 9.11.2 that illustrates changes in natural geologic and hydrologic conditions previously described and shown in Figure 9.11.1. A description of the forces triggered by a lowering of the water table follows.

The loss of buoyant support following a decline in the water table can result in an immediate collapse of the roofs of openings in bedrock or can cause a downward migration of unconsolidated deposits overlying openings in bedrock. The buoyant support exerted by water on a solid (and hypothetically) unsaturated clay overlying an opening in bedrock, for instance, would be equal to about 40 per cent of its weight. This determination is based on the specific gravities of the constituents involved. Site 1 on Figure 9.11.1 shows the unconsolidated deposit overlying a water-filled opening in bedrock. Site 1 on Figure 9.11.2 shows the decline in the water table and the resulting cavity in the deposit formed by the downward migration, of the unconsolidated deposit caused by the loss of support.

The creation of a cone of depression in an area of water withdrawal results in an increased hydraulic gradient toward the point of discharge (Figure 9.11.2) and a corresponding increase in the velocity of movement of water. This force can result in the flushing out of the finer grained unconsolidated sediments that have accumulated in the interconnected openings enlarged by solution. This movement also transports unconsolidated deposits migrating downward into bedrock openings to the point of discharge or to a point of storage in openings at lower altitudes.

The increase in the velocity of ground-water movement also plays an important role in the development of cavities in unconsolidated deposits. Erosion caused by the movement of water through unobstructed openings and against joints, fractures, faults, or other openings filled with clay or other unconsolidated sediments results in the creation of cavities that enlarge and eventually collapse (Johnston, 1933; Robinson and others, 1953).

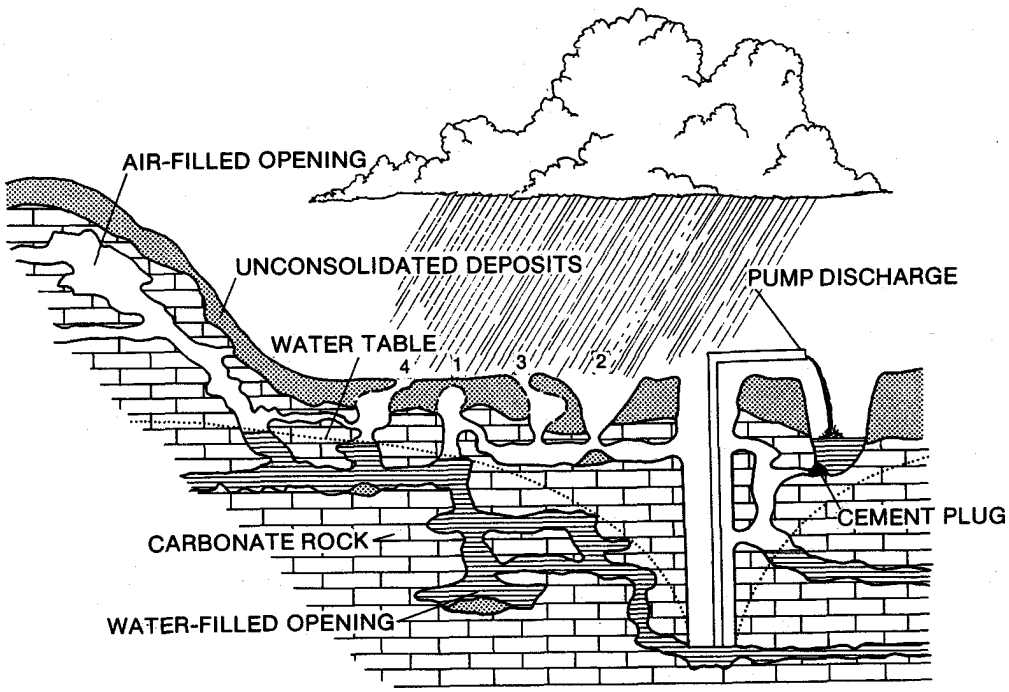

Figure 9.11.2 Schematic cross-sectional diagram of basin showing changes in geologic and hydrologic conditions resulting from water withdrawal. (Numbers apply to sites described in report.)

Pumpage results in fluctuations in ground-water levels that are of greater magnitude than those occurring under natural conditions. The magnitude of these fluctuations depends principally on variations in water withdrawal and on fluctuations in natural recharge. The repeated movement of water through openings in bedrock against overlying residuum or other unconsolidated sediments causes a repeated addition and subtraction of support to the sediments and repeated saturation and drying. This process might be best termed "erosion from below" because it results in the creation of cavities in unconsolidated deposits, their enlargement, and eventual collapse. Fluctuations of the water table against the roof of a cavity in unconsolidated deposits near Greenwood, Alabama, have been observed and photographed through a small collapse in the center of the roof. These fluctuations, in conjunction with the movement of surface water into openings in the ground, resulted in the formation of the cavity and its collapse (Newton and others, 1973).

A drastic decline of the water table in a lowland area (Figure 9.11.2) in which all openings in the underlying carbonate rock were previously water filled (Figure 9.11.1) commonly results in induced recharge of surface water. This recharge was partly rejected prior to the decline because the underlying openings were water filled. The quantity of surface water available as recharge to such an area is generally large because of the runoff moving to and through it from areas at higher altitudes.

The inducement of surface-water infiltration through openings in unconsolidated deposits interconnected with openings in underlying bedrock results in the creation of cavities where the material overlying the openings in bedrock is eroded to lower altitudes. Repeated rains result in the progressive enlargement of this type cavity. A corresponding thinning of the cavity roof due to this enlargement eventually results in a collapse. The position of the water table below unconsolidated deposits and openings in bedrock that is favorable to induced recharge is illustrated in Figure 9.11.2. Sites 2, 3, and 4 on Figure 9.11.2 illustrate a collapse and cavities in unconsolidated deposits that were formed primarily or in part by induced recharge. The creation and eventual collapse of cavities in unconsolidated deposits by induced recharge is the same process described by many authors as "piping" or "subsurface mechanical erosion" where it has been applied mainly to collapses occurring on noncarbonate rocks (Allen, 1969).

In an area of sinkhole development where a cone of depression is maintained by constant pumpage (Figure 9.11.2), all of the forces described are in operation even though only one may be principally responsible for the creation of a cavity and its collapse. For instance, the inducement of recharge from the surface (site 2 on Figure 9.11.2) where the water table is maintained at depths well below the base of unconsolidated deposits, can be solely responsible for the development of cavities and their collapse. In contrast, a cavity resulting from a loss of support (site 1 on Figure 9.11.2) can be enlarged and collapsed by induced recharge if it has intersected openings interconnected with the surface. In an area near the outer margin of the cone (site 4 on Figure 9.11.2), the creation of a cavity and its collapse can result from all forces. The cavity can originate from a loss of support; can be enlarged by the continual addition and subtraction of support and the alternate wetting and drying resulting from waterlevel fluctuations; can be enlarged by the increased velocity of movement of water; and can be enlarged and collapsed by water induced from the surface.

9.11.4 MAGNITUDE AND AREAL EXTENT

It is estimated that more than 4,000 induced sinkholes, areas of subsidence, or other related features have occurred in Alabama since 1900. Most of them have occurred since 1950. Almost all have resulted from a decline in the water table due to ground-water withdrawals.

Dewatering or the continuous withdrawal of large quantities of water from carbonate rocks by wells, quarries, and mines in numerous other areas in Alabama is associated with extremely active sinkhole development. Numerous collapses in these areas contrast sharply with their lack of occurrence in adjacent geologically and hydrologically similar areas where withdrawals of water are minimal. For example, in five areas examined by the author in north-central Alabama in Jefferson and Shelby Counties, an estimated 1,700 collapses, areas of subsidence, or other associated features have formed in a total combined area of about 36 km^2.

In Alabama, most induced sinkholes related to water withdrawals from wells, except those drilled specifically for dewatering purposes, were found within 150 m of the site of withdrawal. The yield of these wells commonly exceeds 22 l/s. Most sinkholes related to quarry operations were found within 600 m of the point of withdrawal; those related to mining operations can occur several kilometres from the point of withdrawal.

Recent collapses forming sinkholes in Alabama in areas in which large quantities of ground

water are being withdrawn generally range from 1 to 90 m in diameter and from 0.3 to 30 m in depth. The largest, located in a wooded area in Shelby County, apparently occurred in a matter of seconds in December 1972. The collapse was about 90 m in diameter and 30 m deep (Figure 9.11.3).

9.11.5 ECONOMIC IMPACT

Costly damage and numerous accidents have occurred or nearly occurred in Alabama as a result of collapses beneath highways, streets, railroads, buildings, sewers, gas pipelines, vehicles, animals, and people. Unfortunately, no inventory of costs or loss in property values has been made. The maintenance and protection of highways in sinkhole prone areas indicate costs resulting from their development. The cost of filling collapses, leveling pavement and monitoring subsidence along less than a kilometre of Interstate Highway 59 in Birmingham, Alabama, during the period 1972-77 is estimated to have exceeded $250,000 (L. Lockell, oral commun.). The estimated cost of bridging a, part of this area, and planned safety measures for highways crossing two similar areas near Birmingham exceeds $4,660,000 (C. Kelly, oral commun.). The need for these protective measures is well illustrated by the damage to a warehouse in 1973 (Figure 9.11.4) that resulted from a collapse adjacent to Interstate Highway 59 in Birmingham.

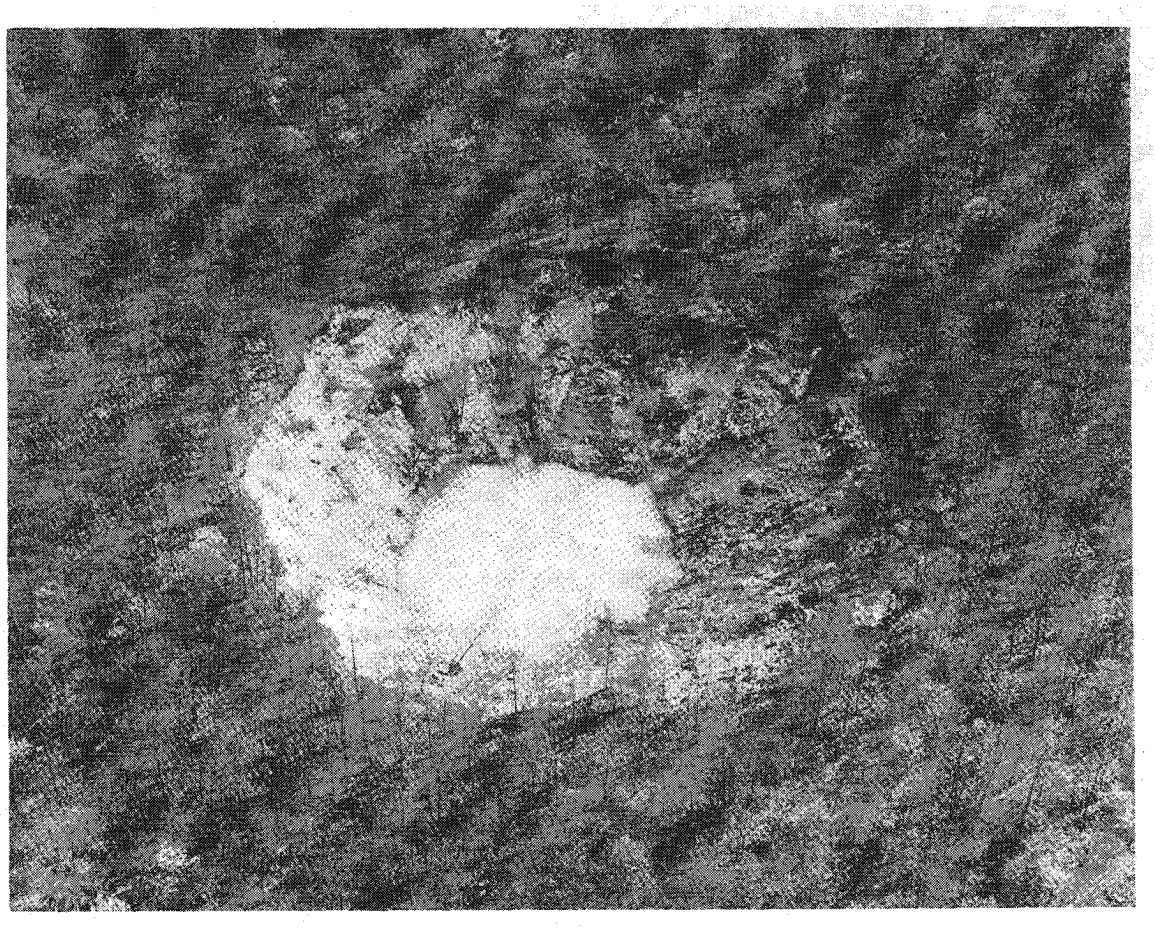

Figure 9.11.3 Sinkhole resulting from collapse near Calera in Shelby County, Alabama (photograph by Curtis Frizzell).

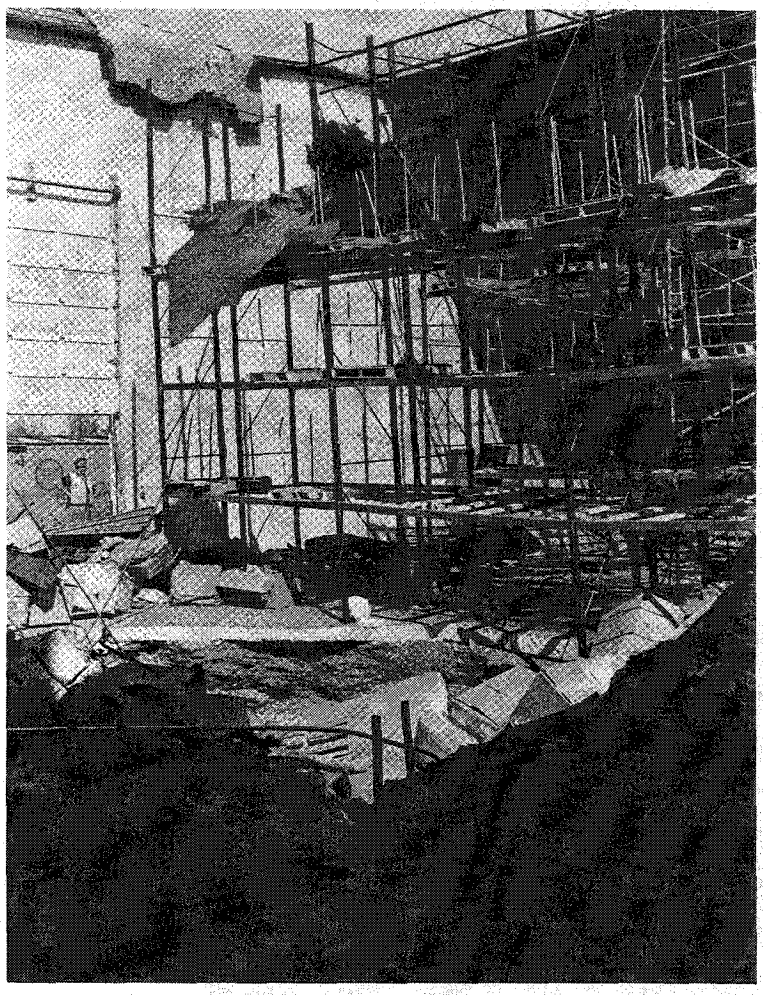

Figure 9.11.4 Collapse in warehouse near Interstate Highway 59 in Birmingham, Alabama (photograph by T. V. Stone).

9.11.6 CORRECTIVE MEASURES

Ideally, the development of sinkholes can be eliminated or minimized by ceasing the pumpage that causes the decline of the water table. The cessation of or drastic decrease in sinkhole activity following a recovery of the water table has been recognized previously (Foose, 1953; Newton and Hyde, 1971; Newton, 1976). Most efforts in Alabama have been directed toward measures minimizing sinkhole development and eliminating potential hazards and damage to structures rather than dealing with the cause. The measures that have been or will be utilized include bridging, adding additional support, the removal of unconsolidated deposits overlying bedrock, grouting, minimizing the diversion of natural drainage, and the construction of flumes and other impermeable drainage systems.

9.11.7 REFERENCES CITED

ALLEN, A. S. 1969. Geologic settings of subsidence, in Reviews in engineering geology: Geol. Soc. America, v. 2, p. 305-342.

DONALDSON, G. W. 1963. Sinkholes and subsidence caused by subsurface erosion: Regional Conf. for Africa on Soil mechanics and Foundation Eng., 3rd, Salisbury, Southern Rhodesia 1963 Proc., p. 123-125.

FOOSE, R. M. 1953. Ground-water behavior in the Hershey Valley, Pennslyvania: Geol. Soc. America Bull. 64, p. 623-645.

JOHNSTON, W. D., Jr. 1933. Ground water in the Paleozoic rocks of northern Alabama: Alabama Geol. Survey Spec. Rept. 16, 441 p.

NEWTON, J. G. 1976. Early detection and correction of sinkhole problems in Alabama, with a preliminary evaluation of remote sensing applications: Alabama Highway Dept., Bur. Research and Devel., Research Rept. No. HPR-76, 83 p.

_____., 1976. Induced and natural sinkholes in Alabama--a continuing problem along highway corridors, in Subsidence over mines and caverns, moisture and frost action, and classification: Natl. Acad. Sci. Transp. Research Rec. 612, p. 9-16.

_____., 1977. Induced sinkholes--a continuing problem along Alabama highways, in Proceedings of second international symposium on land subsidence: Internat. Assoc. Hydrol. Sci. Pub. No. 121, p-. 453-463.

NEWTON, J. G., and HYDE, L. W. 1971. Sinkhole problem in and near Roberts Industrial Subdivision, Birmingham, Alabama--a reconnaissance: Alabama Geol. Survey Circ. 68, 42 p.

NEWTON, J. G., COPELAND, C. W., and SCARBROUGH, L. W. 1973. Sinkhole problem along proposed route of Interstate Highway 459 near Greenwood, Alabama: Alabama Geol. Survey Circ. 83, 53 p.

POWELL, W. J., and LAMOREAUX, P. E. 1969. A problem of subsidence in a limestone, terrane at Columbiana, Alabama: Alabama Geol. Survey Circ. 56, 30 p.

ROBINSON, W. H., IVEY, J. B., and BILLINGSLEY, G. A. 1953. Water supply of the Birmingham area, Alabama: U.S. Geol. Survey Circ. 254, 53 p.

Case History No. 9.12. The Houston-Galveston Region, Texas, U.S.A., by R. K. Gabrysch, U.S. Geological Survey, Houston, Texas

9.12.1 INTRODUCTION

The Houston-Galveston region of Texas, as described in this report, includes all of Harris and Galveston Counties and parts of Brazoria, Fort Bend, Waller, Montgomery, Liberty, and Chambers Counties (Figure 9.12.1). Land-surface subsidence has become critical in parts of the region because some low-lying areas along Galveston Bay are subject to inundation by normal tides, and an even larger part of the region may be subject to catastrophic flooding by hurricane tides. Hurricanes resulting in tides of 3.0-4.6 metres above sea level strike the Texas coast on the average of once every 10 years.

Land-surface subsidence due to fluid withdrawals was first documented in the Goose Creek oil field in Harris County (Pratt and Johnson, 1926). Since then, numerous reports on subsidence in the Houston-Galveston region have attributed subsidence to the compaction of fine-grained material associated with the oil- and water-bearing sands. The more recent reports (Winslow and Doyel, 1954; Winslow and Wood, 1959; Gabrysch, 1969; and Gabrysch and Bonnet, 1975a) present data and interpretations of regional subsidence and its relation to the withdrawals of ground water for municipal supply, industrial use, and irrigation. The authors of these reports recognized that subsidence due to the removal of oil and gas has occurred in the region, but the data are not sufficient to describe in detail the localized areas of occurrence.

9.12.2 GEOLOGY AND HYDROLOGY OF THE HOUSTON-GALVESTON REGION

The aquifers in the Houston-Galveston region are composed of sand and clay beds that are not persistent in either lithology or thickness. The beds grade into each other both laterally and vertically within short distances; consequently, differentiation of geological formations on drillers' logs and electrical logs is almost impossible. However, by use of both the logs and the hydraulic properties of the aquifers, the subsurface units have been divided into three major aquifer systems and one confining system (Jorgensen, 1975).

The age of the geological formations composing the aquifers and the confining layer ranges from Miocene to Holocene. The deepest aquifer containing freshwater is the Jasper aquifer of Miocene age, which is separated from the overlying Evangeline and Chicot aquifers by the Burkeville confining layer. The two principal aquifer systems of the region are the Chicot aquifer of Pleistocene age and the Evangeline aquifer of Pliocene age. The Burkeville confining layer is probably part of the Fleming Formation of Miocene age.

The aquifers are under artesian conditions throughout most of the region, but little information on the hydraulic properties of the Jasper aquifer is available because it is undeveloped. Reports of test holes in the Jasper (W. F. Guyton, oral commun., 1977) indicate that the hydraulic head in the Jasper is above land surface, which probably approximates the original conditions. It is assumed that with no change in head, compaction of the deposits in the Jasper system has not occurred; therefore, the discussion of subsidence in this report will be restricted to a discussion of the Evangeline and Chicot aquifer systems.

The Evangeline aquifer system is composed of the Goliad Sand and possibly the upper part of the Fleming Formation. The system contains sands that yield freshwater of good quality in about the inland two-thirds of the region. The transmissivity of the aquifer system ranges from less than 460m^2/d to about 1,400 m^2d. The horizontal hydraulic conductivity is about 4.57 metres per day, and the storage coefficient ranges from about 0.00005 to more than 0.001.

The Chicot aquifer system is composed of the Willis Sand, Bentley Formation, Montgomery Formation, Beaumont Clay, and the Quaternary alluvium and includes the deposits from the land surface to the top of the Evangeline aquifer. The transmissivity of the Chicot aquifer ranges from 0 to about 1,858 m^2/d. The horizontal hydraulic conductivity is about twice that of the Evangeline aquifer, and the storage coefficient ranges from 0.00004 to 0.20. The larger values

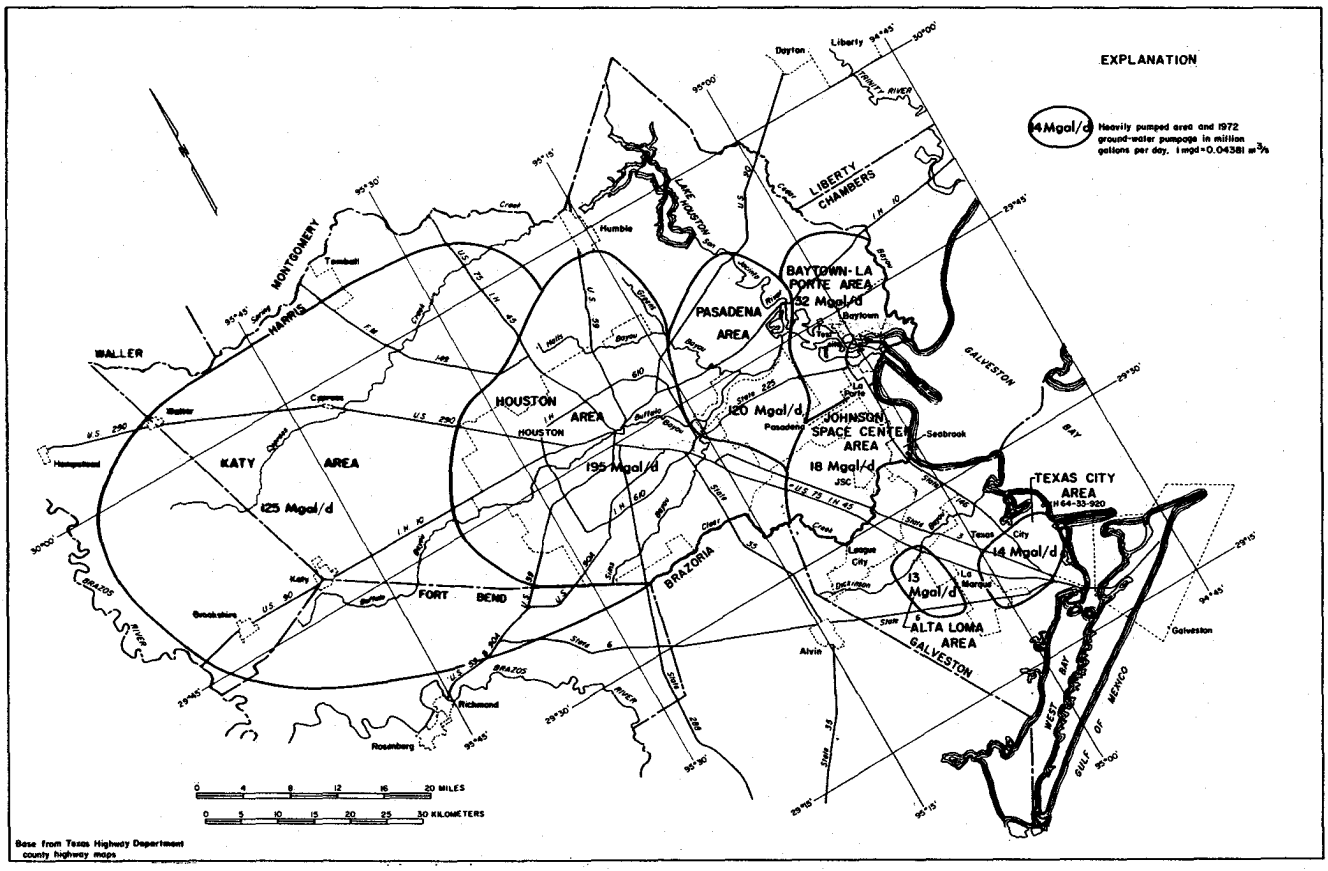

Figure 9.12.1 Locations of principal areas of ground-water withdrawals and average rates of pumping in 1972.

of the storage coefficient occur in the northern part of the region where the aquifer crops out and is partly under water-table conditions.

Both the Evangeline and the Chicot aquifer systems contain many layers of clay interbedded with the water-bearing sands. The clay beds are generally less than 6 metres thick, but locally they retard the vertical movement of water. Every sand bed, therefore, has a different hydraulic head. Data from cores of the clay beds were obtained at six sites for evaluation of subsidence in the Houston-Galveston region. The mineral composition of 27 samples from 5 sites were also determined (Gabrysch and Bonnet, 1975b and unpublished data). Montmorillonite is the principal mineral constituent of the clay beds, which also contain smaller amounts of illite, chlorite, and kaolinite.

9.12.3 DEVELOPMENT OF GROUND WATER

Development of ground water in the Houston-Galveston region for municipal supply and irrigation began in the 1890's. Ground-water withdrawals increased gradually to about 4.4 M^3/s (cubic metres per second) with population growth, increased irrigation, and industrial use until the late 1930's. Construction of the large industrial complex in the region began in 1937, and by 1954 ground-water pumping had increased to about 18 m^3/s.

Ground-water pumping decreased to about 14 m^3/s by 1959 because of the introduction of a supply of surface water in 1954 from nearby Lake Houston on the San Jacinto River. By 1962, ground-water pumping was again at a rate of about 18 m^3/s.

Pumping of ground water for municipal supply, industrial use, and irrigation was approximately 46 per cent, 33 per cent, and 21 per cent, respectively, of the total of 23 m^3/s pumped in 1972. The principal areas of pumping and the average daily rates of pumping in 1972 in each area are shown on Figure 9.12.1. Pumping in 1975 for all uses was 22 m^3/s.

The pumping of larger amounts of ground water has resulted in water-level declines during 1943-73 of as much as 61 metres in wells completed in the Chicot aquifer and as much as 99 metres in wells completed in the Evangeline aquifer (Figures 9.12.2 and 9.12.3). The maximum average annual rate of water-level decline for 1943-73 was 2.0 metres in the Chicot aquifer and 3.3 metres in the Evangeline aquifer. During 1964-73, the maximum rate of decline was 3.0 metres in the Chicot and 5.4 metres in the Evangeline.

9.12.4 SUBSIDENCE OF THE LAND SURFACE

The area of the greatest amount of subsidence coincides with the area of the greatest amount of artesian-pressure decline, which is east-southeast of Houston at Pasadena. Figure 9.12.4 shows that as much as 2.3 metres of subsidence occurred at Pasadena between 1943 and 1973. It should be noted, however, that within the entire region of subsidence, more than one center occurs. These areas are indicated by the closed contours on Figure 9.12.4.

Some of the centers of subsidence may be associated with the pumping of oil and gas and some may be associated with the pumping of ground water. Additional complications in analyzing the causes and areal distribution of subsidence result from the varying thicknesses of individual beds of fine-grained material, the varying total thickness of fine-grained material, the vertical distribution of changes in artesian head, and the relation of compressibility to depth of burial. An example of the effects of compressibility and depth of burial occurs in the southern part of Harris County where about 55 per cent of the subsidence is due to compaction in the Chicot aquifer, which composes only the upper one-fourth of the estimated compacting interval.

Figure 9.12.5 shows subsidence for 1964-73. The maximum amount of subsidence during this period was about 1.1 metres. The indicated maximum average rate for the 9-year period is about 0.12 metre per year as compared to the maximum average rate of 0.08 metre per year for the 30 year period 1943-73. During the last part of the 1943-73 period, the rate of subsidence accelerated, and the area of subsidence increased. The area in which subsidence is 0.3 metre or more increased from about 906 square kilometres in 1954 to about 6,475 square kilometres in 1973.

The maps showing the amounts of subsidence (Figures 9.12.4 through 9.12-6) were constructed from data obtained from the leveling program of the National Geodetic Survey (formerly the U.S. Coast and Geodetic Survey) supplemented by data obtained from local industries. Some subsidence occurred before 1943, but the amount is difficult to determine. However, an approximation of the amount and extent of the subsidence that occurred between 1906 and 1943 is shown on Figure 9.12.6. By 1943, four centers of subsidence were apparent. The centers at Pasadena, Baytown, and Texas City were the result of ground-water pumping; and the center in the Goose Creek oil field resulted from the production of oil, gas, and saltwater.

Because of the nature of deposition of the aquifer systems, each sand bed has a different hydraulic head, and each clay layer is under a different amount of stress. The water-level declines shown by Figures 9.12.2 and 9.12.3 are the maximum declines that have occurred in each of the aquifers. Water-level measurements indicate that the water table is approximately at its original position (about 2 to 6 metres below land surface). Piezometers installed at different depths at each of eight sites are used to define the potentiometric profiles. The differences between the measurements in the piezometers and the original potentiometric surfaces define the stress profile. As an example, at a site in the Pasadena area, the depths to water below land surface in January 1978 were as follows:

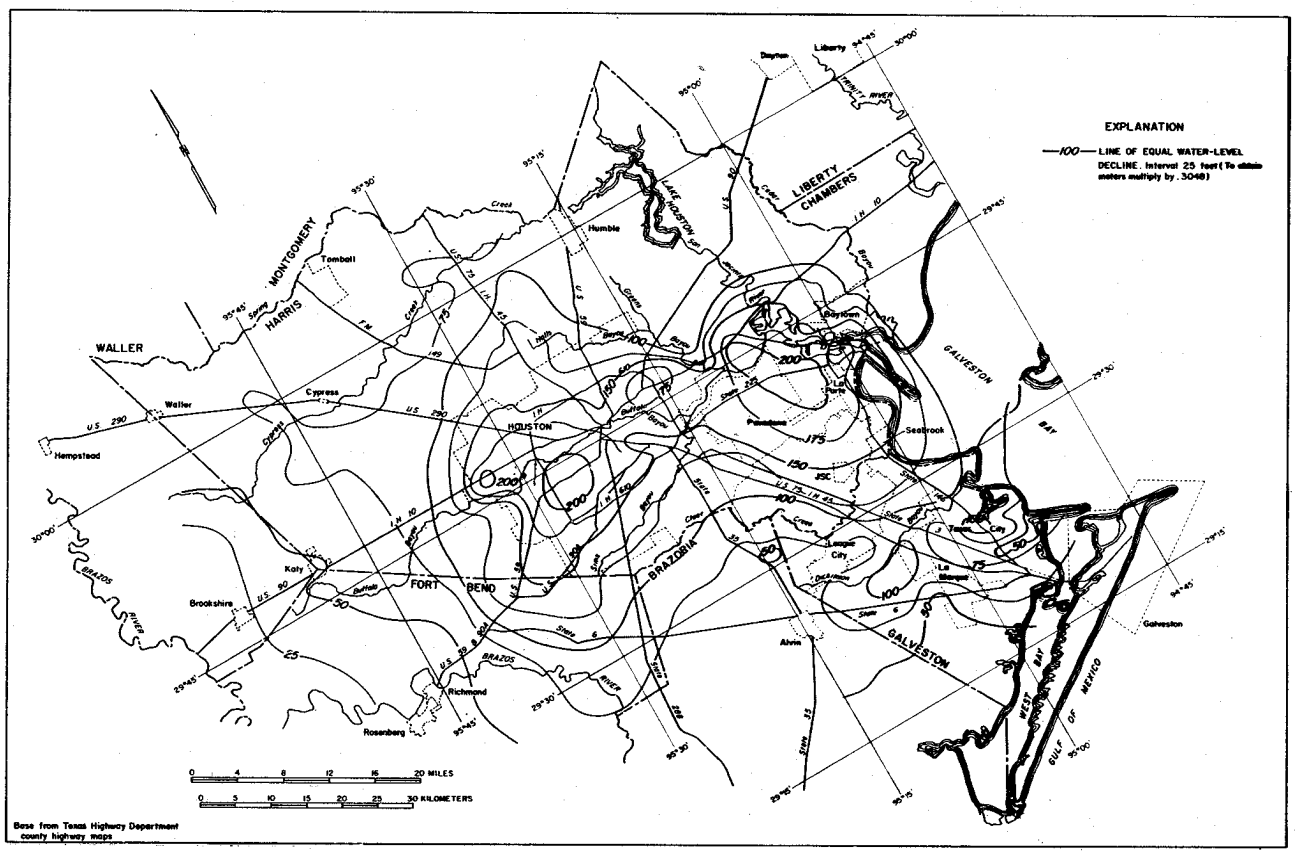

Figure 9.12.2 Approximate declines of water levels in wells completed in the Chicot aquifer, 1943-73.

Piezometer depth (metres)	Depth to water (metres)
10	1.85
30	4.31
119	45.21
221	100.31
284	102.74
403	100.44
552	93.20
828	47.28

The potentiometric surface in each of the two aquifer systems was 15 to 30 metres above land surface before large withdrawals began.

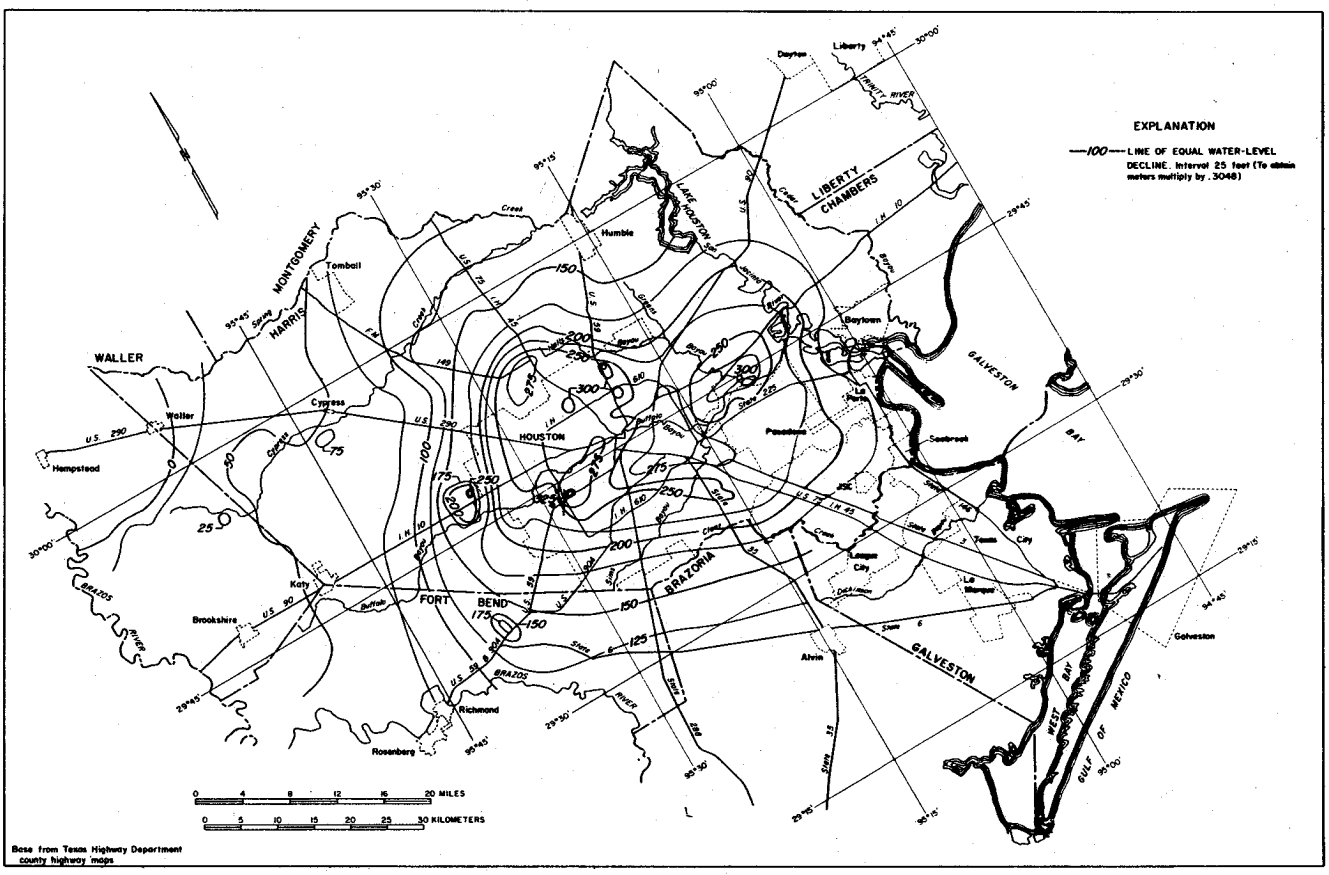

Figure 9.12.3 Approximate declines of water levels in wells completed in the Evangeline aquifer, 1943-73.

The compressibility of the aquifer system has been estimated at two locations. At Seabrook, it is assumed that no compaction due to ground-water pumping occurred below a depth of about 610 metres. Above 610 metres, the sediments include about 243.5 metres of fine-grained material, and the average stress applied to the system during 1943-73 was estimated to be a change in head of 38.6 metres of water. Subsidence during 1943-73 was 0.91 metre; therefore, the compressibility of the fine-grained materials was determined to be

$$0.91\ \text{m}/(243.5\ \text{m})\ (38.6) = 9.7 \times 10^{-5}\text{m}^{-1}.$$

At Texas City, it is assumed that no compaction due to ground-water pumping occurred below a depth of 506 metres. Above 506 metres, the sediments include about 151.5 metres of fine-

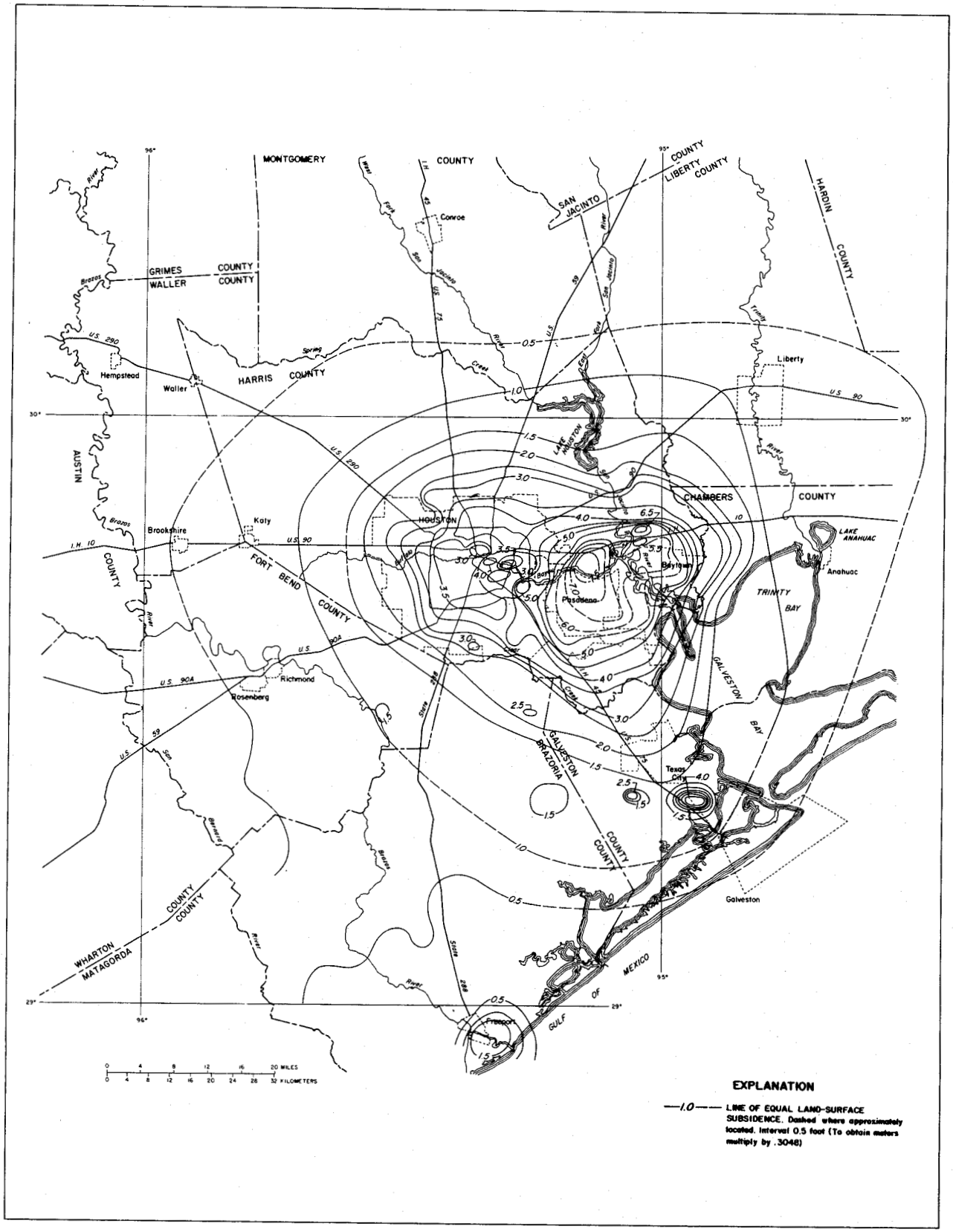

Figure 9.12.4 Subsidence of the land surface, 1943-73.

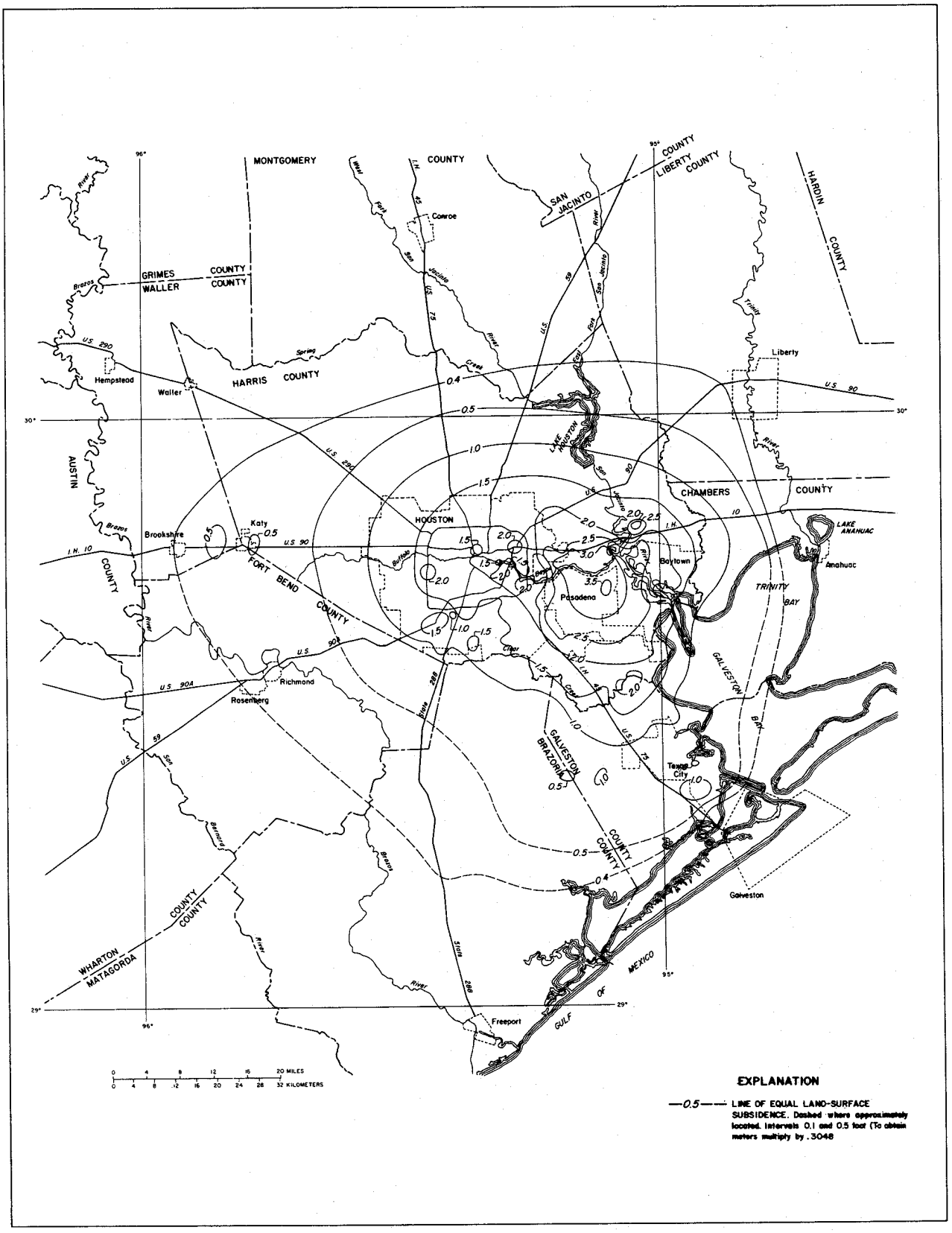

Figure 9.12.5 Subsidence of the land surface, 1964-73.

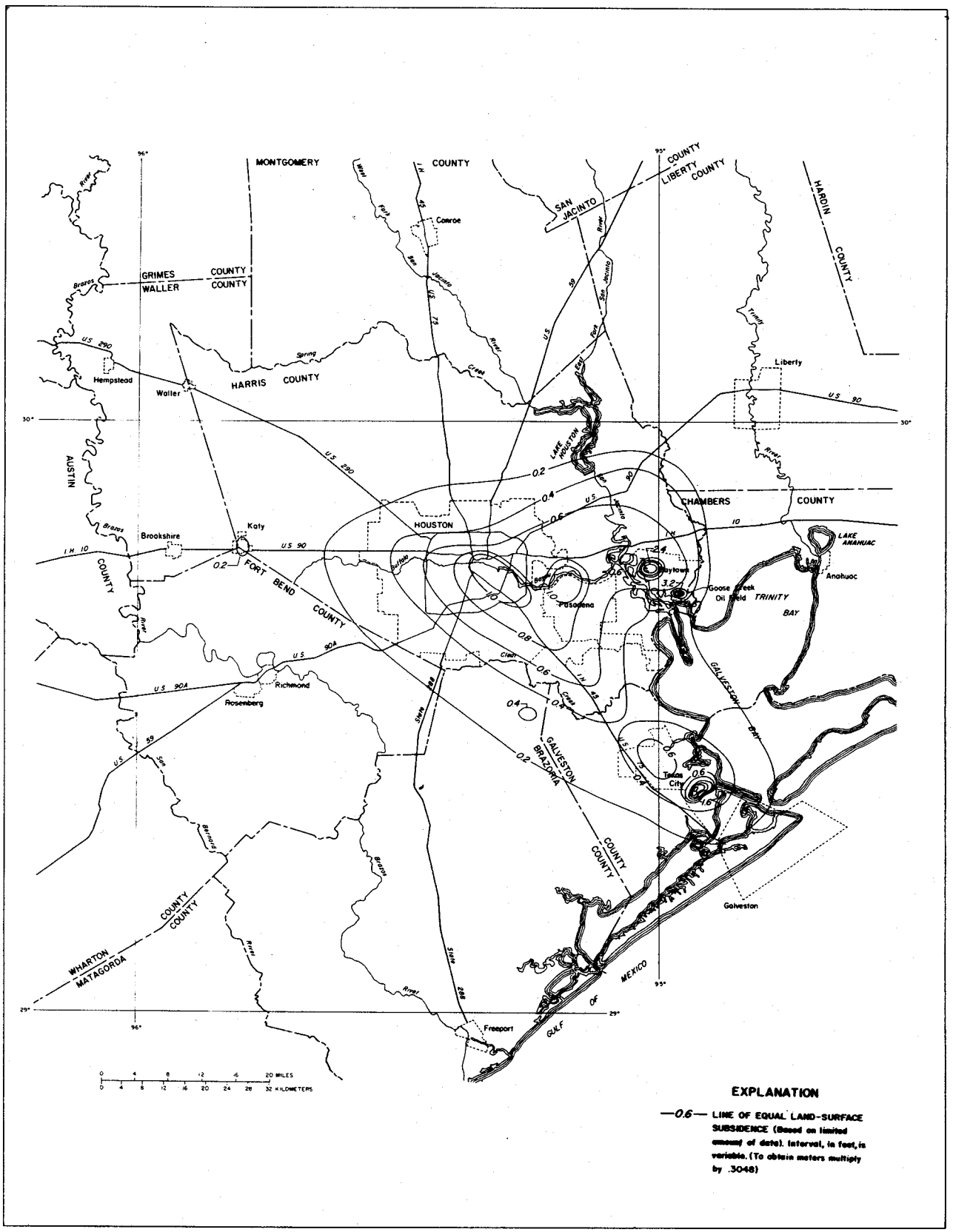

Figure 9.12.6 Approximate subsidence of the land surface, 1906-43.

grained material, and the average stress applied to the system during 1964-73 was estimated to be a change in head of 5.7 metres of water. Subsidence during 1964-73 was 0.18 metre; therefore, the compressibility of the fine-grained material was determined to be:

$$0.18/(151.5\ m)\ (5.7\ m) = 2.1 \times 10^{-4} m^{-1}.$$

The weighted average compressibility as determined by laboratory consolidation tests of 15 cores from three sites was $3.2 \times 10^{-4} m^{-1}$. Because the sediments were still undergoing compression, the compressibilities determined at the Seabrook and Texas City sites are minimum estimates of specific storage.

It has been suggested by some investigators that, in addition to inundation of land by tidal waters, some if not all of the numerous existing faults in the Houston-Galveston region are reactivated by man-caused land-surface subsidence. Attempts have been made to relate the fault activity to subsidence, but because of a lack of data the relationships are not clear.

In 1977, a network of measurement stations, about 0.6 kilometre apart, were established along a line about 70 kilometres long from the approximate center of subsidence westward along U.S. Highway 90 to the Harris County boundary. In addition, closely spaced marks for horizontal and vertical control will be established at three active faults. The purpose of this network is to measure horizontal strain associated with subsidence and to relate this strain to movement along the fault planes.

It has also been hypothesized (Kreitler, 1977) that the numerous faults act as partial barriers to ground-water flow and therefore control or "compartmentalize" subsidence; however, the data on artesian-pressure fluctuations in the area do not support this hypothesis.

Most of the damage resulting from subsidence is related to the lowering of land-surface elevations in the vicinity of Galveston Bay and the subsequent inundation by tidal waters. Several roadways have been rebuilt at higher elevations; ferry landings have been rebuilt; and levees have been constructed to reclaim or protect some areas. The cost of the damages resulting from subsidence have been estimated in some areas, but comprehensive studies for the entire region have not been made. Jones and Larson (1975, table 5) estimated the annual cost of subsidence during 1969-74 to be $31,705,040 in 2,448 square kilometres of the area most severely affected by subsidence. In their estimate of costs, Jones and Larson attributed fault-caused structural damage to man-caused subsidence.

One outstanding example of both the social and economic impacts of subsidence is in the Brownwood subdivision on the west side of Baytown. The area of the subdivision has subsided more than 2.4 metres since 1915, and some homes in the subdivision are permanently flooded by water from the bay. The U.S. Army Corps of Engineers has recommended that the entire subdivision, consisting of 448 homes occupied by 1,550 residents, be purchased by the Federal Government and the inhabitants be relocated at a cost of about $40 million.

9.12.5 FUTURE SUBSIDENCE IN THE REGION

Ground-water pumping in the Houston-Galveston region increased at a rate of about 6 per cent per year before about 1967. Since then, ground-water pumping has been at an almost stable rate, possibly because of recirculation of cooling water by industry and increased use of surface water from Lake Houston. As a result, the rate of decline in water levels has decreased significantly in many parts of the region since the early 1970’s. Records from borehole extensometers (compaction monitors) indicate a decreased rate of subsidence at seven sites scattered throughout the region. The decrease in the rate of subsidence, which began about September 1976, strongly suggests a reflection of the decreased rate of water-level decline.

Water from a new source, Lake Livingston on the Trinity River, about 97 kilometres east of Houston has become available recently; and voluntary commitments to purchase this water have been made by all major industries using ground water in the southern half of Harris County. As a result, ground-water pumping will decrease by about 3.1 m^3/s in the area of maximum artesian-pressure decline and subsidence. An analog-model study of the effects of the decreased pumping suggests a maximum water-level recovery of about 30 metres in the center of the bowl of subsidence. Data are not sufficient to determine the head recovery necessary to stop subsidence, but the rate of subsidence is expected to decrease substantially. By June 1977, the increased use of surface water had caused a decrease in ground-water pumping of about 0.8 m^3/s. Locally, the recovery in artesian head has been as much as 18 metres.

The Harris-Galveston Coastal Subsidence District was created by the Texas Legislature in 1975 to "provide for the regulation of the withdrawal of ground water within the boundaries of

the District for the purpose of ending subsidence which contributes to or precipitates flooding, inundation, or overflow of any area within the District, including without limitation rising waters resulting from storms or hurricanes." The District plans to monitor the stress-strain relationships with additional compaction monitors and piezometers designed for installation prior to the expected voluntary decrease in ground-water pumping. The data collected will be the basis for controlling pumping by the issuance of well permits.

The constitutionality of the subsidence district has been tested in a Texas District Court in a suit titled Sammy Beckendorf, et al., versus the Harris-Galveston Coastal Subsidence District. The District prevailed, but Beckendorf, et al., have appealed the ruling of the court. Other lawsuits against the District have been filed but have not come to trial. Two other lawsuits (Smith-Southwest Industries, et al., versus Friendswood Development Company, et al.; and E. R. Brown, et al., versus Exxon Company, U.S.A., et al.), whereby the plaintiffs seek to establish blame and recover damages from subsidence, have not come to trial.

9.12.6 SELECTED REFERENCES

AMERICAN OIL COMPANY. 1958. Refinery ground subsidence: Plant Engineering Dept., Texas City, Texas, 58p.

GABRYSCH, R. K. 1969. Land-surface subsidence in the Houston-Galveston region, Texas: Internat. Symp. on Land Subsidence, Tokyo, Japan, proc., IASH Pub. no. 88, v. 1, p. 43-54.

GABRYSCH, R. K., and BONNET, C. W. 1975a. Land-surface subsidence in the Houston-Galveston region, Texas: Texas Water Devel. Board Rept. 188, 19 p.

_____. 1975b. Land-surface subsidence at Seabrook, Texas: U.S. Geol. Survey Water Resources Inv. 76-31, 53 p.

JONES, L. L., and LARSON, J. 1975. Economic effects of land subsidence due to excessive ground water withdrawal in the Texas Gulf Coast area: Texas Water Resources Inst., Texas A&M Univ., TR-67, 33 p.

JORGENSEN, D. G. 1975. Analog-model studies of ground-water hydrology in the Houston district, Texas: Texas Water Devel. Board Rept. 190, 84 p.

KREITLER, C. W. 1977. Fault control of subsidence, Houston, Texas: Ground Water, v. 15, no. 3, p. 203-214.

PRATT, W. E., and JOHNSON, D. W. 1926. Local subsidence of the Goose Creek Oil Field: Jour. Geology, v. XXXIV, no. 7, pt. 1, p. 578-590.

WINSLOW, A. G., and DOYEL, W. W. 1954. Land-surface subsidence and its relation to the withdrawal of ground water in the Houston-Galveston region, Texas: Econ. Geology, v. 49, no. 4, p. 413-422.

WINSLOW, A. G., and WOOD, L. A. 1959. Relation of land subsidence to ground-water withdrawals in the upper Gulf coast region, Texas: Mining Eng., Oct., p. 1030-1034; Am. Inst. Mining Metall. Petroleum Engineers Trans., v. 214.

Case History No. 9.13. San Joaquin Valley, California, U.S.A., by Joseph F. Poland, U.S. Geological Survey, Sacramento, California, and Ben E. Lofgren, Woodward-Clyde Consultants, San Francisco, California

9.13.1 INTRODUCTION

The principal areas of land subsidence due to ground-water withdrawal in California are in the San Joaquin Valley and the Santa Clara Valley (Figure 9.13.1). A case history for the Santa Clara Valley is included elsewhere in this publication. In the San Joaquin Valley, subsidence due to ground-water withdrawal occurs in three areas--the Los Banos-Kettleman City area on the central west side, the Tulare-Wasco area on the southeast border, and the Arvin-Maricopa area at the south end (Figure 9.13.1).

Since 1956, the U.S. Geological Survey has carried on two investigative programmes in the San Joaquin Valley. One, a study of land subsidence, was carried on in cooperation with the California Department of Water Resources. The other, a federally financed research project on the mechanics of aquifer systems, had two major goals: to determine the principles controlling the deformation of aquifer systems in response to change in grain-to-grain load, and to appraise the change in storage characteristics as the systems compact under increased effective stress. During the 20 years of research under these two projects, many of the causes and effects of land subsidence have been documented. Sixteen of the principal reports have been pub-

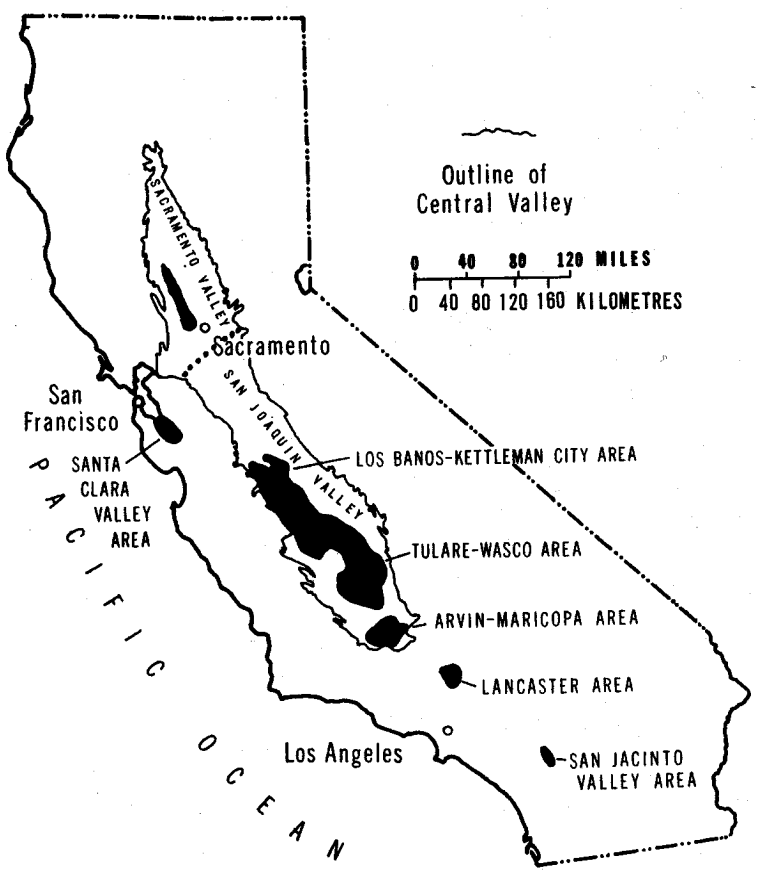

Figure 9.13.1 Areas of land subsidence in California due to ground-water withdrawal.

lished as professional papers of the Geological Survey, the subsidence reports in the Professional Paper 437 series, and the mechanics of aquifer systems papers in the Professional Paper 497 Series. The following case history concerning subsidence in the San Joaquin Valley is taken chiefly from the summary report by Poland, Lofgren, Ireland, and Pugh (U.S. Geol. Survey Prof. Paper 437-H, 1975). More detailed information is available in published reports on the three areas.

9.13.2 GEOLOGY

The San Joaquin Valley includes the southern two-thirds of the Central Valley, an area of 26,000 km^2. It is a broad structural downwarp bordered on the east by the granitic complex of the Sierra Nevada and on the west by the complexly folded and faulted Coast Ranges. The top of the basement complex of the Sierra Nevada block dips gently westward beneath the valley. Late Cenozoic continental deposits form the floor of the valley and attain maximum thickness of 5,000 m near the south edge.

The continental deposits are chiefly of fluvial origin but contain several extensive interbeds of lacustrine origin. The fluvial deposits consist of lenticular bodies of sand and gravel, sand, and silt deposited in stream channels, and sheetlike bodies of silt and clay laid down on flood plains by slow-moving overflow waters.

Along the east side of the valley the sediments deposited by the major streams issuing from the Sierra Nevada--from the Merced River south to the Kings River--have formed a series of coalescing alluvial fans, characterized by a mass of coarse permeable deposits, largely tongues and lenses of sand and gravel, that extend to and beyond the topographic trough of the valley.

In more than half of the San Joaquin Valley area that lies south of Los Banos, the deposits containing freshwater can be divided into: (1) an upper unit of clay, silt, sand, and gravel chiefly alluvial-fan and flood-plain deposits of heterogeneous character, (2) a middle unit consisting of a relatively impermeable diatomaceous lacustrine clay; and (3) a lower unit of clay, silt, sand, and some gravel, in part lacustrine deposits, that extends down to the beds containing saline water. The upper and middle units are Pleistocene age; the lower unit is of Pleistocene and Pliocene age. Together, these three units approximately constitute the Tulare Formation. The middle unit is the Corcoran Clay Member of the Tulare Formation (Miller, Green, and Davis, 1971).

9.13.3 HYDROLOGY

The continental freshwater-bearing deposits can be subdivided into two principal hydrologic units. The upper unit, a semiconfined aquifer system with a water table, also termed the "upper water-bearing zone," extends from the land surface to the top of the Corcoran Clay Member at a depth ranging from 0 to 275 m below the land surface. The lower unit, a confined aquifer system, also termed the "lower water-bearing zone," extends from the base of the Corcoran Clay Member down to the saline water body. The thickness of this confined system ranges from 60 to more than 600 m. The Corcoran Clay Member, which ranges in thickness from 0 to 40 m, is the principal confining bed beneath at least 13,000 km^2 of the San Joaquin Valley. The dotted line in Figure 9.13.2 defines the general extent of this principal confining bed in the valley. South of Bakersfield the confining bed has been designated the E clay by Croft (1972).

Yearly extraction of ground water for irrigation in the San Joaquin Valley increased slowly from 2,500 hm^3 in the middle 1920’s to 3,700 hm^3 in 1940. Then, during World War II and the following two decades, the rate of extraction increased more than threefold to furnish irrigation water to rapidly expanding agricultural demands. By 1966, pumpage of ground water was 12,000 hm^3 per year.

This very large withdrawal caused substantial overdraft on the central west side and in much of the southern part of the valley, mostly within the shaded area of Figure 9.13.2. The withdrawal in these overdraft areas in the 1950’s and early sixties was at least 5,000 hm^3 per year. During the period of long-continued excessive withdrawal, the head (potentiometric surface) in the confined aquifer system between Los Banos and Wasco was drawn down 60 to 180 M. South of Bakersfield the head decline was more than 100 m.

Importation of surface water to these areas of serious overdraft began in 1950 when water from the San Joaquin River was brought south through the Friant-Kern Canal, which extends to the Kern River (Figure 9.13.2).About 80 per cent of the average annual deliveries of 1,250

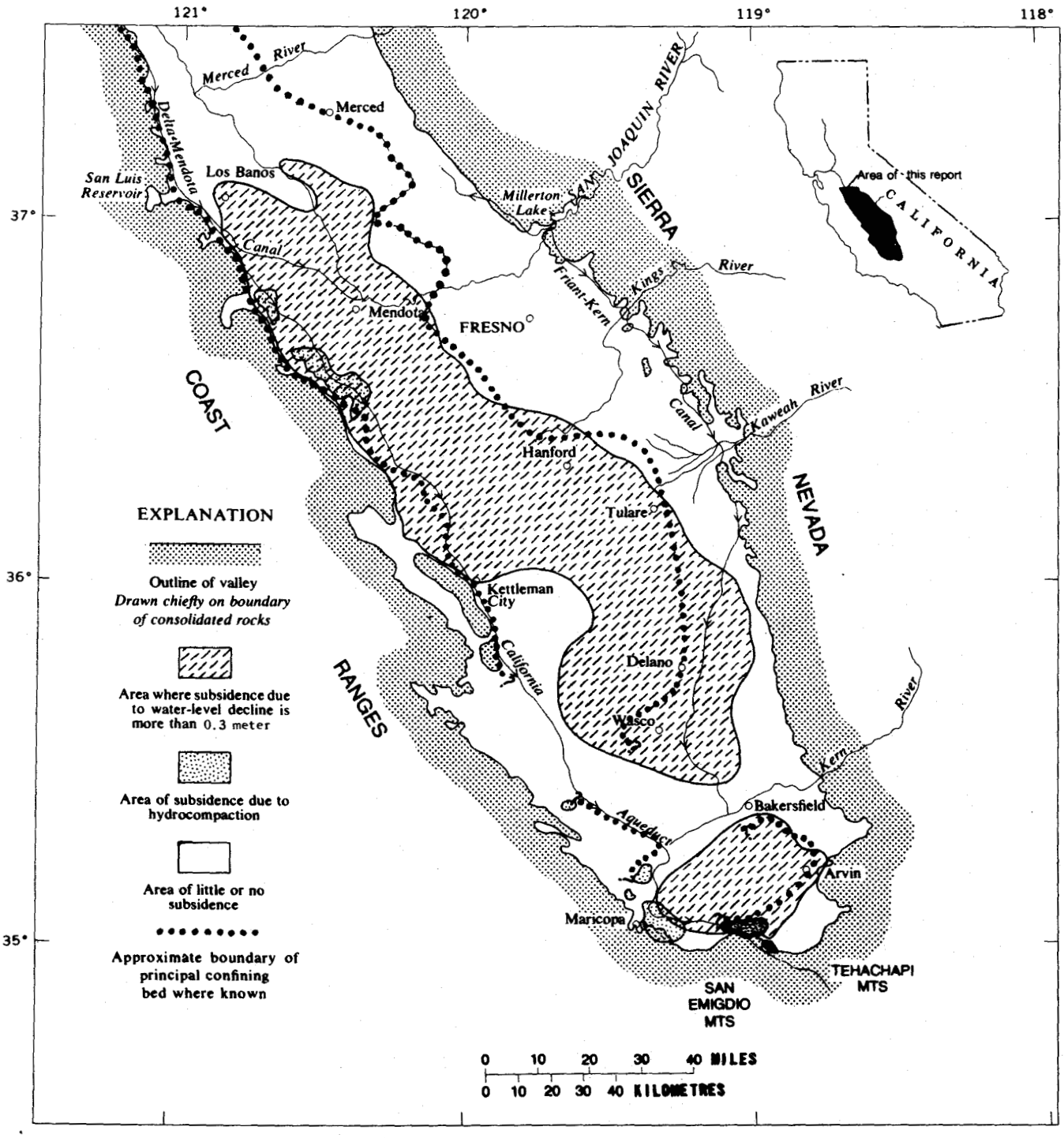

Figure 9.13.2 Pertinent geographic features of central and southern San Joaquin Valley and areas affected by subsidence.

hm^3 of water from this canal is sold to irrigation districts south of the Kaweah River, mostly in the Tulare-Wasco subsidence area.

Large surface-water imports from the northern part of the state to overdrawn areas on the west side and south end of the valley are being supplied through the California Aqueduct (Figure 9.13.2). The joint-use segment of the aqueduct between Los Banos and Kettleman City serves the San Luis project area of the U.S. Bureau of Reclamation and transports State-owned water south of Kettleman City. Surface-water deliveries to the San Luis project area increased from 250 hm^3 in 1968, the first year, to about 1,360 hm^3 in 1974. Also, by 1973 the California Aqueduct delivered 860 hm^3 to the southern part of the San Joaquin Valley (south of Kettleman City), and is scheduled eventually to supply 1,670 hm^3 under long-term contracts.

As a result of these large surface-water imports, the rate of ground-water withdrawal decreased sharply and the decline of artesian head was reversed in most of the areas of overdraft. By the early 1970's many hundreds of irrigation wells were unused, artesian heads were recovering at a rapid rate, and rates of subsidence were sharply reduced.

9.13.4 LAND SUBSIDENCE

Subsidence in the San Joaquin Valley is of three types. In descending order of importance these are (1) subsidence due to the compaction of aquifer systems caused by the excessive withdrawal of ground water; (2) subsidence due to the compaction of moisture-deficient deposits when water is first applied--a process known as hydrocompaction; and (3) local subsidence caused by the extraction of fluids from several oil fields.

Oil-field subsidence is due to the same process as subsidence caused by excessive pumping of ground water--a lowering of fluid level and consequent increase of effective stress on the sediments within and adjacent to the producing beds. However, measured oil-field subsidence in the San Joaquin Valley, which has been discussed briefly by Lofgren (1975), is less than 0.6 m at the few oil fields where periodic releveling has defined its magnitude. This type of subsidence has not created any problems in the valley.

Hydrocompactible deposits occur locally on the west and south flanks of the valley (see Figure 9.13.2). These are near-surface alluvial-fan deposits, largely mud flows, still above the water table. They have been moisture deficient ever since deposition, chiefly because of the low rainfall in the area. When water is first applied, the clay bond is weakened and the deposits compact. Subsidence of 1.5 to 3 m is common and locally it exceeds 4.5 m (Lofgren, 1960; Bull, 1964). The California Aqueduct (Figure 9.13-2) passes through at least 65 km of deposits susceptible to hydrocompaction, and precompaction by prolonged wetting of the aqueduct alinement was carried on for about one year prior to the placing of the concrete lining.

Subsidence due to the compaction of aquifer systems in response to excessive decline of water levels had affected about 13,500 km^2 of the San Joaquin Valley by 1970. Figure 9.13.3 depicts the distribution and magnitude of subsidence exceeding 1 foot (0.3 m) that had occurred by 1970--affecting an area of 11,100 km^2. Three centers of subsidence are conspicuous on this map. The most conspicuous is the long narrow trough west of Fresno that extends 140 km from Los Banos to Kettleman City (referred to subsequently as the west-side area). Maximum subsidence in this area to 1977 was 29.5 feet (9.0 m), 16 km west of Mendota. The second center, between Tulare and Wasco, is defined by two closed 12-foot (3.7-m) lines of equal subsidence, 32 and 48 km south of Tulare, respectively. Maximum subsidence to 1970 was 4.3 m, at a benchmark 32 km south of Tulare. The third center, 32 km south of Bakersfield, has subsided a maximum of 9.2 feet (2-8 m), mostly since World War II. Note that the California Aqueduct was constructed through the full 140 km of the subsidence trough extending from Los Banos to Kettleman City, as well as through the southwestern edge of the subsidence bowl south of Bakersfield.

The cumulative volume of subsidence in the San Joaquin Valley (Figure 9.13.4) grew slowly until the end of World War II. With the great increase in ground-water extraction in the 1940's and 1950's, however, the cumulative volume of subsidence soared to 12,350 hm^3 by 1960, and reached 19,250 hm^3 by 1970. This very large volume is equal to one-half the initial storage capacity of Lake Mead or to the total discharge from all water wells in the San Joaquin Valley for 1.5 years at the 1966 rate. This volume of subsidence represents water of compaction derived almost wholly from compaction of the fine-grained highly compressible clayey interbeds (aquitards), in response to the increase in effective stress as artesian head in the confined system declined. The volume of subsidence for any interval of leveling control was obtained by planimetry of the subsidence map for that period. All leveling data used in the preparation of subsidence maps and graphs were by the National Geodetic Survey (formerly the Coast and Geodetic Survey).

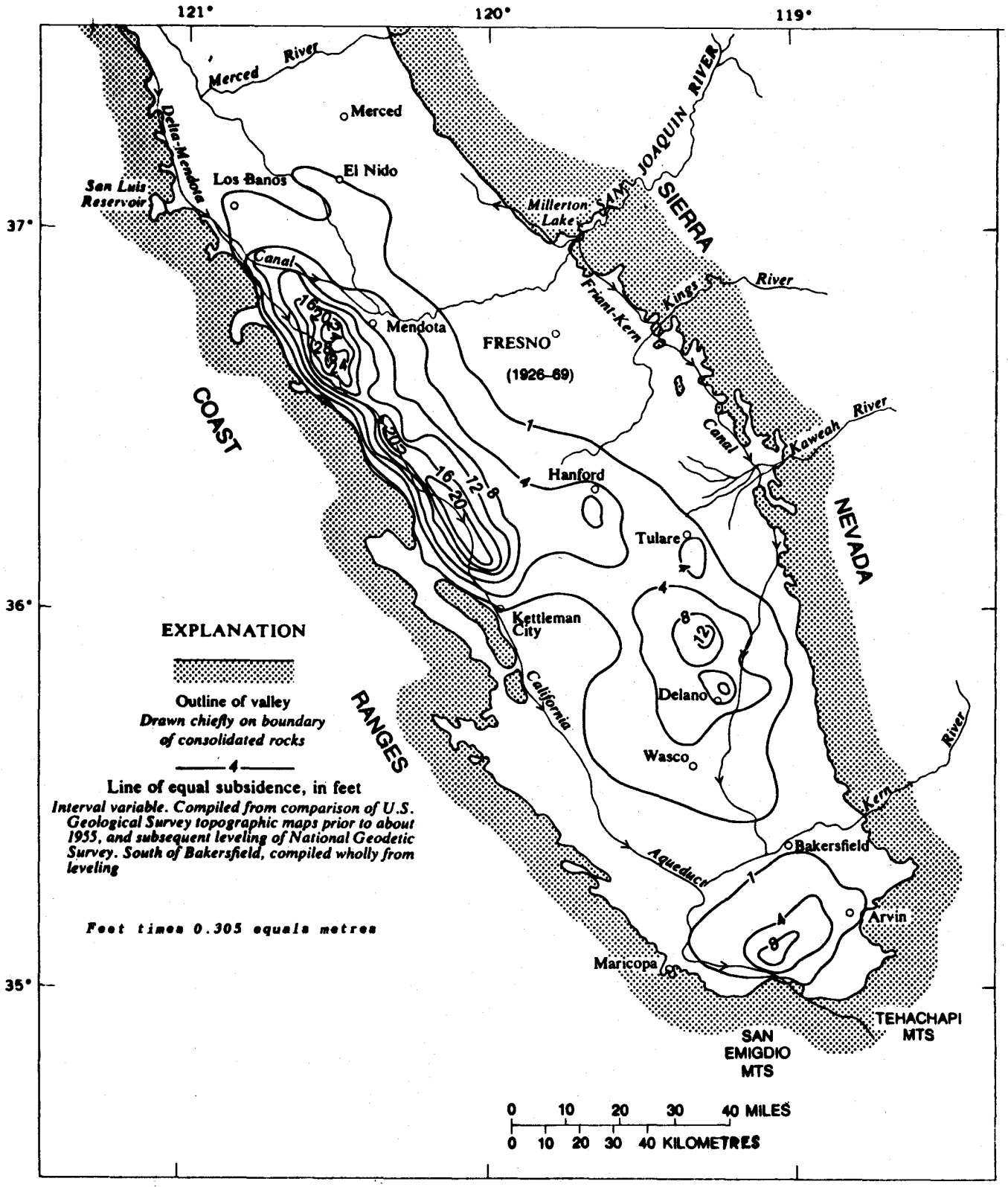

Figure 9.13.3 Land subsidence in the San Joaquin Valley, California, 1926-1970.

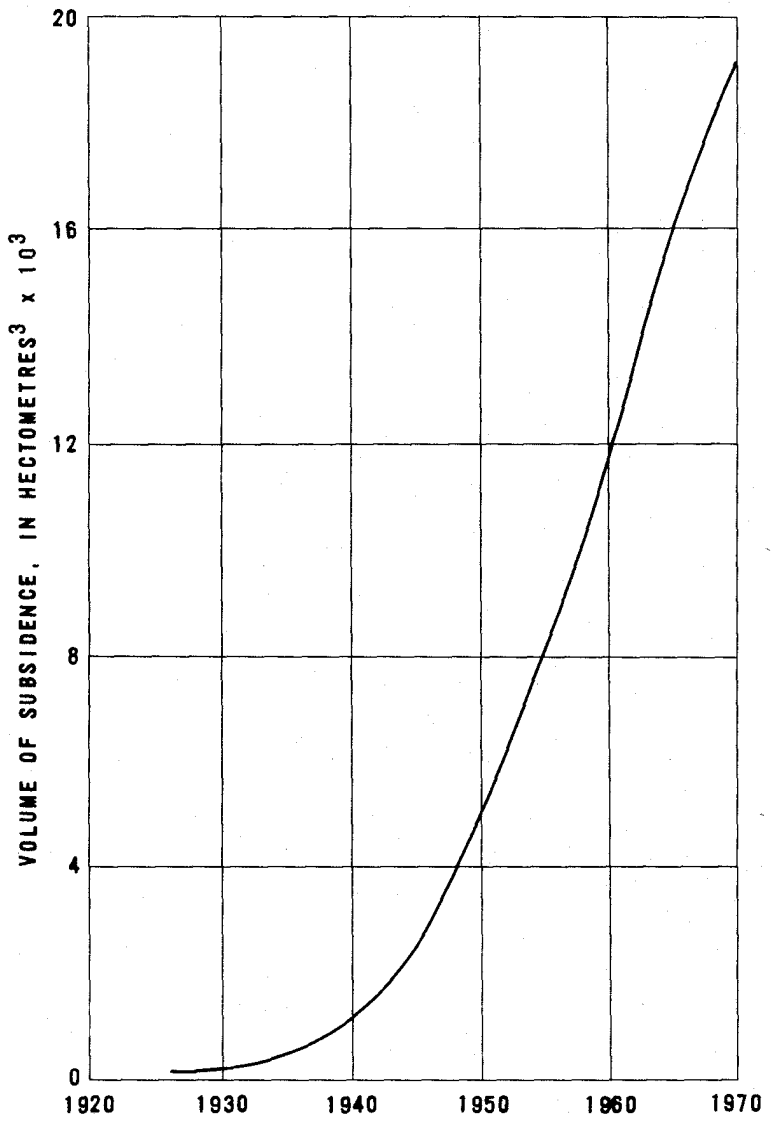

Figure 9.13.4 Cumulative volume of subsidence, San Joaquin Valley, California, 1926-70.

The west-side area has experienced the most severe subsidence (Figure 9.13.5); therefore several illustrations will be presented to show the relation between water-level change (stress change) and compaction or subsidence in that area. Subsidence has affected about 6,200 km^2 and the volume of subsidence, 1926-69, was about 11,850 hm^3, about two-thirds of the valley total. The cumulative volume of ground-water pumpage in the west-side area through March 1969 is estimated as 35,200 hm^3 (Figure 9.13.6). This cumulative pumpage has been plotted with cumulative subsidence at a scale of 3 to 1. The correlation is remarkably consistent, indicating that throughout the 43 years since subsidence began (1926 into 1969), about one-third of the water pumped has been water of compaction derived from the permanent reduction of pore space in the fine-grained compressible aquitards.

Figure 9.13.7 illustrates the relation of subsidence to artesian-head change since 1943 at a site 16 km southwest of Mendota. Bench mark S661, located within the 28-foot (8.5-m) line of equal subsidence in Figure 9.13.5, subsided 8 m from 1943 to 1969, in response to a water-level decline of nearly 125 m as measured in nearby wells. The rate of subsidence at this site reached a maximum of 0.54 m per year between 1953 and 1955 but decreased to 0.04 m per year between 1972 and 1975, due chiefly to substantial recovery of artesian head. Static water level began to recover in 1969 and by 1977 had risen 73 m above the 1968 summer low level because of

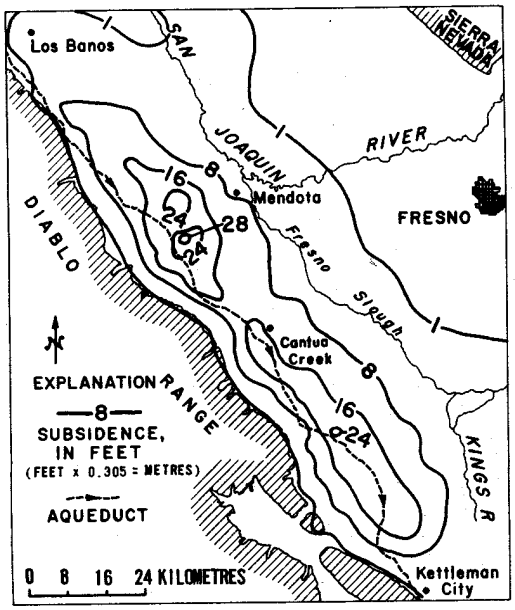

Figure 9.13.5 Land subsidence in the Los Banos-Kettleman City area, California, 1926-69.

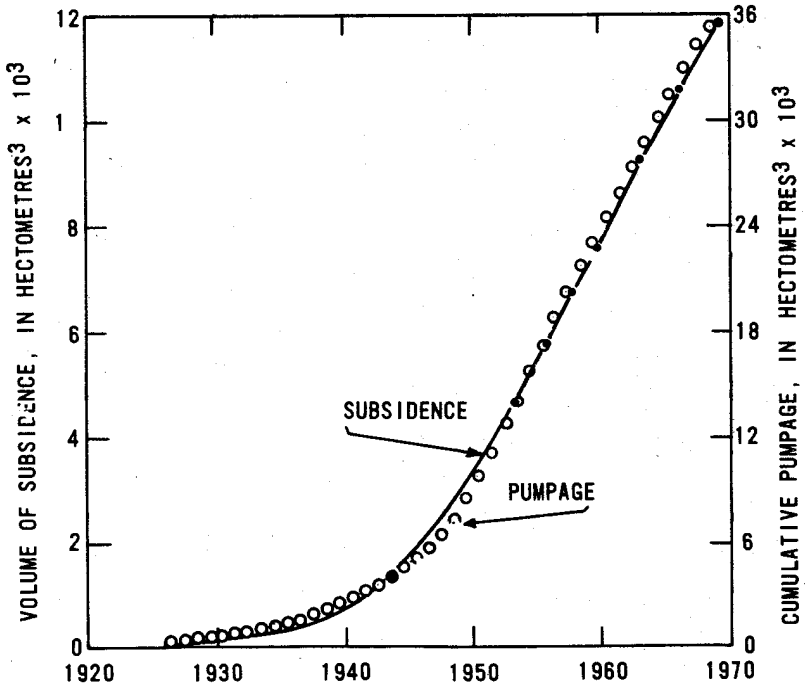

Figure 9.13.6 Cumulative volume of subsidence and pumpage, Los Banos-Kettleman City area, California. Points on subsidence curve indicate times of leveling control.

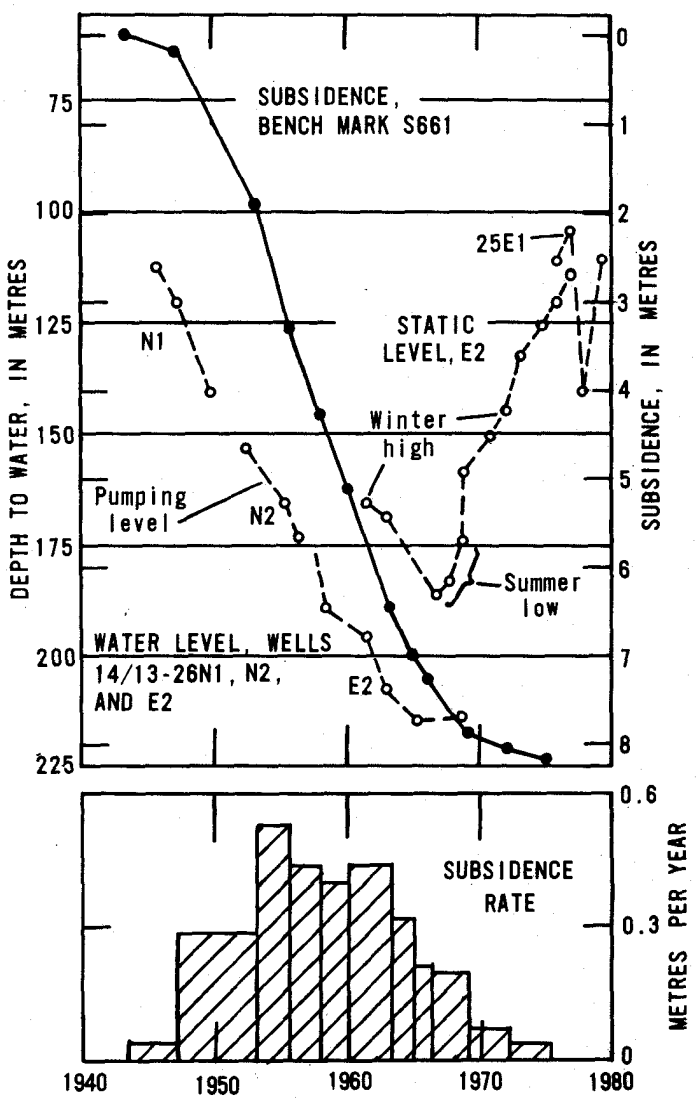

Figure 9.13.7 Subsidence and artesian-head change 16 kilometres southwest of Mendota.

the large imports of surface water through the California Aqueduct and the consequent reduction in pumpage.

If two or more extensometers (compaction recorders) are installed in adjacent wells of different depths, the records from the multiple-depth installation will indicate the magnitude and rate of compaction (or expansion), not only within the total depths of individual wells but also for the depth intervals between well bottoms. Figure 9.13.8 shows the record of compaction from 1958 through 1971 in three adjacent extensometer wells in the west-side area. The site is adjacent to the California Aqueduct at the north end of the southern 16-foot (4.9-m) line of equal subsidence in Figure 9.13.5. The wells are 152, 213, and 610 m deep. Measured compaction in the 13 years was about 0.42 m, 0.97 m, and 3.40 m, respectively. Thus the compaction in the 213-610-m depth interval was 2.43 m. The dashed line represents subsidence of a surface bench mark at this site as determined by repeated leveling from stable bench marks (black dotes on the dashed line show dates of leveling). In the early 1960's the rate of compaction measured in the 610-m well (Nl) was nearly equal to the rate of subsidence. Subsequently the rate of compaction of deposits below the 610-m depth gradually increased, due to increased pumping and declining pore pressures in deeper wells drilled in the 1960's. This deeper compaction caused the departure of the subsidence plot from the compaction plot for well Nl.

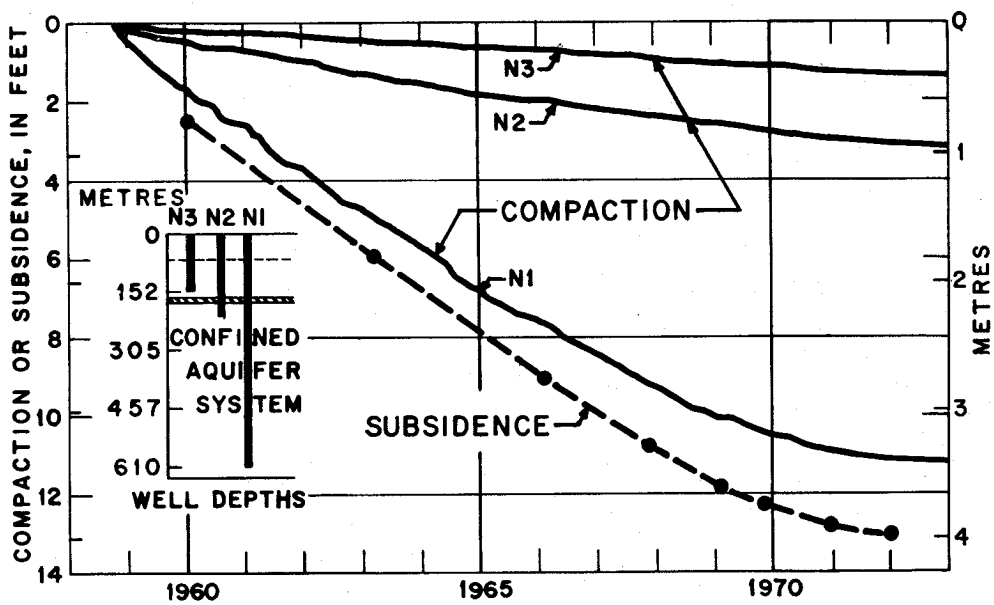

Figure 9.13.8 Compaction and subsidence at Cantua site, 65 kilometres southwest of Fresno, California.

9.13.5 COMPRESSIBILITY AND STORAGE PARAMETERS

In the late 1950's, as one phase of the research on land subsidence and compaction of aquifer sytems, the Geological Survey drilled four core holes in the Los Banos-Kettleman City (west side) area ranging in depth from 305 to 670 m, and two core holes in the Tulare-Wasco area to depths of 232 and 670 m. Cores were tested in the Hydrologic Laboratory for particle-size distribution, specific gravity of solids, dry unit weight, porosity and void ratio, hydraulic conductivity (normal and parallel to bedding) and Atterberg limits. Results have been published (Johnson, Moston, and Morris, 1968). X-ray diffraction studies of 85 samples from the westside cores and 26 samples from the Tulare-Wasco cores indicated that about 70 per cent of the clay-mineral assemblage in these deposits of Pliocene to Holocene age consists of montmorillonite (Meade, 1967, Tables 11-13).

Laboratory consolidation tests were made by the Bureau of Reclamation on 60 fine-grained cores from the four core holes in the west-side area and on 22 fine-grained cores from the two core holes in the Tulare-Wasco area. Parameters tested included the compression index, C_c, a measure of the compressibility of the sample, and the coefficient of consolidation, C_v, a measure of the time-rate of consolidation. Results have been published (Johnson and others, 1968, Tables 8 and 9). The range of the compression index, C_c, was much wider than for samples from the Santa Clara Valley: In the Los Banos-Kettleman City area the range was 0.09 to 1.13; in the Tulare-Wasco area it was 0.25 to 1.53. However, all values greater than 0.47 were either from lacustrine clays or from the fine-grained marine siltstone in the Richgrove core hole 12 km east of Delano.

The subsidence volume represents pore-space reduction occurring chiefly in the fine-grained compressible aquitards. In the west-side area, the volume of subsidence from 1926 to 1969 was about 11,850 hm^3, distributed over 6,200 km^2. If the subsidence had been distributed evenly over this area, it would average about 1.9 m. Roughly half the sediments in the principal aquifer system are fine-grained compressible aquitards. Assuming the average composite thickness of the compacting aquitard is 150 m and the average initial porosity is 40 per cent, a mean subsidence of 1.9 m would represent an average reduction in porosity of roughly 1 per cent in these fine-grained beds (from 40 to 39.2 per cent) - In the small area where the maximum 8.8 m of subsidence has occurred, the local reduction in pore space of aquitards would be roughly 4 per cent (from 40 to 36.3 per cent).

The subsidence/head-decline ratio (specific subsidence) is the ratio between land subsidence and the hydraulic head decline in the coarse-grained permeable beds of the compacting aquifer system, for a common time interval. It can be expressed as the change in thickness per

unit change in effective stress ($\Delta b/\Delta p'$). This ratio is useful as a first approximation of compressibility; it is also useful for predicting a lower limit for the magnitude of subsidence in response to a step increase in virgin stress (stress greater than past maximum). If pore pressures in the fine-grained aquitards were eventually to reach equilibrium with those in adjacent aquifers after a step increase beyond preconsolidation stress, compaction would cease and the subsidence/head-decline ratio would indicate the true virgin compressibility of the system.

In the west-side area during the period 1943-60 the decline of artesian head for the lower zone ranged from 30 to 120 m (Bull and Poland, 1975, Figure 25), resulting in subsidence in the 17-year period of 0.3 to 4.9 m (Bull, 1975, Figure 10). The subsidence/head-decline ratio for that same period ranged areally from 0.01 to 0.08 (Bull and Poland, 1975, Figure 32). In other words, the head decline required to produce 1 metre of subsidence ranged from 100 to 12 m. A subsidence/head-decline ratio can be derived from Figure 9.13.7 for the period 1947 to 1965. In the 18 years, bench mark S661 subsided 6.86 m, and the pumping level in nearby wells declined 95 m. Thus, for that time span the ratio at that site equaled 0.07.

In the Tulare-Wasco area, the subsidence/head-decline ratio ranged from 0.01 to 0.06 (Lofgren and Klausing, 1969, Figure 69). In the Arvin-Maricopa area, the subsidence/head-decline ratio for the 8-year period 1957-65 ranged from 0.01 to 0.05 (Lofgren, 1975, Plate 5B).

Areal variation in the subsidence/head-decline ratio can be produced by one or more of several factors. These include variation in the individual, and gross aggregate thickness of the compacting aquitards and variation in compressibility and vertical hydraulic conductivity of the individual aquitards. Such areal variation in compressibility and hydraulic conductivity can be caused by variation in grain size, in depth of compacting beds (in overburden load), in geologic formation tapped, in existing preconsolidation stress, in clay-mineral assemblage, and in other diagenetic effects. Furthermore, because the subsidence values available for computing the ratio seldom represent ultimate subsidence for a designated change in stress within aquifers, time is an important factor. According to soil-consolidation theory, the time required for an aquitard that is draining to adjacent aquifers to reach a specified percentage of ultimate compaction varies directly as (1) the square of the draining thickness and (2) the ratio of compressibility to vertical hydraulic conductivity. Variation in the thicknesses of the many vertical-draining aquitards encountered at any selected site obviously makes that site unique in its rate of compaction, even if all other factors are equal. In the depth interval 214 to 610 m at west-side well 16/15-34N1, for example, interpretation of the microlog defined 60 aquitards ranging in thickness from 0.6 m to 15 m and averaging 4.5 m.

One other factor directly affecting the accuracy of the subsidence/head-decline ratio is the appropriateness or the accuracy of the change-in-stress value used. Even in a ground-water basin containing a single confined aquifer system it is difficult to obtain measurements of head change that truly represent the average stress change on aquitard boundaries within the full well-depth interval experiencing a measured compaction or subsidence. Thus, observation wells used to derive stress-change values, whether for subsidence/head-change ratios or for stress-strain plots, should be selected or constructed very carefully.

Bull (1975, p. 49-82) made a study of geologic factors that caused areal differences in specific unit compaction in the Los Banos-Kettleman City area for the period 1943-60. The factors included total applied stress, lithofacies, and source and mode of deposition.

Field measurements of compaction or expansion of sediments and the correlative change in fluid pressure(s) can be utilized to construct stress-strain curves and to derive storage and compressibility parameters. One example (Figure 9.13.9) is for a well 176 m deep on the west

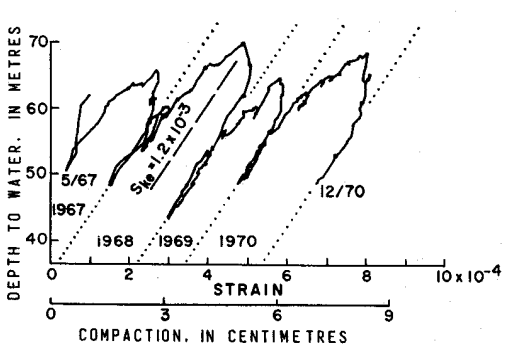

Figure 9.13.9 Stress change, compaction, and strain for a well in western Fresno County, California.

side of the valley. Depth to water is plotted increasing upward (increasing stress). Change in depth to water represents change in effective stress in the aquifers in the confined aquifer system (upper zone) that is 106 m thick. Along the abscissa the lower scale is the measured compaction and the upper scale is the strain (measured compaction/compacting thickness). The yearly fluctuation of water level caused by the seasonal irrigation demand and the permanent compaction that occurs each summer during the heavy pumping season when the depth to water is greatest produce a series of stress-strain loops. The lower parts of the descending segments of the annual loops for the three winters 1967-68 to 1969-70 are approximately parallel straight lines, indicating that the response is essentially elastic in both aquifers and aquitards when the depth to water is less than about 55 m. The heavy dashed line in the 1968 loop represents the average slope of the segments in the elastic range of stress. The reciprocal of the slope of the line is the component of the storage coefficient due to deformation of the aquifer-system skeleton, S_{ke}, and equals 1.2×10^{-3}. The component of average specific storage due to elastic deformation, S_{ske}, equals $S_{ke}/106$ m = $1.1 \times 10^{-5} m^{-1}$. The average elastic compressibility of the aquifer system skeleton, α_{ke}, is S_{ske}/γ_w,; if γ_w, (the unit weight of water) equals 1, the numerical values Of α_{ke} and S_{ske} are identical.

For increase in effective stress in the range of loading exceeding preconsolidation stress, the "virgin" compaction of aquitards is chiefly inelastic--nonrecoverable upon decrease in stress. At Pixley, 27 km south of Tulare (Figure 9.13.3), compaction and change in stress for a confined aquifer system 108-231 m below land surface has been measured since 1958. Riley (1969) showed from a stress-strain plot that the mean virgin compressibility of the aquitards (aggregate thickness 75 m) in this confined aquifer segment 123 metres thick was $7.5 \times l0^{-4} m^{-7}$ and the mean elastic compressibility of the aquifer system was $9.3 \times 10^{-6} m^{-1}$. Thus, for the aquifer system segment 123 metres thick at this site, the mean virgin compressibility of the aquitards is about 80 times as large as the mean elastic compressibility of the confined system.

Figure 9.13.10 shows a generalized plot of water level for the confined aquifer system 32 km south of Mendota (Figure 9.13.5) from 1905 to 1964 and the seasonal high and low in observation well 16/15-34N4 for 1961-77. This well taps the confined system. The regional water level declined about 120 m from 1905 to 1960 and the rate of decline accelerated as the groundwater withdrawal increased. By 1960 the seasonal low had declined below the base of the confining clay, producing a water-table condition. Surface-water imports to the west-side area began in 1968. As the imports increased, ground-water pumpage decreased and water levels recovered sharply. From 1968 to 1976 the water level at well 34N4 rose 82 metres. Then, during 1977, the second of two severe drought years, the imports decreased to 370 hm^3 and pumping draft from both old and newly drilled wells soared to about three times the 1976 rate. As a result the water level in well 34N4 fell 50 m in the 8 months to August 1977.

The changing stress as indicated by the hydrograph of well 34N4 and the resulting strain at this site as measured by an extensometer in well 34Nl since 1959 are clearly displayed in Figure 9.13.11. Well 16/15-34N1, 610 m deep, is equipped with an anchored-cable extensometer.

A time plot of cumulative measured compaction at this site was introduced earlier (Figure 9.13.8). in Figure 9.13.11, the measured compaction is plotted as an annual bar graph for comparison with the fluctuations of the water level in well N4. Note that the water level in well N4 began a sharp rise late in 1968 as surface-water imports began. In response to the sharp recovery of water level, compaction decreased rapidly after 1968 but did not cease until 1975. During this period of rising water levels in the coarse-grained aquifers, nonrecoverable virgin compaction continued through 1974 in the central parts of the thicker aquitards, exceeding the continuing small elastic expansion of the preconsolidated aquifers and the thinner aquitards. The water level in well N4 reached a seasonal high of 107 m below land surface in November 1976. Early in February 1977, when water level was 112 m below land surface (only 5 m below the seasonal high), virgin compaction resumed in well Nl. By March 30, 1977, when water level was 15 m below the seasonal high, the maximum compaction rate of the season was attained. The early February water level 112 m below land surface clearly defined the preconsolidation stress in the central segments of the thickest or least permeable aquitards or both. As the drawdown increased, more and more of the slow draining compressible beds began to contribute water of compaction. By yearend, about 12 cm of renewed nonrecoverable compaction had occurred.

During the first period of water-level decline (1905-68 in Figure 9.13.10), water of compaction represented about one-third of the total water pumped from west-side wells (Figure 9.13.6). By 1968, many of the aquitards were preconsolidated nearly to the 1968 stress level. Early in the second period of water-level decline (in 1977), the response of the preconsolidated sediments was chiefly elastic and the contribution of water of compaction was much less than one-third of the total pumpage. Hence the water level fell very rapidly.

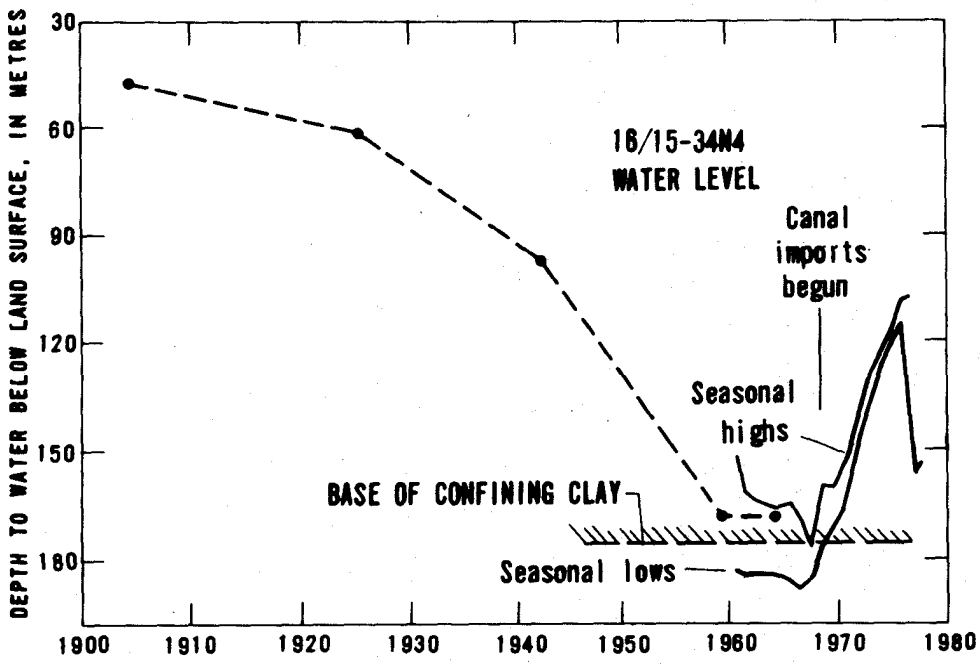

Figure 9.13.10 Long-term trend of water levels near Cantua Creek, and seasonal high and low levels in observation well 16/15-34N4 since 1960. (Modified from Lofgren, 1979,

Figure 9.13.12 displays a similar trend of water-level recovery and reduced compaction, followed by an abrupt head decline and renewed compaction during 1977. Observation well 20/18-6D1 is 25 km north of Kettleman City (Figure 9.13.4) and adjacent to the California Aqueduct. The abrupt head decline of 76 m in 1977 momentarily increased the stress in the aquifers to 1967 levels and stresses in the central parts of the aquitards once again exceeded preconsolidation stresses. In response, virgin compaction of the aquitards exceeded that of 1968. Such stressing and differential compaction in the vicinity of the aqueduct is of concern in sustaining the integrity of such structures. This particular problem appears to be of local extent, however--the intensity of the head decline in well 6Dl is due largely to pumping of a new irrigation well drilled early in 1977 within 60 m of the aqueduct.

9.13.6 ECONOMIC AND SOCIAL IMPACTS

The extensive major subsidence in the San Joaquin Valley has caused several problems. The differential change in elevation of the land surface has created problems in maintenance of water-transport structures, including canals, irrigation and drainage systems, and stream channels. Both the Delta-Mendota Canal and the Friant-Kern Canal (Figure 9.13-3), two major structures of the Central Valley Project of the Bureau of Reclamation, have required remedial work because of subsidence. Also in the period 1926-72, differential subsidence has steepened the channel of the San Joaquin River about 2 m in the 24 km before it reaches the valley trough and has flattened the channel about 2 m in the next 50 km downstream. These changes have affected the transport characteristics of the river and have altered levee requirements.

Another problem common to the subsiding areas in the San Joaquin Valley is the failure of water wells as a result of compressive rupture of casings caused by the compaction of the aquifer systems. In the west-side area, where subsidence has been greatest, many hundreds of deep irrigation wells have required costly repair or replacement. According to Wilson (1968), during 1950-61 approximately 1,200 casing failures were reported in 275 irrigation wells in an area of 1,600 km^2 that spans the region of most intensive subsidence. Well repair and replacement costs attributable to subsidence in the three subsiding areas have been many millions of dollars.

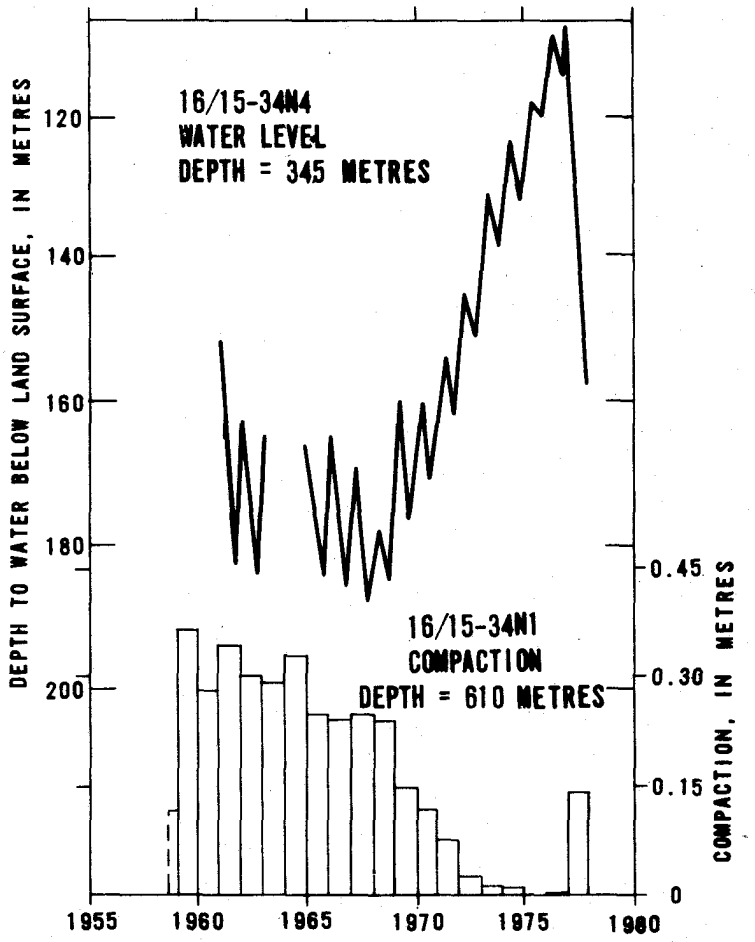

Figure 9.13.11 Seasonal fluctuations of water level in well 16/15-34N4 and measured compaction in observation well 16/15-34N1 near Cantua Creek. (Modified from Lofgren, 1979, Figure 10.)

The need for preconsolidation of deposits susceptible to hydrocompaction substantially increased the construction costs of the California Aqueduct. The aqueduct passes through about 65 km of susceptible deposits. The approximate cost for treatment by prewetting for the reach from Kettleman City to the Tehachapi Mountains has been estimated as $20 million (Lucas and James, 1976, p. 541). Preconsolidation of the susceptible areas between Los Banos and Kettleman City cost an additional estimated $5 million.

The subsidences have increased considerably the number and cost of surveys made by governmental agencies and by private engineering firms to determine the elevations of bench marks or construction sites and to establish grades. In addition, revision of topographic maps has been more frequent and more expensive than in nonsubsiding areas.

9.13.7 LEGAL ASPECTS

So far as known, no legal actions have been taken as a result of the subsidence.

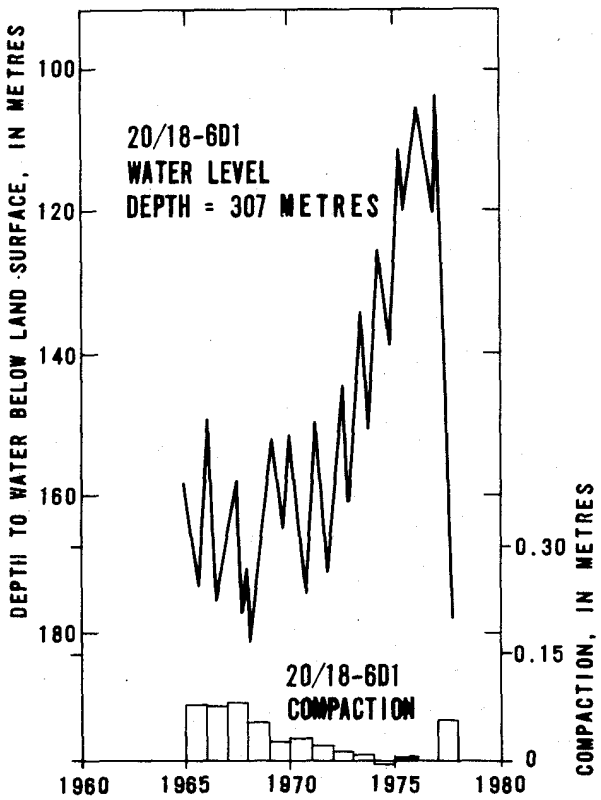

Figure 9.13.12 Seasonal fluctuations of water level and measured compaction in observation well 20/18-6D1 northeast of Huron.

9.13.8 MEASURES TAKEN TO CONTROL OR AMELIORATE SUBSIDENCE

The severe subsidence in all three areas in the San Joaquin Valley has been greatly reduced by the importation of surface water and the consequent decrease in ground-water pumping, as described earlier in this case history.

In the Tulare-Wasco area, the import of surface water from the San Joaquin River through the Friant-Kern Canal began in 1980. In the next 23 years, 1950-1972, the deliveries to this area from the canal averaged about 830 hm^3 per year, roughly 80 per cent of the surface-water supply to the area (Lofgren and Klausing, 1969). In the first 13 years of this period (1950-62), ground-water pumpage averaged about 1,230 hm^3 per year and continued at about this rate into the 1970's. Thus, the water imported from the San Joaquin River to the area during the 23-year period 1950-72 equaled about one-quarter of the total water supply and two-thirds of the ground-water pumpage.

Hydrographs of wells tapping the semiconfined to confined aquifer system in the eastern part of the Tulare-Wasco area show a water-level recovery of about 60 m from 1950 to 1970. As a result, subsidence decreased to less than 3 cm per year in most of the eastern area as 1962-70. On the other hand, hydrographs for wells tapping the confined aquifer system in the western part of the Tulare-Wasco area show continued decline of water levels since the 1950's; the supplemental irrigation supply from the Friant-Kern Canal to the western part has been insufficient to achieve a balance with ground-water pumping. As a result, subsidence has continued at rates locally exceeding 9 cm per year.

In the west-side area, the import of surface water through the California Aqueduct, which began in 1968, soon replaced most of the ground-water pumpage. For example, ground-water pumpage in the west-side area averaged 1,300 hm^3 per year from 1960 to 1967, before the imports began. By 1974, surface water imports to the west-side area reached 1,400 hm^3 per year and pumpage had decreased to roughly 250 hm^3 per year. The great decrease in ground-water pumpage and the consequent recovery of the artesian head in the confined aquifer system have nearly eliminated

the subsidence problem for the present. However, any deficiency in surface-water imports could trigger renewed pumping, renewed head decline, and renewed subsidence, as in the severe drought year of 1977.

9.13.9 REFERENCES

BULL, W. B. 1964. Alluvial fans and near-surface subsidence in western Fresno County, California: U.S. Geol. Survey Prof. Paper 437-A, 71 p.

_____. 1975. Land subsidence due to ground-water withdrawal in the Los Banos-Kettleman City area, California, Part 2. Subsidence and compaction of deposits: U.S. Geol. Survey Prof. Paper 437-F, 90 p.

BULL, W. B., and POLAND, J. F. 1975. Land subsidence due to ground water withdrawal in the Los Banos-Kettleman City area, California, Part 3. Interrelations of water-level change, change in aquifer-system thickness and subsidence: U.S. Geol. Survey Prof. paper 437-G, 62 p.

CROFT, M. G. 1972. Subsurface geology of the Late Tertiary and Quaternary water-bearing deposits of the southern part of the San Joaquin Valley, California: U.S. Geol. Survey Water-Supply Paper 1999-H, 29 p.

JOHNSON, A. I., MOSTON, R. P., and MORRIS, D. A. 1968. Physical and hydrologic properties of water-bearing deposits in subsiding areas in central California: U.S. Geol. Survey Prof. Paper 497-A, 71 p.

LOFGREN, B. E. 1975. Land subsidence due to ground-water withdrawal, Arvin-Maricopa area, California: U.S. Geol. Survey Prof. Paper 437-D, 55 p.

_____. 1979. Changes in Aquifer-System Properties with Ground-Water Depletion, Proceedings, Evaluation and Prediction of Subsidence, American Society of Civil Engineers, p. 26-46.

LOFGREN, B. E., and KLAUSING, R. L. 1969. Land subsidence due to ground-water withdrawal, Tulare-Wasco area, California: U.S. Geol. Survey Prof. Paper 437-B, 103 p.

LUCAS, C. V., and JAMES, L. B. 1976. Land subsidence and the California State Water Project: Internat. Symposium on Land Subsidence, 2d, Anaheim, Calif., Dec. 1976, Proc., p. 533-543.

MEADE, R. H. 1967. Petrology of sediments underlying areas of land subsidence in central California: U.S. Geol. Survey Prof. Paper 497-C, 83 p.

MILLER, R. E., GREEN, J. H., and DAVIS, G. H. 1971. Geology of the compacting deposits in the Los Banos-Kettleman City subsidence area, California: U.S. Geol. Survey Prof. Paper 497-E, 46 p.

POLAND, J. F. 1976. Land subsidence stopped by artesian-head recovery, Santa Clara Valley, California: Internat. Symposium on Land Subsidence, 2d, Anaheim, Calif., Dec. 1976, Proc., p. 124-132.

POLAND, J. F., LOFGREN, B. E., IRELAND, R. L., and PUGH, R. G. 1975. Land subsidence in the San Joaquin Valley as of 1972: U.S. Geol. Survey Prof. Paper 437-H, 78 p.

RILEY, F. S. 1969. Analysis of borehole extensometer data from central California, in Tison, L. J., Ed., Land subsidence, V. 2: Internat. Assoc. Sci. Hydrology, Pub. 89, p. 423-431.

WILSON, W. E. 1968. Casing failures in irrigation wells in an area of land subsidence, California [abs.]: Geol. Soc. America Ann. Mtg., 81st, Mexico City, 1968, Program, p. 324.

Case History No. 9.14. Santa Clara Valley, California, U.S.A., by Joseph F. Poland, U.S. Geological Survey, Sacramento, California

9.14.1 INTRODUCTION

Land subsidence in the central part of the Santa Clara Valley--beneath the southern part of San Francisco Bay and extending to the southern edge of San Jose--was first recognized in 1932-33. Releveling of a line of first-order levels established by the National Geodetic Survey in 1912 showed about 1.2 m of subsidence in downtown San Jose in 1933. The subsiding area extends southward about 40 km from Redwood City and Niles past San Jose, has a maximum width of 22 km, and includes about 750 km^2. As shown by Figure 9.14.1, most of this central area experienced 0.3 to 2.4 m (1 to 8 feet) of subsidence from 1934 to 1967.

9.14.2 GEOLOGY

The Santa Clara Valley is a structural trough extending 110 km southeast from San Francisco. The valley is bounded on the southwest by the Santa Cruz Mountains and the San Andreas fault and on the northeast by the Diablo Range and the Hayward fault. The consolidated bedrock bordering the valley is shown as a single unit in Figure 9.14.1; it ranges in age from Cretaceous to Pliocene and consists largely of sedimentary rocks but includes areas of metamorphic and igneous rocks.

The fresh-water-bearing deposits forming the ground-water reservoir within the valley are chiefly of Quaternary age. They include (1) the semiconsolidated Santa Clara Formation and associated deposits of Pliocene and Pleistocene age and (2) the unconsolidated alluvial and bay deposits of Pleistocene and Holocene age. The Santa Clara Formation, which crops out on the southwest and northeast flanks of the valley, consists of poorly sorted conglomerate, sandstone, siltstone, and clay as much as 600 m thick in outcrop (Dibblee, 1966). Where exposed, this formation has a low transmissivity and yields only small to moderate quantities of water to wells (1 to 6 l/s)--rarely enough for irrigation purposes.

The unconsolidated alluvial and bay deposits of clay, silt, sand, and gravel overlie the Santa Clara Formation and associated deposits their upper surface forms the valley floor. They contain the most productive aquifers of the ground-water reservoir. Wells range in depth from 90 to 360 m. The deeper wells probably tap the upper part of the Santa Clara Formation although the contact with the overlying alluvium has not been distinguished in well logs. Well yields in the valley range from 20 to 160 l/s (Calif. Dept. Water Resources., 1967, pl. 6). The alluvial deposits are at least 460 m thick beneath central San Jose. However, the log of a well drilled to a depth of 468 m revealed a lack of water-bearing material below a depth of 300 M. Coarse-grained deposits predominate on the alluvial fans near the valley margins where the stream gradients are steeper. The proportion of clay and silt layers increases bayward. For example, a well-log section extending 20 km northward from Campbell to Alviso (Tolman and Poland, 1940, Figure 3) shows that to a depth of 150 m, the cumulative thickness of clay layers in the deposits increases from 25 per cent near Campbell to 80 per cent near Alviso.

In 1960, the U.S. Geological Survey drilled core holes to a depth of 305 m at the two centers of subsidence, in San Jose (well 16C6) and in Sunnyvale (well 24C7). (For location, see Figure 9.14.1.) The 305-m depth was chosen because it was the maximum depth of nearby water wells. Cores were tested in the laboratory for particle-size distribution, specific gravity of solids, dry unit weight, porosity and void ratio, hydraulic conductivity (normal and parallel to bedding), Atterberg limits, and one-dimensional consolidation and rebound (Johnson, Moston, and Morris, 1968).

X-ray diffraction studies of 20 samples from the two core holes indicate that montmorillonite composes about 70 per cent of the clay-mineral assemblage in these deposits. Other constituents are chlorite, 20 per cent, and illite, 5-10 per cent (Meade, 1967, p. 44).

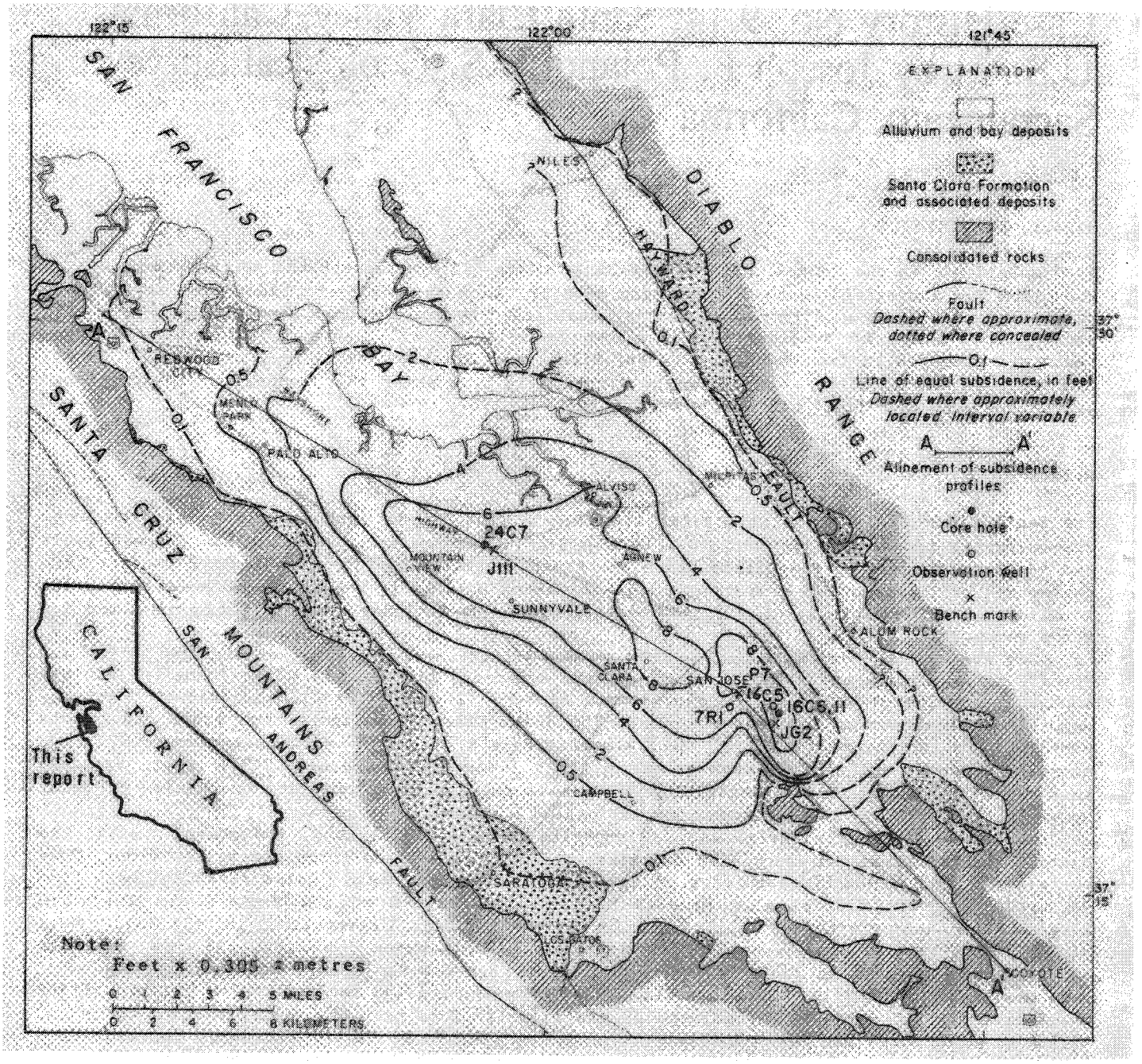

Figure 9.14.1 Land subsidence from 1.934 to 1967, Santa Clara Valley, California. Compiled from leveling of National Geodetic Survey in 1934 and 1967.

9.14.3 HYDROLOGY

In the central part of Figure 9.14.1 and below a depth of 50 to 60 m, ground water is confined. The extent of the confined aquifer system is defined roughly by the 0.6 m (2-ft) 1ine of equal subsidence in Figure 9.14.1. The area of confinement extends southward from beneath San Francisco Bay to San Jose, also west to Palo Alto and east to Milpitas. In the early years of development, wells as far south as San Jose and more than 60 m deep flowed (Clark, 1924, p.1. XV), demonstrating by their areal distribution a minimal extent of the confining sedments. The confined aquifer svstem is as much as 245 m thick. Around the valley margins, ground water is chiefly unconfined and most of the natural recharge to the ground-water reservoir percolates from stream channels in alluvial-fan deposits.

The confining member overlying the confined aquifer system has a thickness ranging from 45 to 60 m. Although predominantly composed of lenses and tongues of clay and silt, it contains some channel fillings and lenses of permeable sand and gravel. This confining member supports a shallow water table distinguished by an irregular surface. As of 1965-70, the shallow water table overlying much of the confined system was less than 10 m below the land surface (Webster, 1973). At least near the Bay, the shallow water table did not fluctuate appreciably during the period of prolonged artesian-head decline terminating in 1966.

The development of irrigated agriculture in the valley began about 1900 and expanded to a maximum about the end of World War II. After 1945, population pressures caused a great transition of land use from agricultural to urban and industrial development. Agricultural pumpage increased from about 50 hm^3 per year in 1915-20 to a maximum of 127 hm^3 per year in 1945-50 (1 cubic hectometre, hm^3, = 1 x $10^6 m^3$ = 810.7 acre-feet). By 1970-75 most of the orchards had been replaced by houses, and agricultural pumpage had decreased to 25 hm^3 per year. Municipal and industrial pumpage, on the other hand, increased from 27 hm^3 per year in 1940-45 to 162 hm^3 per year in 1970-75. Total pumpage (Figure 9.14.2, bottom graph) increased nearly fourfold from 1915-20 to 1960-65--from 60 to 222 hm^3 per year--but then decreased 19 per cent to 185 hm^3 by 1970-75, in response to a rapid increase in surface-water imports, discussed later.

The historical increase in withdrawal of ground water was a principal factor in causing a fairly continuous and severe 50-year decline of artesian head. In the spring of 1916, the artesian head in index well 7Rl in San Jose was 3.7 m above land surface (Figure 9.14.2); by the autumn of 1966 it was 55 m below land surface. The second major factor in this 50-year decline of 59 m was the negative trend of the local water supply. The upper line in Figure 9.14.2 is a plot of the cumulative departure, in per cent, of the seasonal rainfall at San Jose from the 50-year seasonal mean, 1897-98 to 1946-47 (Calif. State Water Resources Board, 1955, p. 26). The 50-year mean is 34.85 cm. Except for the 6-year wet period 1936-42, the departure in the 50

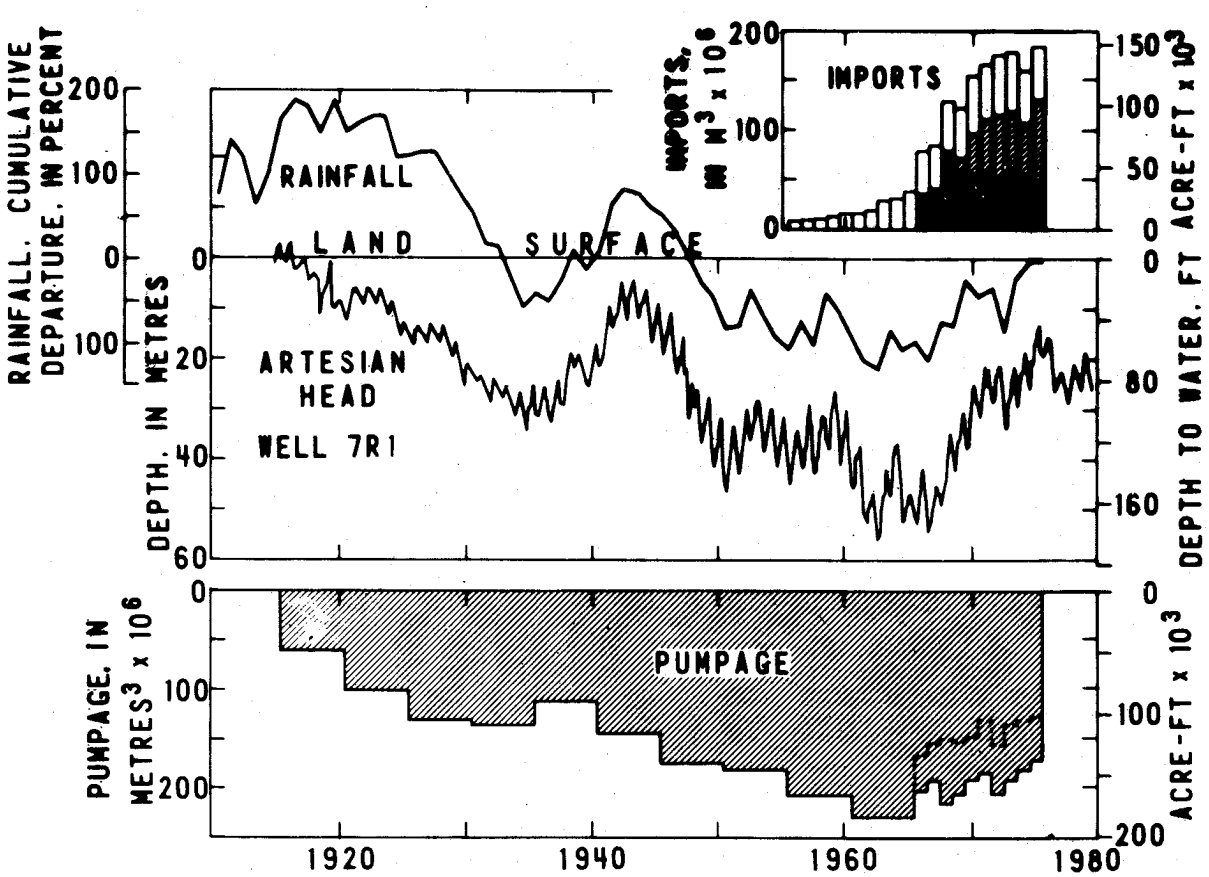

Figure 9.14.2 Artesian-head change in San Jose in response to rainfall, pumpage, and imports.

years 1916--66 was generally negative; the cumulative departure of 310 per cent from 1916 to 1966 represents a cumulative "deficiency" in rainfall of about 108 cm.

The 50-year decline in artesian head from 1916 to 1966 clearly was caused by the cumulative effect of generally deficient rainfall and runoff and a fourfold increase in withdrawals. The plot of artesian-head decline at index well 7R1 conforms in general with the cumulative departure of rainfall at San Jose.

9.14.4 LAND SUBSIDENCE

Land subsidence was first noted in 1932-33 when bench mark P7 in San Jose, established in 1912, was resurveyed and found to have subsided 1.2 m. As a result, a valleywide network of bench marks was established in 1934 (Poland and Green, 1962, Figure 3). The total length of survey lines comprising this bench-mark net was about 400 km. From 1934 to 1967 the National Geodetic Survey (formerly the U.S. Coast and Geodetic, Survey) resurveyed the network from "stable" bedrock ties a dozen times to determine changes in elevation of the bench marks; the latest full survey of the network was in 1967. In the 33 years 1934-67, subsidence along lines of benchmark control ranged from 0.3 to 1.2 m under the Bay to 2.4 m in San Jose (Figure 9.14.1). About 260 km^2 subsided more than 1 m. The subsidence record for bench mark P7 in central San Jose is plotted in Figure 9.14.3, together with the artesian head in nearby index well 7R1, taken from Figure 9.14.2. The black dots on the subsidence curve indicate times of bench-mark surveys. The fluctuations of artesian head represent the change in stress on the confined aquifer system; the subsidence is the resulting strain. Subsidence of bench mark P7 began about 1918 (note dotted inferred segment of subsidence plot representing the period 1912 to 1919) and reached 1.4 m in 1934. From 1938 to 1947 subsidence stopped, during a period of artesian-head recovery, in response to above-normal rainfall and recharge. (The natural recharge was supplemented by controlled percolation releases from newly constructed detention reservoirs on the larger streams.) Subsidence resumed in 1947 as a consequence of a rapidly declining artesian head due to deficient rainfall and increasing demand for ground water (Figure 9.14.2); it attained its fastest average rate in 1960-63 (0.22 m/year), in response to the rapid head decline of 1959-62 during a drought period (see Figure 9.14.2). By 1967 bench mark P7 had subsided 3.86 m.

Figure 9.14.4 shows land-subsidence profiles along line A-A′ from Redwood City to Coyote from 1912 through 1969 (for location, see Figure 9.14.1). The spring 1934 leveling was used as a reference base because this was the first complete leveling of the net. Note that from 1934 to 1967, maximum subsidence of 2.6 m was near bench mark W111, 4.8 km northwest of bench mark P7; also that from 1934 to 1960 the greatest subsidence along line A-A′ was 1.7 m, at bench mark

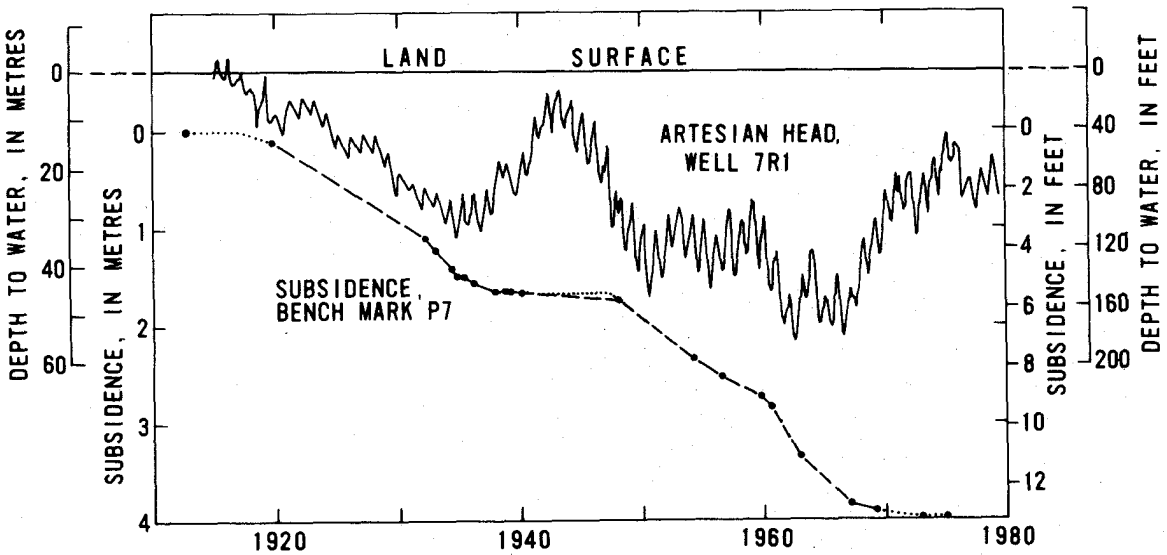

Figure 9.14.3 Artesian-head change and land subsidence, San Jose.

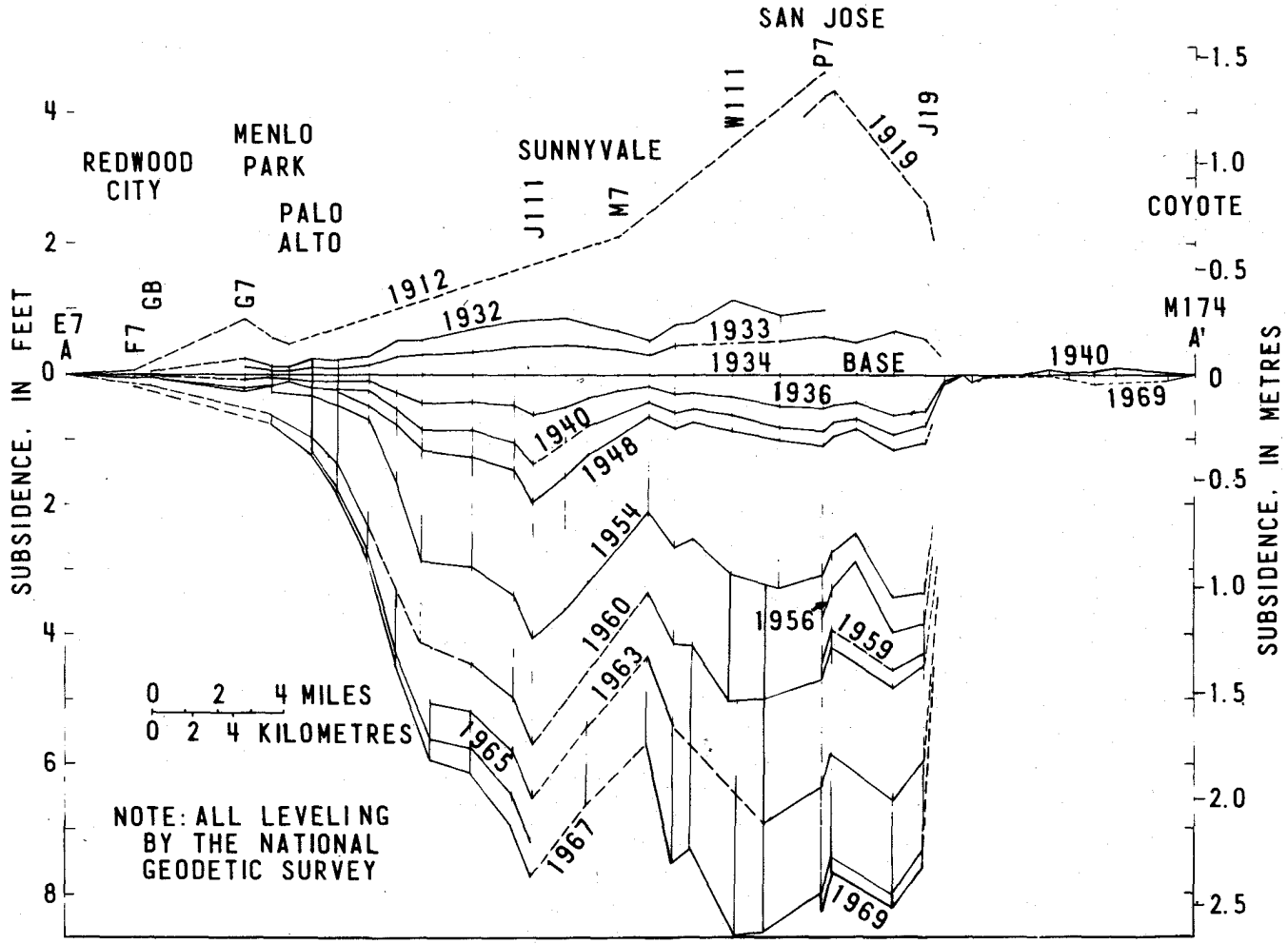

Figure 9.14.4 Profiles of land subsidence, Redwood City to Coyote, California, 1912-69.

J111 in Sunnyvale. Changes in the rate and magnitude of artesian-head decline doubtless have caused such geographic variations in subsidence rate and magnitude with time.

The volume of subsidence (pore-space reduction) planimetered from the 1934-67 subsidence map (Figure 9.14.1) was about 617 hm^3. If the ratio of the pre-1934 subsidence volume to the 1934-67 subsidence volume is assumed to be equal to the ratio of the pre-1934 subsidence of bench mark P7 to the 1934-67 subsidence of that bench mark, then the total subsidence volume from 1912 to 1967 is about 975 hm^3. Protrusion of well casings above the land surface and inundation of lands near the south end of San Francisco Bay also have furnished evidence of subsidence. Protrusion of well casings has been common in the subsiding area (Tolman, 1937, p. 345). Many of the casings gradually protruded 0.6-1 m above ground level but usually were cut off before protruding higher. This protrusion indicates that compaction of the deposits occurred in the depth interval above the bottom of the protruding casing. However, such protrusion often is accompanied by compression and rupture of the casing at depth and thus supplies only a minimal value of subsidence. In general, the deeper the compacting interval, the smaller will be the protrusion in proportion to the subsidence, because the frictional drag of the formation or the gravel-pack on the casing wall should increase proportionately with depth.

Although some horizontal movement doubtless has occurred in the subsidence area in association with the subsidence, no surveys or evidence of horizontal movement are known to the author.

The comparison of artesian-head change and subsidence from 1916 to 1967 (Figure 9.14.3) demonstrates beyond a reasonable doubt that the increase in effective stress resulting from the declining artesian head caused the compaction and the subsidence.

9.14.5 EXTENSOMETERS TO MEASURE COMPACTION

Extensometers (compaction recorders) were installed by the Geological Survey in 1960 in the cased core holes 305 m deep in San Jose (16C6) and in Sunnyvale (24C7) and in several unused water-supply wells. (For location, see Figure 9.14.1.) The purpose of this equipment was to measure the rate and magnitude of compaction occurring between the land surface and the well bottom. When first installed, the extensometer consisted of an anchor placed in the formation below the casing bottom, attached to a cable that passed over sheaves at the land surface and was counterweighted to maintain constant tension (Figure 2.5A). A recorder actuated by cable movement yields a time graph of the movement of land surface with respect to the anchor--the compaction or expansion of the deposits within that depth range. To reduce friction and increase the accuracy of measurement four of the extensometers were modified in 1972 by replacing the cable with a free-standing pipe of 3.8-cm diameter (Figure 2.5B) within the well casing of 10-cm diameter. The records obtained from these instruments show that the measured compaction to the depth of 305 m is nearly equal to the land subsidence as measured periodically by releveling of the bench-mark network. Thus, these instruments function as continuous subsidence monitors.

Figure 9.14.5 shows the measured compaction in the 305-m well in San Jose (well 16C6) and the compaction and artesian-head fluctuation in adjacent unused well 16C5 (depth 277 m) through 1975. The dashed line represents subsidence of adjacent bench mark JG2 as determined by periodic releveling from stable bench marks. Measured compaction of the confined aquifer system to the 305-m depth from July 1, 1960, to December 31, 1976, was 1.4 m.

9.14.6 MEASURES TAKEN TO CONTROL SUBSIDENCE

Local agencies have been working since the 1930's to conserve water and to obtain water supplies adequate to stop the ground-water overdraft and raise the artesian head. Their program has involved (1) salvage of flood waters from local streams that would otherwise waste to the Bay and (2) importation of water from outside the valley. In 1935-36 five storage dams were built on local streams to provide detention reservoirs with combined storage capacity of about 62 hm^3 to retain floodwaters and permit controlled releases to increase streambed percolation (Hunt, 1940). The storage capacity of detention reservoirs was increased to 178 hm^3 in the early 1950's (Calif. State Water Resources Board, 1955, p. 51).

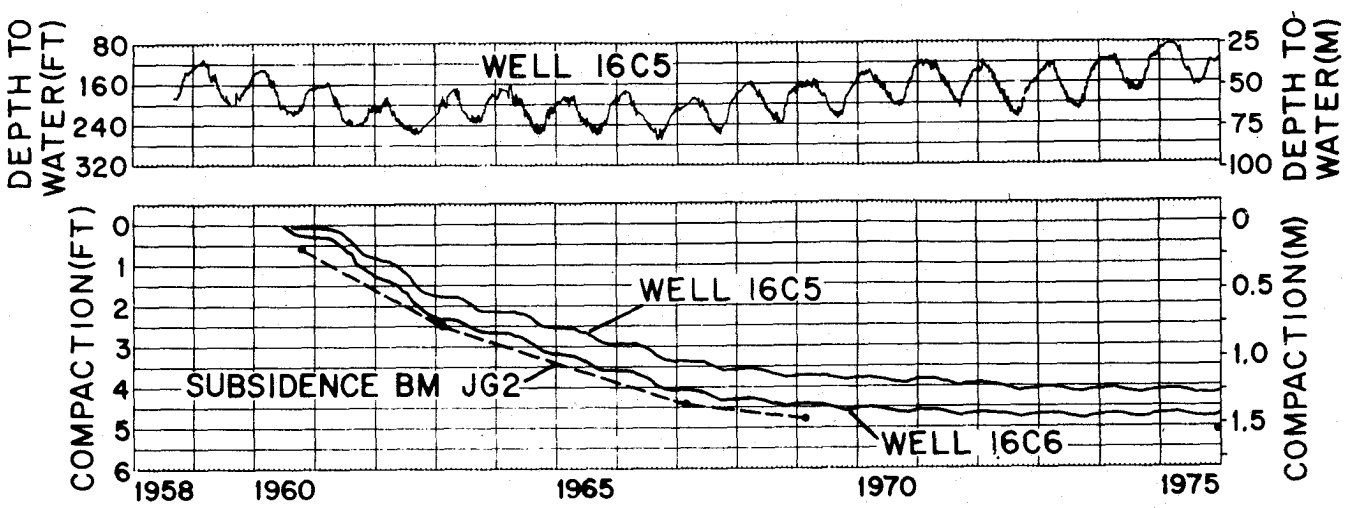

Figure 9.14.5 Measured water-level change, compaction, and subsidence in San Jose.

By 1960, sharply declining water levels furnished evidence that local resources were not adequate to supply present and future water needs. Steps were taken to increase water imports to the County. The import of surface water to Santa Clara County began about 1940 when San Francisco commenced selling water imported from the Sierra Nevada to several municipalities. This import increased to 15 hm^3 in 1960 and to 54 hm^3 by 1975 (see blank segments of yearly bars, upper right graph, Figure 9.14.2). Surface water imported from the Central Valley through the State's South Bay Aqueduct first became available in 1965; by 1974-75, the aqueduct import was 128 hm^3 (see cross-hatched plus diagonally ruled segments of yearly bars, upper right graph, Figure 9.14.2). As a result, total imports to Santa Clara County increased five-fold from 1964-65 to 1974-75--from 37 to 183 hm^3 per year.

The recovery of water level since 1967 has been dramatic. By 1975, the spring high water level at index well 7R1 (Figure 9.14.2) was 32 m above that of 1967, and about equal to the level in this well in 1925. This major recovery of head was due primarily to the fivefold increase in imports from the Central Valley. Two other favorable factors were the above-normal rainfall and the decreased pumpage (Figure 9.14.2).

The average seasonal rainfall at San Jose was 13 per cent above normal in the period 1966-75. The cumulative departure graph (Figure 9.14.2) indicates an increase of 120 per cent or a cumulative excess of about 41 cm above normal in the 9-year period.

The average yearly pumpage of ground water, which had reached its peak of 228 hm^3 in 1960-65, decreased to 185 hm^3 in 1970-75. A principal reason for this 19-per cent decrease was a use tax levied on ground-water pumpage since 1964. In 1977, for example, the ground-water tax was levied at $8.50 per unit (1 acre-ft. or 1234 m^3) for ground water extracted for agricultural purposes and at $34 per unit for ground water extracted for other uses. The energy cost to the consumer for pumping ground water in the Santa Clara Valley at 1977 prices was $10 to $15 per unit. Thus, the average total cost for ground water pumped for agricultural purposes was about $20 per unit and for other uses was about $45 per unit. The price for surface water delivered in lieu of extraction was $14 per unit for water used for agriculture and $39.50 per unit for water used for other purposes. The economic advantage of buying surface water, where available, is obvious.

Recharge to the ground-water reservoir from regulated local runoff released to stream channels and percolation ponds has been augmented since 1965 by water from the South Bay Aqueduct that could not be delivered directly to the user. The quantity diverted to recharge areas (cross-hatched segment of yearly bars, upper right graph, Figure (9.14.2) in the 10 years to 1975 averaged about 50 hm^3 per year and represents 56 per cent of the total import from the South Bay Aqueduct.

The marked decrease in rate of subsidence in response to the dramatic head recovery from 1967 to 1975 is demonstrated graphically by the compaction records from the two deep extensometers in San Jose and Sunnyvale (Figure 9.14.6). The rate of measured compaction in well 16C6 in San Jose decreased from about 30 cm per year in 1961 to 7.3 cm in 1967 and to 0.3 cm in 1973. Net expansion (land-surface rebound) of 0.6 cm occurred in 1974. In Sunnyvale, compaction of the sediments above the 305-m anchor in well 24C7 decreased from about 15 cm per year in 1961 to 1.2 cm in 1973; net expansion of 0.5 cm and 1.1 cm occurred in 1974 and 1975, respectively. Very deficient rainfall in 1975-76 and in 1976-77 virtually eliminated runoff and recharge from local sources, and water levels started to decline once more in 1976. In response, compaction and subsidence resumed once again. In San Jose at well 16C6, compaction in 1976 was 3.5 cm, about equal to that in 1968; in Sunnyvale, compaction was 1.6 cm.

9.14.7 COMPRESSIBILITY AND STORAGE PARAMETERS

Compressibility characteristics of fine-grained compressible layers (aquitards) can be obtained by making one-dimensional consolidation tests of "undisturbed" cores in the laboratory. As one phase of the research on compaction of the aquifer system, laboratory consolidation tests were made on 21 selected fine-grained cores from the two core holes. These tests were made in the Earth Laboratory of the United States Bureau of Reclamation at Denver, Colorado. Parameters tested included the compression index, C_c, a measure of the nonlinear compressibility of the sample, and the coefficient of consolidation, C_v, a measure of the time rate of consolidation. Complete results of these laboratory tests have been published (Johnson and others, 1968, Tables 8 and 9 and Figure 21). The 21 samples tested spanned a depth range from 43 to 292 m below land surface. The range of the compression index, C_c, was small compared to the range in the San Joaquin Valley: the maximum value was 0.33, the minimum 0.13, and the mean was 0.24. Of the 21 samples, 15 had C_c values falling between 0.20 and 0.30. This suggests that the nonlinear

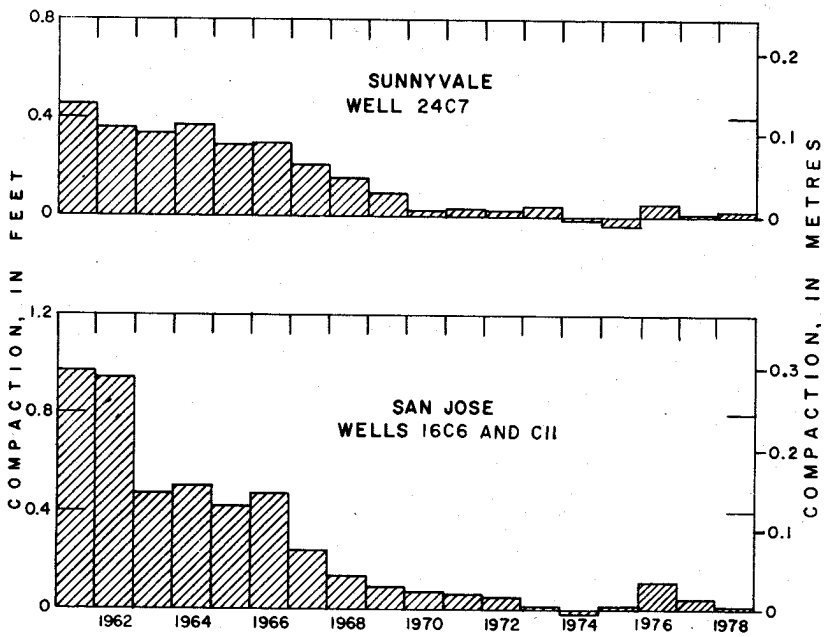

Figure 9.14.6 Measured annual compaction to 305-m (1,000-ft) depth.

compressibility characteristics of the aquitards in the confined aquifer system do not vary widely.

The plot of void ratio against the log of load (effective stress), known as the e-log p plot, can be used to obtain a graphic plot of compressibility versus effective stress. Such a graph can be used to estimate ultimate compaction due to a step increase in effective stress. This procedure applied to the laboratory consolidation tests at the Sunnyvale and San Jose core holes produced estimates of ultimate compaction that were only about one-third to one-half the values obtained by summing field measurements of compaction to date with residual compaction estimated from a one-dimensional simulation of the field observations (Helm, 1976). The reason for this disparity is not known. Apparently the samples tested were not representative of the aquitards that contributed most to the observed compaction.

Subsidence represents pore-space reduction which occurs almost wholly in the fine-grained compressible aquitards. At well 16C6 in San Jose the confined aquifer system is 244 m thick, from 61 to 305 m below land surface. Based on study of the microlog, the confined system contained 38 aquitards with a combined thickness of 145 m. The mean porosity of 27 core samples, determined in the laboratory, was 37 per cent. The total subsidence to date at well 16C6 is about 4 m. A reduction of 4 m in the thickness of the confined system requires about 1.8 per cent reduction in the porosity of the aquitards--for example, from 37 to 35.2 per cent.

The subsidence/head-decline ratio is a useful parameter in subsidence studies. The ratio is a rough approximation of the response of the aquifer system to a given change in stress. At San Jose, referring to the plot of subsidence for bench mark P7 and the artesian-head change in well 7R1 (Figure 9.14.3), the artesian head declined from 6 m below land surface in 1918 (approximate preconsolidation stress) to 55 m below land surface in 1966, for a net change of 49 m. Subsidence at bench mark P7 from 1918-66 was about 3.84 m. This means that as of 1966 the empirical ratio is 3.84 m/49 m = 0.08. The ratio of ultimate subsidence to head decline must therefore be larger than 0.08 at this site. Artesian head as measured in a well casing represents a composite pore pressure of all aquifers in the confined system that are tapped by the observation well. If and when the pore pressures in fine-grained aquitards reach equilibrium with those in the adjacent aquifers, compaction will cease, and the ratio of ultimate subsidence to head decline will be a true measure of virgin compressibility for the entire interval being stressed. Such an ultimate value is analogous to a storage coefficient.

Helm (1977), by means of a one-dimensional simulation of the long-term field observations of subsidence at bench march P7 and artesian head at well 7RI, provided the parameters used for estimating the ultimate compaction (subsidence) resulting from a step change in head of 49 m;

the computed compaction is about 5.3 m. Thus, on the basis of Helm's parameter values, the ultimate subsidence/head-decline ratio would be 5.3 m/49 m = 0.11. If we divide the ratio by the thickness of compacting aquitards, 145 m, we obtain the virgin compressibility (for stress increase beyond preconsolidation stress) of the aquitards:

$$5.3\ m/(145\ m \times 49\ m) = 7.4 \times 10^{-4} m^{-1}$$

As the water levels in the San Jose area rose rapidly after 1967 (Figure 9.14.2), the stress-strain curves obtained from paired measurements of compaction and artesian head began to show seasonal expansion during the winter months when the water level was highest and the effective stress on the confined system was lowest. These stress-strain loops can be used to obtain the compressibility of the confined system in the recoverable or elastic range of stresses (less than preconsolidation stress). One example (Figure 9.14.7) shows the stress-compaction plot for a pair of wells in San Jose from 1967 through 1974. Compaction was measured in well 16C6,11, 305 m deep, and stress in nearby well 16C5. Depth to water is plotted increasing upward. Change in depth to water represents an average change in stress in all aquifers of the confined aquifer system tapped by well 16C5. The lower parts of the descending segments of the annual loops for the winters of 1967-68, 1969-70, and 1970-71 are approximately parallel, as shown by the dotted lines, indicating that the response is essentially elastic in both aquifers and aquitards when the depth to water is less than about 55 m. The heavy dashed line drawn parallel to the dotted lines represents the average slope of the segments in the range of stresses less than preconsolidation stress. The reciprocal of the slope of this line is the component of the storage coefficient attributable to elastic or recoverable deformation of the aquifer-system skeleton, S_{ke}, and equals 1.5×10^{-3}. The component of average specific storage due to elastic deformation, S_{ske}, equals $S_{ke}/244\ m = 6.15 \times 10^{-6} m^{-1}$, if stresses are expressed in metres of water, and if γ_w (the unit weight of water) = 1, the average elastic compressibility of the aquifer system skeleton, α_{ke}, is equal numerically to S_{ske}.

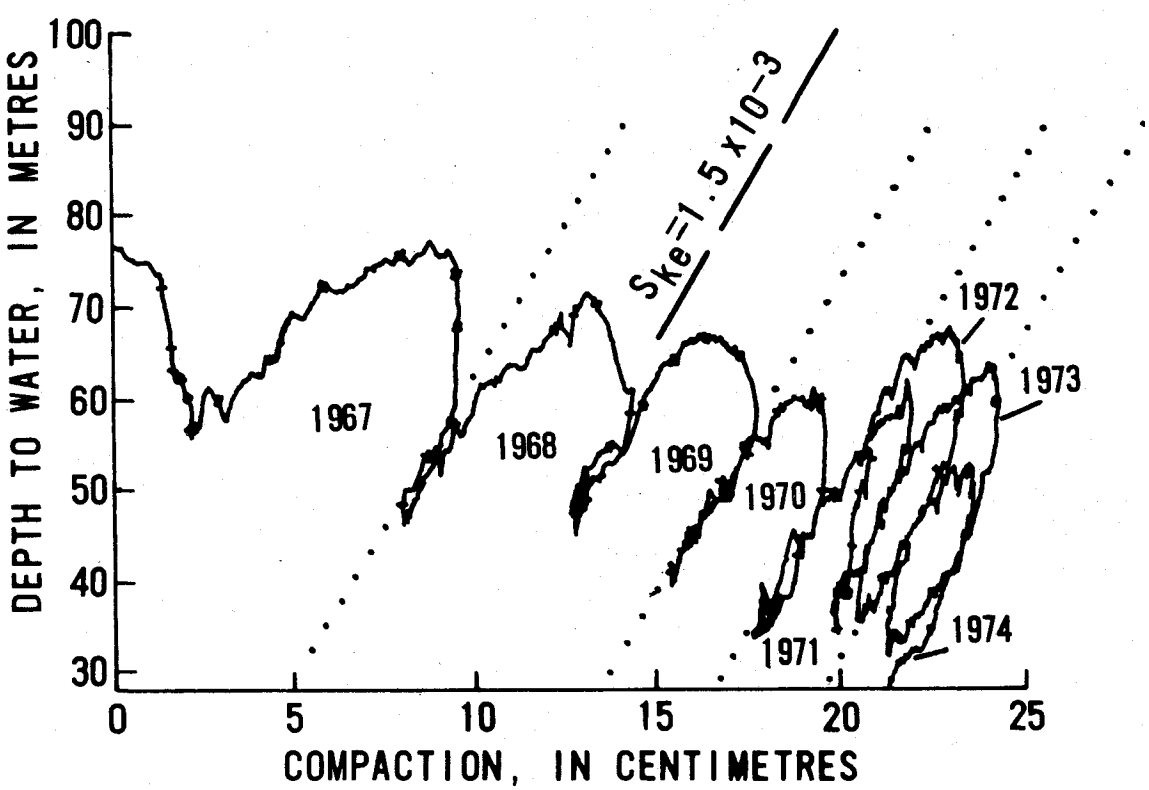

Figure 9.14.7 Stress change and compaction, San Jose site.

In these computations I have assumed that in the range of stresses less than preconsolidation stress, the compressibility of the aquitards and the aquifers is the same. Therefore, the full thickness of the confined aquifer system, 244 m, was used to derive the specific storage component, S_{ske}, in the elastic range of stress.

At these San Jose sites, then, the average compressibility of the aquitards in the virgin range of stress, 7.4×10^{-4} m^{-1}, is 120 times as large as the average compressibility of the confined aquifer system in the elastic range of stress, 6.15×10^{-6} m^{-1}. This great difference in response to stressing should be kept in mind when considering use of aquifer tests to derive hydrologic parameters, as well as in appraisal of subsidence potential.

9.14.8 ECONOMIC AND SOCIAL IMPACTS

Subsidence has created several major problems. Lands adjacent to San Francisco Bay have sunk as much as 2.4 m since 1912, requiring construction and repeated raising of levees to restrain landward movement of the saline bay water onto 44 km2 of land below high-tide level in 1967. Also, flood-control levees have been built and maintained near the bayward ends of the depressed stream channels. About $9 million of public funds had been spent to 1974 on such flood-control levees to correct for subsidence effects, according to Lloyd Fowler, former Chief Engineer of the Santa Clara Valley Water District. In addition, a major salt company has spent an unknown but substantial amount maintaining levees on 78 km2 of salt ponds to counter as much as 2.4 m of subsidence. Several hundred water-well casings have failed in vertical compression, due to compaction of the sediments. The cost of repair or replacement of such damaged wells has been estimated as at least $4 million (Roll, 1967). Including funds spent on maintaining the salt-pond levees, establishing and resurveying the bench-mark net, repairing railroads, roads, and bridges, replacing or increasing the size of storm and sanitary sewers, and making private engineering surveys, the direct costs of subsidence must have been at least 35 million dollars to date.

A major earthquake could cause failure of the bay-margin levees, resulting in the flooding of areas presently below sea level. The levees were constructed of locally derived weak materials and were designed only to retain salt-pond water under static conditions (Rogers and Williams, 1974). The potential for such an earthquake poses a continuing threat to flooding of the estimated 44 km^2 (4400 hectares) of land standing below high tide level as of 1967. Such a threat must have reduced the value of this land very substantially compared to the value if it all still stood above mean sea level as it did in 1912. This decrease in land value should be included in the gross costs of subsidence.

9.14.9 LEGAL ASPECTS

The successful management of a highly variable water supply to achieve a balance with an ever-increasing demand for water in Santa Clara County (not shown on map) has been remarkable for several reasons. First, maximum development of local water supplies and importation of water from two sources have momentarily brought supply and demand into balance. Secondly, by building up the ground-water storage in the recharge area, and thus the artesian head in the confined system, land subsidence was stopped, at least temporarily, by 1973. Thirdly, all this has been accomplished by bond issues, revenue from taxes, and water charges, thus avoiding a drawn-out expensive legal adjudication of the ground-water supply such as occurred in southern California, in the Raymond Basin (Pasadena vs. Alhambra, 1949).

9.14.10 CONCLUSIONS

Both the cause of subsidence and the means of its control are known. The evidence given here proves that the subsidence is caused by decline of the artesian head and the resulting increase in effective overburden load or grain-to-grain stress on the water-bearing beds in the confined system. The sediments compact under the increasing stress and the land surface sinks. Most of the compaction occurs in the fine-grained clayey beds (aquitards) which are the most compressible but have low permeability. Therefore, the escape of water from these slow draining aquitards (decay of excess pore pressure) and the increase in effective stress are slow and time-dependent, but the ultimate compaction is large and chiefly permanent.

The subsidence has been stopped by raising the artesian head in the aquifers until it equaled or exceeded the maximum pore pressures in the aquitards. The compaction and water-level records being obtained by the Geological Survey indicate that if the artesian head can be maintained 3 to 6 m above the levels of 1971-73, subsidence will not recur. On the other hand, subsidence will recommence if artesian head is drawn down as much as 6 to 9 m below the 1971-73 levels.

9.14-11 EPILOGUE

Recently the Santa Clara Valley Water District was given Historical Landmark status by the American Society of Civil Engineers for its major contributions to the development of the region. It was acknowledged that the district's system is "the first and only instance of a major water supply being developed in a single ground-water basin involving the control of numerous independent tributaries to effectuate almost optimal conservation of practically all of the sources of water flowing into the basin."

9.14.12 REFERENCES

CALIFORNIA DEPARTMENT OF WATER RESOURCES. 1967. Evaluation of ground-water resources, South Bay: Calif. Dept. Water Resources Bull. No. 118-1, Appendix A, Geology, 153 p.

CALIFORNIA STATE WATER RESOURCES BOARD. 1955. Santa Clara Valley Investigation: Calif. State Water Resources Board Bull. No. 7, 154 p.

CLARK, W. 0. 1924. Ground water in Santa Clara Valley, Calif.: U.S. Geol. Survey Water-Supply Paper 519, 207 p.

DIBBLEE, T. W. 1966. Geologic map of the Palo Alto 15-minute quadrangle, California: Calif. Div. Mines and Geology, Map sheet 8.

HUNT, G. W. 1940. Description and results of operation of the Santa Clara Valley Water Conservation Districts project: Am. Geophys. Union Trans., pt. 1, p. 13-22.

HELM, D. C. 1977. Estimating parameters of compacting fine-grained interbeds within a confined aquifer system by a one-dimensional simulation of field observations: Internat. Symposium on Land Subsidence, 2d, Anaheim, Calif., Dec. 1976, Proc., p. 145-156.

JOHNSON, A. I., MOSTON, R. P., and MORRIS, D. A. 1968. Physical and hydrologic properties of water-bearing deposits in subsiding areas in central California: U.S. Geol. Survey Prof. Paper 497-A, 71 p.

MEADE, R. H. 1967. Petrology of sediments underlying areas of land subsidence in central California: U.S. Geol. Survey Prof. Paper 497-C, 83 p.

PASADENA v. ALHAMBRA (33 Cal. 2d 908 207 Pac. 2d 17) 1949; certiorari denied (339 U.S. 937) 1950.

POLAND, J. F. 1969. Land subsidence and aquifer-system compaction, Santa Clara Valley, California, USA, in Tison, L. J., ed., Land Subsidence, Vol. 2: Internat. Assoc. Sci. Hydrology, Pub. 88, p. 285-292.

_____. 1977. Land subsidence stopped by artesian-head recovery, Santa Clara Valley, California.: Internat. Symposium on Land Subsidence, 2d, Anaheim Calif., Dec. 1976, Proc., p. 124-132 (I.A.H.S., Pub. 121).

POLAND, J. F., and Green, J. H. 1962. Subsidence in the Santa Clara Valley, California--A progress report: U.S. Geol. Survey Water-Supply Paper 1619-C, 16 p.

ROGERS, T. H., and Williams, J. W. 1974. Potential seismic hazards in Santa Clara County, Calif.: Calif. Div. Mines and Geology, Special Report 107, 39 p. 6 pl.

ROLL, J. R. 1967. Effect of subsidence on well fields: Am. Water Works Assoc. Jour., v. 59, no. 1, p. 80-88.

TOLMAN, C. P. 1937. Ground Water: New York, McGraw-Hill Book Co., 593 p., lst ed.

TOLMAN, C. P., and Poland, J. F. 1940. Ground-water, salt-water infiltration, and ground-surface recession in Santa Clara Valley, Santa Clara County, California: Am. Geophys. Union Trans., p. 23-35.

WEBSTER, D. A. 1973. Map showing areas bordering the southern part of San Francisco Bay where a high water table may adversely affect land use: U.S. Geol. Survey Misc. Field Studies Map MF 530.

Case History No. 9.15. Ravenna, Italy, by Laura Carbognin, Paolo Gatto, and Giuseppe Mozzi, National Research Council, S. Polo 1364, Venice, Italy

9.15.1 INTRODUCTION

Ravenna is about 60 km south of the Po delta, in a symmetric position with respect to Venice (Figure 9.15.1). Land subsidence in this area has been observed for a long time but only recently did the related consequences become critical. Progressively affecting the entire territory of about 700 km^2 (Figure 9.15.2), the subsidence increasingly threatens not only the industrial area, and the urban zones, but also the surrounding vast marshland reclamations which could be submerged once again. The existence of several buildings and historical monuments is jeopardized as well, since their foundations have to be kept dry by pumping out water continuously.

It became clear from the first analysis, started in 1970 by the National Research Council of Venice at the request of the Municipality of Ravenna, that the causes of land subsidence had to be mainly ascribed to the removal of fluids from the subsurface (Bertoni, et al., 1973).

The investigation began with the inventory of available stratigraphic, hydrological, geotechnical, and geodetic data. Unfortunately no information was available concerning physical and mechanical properties of the formations. Good historical data are available for both piezometry of the aquifers and subsidence. Field measurements such as leveling and hydraulic head records were carried out almost annually, using networks of suitably placed bench marks and piezometers, similarly to what was done for Venice. The preliminary hydrogeological in-

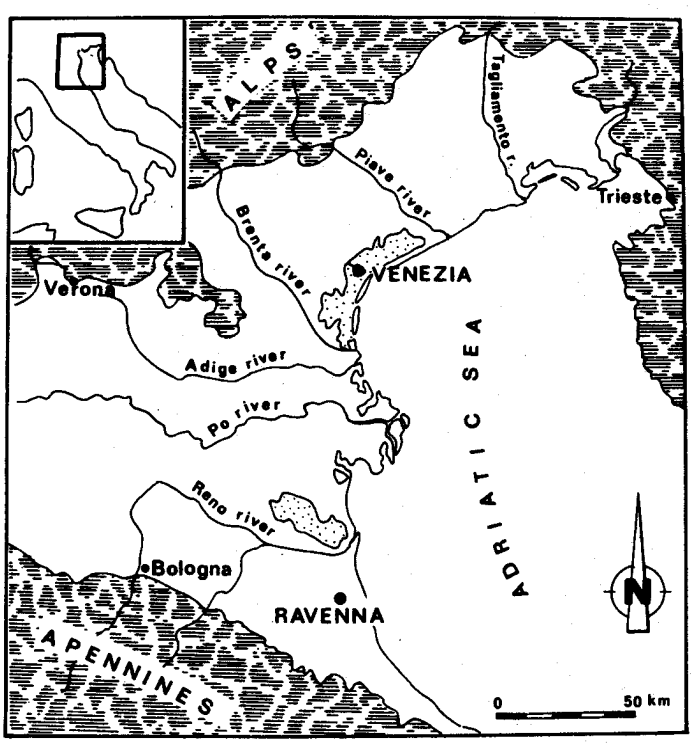

Figure 9.15.1 Areas of Ravenna and Venezia. They are symmetric with respect to the Po delta. (From Carbognin, et al., 1978, Figure 13; published with permission of the American Society of Civil Engineers.)

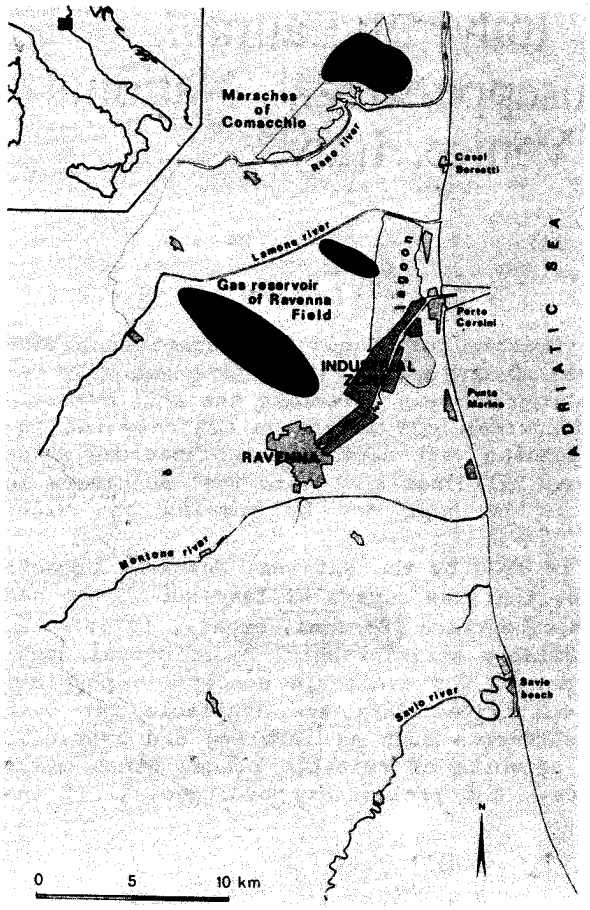

Figure 9.15.2 Map of the area under investigation (District of Ravenna). (From Carbognin, et al., 1978, Figure 1; published with permission of the American Society of Civil Engineers.)

vestigation will be further improved by using the information obtained through specifically programmed test holes. The research already undertaken has, however, provided a good understanding of the overall subsidence occurrence.

After a preliminary description of the geological environment, this paper presents the history of the pressure decline in the aquifer and land settlement and discusses their relationships.

9.15.2 HYDROLOGICAL FEATURES

The total thickness of Quaternary sediments in the Ravenna area ranges between 1500 and 3000 metres and mostly consists of sandy and silty-clay layers of alluvial and marine origin. The bottom of the Quaternary sediments follows the structure of the pre-Quaternary substratum, characterized by folds and faulted overfolds which are parallel to the main tectonic profiles of the Apennines and include several gas-bearing traps at depths on the order of 2000 m (Figure 9.15.3) (Agip Mineraria, 1969a).

The presence of massive Quaternary deposits confirms that in the past the geologic subsidence was quite pronounced in this area and is still rather active (Salvioni, 1957); it is apparent that the tectonic stresses acting along a SW direction tend to increase the Po basin curvature. The deep structure has influenced the thickness of the Neozoic formations and consequently the subsidence rate exhibits a non-uniform space distribution (Dal Piaz, 1969).

The stratigraphy of the upper Quaternary sediments is not defined with accuracy, due to the partial lack of information. However, it has been possible to reconstruct schematically the map

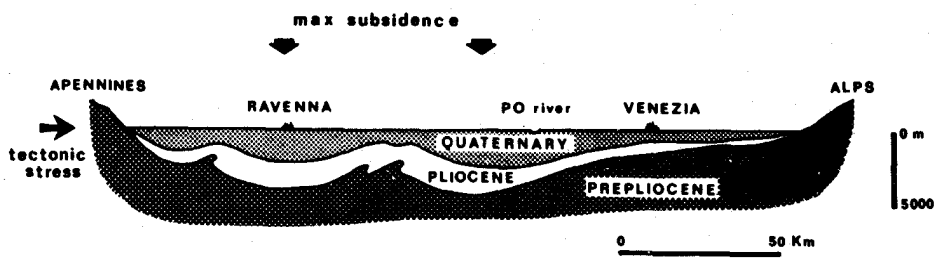

Figure 9.15.3 Very schematic cross-section of the Po Valley between Venezia and Ravenna (Agip Mineraria, 1969a).

of the aquifer system down to 500 m using the relative positions of the intakes of several pumping wells and other sparse lithological information.

Between 90 and 430 m the confined units are well identified and rather continuous (Figure 9.15.4) (Bertoni, et al., 1973). In the upper 90 m the areal continuity of the sands is quite limited and the definition of large important formations is uncertain. This portion of the system is little exploited due both to reduced productivity and possible water pollution from the overlying polluted unconfined aquifer. Below 430 m the salt content becomes very high (Agip Mineraria, 1972) and the water cannot be used any longer for industrial and/or agricultural purposes.

From the information available, the aquitards separating the various sandy formations appear to be rather continuous with very low permeability. The logs suggest that large amounts of silty sediments are present. The aquifers shown in Figure 9.15.4 consist mostly of fine and medium sands with occasional shells. However, clayey or silty sands also may be found which locally reduce the aquifer transmissivity.

The recharge of this confined multi-aquifer system comes mainly from the foothills of the Apennines as well as from the Po River basin (Figure 9.15.5) (Carbognin, et al., 1978). It is clearly impossible on the basis of the available records to quantify the respective contributions.

9.15.3 SUBSOIL RESOURCES EXPLOITATION AND SUBSIDENCE

It was soon quite clear that as in the Venice case the surface settlement was caused by the removal of subsoil fluids. Since the withdrawal rate is hard to assess with accuracy, the behaviour of the subsurface flow field was kept under periodic observation through a network of 120 piezometers (Figure 9.15.6). A 1972 survey of the area revealed that 877 active wells tapped the 9 confined aquifers. These wells were scattered across the area, but the most recent and productive ones were concentrated on the industrial zone (Bertoni, et al., 1973).

Figure 9.15.7 shows the behavior of the piezometric levels of the various aquifers underlying the historical center (Carbognin, et al., 1978). It is evident from this figure that:

- there was a lowering of the hydraulic head below the ground level beginning in the 1950's;
- the greatest decline occurred after 1960, simultaneously with the development of the nearby industrial zone;
- aquifers 4 and 5 are the most intensively exploited;
- among the head gradients found in the aquitards the highest occurs between aquifers 3 and 4, with a difference of head of 22.50 m;
- in recent years the piezometric level tends to be constant;
- aquifers exhibit a somewhat independent hydraulic behavior (except perhaps aquifers 1 and 2). This is further evidence that the basin underlying Ravenna is a real multi-aquifer system.

Piezometric records permitted periodical plotting of equipotential lines. As an example, Figure 9.15.8 gives the piezometric surface in 1977 averaged over all the aquifers between 100 and 430 m (Carbognin, et al., 1978). It may be observed that the maximum drawdown of about 40 m occurs in the industrial zone (it was the same in 1972). Today, however, a large decline extends even

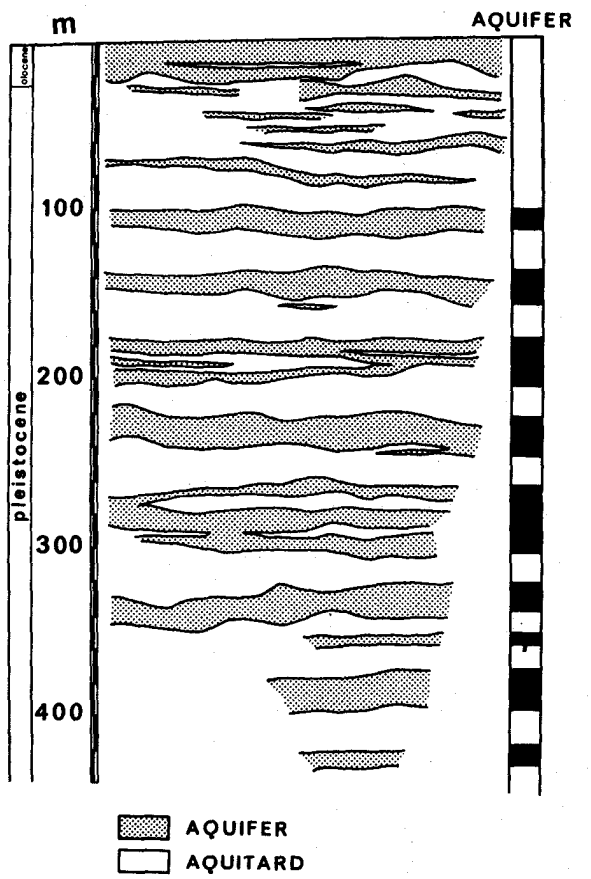

Figure 9.15.4 Schematic cross-section of the Ravenna aquifer system. (From Carbognin, et al., 1978, Figure 3; published with permission of the American Society of Civil Engineers.)

to the western and southern parts of the territory due to the increase of water withdrawn for agricultural uses, seaside resorts, and new industrial parks springing up on the outskirts of Ravenna.

The asymmetric cone of depression develops with its major axis from NW to SE, greatly affecting the coastline. A strong gradient appears in the southern part, corresponding to the direction of the Apennines recharge.

Between 1972 and 1977, the maximum decline of the piezometric head has not changed substantially (see Figure 9.15.7). Nevertheless, even if encouraging, this does not correspond to the arresting of land subsidence, as will be seen later.

So far as the geodetic survey of the area is concerned, it was not homogeneous in time. Although the land subsidence began in the early 1950's, only since 1970 have land levelings been systematically carried out at the same time as the measurement of the piezometric levels. As an example, Figure 9.15.9 shows the subsidence experienced from 1972 to 1977. The general increase of the subsidence in these years is shown by the two maps of Figure 9.15.10. In the evaluation of the rate of subsidence linear trends are assumed. It may be noted that the area experiencing subsidence exceeding 3 cm/y in the latter period is about 30 times greater than the corresponding area in the former one. Moreover, a settlement rate exceeding 5 cm/y was experienced in the last few years (Figure 9.15.10b). The maximum rate of about 11 cm was recorded in the industrial zone between 1972 and 1973 and in Ravenna's historical center about 8 cm was observed.

The shape of the subsiding areas is in close correspondence with the cone of depression of the aquifers in both periods. The time and space correlation between ground sinking and water withdrawals is clearly evidenced in Figure 9.15.11, which shows the average piezometric level and subsidence from 1950 to 1977 along a line crossing the city and extending to the country

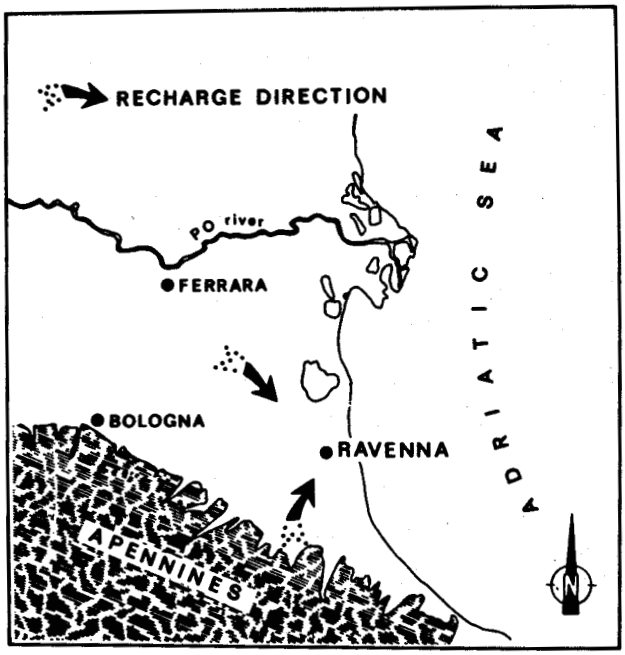

Figure 9.15.5 Map of the recharge areas of the Ravenna aquifer system. (From Carbognin, et al., 1978, Figure 4; published with permission of the American Society of Civil Engineers.)

side. This comparison stresses the nearly absolute behavioral identity of these parameters (Carbognin, et al., 1978).

From 1949 to 1977 maximum subsidence of about 1.20 m was recorded in the industrial zone, but in general and especially in recent years (1972-1977) the entire area has been affected at alarming rates. Bearing in mind that the ground elevation of 90 per cent of the land between the city and the coastline does not exceed 1 m above sea level and that 20 per cent of the latter is below mean sea level, the situation is becoming more and more serious.

In the past, the main cause of subsidence was wrongly ascribed to gas exploitation. The analyses carried out, though not precisely quantified, allowed us to estimate its effective contribution to the subsidence. With no doubt gas extraction from the natural deposits contributes in some zones to increase land settlement, but it has had limited effects. For instance, by superimposing the subsidence contour map of the period 1949-1972 on that of the gas reservoir of Ravenna Field, a good correspondence is observed between the area of the traps and area of the lines of equal subsidence, both being elliptic and with their major axes oriented in a NW-SE direction (Bertoni, et al., 1973) (Figure 9.15.12).

Likewise a comparison of land subsidence and the piezometric level recorded between 1949 and 1972 along a line crossing the Ravenna Field and industrial zone (Figure 9.15.13) shows a secondary local maximum, A, of subsidence corresponding to the location of the gas reservoir, but there is no corresponding piezometric decline [for which a minimum does not exist]. On the other hand, the maximum, B, of subsidence over the industrial zone corresponds to the maximum of drawdown. However, this gas reservoir is practically depleted and in 1972 its development had already achieved 95 per cent of the potential productivity: therefore the present contribution of gas withdrawal is probably negligible.

Unfortunately little is known about the more recent offshore gas exploitations and consequently it is impossible to say how much they influence the sinking of the coastal areas. This matter requires further investigation.

Among the man-induced causes of subsidence it must be remembered that marsh-land reclamation occurred on a large scale in this territory. Since the reclamation works were completed a long time ago (over 50 years), the contribution of the fill should no longer have any influence in the subsidence occurrence.

Natural subsidence gives a nonnegligible contribution in the overall occurrence. The bench mark of Porta Adriana in the historical center provides a useful indication to quantify this

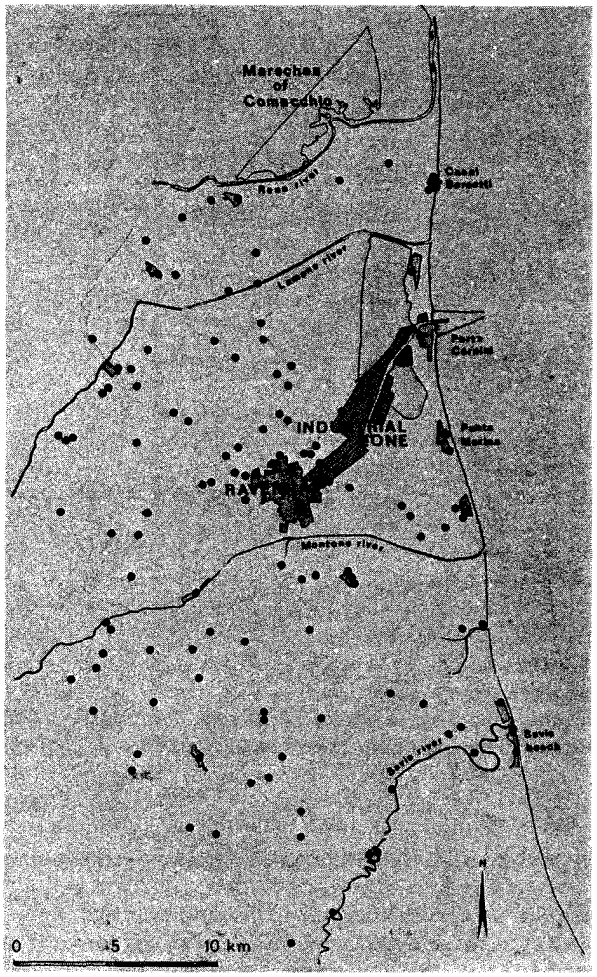

Figure 9.15.6 Map of the network of piezometers in the Ravenna area. (From Carbognin, et al., 1978, Figure 5; published with permission of the American Society of Civil Engineers.)

component since its elevation was recorded for the first time as early as 1902 (Figure 9.15.14). The data points of Figure 9.15.14 show that from 1902 to 1950 the subsidence rate was 5.14 mm/y (assuming as usual a linear trend in this period), while later on the rate has increased greatly due to the intensive exploitation of the subsurface resources. Since before 1950 water consumption was very small, the value of 5.14 mm/y may be considered as indicative of the geologic component of the subsidence in Ravenna.

To the present time the dominant factor of Ravenna subsidence is the intensive withdrawal of artesian water in the industrial zone, where the apex of the cone of depression is always found. The minimal piezometric levels reached in 1972 in the industrial zone have not changed but in spite of this additional subsidence occurred in the following years (Figure 9.15.15). This fact is partly explainable by a delay between the head declines in the aquifers and the resulting subsidence. As a second partial explanation it seems likely also that the maintenance of a very strong depression in the deepest aquifer over the last five years has introduced a secondary phenomenon of an upconing from the salt-water aquifers lying below 430 m, i.e., an irreversible pollution of the fresh-water system and a further compaction of the clayey soil aquitard. It is known in fact that some chemical variations of interstitial water in the clay soils can cause a change in the electrochemical equilibrium and therefore a collapse.

This contamination by salt water has been confirmed by the chemical analyses of the aquifer waters which evidence a progressive pollution in the industrial zone; this intrusion happened from the underlying saline water. In the nearby littoral, salt pollution of the same aquifer

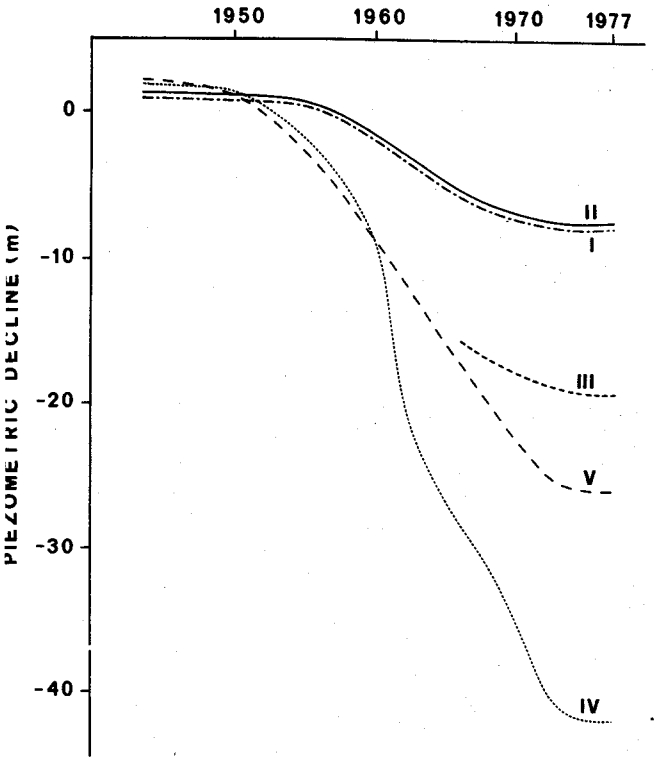

Figure 9.15.7 Piezometric levels from 1944 to 1977 of the various aquifers below the historical center of Ravenna. (From Carbognin, et al., 1978, fig. 6; published with permission of the American Society of Civil Engineers.)

occurred later but never reached the high values recorded in the industrial zone. In the coastal areas, salt water intrusion would also occur laterally.

As already shown in Figure 9.15.10b, the greatest sinking area after 1972 includes the coastline. The consequences are indeed very serious. In fact a striking regression of the shoreline and in some places the vanishing of the famous beaches of Romagna are the most severe effect of the sinking of the littoral. Not only coastal processes are responsible for it, as was believed before.

The following examples confirm the statement:

> Area of Lido Adriano: From 1957 to 1977 the regression of the shoreline has been 126 m. In the same period this zone has experienced a subsidence of about 45 cm. With a 4 per mill mean average beach slope (computed up to the isobath -8), the subsidence prevails on the process of beach regression (Figure 9.15.16).
>
> Area of Punta Marina: Between 1957 and 1977, the reported shoreline regression has been 70 m south of Punta Marina. The subsidence during these years has been 35 cm. Here the mean slope is around 4-5 per mill, and the beach regression is mostly attributable to the subsidence.

9.15.4 CONCLUSIONS

It is now clear that subsidence in the territory of Ravenna is mostly due to the intensive artesian water exploitation for industrial purposes, and, in more recent time, for agricultural uses. In some places the salt water intrusion has caused further compaction.

The exploitation of the gas reservoir of Ravenna Field has provided a minor local contribution to the subsidence; the possibility of a greater influence from the very active offshore gas fields is recognized and should be monitored.

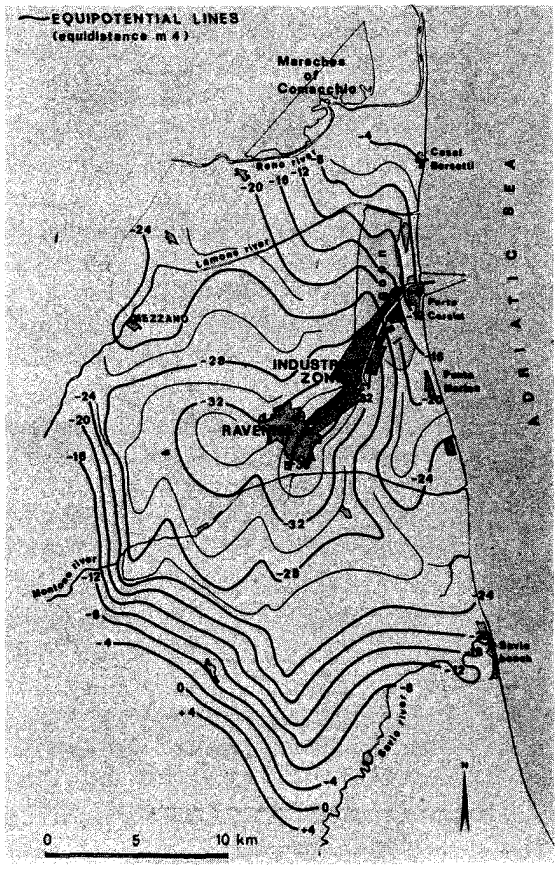

Figure 9.15.8 Average piezometric surface in 1977; datum is mean sea level. (From Carbognin, et al., 1978, Figure 7; published with permission of the American. Society of Civil Engineers.)

Since 1949 the average piezometric decline has nearly reached 45 m in the industrial area; correspondingly the average subsidence has been about 1 m. The close relationship between land settlement and water withdrawals has been clearly proven by the present analysis. Moreover if z indicates the land subsidence induced by man (i.e., the overall sinking minus geological component) and Δh is the piezometric decline expressed in the same units, we obtain a value $z/\Delta h$ approximately equal to 1/52. This result means that every 52 cm of withdrawal has produced 1 cm of subsidence. These values related to the environmental conditions place the Ravenna case among the more alarming in the world.

Apart from the values themselves, it is interesting to examine the trend of the occurrence. It is a matter of concern to find that while the subsidence still seemed quite localized around the industrial zone until 1972, it has assumed a broad increase since 1972. At present, the subsidence is affecting wide areas at a large rate and the related consequences are becoming highly critical for the survival of the whole physical and human environment.

The situation is very precarious along the littoral areas where a regression of the coastline over 150 m has been observed in some points. This threatens the most profitable industry of Romagna, i.e., the tourism.

The lands lying behind the coastal areas are in danger too. Bearing in mind that they lie at a height of less than 1 m above m.s.l., if the present trend is maintained for 10 years and if some sea storm would destroy the remaining dunes, 70 per cent of the territory between Ravenna and the beach (about 200 km^2) would permanently be inundated by the sea. Some urban zones, the industrial area, all harbor structures and several beach resort centers are in this part of the municipality. The damages would be incalculable. It is only a hypothesis, but not altogether unlikely.

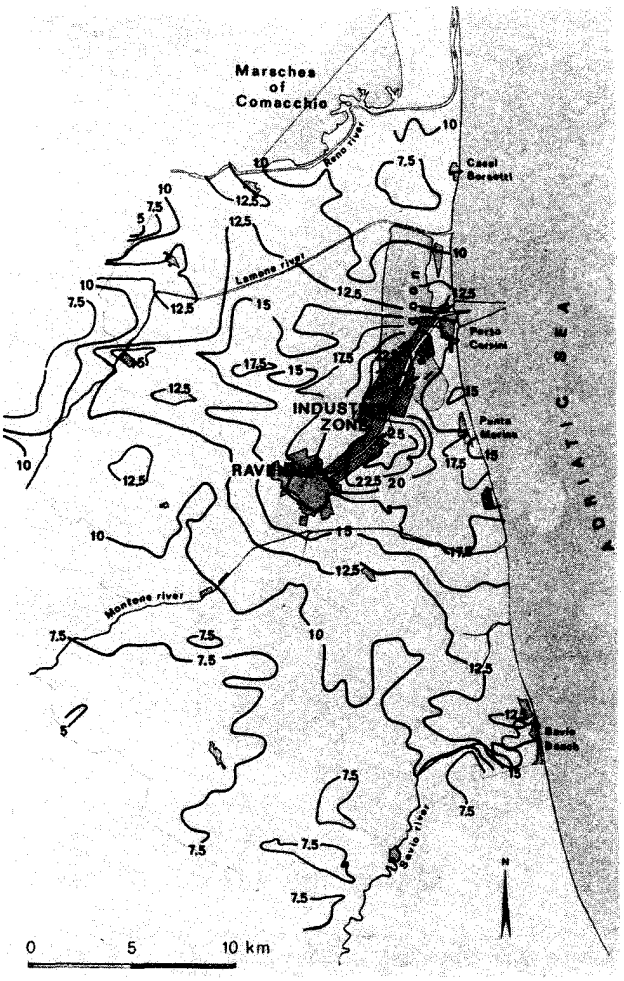

Figure 9.15.9 Land subsidence in the Ravenna area from 1972 to 1977, expressed in cm. (From Carbognin, et al., 1978, Figure 8; published with permission of the American Society of Civil Engineers.)

All this, however, is a simple projection of the present trend: a precise modeling is now in order. With enough information on physical and mechanical characteristics of the soils it would be possible to implement a mathematical simulation of the subsidence which would allow us to make real predictions on a long-term basis and understand the actual behavior of the system. In 1974 the authors (Carbognin, et al., 1974) suggested the necessary operations for investigating the knowledge on subsoil and improving the control of phenomenon evolution. In any case the subsidence control is today no longer achievable by local intervention, but only on a regional scale because of the vastness of the subsidence occurrence.

9.15.5 REFERENCES

AGIP MINERARIA. 1969a. "Relazione sull'incontro della Commissione veneziana con la Direzione Agip." Agip Mineraria, S. Donato Milanese.

_____. 1969b. "La pianura Padana-Veneta," in Italia, Geologia e ricerca petrolifera, Enciclopedia Petrologia e Gas Naturali, ENI, Colombo Ed., Milano.

_____. 1972. "Acque dolci sotterranee," Inventario dei dati raccolti dall'Agip durante la ricerca di idrocarburi in Italia, S. Donato Milanese.

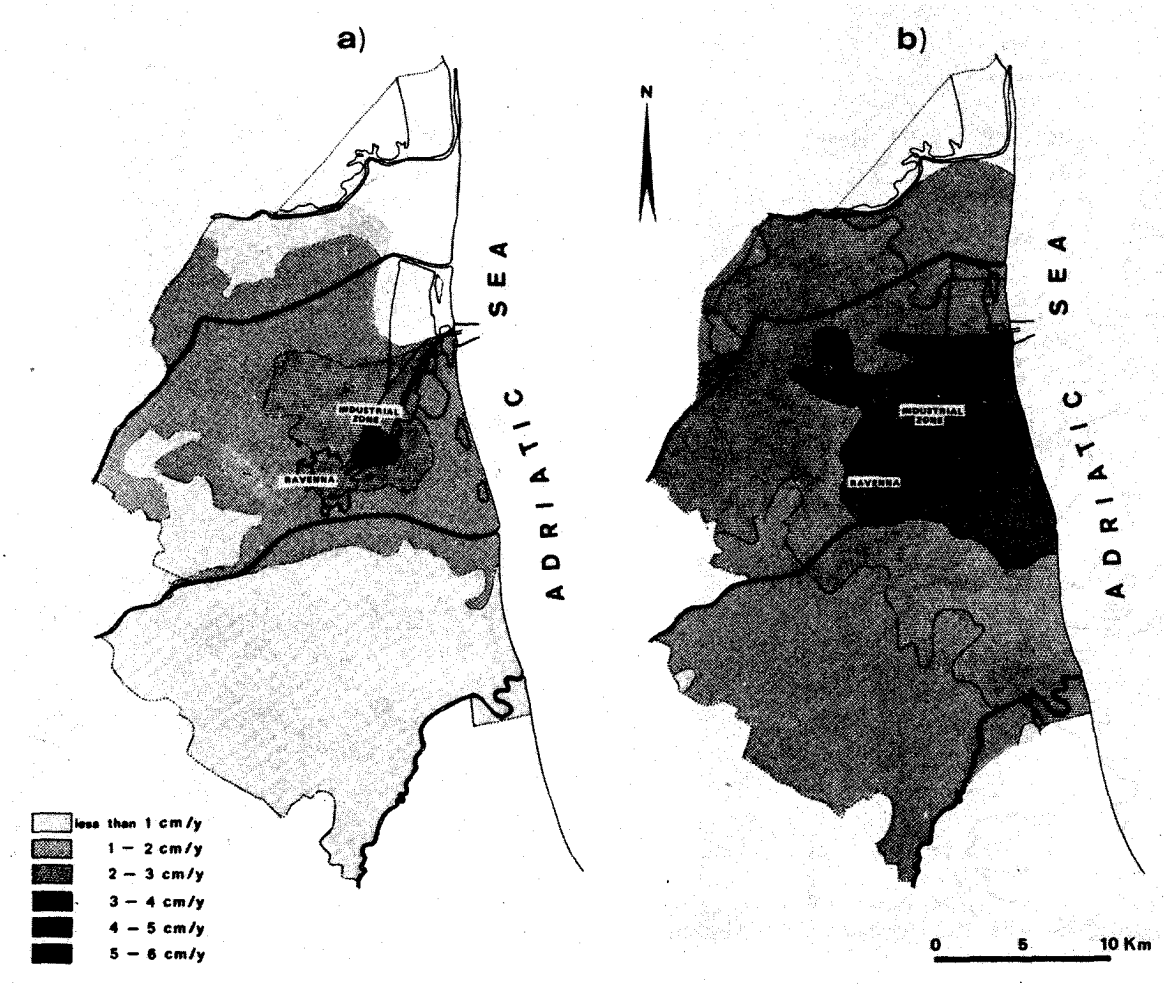

Figure 9.15.10 Space distribution of the subsidence rate between 1949-1972 (a) and 1972-77 (b). (From Carbognin, et al., 1978, Figure 10; published with permission of the American Society of Civil Engineers.)

BERTONI, W., L. CARBOGNIN, P. GATTO, and G. MOZZI. 1973. "Note interpretative preliminari sulle cause della subsidenza in atto a Ravenna," C.N.R., Lab. per lo Studio della Dinamica delle Grandi Masse, Tech. Rep. 65, Venezia.

CARBOGNIN, L., P. GATTO, and G. MOZZI. 1974. "Ricerca sulla subsidenza in atto nel Ravennate. Programma per la realizzazione della III e IV fase di studio e relativo piano finanziario," C.N.R., Lab. per 16 Studio della Dinamica delle Grandi Masse, Tech. Note 56, Venezia.

CARBOGNIN, L., P. GATTO, G. MOZZI, and G. GAMBOLATI. 1978. "Land subsidence of Ravenna and its similarities with the Venice case," Proceedings of the Engineering Foundation Conference on "Evaluation and Prediction of Subsidence," pp. 254-266, ASCE, New York.

DAL PIAZ, G. 1969. "Il bacino quaternario polesano-ferrarese e i suoi giacimenti gasseferi," Atti Convegno Giacimenti Gassiferi Europa Occidentale, Vol. 1, Roma.

SALVIONI, G. 1957. "1 movimenti del suolo nell'Italia centro-settentrionale," Boll. di Geo desia e Scienze Affini, I.G.M., anno XVI, Firenze.

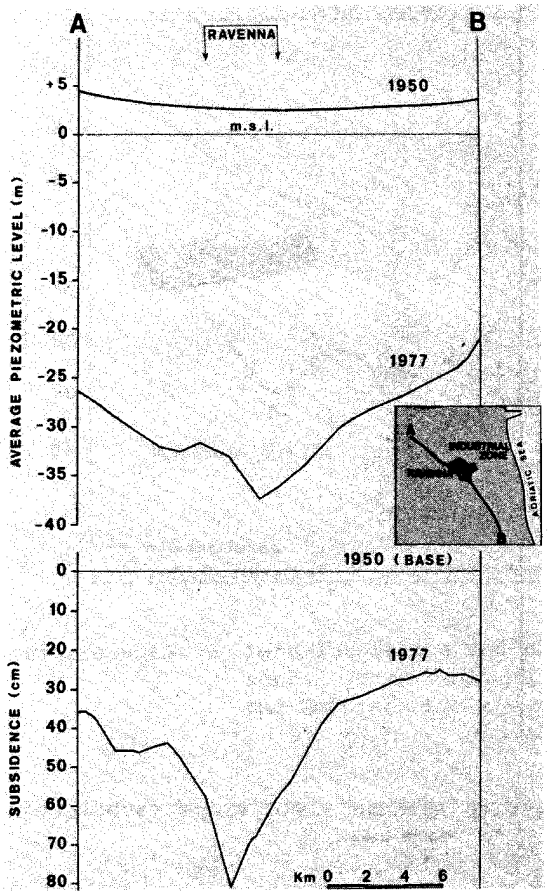

Figure 9.15.11 Comparison between the average piezometric level and the ground level over the city of Ravenna and its rural area. (From Carbognin, et al., 1978, Figure 9; published with permission of the American Society of Civil Engineers.)

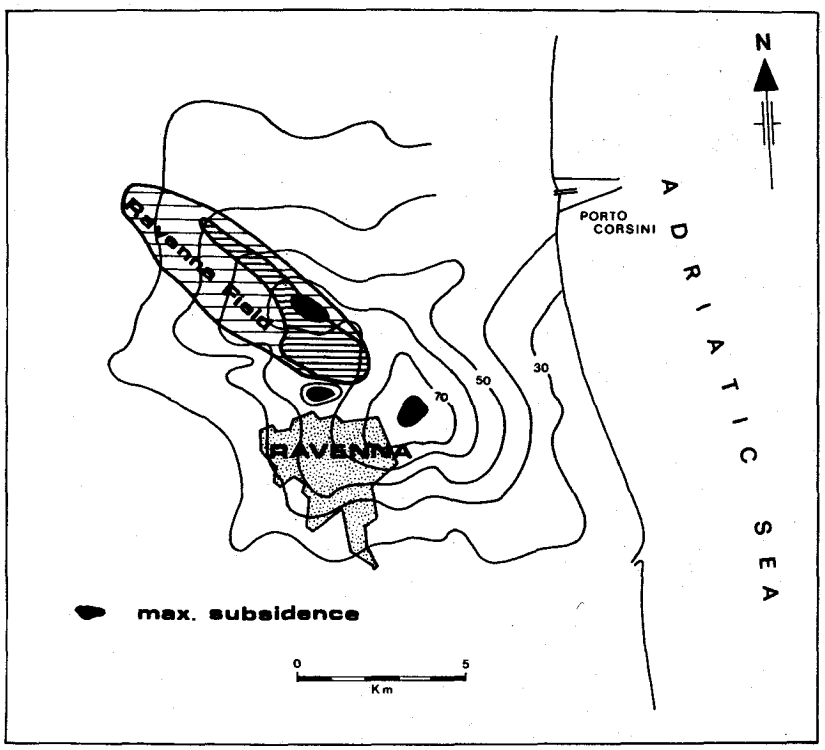

Figure 9.15.12 Comparison of development of sinking area with Ravenna Field traps (subsidence in cm).

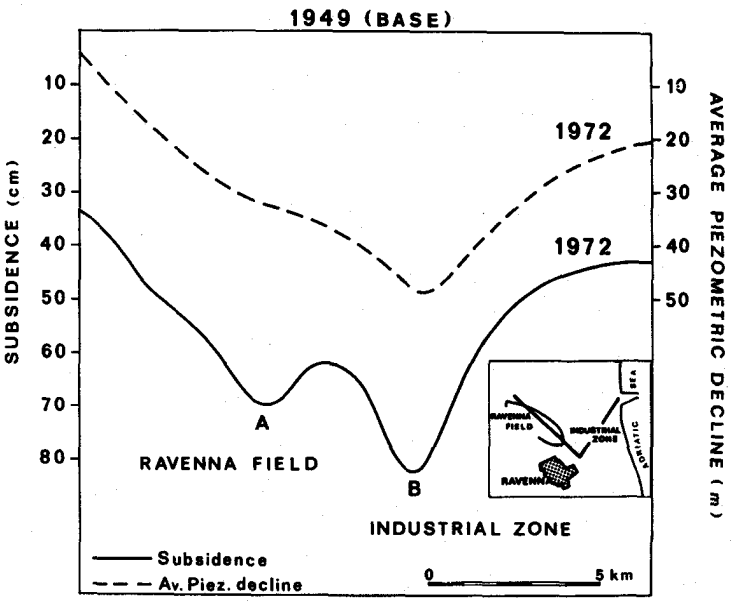

Figure 9.15-13 Land subsidence and piezometric level over the Ravenna Field and the industrial zone. (From Carbognin, et al., 1978, Figure 11; published with permission of the American Society of Civil Engineers.)

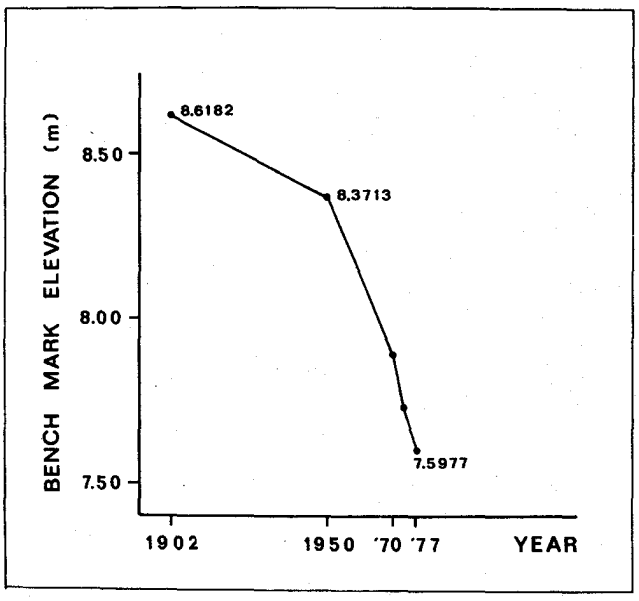

Figure 9.15.14 Elevation of bench mark of Porta Adriana (historical center) from 1902 to 1977.

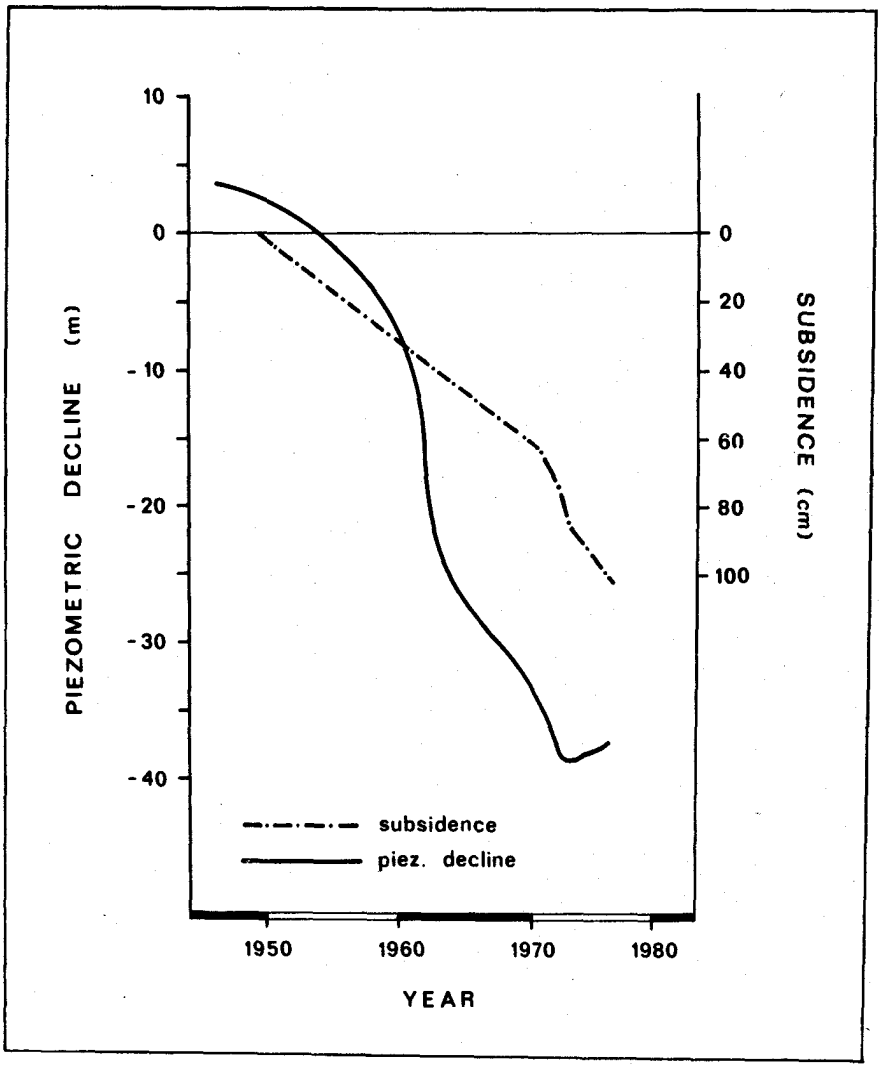

Figure 9.15.15 Comparison between subsidence and drawdown in the industrial area.

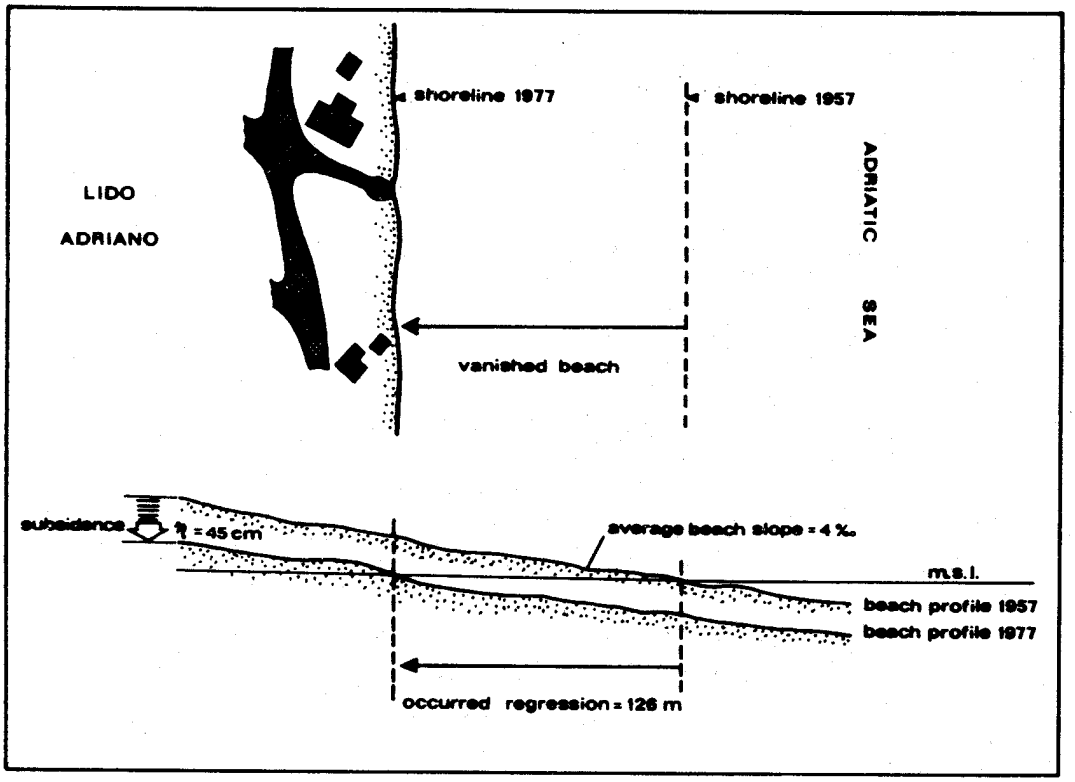

Figure 9.15.16 Schematic representation of the process of the beach regression at Lido Adriano area.

Appendixes

Appendix A. Instrument capabilities for measuring land-surface displacement

INSTRUMENT	AVAILABILITY	INSTRUMENT CHARACTERISTICS	DATA COLLECTION CHARACTERISTICS		RANGE	ACCURACY	SENSITIVITY TO ENVIRONMENT	CALIBRATION AND MAINTENANCE	EASE/COST OF INSTALLATION	EASE/COST OF OPERATION	POWER REQUIREMENTS	EASE/COST OF DATA REDUCTION	COST OF INSTRUMENT
			REMOTE OR DIRECT	ENTER SUBSIDENCE AREA									
Steel tape (structure and surface strain, surface and structure crack movement)	Lufkin; Chesterman; Kueffel & Esser	Portable, rugged, long life	Direct	Yes	100 ft usually; available in 3 to 300 ft lengths	±0.01 ft	Temperature; wind; tension	Periodically clean, oil, and calibrate against standard tape	Install reference points	2 tapemen plus 1 man to set stakes; use with tensioning device, taping pins, plumbbob	None	Simple	100 ft: $30 to $300
Invar tape (structure and surface strain, surface and structure crack movement)	Keuffel & Esser	Portable, prone to breaking	Direct	Yes	50 ft to 100 ft	±0.005 ft	Wind; tension	Clean periodically	As above	2 tapemen; use with tension frames and weights; for high accuracy repeat readings with 3 tapes	None	Simple	100 ft: $300 150 ft: $400
Precision level (automatic or tilting with optical micrometer) with invar rod (structure and surface settlement; with tape or tape extensometer for ground tilt)	Jenoptik; Kern; Wild; Leitz; Zeiss	Portable, rugged, long life	Direct	Yes	Maximum change in elevation between sights approx. 13 ft; sight length greater than 7 ft and less than 150 ft	±0.002 ft to ±0.005 ft over mile circuit	Wind; bright sunlight	Check telescope alignment annually	Install reference points and bench marks	1 instrument man; 1 rod man	None	Simple; need 1 engineer; may use computer to reduce large volume of data	Level: $850 to $1500; rod: $700
Precision theodolite with tape for baseline (triangulation) (surface and structure settlement and strain)	Kern; Wild; Jenoptik; Leitz	As above	Direct	No		1 sec instrument read to 0.2 sec by angle repetition: 1:20,000 to 1:50,000; best positional accuracy ±0.001 in ±0.005 ft	Temperature; wind; vibration; direct sun; temperature sensitivity minimal with invar tape	As above	Install reference points and 3 instrument stations	1 surveyor; and 1 rod man if targets not fixed; 2 men needed for taping of baselines between instrument piers	None	As above; computer programs readily available	Precision Theodolite: $3000 to $9000
Optical electronic distance measurement device (EDM) (use with theodolite if not built-in) (structure and surface strain)	First developed 1948; AGA; Kern	Portable; retroreflectors may be portable or fixed to reference point	Direct	Yes-rod man only	20,000 ft	±0.02 to 0.2 ft plus 1:25,000 to 1:650,000 Mekometer 3000: ±0.0007 ft plus 1:1,000,000 (as good as invar)	Temperature and pressure along line of sight; smog can disrupt readings; may be used day or night	Calibrate against 50 meter invar tape every two years	Install reference points	1 surveyor plus 1 laborer if retroreflectors portable or adjustable; lower cost per mile of traverse than conventional methods	Rechargeable battery for 1 day's work	Distance usually automatic; a few provide only phase shift and surveyor must convert to distance	Typical EDM: Mekometer 3000: $34,000; reflectors: $0.50 to $410
Infrared EDM (use with theodolite if not built-in) (structure and surface strain and settlement)	Wild; AGA; Kern; Keuffel & Esser; Zeiss; HP; Precision; Cubic Corp; Telluro-meter	As above	Direct	Yes-rod man only	1000 to 16,000 ft; minimum; 1 ft	Typically 0.02 ft plus 1:100,000 to 1:300,000; Telluro-meter MA 100; 0.002 ft over 300 ft	Temperature and pressure; less sensitive than other EDM's; can use day or night and in bright sun	As above	As above	As above	Rechargeable battery for 1 day's work	Distance usually automatic; most have automatic correction for temperature and pressure	Reflectors: $0.50 to $260 each; EDM: $3000 to $7000 without theodolite; Tellurometer MA 100.
Infrared EDM (3-D trilateration) (structure and surface settlement and strain)	As above	As above	Direct	No	As above	As above	As above	As above	Install reference points and instrument stations	1 surveyor	As above	As above; reduce distances to EDM to coordinates	As above
Laser EDM (structure and surface strain)	Developed late 1960's; AGA	As above	Direct	Yes-rod man only	5000 to 20,000 ft	±0.01 to 0.08 ft and 1:1,000,000; ±0.015 over 19 miles	Temperature and pressure; smog; dust; fog; air turbulence; sensitive to vibration	As above	As above	1 surveyor and 1 rod man	Lower power consumption than other EDM's; rechargeable battery for 1 day's work	Distance automatic	
EDM tachymeter (distance, angles, horizontal distance and elevation automatically computed) (structure and surface settlement; and strain)	AGA geodimeter models 700 and 710; Wild model DI-3S	Portable	Direct with portable reflectors Remote with fixed reflectors	Yes-rod man only	1000 to 15,000 ft	.02 ft plus 1:1,000,000 to .02 ft plus 5:1,000,000	Temperature; pressure; vibration; dust	As above	Install reference points; install instrument stations if used	1 surveyor and 1 rod man, if targets not fixed	Rechargeable battery for 1 day's operation	Automatic data reduction; surveyor may have to enter horizontal or vertical angle to get horizontal distance and elevation (DI-3S only)	$18,000; $10,000 (DI-3S without theodolite); reflectors $0.50 to $260 each

INSTRUMENT	AVAILABILITY	INSTRUMENT CHARACTERISTICS	DATA COLLECTION CHARACTERISTICS: REMOTE OR DIRECT	DATA COLLECTION CHARACTERISTICS: ENTER SUBSIDENCE AREA	RANGE	ACCURACY	SENSITIVITY TO ENVIRONMENT	CALIBRATION AND MAINTENANCE	EASE / COST OF INSTALLATION	EASE/COST OF OPERATION	POWER REQUIREMENTS	EASE / COST OF DATA REDUCTION	COST OF INSTRUMENT
Rod extensometer with dial gauge (ground or structure strain and crack movement)	Terrametrics; Structural Behavior Engineering Laboratories or user fabricated; Nason (1971)	Permanent for monitoring period; recoverable rugged and dependable	Direct	Yes	Displacement ranges to 1.0 in., resettable gauge length 10 in. to 20 in.; if user fabricated gauge length may be 10 feet	Sensitivity of 0.0001 in.	Susceptible to vandalism unless protected; sensitive to temperature	Calibrate with standard reference bar; easy to replace	Embed reference points in soil, rock or structure and attach bar; provide protection for instrument	Simple; one person to read; can use camera recorder and replace film periodically	Battery for camera	Convert dial readings to displacement; temperature correction	$100 to $800
Steel tape extensometer (ground or structure strain, convergence)	Sinco; Irad; Terrametrics; Interfels; Soiltest	Portable; dependable	Direct	Yes	Displacement ranges of 0.01 in. to 100 ft; gauge length 2 ft to 100 ft	±0.01 in.	Reference points susceptible to damage; sensitive to temperature	Problems with tape breaking; calibrate with standard reference bar; oil periodically and check tensioning device	Embed reference points in soil, rock or structure	Simple; one or two people to attach extensometer to reference points, apply tension and read; two people need two hours for 15 readings	None	Direct readout of distance makes data reduction simple; temperature corrections	$500 to $1500
Invar wire extensometer (ground or structure strain, convergence)	Telemac; Kern	Portable	Remote	Yes	Displacement ranges of 2.5 in. to 4.0 in.; gauge length of 3 ft to 150 ft	±0.0008 in. to 0.002 in.	Reference points susceptible to damage; insignificant temperature effects	Calibrate with standard reference bar; clean periodically and check tensioning device as well as zero drift of readout	As above	As above	12 VDC	Digital readout of distance makes data reduction simple	$4800
Rod extensometer with LVDT (ground and structure strain and crack movement)	User fabricated; Kennedy (1971)	Permanent for monitoring period; may be recoverable; suitable for long-term monitoring	Remote	No	Displacement ranges of 0.10 in. to 6 in.; gauge length 5 ft to 10 ft	±0.001 in. possible; infinite resolution	Electronics not very sensitive to vibration or temperature, but susceptible to changes in line resistance, cable length, or input voltage variance; may be subject to corrosion, vandalism and sensitive to temperature	Check for zero drift; easy to replace; calibrate with standard reference bar	Embed reference points in soil, rock or structure, and attach bar; provide protection for instrument; establish zero reading; enclose in telescoping casing for monitoring convergence	Simple, one person to take reading	None	Direct reading of distance makes data reduction simple; apply temperature correction	LVDT $200; transducer amplifier and recorder readout $800; cable $14/20 ft
Rod extensometer with machinist's scale (ground and structure strain and crack movement)	User fabricated; Utter and Tescn (1965)	May be permanent for monitoring period or may be portable	Direct	Yes	Displacement ranges of 0.1 in. to 10 ft; typical gauge length 3 ft to 10 ft	Sensitivity of 0.01 in.	Susceptible to corrosion, vandalism and sensitive to temperature	Clean periodically, calibrate with standard reference bar; easy to repair	Embed reference points in soil, rock or structure; provide protection for instrument	Simple; one person to take reading	None	As above	Materials and labor $500
Rod extensometer with micrometer (surface or structure strains and crack movement)	Micro-precision Engineering Livermore, CA Burland and Moore, 1973	Portable	Direct	Yes	Displacement ranges of 0.001 in. to 3.0 in.; typical gauge length 10 ft	±0.005 in.; sensitivity of 0.0004 in.	Reference points susceptible to damage; sensitive to temperature unless invar	Clean periodically; calibrate with standard reference bar; easy to repair	Embed reference points in soil, rock, or structure	One or two people to move bar, adjust micrometer and take reading	Penlight battery	Direct readout of distance makes data reduction simple, temperature correction	Materials and labor $600

INSTRUMENT	AVAILABILITY	INSTRUMENT CHARACTERISTICS	DATA COLLECTION CHARACTERISTICS: REMOTE OR DIRECT	DATA COLLECTION CHARACTERISTICS: ENTER SUBSIDENCE AREA	RANGE	ACCURACY	SENSITIVITY TO ENVIRONMENT	CALIBRATION AND MAINTENANCE	EASE/COST OF INSTALLATION	EASE/COST OF OPERATION	POWER REQUIREMENTS	EASE/COST OF DATA REDUCTION	COST OF INSTRUMENT
Single point or multi-point Terzaghi differential settlement manometer (structure settlement)	Serata; Galileo	Readout and hoses can be permanent or portable	Direct	Yes	Up to 50 ft of settlement; distances up to 1000 ft between reference points	±0.25 in.	Susceptible to barometric pressure variation, heating due to sunlight, temperature variations, and vandalism; water cannot be used in freezing conditions	Hoses must be free of air bubbles, dirt, algae, little difficulty to repair or replace hoses; survey elevation of readout stations before each observation	Install reference points on structure; provide protection for readout and hoses if permanent installation	Simple; two technicians for portable system, one for permanent installation; repeat measurement for each data point, and allow ample time for stilling oscillations	None	Convert pressure differences or graduated scale reading to elevation	Multiple points and terminal point apparatus $150 to $500; deairing unit $300 to $800
Single point simple hose manometer (structure or surface settlement)	Soil and rock instrumentation; also user fabricated; Dunnicliff (1971)	Permanent for monitoring period; may be recoverable	Direct	No, if hose is long enough	Up to 20 ft of settlement	±0.50 in.	As above	Hoses must be free of air bubbles, dirt, algae; difficult to repair or replace hoses; survey elevation of readout station before each observation	Hose placed in trench of uniform grade below frost depth and buried; provide protection for readout device; readout must be installed below lowest point along hose	Simple; one person to take reading	None	As above	Readout $150; tubing $0.30/ft deairing unit $300 to $800
Single point or multi-point electrical contact type hose manometer (structure or surface settlement)	Soil and Rock instrumentation; Soil Instruments	As above	Direct	As above	Up to 3 ft of settlement	±0.10 in.	As above; problems with electronics likely; mercury is used in freezing temperatures	As above	As above; install readout at same elevation as manometer hose	Simple; one person to adjust readout, establish electric contact, and take reading	Battery	As above	100 ft long manometer with readout, electronics, mercury and nitrogen regulation, single point $250, multi-point $450; deairing unit $300 to $800
Single point overflow type manometer (structure or surface settlement)	Telemac; Soil Instruments; Galileo	As above	Direct	As above	Up to 3 ft of settlement	±0.20 in.	Susceptible to barometric pressure variation, heating due to sunlight, temperature variations, freezing conditions and vandalism	As above	As above; overflow cell is buried; readout must be installed below lowest point along hose	Simple, one person to add water, confirm overflow and get reading	None	Convert graduated standpipe or pressure gage reading to elevation	Overflow cell $32; graduated standpipe $35; tubing $25/100 ft; deairing unit $300 to $800
Full profile overflow type manometer (structure or surface settlement)	Telemac	Permanent for monitoring period; recoverable	Direct	As above	Up to 10 ft of settlement	±0.30 in	As above	As above	Casing is placed in trench and buried; readout and pulley system installed in pit with protection provided	One person to move prove, add water, confirm overflow and get reading	None	As above	Readout: manual $3000; digital $4500
Full profile air balloon in liquid filled tube settlement device (structure or surface settlement)	Soil Instruments	Probe and readout are portable	Direct	As above	Up to 10 ft of settlement	±0.60 in.	Susceptible to variations in temperature and pressure; cannot be used in freezing conditions; possible electric problems with transducer and readout	Periodic calibration of transducer; calibrate steel tape with reference tape or bar; survey elevation at each readout station before each observation	Tube placed along trench, kept straight, brought to surface on gentle curve, and buried	One person to move probe and take reading	Battery	Convert electric readouts to elevation	Available with electromagnetic torpedo to monitor horizontal movement $1500; casing $3/ft
Full profile two liquid pressure balance manometer (structure or surface settlement)	User fabricated; O'Rourke (1977)	Permanent for monitoring period; may be recoverable	Direct or Remote	As above	Up to 20 ft of settlement	±0.25 in.	As above	As above; calibration risers along tube allow for in-situ calibration along profile	Tubing with calibration risers placed along trench of uniform grade below frost depth and buried	One person to move two liquid interface along tube, calibrate and take readings	None for manual readout; battery for automatic readout	Convert readings on pressure gage to elevation for manual readout. Automatic readout gives scaled chart recording of tubing elevation	Tubing $0.30/ft; manual readout $4000; automatic readout $5500
MPBI with fixed electrolytic level sensors (surface settlement)	User fabricated; Cooke and Price (1973)	Permanent for monitoring period; recoverable	Remote	No	±30 minutes; can be mechanically extended to: 6 degrees down, 3 degrees up	3 min.	Sensitive to moisture, changes in line resistance and cable length; temperature does not affect calibration, but zero reading is sensitive to temperature variation and twist of casing	None; difficult to remove sensors for repair or replacement	Install sensors in flexible casing along trench and bury	Simple, one person to adjust levels and take reading	Battery or AC main	Convert voltage or digital readout to displacement	

INSTRUMENT	AVAILABILITY	INSTRUMENT CHARACTERISTICS	DATA COLLECTION CHARACTERISTICS		RANGE	ACCURACY	SENSITIVITY TO ENVIRONMENT	CALIBRATION AND MAINTENANCE	EASE/COST OF INSTALLATION	EASE/COST OF OPERATION	POWER REQUIREMENTS	EASE/COST OF DATA REDUCTION	COST OF INSTRUMENT
			REMOTE OR DIRECT	ENTER SUBSID-ENCE AREA									
Electrolytic type tiltmeter (ground tilt)	BAC	Portable; long service records; permanent installation for best accuracy	Remote	Yes	0.5 to 1.0 degree	1.0 to 2.0 seconds of arc	Sensitive to temperature; possible electric problems including zero drift due to residual instability of metals and cements; permanent installation may be subject to vandalism	Check for zero drift	Install base plates on reference stations	One person with moderate training to take reading; portable device must be mounted on base plate for each reading	Battery	Convert digital readout to tilt angle	readout $1500; stations to $100 each
Spirit level type tiltmeter (ground tilt)	Galileo	Portable; rugged long operating life	Direct	Yes	0.5 to 1.0 degree	5.0 to 10.0 seconds of arc	Moderately sensitive to temperature; reference points may be subject to vandalism	Check zero by readings at 180 degrees	As above	Simple; one person to mount level and read	None	Simple; direct readout of tilt angle is given	readout $1200; stations to $100 each
Vibrating wire type tiltmeter (ground tilt)	Telemac; Maihak	Portable, rugged long term stability	Remote	Yes	1.5 degree	0.3 to 10.0 seconds of arc	Relatively insensitive to temperature or moisture; reference points may be subject to vandalism	None	As above	One person to mount tiltmeter and take reading; time and training required depends on readout device used	Battery	Convert vibrating frequency, analog reading, or digital readout to tilt angle	Tiltmeter $1200; readout $3000 to $4500
Force balance servo-accelerometer type tiltmeter (ground tilt)	Sinco; Terra; Technology; Schaevitz; Geotesting	Portable; moderately delicate	Remote	Yes	±30 degrees	10.0 to 80.0 seconds of arc	As above	None	As above	One person with moderate training to mount tiltmeter and take reading	Battery	Convert digital readout to tilt angle	Tiltmeter $2900; readout $1100
Rod extenso-meter with micrometer and spirit level (ground tilt)	Micro Precision Engrg; Galileo	Portable; rugged	Remote	Yes	0.5 to 1.0 degree	5.0 to 10.0 seconds of arc	Moderately sensitive to temperature; reference points may be subject to vandalism	Check zero by readings at 180 degrees	Reference points embedded in soil, rock or structure	One person with moderate training to mount bar, adjust level and read	None	Simple; direct readout of tilt angle is given	$3500
Rod extenso-meter with leveling bubble and levelling screw, and linear potentiometer, LVDT, or dial gauge (ground tilt)	User fabricated; Hendron, et al, (1975), Nason (1971)	Permanent for monitoring period	Direct	Yes	5.0 degrees	50.0 seconds of arc	Susceptible to corrosion and vandalism unless protected	None	Extensometer mounted on reference points embedded in soil, rock or structure	Simple, one person to adjust screw and take reading	None	Convert leveling screw reading to tilt angle	$1500 to $3500

Appendix B. Capabilities of existing subsidence monitoring instruments

PROPERTIES / INSTRUMENT	AVAILABILITY	OPERATING PRINCIPLE	DEPTH RANGE	RANGE OF VERTICLE DISPLACEMENT	MANUFACTURER'S SENSITIVITY	ACCURACY	MAXIMUM DOWNHOLE TEMPERATURE: RATED OR (ESIMATED)	MAXIMUM DOWNHOLE PRESSURE: RATED OR (ESTIMATED)	MATERIAL COMPOSITION	OPERATION and INSTALLATION (IMPORTANT FEATURES)	MAINTENANCE REQUIREMENTS & ESTIMATED SERVICE LIFE	SELECTED REFERENCES
WIRE-TYPE BOREHOLE EXTENSOMETER: weight-tensioned: weight anchored; with rotary potentiometer or water-level recorder at surface (USGS compaction meter)	Sinco; user-fabricated (4)	Note (a) Measure vertical-displacement between two markers at depth by comparing results of adjacent installation; access to borehole not necessary but wire must be free to move between borehole and transducer outside well. A straight hole (<1/2° inclination) is desirable to reduce friction (3)	Maximum: 600m; Typical; up to 300m	Total: 25-50mm, resettable with water-level recorder; 2.7m maximum with rotary potentiometer.	±0.3mm	Total 1 to 1.5 mm (3) reported. Note: friction drag at stress reversals may limit total length accuracy to ±3 to ±8 mm (5)	(500° C. (2) above which strength loss may become important); no provision for downhole temperature measurement.	not applicable	wire usually stainless steel; may be plastic coated; typically 1/8 in. AISI 302 stranded aircraft cable	Movement between surface and anchor seen as rotation of pulley at surface; counter-weight at surface maintains constant tension on wire ideally, but friction of wire may affect tension (6)	Weight anchors maybe lifted out of borehole to replace wire; Under severe geothermal conditions, pitting corrosion rate may be 0.15 mm•month. So a 3 mm wire would sever in 1-1/2 years. Note: Due to general corrosion, the wire may last 100 years, given a rate of 0.5g/m^2•day	(1) Toliva, 1970 (2) Phillips and Sykes, 1970 (3) De Lois, 1973 (4) Lofgren, 1969 (5) Riley, 1969 (6) Bull and Miller, 1975 (7) Lofgren, 1961
WIRE-TYPE BOREHOLE EXTENSOMETER; weight-tensioned; with grout or mechanical anchor; dial gauge or sensor at surface	Interfels; user-fabricated (1), (2)	as above	Typical: up to 100m	Total: 10-50mm resettable	±0.5 to 1.0mm	Total: 1.5 to 3mm estimated	as above	not applicable	as above; wire may be encased inplastic tubing	Multiple wire installations possible, but may not be practical in deep holes; see note a; easy to reset range	Anchor and wire system usually not removeable; life under severe geothermal conditions may be 1-1/2 years	(1) Waddell, 1964 (2) Sellers, 1969 (3) Cording et al, 1975
WIRE-TYPE BOREHOLE EXTENSOMETER; spring-tensioned; with grout or mechanical anchor; and dial gauge or micrometer sensor at surface	Terrametrics; Peter Smith; Serata	Wire stretched between anchor at depth and spring-loaded reference point at surface. Movement between surface and anchor seen as displacement of sensing rod contact spring	Maximum: 450m Typical: 15-90m	Total: 90-150mm	±0.03mm	Total: ±0.1mm to 2.5mm reported; Under mining conditions, accuracy of single measurment reported to be ±0.2 to 3mm, while survey accuracy tying in borehole collars was ±6mm	as above	not applicable	as above	Multiple wire installations possible, but may not be practical in deep holes; see note a; easy to reset range. Relatively rugged compared to electrical transducers. Stretch of wire due to change in spring tension added to readout value.	as above	(1) Potts, 1964 (2) Dunnicliff, 1970
WIRE-TYPE BOREHOLE EXTENSOMETER; cantilever tensioned; with grout or mechanical anchor; and cantilever-mounted electrical resistance strain gauge sensor at surface	Terrametrics	Wire stretched between anchor and cantilever spring at surface. Movement between surface and anchor causes bending of cantilever and resistance change in strain gauge	Typical: 150m	Total: 15mm resettable	±0.01mm	Total: ±0.5mm estimated	as above	not applicable	as above	Multiple wire installations possiblem but may not be practical in deep holes. See note a. Sensitive to moisture; zero drift can cause problems	as above; except sensor may require recalibration or replacement at more frequent intervals	(1) Sellers, 1969 (2) Dunnicliff, 1970
WIRE-TYPE BOREHOLE EXTENSOMETER; spring tensioned; mechanical or grout anchor; rotory potentiometer sensor at surface	Sinco	Wire stretched from anchor, over pulley (to which potentiometer is coupled)to spring. Movement between surface and anchor seen as pully rotation	Typical: 100m assumed	Total: 50mm resettable	±0.05mm	Total: ±1.5mm estimated	as above	not applicable	as above	as above	as above	(1) Dunnicliff, 1970
WIRE-TYPE BOREHOLE EXTENSOMETER; cantilever tensioned; mechanical or grout anchor; cantilever-mounted vibrating-wire strain gauge sensor at surface	Telmac	Wire stretched between anchor and cantilever spring at surface. Movement between surface and anchor causes bending at cantilever and changes natural frequency of vibrating wire	Typical: 100m	Total: 50mm	±0.01mm	Total: ±1.5mm estimated	as above	not applicable	Stainless steel wires	as above; but somewhat more resistant to environmental problems	as above	(1) Dunnicliff, 1970
ROD-TYPE BOREHOLE EXTENSOMETER; with mechanical or grout anchor; with dial gauge or micrometer sensor	Irad; Interfels; Terrametrics: Huggenberger Soil Instruments	Movement between anchor and surface appears as translation of top of rod relative to surface; Displacement of top of rod detected by sensor	Maximum: 500m Typical: 30-180m	Total: 10-50mm resettable Add rod lengths as required in extention: in compression, can cut rod as needed	±0.01mm to ±0.03mm	Total: ±0.02mm to ±0.6mm estimated	as above	not applicable	Rod generally stainless steel; occasionally aluminum. May be plastic coated of cased in plastic tube. Anchor usually cadmium plated mild steel, or cast iron. Rod is typically small diameter 6mm solid rod - 17mm pipe.	Note C: Access to borehole not required; but top of rod must be free to move between borehole and transducer. Rod installed in flexible tube if hole unstable and requires grouting. A straight hole (1/2° inclination) is desirable to reduce friction. If multiple installation not practical for deep hole, measure vertical displacement between 2 markers at depth by comparing results of adjacent installations.	Typical rod (pipe) wall thickness is 3mm. Based on pitting corrosion rate of 0.15mm/mo(1). The service life would be about 1-1/2 years. If some pinholes can be tolerated, service life may be as long as 100yrs., based on a general corrosion rate of 0.5m^2/day.(1)	(1) Toliva, 1970 (2) Cording, et al., 1975 (3) Seller, 1969
ROD-TYPE BOREHOLE EXTENSOMETER; with mechanical or grout anchor; with linear potentiometer sensor	Interfels; Sinco; Irad; Soil Instruments	as above	Typical: 30m to 180m	total: 10-150m	±0.01mm to 0.1mm	Total: ±0.2 to ±2mm, estimated	as above	not applicable	as above	as above	as above; Wiper-contacts of potentiometer may degrade and wear and require replacement or recalibration within 1 year.	
ROD-TYPE BOREHOLE EXTENSOMETER; with mechanical or grout anchor; with LVDT sensor	Interfels	as above	Typical: 30m to 180m	Total: 12 mm, resettable	±0.01mm to ±0.1mm	Total: ±0.2 to +2mm estimated	as above	not applicable	as above	as above	as above; except service life of LVDT should be somehat longer than for potentiometer if adequately sealed.	
ROD-TYPE BOREHOLE EXTENSOMETER; with mechanical or grout anchor; with vibrating wire strain gauge sensor	Maihak	as above	Typical: 30m to 180m estimated	Total: 6 to 100mm	±0.003mm to ±0.03mm	Total: ±0.05 to ±1.25mm reported; but friction may make +0.05mm unrealistic	as above	not applicable	as above	as above	as above; except service life of vibration wire strain gauge should be several years	

TABLE 2.11 CAPABILITIES OF EXISTING SUBSIDENCE MONITORING INSTRUMENTS •VERTICAL DISPLACEMENTS• Sheet 2 of 4

PROPERTIES / INSTRUMENT	AVAILABILITY	OPERATING PRINCIPLE	DEPTH RANGE	RANGE OF VERTICLE DISPLACEMENT	MANUFACTURER'S SENSITIVITY	ACCURACY	MAXIMUM DOWNHOLE TEMPERATURE: RATED OR (ESIMATED)	MAXIMUM DOWNHOLE PRESSURE: RATED OR (ESTIMATED)	MATERIAL COMPOSITION	OPERATION and INSTALLATION (IMPORTANT FEATURES)	MAINTENANCE REQUIREMENTS & ESTIMATED SERVICE LIFE	SELECTED REFERENCES
ROD-TYPE BOREHOLE EXTENSOMETER, with mechanical or grout anchor; attached wire at surface with scale readout	User fabricated (1)	Movement between surface and anchor seen as translation of top of rod relative to surface; wire attached to rod goes over pulley and is tensioned by a weight. Elevation of wt or rotation of pulley also are measurements of displacement	Typical: 100m	1m	±2.5mm	Total: ±15mm estimated	as above	not applicable	as above	as above	as above	(1) Howell, Wright, and Dearinger, 1976
ROD-TYPE BOREHOLE EXTENSOMETER, with two concentric rods; mechanical anchors; and dial gauge readout (DOUBLE-POINT BOREHOLE EXTENSOMETER)	Irad: Telemetrics	Inner rod anchored at base of borehole. Outer rod extends only partway down the hole and is anchored. Movement between surface and other anchor seen as translation of top of appropriate rod relative to surface; position of inner or outer rod relative to fixed measuring surface read with dial gauge	Maximum: 15m	Total: 100-300m Can be increased in extension with extension rods by 600m	±0.01	Total: ±0.5mm estimated	as above	not applicable	Outer rod: galvanized steel (Irad); probably 15mm. Inner rod: stainless steel.	See note (c): Hole can be grouted if extensometer tools placed in protective tubes; not for use in cased holes	Probably not recoverable for replacement. Corrosion resistance will be higher for all stainless steel assembly; removal of galvanized coating will be rapid; sealing may impede movement between concentric pipes. Service life probably less than 1 year due to corrosion of outer rod and due to scaling	
PIPE-TYPE BOREHOLE EXTENSOMETER, anchored by own weight. attached wire at surface with water level recorded readout	User fabricated (1), (2), (3)	Movement between surface and anchor seen as translation of top of pipe relative to surface; wire attached to pipe goes over pulley and is tensioned by weight. Elevation of weight or rotation of pulley are also measurements of displacement	Maximum: (3)1200m Typical: 300-600m	Total: 25-50mm resettable	±0.01mm to ±0.03mm	Total: 0.2 to 0.6mm estimated	as above	not applicable	Cast iron (3); low alloy steel possible; pipe typically 50mm to 100mm diameter	Pipe usually installed in metal cased hole, often abandoned well; pipe usually found ~5 to 10m below base of casing. See note (c)	Pipe stands on shoe: can probably be removed for replacement, but with difficulty. Typical wall thickness for pipe cited is 4mm for general corrosion rate of 6u/m*d(4); it would last a maximum of 10 years in a sever geothermal environment.	(1) Fulchner, 1977 (2) Komaki, 1969 (3) Hirono, 1969 (4) Toliva, 1970
MULTIPLE BASE LENGTH EXTENSOMETER, with inductance sensors, mechanical metal anchors	Telmac	Central rod, able to move freely in hole, contains inductance-type sensors. When rod moves relative to concentric anchors, inductance sensors detect relative position of each anchor	50m estimated: Maximum of 1 sensor per meter	Maximum: 125mm	0.01mm	Total and interval: 0.02 mm claimed	50°C	(500 KN/m^2 estimated)	Probably stainless steel	Access to hole not necessary, but instrumented rod must be free to displace toward surface. Will not work in metal casing; probably o.k. if anchors installed outside flexible plastic casing	Central rod containing electronics has no mechanical coupling to anchors, so probably could be replaced. Under geothermal conditions, central rod and electronics housing may suffer pitting and corrosion. Electronics as designed not suitable for geothermal environment: life in non-geothermal environment probably 1 yr. Longer if rod replaced	
MULTIPLE BASE LENGTH EXTENSOMETER, with reed switch sensors; and magnetic markers	User fabricated (1, 2, 4)	Permanent, moveable central rod contains reed switches, at approximately same spacing as magnets anchored outside borehole casing. Reed switches may be paired or single. Rod installed so initially each reed switch approximately opposite magnet. Movement of measuring rod needed to align reed switch with corresponding magnet measured with micrometer. Can replace rods with tape for easier handling	30-70m	Total: 150-250mm Intervals: 150-250mm	±0.02mm to ±0.1mm	±0.1mm(1) reported with rods ±0.15mm(2) with tape	(50°C estimated: possibly higher since reed switches can operate to 200°C)	(700 KN/m^2 estimated based on depth range)	Rod: thin-walled stainless steel tube with precision connectors. Tape: Stainless steel. Brass housing for reed switches	Access to hole not necessary, but instrument must be free to displace toward surface. May be slightly influenced by steel casing and accuracy reduced due to distortion of magnetic field.	Central rod can be withdrawn or replaced but with loss of accuracy. Stainless steel tape or tube would become severely pitted in 1 1/2 years of service, based on pitting corrosion rate of 0.15mm/month. (3) Electronics as designed not suitable for geothermal environment Life probably 1 yr under non-geothermal conditions; longer if rod replaced	(1) Burland, Moore and Smith, 1972 (2) Smith and Burland, 1976 (3) Toliva, 1970 (4) Burland and Moore, 1973

TABLE 2.11 CAPABILITIES OF EXISTING SUBSIDENCE MONITORING INSTRUMENTS •VERTICAL DISPLACEMENTS• Sheet 3 of 4

PROPERTIES / INSTRUMENT	AVAILABILITY	OPERATING PRINCIPLE	DEPTH RANGE	RANGE OF VERTICLE DISPLACEMENT	MANUFACTURER'S SENSITIVITY	ACCURACY	MAXIMUM DOWNHOLE TEMPERATURE: RATED OR (ESIMATED)	MAXIMUM DOWNHOLE PRESSURE: RATED OR (ESTIMATED)	MATERIAL COMPOSITION	OPERATION and INSTALLATION (IMPORTANT FEATURES)	MAINTENANCE REQUIREMENTS & ESTIMATED SERVICE LIFE	SELECTED REFERENCES
CHAIN-TYPE EXTENSOMETER, mechanical or grout anchor, with linear potentiometer or LVDT sensor	Soil Instruments; Interfels	Device consists of a linear sensor housing in a steel case, and fixed to a concrete anchor or anchor plate. A moveable rod extends from the sensor case at 2nd anchor, 1 m or more away. Movement between anchored sensor case and 2nd anchor detected by sensor. Extensometers can be coupled by using 2nd anchor of 1st extensometer to anchor sensor case of next extensometer	Typical: 60-100m, but lead wire could extend several hundred m. from last sensor to readout	Maximum: 10mm to 300mm per sensor	±0.1mm to ±1.0mm	Interval: ±2 to 5mm estimated Total: assuming 10 sensors @10 ft centers, ±7 to ±16mm estimated	(0-50°C, estimated)	(1000KN/m^2 estimated)	Probably stainless steel	Generally used in dams or fills. Requires well compacted fill or soft grout around anchors and no casing in hole. Rods may be protected by flexible plastic casing. Only lead wires exit at surface; no access to borehole necessary	Cannot be repaired or replaced. Life limited by sensors; LVDT probably more reliable than linear potentiometer. Life probably 1 year under non-geothermal conditions	
SONDE-TYPE EXTENSOMETER, with induction sensor and metal markers	Telmac; Maihak; Terrametrics; Sinco; Soil Instruments	Probe lowered down hole on cable; when it passes anchored metal marker, current change induced in secondary coil and detected at surface. Depth of marker is length of cable played out	Typical: 75m to 100m; Maximum: 300m	Ideally unlimited; but depends on casing; up to ~ 17% strain possible, based on typical elastic compressibility of casing	±0.1mm to ±1.5mm	Interval: 1.25 to 5mm reported Total: 5 to 10 mm estimated	up to 110°C	(3000KN.m^2 estimated, based on depth range)	Casing usually plastic. Metal markers may be any common metal. Instrument housing stainless steel	Best when hole within 3° of vertical. Markers anchored outside flexible plastic casing. Access to hole required. Not for use in metal casing	If probe can be modified to take geothermal conditions, will be easy to maintain since removed between readings	
SONDE-TYPE EXTENSOMETER, with 2 or 3 induction sensors; and "casing collars" as markers (CASING COLLAR LOCATOR)	Provided as a service only; by Dresser-Atlas, Schlumberger, and others	Sonde consists of 2 or 3 probes rigidly connected in series. Works like above sonde but senses change in metal thickness at collars; distance between adjacent markers determined by cable played out between probe detection upper marker (collar) and lower probe detecting lower marker (collar). Depth of probe also determined by wheel on tool which tracks against edge of casing. Wheel has several attached magnets, and each partial rotation of wheel detected by reed switch tool. With triple sensor data can be calibrated in-situ using known distance between 1 pair of sensors	Maximum: 1500m	Ideally unlimited; but depends on compressibility of metal casing and casing/ground bond	±3mm[4] improved to about ±0.1mmat Gronigen[2]	Interval: ±15mm reported (1) for double; ±3.5mm for triple (2) Total: ±0.05m(2)	(Probably up to 120°C; typical for production logging tools.) At Gronigen[2], induction sensors connected by invar mandrel to minimize temperature effect	(Probably 70,000KN/m^2 maximum typical for production logging tools)	Instrument housing stainless steel. Casing: low-alloy steel, standard oil-well casing	Operates in cased hole. Accessible hole required. Works best in holes where casing collar has a recess to provide sharp signal [2]	as above	(1) Allen, 1960 (2) deLoos, 1973 (3) Allen, 1971 (4) Allen, 1968
SONDE-TYPE EXTENSOMETER, with reed switch sensor (lowered on cable) and magnetic markers	Soil Instruments; Terra Technology; ELE	Probe lowered down hole on cable. When it passes anchored magnetic marker, reed switch closes and detected at surface. Depth of marker is length of cable played out, and is measured with steel tape	Typical: 100m	Ideally unlimited, but depends on casing. Up to 17% strain possible.	±1-2mm[1]	Interval: 1-2mm reported[1]; Total: ±2.5mm reported for 30m; ±5mm estimated for 100m. Accuracy limited by steel tape	(Probably up to 120°C as above; Reed switched can tolerate up to 200°C)	(1000 KN/m^2 estimated; based on depth range)	Probe in brass or stainless steel housing. Magnet probably Alnico. May be coated with epoxy[1]	Operates in hole cased with non-magnetic casing. Accessible hole required; Magnets anchored to ground outside casing or attached to flexible casing cemented to ground. Magnets may also be pneumatically forced into ground.	as above	(1) Burland, Moore, and Smith, 1972 (2) Marsland and Quarterman, 1974
SONDE-TYPE EXTENSOMETER, with two reed switch sensors and magnetic markers (lowered on rods)	Soil Instruments;	Probe lowered down hole on coupled rods. Probe consists of two reed switches spaced 0.5-1.0m apart; magnets also spaced at this depth. Depth of marker determined by rod used to lower probe. Distance between adjacent markers determined by rod movement between upper reed switch detecting lower magnet. Incremental rod travel measured with micrometer	30m estimated	Total: as above Interval: 150-250mm	±0.05mm	±2mm estimated ±0,1mm claimed by mfg.	(50°C, estimated)	(300KN/m^2 estimated based on depth)	Stainless steel rods; stainless steel housing	As above; requires hole with minimal curvature since not very flexible	as above	
SONDE-TYPE EXTENSOMETER, with radioactive bullet markers and 2 or 3 gamma-ray detectors (GAMMA-RAY LOGGER)	Provided as a service only; by Dresser-Atlas, Schlumberger, and others	Sonde consists of 2 or 3 probes (usually rigidly) connected in series. Signal is sent to surface when x-ray detector locates bullet. Depth determined by amount of cable played out and rotation of tracking wheel-(see casing-collar locator). Distance between adjacent markers determined by amount of cable played out between upper probe detection of upper bullet and lower probe detection of lower bullet. With 3 detectors, can use 1 pair for in-situ calibration	1500m	Unlimited because bullets outside casing in formation	±0.1mm	Depends on logging rate; works best at slow rate (1.5m/min[1]or less[4]). Accuracy probably higher than for casing collar locator once strain exceeds elastic limit of casing; Interval: ±30mm error in 2-detector tool[2] can be reduced to ±3mm error in 3-detector tool[1]; Total: ±10 to 120mm[1]	(200°C, estimated; typical for x-ray logging tools) Tool cooled with dry ice (3)	(140,000 kN/m^2; typical for x-ray logging tools)	Bullets are 10μ Curie Cesium 137(1) at Gronigen and 1-6μ Curie in Japan(4) Invar housing[1][1cp]	Operates in cased, open hole; since bullets are shot into formation with perforating gun, best to them install before casing. Otherwise, to prevent leakage, only production zone can be marked. May be impossible to place bullets in hard formations such as anhydrite and dolomite.(1) Can install free-hanging casing length inside completed borehole with R/A bullets welded at known intervals to use as in-situ calibration for tool. In Japan, welded buttons to production casing to get compaction of casing as well as ground(4).	If tool can be modified to meet geothermal environment, should be easy to maintain since portable. Some problem may arise if R/A bullets are dislodged or diffuse into formation	(1) deLoos, 1973 (2) Allen, 1969 (3) Allen, 1977 (4) Sano, 1969 (5) Allen, 1971
SONDE-TYPE EXTENSOMETER, with latching pawls to detect casing collars	Soiltest; Sinco; Soil Instruments; Geotesting	When probe lowered down through small dia,. coupling into larger diameter casing, pawls will lock if pulled upward against smaller x-section. Depth measured on graduated tape at these x-sections	Typical: 100m	Total interval: 3-6% vertical strain; limited to allowable movement per coupling	±1 to ±3mm	Interval: ±10m estimated Total: ±40mm estimated Best when hole within 25° of vertical	(50°C, estimated)	(1000 kN/m^2 estimated; but should operate if some leakage occurs)	Chrome/brass or galvanized steel	Requires cased hole with telescoping tubing and collars which have a different I.D. from casing. Latching mechanism released when probe hits hole bottom, allowing withdrawal. Requires applied upward force at regular intervals to detect collars	Tool has moving mechanical parts; although portable, may be difficult to modify for geothermal conditions	

PROPERTIES / INSTRUMENT	AVAILABILITY	OPERATING PRINCIPLE	DEPTH RANGE	RANGE OF VERTICLE DISPLACEMENT	MANUFACTURER'S SENSITIVITY	ACCURACY	MAXIMUM DOWNHOLE TEMPERATURE: RATED OR (ESIMATED)	MAXIMUM DOWNHOLE PRESSURE: RATED OR (ESTIMATED)	MATERIAL COMPOSITION	OPERATION and INSTALLATION (IMPORTANT FEATURES)	MAINTENANCE REQUIREMENTS & ESTIMATED SERVICE LIFE	SELECTED REFERENCES
SONDE-TYPE BOREHOLE INCLINOMETER; with pendulum and LVDT sensor	Galileo; Dames and Moore	As probe inclines, pendulum remains vertical. The LVDT measures the displacement of the bottom of the pendulum relative to the instrument case. Depth determined by amount of cable played out at measuring point.	300m estimated	12°	±1 min	±10 min estimated	(50°C, estimated based on typical electronics)	(3000 KN/cm^2, estimated based on depth)	Probably stainless steel housing; casing usually grooved PVC.	To get orientation, must install in grooved or square casing, survey initially for spiral; for best results, casing should be tele-scoping if cemented or keyed to surrounding ground. Casing may be inserted inside flexible grouted casing. Take readings at intervals corresponding to tool length.	Probe temporary; if it can be modified to meet geothermal conditions, it should be easily maintained. Scaling and distortion of casing groves may limit life. Casing materials now used not suitable for geothermal environment.	
SONDE-TYPE BOREHOLE INCLINOMETER; with pendulum and linear potentiometer sensor	Sinco	As probe inclines, pendulum remains vertical. Pendulum contacts resistance element fixed to case. Resistance varies with angle between pendulum and instrument case. Depth determined by amount of cable played out at measuring point.	300m	12° - 25°	3 min	±20 min estimated	(as above)	1400 KN/m^2	Probe has brass housing, casing usually aluminum or plastic	as above	as above	Wilson, 1962
SONDE-TYPE BOREHOLE INCLINOMETER; with pendulum and servo-accelerometer	Terra-Technology; Geo-Testing; Sinco	As probe inclines, pendulum remains vertical. This system measures force required to return pendulum to initial alignment in probe. Depth determined by amount of cable played out at measuring point.	300m	Typical: 25° 45-90° available	±10 sec	±1 min reported (1)	Typical: 50°C, up to 90°C available	Typical: 3500 KN/m^2 up to 140,000 KN/m^2 available	Probe has stainless steel housing; wheel may be aluminum, stainless steel, or hard plastic; cable cased in hard polyurethane or neoprene.	as above	as above	(1) Brownwell, Ryan and Toth, 1971
SONDE-TYPE BOREHOLE INCLINOMETER; with pendulum and air pressure device	TerraTech, developmental	As above except: Tilt measured by pneumatic force (air pressure) required to return pendulum to original alignment in probe.	100m estimated		±35 sec	±3 deg estimated	(50°C estimated)	(1000 KN/m^2 estimated	Probably stainless steel housing	as above	as above	Durmicliff, 1970
SONDE-TYPE BOREHOLE INCLINOMETER; with cantilevered pendulum and vibrating wire strain gauges	Maihak; Telemac; Geonor; ELE	Cantilever with weight at unsupported end bends as probe tilts. Bending of cantilever measured by vibrating wire strain gauge.Depth determined by amount of cable played out at measuring point.	300m estimated	Typical: 6-30°	±30 sec - ±2 min	±3 to 4 min reported	(50°C estimated based on typical electronics)	(3000 KN/m^2, estimated based on depth)	Probably stainless steel housing. Casing usually grooved, PVC.	as above	as above	
SONDE-TYPE BOREHOLE INCLINOMETER; with cantilevered pendulum and bonded electrical resistance strain gauges	Soil Instruments: Soiltest	Cantilever with weight at unsupported end bends as probe tilts. Bending of cantilever measured by electrical resistance strain gauges.Depth determined by amount of cable played out at measuring point.	200m	5° to 30°	±15 sec to ±40 sec	±1 min(1) reported for shallow depths	(as above)	(2000 KN/m^2, estimated based on depth)	Chrome plated brass or stainless steel housing; neoprene sheathed cable, stainless steel wheels.	as above	as above	(1) Kallstenius and Bergau, 1961
SONDE-TYPE BOREHOLE INCLINOMETER; with pendulum, compass and camera	Sperry Sun; Schlumberger	As probe inclines, pendulum remains vertical. Camera photographs pendulum position relative to compass fixed to case. Depth determined by amount of cable played out at measuring point.	Deep holes more than 6km	2° to 130° available			Maximum: 315°C for 5hrs; with special instrumentation; Typical: 175°C	140,000 KN/m^2	Probably stainless steel housing.	Instrument determines both orientation and tilt; camera operated by timer; accuracy of depth measurement associated with angle measurement will be low unless used as a single-shot device.	Probe temporary; if can be modified to meet geothermal conditions, should be easily maintained	
SONDE-TYPE BOREHOLE INCLINOMETER; pendulum, linear potentiometer, compass and rotary motor	Eastman	For compass orientation, rotary motor rotates mirror until indicator facing north. For angle from vertical as probe tilts, pendulum remains vertical. Pendulum contacts resistor fixed to case. Resistance varies with angle between pendulum and instrument case.	450m - 540m	more than 30°; can used at any angle	1° for tilt; 2° for orientation		(50°C estimated)	6300 KN/m^2	Chrome plated bronze case	Determines inclination and orientation; device also contains TV camera	as above	
SONDE-TYPE BOREHOLE INCLINOMETER; with gyro-compass camera, and pendulum	Service tool only; by Sperry Sun, Schlumberger	As probe inclines, pendulum remains vertical. Camera photographs pendulum position relative to gyro-compass, fixed to case.	6.2km reported; maximum range probably 9km	2° to 90°		±15 min tilt; 1° to 3° orientation	190°C reported, with thermal shield for up to 11.5 hrs.	(112,000 KN/m^2 estimated, based on depth and muds reported)	Housing K-Monel	Determimes inclination and orientation	as above	Oil and Gas Journal, 1971
SONDE-TYPE BOREHOLE INCLINOMETER; with needle-pointed pendulum and punchable chart	Totco	as probe inclines pendulum remains vertical. At pre-set time point of pendulum punched chart fixed to probe, giving inclination of probe. Depth determined by amount of wire-line played out.	6-10Km estimated	7, 14, 21 deg	8 min	15 min estimated	Special models available for warm(<150°C and hot(<300°C estimated) holes.	(100,000 KN/m^2 estimated, based on depth)	Probably stainless steel housing	Make reading at one depth only - gives tilt only - not orientation. Must be retrieved to determine tilt. Tilt simply determined by examining chart with magnifying glass, will operate in any type of hole, cased or uncased.	as above	
FIXED BOREHOLE DEFLECTOMETER with cantilever mounted electrical resistance strain gauge sensors	Telemetrics	Steel tubes anchored in hole and connected to adjacent tubes by cantilever. Angular movement between two tubes causes cantilever to bend. Bending sensed by strain gauges.	54m with 6m intervals between cantilevers		±3 sec	±20 sec	90°C	(540 KN/m^2 estimated based on depth)	Tubes are stainless steel	Designed for use in uncased hole but could be installed in flexible casing. Orientation must be determined when installed	Permanent; may be impossible to recover or repair; electronics will require modification for geothermal environment; stainless steel housing may leak after several years service, due to pitting or corrosion.	
FIXED BOREHOLE DEFLECTOMETER with inductive sensor	Interfels	Steel tubes anchored in hole and connected by tensioned wire. Position of wire changes as angular movement between tubes occur. Movement detected by inductive sensors	54m with up to 8 measuring elements	35min/element; resettable	±2 to ±20 sec	±1 to 3 min estimated	(50°C estimated)	(540 KN/m^2 estimated based on depth)	Probably stainless steel housing	as above	as above	
FIXED BOREHOLE DEFLECTOMETER with pendulum, electrical contacts with micrometer	SGI	Pendulum remains vertical as probe tilts. When tilt exceeds a preset value, pendulum has swing far enough to touch electrical contact and complete circuit. Micrometer can be turned from surface to deflect pendulum to determine angle	10m estimated	0 - 1 deg. to several degrees(1)	±6 min to ±7 sec	± 3 deg estimated	(50°C estimated)	(100 KN/m^2 estimated based on depth)	Probably stainless steel housing	Install in flexible tube. Determine orientation when instrument installed. Requires mechanical connection between surface and instrument	as above; probably not suitable for geothermal environment	(1) Kallstenius and Bergau, 1961

Appendix C. List of symbols used in text, part I

Symbol	Term
A	Cross-sectional area
A_P	Area of point of sampling spoon
a	Area of manometer
b	Thickness; effective stress due to buoyant weight of submerged deposits
b'	Thickness of aquitard
C	D/R
C_C	Compression index
C_V	Coefficient of consolidation
D	Depth to compressing beds
dh/dt	Rate of subsidence
E	Young's modulus
e	Void ratio; e_0, initial void ratio
G	Specific gravity
H	Total subsidence
H_0	Initial thickness
h	Applied stress; difference in head; head at given elapsed time
h_a	Average head in aquitard
h_C	Head in confined system
h_0	Head at zero time
h_u	Head in unconfined system
J	Seepage stress
K	Hydraulic conductivity
K'	Vertical hydraulic conductivity
L	Length of flow
M_V	Coefficient of volume compressibility

Symbol	Term
$\overline{N}$	Average of N (blows)
n	Porosity
p	Total stress (geostatic pressure); water level
p′	Effective stress (effective overburden pressure)
p_a	Applied stress
P_0	Reference water level
Q	Amount of liquid production; quantity of water discharged in unit time
R	Radius of stressed system
R_u	Ultimate bearing resistance
r_s	Specific retention
S	Storage coefficient; effective stress due to weight of unsaturated deposits
S_c	Final subsidence
S_o	Sorting coefficient
S_s	Specific storage
S'_s	Specific storage of aquitard (compressible bed)
S_{ke}	Component of S attributable to elastic deformation of the aquifer-system skeleton
S_{ske}	Component of S_s due to elastic deformation of aquifer-system skeleton
S_{kv}	Component of S attributable to inelastic (virgin) deformation, of aquifer-system skeleton
S_{skv}	Component of S_s due to inelastic (virgin) deformation of aquifer-system skeleton
S_{sw}	Component due to compressibility of water
S'_{sk}	Component of specific storage due to compressibility of aquitard
S'_{skv}	S_{kv}/b'; b′ is aggregate thickness of aquitards
s	Amount of subsidence; drawdown
T	Transmissivity; time factor
t	time
U	Degree of consolidation
U_t	Excess pore pressure at time t
U_W	Pore pressure (fluid pressure or neutral stress)

Symbol	Term
∇	Flow velocity vector
w	Moisture content, per cent of dry weight
w_L	Liquid limit
w_P	Plastic limit
Y_s	Specific yield
z	Depth
αke	Compressibility of aquifer-system skeleton in elastic range of stress
αkv	Compressibility of aquifer-system skeleton in virgin range of stressing
β_w	Compressibility of water
γ	Submerged unit weight
γ_b	Buoyant unit weight of saturated deposits
γ_d	Dry unit weight
γ_m	Moist unit weight
γ_s	Unit weight of solids
γ_w	Unit weight of water
$\Delta p'$	Change in effective stress
ν	Diffusivity; Poisson’s ratio
τ	Time constant

Appendix D. Glossary, by Laura Carbognin and Working Group

The purpose of this glossary is to explain the meaning of terms currently recurring in studies on land subsidence due to ground-water withdrawals. Because this volume is for readers with diverse backgrounds and for interested untrained personnel, the definitions given here are simplified. For a more detailed explanation, the bibliography suggests some books which will help the reader.

AQUICLUDE

An areally extensive body of saturated but relatively impermeable material that does not yield appreciable quantities of water to wells. Aquicludes constitute boundaries of aquifer flow systems; term is synonymous with confining bed.

AQUIFER

An areally extensive body of saturated permeable material that will yield significant quantities of water to wells and springs. An aquifer includes the unsaturated part of the permeable body. Aquifers may be classed as unconfined or confined, depending upon the presence or absence of a water table. An aquifer may also be called a water-bearing stratum. Unconsolidated alluvial deposits of sand and gravel, porous sandstones, or fractured limestones are examples of water-bearing formations

AQUIFER SYSTEM

A heterogeneous body of interbedded permeable and poorly permeable layers that functions regionally as a water-yielding hydraulic unit. It comprises two or more aquifers (permeable formations) separated by laterally discontinuous aquitards that locally impede ground-water movement but do not greatly affect the overall hydraulic continuity of the system.

AQUITARD

A saturated, but poorly permeable, bed that locally impedes ground-water movement and does not yield water freely to wells, but which may transmit appreciable water, to or from adjacent aquifers.

ARTESIAN

The term artesian derives from Artois (Lat. Artesium), a northern province of France where naturally flowing wells were drilled in 1750. Today the term artesian is applied to any well tapping a pressure aquifer or simply to the aquifer itself. Artesian is synonymous with confined.

ARTESIAN AQUIFER

An aquifer in which the water level rises above the base of the upper confining bed when penetrated by a well. In recent years artesian aquifer has been used as a synonym for confined aquifer.

BENCH MARK

A relatively permanent mark, natural or artificial, furnishing a survey point at a known elevation in relation to an adopted datum. Bench marks, or marked points, connected by precise leveling, constitute the control of land-surface settlement.

COEFFICIENT OF COMPRESSIBILITY (L^2F^{-1})

Compressibility is the aptitude of the soil to be deformed. It is expressed by means of a coefficient which is the ratio between a void ratio decrease from e_o to e and an increase in effective stress. The value $a_v = e_0 - e\Delta p$ represents the coefficient of compressibility for the range p_0 to $p_0 + p$. Units usually are cm^2kg^{-1}.

COEFFICIENT OF VOLUME COMPRESSIBILITY (L^2F^{-1})

The compression of a clay (aquitard) per unit of original thickness, due to a unit increase of effective stress, in the load range exceeding preconsolidation stress. It is expressed by the equation

$$m_v = \frac{a_v}{1 + e_0}$$

in which e_0 is the initial void ratio. Units usually are $cm^2\ kg^{-1}$.

COMPACTION

A decrease in the volume of a mass of sediments from any cause. In this guidebook, compaction is defined as the decrease in the thickness of sediments, as a result of an increase in vertical compressive stress, and is synonymous with "one-dimensional consolidation," as used by engineers. The term compaction is applied both to the process and to the measured change in thickness.
In thick fine-grained beds, compaction is a delayed process involving the slow escape of pore water and the gradual transfer of stress from neutral to effective. Until sufficient time has passed for excess pore pressure to decrease to zero, measured values of compaction are transient.

COMPACTION, RESIDUAL

Compaction that would occur ultimately if a given increase in applied stress were maintained until steady-state pore pressures were achieved, but had not occurred as of a specified time because excess pore pressures still existed in beds of low diffusivity in the compacting system. It can also be defined as the difference between (1) the amount of compaction that will occur ultimately for a given increase in applied stress, and (2) that which has occurred at a specified time.

COMPACTION, SPECIFIC (L^3F^{-1})

The decrease in thickness of deposits, per unit of increase in applied stress, during a specific time period.

CONE OF DEPRESSION

A cone of depression in the water table, developed around a pumping well and extending throughout the area of influence of a well (also see drawdown). For an artesian aquifer, this can be called the "cone of pressure relief" (Tolman, 1937).

CONFINED AQUIFER

Same as artesian aquifer.

CONSOLIDATION

The gradual reduction in the water content (void ratio) of a saturated soil, as a result of an increase in the pressure acting on it, because of the addition of overlying sediments or the application of an external load. A laboratory test called a one-dimensional consolidation test (odometric test), is performed on soil samples to evaluate consolidation. From such a test the coefficient of consolidation, c_v, usually reported in $cm^2 sec^{-1}$, is calculated as the ratio

$$c_v = \frac{K}{m_v \gamma_w} \frac{1}{}$$

where K is the hydraulic conductivity, m_v is the coefficient of volume compressibility, and γ_w is the unit weight of water. The theory of consolidation, developed by Terzaghi, leads to a relation between degree of consolidation and time:

$$U\% = \frac{c_v t}{H^2}$$

In this expression U is the degree of consolidation, that is, the percentage of total consolidation occurring in some time t; c_v is the coefficient of consolidation; and H is half of the sample's thickness when the odometric test is performed.

DRAWDOWN

As water is withdrawn from an aquifer by a pumped well, the ground-water level is lowered. Drawdown is the distance the water table or pressure surface is lowered at a given point (see also cone of depression).

EXTENSOMETER

An instrument used for measuring vertical deformation of fine-grained beds in the subsoil under stress. Vertical extensometers commonly are installed when land subsidence follows ground-water withdrawal. Extensometers also are used to measure small horizontal displacements.

HEAD, HYDRAULIC, OR STATIC

The static head is the height, referred to a standard datum, of the surface of a column of water that can be supported by the static pressure at a given point. The static head is the sum of the elevation head and the pressure head.

HYDRAULIC CONDUCTIVITY, K (LT^{-1})

If a porous medium is isotropic and the fluid is homogeneous, the hydraulic conductivity of the medium is the volume of water at the existing kinematic viscosity that will move in unit time under a unit hydraulic gradient through a unit area measured at right angles to the direction of flow. In the metric system it may be expressed in cm sec^{-1}; in English units it may be expressed in feet day^{-1} (see also permeability).

HYDRAULIC GRADIENT

The change in static head per unit of distance in the direction of the maximum rate of decrease in head if not specified. If different, direction is specified.

HYDROCOMPACTION

The process of volume decrease and density increase that occurs when moisture-deficient deposits compact as they are wetted for the first time since burial. This type of land settlement has also been called "shallow subsidence."

LAND SUBSIDENCE

Sinking or settlement of the land surface, due to diverse causes and generally occurring on a large scale. Usually the term refers to the vertical downward movement of the land surface although small-scale horizontal movements may be present. The term does not include landslides which have large-scale horizontal displacements, or settlement of artificial fills.

PERMEABILITY

The capacity of rock or soil to transmit fluid under the combined action of gravity and pressure. Permeability is expressed as the velocity with which water, under the influence of a given difference in head, passes through a porous medium having a certain cross section and thickness. Permeability is dependent on the size and shape of the pores of the porous medium and it can be reduced by compaction (see also hydraulic conductivity).

PHREATIC AQUIFER

Same as unconfined aquifer.

PHREATIC SURFACE

Same as water table.

PIEZOMETRIC SURFACE

An imaginary surface coinciding with the head of the water in an aquifer. (Also see potentiometric surface.)

POTENTIOMETRIC SURFACE

A surface which represents the static head. As related to an aquifer, it is defined by the levels to which water will rise in tightly cased wells (USGS) Also called piezometric surface in many countries.

REBOUND

An upward movement of soil as a consequence of a decrease in effective stress. In fine-grained soils, rebound is usually much less than the amount of compaction, since the latter is mostly irreversible.

RECOVERY

The water-level rise in a well occurring upon the cessation of discharge from that well or a nearby well.

STRESS, APPLIED (FL^{-2})

The downward stress imposed at an aquifer boundary. It differs from effective stress in that it defines only the external stress tending to compact a deposit rather than the grain-to-grain stress at any depth within a compacting deposit.

STRESS, EFFECTIVE (FL^{-2})

Stress (pressure) that is borne by and transmitted through the grain-to-grain contacts of a deposit, and thus affects its porosity or void ratio and other physical properties. In one-dimensional compression, effective stress is the average grain-to-grain load per unit area in a plane normal to the applied stress. At any given depth, the effective stress is the weight (per unit area) of sediments and moisture above the water table, plus the submerged weight (per unit area) of sediments between the water table and the specified depth, plus or minus the seepage stress (hydrodynamic drag) produced by downward or upward components, respectively, of water movement through the saturated sediments above the specified depth. Thus, effective stress may be defined as the algebraic sum of the two body stresses, gravitational stress and seepage stress. Effective stress may also be defined as the difference between geostatic and neutral stress.

STRESS, GEOSTATIC (FL^{-2})

The total load per unit area of sediments and water above some plane of reference. It is the sum of (1) the effective stress and (2) the neutral stress.

STRESS, NEUTRAL (FL^{-2})

Fluid pressure exerted equally in all directions at a point in a saturated deposit by the head of water. Neutral pressure is transmitted to the base of the deposit through the pore water, and does not have a measurable, influence on the void ratio or on any other mechanical property of the deposits.

STRESS, PRECONSOLIDATION.(FL^{-2})

The maximum antecedent effective stress to which a deposit has been subjected, and which it can withstand without undergoing additional permanent deformation. Stress changes in the range less than the preconsolidation stress produce elastic deformations of small magnitude. In fine-grained materials, stress increases beyond the preconsolidation stress produce much larger deformations that are principally inelastic (nonrecoverable).

STRESS, SEEPAGE (FL^{-2})

When water flows through a porous medium, force is transferred from the water to the medium by viscous friction. The force transferred to the medium is equal to the loss of hydraulic head. This force, called the seepage force, is exerted in the direction of flow.

SUBSIDENCE/HEAD-DECLINE RATIO

The ratio between land subsidence and hydraulic head decline in the coarse-grained beds of the compacting aquifer system.

UNCONFINED AQUIFER

A geologic formation of permeable material that has a water table as the upper surface.

WATER TABLE

The upper surface of the zone of saturation in a phreatic aquifer in which the pressure is atmospheric.

WELL, ARTESIAN

A well that takes water from a pressure water body.

REFERENCES

AMERICAN SOCIETY FOR TESTING AND MATERIAL. 1980. Standard definitions of terms and symbols relating to soil and rock mechanics. ASTM C.653-80, p. 29.

CHOW, V. T. 1964. Handbook of applied hydrology, Ch. 13. New York, McGraw-Hill, 55 p.

KEZDI, A. 1974. Handbook of soil mechanics. Vol. 1, Soil physics. New York, Elsevier, 294 P.

LOFGREN, B. E., and KLAUSING, R. L. 1969. Land subsidence due to ground-water withdrawal, Tulare-Wasco area, California. U.S. Geological Survey water-supply paper 1988, 21 p.

MEINZER, O. E. 1923. Outline of ground-water hydrology with definitions. U.S. Geological Survey water-supply paper 494, 71 p.

POLAND, J. F., LOFGREN, B. E., and RILEY, F. S. 1972. Glossary of selected terms useful in studies of the mechanics of aquifer systems and land subsidence due to fluid withdrawal. U.S. Geological Survey Water-Supply Paper 2025, 9 p.

PROKOPOVICH, N. P. 1963. Hydrocompaction of soils along the San Luis Canal alignment, western Fresno County, California. In Abstracts for 1962. Geol. Soc. America spec. paper 76, p. 70.

TERZAGHI, K., and PECK, R. B. 1967. Soil mechanics in engineering practice, 2nd ed. New York, John Wiley, 729 p.

TODD, D. K. 1959. Hydrology. New York, John Wiley, 336 p.

TOLMAN, C. F. 1937. Ground water. New York, McGraw-Hill. 593 p.

UNITED NATIONS EDUCATIONAL, SCIENTIFIC AND CULTURAL ORGANIZATION. 1978. International glossary of hydrology, 2nd ed., WMO/UNESCO.

Appendix E. Metric conversion table

Multiply inch-pound unit	By	To obtain metric unit
inch	25.4	millimetre (mm)
foot (ft)	0.3048	metre (m)
foot per mile (ft/mi)	0.1894	metre per kilometre (m/km)
mile (mi)	1.609	kilometre (km).
pound ----------	0.45 ----	kilogram (kg)
square foot (ft^2)	0.0929	square metre (m^2)
square mile (mi^2)	2.590	square kilometre (km^2)
acre	0.405	hectare (ha)
acre-foot (acre-ft)	1,233	cubic metre (m^3)
gallon (gal) ----------	3.785 ----	litre (l)
	0.003785	cubic metre(m^3)
cubic foot (ft^3)	0.0283	cubic metre (m^3)
acre-foot per square mile ($acre\text{-}ft/mi^2$)	476	cubic metre per square kilometre (m^3/)km^2)
gallon per minute (gal/min)	6.309×10^{-5}	cubic metre per second (m^3/s)
cubic foot per second per square mile [(ft^3/s)/mi^2]	0.0109	cubic metre per second per square kilometre [(m^3/s)/km^2]
ft per year (ft/yr) ----------	9.7×10^{-7} ---	centimetres per second (cm/s)
gallon per day per square foot (gal/d/ft^2)	4.716xlO-5	centimetre per second (cm/s)
ton (short)	0.9072	metric ton (t)
gallon per day per foot (gal/d/ft)	1.433×10^{-3}	square centimetre per second (cm^2/s)
pound per cubic foot (lb/ft^3)	16.05	kilogram per cubic metre (kg/m^3)
pounds per square inch (psi)	0.07	kilograms per square centimetre (kg/cm^2)

ISBN 92-3-102213-X